Organizational Results Research Report

January 2007
OR07.006

Slope Stabilization Using Recycled Plastic Pins Phase III

Prepared by Missouri Transportation Institute and Missouri Department of Transportation

FINAL REPORT

RI98-007D

Slope Stabilization Using Recycled Plastic Pins – Phase III

Prepared for the
Missouri Department of Transportaion
Organizational Results

by
J. Erik Loehr, Ph.D.
Assistant Professor of Civil Engineering
and
John J. Bowders, Ph.D., P.E.
Professor of Civil Engineering

Department of Civil and Environmental Engineering
University of Missouri - Columbia

January 2007

TECHNICAL REPORT DOCUMENTATION PAGE

1. Report No.	2. Government Accession No.	3. Recipient's Catalog No.
4. Title and Subtitle Slope Stabilization Using Recycled Plastic Pins – Phase III		5. Report Date January 2007
		6. Performing Organization Code
7. Author(s) J. Erik Loehr and John J. Bowders		8. Performing Organization Report No.
9. Performing Organization Name and Address University of Missouri – Columbia Department of Civil and Environmental Engineering; E2509 Lafferre Hall Columbia, Missouri 65211-2200		10. Work Unit No. 11. Contract or Grant No. RI98-007D
12. Sponsoring Agency Name and Address Missouri Department of Transportation Research, Development and Technology Division P. O. Box 270-Jefferson City, MO 65102		13. Type of Report and Period Covered Final Report 14. Sponsoring Agency Code

15. Supplementary Notes
The investigation was conducted in cooperation with the U. S. Department of Transportation, Federal Highway Administration.

16. Abstract

A new technique for stabilizing surficial slope failures using recycled plastic reinforcing members has been developed. The objective of the project described in this report has been to develop, evaluate, and document a technique for stabilization of surficial slope failures using recycled plastic reinforcing members. The project has been undertaken in three sequential phases to provide for logical evaluation of project accomplishments and refinement of the scope of work based on results of activities undertaken throughout the project. This report is the final technical report for the entire three phase project, which describes the accumulated activities performed throughout all three phases of the project.

The principal project tasks undertaken include development of a general design methodology, evaluation of the material properties of recycled plastic members from several different manufacturers, establishment of full-scale field test sections at five different sites, monitoring the performance of these sites for periods ranging from two to five years, evaluation and interpretation of field observations, "calibration" of the developed design method, and finally, development of technology transfer materials.

The following conclusions are drawn from the work performed as part of this project: (1) the technique of using recycled plastic reinforcement to stabilize surficial slope failures has proven to be effective at providing long-term stabilization; (2) observed performance at the test sites suggests a typical behavioral pattern consisting of an initial period in which little movement is observed and little load is transferred to the reinforcement, a period of increasing movement and increasing mobilized loads in the reinforcement, followed by a period of stabilized movements and loads in the reinforcing members as a result of the slope coming to equilibrium; (3) while the required member spacing depends on the conditions present at a site, a "standard" pattern that appears sufficient for most sites consists of using recycled plastic reinforcing members placed in a 3-ft by 3-ft (0.9-m by 0.9-m) staggered arrangement over the entire slide area; (4) reliable installation can be accomplished with either a percussion hammer similar to what is used on many drill rigs, or a simple drop-weight hammer similar to what is used to install guard rail posts; (5) care must be used when selecting recycled plastic products for use in slope stabilization applications as the properties of these materials can vary substantially from product to product; and (6) costs for the technique vary with the reinforcement pattern selected but appear to be substantially less than those for most other competing slope stabilization technologies.

Given the cost effectiveness and successful demonstration of the technique, it is recommended that the technique be implemented in "production" operations. The primary challenges to implementation are likely to involve developing appropriate contracting methods for selection of qualified installation contractors and for acquisition of suitable recycled plastic product. In the early phases of implementation, it is further recommended that limited monitoring be performed of both construction operations as well as post construction performance to further expand the database of cases where the technique has been used and to provide for reliable evaluation of the technique in production operations.

17. Key Words	18. Distribution Statement
Geotechnical Engineering, slope stability, slope stabilization, recycled plastic, maintenance, repair, field demonstration	No restrictions. This document is available to the public through National Technical Information Center, Springfield, Virginia 22161

19. Security Classification (of this report)	20. Security Classification (of this page)	21. No. of Pages	22. Price
Unclassified	Unclassified	289	

Executive Summary

The objective of the project entitled "Slope Stabilization Using Recycled Plastic Pins" has been to develop, evaluate, and document a technique for stabilizing surficial slope failures using recycled plastic reinforcing members. The project has been undertaken in three sequential phases to provide for logical evaluation of project accomplishments and refinement of the scope of work based on results of activities undertaken throughout the project. This report is the final technical report for the entire three phase project, which describes the accumulated activities performed throughout all three phases of the project.

Phase I of the project was initiated in January 1999 and served as a "proof of concept" phase, wherein a single slope was stabilized using recycled plastic reinforcement. The proof of concept site, located on Interstate 70 near Emma Missouri, was successfully stabilized in November 1999. Additional activities undertaken during Phase I included basic characterization of the engineering properties of recycled plastic members, evaluation of the long-term stability of recycled plastics when subjected to potentially detrimental environmental conditions, and installation of instrumentation for monitoring the performance of the stabilized slope. Phase I was completed in June 2000.

Phase II of the project was initiated in October 2000 to expand the evaluation and demonstration of the technique. In this phase, test sections were established at five sites selected from well over 50 candidate test sites to provide for evaluation of the stabilization technique in a variety of different conditions (e.g. slope type, slope height, slope inclination, water conditions, etc.) while at the same time providing opportunity to evaluate alternative stabilization schemes. Two of the selected sites were located in District 4 on Interstate 435 in southern Kansas City. Additional sites were located in District 1 on U.S. Highway 36 near Stewartsville Missouri, in District 2 on Interstate 70 near Emma Missouri, and in District 5 on U.S. Highway 54 near Fulton Missouri. Following installation, each of the sites were monitored for periods ranging from two to five years using various types of field instrumentation. Phase II was completed in December 2003.

Phase III was initiated in November 2003. The focus of the final phase of the project was to complete field monitoring activities at the test sites, to analyze and assimilate the observed field performance into practical and implementable design and construction tools and procedures, and to develop practical technology transfer materials to facilitate widespread implementation of the technique. Field monitoring was completed in February 2005. This report serves as the final deliverable for the project and as documentation of the entire three phase project.

The principal conclusions derived from the project are as follows:

(1) The technique of using recycled plastic reinforcement to stabilize surficial slope failures in excavated and embankment slopes has proven to be effective at providing long-term stabilization. To date, slopes stabilized as a part of this project have been in place for up to six years. Control sections established at several of the sites have failed, which demonstrates that these sites have very likely been subjected to conditions that are at least as bad as those that caused the original failures and that the installed reinforcement is in fact providing additional stabilization.

(2) Observations from field instrumentation measurements taken at the field test sites provide a consistent picture of how the reinforcement effects stabilization. The observed performance has generally followed a three-stage behavioral pattern. In the first stage, the stabilized slopes are observed to experience little movement and little resistance is provided by the reinforcing members. In Stage 2, slope movements are observed to increase substantially in response to increased pore water pressures within the slope at the same time as loads in the reinforcing members are observed to increase. These movements are believed to simply be movement required to mobilize resistance in the reinforcing members. Finally, Stage 3 is characterized by diminishing movement that is simultaneously accompanied by stabilization of the loads in the reinforcing members. This stage is believed to be a result of the slope and reinforcement coming to equilibrium.

(3) The required spacing of reinforcing members depends on the specific conditions encountered at a particular site. A "standard" reinforcement pattern that appears to be sufficient for the vast majority of cases encountered consists of a distributed pattern of reinforcing members placed across the entire slide area on a staggered grid with members spaced at 3-ft centers. In some cases, appropriate stabilization can also be accomplished with members placed at greater spacing.

(4) Recycled plastic reinforcing members can be efficiently and reliably installed using either a percussion hammer found on many drilling rigs or a simple drop-weight type of hammer. Experience acquired to date has shown that the critical feature of installation equipment is having a mast to maintain the alignment between the hammer and the reinforcing member.

(5) Costs for stabilization of slopes using recycled plastic reinforcing members were relatively consistent throughout the project. Nominal costs for materials and installation are approximately $40/member with the costs being approximately equally split between material costs and installation costs. Unit costs per unit area of the slope face vary significantly with the spacing of the reinforcing members.

(6) Field performance data acquired at the respective test sites provide a strong basis for "calibration" of the general design methodology developed as part of this project to establish specific recommendations for application of the method for future design. Recommendations developed based on these analyses include:
- that Broms' (1964) method be used for predicting the limit soil pressure,
- that axial resistance be ignored in the analyses,
- that the member capacity used for prediction of member resistance be taken as the nominal measured capacity when members are to be placed at spacings of 3-ft or less and as 60% of the nominal measured capacity when members are to be placed at spacings greater than 3-ft.

(7) The material properties of recycled plastic members vary with the manufacturing process used and the specific blend of constituents used.

(8) The properties of all recycled plastic members are dependent on the specific loading rate adopted for testing and the magnitude of loading rate effects can vary from product to product. As such, care must be applied when reviewing material properties from different manufacturers and for different products to ensure that acceptable performance can be achieved with a particular product.

Acknowledgements

This project could not have been accomplished without the assistance of numerous individuals who contributed their time, efforts, and expertise to the project. The assistance of all of these individuals is gratefully appreciated. Particular acknowledgement is due to Thomas Fennessey, Bill Billings, Bruce Harvel, Ken Markwell, Barry Arthur, Mike McGrath, Steve Giffen, Gary Goessmann, Chuck Sullivan and many others with the Missouri Department of Transportation for identifying candidate sites and facilitating the project in many ways. Pat Carr, Terrell Waller, and several others from The Judy Company provided much needed expertise, equipment, and assistance with installation at each of the test sites. Professor Hani Salim of the University of Missouri Department of Civil and Environmental Engineering provided sound guidance for evaluating the structural properties of the recycled plastic members. Randy Jolitz of Epoch Composite Products, Rachel Aanenson of Bedford Technology, and Sabine Zink of Resco Plastics provided recycled plastic members for testing. The Recycled Materials Resource Center provided supplemental funding to the project to support development of a draft specification for recycled plastics for use in slope stabilization. The MoDOT Geotechnical Technical Advisory Group is acknowledged for their thoughtful review of project reports and pertinent comments and suggestions for the project. The support of the University of Missouri College of Engineering and Department of Civil and Environmental Engineering is also appreciated. Finally, the assistance of numerous undergraduate and graduate student research assistants including: Jorge Parra, Eng Chew Ang, David Hagemeyer, Paul Denkler, Lee Sommers, Awilda Blanco, Daniel Huaco, Joseph Chen, Glen Bellew, Todd Dwyer, Andy Boeckmann, Nick Roth, Deepak Neupane, Graham Jones, Tim Morgan, Abe Smith, Katy Chandler and many others was integral to completion of the project.

Table of Contents

Chapter 1. Introduction

The objective of the project entitled "Slope Stabilization Using Recycled Plastic Pins" has been to develop, evaluate, and document a technique for stabilization of surficial slope failures using recycled plastic reinforcing members. The project has been undertaken in three sequential phases to provide for logical evaluation of project accomplishments and refinement of the scope of work based on results of activities undertaken throughout the project. This report is the final technical report for the entire three phase project, which describes the accumulated activities performed throughout all three phases of the project.

1.1. Motivation

Slope failures and landslides constitute significant hazards to all types of both public and private infrastructure. Total direct costs for maintenance and repair of landslides involving major U.S. highways alone (roughly 20 percent of all U.S. highways and roads) were recently estimated to exceed $100 million annually (TRB, 1996). In the same study, indirect costs attributed to loss of revenue, use, or access to facilities as a result of landslides were conservatively estimated to equal or exceed direct costs. Costs for maintaining slopes for other highways, roads, levees, and railroads maintained by government and private agencies such as county and city governments, the U.S. Forest Service, the U.S. Army Corps of Engineers, the National Parks Service, and the railroad industry significantly increase the total costs for landslide repairs.

A significant, but largely neglected, toll of landslides is the costs associated with routine maintenance and repair of “surficial” slope failures. Costs for repair of such slides were not explicitly included in the above referenced study because of limited record keeping for these types of slides by most state departments of transportation. However, the authors of the TRB study conservatively estimated that costs for repair of minor slides equal or exceed costs associated with repair of major landslides. This estimate is supported by the Missouri Department of Transportation’s (MoDOT) experience with surficial slide problems, which are estimated to cost on the order of $1 million per year on average. Many other state departments of transportation have similar problems with similarly high, or even higher annual costs. All available evidence clearly indicates that the cumulative costs for repair of many surficial slides can become extremely large, despite the fact that costs for repair of individual slides are generally low. In addition, minor failures often constitute significant hazards to infrastructure users (e.g. from damage to guard rails, shoulders, or portions of road surface) and, if not properly maintained, often progress into more serious problems requiring more extensive and costly repairs.

The premise of the project is that slender structural members manufactured from recycled plastics can be used to effectively reinforce slopes as illustrated in Figure 1.1. As shown in the figure, recycled plastic reinforcing members are installed in the slope to intercept potential sliding surfaces and provide the resistance needed to maintain the long-term stability of the slope. Using recycled plastic members for stabilization has several potential advantages over more common civil engineering materials. Plastic members are less susceptible to degradation by chemical and biological attack than other structural materials and are lightweight, meaning smaller installation equipment and lower transport costs. Plastic members also present less of an obstruction if future construction (e.g.

underground utilities) must traverse a stabilized site. Using recycled plastics also has environmental and political benefits as it reduces the volume of waste entering landfills and provides additional markets for recycled plastic. Development of a cost effective means for using these materials while providing long-term stabilization therefore clearly has numerous advantages for agencies like MoDOT.

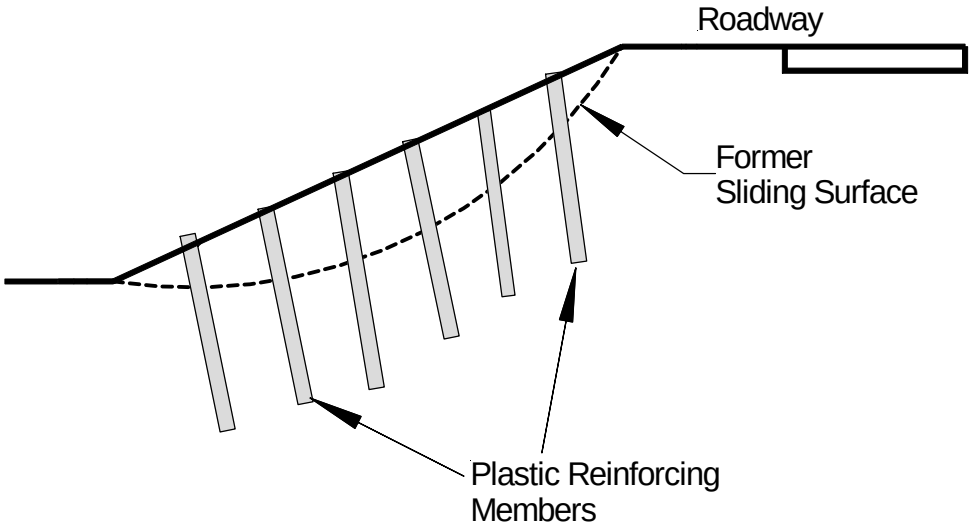

Figure 1.1 Stabilization of surficial slope failures with recycled plastic reinforcement.

1.2. Background

Because no previous attempts to utilize recycled plastic members in similar applications had been undertaken, the project was developed to be performed in three phases. Phase I of the project was initiated in January 1999 and served as a "proof of concept" phase, wherein a single slope was stabilized using recycled plastic reinforcement. The proof of concept site, located on Interstate 70 near Emma Missouri, was successfully stabilized in November 1999. Additional activities undertaken during Phase I included basic characterization of the engineering properties of recycled plastic members, evaluation of the long-term stability of recycled plastics when subjected to potentially detrimental environmental conditions, and installation of instrumentation for monitoring the performance of the stabilized slope. Phase I was completed in June 2000.

Phase II of the project was initiated in October 2000 to expand the evaluation and demonstration of the technique and to begin addressing four key issues deemed critical to successful implementation of the technique on a widespread basis. These issues included:

- Determining the range of applicability for using recycled plastic members for slope stabilization (e.g. soil type, slope geometry, etc.),
- Validating the assumptions inherent in the design methodology and optimizing placement of reinforcing members,
- Establishing the economics of stabilization with slender reinforcement as compared to other current and potential stabilization measures, and

- Developing and documenting formal procedures for design and construction of slope stabilization measures and developing technology transfer materials.

The predominant activities undertaken in Phase II included establishing additional test sites in differing site conditions, initiating additional performance monitoring to determine the load transfer mechanisms for recycled plastic reinforcement, and acquiring additional cost data for the technique. Phase II was completed in December 2003.

Phase III was initiated in November 2003. The focus of the final phase of the project was, in essence, to address the remaining issues for successful widespread implementation. The primary objectives of Phase III have been to complete field monitoring activities at the field test sites, to analyze and assimilate the observed field performance into practical and implementable design and construction tools and procedures, and to develop practical technology transfer materials to facilitate widespread implementation of the technique. Field monitoring was completed in February 2005. This report serves as the final deliverable for the project and as documentation of the entire three phase project.

1.3. Structure of Report

Because of the critical role played by full-scale field evaluations at the test sites, this report is generally organized with respect to the different test sites with several additional chapters to describe other pertinent activities and findings. In Chapter 2, the general objectives and the adopted approach for design of slopes reinforced using recycled plastic reinforcement are presented followed by descriptions of several specific issues associated with predicting the resistance provided by reinforcing members. Evaluations undertaken to determine the engineering properties of recycled plastic members are then described in Chapter 3. The general process and criteria used for selection of the respective field test sites are described in Chapter 4. Chapter 5 describes the instrumentation used to monitor performance at the respective field test sites.

Activities undertaken to establish each of the respective test sites are described in Chapters 6 through 9. Each of these chapters contain general descriptions of the site, a summary of soil properties determined for the sites, a summary of the stability analyses performed, a description of the selected stabilization scheme(s), descriptions of specific instrumentation, and finally a summary of observations obtained from instrumentation. Chapter 10 then describes the construction methods used and the installation monitoring performed for each of the respective field test sites.

Chapter 11 contains a summary of observations drawn from collective interpretation of observations from the test sites and description of a series of "calibration" analyses used to refine the general design method based on the observed field performance at the field sites. Recommendations regarding design of slope stabilization schemes using recycled plastic reinforcement are also provided in Chapter 11. Finally, Chapter 12 contains a summary of the report along with overall conclusions from the project effort.

1.4. Other Project Documentation

In addition to this report, a series of other publications have been prepared during different stages of the project to document project activities and findings at interim stages of the project, to document more narrowly focused tasks performed as part of the project, or to facilitate implementation of the slope stabilization technique. These publications include

project reports, draft specifications, student theses, and several peer-reviewed publications published in scholarly journals or conference proceedings.

Project Reports

- Phase I Technical Report – *Slope Stabilization Using Recycled Plastic Pins – Constructability* (Loehr et al., 2000)
- Phase II Technical Report – *Slope Stabilization Using Recycled Plastic Pins: Phase II – Assessment in Varied Site Conditions* (Loehr and Bowders, 2003)
- Material Properties Evaluation Report – *Evaluation of Recycled Plastic Products in Terms of Suitability for Stabilization of Earth Slopes* (Bowders et al., 2003)

Technology Transfer Documents

- Draft AASHTO Material Specification – *Standard Specification for Recycled Plastic Pins Used to Stabilize Slopes*
- Draft MoDOT Construction Specification – *Standard Specification for Construction of Slope Stabilization Measures Using Recycled Plastic Reinforcement*
- Design and Construction Guide – Guide for Design and Construction of Slope Stabilization Measures Using Recycled Plastic Reinforcement (Loehr and Bowders, 2006)
- One-half day workshop – "Design and Construction Guidance for Slope Stabilization Using Recycled Plastic Reinforcement", (Loehr and Bowders, 2005)

Student Theses

- *Stability Analysis of Slopes Reinforced with Recycled Plastic Pins*, (Liew, 2000)
- *Reliability-based Analysis of Three Alternative Methods for Repair of Surficial Slope Failure*, (Sommers, 2001)
- *Engineering Properties of Recycled Plastic Pins for Use in Slope Stabilization*, (Chen, 2003)
- *Evaluation of Uncertainties in the Resistance Provided by Slender Reinforcement for Slope Stabilization*, (Parra, 2004)
- *Calibration of Resistance Provided by Slender Reinforcing Members in Earth Slopes*, (Chandler, 2005)
- *Numerical Investigation of Load Transfer Mechanism in Slopes Reinforced with Piles*, (Ang, 2005)

Scholarly Articles

- "Stabilization of Slopes Using Recycled Plastic Pins," *Transportation Research Record: Journal of the Transportation Research Board*, (Loehr et al., 2000)

- "Construction Methods for Slope Stabilization Using Recycled Plastic Pins," *Proceedings of the Mid-Continent Transportation Symposium*, (Sommers et al., 2000)
- "Stabilization of Infrastructure Slopes Using Recycled Plastic Pins," Extended Abstract published in *Proceedings of Transportation Systems 2000 Workshop*, (Loehr, 2000)
- "Slope Stabilization with Recycled Plastic Pins," *Geotechnical News*, (Bowders and Loehr, 2000)
- "Stabilization of Slopes with Recycled Plastic Pins," *Proceedings of the NSF Workshop on Geotechnical Composite Systems*, (Loehr, 2002)
- "Engineering Properties of Recycled Plastic Pins for Use in Slope Stabilization," *Transportation Research Record: Journal of the Transportation Research Board*, (Bowders et al., 2003)
- "Field Performance of Embankments Stabilized with Recycled Plastic Reinforcement," *Transportation Research Record: Journal of the Transportation Research Board*, (Parra et al., 2003)
- "Mechanical Stabilization of Earth Slopes Using Recycled Materials," *Proceedings of Beneficial Use of Recycled Materials in Transportation Applications*, (Loehr et al., 2003)
- "Design Method for Slope Stabilization Using Recycled Plastic Pins," *Proceedings of Geo-Trans 2004: Geotechnical Engineering for Transportation Projects*, (Loehr et al., 2004)
- "Sources of Uncertainty in Lateral Resistance of Slender Reinforcement Used for Slope Stabilization," *Proceedings of Geo-Support 2004: Drilled Shafts, Micropiling, Deep Mixing, Remedial Methods, and Specialty Foundation Systems*, (Parra et al., 2004)
- "Slope Stabilization Using Recycled Plastic Pins," *Proceedings of the 55th Highway Geology Symposium*, (Loehr et al., 2004)
- "Numerical investigation of limit soil pressure for design of pile stabilized slopes," *Prediction, Analysis, and Design in Geomechanical Applications*, (Ang et al., 2005)
- "Creep Behavior of Recycled Plastic Lumber in Slope Stabilization Applications," *Journal of Materials in Civil Engineering,* (Bowders et al., 2006)

The technical reports for Phase I and II (Loehr et al, 2000, and Loehr and Bowders, 2003) serve as formal documentation of progress and results for the project at the completion of the respective phases. The material properties evaluation report (Bowders et al., 2003) documents efforts undertaken to develop knowledge of the behavior of a range of recycled plastic products and to develop a draft material specification for the products when used for the slope stabilization application. Pertinent content from these reports is included in the present report to provide for a complete technical reference on the entire project effort. The

technology transfer documents were generally developed during Phase III of the project. These documents represent the most up-to-date guidance available based on the lessons learned throughout the entire project. All of the project reports and technology transfer materials are available from the Missouri Department of Transportation or from project investigators.

The student theses and scholarly articles generally describe specific aspects of the project, often supplemented with related work outside of the project scope, and represent the state of knowledge at the time of publication. All of the student theses are available from the University of Missouri. The scholarly articles are available from the publishers of the respective articles or through common literature sources.

Chapter 2. General Analysis Methodology and Design Issues

The general approach taken for analysis of reinforced slopes, and the one adopted in this work, is to first establish the resistance provided by individual reinforcing members and then to incorporate that resistance into classic slope stability analysis procedures to determine the factor of safety for the reinforced slope. Given the resistance provided by individual reinforcing members, the mechanics of stability analyses incorporating these forces is relatively well established. Development of the distribution of resistance provided by a single member is less well established. In this chapter, the general approach taken to analyze the stability of slopes reinforced with recycled plastic and "strong" reinforcing members is described with particular focus on development of the distribution of resisting force along reinforcing members. The developed method utilizes a limit state design approach that considers a series of potential failure modes.

2.1. General Approach to Stability Analysis

The general approach adopted for evaluating the stability of reinforced and unreinforced slopes is to first assume a potential sliding surface and then calculate a factor of safety for that sliding surface based on consideration of the equilibrium of the free body formed by the sliding surface and slope surface as shown in Figure 2.1. For most slope stability analyses, the factor of safety, F, is defined as

$$F = \frac{\int s}{\int \tau} \tag{2.1}$$

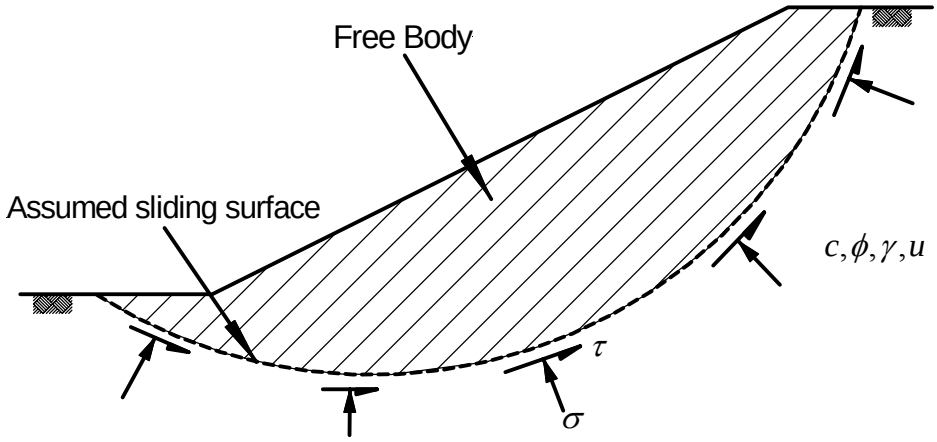

Figure 2.1 Free body diagram considered for equilibrium in slope stability analysis.

where s is the available shear strength and τ is the mobilized shear stress (stress required to maintain equilibrium) on the assumed sliding surface. In the general case, the available shear strength (s) is a function of the normal stress, σ, on the sliding surface and is often expressed using the Mohr-Coulomb failure criterion

$$s = c + \sigma \tan \phi \tag{2.2}$$

where c is the cohesion intercept and ϕ is the angle of internal friction for the soil on the sliding surface. In terms of effective stresses, the Mohr-Coulomb criterion is expressed as

$$s = \bar{c} + (\sigma - u)\tan\bar{\phi} = \bar{c} + \bar{\sigma}\tan\bar{\phi} \qquad (2.3)$$

where u is the pore pressure on the sliding surface, $\bar{\sigma}$ is the effective stress on the sliding surface, and $\bar{c}$ and $\bar{\phi}$ are respectively the cohesion intercept and angle of internal friction expressed in terms of effective stresses. Substituting Equation 2.3 into Equation 2.1 results in the following expression for the factor of safety in terms of effective stresses

$$F = \frac{\int\left(\bar{c} + (\sigma - u)\tan\bar{\phi}\right)}{\int\tau} = \frac{\int\left(\bar{c} + \bar{\sigma}\tan\bar{\phi}\right)}{\int\tau} \qquad (2.4)$$

Equation 2.4 indicates that the factor of safety along an assumed sliding surface is dependent on (1) the Mohr-Coulomb strength parameters ($\bar{c}$ and $\bar{\phi}$) for the soil on the sliding surface, (2) the normal stress (σ) on the sliding surface, (3) the pore pressure (u) on the sliding surface and (4) the mobilized shear stress (τ) on the sliding surface. The Mohr-Coulomb strength parameters ($\bar{c}$ and $\bar{\phi}$) and the pore pressure (u) are assumed to be known. The distribution of normal stress (σ) and shear stress (τ) along the potential sliding surface are unknown and must be determined from equilibrium of the sliding body.

The most common approach to determine the distribution of normal and shear stress is to use a "method of slices" as depicted in Figure 2.2. In this approach, the sliding body is divided into a number of vertical slices and equilibrium of the individual slices is considered to determine the normal and shear forces (or stresses) on the sliding surface and the factor of safety for an assumed sliding surface. The process is then repeated for other potential sliding surfaces until the most critical sliding surface – the surface giving the lowest value of the factor of safety – is found. The factor of safety associated with the most critical sliding surface is taken to represent the stability of the slope.

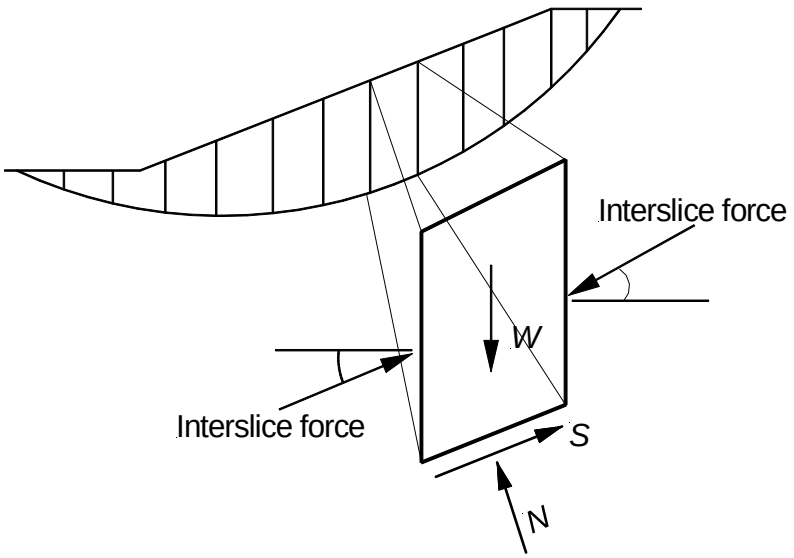

Figure 2.2 Static equilibrium of individual slice in the Method of Slices.

2.2. Stability of Reinforced Slopes

A similar approach is adopted for reinforced slopes except that a force due to a reinforcing member, F_R, is added to the other forces on the slices that are intersected by reinforcing members as shown in Figure 2.3. This force is included in development of equilibrium equations that are used to solve for the overall factor of safety for the slope. It is important to point out that the reinforcement force (F_R) may have components both perpendicular and parallel to the reinforcing member and that F_R is considered a known quantity and must be provided for the stability analysis.

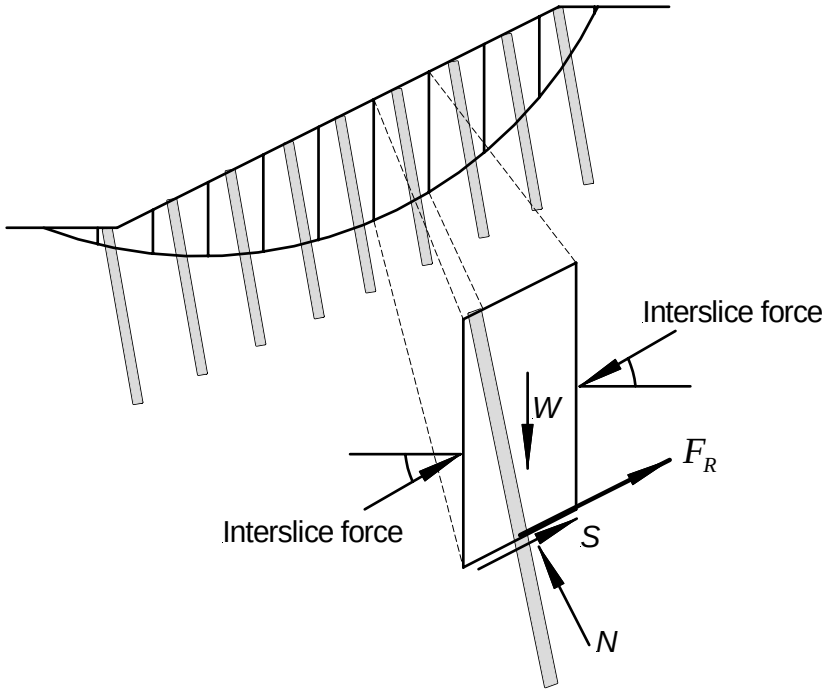

Figure 2.3 Reinforcement force (F_R) on an individual slice in the Method of Slices.

The reinforcement force modifies the factor of safety in several ways. First, the reinforcement force provides a direct resistance to sliding. This direct resistance will always tend to increase the factor of safety over that for the unreinforced slope. In addition, the reinforcement force can modify the computed equilibrium normal and shear forces on the sliding surface and thereby change the factor of safety as compared to an unreinforced slope. These forces can either increase or decrease the factor of safety depending on the inclination of the reinforcement force with respect to the sliding surface and the respective magnitudes of the axial and lateral components of the reinforcement force. Note that for limit equilibrium analyses, forces due to reinforcement are generally taken as the maximum resisting force that can be developed for the reinforcing element. The forces are therefore referred to as "limit resistances" in this report.

In general, the magnitude of the resisting force that is included in the stability analysis varies with position along the reinforcing member. The distribution of the reinforcement force is described by a "limit resistance curve" as shown conceptually in

Figure 2.4. The limit resistance curve defines the magnitude of the resisting force provided by the reinforcing member as a function of the location where a potential sliding surface crosses the member. As illustrated in Figure 2.5, each reinforcing member on a slope will provide a resisting force based on the location of the intersection of the sliding surface and the reinforcing member. The method adopted for computing the limit resistance distribution for reinforcing members is described in the following section.

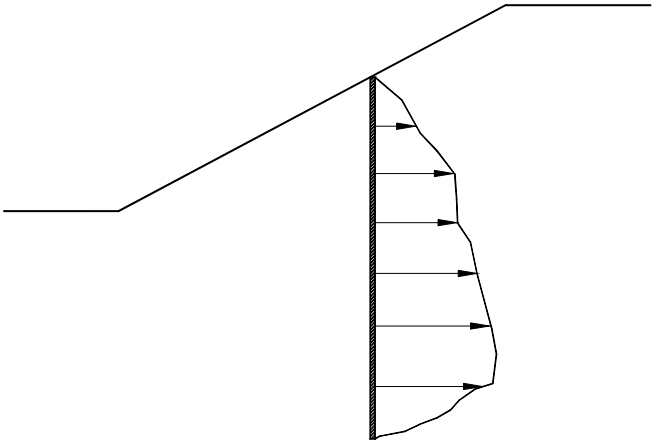

Figure 2.4 Conceptual distribution of limit resistance along a reinforcing member in a slope.

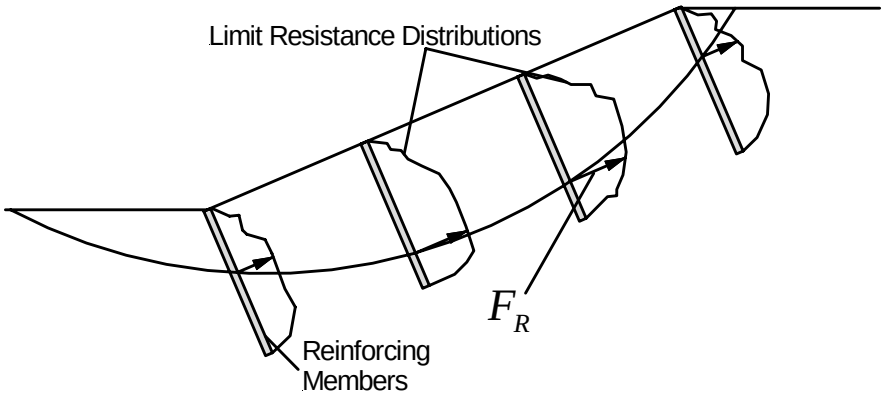

Figure 2.5 Example of distributions of limit resistance for multiple members in a reinforced slope.

2.3. Calculation of Limit Lateral Resistance

Because the resistance provided by reinforcing members is assumed known from the perspective of stability analysis, it is necessary to establish the resistance provided by reinforcing members prior to performing stability analysis. The resistance is generally estimated using a limit state design approach, and is therefore referred to as the limit resistance. The general method used to estimate the limit resistance is described in this chapter. Specific details recommended for use in estimating the limit resistance for recycled plastic reinforcing members are then discussed further in Chapter 11.

In the method adopted for this work, two general failure mechanisms are considered to determine the distribution of limit lateral resistance along the reinforcing members: failure of soil around or between reinforcing members and structural failure of the reinforcing member due to mobilized forces from the surrounding soil. The method only considers the lateral resistance provided by the reinforcing members; axial contributions are ignored although it is clear that axial forces can have an effect on stability. Axial contributions of the reinforcing members are discussed further later in this chapter and in subsequent chapters.

Four specific limit states, or failure modes, are considered in determining the distribution of limit resistance along the reinforcing member as summarized in Table 2.1. The failure mode producing the least limit resistance at each potential sliding depth governs the magnitude of the overall limit resistance. The following sections describe this process in more detail.

2.3.1. Calculation of Limit Resistance Based on Soil Failure Modes

The limit lateral soil pressure is the maximum lateral pressure that the soil adjacent to the reinforcing member can sustain before failure, either by flowing around or between reinforcing members. The two soil failure modes considered in the method are referred to as Failure Mode 1 and Failure Mode 2. In Failure Mode 1, the soil above the sliding surface is considered to fail by flowing between or around the reinforcing members. In Failure Mode 2, the soil below the sliding surface adjacent to the reinforcing member is assumed to fail, resulting in the reinforcing member passing through the soil. The limit resistance corresponding to each of these failure modes is computed based on the limit soil pressure.

Table 2.1 Summary of soil and member failure modes for establishing limit lateral resistance of reinforcing members.

Failure Mode	Description
Mode 1	Failure of soil above sliding surface around or between reinforcing members
Mode 2	Failure of soil below sliding surface due to insufficient anchorage length
Mode 3	Structural failure of member in bending
Mode 4	Structural failure of member in shear

The limit soil pressure (a stress) and limit lateral resistance (a force) acting on a reinforcing member for an assumed sliding depth are illustrated in Figure 2.6. The limit resistance (a force) is computed by integrating the limit soil pressure over the length of the reinforcing member above the depth of sliding, assuming that the limit soil pressure is fully mobilized along the entire length of the member above the sliding surface. The limit resistance force is assumed to act perpendicular to the reinforcing member at the sliding surface. Since the depth of the critical sliding surface is unknown, the limit resistance is computed for varying sliding depths to establish the limit resistance as a function of position along the length of the reinforcing member.

In Failure Mode 1, the soil above the sliding surface is assumed to fail by flowing between or around the reinforcing members. The reinforcing member is assumed sufficiently anchored into stable soil below the sliding surface. A schematic depicting this idea is shown

in Figure 2.7. A limit resistance curve describing the magnitude of the limit lateral resistance as a function of position along the reinforcing member for Failure Mode 1 is shown in Figure 2.8.

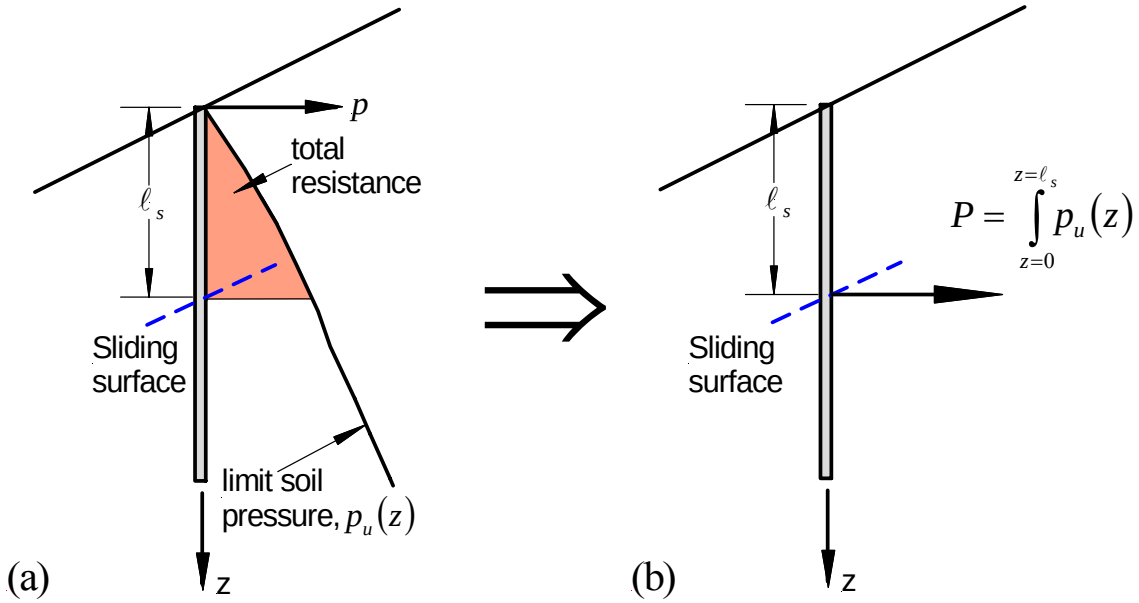

Figure 2.6 Schematic illustrating calculation of limit resistance force: (a) limit soil pressure and (b) equivalent lateral resistance force

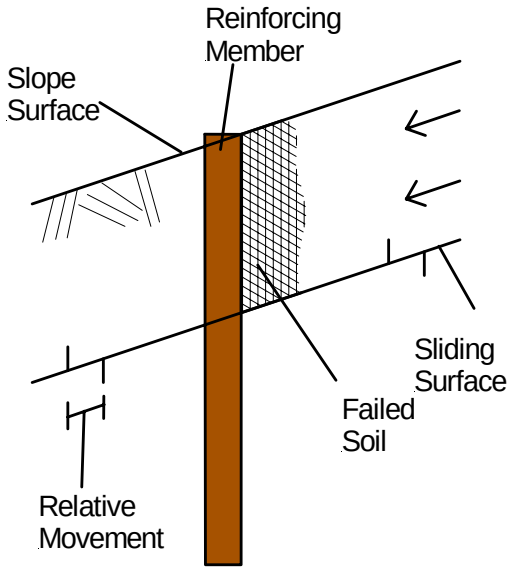

Figure 2.7 Schematic illustrating Failure Mode 1.

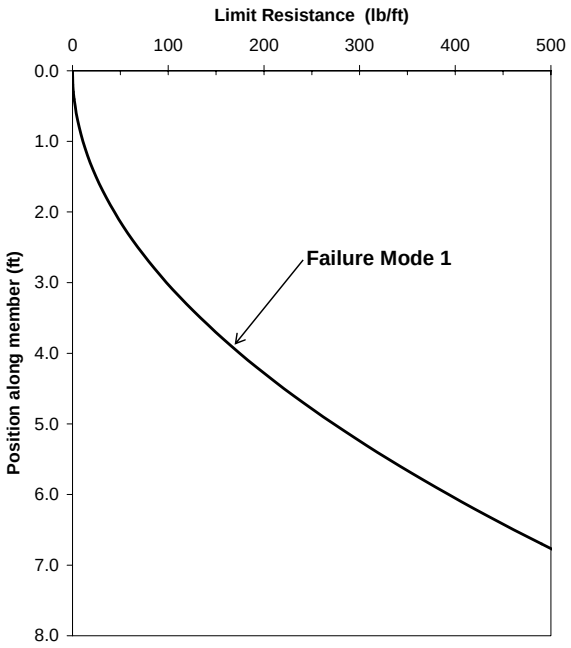

Figure 2.8 Limit resistance curve for Failure Mode 1.

A similar process is used to calculate the resistance for Failure Mode 2, except that the soil below the sliding surface adjacent to the reinforcing member is assumed to fail while

the member is sufficiently anchored in the moving soil above the sliding surface. The reinforcing member is essentially flowing through the soil below the sliding surface, as illustrated in Figure 2.9. The limit resistance for Failure Mode 2 is determined by integrating the limit soil pressure along the reinforcing member below the depth of the sliding surface, again assuming that the limit soil pressure is fully mobilized along the length of member below the sliding surface. This calculation is again repeated for varying depths of sliding to develop a curve describing the magnitude of the limit resistance along the length of the reinforcing member for Failure Mode 2, as shown in Figure 2.10.

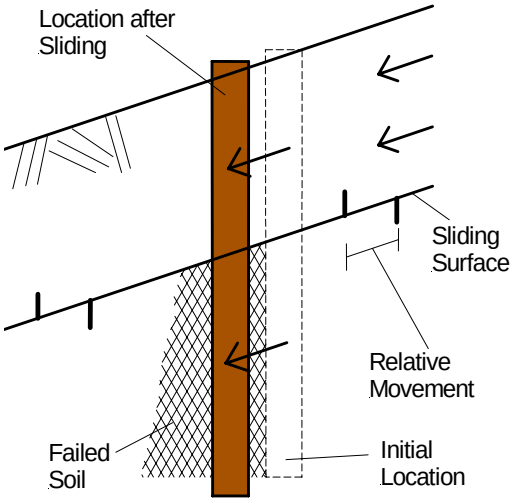

Figure 2.9. Schematic illustrating Failure Mode 2.

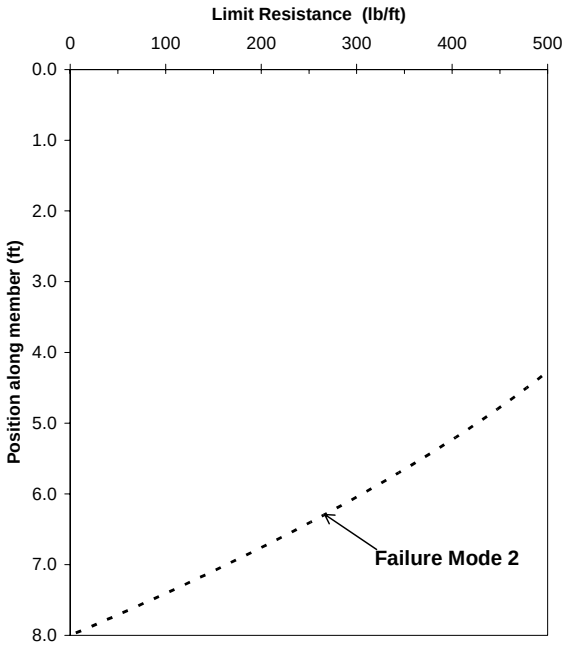

Figure 2.10 Limit Resistance curve for Failure Mode 2.

Combining the two soil failure modes, a composite curve can be developed by taking the least resistance for the two failure modes to produce the limit resistance along the length of the reinforcing member. A typical composite limit resistance curve considering the two soil failure modes is shown in Figure 2.11. The limit resistance computed in this manner is suitable for cases where the structural capacity of the reinforcing member is such that failure of the soil completely controls the resistance.

2.3.2. Structural failure modes

Under some conditions, the limit soil pressure may be great enough that the reinforcing member will fail structurally prior to complete mobilization of the soil resistance. Two potential modes of structural failure exist: failure of the member in bending (Failure Mode 3) and failure of the member in shear (Failure Mode 4). Failure Mode 3 can be further broken into two subcategories: failure due to excessive moments from the applied soil pressure above sliding surface (Failure Mode 3a) and failure due to excessive moments from the soil pressure below the sliding surface (Failure Mode 3b). Failure mode 3a and the limit resistance curve for Failure Mode 3a are shown in Figures 2.12 and 2.13, while the schematic and limit resistance curve for Failure Mode 3b are shown in Figures 2.14 and 2.15.

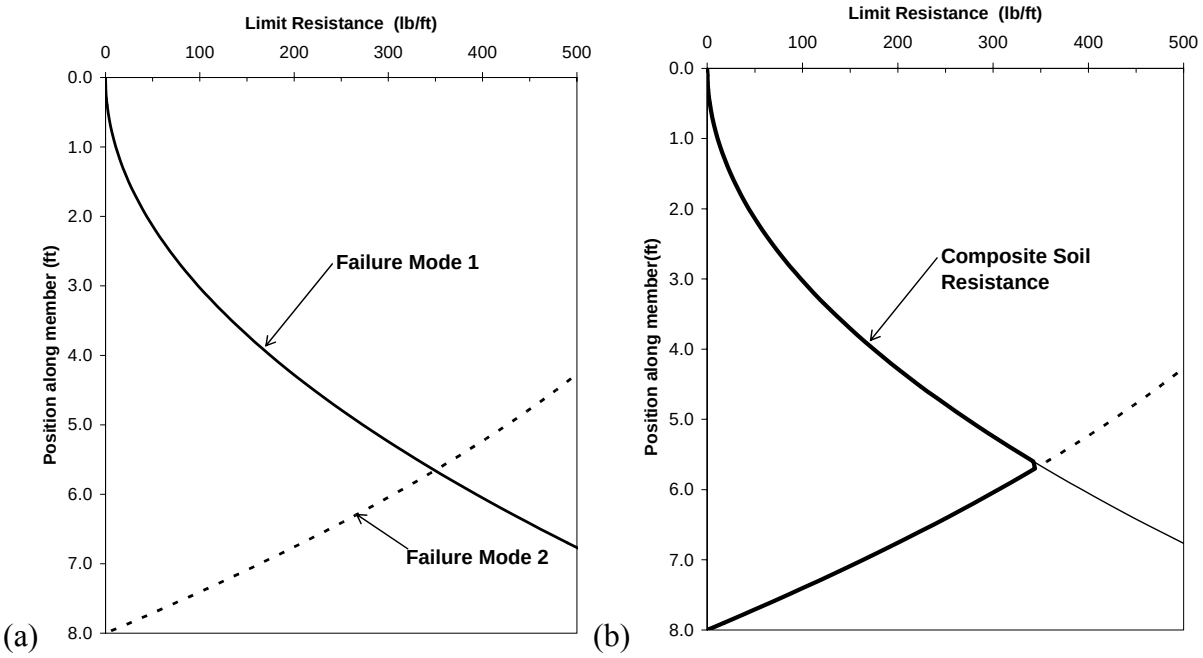

Figure 2.11 Determination of composite resistance based on failure of the soil: (a) Limit resistance curves of Failure Modes 1 and 2 and (b) composite limit resistance curve of Failure Modes 1 and 2.

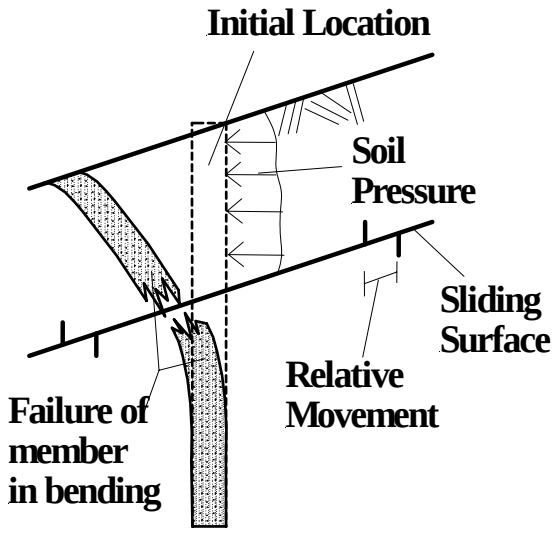

Figure 2.12 Schematic illustrating Failure Mode 3a

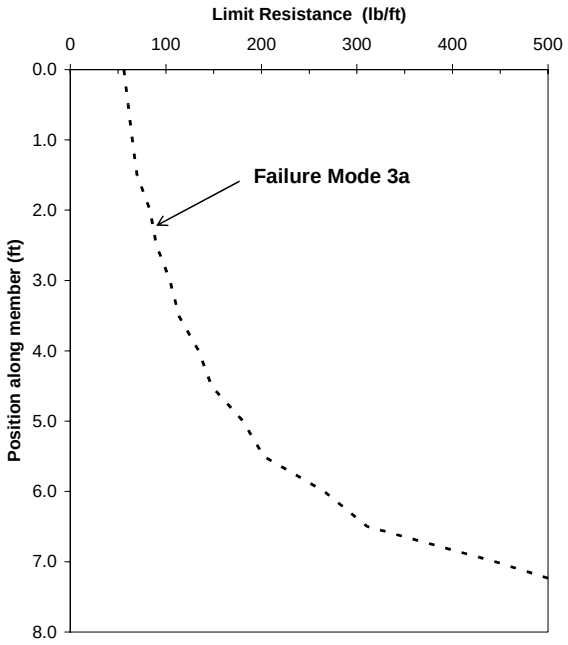

Figure 2.13 Limit Resistance Curve for Failure Mode 3a

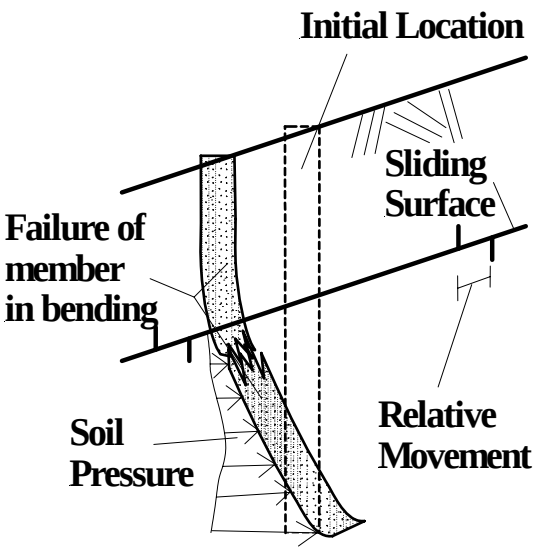

Figure 2.14 Schematic illustrating Failure Mode 3b

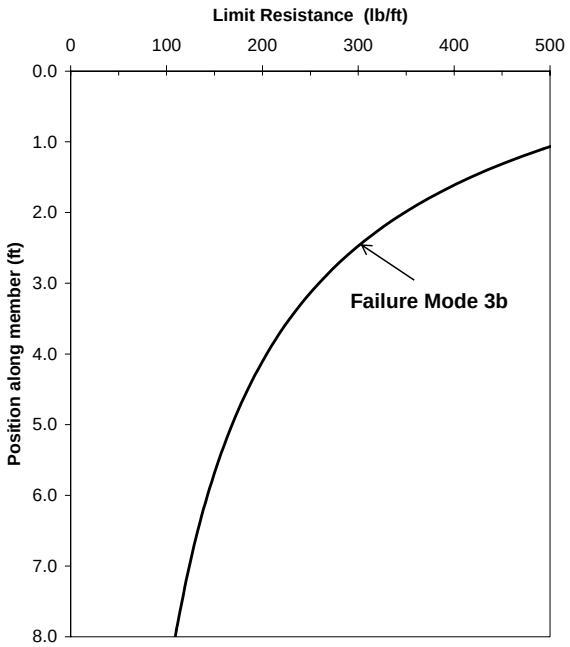

Figure 2.15 Limit Resistance curve for Failure Mode 3b

To calculate the limit resistance corresponding to structural failure of the member in bending, the maximum moment (M_{max}) in the reinforcing member is calculated from elastic theory or numerical methods using the computed limit soil pressures. A scaling factor, α, is then calculated as:

$$\alpha = \frac{M_{\max}}{M_{ult}} \tag{2.5}$$

where M_{ult} is the ultimate design moment of the reinforcing member. This scaling factor is then used to produce a factored soil pressure that approximately produces a maximum moment, M_{max}, equal to M_{ult}. A typical distribution of moment versus depth for a sliding depth of 3.5-ft. is shown in Figure 2.16. The computed maximum moment using the limit soil pressure exceeds the capacity of the reinforcing member. The moment is scaled down so that the maximum moment is equal to the ultimate moment of the reinforcing member, as shown in Figure 2.16a. This scaling factor is then applied to the limit soil pressure, as shown in Figure 2.16b, to produce the factored soil pressure. This factored soil pressure is then used to compute a limit resistance by integrating the factored pressure over the length of member above (mode 3a) or below (mode 3b) the sliding surface as was done for Failure Modes 1 and 2. This process is repeated for varying depths of sliding to produce a curve of the limit resistance corresponding to failure of the reinforcing member. A typical plot of this limit resistance for Failure Modes 3a and 3b is shown in Figure 2.17.

The limit resistance due to failure of a reinforcing member in shear can be evaluated in a similar manner to failure of the reinforcing member in bending by determined the factored soil pressure that causes the computed maximum shear to equal the shear capacity of

the reinforcing member. For the members considered in this research, the shear capacity is not a controlling limit state at any point along the length of the reinforcing member.

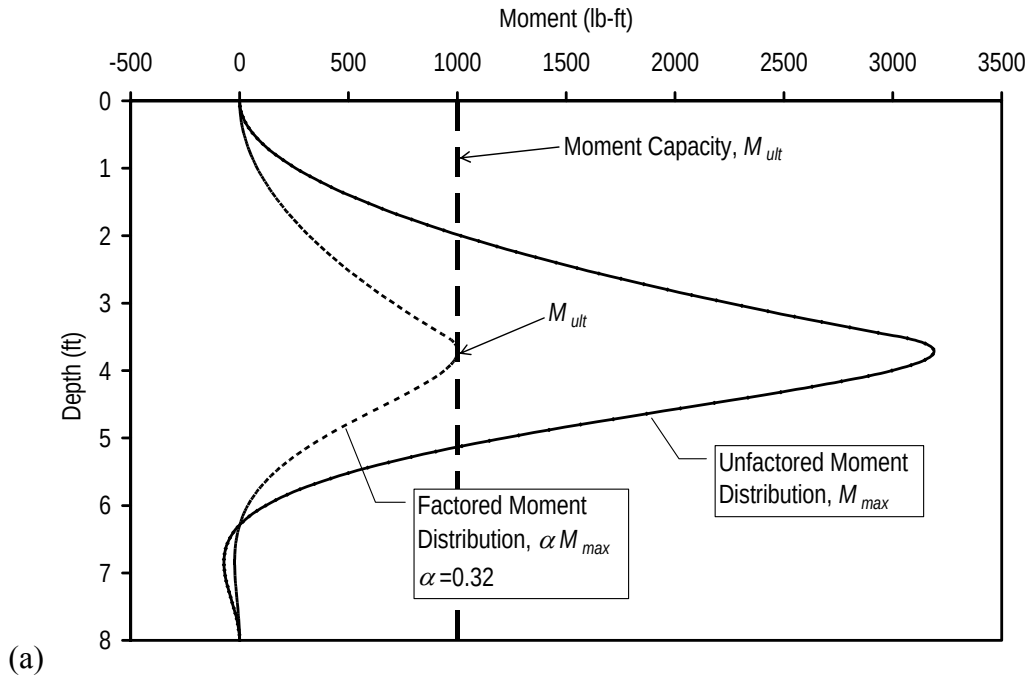

(a)

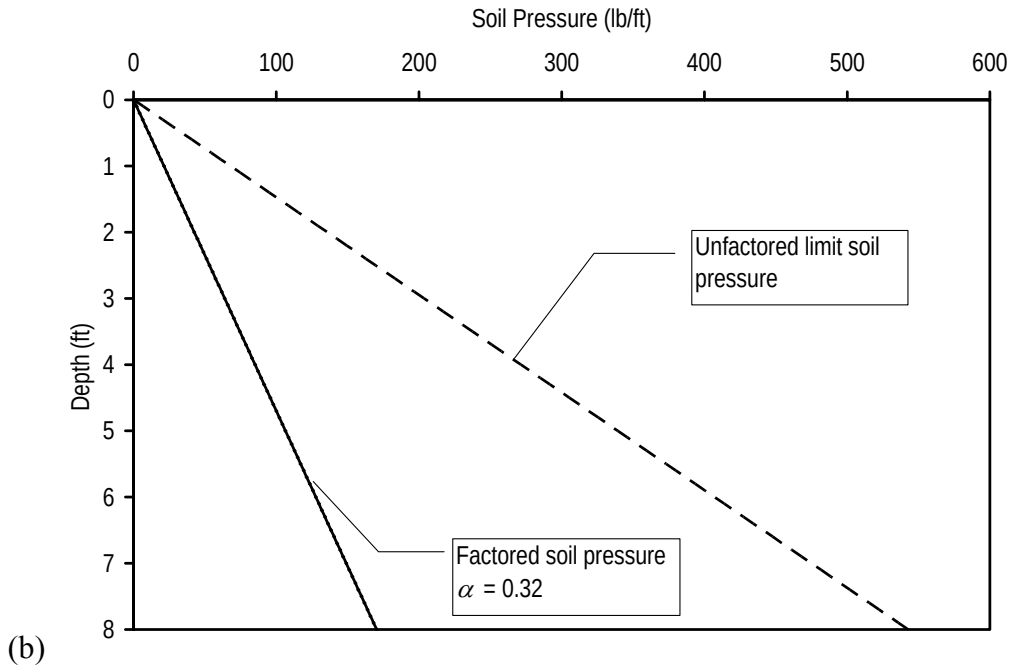

(b)

Figure 2.16 Illustration of method for computing resistance based on bending failure of members: (a) factored moment distribution and (b) factored limit soil pressure

Combining the limit resistance curves due to soil failure and the failure of the member in bending, a composite limit resistance curve that accounts for all failure modes can

be established, as shown in Figure 2.18. The controlling failure mode is dependent on the depth of sliding. For sliding surfaces passing through the upper 2- to 3-ft. of the reinforcing member, Failure Mode 1 typically controls. Failure Mode 3 controls for sliding surfaces passing through depths of 3- to 7.5-ft. along the reinforcing member. Below that depth, Failure Mode 2 typically controls. These depths are approximate and vary with the properties of the reinforcing members, the spacing of the members, and the soil properties.

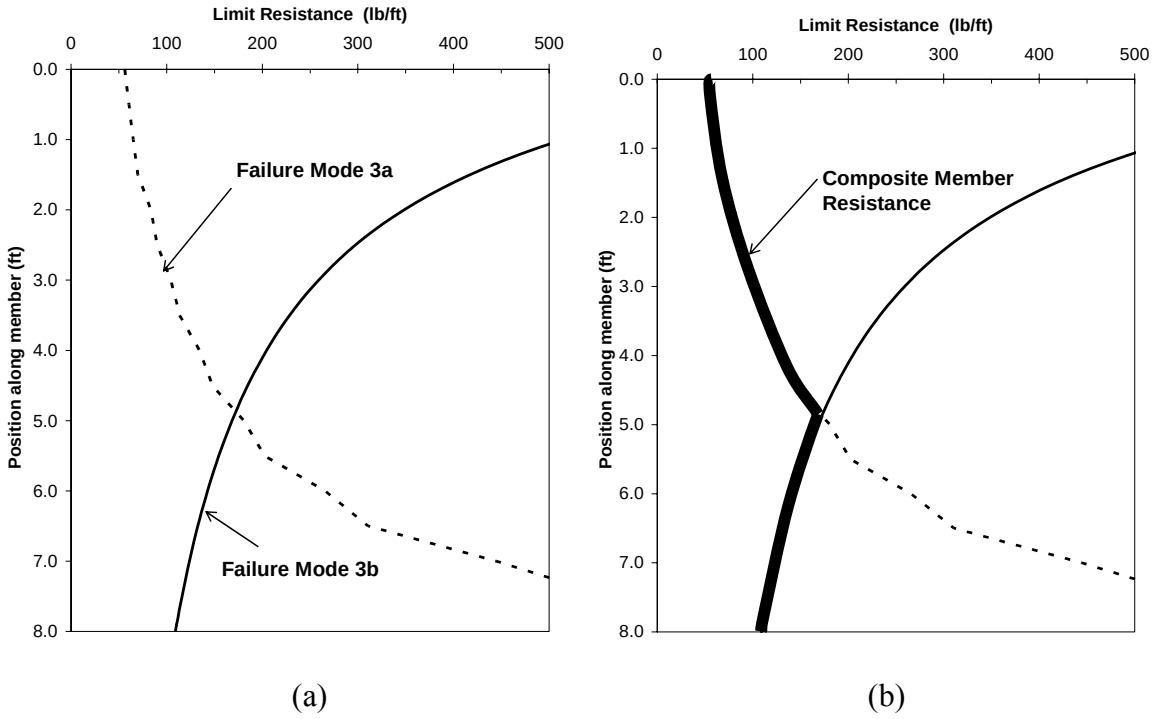

Figure 2.17 Limit resistance for structural failure of member in bending: (a) limit resistance of Failure Modes 3a and 3b and (b) composite member resistance

For "strong" reinforcing members, the limit soil resistance is not great enough to result in structural failure of the member. In such cases, the composite limit resistance curve is solely a function of the limiting soil resistance as shown in Figure 2.11b. The limit resistance curve for a "weak" reinforcing member, e.g. Figure 2.18b, is dependent on all four limit states. The increased resistance of "strong" reinforcing members as compared to that of "weak" members only produces additional stability if the depth of the critical sliding surface passes in the range where the structural capacity of the weak reinforcing member would control (Parra, 2004).

2.4. Calculation of Factor of Safety

Once the overall limit lateral resistance distribution is developed for individual reinforcing members, the mechanics of stability analysis for slopes reinforced with structural members are relatively straightforward and well established. The commercial slope stability analysis programs, UTEXAS4 and Slide 5.0, were used to perform all of the stability analyses presented in this report. Both programs have the ability to search for the most

critical sliding surface and the minimum factor of safety with or without reinforcing elements.

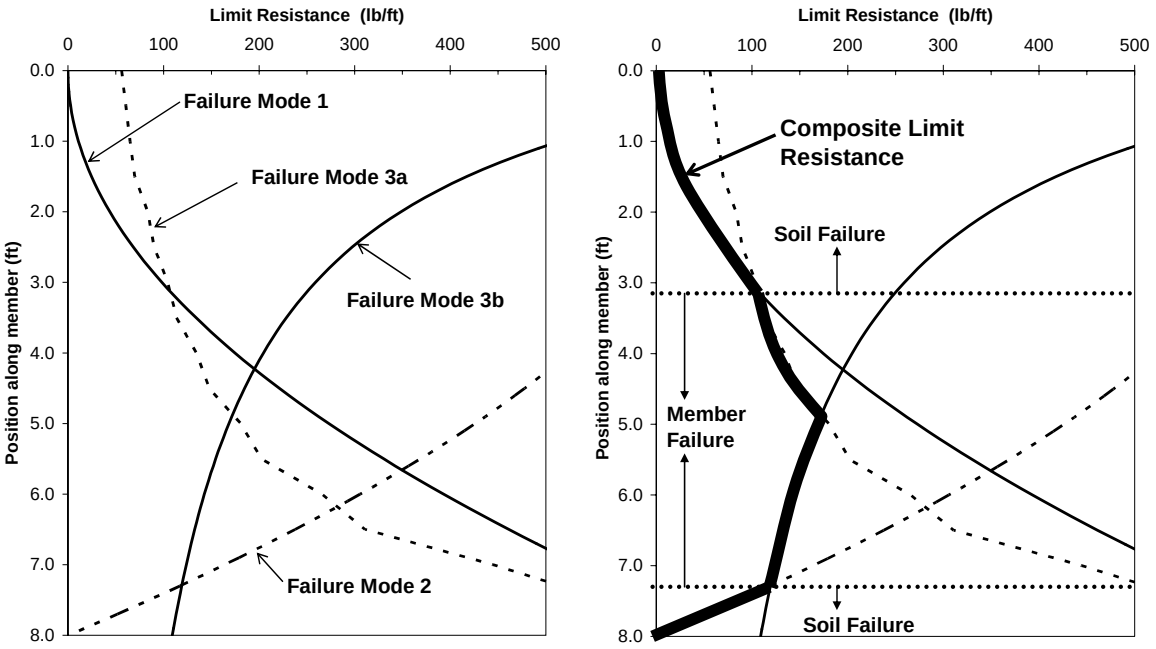

(a) (b)

Figure 2.18 Determination of composite limit resistance curve for all failure modes: (a) limit resistance curves for Failure Modes 1, 2, and 3 and (b) Composite limit resistance curve

Although the process of calculating the factor of safety using UTEXAS4, Slide, or other suitable software is straightforward once the overall limiting lateral resistance curve is developed, the searches for the most critical sliding surface (the surface giving the minimum factor of safety for a particular set of slope conditions) proved to be difficult as numerous "local minima" exist as sliding surfaces passing through different zones of the reinforcement are considered. To ensure that the overall most critical sliding surface was found for all analyses, a rigorous search procedure was developed. The procedure consisted of:

1. selecting several starting centers of circles for the searches (6-10) around the toe, face and crest of slope;
2. for each center of circle chosen, trying a radius crossing reinforcement with the sliding surfaces less than 4 ft (1.2-m) and 8 ft (2.4-m) below the face of the slope;
3. from the most critical circle found from step (2), repeat searches by starting the search using circles with the same center and varying the radius within approximately 2-ft (0.6-m) of the radius of that previous critical circle. The critical circle was determined to a precision of 0.5 ft (0.15-m). This procedure proved to be effective for finding the minimum factor of safety within a tolerance of 0.001.

2.5. Issues Associated with Estimation of Limit Lateral Resistance

While the procedure described in Section 2.3 for estimating the limit lateral resistance for reinforcing members is sound, the mechanics of load transfer in reinforcing members are complex and require careful consideration of several potentially important issues. Foremost among these are:

1. the properties of the recycled plastic reinforcing members;
2. the magnitude of the limit soil pressure and how it is affected by member spacing; and
3. the effect of member inclination, particularly in regards to the relative magnitudes of axial and lateral resistance.

Further discussion of the properties of recycled plastic members is provided in Chapter 3. The following sections provide additional discussions about the magnitude of the limit soil pressure and the effects of member spacing and inclination. Subsequent chapters then provide further discussion of these issues based on observations made at field test sites during this project.

2.6. Methods for predicting limiting soil pressure

As described in previous sections, the limit soil pressure is a key parameter for predicting the resistance provided by reinforcing members. Unfortunately, the limit soil pressure resulting from mass movement of soil adjacent to reinforcing members is difficult to predict. A variety of methods exist to estimate the limit soil pressure. However, the limit soil pressures predicted by these methods vary by a significant amount. Three of the most commonly cited methods, by Ito and Matsui (1975), Broms (1964), and Poulos and Davis (1980), are described here.

2.6.1. Ito and Matsui

Ito and Matsui (1975) proposed a method to determine the limit lateral force on stabilizing piles in a slope. The method was established based on soil failure between piles assuming the soil between the piles to be in a plastic state according to the Mohr-Coulomb failure criterion. This method is referred to as the "theory of plastic deformation".

The assumed region of plastic behavior is shown in Figure 2.20. The following assumptions are also made:

4. Under deformation, two sliding surfaces occur along lines AEB and A'E'B'.
5. The soil is plastic only in region AEBB'E'A'
6. No frictional forces act on the surface of the pile.
7. The soil is assumed to be in a plane strain condition in the vertical direction.
8. The piles are rigid.
9. The ground surrounding the piles is horizontal.

The lateral force provided per unit length of pile is taken to be the difference in soil pressures acting on surfaces BB' and AA' when the soil is in a plastic state.

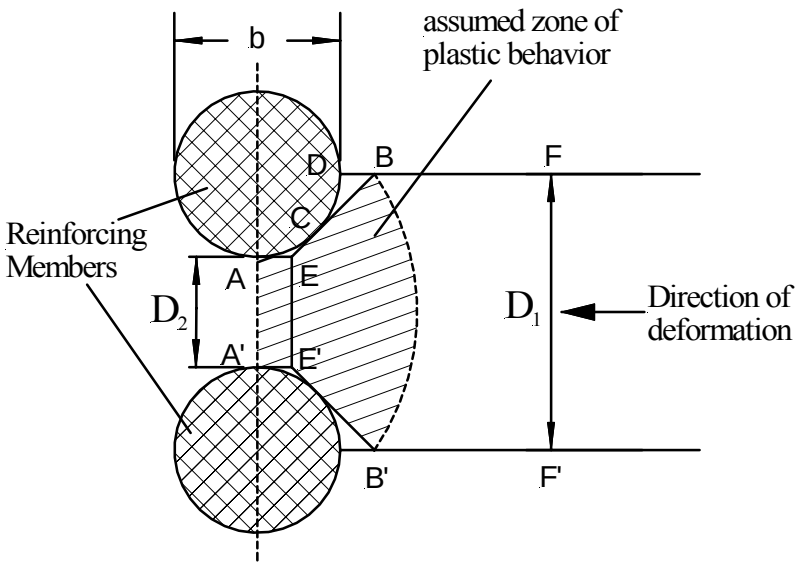

Figure 2.20 Schematic showing assumed region of plastic deformation for theory by Ito and Matsui (after Ito and Matsui, 1975).

The resulting force per unit length of pile at a given depth, *z*, is obtained by the following equation:

$$P(z) = cD_1\left(\frac{D_1}{D_2}\right)^{\left(N_\phi^{1/2}\tan\phi+N_\phi-1\right)}\left[\frac{1}{N_\phi\tan\phi}\left\{\exp\left(\frac{D_1-D_2}{D_2}N_\phi\tan\phi\times\tan\left(\frac{\pi}{8}+\frac{\phi}{4}\right)\right)-2N_\phi^{1/2}\tan\phi-1\right\}+\frac{2\tan\phi+2N_\phi^{1/2}+N_\phi^{-1/2}}{N_\phi^{1/2}\tan\phi+N_\phi-1}\right] \quad (2.6)$$
$$-c\left\{D_1\frac{2\tan\phi+2N\phi^{1/2}+N_\phi^{-1/2}}{N_\phi^{1/2}\tan\phi+N_\phi-1}-2D_2N_\phi^{-1/2}\right\}+\frac{\gamma z}{N_\phi}\left\{D_1\left(\frac{D_1}{D_2}\right)^{\left(N_\phi^{1/2}\tan\phi+N_\phi-1\right)}\times\exp\left(\frac{D_1-D_2}{D_2}N_\phi\tan\phi\tan\left(\frac{\pi}{8}+\frac{\phi}{4}\right)\right)-D_2\right\}$$

where $N_\phi = \tan^2\left(\pi/4+\phi/2\right)$,

D_1 is the center to center pile spacing, D_2 is the inner distance between piles, c is the cohesion intercept of the soil, γ is the unit weight of the soil, and ϕ is the angle of internal friction of the soil.

The limit lateral force on the pile, *P*, increases linearly with increasing γ or *z*. For a constant pile diameter, the limit lateral force also increases as the distance between piles decreases. Thus, more closely spaced piles will produce higher limit loads and conversely more widely spaced piles produce lesser limit loads. The limit lateral force also increases as c or ϕ increases. This is attributed to soils with higher strengths being harder to pass between the piles.

2.6.2. Broms' Method

Broms (1964) presents a method for determining the limit lateral resistance for cohesionless soil surrounding a pile. Different pile lengths and different pile head conditions were evaluated. The ultimate lateral pressure was assumed to equal three times the Rankine passive pressure of the soil. Broms assumed that passive lateral earth pressures develop at the front of the pile (upstream side) and active pressures develop at the back (downstream

side). The active lateral earth pressures are small compared to the passive lateral pressures and are neglected. The lateral earth pressure developed at failure is assumed to be independent of the cross sectional area of the pile. The limit lateral force per unit depth increases linearly from zero at the ground surface, with the distribution, *P*, given by the following equation:

$$P(z) = 3D\sigma_v' K_p \tag{2.7}$$

where *D* is the pile diameter, σ_v' is the effective vertical stress at the depth of interest, and K_p is the coefficient of passive earth pressure calculated by the following equation:

$$K_p = \frac{1+\sin\phi}{1-\sin\phi} \tag{2.8}$$

where ϕ is the angle of internal friction of the soil. Broms' method assumes lateral deflections are large enough to develop full passive pressure adjacent to the pile.

2.6.3. Poulos and Davis Method

Poulos and Davis (1980) estimated the limit lateral resistance for purely cohesive (ϕ = 0) soils and *c*-ϕ soils. For purely cohesive soils, the ultimate lateral soil resistance is assumed to increase from the surface down to a depth of three pile diameters and to remain constant at depths below three pile diameters. When the ultimate lateral resistance becomes constant, failure consists of plastic flow of soil around the pile. At the surface, the limit resistance is approximately $2c_u$, where c_u is the undrained shear strength of the soil. The limit resistance then increases to a constant resistance of 8 to $12c_u$ at depths of three or more pile diameters below the surface, as shown in Figure 2.21.

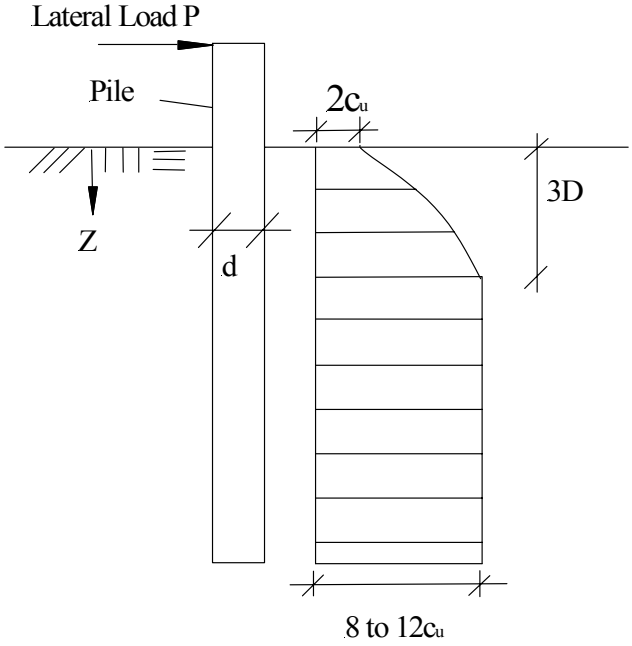

Figure 2.21 Distribution of lateral soil resistance for purely cohesive soils according to Poulos and Davis (after Poulos and Davis, 1980).

For purely cohesive soils, the limit soil pressure, p_u, is determined by the following equation:

$$p_u = K_c c_u \tag{2.9}$$

where K_c is a lateral resistance factor and c_u is the undrained shear strength of the soil. K_c depends on the ratio of pile adhesion to soil cohesion (c_a/c) and on the aspect ratio of the pile cross section (d/b) where d and b are the length and width of the pile cross section. The variation of the lateral resistance factor, K_c, for rough (c_a/c=1.0) and smooth (c_a/c=0) piles is shown in Figure 2.22.

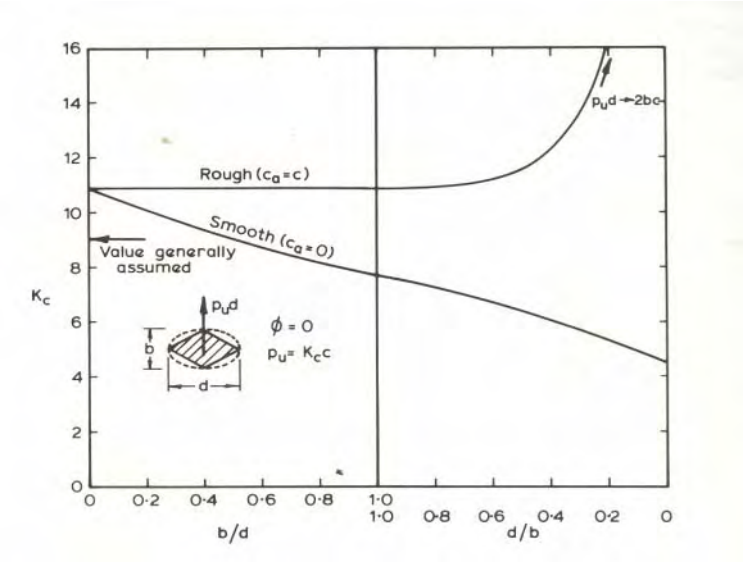

Figure 2.22 Lateral resistance factors for rough and smooth piles in purely cohesive soils (from Poulos and Davis, 1980).

For soils having both a cohesion intercept and an angle of internal friction, the ultimate resistance at any depth can be determined by the following expression:

$$p_u = qK_q + cK_c \tag{2.10}$$

where q is the vertical overburden pressure and c is the cohesion intercept of the soil. K_c and K_q are lateral resistance factors taken to be a function of the friction angle of the soil and the ratio of the depth of interest to the width of the pile (z/d). K_c and K_q are plotted in Figure 2.23.

2.6.4. Comparison of Methods

Parra (2004) compared methods for predicting the limit soil pressure for slender reinforcing members. A typical plot showing the variation of limit soil pressure among methods is shown in Figure 2.24. The variability in the predicted limit soil pressures by the three methods presented is approximately an order of magnitude. One of the objectives of the work described in this report is to evaluate the appropriateness of these methods for predicting the limit soil pressure based on performance of several field test sites reinforced with slender reinforcing members.

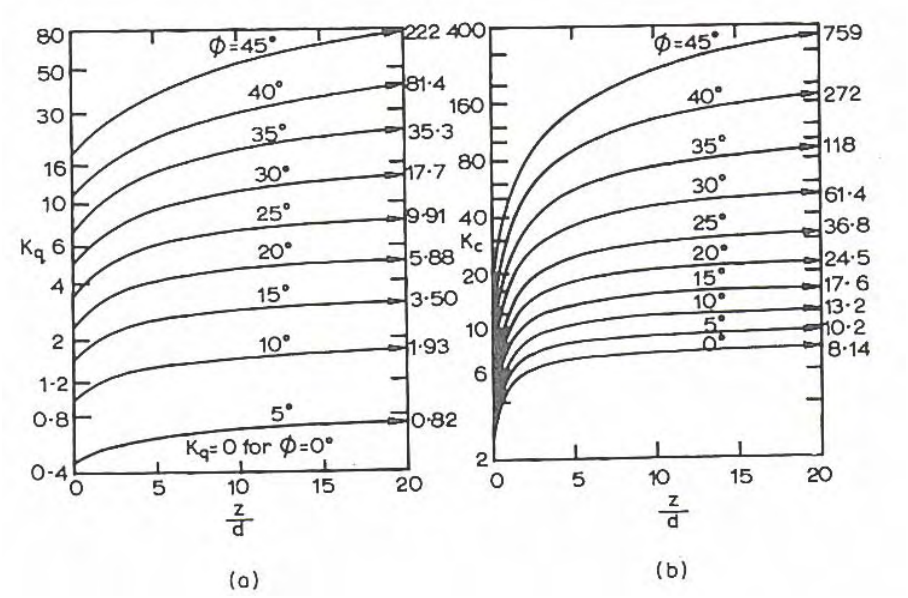

Figure 2.23 Lateral resistance factors for c-ϕ soils (from Poulos and Davis, 1980).

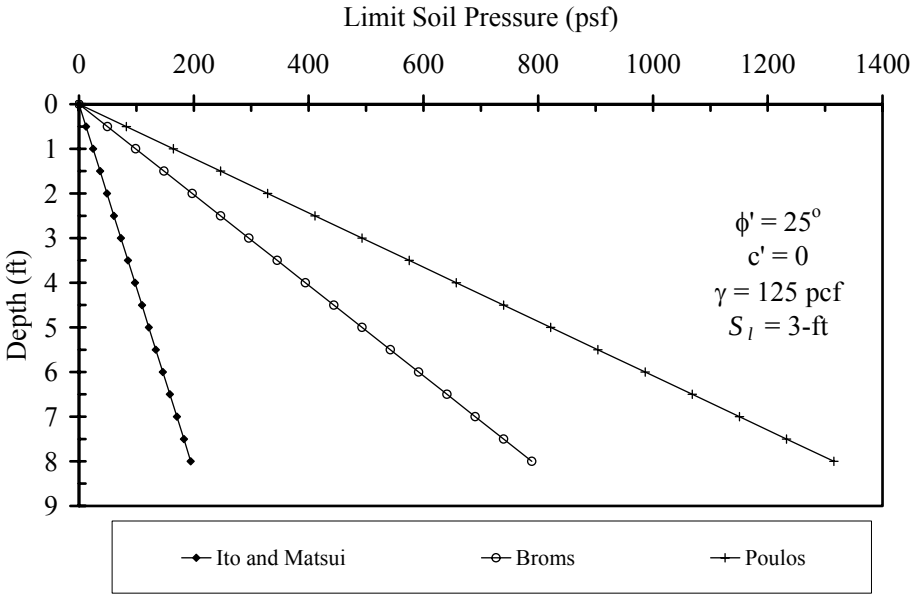

Figure 2.24 Variation in limit soil pressure predicted by different methods (from Parra, 2004)

2.7. Calculation of Limit Resistance for Inclined Reinforcing Members

The limit soil pressure utilized in computing the limiting resistance distributions as described in Section 2.3 is based on the assumption of vertical reinforcing members in horizontal ground as shown in Figure 2.25. How the limit soil pressure changes for vertical reinforcing members in a slope (Figure 2.26) or for inclined reinforcing members (Figure

2.27) is not well understood. No other methods appropriate for these conditions were found in the literature. As such, several approximations were made for using the limit soil pressures for vertical members in sloping ground and for inclined members. Analyses were then performed to study the impact of the modification in calculating limiting soil pressure.

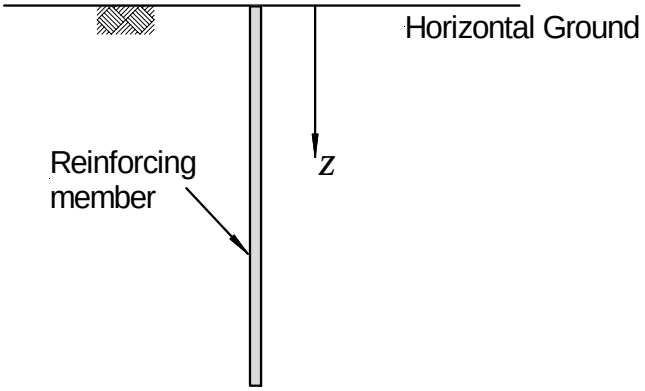

Figure 2.25 Reinforcing member and ground geometry generally assumed in calculation of limit soil pressure (vertical member in horizontal ground).

For vertically oriented reinforcing members in sloping ground, the limit soil pressure was assumed to be identical to that computed for vertical members in horizontal ground. While the influence of this approximation is not known at this time, it is believed to have negligible effect on the limiting resistance of reinforcing members since the effective overburden stress (γz) acting on a reinforcing member at a depth z is similar to that which would be computed for horizontal ground (Figure 2.26).

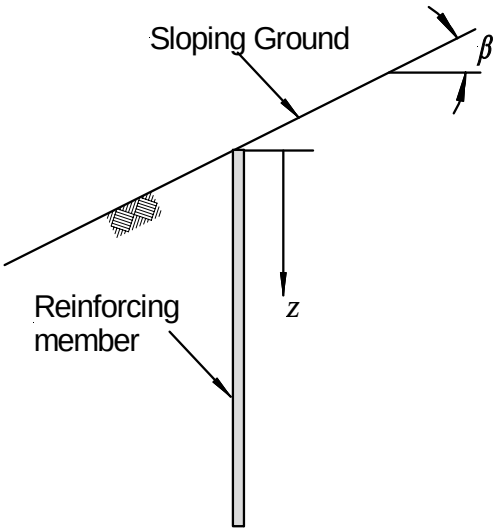

Figure 2.26 Vertical reinforcing member in sloping ground.

For inclined reinforcing members, the picture is much less clear. As shown in Figure 2.27, the effective overburden pressure at a point at distance z from the top of the reinforcing member is not given by γz, but rather is a function of the relative inclination of the slope and

the reinforcing member. Two alternative methods for calculating the limit soil pressure were therefore evaluated for use with inclined reinforcing members. The first alternative used was to simply ignore the influence of inclination and use the limiting resistance distribution for the reinforcing members as if they were placed vertically. The second alternative used was to compute the limiting soil pressure assuming that the effective overburden stress is given by the height of soil above a particular point on the reinforcing member as shown in Figure 2.27. For reinforcing members placed perpendicular to the face of the slope, the vertical overburden pressure for the second alternative is given by

$$\overline{\sigma_v} = \frac{\gamma z}{\cos\beta} \tag{2.11}$$

where γ is the unit weight of the soil, z is the distance from the ground surface to the point of interest measured along the reinforcing member, and β is the inclination of the slope.

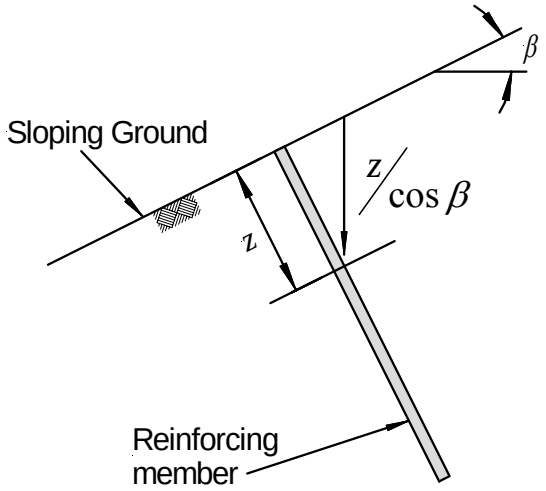

Figure 2.27 Inclined reinforcing member in sloping ground.

Figures 2.28 and 2.29 show limit resistance curves for "weak" and "strong" reinforcing members respectively placed perpendicular to the face of the slope using the two alternative methods for computing the limit soil pressure. As shown in the figures, the differences in the computed limit resistance curves are small and therefore are not likely to significantly influence the computed factors of safety. Additional calculations comparing factors of safety computed using the two alternative methods described above suggest a similar conclusion (Liew, 2000).

2.8. Unresolved Issues

The general approach described in this chapter provides the basis for evaluating the stability of slopes reinforced with recycled plastic members. However, several specific issues associated with the analysis procedure remain unresolved. The two most significant issues are:

1. Which method for predicting the limit soil pressure is most appropriate, and
2. What is the influence of member inclination, particularly as related to relative axial and lateral resistance components?

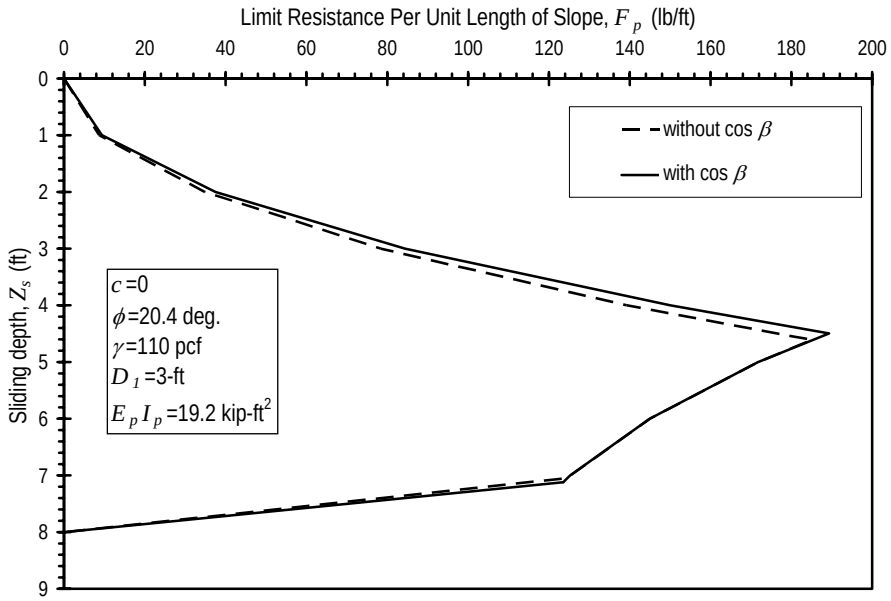

Figure 2.28 Limit resistance curves for "weak" reinforcing members placed perpendicular to the face of the slope computed using two alternative methods.

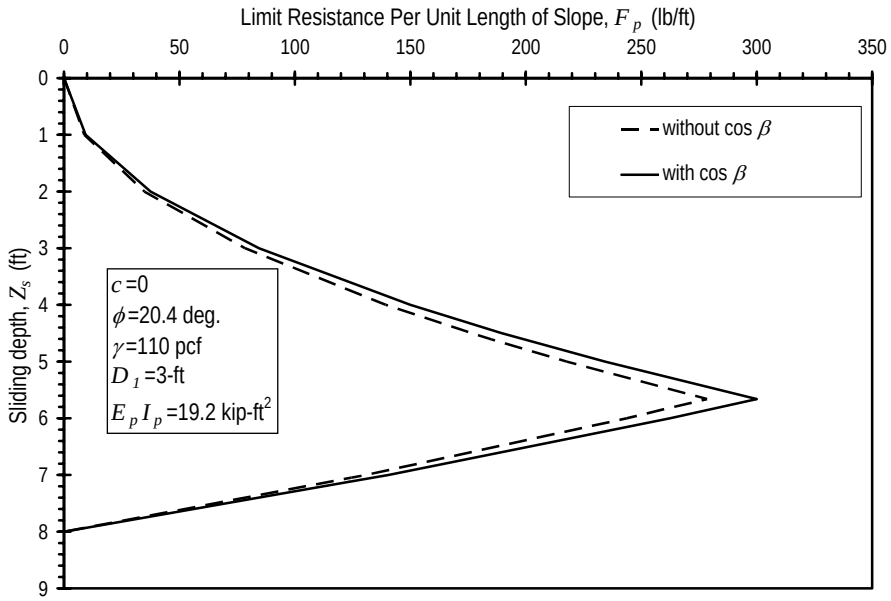

Figure 2.29 Limit resistance curves for "strong" reinforcing members placed perpendicular to the face of the slope computed using two alternative methods.

Both of these issues are also largely unresolved for other types of reinforcement so little guidance on these issues is presently available. The limit soil pressure can have a substantial effect on the computed lateral resistance of members and thus plays a pivotal role in calculating lateral resistance for members, particularly for the range in values predicted by

the different available methods. The effect of member inclination is less well understood. While the results presented by Liew (2000) suggest that member inclination has little effect on the computed limit soil pressure, the more important issue associated with member inclination is the relative contributions of axial and lateral resistance for different member inclinations. It is certainly possible that different member inclinations may provide different lateral resistance mobilization. Even more importantly though is the contribution of mobilized axial forces and how these components change with inclination. So while it is a relatively simple matter to compute axial capacities of reinforcing members in slopes, it is a much more difficult matter to determine how axial resistance will be mobilized as compared to how lateral resistance will be mobilized. This issue has, to date, received little attention with most methods simply ignoring either axial or lateral contributions (the one presumed to be smaller in magnitude) to stability.

As a result of these unresolved issues, the "baseline" method utilized throughout the project, both for parametric analyses and for design of the stabilization schemes utilized at the test sites, has utilized the Ito and Matsui (1975) method for predicting limit soil pressures and has ignored potential contributions from mobilized axial resistance. Use of the Ito and Matsui method is believed to introduce some conservatism into the analysis method. Ignoring axial contributions can be conservative or unconservative, depending on the orientation of the member with respect to the direction of soil movement.

A final issue that remains with regard to predicting the resistance provided by the reinforcement is estimation of the bending and/or shear capacity of the members over the service life of the stabilization scheme. Several phenomena could lead to reduction of the capacity of the members once installed. Of particular note are the potential for creep of the plastic members, the potential for degradation of the members over time, and the potential for damage to the members during installation. Test results presented in Chapter 3 suggest that degradation from exposure and damage from installation are likely to have little effect on the capacity of the members. There is also evidence that creep will have only a minor influence, at least when the mobilized stresses in the members are low. However, field evidence described in subsequent chapters also suggests that creep may be occurring so this issue remains somewhat unresolved. Fortunately, the performance data acquired in this project provides ample data with which to begin addressing these issues.

2.9. Summary

In this chapter, the limit equilibrium method of stability analysis for reinforced and unreinforced slopes was described. While inclusion of the resisting force provided by reinforcement into limit equilibrium stability analyses is conceptually simple, the determination of that force is difficult. The general procedure proposed by Loehr and Bowders (2003) for computing composite limit resistance curves based on several potential failure modes was described in this chapter. The failure modes considered include: (1) failure of soil around or between reinforcing members above the sliding surface, (2) failure of soil around or between reinforcing members below the sliding surface, and (3) structural failure of the reinforcing members. Three methods for predicting the limit soil pressure for use in this procedure were also presented. One of the objectives of this work is to evaluate these methods based on performance of several field test sites reinforced with recycled plastic reinforcing members.

Chapter 3. Properties of Recycled Plastic Reinforcement

The engineering properties of reinforcing members are of paramount importance for slope stabilization because of the potential for structural failure of members due to the loads imposed by moving soil and due to stresses imparted on the members during field installation. Due to the variety of manufacturing processes and constituent mixes used in the manufacture of recycled plastic products, the engineering properties of commercially available members can vary substantially.

In order to gain a proper perspective of the engineering properties of recycled plastic members used for slope stabilization, an extensive testing and analysis program was undertaken. The program included:

1. determining the basic engineering and material properties of commonly available recycled plastic lumber products;
2. determining the potential variability of these properties within one product and among various products and manufacturers; and
3. determining how these properties change when the material is subjected to various potentially detrimental environments.

This chapter provides background information regarding common recycled plastic products, describes several pertinent standardized test procedures for measuring properties of recycled plastic products, and describes results obtained from the testing and analysis program.

3.1. Sources and Manufacturing of Recycled Plastic Lumber

There are many manufacturers of recycled plastic lumber in the United States. The number is currently more than 30, but is variable due to the nature of start-up businesses. Recycled plastic lumber products vary not only due to different manufacturing methods but also due to the proprietary blends of materials incorporated into the products, which can vary at their source.

Recycled plastic lumber products are manufactured from industrial or post-consumer waste consisting predominantly of polymeric materials (usually high or low density polyethylene). Typically, recycled plastic lumber is composed of the following resins (McLaren, 1995):

- High Density Polyethylene (HDPE) – 55 percent to 70 percent,
- Low Density Polyethylene (LDPE) – 5 percent to 10 percent,
- Polystyrene (PS) – 2 percent to 10 percent,
- Polypropylene (PP) – 2 percent to 7 percent,
- Polyethylene-terephthalate (PET) – 1 percent to 5 percent, and
- varying amounts of additives (sawdust, fly ash, and other waste materials) – 0 percent to 5 percent.

Table 3.1 shows the common resins, their positive characteristics, common uses, and recycling rate for 2001. In the United States, post-consumer waste has increased at a faster rate than industrial waste. Post-consumer, plastic bottle recycling increased by 80 million pounds in 2001 to an all time high of 1,591 million pounds (APC, 2002). The HDPE raw material comes primarily from post-consumer milk jugs while PET comes primarily from

post-consumer soft drink bottles. Assuming a 50 percent recycling rate for all waste plastics, the total production of the recycled plastic lumber is estimated to approach 25 billion board feet (6254 m^3) per year (McLaren, 1995). Therefore, the importance of the recycled plastic lumber industry in recycling of plastics cannot be overemphasized.

Table 3.1 Common recycled plastics used in recycled plastic lumber products (Osman et al., 1999)

Resin Type	Positive Characteristics	Common Original Use	Common Recycled Use	Quantity Recycled[1] , lbx10^6 (Rec. rate[2], %)
Polyethylene terephthalate (PET)	High strength, excellent moisture barrier, good clarity	Soft drink bottles, juice containers, food packaging	Bottles, paint brushes, geotextiles, carpeting	834.3 (22.1%)
High Density Polyethylene (HDPE)	High strength and melting point, good ductility	Milk containers, oil bottles, films and pipes	Plastic lumber, motor oil containers, bottles, drainage pipes	750 (23.2%)
Low Density Polyethylene (LDPE)	Excellent clarity, toughness and flexibility, easy to process	Bottles, trash bags, cable sheathing, sheets and films	Films, plastic bags, bottles	0.2 (0.5%)
Polypropylene (PP)	Low density, high melting point, and excellent chemical resistance	Carpeting, netting, geotextiles, heavy-duty bags	Flexible packing containers	5.7 (3.8%)
Polystyrene (PS)	Low cost, low density, good weathering resistance	Cups, water bottles, outdoor furniture	Egg cartons, video tape cases	0.1 (1.1%)

[1]: Data from American Plastic Council survey results (APC, 2002)

[2]: Percentages shown for PET and HDPE based on virgin resin sales plus recycled resin used in manufacture of bottles.

Manufacturers also use different processes to produce their product (Bruce et al., 1992). The two main processes commonly used are compression molding and extrusion forming. In compression molding, the constituent waste streams are pulverized, blended together, heated until partially melted, and then compression formed in molds. In this process, the raw material is compressed into desired shapes and dimensions and is cured with heat and pressure. Extrusion forming includes similar steps; however, the molten composite material is forced through a die of the desired cross-section for the member being produced

in lieu of compression into a mold. An advantage of the extrusion process is that it is relatively easy to manufacture members of any desired length while the compression molding process requires different molds for each different member length. Extrusion forming is generally a more efficient process, allowing greater production rates, but is more challenging technically. Owing to the endless variety of possible constituents and manufacturing processes, the resulting recycled plastic products (often seen in park benches, picnic tables, and decks for homes and marine setting) can have very different engineering properties, even among apparently similar materials and sections.

Table 3.2 summarizes the composition and engineering properties of plastic lumber products from several different manufacturers reported by Breslin et al. (1998). Manufacturers use materials including virgin plastics, post-consumer waste plastics, and various plastic mixtures. Breslin et al. (1998) concluded that the engineering properties of plastic lumber vary depending on the composition of the polymers and additives used in lumber manufacturing. Unit weights ranged from 47 pcf to 60 pcf (7 KN/m^3 to 9.5 KN/m^3) for different manufacturers. Compressive strength varied from 1700 psi to 3800 psi (11.7 MPa to 26.2 MPa). They also found that use of a single polymer (HDPE) and glass fiber additive resulted in significantly higher modulus of elasticity for plastic lumber (Breslin et al., 1998).

Lampo and Nosker (1997) performed compression tests on recycled plastic lumber products from multiple manufacturers. Table 3.3 shows a summary of results provided, which clearly demonstrates that products produced by different manufacturers can have substantially different material properties. The significant variation in properties shows that these materials cannot be considered identical, and they cannot be assumed to perform similarly in many applications (Lampo and Nosker, 1997).

3.2. Standard Test Methods for Recycled Plastic Lumber

Manufacturers of recycled plastic products will generally document a wide variety of properties for their products including strength, dimensional stability, water absorption, nail and screw withdrawal, density, and other properties. For slope stabilization applications, the key properties of interest are strength and stiffness (both axial and bending), and resistance to installation stresses as illustrated in Figure 3.1.

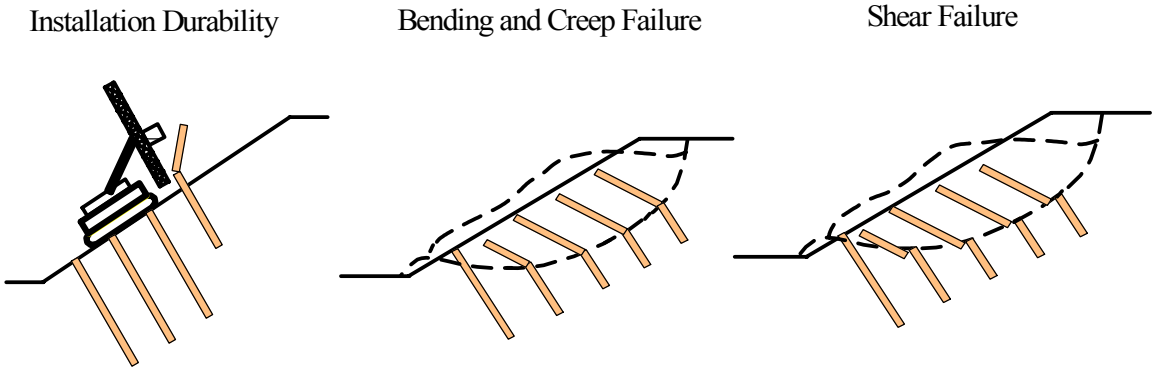

Figure 3.1 Three potential modes of failure for reinforcing members in slope stabilization applications.

Table 3.2 Engineering Properties of Plastic Lumber Products (Breslin et al., 1998)

Product	Composition	Specific Gravity	Unit Weight[1] (lb/ft^3)	Compressive Strength (psi)	Young's Modulus (ksi)	Tensile Strength (psi)
TRIMAX	HDPE/Glass fibers	0.75	46.80	1740	450	1250
Lumber last	Commingled recycled plastic	0.86	53.66	3755	140	1453
Earth care recycle maid	Post-consumer milk jugs	0.79	49.30	3205	93 - 102.5	2550
Earth care products	HDPE	0.909	56.72	- - [2]	173.4	- -
Superwood Selma, Al	33% HDPE, 33% LDPE, 33% PP	0.82-0.87	51.2-54.3	3468	146.2	- -
Rutgers University	100% Curb tailings	0.944	58.9	3049	89.5	- -
	60% Milk bottles, 15% Detergent bottles, 15% Curb tailings, 10% LDPE	0.883	55.1	3921	114.8	- -
	50% Densified PS	0.806	50.3	4120	164	- -
BTW Rec. plastic lumber	Post-consumer	0.88-1.01	54.9-63.0	1840-2801	162	- -

[1]: calculated by present authors
[2]: data not available
Conversion: 1MPa = 145 psi, 1ksi = 6.9 MPa

Axial and flexural strength and stiffness are commonly measured by most manufacturers and provided in their advertising literature and on company web sites. These properties are generally obtained from tests performed in accordance with three different ASTM standards:

- ASTM D6108 – Standard Test Method for Compressive Properties of Plastic Lumber and Shapes (ASTM, 2003);
- ASTM D6109 – Standard Test Method for Flexural Properties of Unreinforced and Reinforced Plastic Lumber and Related Products (ASTM, 2005); and
- ASTM D6112 – Standard Test Methods for Compressive and Flexural Creep and Creep Rupture of Plastic Lumber and Shapes (ASTM, 1997).

Additional information regarding these standards is summarized in Table 3.4. These standards have served to make properties reported by different manufacturers consistent and have therefore improved comparisons among different products for a particular application. However, the standard test methods were primarily developed for above ground applications such as decks, and are therefore not perfectly suited to the application of slope stabilization

where conditions and loads differ from above ground applications. Of particular importance is the fact that the ASTM standard test methods require very high loading rates for measurement of member strength and stiffness. Since the strength and stiffness of plastics are sensitive to loading rate, and since loading in the slope stabilization application is much slower than what is used in the standard test methods (on the order of weeks or months as compared to minutes), it is not reasonable to assume that properties measured using the ASTM standards will be appropriate for predicting performance in slope stabilization applications. This issue is further complicated by the fact that some products are more sensitive to loading rate than others so it is difficult to convert properties established using the standard test methods to properties needed for design of slope stabilization measures. Nevertheless, these standards do provide a baseline for comparison of different products. Some modifications to the ASTM procedures were employed in the testing program described subsequently.

Table 3.3 Specific Gravity and Results of Compression Tests on Recycled Plastic Lumber (Lampo and Nosker, 1997)

Sample	Specific Gravity	Unit Weight[1] (lb/ft^3)	Yield Strength (at 2 % strain) (psi)	Ult. Strength (at 10 % strain) (psi)	Young's Modulus (ksi)
51A	0.28	17.4	709	785	38.0
1B	0.70	43.8	1381	1885	61.9
2D (br)	0.86	53.9	1668	2321	85.3
2D (g)	0.81	50.5	2103	2857	116.0
1E	0.86	53.8	1769	2422	80.8
1F	0.79	49.2	2190	2814	108.2
1j (b)	0.75	47.0	1900	2364	93.3
1j (w)	0.91	56.7	2161	2828	110.1
23L	0.79	49.0	1711	1929	191.4
1M	0.57	35.3	964	1226	57.9
1S	0.91	56.7	1668	2045	80.5
1T	0.88	54.9	2248	3118	117.9
9U	0.77	48.3	1827	2408	86.7
Range	0.28-0.91	17.4-56.7	709-2248	785-3118	38-191.4
Mean	0.76	47.4	1715	2231	94.5
Std. Dev.	0.17	10.8	465	666	37.6

[1]: Calculated by present authors

Conversion: 1MPa = 145 psi, 1ksi = 6.9 MPa

3.3. Testing Program

For this project, an extensive series of laboratory tests were performed to evaluate the engineering properties of recycled plastic products from three different manufacturers. Laboratory tests performed included uniaxial compression tests, four-point flexure tests,

compressive creep tests, and flexural creep tests. Detailed procedures and results for each set of tests are described in this section.

Table 3.4 ASTM Standard Test Methods for Plastic Lumber

ASTM Designation	Test Method	Primary Constraints
D6108 Standard Test Method for Compressive Properties of Plastic Lumber and Shapes	Uniaxial Compression Test	• Specimen length = 2 x minimum width. • Compressive stress = compressive load divided by minimum or effective original cross-sectional area. • Compressive strength taken at 3% strain if no clear yield point. • Strain rate = 0.03 ± 0.003 in/in/min (mm/mm/min) and testing time ~ 1 to 5 min. • Secant Modulus @ 1% strain.
D6109 Standard Test Method for Flexural Properties of Unreinforced and Reinforced Plastic Lumber and Related Products	Four-point Flexure Test	• Support span (length) divided by minimum width = 16 (nominally). • Imposed rate of crosshead motion from equation listed in the standard. • Flexural strength = maximum stress at the moment of rupture. • Secant Modulus of elasticity in flexure from equation provided.
D6112 Standard Test Methods for Compressive and Flexural Creep and Creep-Ruptured of Plastic Lumber and Shapes	Compressive Creep and Flexural Creep	• Uniaxial loading for compressive creep. • Plot successive creep modulus versus time at various stresses for linear viscoelastic materials. • Four-point loading for flexural creep. • Approximate time schedule for compressive or flexural creep tests: 1, 6, 12, and 30 min; 1, 2, 5, 20, 100, 200, 500, 700, and 1000 hours.

Tests were performed on specimens from three different manufacturers, denoted as manufacturers A, B, and C, as summarized in Table 3.5. All members were nominally 3.5 in. x 3.5 in. (90 mm x 90 mm) in cross-section by 8 feet (2.4 m) in length. Details of the member compositions and manufacturing processes were not provided, but members were separated into "batches" to ensure consistency within a single batch. One manufacturer (manufacturer A) provided members manufactured in seven different batches, denoted batches A1 through A6 and A10, over a period of three years. Members in batches A1 through A4 were compression-molded products while members from batches A5, A6 and A10 were extruded products. The constituent formula among the first five batches (A1 to A5) was similar with approximately 60 percent low-density polyethylene (LDPE) and 40 percent filler material (primarily sawdust). Batches A6 and A10 were produced using a

higher percentage of high-density polyethylene (HDPE). Two additional manufacturers (manufacturers B and C) provided specimens of unreinforced members composed of HDPE with negligible filler and additives. These specimens are denoted as batches B7 and C9. Manufacturer B also provided specimens composed of HDPE reinforced with cut-strand fiberglass reinforcement (batch B8).

Table 3.5 Summary of recycled plastic products tested for this project.

Specimen Batch	Principal Con-stituent	Mftg. [1] Process	Condition	Depth (in)	Width (in)	Length[2] (in)	Unit weight (lb/ft^3)
A 1	LDPE	CM	Virgin	3.6	3.6	7.0	61.2
A 2	LDPE	CM	Virgin	3.5	3.5	6.9	63.4
A 3	LDPE	CM	Virgin	3.6	3.6	7.1	64.5
A 4	LDPE	CM	Virgin	3.6	3.4	7.0	64.6
A 5	LDPE	EX	Virgin	3.4	3.4	7.1	58.9
A 6	HDPE	EX	Virgin	3.4	3.4	7.0	60.9
A10	HDPE	EX	Virgin	3.5	3.5	7.0	67.6
A11	HDPE	EX	Installed	3.5	3.5	7.0	68.3
A12	HDPE	EX	Installed	3.5	3.5	7.0	68.5
A13	HDPE	EX	Installed	3.5	3.5	7.0	66.8
B 7	HDPE	EX	Virgin	3.4	3.4	6.9	52.9
B 8	HDPE + Fiber glass	EX	Virgin	3.4	3.4	6.9	51.9
C 9	HDPE	EX	Virgin	3.5	3.5	7.0	67.9

[1]: CM – compression molded, EX - extruded

[2]: for uniaxial compression tests.

Conversion: 1 in = 2.54 cm, 1 lb/ft^3 = 0.1572 kN/m^3

Specimens from batches A1 through A6, A10, B7, B8 and C9 were manufactured at company facilities and shipped to the University of Missouri Geotechnical Laboratories for testing or to the contractor for installation at the field test sites. Each of these batches is considered "virgin" material in that they represent materials just following manufacturing. In contrast, batches A11, A12 and A13 were composed of specimens that had been subjected to driving stresses during installation at field test sites[1]. All specimens in these batches were manufactured during the same period as batch A10, and thus have a similar constituent formula. Batches A11 and A12 were installed at the I70-Emma site in January 2003 using two distinct methods of installation. Batch A13 was installed at the US54-Fulton site in January 2003.

3.4. Uniaxial Compression Tests

Uniaxial compression tests were performed on specimens cut from full size recycled plastic members. The member cross-section was square with side dimensions of 3.5 inches (90 mm) and a nominal length of 7 inches (180 mm) – twice the minimum width. The tests were conducted using a stress controlled universal compression machine. As shown in Figure 3.2, a steel plate was placed on top of the specimen to make sure the compressive load

[1] Specimens were taken from exposed portions of members remaining above ground following installation

was uniformly distributed across the whole cross-sectional area of the specimen. A dial gage was placed beneath the steel plate to measure displacement during the test.

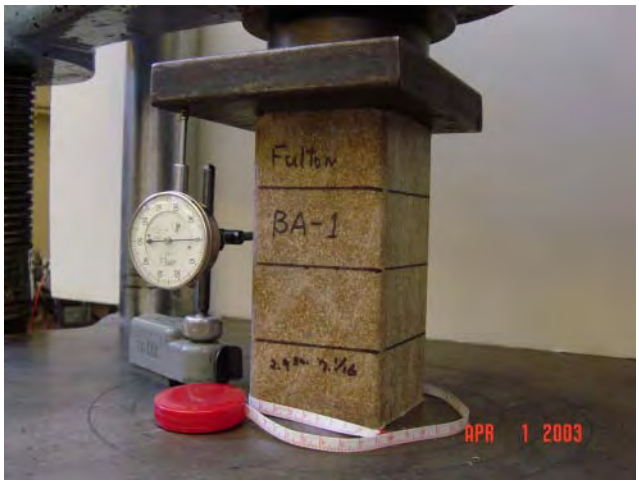

Figure 3.2 Setup for uniaxial compression tests.

Axial strain was computed by dividing the incremental displacement of the loading head by the initial height of each specimen. A strain rate was determined by dividing the incremental strain by the elapsed testing time. Secant moduli were established at one and five percent strain as shown in Figure 3.3 from the slope of the straight line connecting zero percent strain to the corresponding stresses at one percent and five percent strain. The average strain rate was determined by taking the average of all strain rates before the peak stress was reached, as illustrated in Figure 3.4. An average strain rate of approximately 0.006 in/in/min (mm/mm/min) was typically used, except for tests performed to evaluate strain rate effects.

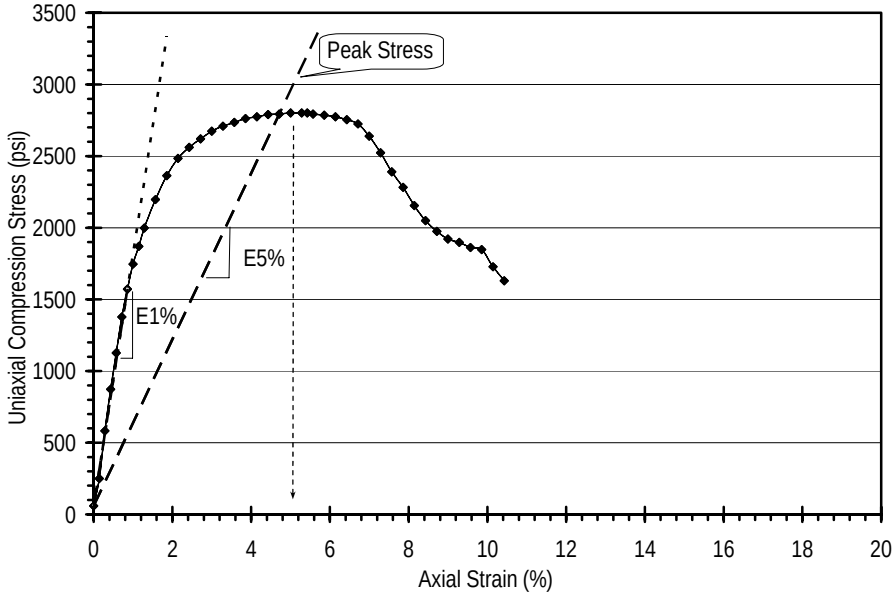

Figure 3.3 Typical stress-strain curve showing computation of secant moduli (batch A3).

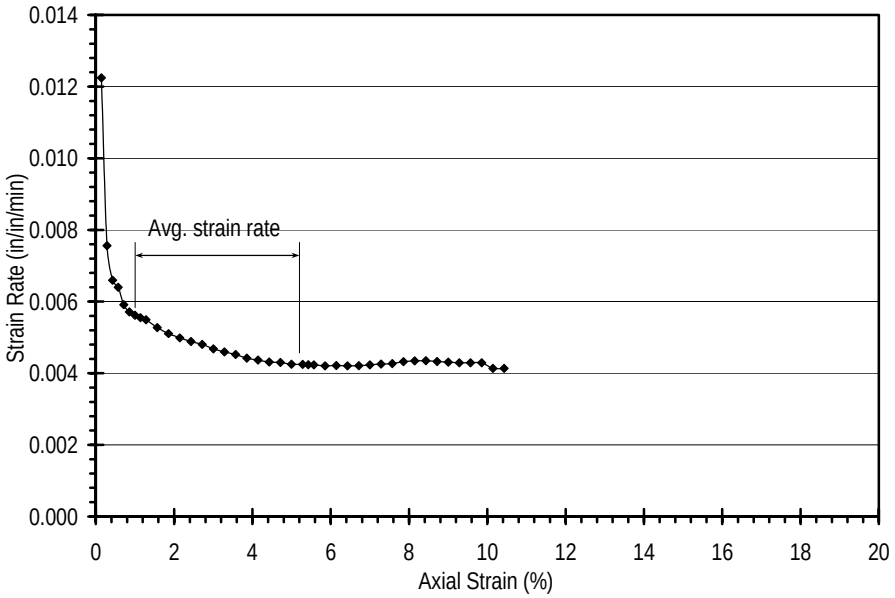

Figure 3.4 Typical plot of axial strain rate versus axial strain showing method used to establish strain rates for each test (Batch A3).

Two failure criteria were used to establish the compressive strength of the recycled plastic members. The first one was based on using the original cross-sectional area (A_o) of the specimen to calculate the compressive stress and using a five percent strain limit as the baseline to choose the compressive strength. The second criterion was based on using a corrected cross-sectional area (A_c) based on the measured perimeter of the specimen during testing to calculate the compressive stress and choosing the peak stress as the compressive strength. A measuring tape was used to measure the perimeter of the middle section of specimens during the compression test (Figure 3.2). The corrected cross-sectional area (A_c) was calculated by assuming the measured perimeter was that of a square section, so that

$$A_c = \left(\frac{Measured\ Perimeter}{4} \right)^2 \tag{3.1}$$

3.4.1. Stress-Strain Response

Figure 3.5 shows typical uniaxial compressive stress versus axial strain response for both extruded and compression molded specimens from different manufacturers. As shown in the figure, specimens provided by manufacturer A exhibited a clear peak in the stress-strain response, whereas specimens from manufacturers B and C produced no clear peak in the stress-strain curves when the original cross-sectional area (A_o) is used to compute stress. The observed peak stress for compression molded specimens from manufacturer A occurs at approximately 5% strain while the peak for extruded specimens occurs at substantially larger strains. Figure 3.5 also shows that stresses computed using measured cross-sectional areas throughout testing are substantially lower than those computed using the initial cross-sectional area.

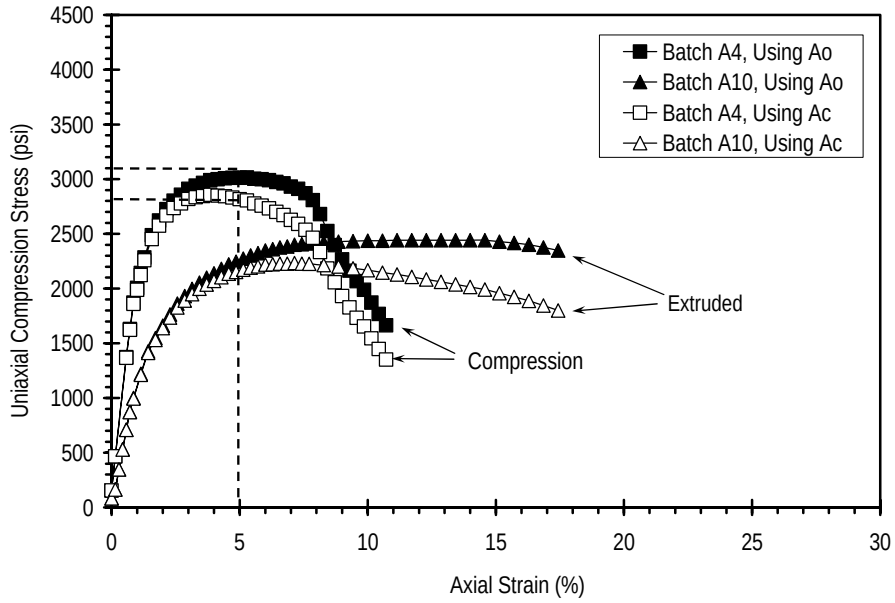

(a) typical stress-strain response for specimens from manufacturer A.

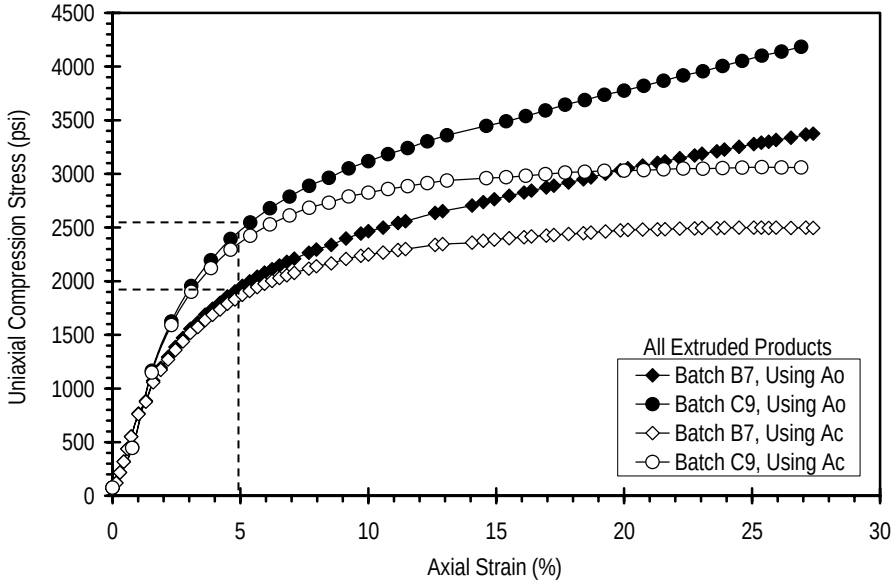

(b) typical stress-strain response for specimens from manufacturers B and C.

Figure 3.5 Typical uniaxial compressive stresses versus axial strain behavior for recycled plastic specimens.

Figure 3.6 shows typical deformed specimens at the completion of uniaxial compression tests for compression molded specimens from manufacturer A and extruded products from manufacturers B and C. These photographs reveal that compression molded specimens from manufacturer A developed clearly defined failure planes, while specimens from manufacturers B and C developed no clear failure planes, but exhibited a bulging type of failure mode. Both observations are consistent with the observed stress-strain response

where compression molded specimens exhibited a clear peak in the stress-strain curves while extruded products did not exhibit a clear peak. Observed behavior for extruded specimens from Manufacturer A was generally more similar to that shown in Figure 3.6b for other extruded specimens.

(a) Typical failure mode for compression molded specimens from manufacturer A.

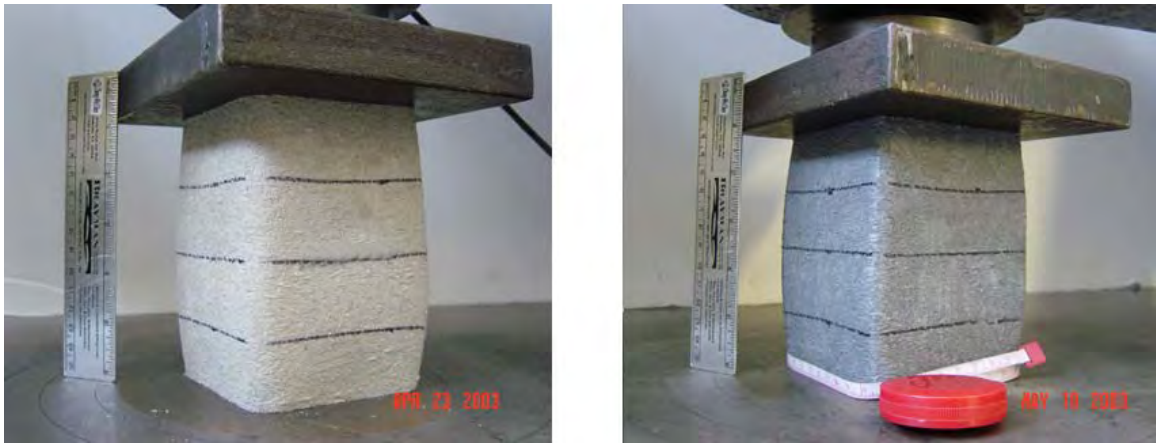

(b) Typical failure mode for extruded products from manufacturers B and C.

Figure 3.6 Failure modes for recycled plastic specimens during uniaxial compression tests.

3.4.2. Uniaxial Compressive Strength

Observations from the laboratory testing suggest that a corrected cross-sectional area should be used in the determination of the compressive strengths, but no standard area correction has been established. If one assumes a constant specimen volume and that the cross-section remains uniform during compression, a corrected cross-sectional area can be computed as:

$$A_e = A_0 / (1 - \varepsilon) \tag{3.2}$$

where A_e is the corrected cross-section area, A_o is the original cross-sectional area, and ε is axial strain. However, observation of specimens during testing indicate that the cross-

sectional areas do not remain uniform and the volume is likely not constant during deformation, thus invalidating the use of Equation 3.2 for area corrections. Since no consistent area correction has been agreed upon, the compressive strengths reported subsequently were taken to be the compressive stress at five percent axial strain for all specimens *without area corrections*. In cases where a peak stress was exhibited at strains of less than five percent, the compressive strengths were taken to be equal to the peak stress. The five percent strain limit serves to limit the magnitude of errors associated with the specimen area and provides a consistent basis for comparison of strengths for different specimens. The five percent strain limit also serves as a basis for limiting deformation in the field applications.

Figure 3.7 shows the difference between the "measured" cross sectional area (A_c) determined from the measured perimeter during the testing and the original area (A_o) versus axial strain for specimens from several batches. In general, the cross-sectional area is a function of axial strain with the area increasing with axial strain for all specimens from all three manufacturers. The cross sectional area for batches A4 (compression molded) rapidly increases while the cross sectional area for batches B7, B8, and C9 increased at a lower rate. The cross sectional areas for batches A5, A6, and A10 (all extruded products from manufacturer A) have intermediate increases. Application of this correction produces a more clearly defined peak in the stress-strain response for specimens from manufacturers A, B, and C (Figure 3.5).

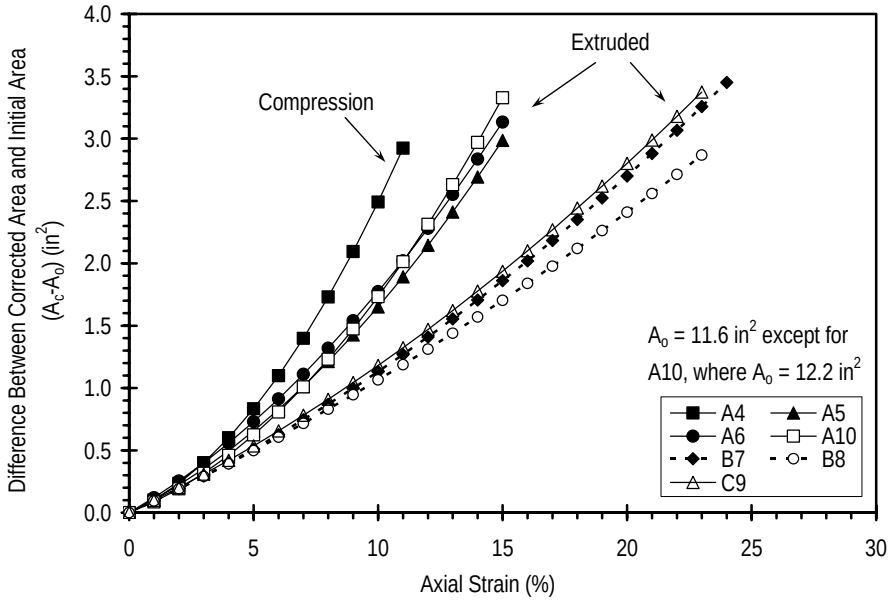

Figure 3.7 Difference calculated from measured perimeter versus axial strain during compression tests (Mftg A, B, and C).

Table 3.6 shows a summary of uniaxial compressive strengths determined from each batch. Overall, measured average compressive strengths range from 1600 psi to 3000 psi (11 MPa to 21 MPa) when established using the original cross-sectional area. The results shown are for specimens loaded using a nominal strain rate equal to 0.006 in/in/min (0.006 mm/mm/min).

Specimens from batches A1 to A4 are compression-molded products with dates of manufacture spanning two years. The average strength of these specimens is 2800 psi (19 MPa) with a standard deviation of about 150 psi (1 MPa). This shows a good consistency of product over the two-year period. Specimens from batches A5 and A6 were manufactured using the extrusion process with a slightly lower amount of "filler" material (primarily sawdust). The average compressive strength of these specimens was 1600 psi (11 MPa), approximately 40 percent lower than specimens from batches A1 to A4. Most of the reduction in strength among specimens in batches A1-A4 and batches A5-A6 is attributed to the manufacturing process. However, specimens in batches A5 and A6 represent the initial attempts by manufacturer A at extruded products. Specimens from batches A10 to A13 were also manufactured using the extrusion process. The average strength of these specimens is 2200 psi (15 MPa), approximately 20 percent lower than specimens from batches A1 to A4. The subsequent products (Batches A10 to A13) show about a 30 percent increase in the average compressive strength of batches A5 and A6. This demonstrates that the manufacturer can modify the process and the constituent mixture to produce materials with comparable strengths to the compression-molded product.

Table 3.6 Summary of Uniaxial Compressive Strengths.

Specimen Batch	# Specimens	Nominal Strain Rate (in/in/min)	Uniaxial Compressive Strength (psi)			
			Using A_o [1]		Using A_c [2]	
			Avg.	Std. Dev.	Avg.	Std. Dev.
A1	10	NA	2784	128	- - [3]	- -
A2	7	0.005	2948	117	- -	- -
A3	6	0.005	2824	88	- -	- -
A4	6	0.005	2621	295	2486	271
A5	6	0.007	1634	200	1578	189
A6	14	0.007	1602	105	1521	102
A10	15	0.006	2219	154	2152	136
A11	15	0.006	2301	139	2217	140
A12	8	0.007	2085	84	1931	199
A13	15	0.007	2380	330	2310	318
B 7	15	0.007	2080	69	2331	134
B 8	15	0.006	2500	191	2505	195
C 9	15	0.007	2315	209	2556	322

[1]: stress calculated using original cross-sectional area (A_o)
[2]: stress calculated using corrected cross-sectional area (A_c)
[3]: Data not available
Conversion: 1 MPa =145 psi

The specimens used to represent the strength for batches A11, A12 and A13 were taken from portions of field installed members that remained above the ground surface after installation. Thus, these specimens are considered "disturbed", having been subjected to driving stresses indicative of other members installed in the field. Batch A10 specimens were identical specimens to batches A11, A12, and A13 except that A10 specimens were delivered directly to the laboratory and are considered "virgin" materials. The similarity of the average compressive strengths for these batches suggests there is no discernable

difference in the average compressive strength between specimens in the virgin condition and those in the disturbed condition, which further suggests that the installation process utilized (described in more detail in Chapter 10) does not have deleterious effect on the compressive strength of the members. Batches A11 and A13 are specimens that were installed using a pneumatic hammer while batch A12 specimens were installed using an impact hammer. Batch A12 was found to have slightly lower strengths (about 10 percent lower) than the virgin specimens from batch A10. However, it should be noted that Batch A12 was composed of a data set that is substantially smaller than the data sets for other batches.

The average compressive strength for specimens from manufacturers B and C ranged from 2000 psi to 2500 psi (14 MPa to 17 MPa), approximately 10 percent to 30 percent lower than specimens from batches A1 to A4. Batch B8 with the fiberglass-reinforced specimens shows about 20 percent increase in compressive strength when compare to the unreinforced specimens (Batch B7).

The average compressive strengths for materials from the three manufacturers determined at five percent strain with no area correction (A_o) and at the peak stress with area correction (A_c) are shown as bar graph in Figure 3.8. In general, the strengths at $A_{o\text{-}(5\%)}$ are higher than those with area correction (A_c). The difference is approximately five percent. In two instances, batches B7 and C9, the strength with the area correction was higher (by approximately 10 percent) than the specimens without area correction. The close agreement between the strengths indicates that using the strength at five percent strain without corrected cross-sectional area provides a reasonable value for the peak strength.

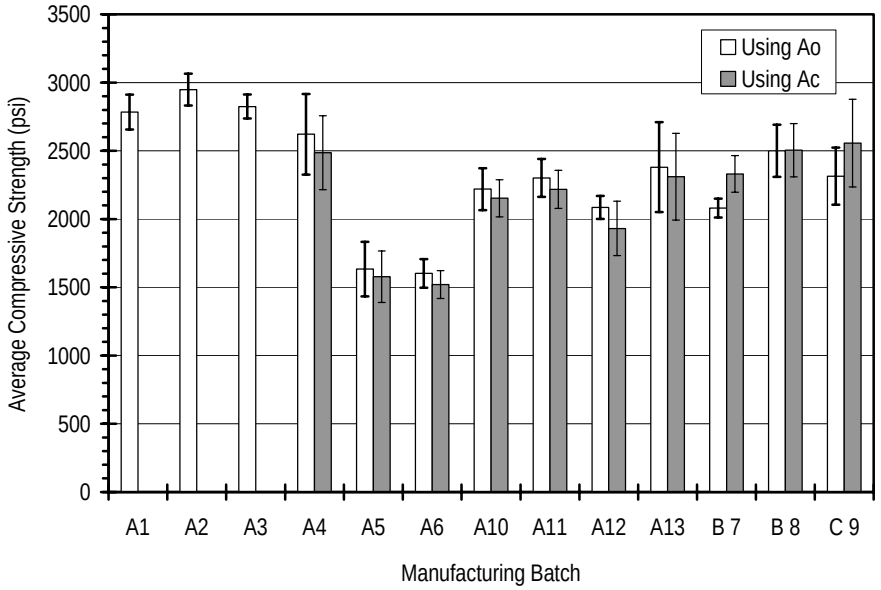

Figure 3.8 Comparison of average compressive strengths with and without cross-sectional area corrections for materials from all manufacturers.

Figure 3.9 shows a plot of the average compressive strength versus average unit weight for materials from three manufacturers. The solid data points represent strengths calculated based on original cross-sectional area (A_o), and open data points represent

strengths calculated from corrected cross-sectional area (A_c). The average strengths ranged from 1500 psi to 3000 psi (10 MPa to 21 MPa) within a unit weight range of 50 pcf to 70 pcf (8 kN/m^3 to 11 kN/m^3). There is little correlation between strengths and unit weights.

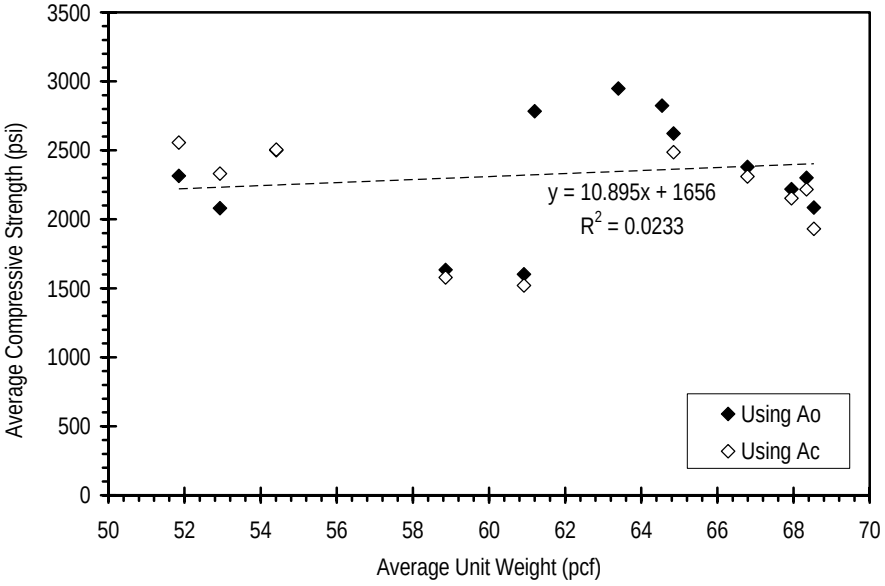

Figure 3.9 Average compressive strength versus average unit weight for materials from all manufacturers.

3.4.3. Modulus of Elasticity

Average values and standard deviations of the secant modulus of elasticity, E, determined from the uniaxial compression tests at one percent strain and five percent strain are shown in Table 3.7. The moduli were calculated using the original cross-sectional area (A_o) and corrected cross-sectional area (A_c). The moduli determined at one percent strain generally ranged from 80 ksi to 190 ksi (552 MPa to 1310 MPa) for both failure criteria. The moduli of the extruded products was generally on the order of one half that determined for the compression-molded products. For example, batch B8 (fiberglass-reinforced) show the stiffness about 20 percent lower than the compression-molded products. The average secant modulus for batch B8 (fiber-reinforced) at one percent axial strain was 138 ksi (951 MPa), approximately 60 percent higher than specimens from batch B7 (unreinforced).

The average results and range for each batch are shown as a bar graph in Figure 3.10 ($E_{@1\%}$) and Figure 3.11 ($E_{@5\%}$). The secant moduli at one percent axial strain show little difference between original and corrected area. At five percent axial strain (Figure 3.11), the moduli calculated using the original cross-sectional area are about five percent greater than those calculated using the corrected area. This behavior is similar to that for the compressive strength and further indicates that the strength and modulus calculated using the original area at five percent strain are a reasonable representation of the peak strength.

The average secant moduli at one percent strain for batches A10 – A13 ranged from 110 ksi to 120 ksi (758 MPa to 827 MPa). For Batches A5 and A6 the average secant moduli at one percent strain ranged from 80 ksi to 90 ksi (552 MPa to 621 MPa). The secant moduli at one percent strain for batches B7 and B8 were quite different from manufacturer A. The

secant moduli at one percent strain for batches B7 and C9 were almost identical and both are unreinforced material. The unreinforced material (Batch B7) had a secant modulus of 90 ksi (621 MPa) while the reinforced material (Batch B8) had a secant modulus of 140 ksi (965 MPa). Obviously, the reinforcing fibers significantly stiffen the material.

Table 3.7 Summary of Secant Moduli from Uniaxial Compression Tests

			Secant Modulus							
			Using A_o[1]				Using A_c[2]			
		Nom.	$E_{1\%}$ (ksi)		$E_{5\%}$ (ksi)		$E_{1\%}$ (ksi)		$E_{5\%}$ (ksi)	
Spec. Batch	# Spec.	Strain Rate (in/in/min)	Avg.	Std. Dev.	Avg.	Std. Dev.	Avg.	Std. Dev.	Avg.	Std. Dev.
A1	10	NA	134	8	57	4	- -[3]	- -	- -	- -
A2	7	0.005	184	9	55	3	- -	- -	- -	- -
A3	6	0.005	164	29	57	3	- -	- -	- -	- -
A4	6	0.005	186	20	52	4	185	20	49	4
A5	6	0.007	84	16	33	4	84	16	31	3
A6	14	0.007	93	8	32	2	92	8	30	2
A10	15	0.006	114	12	45	3	113	12	43	3
A11	15	0.006	119	11	47	3	119	11	45	3
A12	8	0.007	108	11	40	4	107	11	38	4
A13	15	0.007	110	21	48	6	110	21	45	6
B 7	15	0.007	87	10	42	2	85	11	39	3
B 8	15	0.006	138	27	49	4	136	26	47	4
C 9	15	0.007	87	12	46	4	86	12	45	4

[1]: Use initial cross-sectional area (A_0) to calculated stresses
[2]: Use corrected cross-sectional area (Ac) to calculated stresses
[3]: Data not available

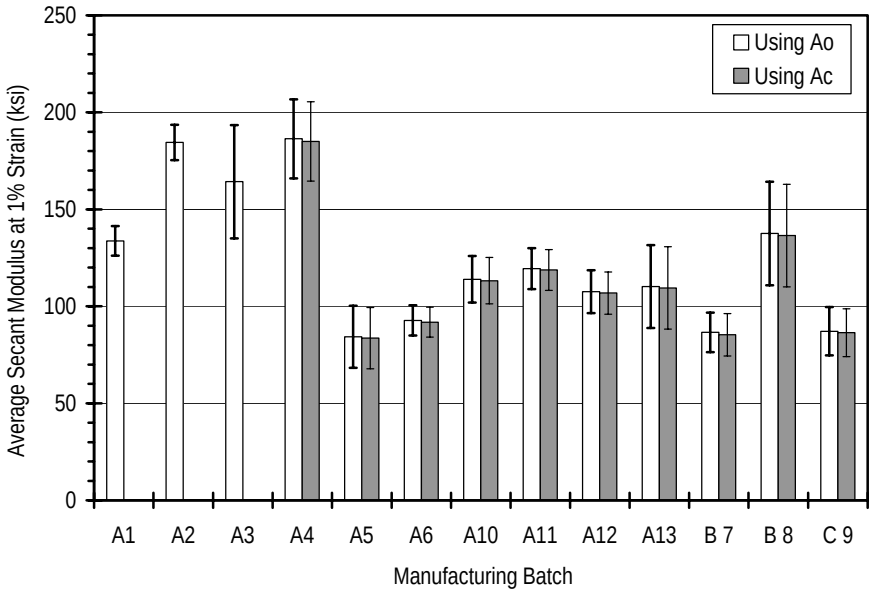

Figure 3.10 Comparison of average secant modulus at 1% axial strain ($E_{@1\%}$) for all manufacturers.

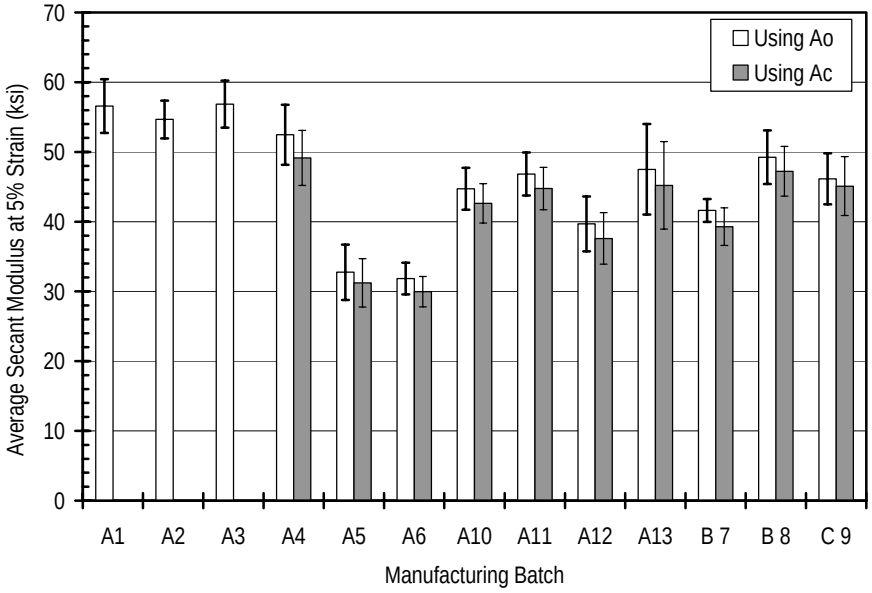

Figure 3.11 Comparison of average secant modulus at 5% axial strain ($E_{@5\%}$) of all manufacturers.

The modulus values determined at five percent strain ranged from 30 ksi to 60 ksi (207 MPa to 414 MPa), indicating that all of the products exhibited significant softening (decreasing stiffness) with increasing strain. The secant moduli at five percent strain were similar for batches A10 through A13, manufacturer B, and manufacturer C, and were in the range of 40 ksi to 50 ksi (276 MPa to 345 MPa).

3.4.4. Strain Rate Effects

The properties of plastic materials are dependent on the rate of loading (Birley et al, 1991). The behavior of the recycled plastic lumber is that the more rapidly it is loaded, the stronger and stiffer the material behaves (McLaren, 1995). To evaluate this effect, a series of tests were performed for a range in strain rates for specimens provided by all three manufacturers. All compressive strengths were calculated using the original cross-sectional area (A_o).

The results of tests for several batches of "virgin" specimens from manufacturer A are plotted in Figure 3.12. It is of interest to see that the trend line of batch A4 (compression molded) is almost parallel to the trend line of batch A10 (extruded products). Batch A4 shows that the measured compressive strength increased from 2100 psi to 2900 psi (14 MPa to 20 MPa) (a 30 percent change) as the strain rate was varied from 0.0006 in/in/min to 0.02 in/in/min (0.0006 mm/mm/min to 0.02 mm/mm/min). This corresponds to a drop in compressive strength of approximately 18 percent for each log cycle reduction in strain rate. Batch A10 had a drop in compressive strength of approximately 22 percent for each log cycle reduction in strain rate. Batches A5 and A6 had slightly smaller, but similar strain rate effects. In these tests, the specimen tested at the lowest strain rate (0.0006 in/in/min) reached peak stress in about two hours while specimens tested at the highest strain rate (0.021 in/in/min) reached failure in approximately 6 minutes. Because of the significance of strain rate effects and practical issues involved with developing a specification, a strain rate of

approximately 0.006 in/in/min (testing time of approximately 20 minutes) was chosen as a baseline for comparing the remaining test specimens.

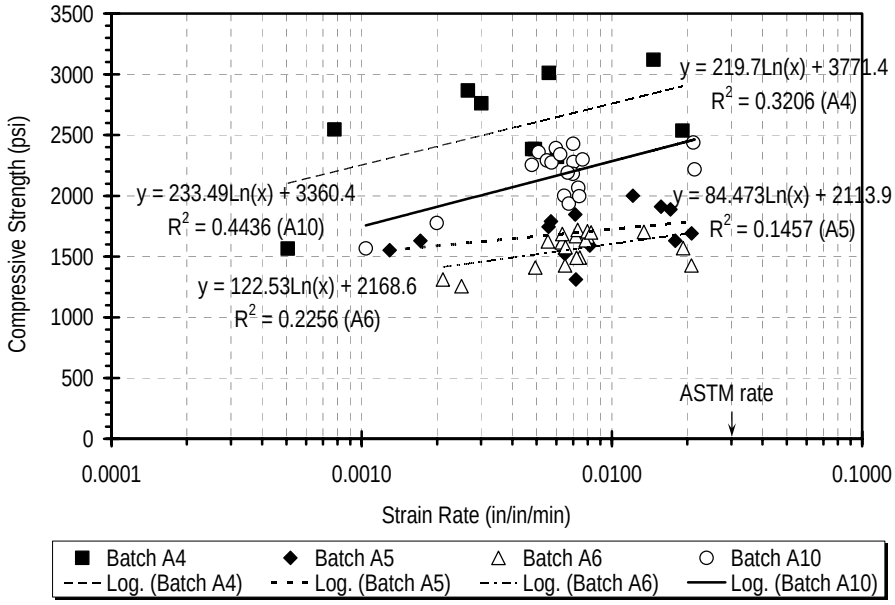

Figure 3.12 Compressive strength versus strain rate for tests on RPPs (Mftg A – virgin specimens).

Figure 3.13 shows that the compressive strength versus strain rate for batch A10 (virgin specimens) and for batches A11 to A13 (disturbed specimens). In general, the differences in strain rate effects between virgin and disturbed specimens were small. Batches A11 and A13, which were installed using the same type of equipment, show that the measured compressive strength increased from 1800 psi to 2500 psi (12 MPa to 17 MPa) (a 30 percent change) as the strain rate was varied from 0.0003 in/in/in to 0.02 in/in/min (0.0003 mm/mm/min to 0.02 mm/mm/min). This corresponds to a drop in compressive strength of approximately 15 percent for each log cycle reduction in strain rate, which is lower than that for batch A10, which had a 22 percent decrease in strength for each log cycle reduction in strain rate. The variation in stain rate effects between the three disturbed batches is not significant enough to indicate again that either driving method is more or less deleterious to the member strength.

Figure 3.14 shows the compressive strength versus strain rate for specimens from manufacturer B and manufacturer C. Note that the slope of strain rate relations are almost identical, although these materials come from different manufacturers. In general, these three batches show that the strength increased from 1800 psi to 2700 psi (12 MPa to 19 MPa) (a 30 percent change) as the strain rate was varied from 0.0003 in/in/min to 0.02 in/in/min (0.0003 mm/mm/min to 0.02 mm/mm/min). This corresponds to a drop in compressive strength of approximately 20 percent for each log cycle reduction in strain rate. It can be concluded that the drop in compressive strength for RPPs from all three manufacturers ranged from 15 percent to 25 percent for each log cycle reduction in strain rate.

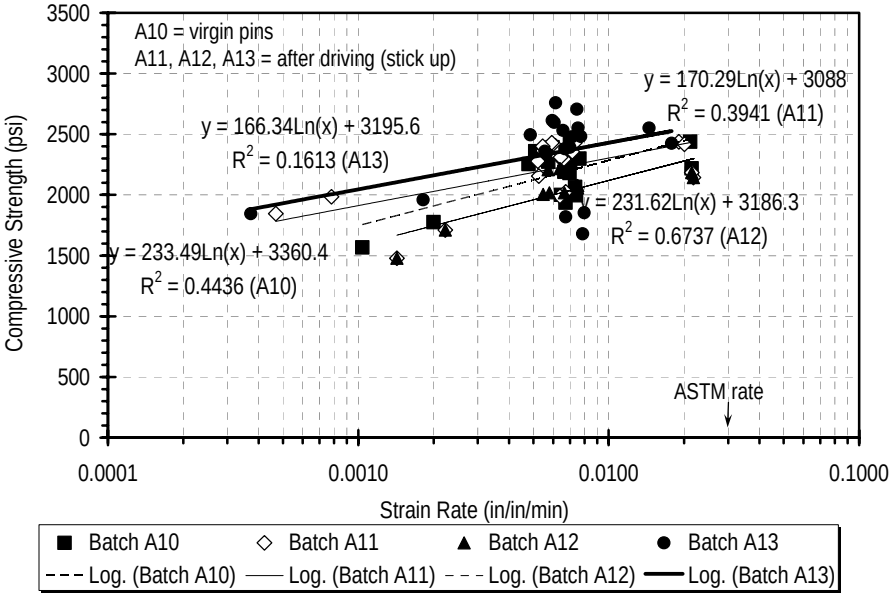

Figure 3.13 Compressive strength versus strain rate for materials from Mftg A (virgin specimens versus disturbed specimens).

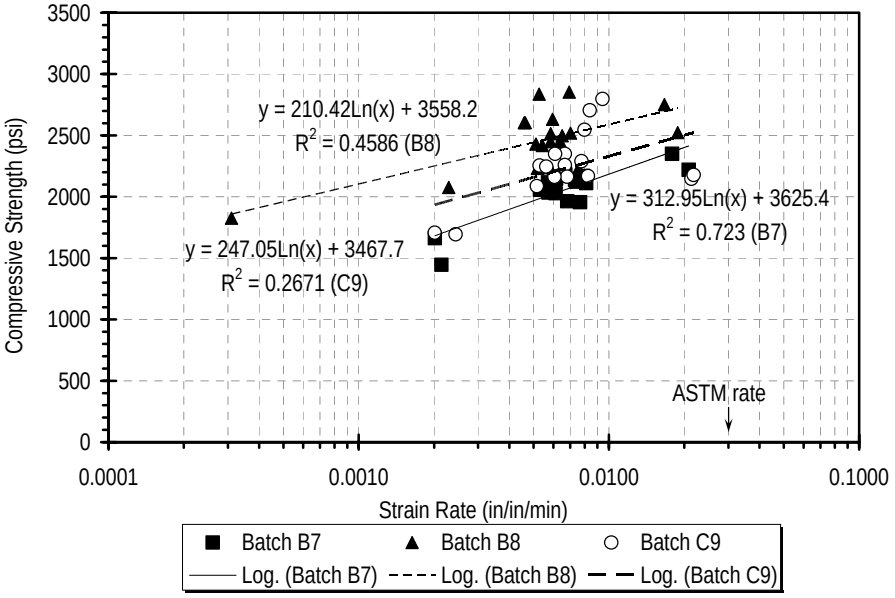

Figure 3.14 Compressive strength versus strain rate for uniaxial compression tests on specimens from manufacturers B and C.

In order to try to normalize the strain rate effects observed for different materials, a "standard compressive strength" (σ_{std}) was defined as the compressive strength at a strain rate of 0.03 in/in/min (the ASTM specified rate), based on the compressive strength versus strain rate plot (Figure 3.15). For example, results of the compressive strengths versus strain rates from batch A10 were plotted in Figure 3.15. The standard compression strength was taken equal to 2540 psi at a strain rate equal to 0.03 in/in/min (0.03 mm/mm/min). Note that,

every batch has a different standard compressive strength as measured at a strain rate of 0.03 in/in/min (0.03 mm/mm/min).

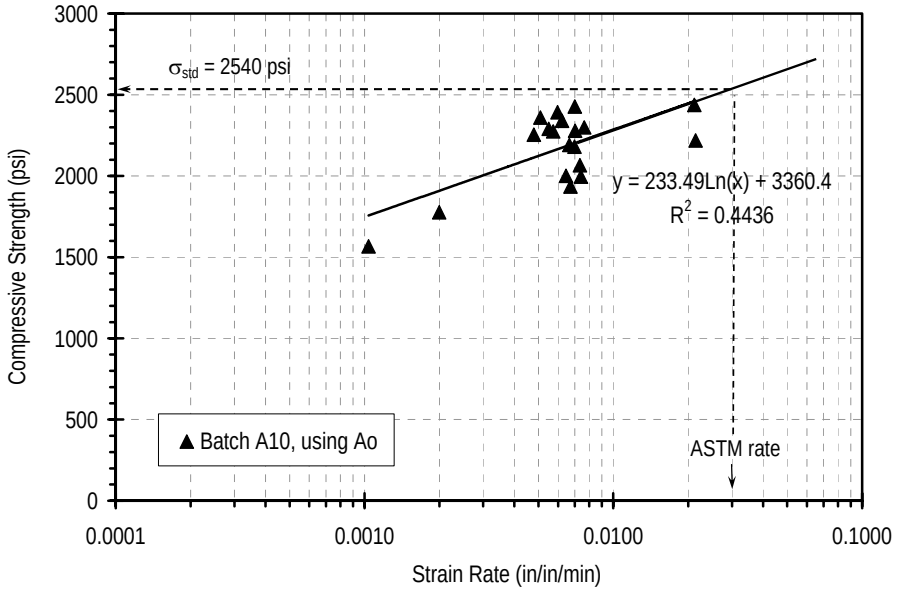

Figure 3.15 Establishing "standard compressive strength" (σ_{std}) from tests on specimens at different strain rates (Batch A10).

The ratio of the compressive strength (at a given strain rate) to the standard compressive strength (σ_{std}) as a function of strain rate for the RPPs from all three manufacturers is plotted in Figure 3.16. As shown in this figure, the compressive strength decreases with decreasing strain rate in terms of the standard compressive strength (σ_{std}) of percentage reduction. Batch A5 has the flatter slope and serves as an "upper-bound" on the reduction in compressive strength with strain rate. Batch B7 has the steepest slope and serves as a "lower-bound" reduction. The average slope was computed by taking average value of all the data, thus making it easy to compare all possible strain rates that might occur in the field in terms of reductions of the standard compression strength (σ_{std}). For example, the compressive strengths decrease by approximately 30 percent (average slope) of standard strengths at one-day testing rate, while the strengths reduce about 60 percent (average slope) of standard strengths at one-week testing rate. From this strain rate relationship (Figure 3.16), specimens can be tested at any strain rate to establish the corresponding compressive strengths at other strain rates of interest.

Strain rates have particular significance in developing a suitable specification for recycled plastics in the slope stabilization application. Recently developed ASTM standards dictate strain rates that are approximately 1.5 times greater than the highest strain rate shown in Figures 3.12, 3.13, and 3.14. While the value of standardized test procedures is acknowledged, current standardized tests were developed with typical building applications in mind. The loading rates specified in these standards is therefore very high. In the slope stabilization application, the members are called upon to resist sustained bending loads over time, which may cycle from negligible load to the limit loads of the members as load is transferred from the moving soil in response to environmental conditions in the slope. In this

application, the loading rate is likely to be very slow, on the order of months (seasonal). The evaluation program included tests performed at a range of loading rates to establish relationships between the properties of interest (primarily strength and stiffness) and loading rate.

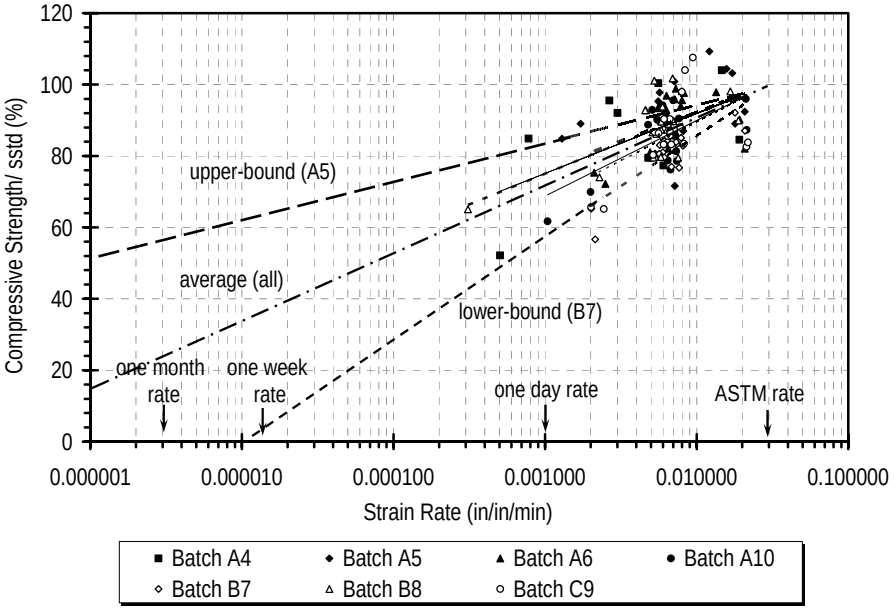

Figure 3.16 Ratio of compressive strength to standard compressive strength versus strain rate for several different batches of product.

3.5. Four-Point Flexure Tests

Four-point flexure tests were used to determine the flexural strength and stiffness of the different products evaluated. Specimens were cut to lengths of approximately 6 feet (~2 m). The support span to depth ratio used was 16:1 (ASTM, 2005). A schematic drawing of the setup is shown in Figure 3.17 and a photograph of the setup in the laboratory is shown in Figure 3.18. The tests were conducted using a stress controlled universal testing machine with a four-point bending attachment. The support span length (L) ranged from 4 feet to 5 feet (1.2 m to 1.5 m) with a load span ($L/3$) of 16 inches to 20 inches (0.4 m to 0.5 m). The rate of crosshead motion ranged from 1.2 in/min to 1.9 in/min (30 mm/min to 48 mm/min) as stipulated in the ASTM standard (ASTM, 2005). During loading, the deflection at the middle point of the load span and corresponding load applied to the specimen were recorded.

The typical response observed in the four-point flexure tests is shown in Figure 3.19. The flexural stress is plotted as a function of the extreme fiber strain at the center of the specimen ("center" strain). These data were derived from the applied loads and measured deflections as follows. Flexural stress (or bending stress), σ_b, was calculated as

$$\sigma_b = \frac{Mc}{I} \tag{3.3}$$

where M is the bending moment, c is distance from the neutral axis to the extreme fiber, and I is the moment of inertia of the cross-section. The maximum deflection at the center of the load span, Δ_{max}, is given as:

$$\Delta_{max}\ (at\ center) = \frac{\left(P/2\right)\ a\ \left(3L^2 - 4a^2\right)}{24E_bI} \tag{3.4}$$

where P is the applied load, L is the total span length, a is the distance from the outer support to the loading point ($L/3$), Δ is the deflection at the center of load span, and I is the moment of inertia. Equation 3.4 is merely a modification of the general equation for the center deflection (Δ) of a beam being tested in a four-point flexure test (Timoshenko and Gere, 1972). From Eq. 3.4, the flexural or bending modulus for each specimen was calculated as:

$$E_b = \frac{\left(P/2\right)\ a\ \left(3L^2 - 4a^2\right)}{24 * \Delta * I} \tag{3.5}$$

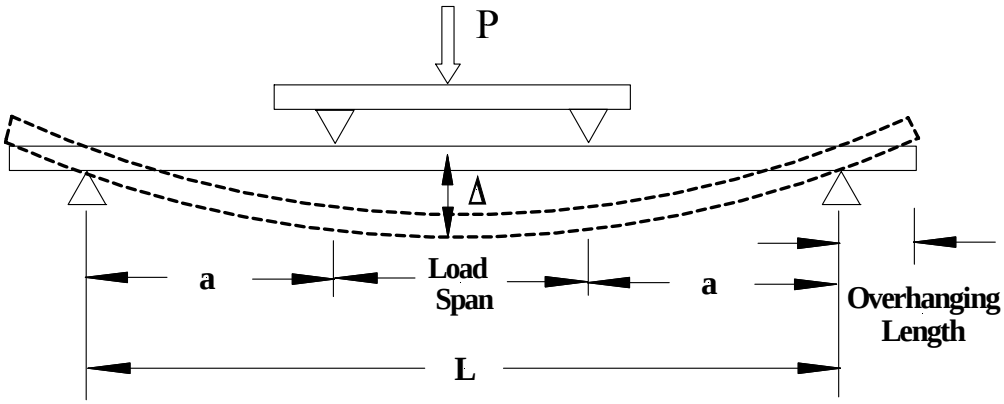

Figure 3.17 Loading diagram for four-point flexure test.

Figure 3.18 Photograph of four-point flexure test in progress.

If the material is assumed elastic with a linear stress-strain relationship, Hooke's law can be used to calculate the strain. In these tests, the center strain, ε_b , was calculated as:

$$\varepsilon_b = \frac{\sigma_b}{E_b} = \frac{12 * \Delta * h}{\left(3L^2 - 4a^2\right)} \tag{3.6}$$

where h is the depth of the specimen, L is the total span length, and a is the distance between the loading supports (L/3). A deformation rate was calculated by dividing the central deflection by the elapsed testing time. The average deformation rate was computed by taking the average of all deformation rates at center strains of less than two percent, as illustrated in Figure 3.20. A nominal deformation rate for the four-point flexure tests was 0.2 in/min (5.1 mm/min). Because the members tended to soften with increasing strain, secant values of the flexural modulus were computed at center strains of one and two percent, as shown in Figure 3.19.

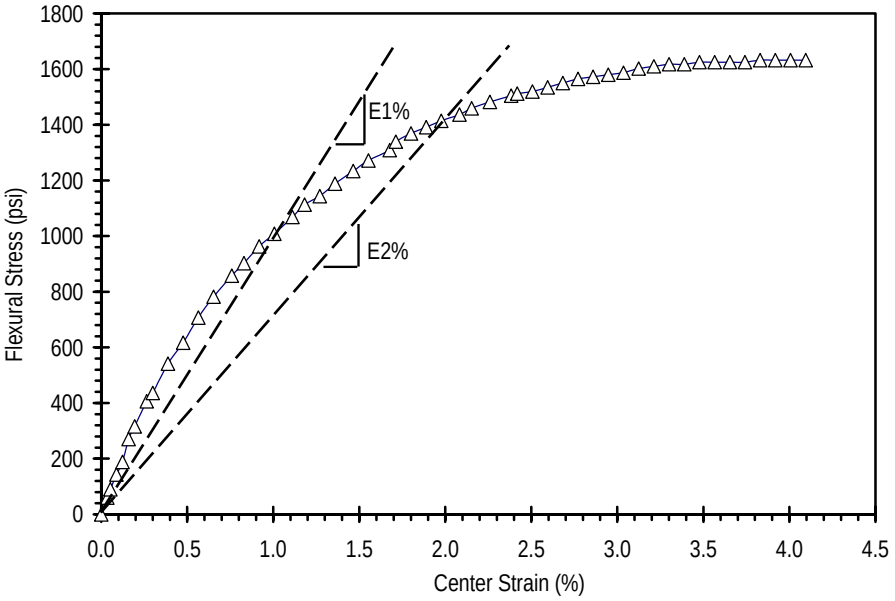

Figure 3.19 Illustration of typical flexural stress versus center strain response and method for establishing secant moduli for recycled plastic specimens loaded in four-point bending.

3.5.1. Flexural Stress- Center Strain Curves

Typical results of flexural stress versus center strain are plotted in Figure 3.21 for specimens from batches A4, A10, and B8. Specimens from batches A10 and B8 (extruded products) tolerated more than two percent center strain while specimens from batch A4 (compression-molded) ruptured prior to reaching two percent strain. Specimens from batch A10 showed a flatter curve after passing two percent strain and ruptured before reaching three percent strain, while specimens from batch B8 showed increasing stress with increasing strain until reaching three percent strain, when the tests were stopped.

3.5.2. Flexural Strengths

Results of the four-point flexure tests are summarized in Table 3.8. Since the number of tests on batches A11 and A12 were limited, no standard deviation is reported. Extruded members showed continually increasing stress with increasing deflection/strain without experiencing rupture of the member, while the compression molded members ruptured at

approximately two percent strain. The flexural strength for comparison of the different products was therefore taken to be the flexural stress at center strains of two percent or the stress at rupture for members that failed at center strains of less than two percent so that consistent strengths were established for all specimens. The measured flexural strengths for specimens loaded to failure or two percent center strain ranged from 1300 psi to 3600 psi (9 MPa to 25 MPa) under a nominal deformation rate 0.2 in/min (5.1 mm/min). The key finding from these tests is that there is significant variability, a factor of 2.8, in the flexural strength among the products tested.

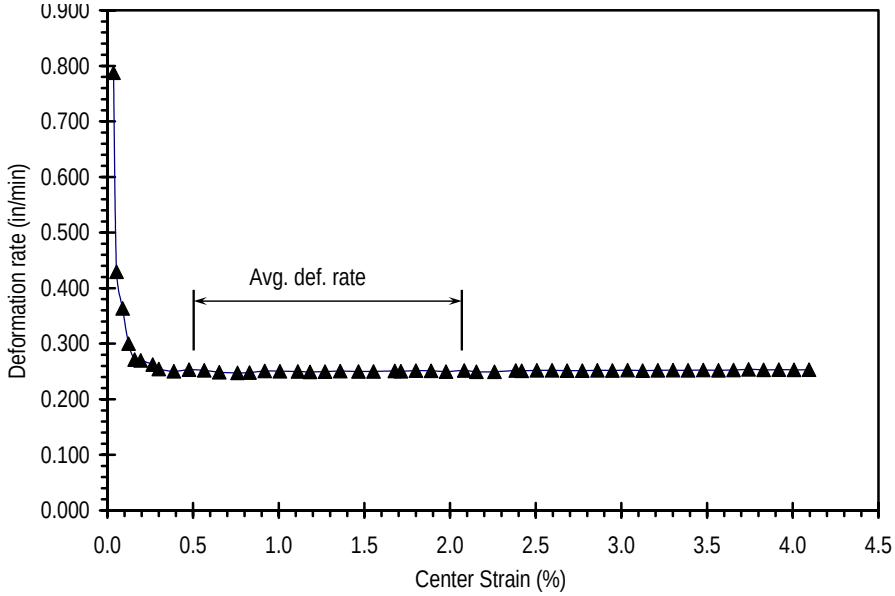

Figure 3.20 Illustration of method used to establish average deformation rate (Batch A5).

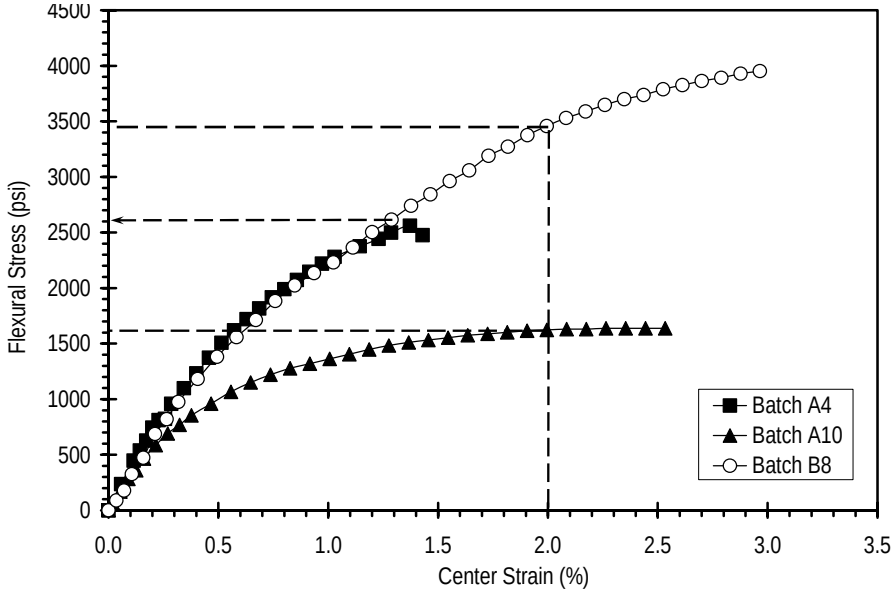

Figure 3.21 Typical flexural stresses versus center strain behavior for recycled plastic members.

Table 3.8 Summary of Four-Point Flexure Test results.

Spec. Batch	# Spec.	Nom. Def. Rate (in/min)	Flexural Strength [1] (psi)		Secant Flexural Modulus $E_{1\%}$ (ksi)		Secant Flexural Modulus $E_{2\%}$ (ksi)	
			Avg.	Std. Dev.	Avg.	Std. Dev.	Avg.	Std. Dev.
A1	13	- - [2]	1574	342	103	8	88 [3]	- -
A4	3	0.17	2543	260	213	13	- -	- -
A5	5	0.23	1542	188	98	14	73	2
A6	7	0.14	1360	118	95	12	68	6
A10	6	0.18	1596	137	123	22	76	10
A11	1	0.19	1679	- -	135	- -	81	- -
A12	1	0.19	1448	- -	115	- -	71	- -
B 7	6	0.17	1505	112	90	7	69	4
B 8	6	0.17	3589	358	243	24	179	13
C 9	7	0.16	1696	39	107	4	83	2

[1]: all results based on stress at 2% center strain or center strain at rupture of less than two percent
[2]: data not available
[3]: result of 2 specimens, others ruptured prior to reaching two percent center strain
Conversion: 1 MPa = 145 psi, 1 ksi = 6.9 MPa

A comparison the average flexural strength among all batches is plotted as a bar graph in Figure 3.22. This graph shows a tendency for the extruded products to have lower flexural strengths, except for batch B8 that contained reinforcing fibers. The average flexural strength for extruded products is about 1500 psi (10 MPa) and for compression-molded products is about 2500 psi (17 MPa) (a 40 percent change); however, this conclusion must be tempered because only three specimens were tested from batch A4. The only exception is batch B8 that has the flexural strength of approximately 3600 psi (25 MPa). The reinforced products of batch B8 showed a little increase in uniaxial compression strength (Table 4.1), but a large increase in flexural strength relative to other materials.

3.5.3. Flexural Modulus

Average values of the secant flexural modulus for each batch of specimens are shown in Table 3.8. In general, the flexural moduli varied from approximately 90 ksi to 250 ksi (621 MPa to1724 MPa) at one percent strain, similar to the values observed in the uniaxial compression tests with the exception of batch B8.

Results from batches A4 and B8 have significantly higher flexural stiffness than the other batches by a factor of two. This may potentially be a result of being compression molded or reinforced as compared to being on extruded products. Breslin et al. (1998) concluded that the use of glass and wood fiber additives significantly improves the modulus of elasticity for plastic lumber. Batch A10 (virgin specimens), and batches A11 and A12 (disturbed specimens) have similar flexural strength and flexural moduli, which again suggests little effect on properties due to installation stresses. Flexural moduli at two percent center strain were consistently lower than those determined at one percent center strain, because members tend to soften with increasing strain. The clear difference is shown as a

bar graph in Figure 3.23. Secant flexural modulus at two percent was not available for batch A4, because the specimens ruptured before two percent center strain.

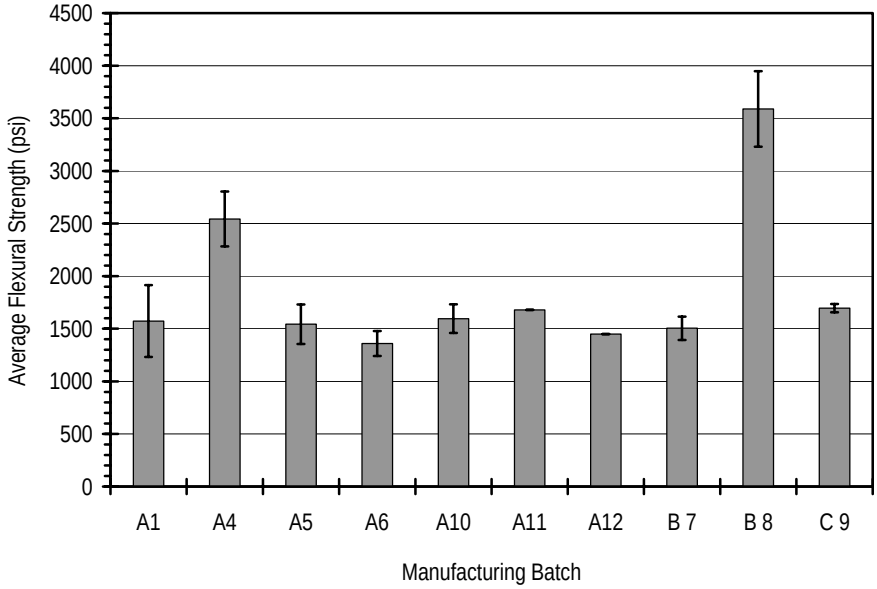

Figure 3.22 Comparison of average flexural strengths for all manufacturers.

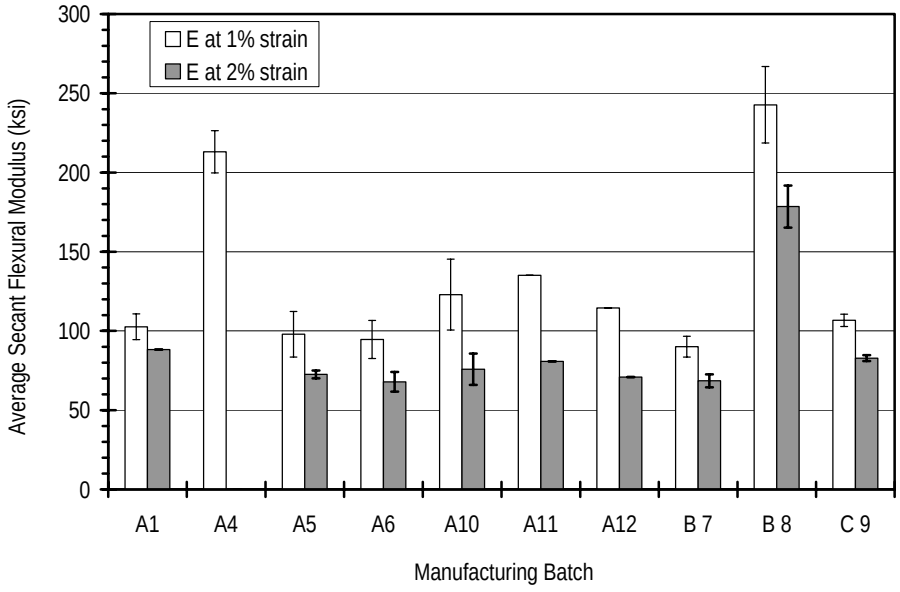

Figure 3.23 Comparison of average secant flexural modulus at one percent center strain ($E_{1\%}$) and two percent strain ($E_{2\%}$).

3.6. Flexural Creep Tests

Flexural creep response testing was performed on scaled members having nominal dimensions of 2 in. x 2 in. x 24 in. (51 mm x 51 mm x 61 cm). A cantilever setup was conceived to achieve the desired field loading. The creep frame that was designed and built

resembled a pommel horse; a schematic drawing is shown in Figure 3.24. Two steel channels (C8 x 14) were welded together with the channels facing in. A gap of approximately two inches was left between channels for a fastening position. The channels were welded to a two-inch (51 mm) steel pipe stand that was threaded together to accommodate moving the creep frame from place to place. The overall dimensions of the frame are approximately 41-inch (104 cm) long by approximately 42-inch (107 cm) tall. Fixing the specimens to the frame was achieved using several all thread bolts approximately nine-inch (23 cm) long, 1 in. x 6 in. (25 mm x 152 mm) wood boards and a 1 in. x 6 in. (25 mm x 152mm) steel plate with the same length as that of the creep frame. The wooden boards and steel plate had holes drilled in them at the positions that the all thread bolts would be used to clamp the specimens. A wood board was placed on the creep frame and on top of the creep specimens to protect the specimens from melting on the steel at high temperatures. The 1 in. x 6 in. (25 mm x 152 mm) steel plate was place on top to provide rigidity to the clamping mechanism. The creep frame was designed to hold eight specimens at various loads.

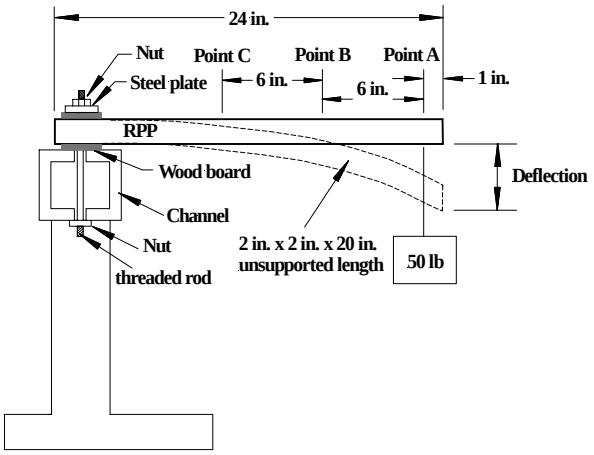

Figure 3.24 Setup for testing flexural creep of recycled plastic members.

Table 3.9 shows the temperature and loading setup for the flexural creep tests. It was determined that five temperatures would be needed to achieve continuity throughout testing. Temperatures of 21°, 35°, 56°, 68°, and 80° Celsius (70°, 95°, 133°, 154°, and 176° Fahrenheit) were easily obtained in elevated temperature controlled environmental rooms. Humidity levels were not monitored. Eight specimens at each temperature were tested for a total of thirty-six specimens with the exception that only four specimens were tested at 35°C (95°F). Two specimens were equally loaded at the same temperature to assure reproducibility. Specimens were loaded with either single (21 lbs, 35 lbs or 50 lbs) or multiple point loads along their length (five 10-Lb loads distributed evenly). The deflections at three points (points A, B, C as shown in Figure 3.24) along the cantilever were measured and recorded over time. Typical results are shown in Figure 3.25, which shows the creep deflection versus time response.

By its very nature, creep is a long-term phenomenon. For example, members being tested at 21°C (70°F) have been under load for more than five years but have not ruptured. Tests at elevated temperatures were established in order to accelerate the creep process.

Results from the accelerated testing were used along with the Arrhenius method (Koerner et al., 1990) to estimate the long-term creep behavior for members in the field.

Table 3.9 Temperature and Loading Details for Flexural Creep Tests

Temperature (°C)	# Specimens Tested	Point Load (lbs)	Disturbed Load (lbs)
21	8	21, 35, 50	10 lbs @ 5 points
35	4	50	- - [1]
56	8	21, 35, 50	10 lbs @ 5 points
68	8	21, 35, 50	10 lbs @ 5 points
80	8	21, 35, 50	10 lbs @ 5 points

[1]: data not available

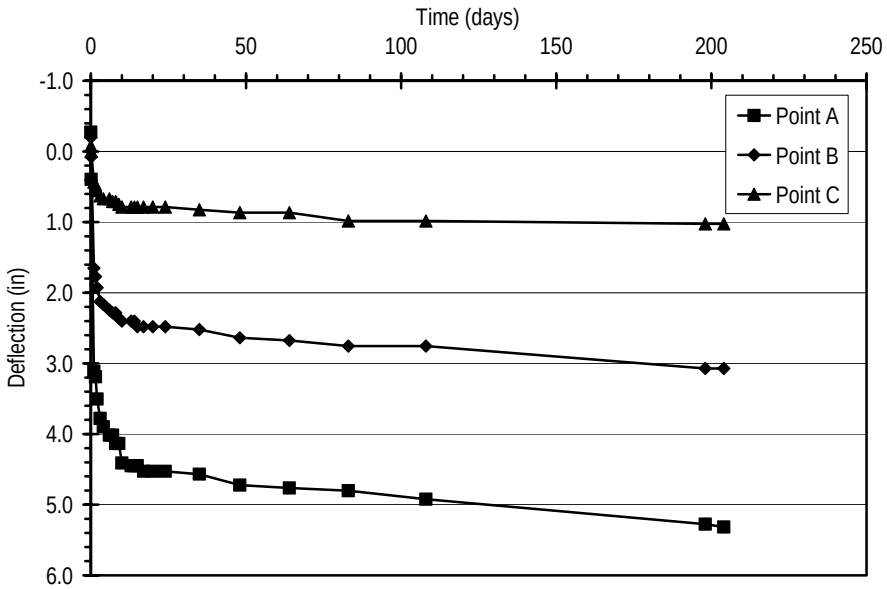

Figure 3.25 Deflection versus time response for recycled plastic members with five 10-Lb loads at even spacing in 56°C environment. Specimen failed after 210 days.

Arrhenius modeling provides a method to accelerate the creep rate of materials and to predict performance at field temperatures. An example of an Arrhenius plot is shown in Figure 3.26. The following steps explain the method:

1. Results from flexural creep tests at several different temperatures are presented in a plot of the natural logarithm of the inverse of the time required for the member to rupture (failure) versus the inverse of the temperature at which the test was conducted (Figure 3.26).
2. The negative slope of the line on the Arrhenius plot is known as the activation energy (E_{act}) divided by the universal gas constant (R=8.314 J/mol-ºK). Knowing the value of negative slope ($-E_{act}/R$), the reaction rate intercept on the Arrhenius plot (ln A) and the temperature of an actual site (T_{site}), the time

for the member to reach the breaking point under field conditions for a members stressed to the same level as those used to develop the Arrhenius plot can be determined.

3. Step 3: The reaction rate for the field condition, ln (R_{site}), can be calculated as:

$$\ln\left(\frac{1}{t}\right) = \ln A - \left(\frac{E_{act}}{R}\right)\left(\frac{1}{T_{site}}\right) \tag{3.7}$$

For this project, flexural creep tests at different temperatures were completed and the parameters for the Arrhenius model were calculated to allow estimation of the time for the member to reach failure.

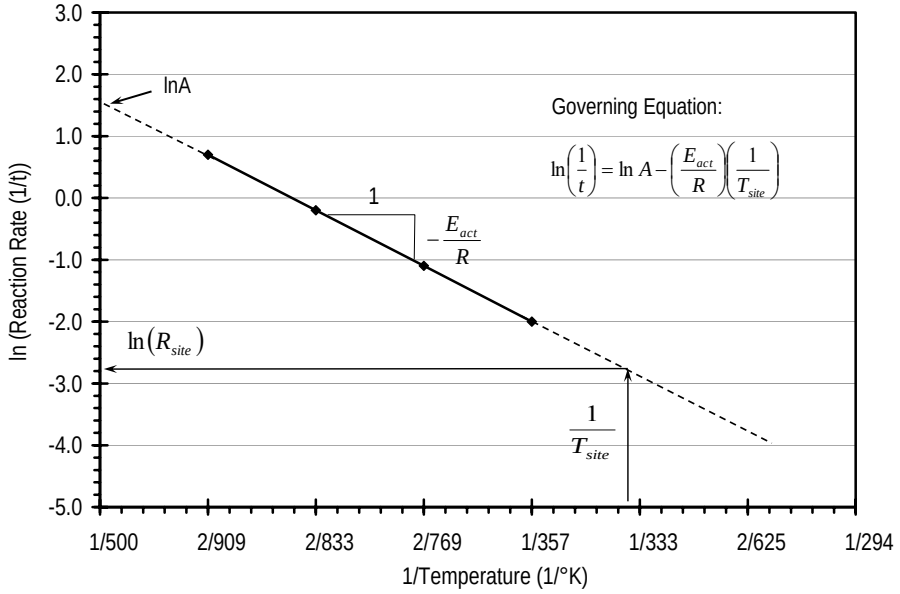

Figure 3.26 Arrhenius plot of inverse reaction rate versus inverse temperature (Koerner, 1998).

3.6.1. Flexural Creep Test Results

Typical results of deflection versus time for specimens under a sustained load are shown in Figure 3.27. The behavior shown is typical of the members tested at the various temperatures. The specimens were loaded with 50 lbs (23 kg) at the free end of a simple cantilever (Figure 3.24). All specimens failed after the final data point, with the exception of the specimens at 21°C (70°F), which have been under load for more than five years but have not failed.

Table 3.10 shows a summary of results for flexural creep tests under various loading conditions and temperatures. Specimens at elevated temperatures of 56°C, 68°C, and 80°C (133°F, 154°F, and 176°F) failed under four types of loading conditions. As the temperature increased, the time to reach failure decreased for the same load condition. Results show that the loading levels, along with temperature, affect the creep behavior of the recycled plastic specimens. The higher load levels or those closer to the ultimate strength of the material, the faster the creep rate and shorter time to reach failure.

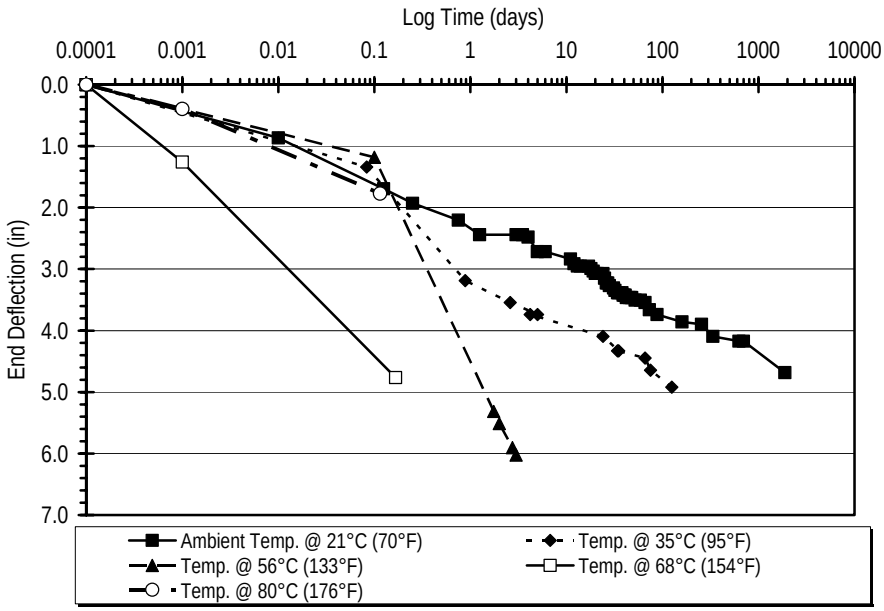

Figure 3.27 Deflection versus time response for recycled plastic members loaded with 50 lbs at the free end of a simple cantilever under various temperatures.

Table 3.10 Summary of Flexural Creep Tests on Recycled Plastic Specimens

# Specimens Tested	Temperature (°C)	# Specimens Tested	Average Time to Reach Failure (days)	Comments[2]
10 lbs @ 5 points	21	2	1185[1]	Not failed
	56	2	194.5	Failed
	68	2	3.5	Failed
	80	2	0.8	Failed
21 lbs single load	21	2	1185[1]	Not failed
	56	2	574	Failed
	68	2	17.5	Failed
	80	2	8.5	Failed
35 lbs single load	21	2	1185[1]	Not failed
	56	2	71.5	Failed
	68	2	0.6	Failed
	80	2	0.75	Failed
50 lbs single load	21	2	1185[1]	Not failed
	35	4	200	Failed
	56	2	3.1	Failed
	68	2	0.4	Failed
	80	2	0.75	Failed

[1]: the last day of testing, specimens have not ruptured
[2]: failure is defined as breakage of the specimens

An example of an Arrhenius plot for the members is shown in Figure 3.28. The plot includes data for tests at 35°C, 56°C, 68°C, and 80°C (95°F, 133°F, 154°F, and 176°F) with a 50-lbs(23 kg) single load at the end of a simple cantilever. Results show that recycled plastic members were all broken under this loading condition except for the members tested at 21°C (70°F), which have been under load for more than five years. The data point for tests at 21°C (70°F) is therefore not plotted in the Arrhenius plot (Figure 3.28).

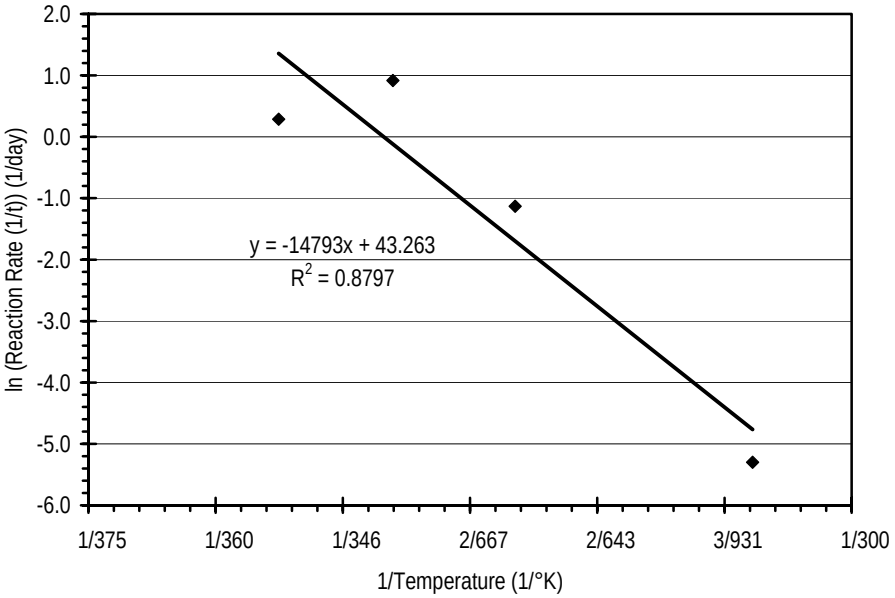

Figure 3.28 Typical Arrhenius Plot for flexural creep test on 2 in. x 2 in. x 24 in. member loaded with a 50-lb weight at the end of a simple cantilever under various temperatures.

From the slope and intercept of the line in the Arrhenius plot, the time to achieve creep failure under this loading level at field temperature conditions can be estimated from

$$\ln\left(\frac{1}{t}\right) = -14793\left(\frac{1}{T_{site}}\right) + 43.263 \qquad \text{(From Eq. 3.7)}$$

From this relation (assuming T_{site}=21°C = 294°K), the time required for the members to creep to the failure point is estimated to be approximately 1157 days (3.2 years) under this level of load. However, observations from laboratory tests under similar loads at this temperature show that the members remain stable and have steady creep rate. Thus the Arrhenius modeling would appear to underestimate the time to reach failure. Arrhenius plots for other loading conditions are provided in Chen (2003).

Because creep rate is dependent on load level, a similar process was used for the other loading conditions to predict estimated time to reach failure at field temperatures over a range in load levels. The results of these analyses are summarized in Table 3.11. In the table, load level is represented by three quantities: the maximum moment in the test member, the maximum flexural (extreme fiber) stress in the test member, and by the maximum flexural stress normalized with respect to a nominal flexural strength of recycled plastic

members (here taken to be 1500 psi based on results presented in Figure 3.22). Considering the specimens loaded with a single 50-lb load as an example, the maximum moment is:

$$M_{\max} = 50\ lbs * 19\ in = 950\ in - lb \tag{3.8}$$

From mechanics of materials theory, the corresponding flexural stress, σ_{flex}, is:

$$\sigma_{flex} = \frac{M_{\max} * y}{I} = \frac{950\ in - lbs * 1\ in}{1.33\ in^4} = 714\ psi \tag{3.9}$$

where y is the distance from the neutral axis to the extreme fiber and I is the section moment of inertia for the test section. Adopting an average flexural strength of 1500 psi, the normalized flexural stress level is:

$$\frac{\sigma_{flex}}{\sigma_{flex-\max}} = \frac{714}{1500} = 0.476 \cong 48\% \tag{3.10}$$

Figure 3.29 shows the estimated times to reach creep failure at field temperatures as a function of the mobilized load level as represented by the flexural stress in the members. The graph is subsequently used to predict the effective creep lifetime of recycled plastic members under field loads as described in the following section.

Inspection of the estimated times to reach creep failure in Table 3.11 reveal periods of at least several years for specimens loaded to flexural stresses approaching 50 % of the flexural strength (recalling that the estimates are believed conservative) to several thousand years for specimens loaded to only 20% of the flexural strength. The estimate determined for the distributed loading case also suggests a substantially longer time to failure for distributed loading as compared to single point loading at similar stresses. It is not clear whether this result is simply a result of variability in materials or a result of different creep behavior for different forms of loading. Additional testing is needed to better define the relations for different loading conditions.

Table 3.11 Summary of estimated time to creep rupture for various loading conditions based on flexural creep tests

Loading Condition	Max. Moment, M_{max} [1] (in-lb)	Flexural Stress, σ_{flex} [2] (psi)	Flex. Stress Ratio (σ_{flex} / $\sigma_{flex\text{-}max}$) [3] (%)	Time to Failure at 21°C[4] (years)
50 lb Single	950	714	48	3.2
35 lb Single	665	500	33	290
21 lb Single	399	300	20	2317
Five 10 lb loads Equally Spaced	590	444	30	6515

[1]: moment arm = 19 inches
[2]: use Eq 3.9 to calculate stress
[3]: average flexural strength = 1500 psi (measured in laboratory)
[4]: calculation from Chen (2003)

3.6.2. Estimation of Creep Life in the Field

Figure 3.29 provides a method for estimating the expected "field life" of stabilization measures using recycled plastic reinforcement, if the level of loading is measured or estimated. Figure 3.30 shows a sample of measured bending moments that were mobilized in two instrumented reinforcing members at the I70-Emma test site. Considering the largest measured moments of nominally 350 ft-lb, the maximum mobilized flexural stress is nominally 500 psi, or about 33% of the ultimate flexural stress. From Figure 3.29, this would suggest that the time to creep rupture would be on the order of several decades, or even longer for distributed loading. If the lower measured moment is considered, the estimated time to creep rupture is significantly longer.

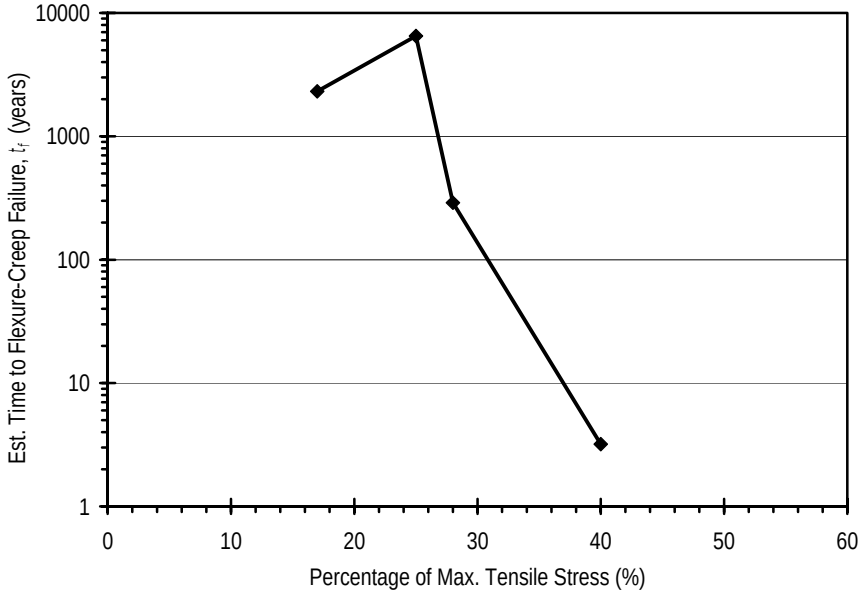

Figure 3.29 Relation between loading level and estimated time to creep rupture based on Arrhenius modeling of flexural creep tests.

The above procedure can be used to estimate the design life of slope stabilization measures utilizing recycled plastic reinforcement. Such estimates are presented and discussed in the subsequent chapters. If the estimated time to failure is too low, designers can modify the design to reduce the stress level in individual members to increase the design life. Options for reducing the stress include increasing the number of members (thereby reducing the force required to achieve stability), increasing the size of the pins (thereby reducing the flexural stress for a given force), changing the constituent blend to make members less creep susceptible, or changing the cross-section to increase their moment of inertia.

It is possible, perhaps even likely, that the method described is conservative, since it is entirely based on laboratory tests and the Arrhenius method, which tends to underestimate the time to reach failure. In the testing program various single point loads were used to generate the creep deformation with breakage time. The data in Table 3.11 shows that for similar specimens, loaded with five 10 lb at equally spacing, the time to reach failure due to flexural creep at 21°C is about 6500 years, much longer than that for single point loaded

specimens. However, the loading conditions in the field are much closer to distributed loading than to point loading. Additional testing programs, preferably involving a range of commercially available products, are recommended to develop further knowledge regarding this important issue.

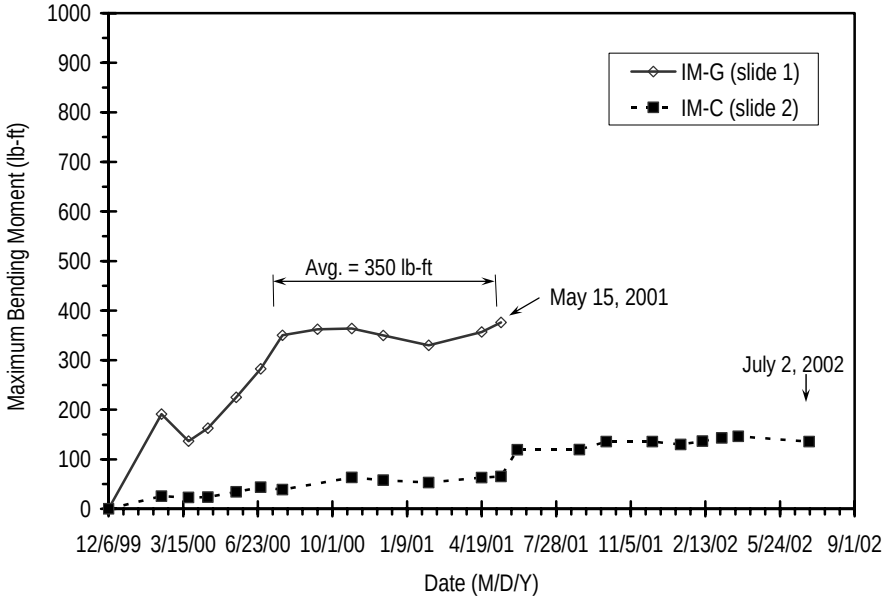

Figure 3.30 Maximum mobilized bending moments from instrumented members at I70-Emma site (Parra et al., 2003).

3.7. Evaluation of Material Exposure to Potentially Detrimental Environments

Because there is some potential for polymeric materials to degrade when placed in certain exposure environments, a series of tension and compression tests were performed on specimens subjected to a series of environmental conditions. All specimens were from Batch A1. Specimens were prepared from the recycled plastic material and placed in several exposure environments for up to one year in order to evaluate the durability of the material. The environments included: submergence in an acidic solution (pH 5), ultraviolet (UV) exposure, submergence in tap water, submergence in kerosene, and exposure to a series of freeze/thaw cycles. At selected times (7, 14, 28, 63, 330 and 375 days), one specimen was removed from each environment and tested. The measured tensile and compressive strengths after one year of exposure are summarized in Table 3.12. These data show very little impact for the compressive strengths. The tensile strength was impacted slightly, especially for specimens exposed to Kerosene. However, it is important to note that it is highly unlikely that the members would be subjected to such high concentrations of kerosene or other hydrocarbons, even in the unlikely event of a direct spill from a tanker truck or rail car so the potential for dramatically impacting a stabilized site is very remote. Overall, the results indicate that the recycled plastics tested are generally resilient to a broad range of exposure conditions, especially when compared to more common civil engineering materials such as steel and concrete.

Table 3.12. Summary of tension and compression properties of recycled plastic material subjected to various exposure environments.

Exposure Environment[1]	Tension		Compression	
	Young's Modulus (ksi)	Peak Stress (ksi)	Young's Modulus (ksi)	Peak Stress (ksi)
No Exposure	129	1.8	107	3.0
pH 5	114	1.5	106	2.5
UV	112	1.4	91	2.5
Tap Water	112	1.5	104	2.4
Kerosene	97	0.9	86	2.2
Freeze/Thaw[2]	105	1.6	100	3.0

[1]Data shown are for tests conducted on specimens after 375 days of exposure in the noted environment with the exception of the tension values, which are for specimens after 330 days of exposure.
[2]Data are for specimens subjected to 334 freeze/thaw cycles (-15 to +45 F degrees)

3.8. Significant Conclusions from Materials Testing Program

Results presented in this chapter from an extensive series of tests on recycled plastic members from three different manufacturers lead to a number of important observations and conclusions. These include:

- Compressive strengths of recycled plastic members ranged from 1600 psi to 3000 psi (11 MPa to 21 MPa) with no cross-sectional area correction and tested at a nominal strain rate of 0.006 in/in/min (0.006 mm/mm/min).
  - The average compressive strengths of the extruded products (2200 psi) are approximately 20 percent lower than the compressive strength of the compression-molded products (2800 psi).
  - Manufacturers of extruded products can modify their processes and constituent mixtures to produce materials with comparable strengths to the compression molded products.
  - There is no discernable change in the average compressive strength between specimens in the virgin condition (before installation) and those in the disturbed condition (after installation) indicating that the installation techniques used to date (described in subsequent chapters) do not have a deleterious effect on the material properties.
  - There is little correlation between the measured compressive strengths and unit weights of the specimens.
- Compression moduli determined at one percent strain ranged from 80 ksi to 190 ksi (552 MPa to 1310 MPa).
  - Compression moduli of the extruded products (90 ksi) was generally on the order of one half that determined for the compression-molded products (180 ksi).
  - Compression moduli for the reinforced products had a secant modulus of 140 ksi (965 MPa) while the secant modulus of a similar unreinforced material was only 90 ksi (621 MPa).
- Strain rate has a significant impact on the measured strengths of the products.
  - For each order of magnitude decrease in strain rate, the measured compressive strength was found to decrease by nominally 20 percent.

  - Strain rate relations for different material products varied substantially, so product specific tests are desirable to establish appropriate relations
- Flexural strengths for specimens loaded to failure or two percent center strain ranged from 1300 psi to 3600 psi (9 MPa to 25 MPa) under a nominal deformation rate 0.2 in/min (5.1 mm/min).
  - There is significant variability, a factor of 2.8, in the flexural strength among the products tested.
  - Extruded members showed continually increasing stress with increasing deflection/strain without experiencing rupture of the member while compression molded members ruptured at approximately two percent strain.
- Flexural moduli varied from 90 ksi to 250 ksi (621 MPa to 1724 MPa) at one percent strain, similar to the values observed in the uniaxial compression tests with the exception of the fiberglass-reinforced material.
- Flexural creep tests revealed the recycled plastics to be creep sensitive.
  - Creep tests were highly dependent on the temperature and stress level in the specimens.
  - Arrhenius modeling can be used to conservatively estimate the time to creep rupture under various load levels.
  - Additional creep testing of different products is recommended to better address this important issue.

Chapter 4. Site Selection

The most critical element of the project was establishing a series of field test sites where full-scale use of the technique was implemented. A vital portion of this task was selection of the particular sites to be included in the field testing program. Well over fifty different sites where surficial slope failures had recently occurred were considered for stabilization as a part of the project. Candidate sites were identified from a variety of sources including project investigators, MoDOT geotechnical personnel in Jefferson City, and other MoDOT personnel located in districts throughout the state. While the overall objective of site selection was to select sites that would establish the range of site conditions over which recycled plastic reinforcement is viable, other criteria were also considered to ensure the success of the project. In this chapter, the criteria and process utilized for selecting the demonstration sites are described along with a brief summary of the characteristics of the sites selected for stabilization during the project. Detailed characteristics for each selected site are provided in subsequent chapters.

4.1. Criteria for Site Selection

Selection of the sites to be stabilized was a complicated issue. The constructability and performance of the technique is likely to be affected by soil type, slope geometry, stabilization scheme, construction method, and climatic conditions, among many others. Addressing all of these issues with a limited number of additional test sites was not feasible. Furthermore, the "available" sites at any given time may have characteristics that are better suited to evaluating some of these issues, but not others. Site selection activities therefore focused on selecting sites that would maximize the number of different issues that could be addressed while also addressing the specific issues that were considered to be most important. Specific project constraints such as schedule, budget, and convenience for long-term monitoring also had to be considered.

The criteria considered for selecting the test sites are listed in Table 4.1 along with the issues to be evaluated for each criterion. In general, preference was given to selection of slopes with a range of different geometries and soil types, having both excavated and embankment slopes, and to slides of reasonable size so that different stabilization schemes could be evaluated at a single site while still remaining within the project budget. Other criteria were then considered in a secondary manner.

4.2. Site Selection

Based on these criteria, candidate sites were identified by project and MoDOT personnel. Each of the sites was then screened based on general characteristics such as size, expected soil type, apparent depth of slide, and location. Well over fifty promising sites were then visited by project personnel to photograph the slope, map the surface features, and in some cases collect samples of soil for preliminary classification and testing. More detailed investigations were then performed for the seven sites deemed to be most promising as summarized in Table 4.2.

Five of these sites were ultimately selected for stabilization as a part of the project. General locations of the selected sites are shown in Figure 4.1. The first test site selected is the I70-Emma site, located on Interstate 70 approximately midway between Columbia and

Kansas City in west-central Missouri. This site was the "proof of concept" site stabilized during Phase I of the project; additional stabilization was then installed in adjacent areas of the site during Phase II. Two of the selected sites are located on Interstate 435 in Kansas City Missouri. One of the sites is located on U.S. Highway 36 in northwestern Missouri. The final selected site is located on U.S. Highway 54 in the central part of the state. With the exception of the proof-of-concept stabilization, all sites were established during Phase II of the project.

Table 4.1 Criteria used for evaluation of sites considered for Phase II.

Criteria (Variable)	Issue
Embankment or Cut Slope	Performance
Angle of Slope	Constructability, performance
Soil Type	Constructability, performance
Stratigraphy	Constructability, performance
Depth of Slide	Applicability
Size of Slide Area	Stabilization scheme, Budget, Economics
Presence of Debris in Slope	Constructability
Location of Slope Relative to Pavement	Constructability, Safety
Geographic Location of the Slope	Climate, convenience for monitoring

Table 4.2 Summary of most promising sites considered for stabilization.

Site	MoDOT District	Slope Inclination (H:V)	Slope Height (ft)	General Characteristics
I70-Emma	2	2.5:1	22	Embankment slope with lean to fat clay
I435-Wornall Road	4	2.2:1	32	Embankment with lean clay over clay shale fill
I435-Holmes Road	4	2.2:1	15	Embankment with lean clay over clay shale fill
MO13-Bolivar[1]	8	1.7:1	20	Embankment slope with lean to fat clays
US36-Stewartsville	1	2.2:1	29	Excavated slope with lean clay over fat clay
US54-Fulton	5	3.2:1	46	Excavated slope in "ablation" till
US63-Columbia[1]	5	2.5:1	25	Excavated slope over rock ledge
I44-Sarcoxie[1]	7	2.0:1	24	Excavated slope in gravelly clay

[1] site not ultimately selected for stabilization

The selected sites include three embankment slopes and two excavated slopes. Each of the slopes are large enough to represent typical slopes in the State of Missouri. The inclinations of the slopes vary from 2.2H:1V (horizontal:vertical) to 3.2H:1V with heights ranging from 15- to 46-ft (4.5- to 14-m). The soil types generally include lean and fat clays with two of the slopes having layered stratigraphies consisting of a relatively thin surficial layer of lean to fat clay overlying much stiffer fat clay or clay shale. Several of the slopes contain scattered gravel and cobbles and the I70-Emma site contains significant construction

debris and rubble fill placed in previous stabilization attempts. More detailed descriptions of each of the selected sites are provided in Chapters 6 through 9.

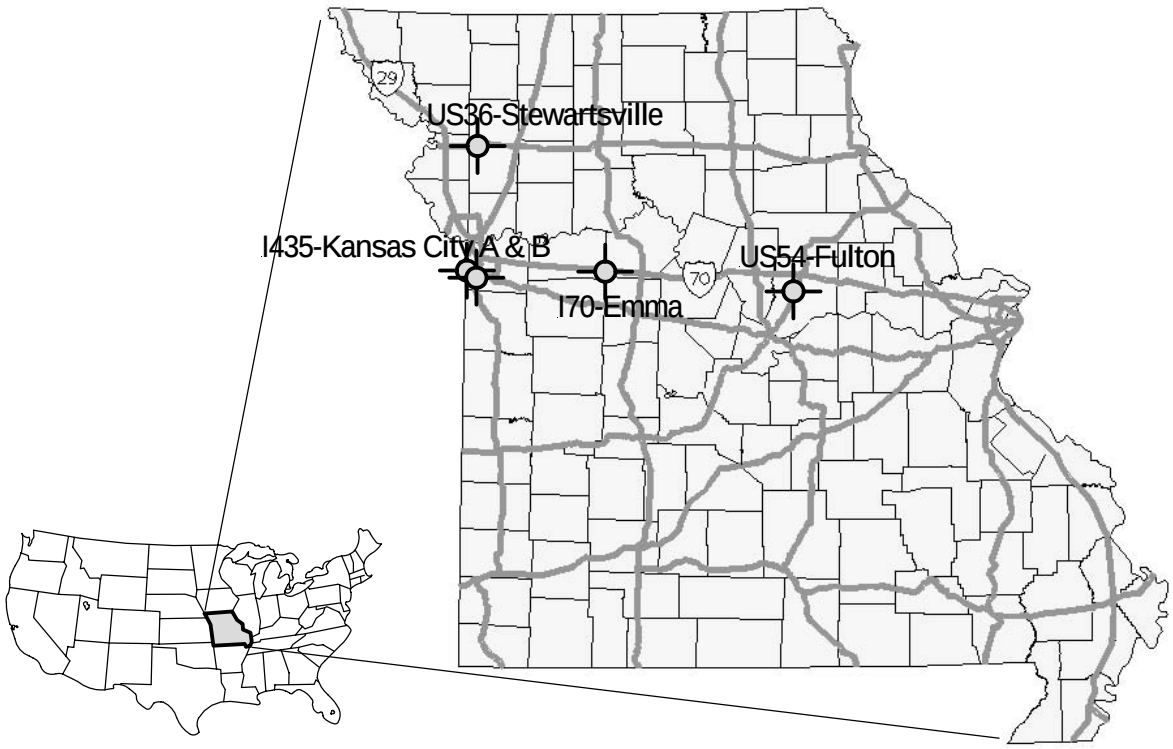

Figure 4.1 Map of the State of Missouri showing locations of the selected stabilization sites.

The reasons for not selecting the remaining sites in Table 4.2 varied. The MO13-Bolivar site was a very attractive site because the embankment contained significant gravel and the slope was very steep, both of which would provide a challenge for stabilization using recycled plastic members. However, the area to be stabilized was larger than could be accommodated within the project budget; additional funding from MoDOT District 8 was therefore needed to stabilize the entire slide area. The roadway was also scheduled for widening in the near future, which meant that the length of time available for monitoring would be limited. Because of these issues, MoDOT District 8 personnel decided to accelerate the construction schedule and simply flatten the slope during the roadway widening project.

The I44-Sarcoxie site was initially also very attractive because of the presence of significant gravel in the surficial soils sampled during the site visit. However, boring and sampling activities revealed that the slope was actually composed predominantly of high plasticity clay soils and, as such, was similar to other sites being considered. The failure also appeared to be relatively deep and the site is located a significant distance from the University of Missouri campus, which meant that field performance monitoring would be difficult. The site was therefore eliminated in favor of other sites. The US63-Columbia site was attractive because of its close proximity to the University, which would permit the site to

be frequently monitored. However, other sites seemed to have more significant advantages so the US63-Columbia site was not selected in the final evaluation.

Perhaps the two most significant limitations of the five selected sites is that none of the selected slopes contain significant gravel and none have slope angles greater than 2H:1V. Both of these characteristics would serve as a significant test of the installation method. However, very few slopes with these characteristics were identified during the site selection process, and none of the identified sites could be utilized for the project for varied reasons. However, it is important to note that the lack of a significant number of potential sites with such characteristics is an indication that (1) there are few slopes in Missouri with these characteristics or (2) that few surficial slides occur in slopes with these characteristics. This is not altogether unexpected due to the inherent strength of most gravelly soils and because MoDOT constructs very few permanent slopes steeper than 2:1.

4.3. Summary

In this chapter, the process used to select the five sites for stabilization was described. The selected slopes share characteristics with the majority of slopes that experience surficial slides in the State. As such, the effectiveness of the stabilization measures installed at the selected sites is expected to be representative of the effectiveness that can be achieved for most surficial slides within the State. The slopes share some similarities but also have distinct differences, which allows for direct evaluation of the effectiveness of alternative stabilization schemes, e.g., different reinforcement placements, while still evaluating the range of applicability.

Chapter 5. Field Instrumentation

Several different types of field instrumentation were used at the respective field test sites to monitor performance of the stabilized and control slide areas. In this chapter, the different types of instrumentation utilized at the field test sites are described along with methods used for calibration, analysis, and interpretation of the different types of instrumentation. Specific instrumentation installed and monitored at the respective field test sites is described in subsequent chapters.

5.1. Types of Instrumentation

Several different types of instrumentation were installed in the stabilized and control test areas to monitor field performance over time. Specifically, instrumentation was installed to monitor lateral deformation, pore water pressure, and moisture content within the slopes at selected locations; selected reinforcing members were also instrumented to monitor the loads developed in the members. Lateral displacements were monitored with conventional slope inclinometers. Pore water pressures were monitored with conventional standpipe piezometers screened at selected depths. In addition, moisture content or soil suction was monitored using three different types of devices: ThetaProbes®, Equitensiometers®, and Profile Probes®. Loads in the reinforcing members were monitored using electrical resistance strain gages and "force-sensing resistors" (FSR). Details of each type of instrument are provided in the following sections. In general, instrumentation used at all similar was similar, except where noted otherwise in subsequent chapters.

5.2. Measurement of Lateral Deformations

Lateral deformations were measured at each site using conventional slope inclinometers. Standard 2.5-in (6.4-cm) diameter inclinometer casing was generally installed in 4-in (10-cm) or 6-in (15-cm) diameter boreholes and backfilled with clean sand or pea gravel. Experience using inclinometer casings installed in 4-in (10-cm) diameter boreholes backfilled with clean sand during Phase I was less than satisfactory. As a result, all inclinometer casings installed at field test sites during Phase II of the project were placed in larger 6-inch (15-cm) diameter boreholes backfilled with clean pea gravel. Where possible, each casing was extended to approximately 5-ft (1.5-m) below the toe of the slope. In cases where very stiff soil was encountered at shallower depths, the casing was extended at least 3-ft (0.9-m) into the stiff soil to ensure adequate founding of the inclinometer casings. Following installation, lateral deformations were regularly measured using an inclinometer probe provided by MoDOT.

5.3. Measurement of Loads in Instrumented Reinforcing Members

Several members within the stabilized areas at each site were instrumented with strain gages and force-sensing resistors (FSR) to monitor the loads mobilized in the reinforcing members. Figure 5.1 shows a typical schematic of the instrumented recycled plastic reinforcing members installed in the stabilized slopes and a photograph of a 4-ft (1.2-m) long "test" member containing these sensors. Each instrumented member generally contained six pairs of strain gages placed on opposite (uphill and downhill) sides of the member. Strain gage pairs were placed at 1-ft (0.3-m) intervals over the top 4-ft (1.2-m) of each member and at 1.5-ft (0.45-m) intervals below this point. Five pairs of FSR were also placed on opposite

sides of the members halfway between each pair of strain gages. Several steel pipe members were also instrumented with a similar array of strain gages but without the FSR.

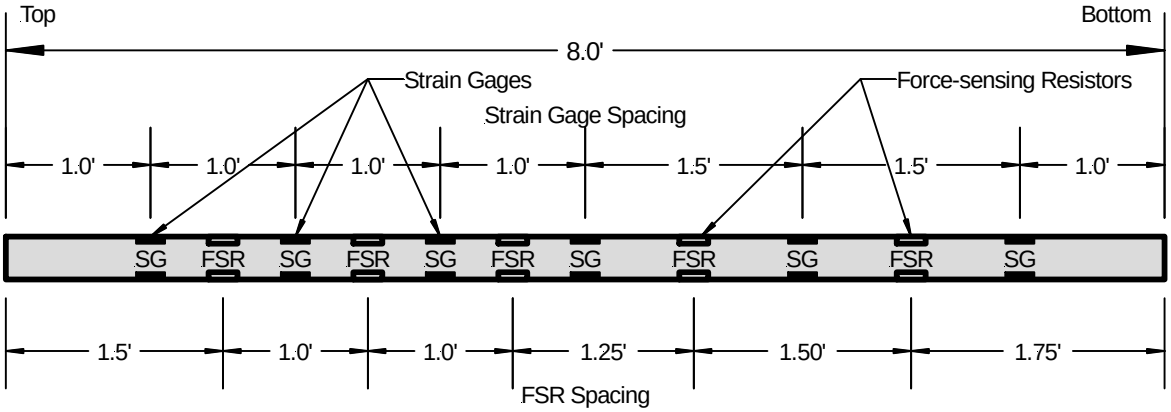

(a) schematic

(b) photograph

Figure 5.1 Instrumentation used to monitor loads in recycled plastic reinforcing members: (a) schematic of instrumented member and (b) photograph of an instrumented test member.

5.3.1. Strain gages

The strain gages used were the electrical resistance type similar to those frequently used to measure strains in concrete and steel members for structural applications. These gages have the advantage of being inexpensive and commercially available with strain ranges suitable for the project. The disadvantage of this type of gage is that they are not generally well-suited for long-term monitoring, particularly in a buried environment. Several alternative types of strain gages were also considered including vibrating-wire and fiber-optic strain gages. However, these gages are substantially more expensive than electrical resistance gages and were not available with strain ranges needed for the project. There was also significant concern regarding whether these gages could survive installation. The decision was therefore made to use relatively large numbers of electrical resistance type gages with the hope that a sufficient number of them would survive long enough to enable conclusions to be drawn regarding the loads in the members.

The strain gages used to instrument the recycled plastic members were generally 350-Ohm electrical resistance gages (Vishay Measurements Group part number EP-08-500BL-

350) with a working range of 15000 microstrains and a gage length of 0.5-in (1.3-cm) as shown in Figure 5.2. Several 120-Ohm gages (part number EP-08-500AF-120) with similar characteristics were also used for selected members. Gages were placed on the recycled plastic members in 0.125-in (0.3-cm) deep recesses machined into the members to prevent the gages from being ripped off during installation. Gages were attached using a special adhesive (M-bond Type AE resin with Type 15 curing agent) selected to be compatible with the plastic members. The adhesive requires curing at elevated temperatures while the gages are under a nominal normal load. The gages were therefore applied to one side of the member at a time and then placed in a controlled temperature box for curing as shown in Figure 5.3. Following curing, all gages were wired and the wires placed in machined grooves running along the neutral axis of the member. The gages were then sealed with Vishay Measurements Group 3145 RTV sealant (for insulation and waterproofing) and the recessed areas for the gages and wires filled with common silicon caulk to provide a secondary seal against moisture and to hold the wires in place.

Figure 5.2 Photographs of 350-Ohm electrical resistance strain gages used to monitor strains in the recycled plastic reinforcing members.

Figure 5.3 Photographs of temperature controlled box utilized for curing the adhesive used to attach strain gages to recycled plastic members.

The strain gages used for the steel members installed at several sites were 350-Ohm electrical resistance gages (part number CEA-06-250UN-350) with a strain range of 5000 microstrains and a gage length of 0.25-in (0.64-cm). The gages were attached using conventional adhesives that cure at room temperature. Since recessed areas for the strain gages could not be efficiently made, the gages were attached to the surface of the steel pipe and covered with 0.5-in (1.3-cm) angle sections as shown in Figure 5.4, which were tack welded to the pipe to protect the gages during installation.

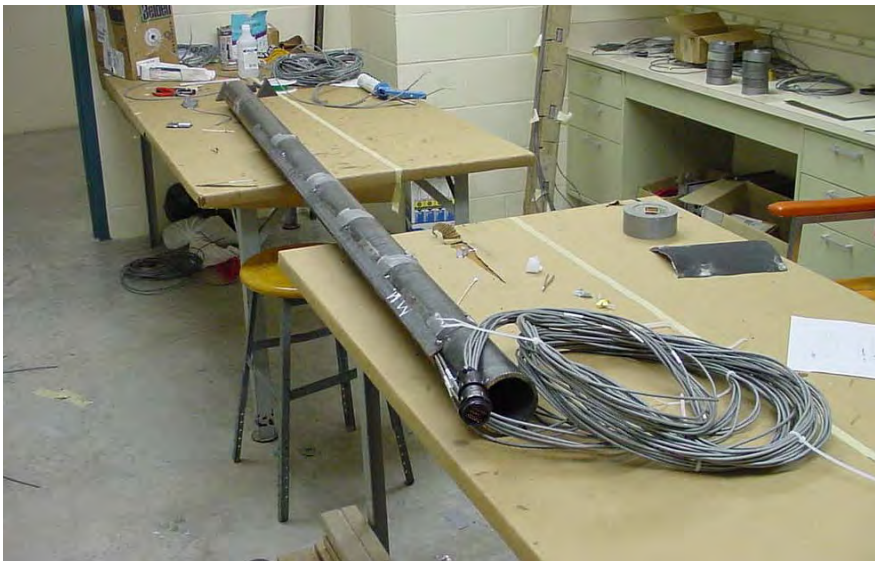

Figure 5.4 Photograph of instrumented steel pipe member with 0.5-in angle section to protect gages during installation.

5.3.2. Interpretation of strain gage readings

Readings from instrumented reinforcing members were processed and interpreted to establish the magnitudes of axial stresses and bending moments mobilized in the reinforcing members at each reading. However, it is important to note that reduction of the strain gage data requires that potentially significant assumptions be made in order to interpret the data. Two basic assumptions that were made include: (1) bending was assumed to be uniform when separating out axial strains from bending strains and (2) all strains were assumed to produce changes in stress (i.e. no creep or thermal strains). While these assumptions may be questioned, it is not clear that other assumptions could be made to reduce the data with the information currently available. Furthermore, there is no compelling evidence to suggest that these assumptions will have a noticeable impact on the interpretations made.

Of somewhat more importance in the current context, however, are assumptions made regarding which gages were providing accurate data and which gages were not. To address this issue, several different interpretations were developed for many of the instrumented reinforcing members (generally denoted as interpretation A, B, C, etc.) and significant effort was put into selecting the most appropriate of these interpretations that is both reasonable and consistent with observations from other instrumentation. The interpretations presented in subsequent chapters are the ones deemed to be the most appropriate among several different interpretations that can be made.

One particular issue that came to light during interpretation of data from instrumented reinforcing members is the issue of initial stresses and bending moments imposed during installation. Data obtained from members where readings were taken prior to and just after installation indicate that significant initial stresses and moments were often developed in the members due to the installation process. The existence of such stresses is not difficult to accept given the method of installation. However, the distribution of such stresses is in no way connected to the mechanisms by which load is transferred to the reinforcing members due to slope movements. It is therefore unreasonable to expect that the *overall* stresses and moments determined *including the initial stresses* should have distributions that are consistent with what one would expect from slope movements. However, it is reasonable to expect that the *incremental* stresses imposed *since installation* should have distributions that are consistent with those expected from slope movements. Because both the overall and incremental stresses are of importance in establishing the patterns of behavior in the slopes, two sets of interpretations were made: one set including any initial strains/stresses developed during installation and another that only includes the strains/stresses developed since installation was complete. In subsequent chapters, the term "overall" is used to refer to stresses and bending moments determined to include any stresses or moments developed during installation (i.e. with reference to the unstressed member prior to installation) while the term "incremental" is used to refer to stresses and bending moments developed since installation (i.e. with reference to the member stresses just after installation).

5.3.3. Force-sensing Resistors

In addition to the strain gages, each of the instrumented recycled plastic members was also fitted with several "force-sensing resistors", or FSR. These sensors are thin, 1.5-in by 1.5-in (3.8-cm by 3.8-cm) square electrical pads shown in Figure 5.5 that have a resistance that is proportional to the force applied to the sensor. These sensors are commonly used in touch pads for automated teller machines and other similar equipment. They are not intended for use as pressure sensors. However, they do have a resistance that is proportional to the applied pressure and thus can provide at least a qualitative measure of the lateral pressures being imposed on the reinforcing members. Experience gained from analyzing the strain gage data obtained from the I70-Emma site during Phase I (where FSR were not used) demonstrated the benefit that could be gained by having some measure of the distribution of lateral pressures, even if only a qualitative measure. Several different types of total stress cells were investigated for this purpose. However, all available cells were generally too large for use on the recycled plastic members and were generally believed to be cost prohibitive. Given that the FSR are inexpensive (approximately $5/each) it was decided to try these sensors in the hope that they could provide some information during analysis and interpretation of the strain gage data.

Since the sensors are intended to measure normal loads, it is not necessary to firmly bond the FSR to the member. FSR were therefore simply applied to the members using the adhesive backing that comes on the sensors from the manufacturer. The sensors were placed in 0.0625-in (0.16-cm) deep recesses, wired for connection to the data acquisition system, and then covered with a thin layer of common silicon caulk to provide a seal against water. Wiring for the sensors was placed in machined grooves and caulked into place in a manner similar to that for the strain gages.

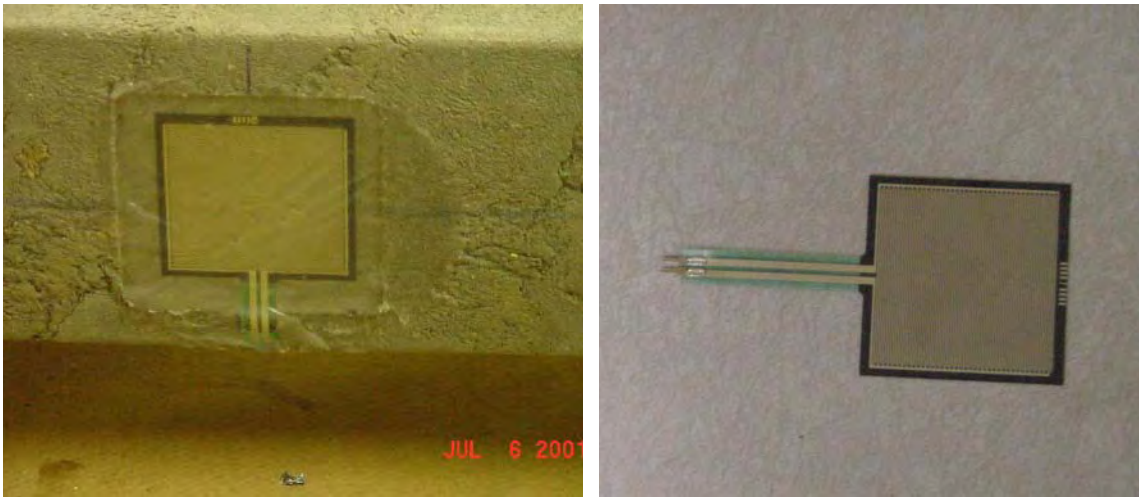

Figure 5.5 Photograph of force-sensing resistor used to measure applied pressure on instrumented recycled plastic members.

Except for strain gages used during Phase I, readings for the strain gages and FSR were acquired using the data acquisition system shown in Figure 5.6 that was specifically designed and built for this project. This system permits readings for all strain gages and FSR for a member to be taken in approximately one minute as compared to the 60 minutes required to manually read all sensors for a single member as was done in Phase I. The system therefore permitted more frequent readings to be taken and permitted readings from several sites to be taken in a single day.

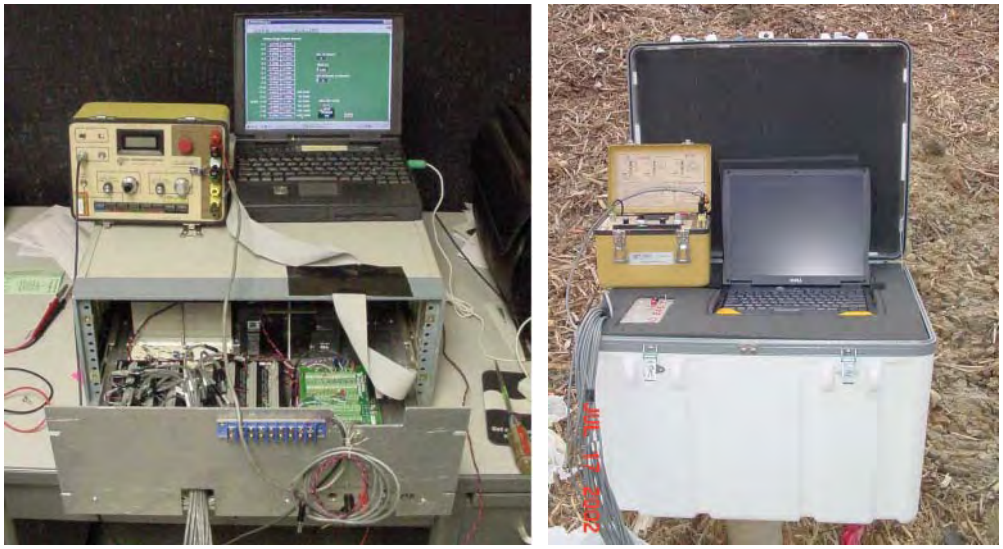

Figure 5.6 Data acquisition system developed, constructed, and used in this project to acquire readings from instrumented reinforcing members.

5.3.4. Interpretation of force-sensing resistor readings

The data acquisition system measures a voltage differential across each sensor. In the case of the strain gages, the voltages are directly proportional to the strain in the sensors and

thus can be directly converted to strain. In the case of the FSR however, it is necessary to determine resistance in each sensor prior to converting that resistance to an applied pressure. To do this, the data acquisition system was outfitted with a series of six fixed resistors with resistances of 100, 1000, 5000, 10000, 50000, and 100000 ohms, respectively. The voltage differential across each of these fixed resistors was then measured each time a set of readings was taken to establish the relation between measured voltage and known resistances for that set of readings. Measured voltages for each FSR were then converted to resistances using a non-linear least-squares fit of the voltage-resistance relation for that particular reading. Figure 5.7 shows the relation between voltage and resistance determined in this manner for one set of readings.

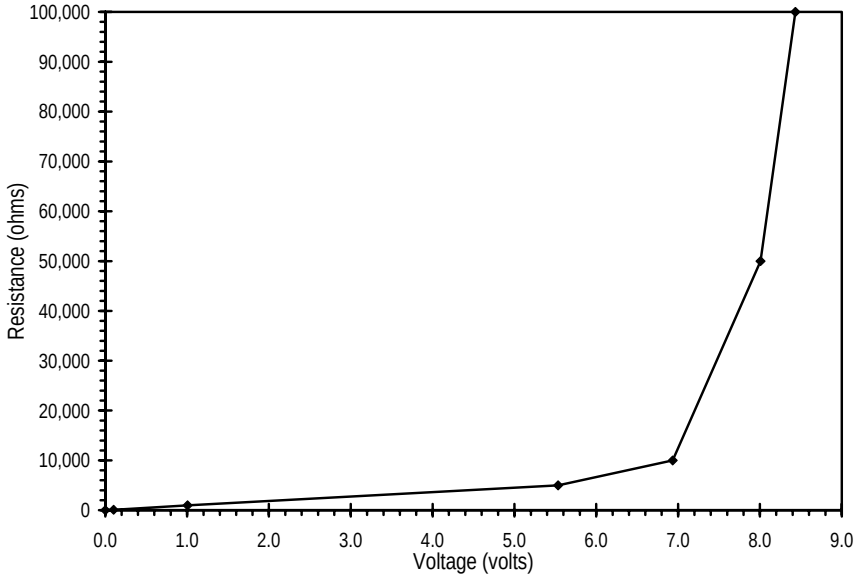

Figure 5.7 Sample of relation between measured voltage and resistance for fixed resistors in data acquisition system.

Once the resistance for each sensor is determined, the corresponding pressure is established based on the relation between resistance and applied pressure determined in several laboratory calibration tests. The calibration was established by loading several FSR in a laboratory loading apparatus over pressures ranging from 1150- to 14000-psf (55- to 670-kPa). The laboratory loading apparatus, shown in Figure 5.8, consisted of an FSR mounted on a piece of recycled plastic and covered with a thin layer of common silicon caulk to mimic the conditions used to mount the sensors on the reinforcing members. The FSR and plastic piece were then placed within a 4-in (10-cm) diameter PVC confining ring and covered with approximately 0.75-in (1.9-cm) of concrete sand. The entire assembly was then placed in a load frame and loaded incrementally. Resistance readings were determined for each load for several sets of tests including several load-unload cycles.

Figure 5.9 shows the results of the calibration tests along with the least-squares relation used to convert measured resistance to applied pressure. At relatively high pressures, very little scatter was observed in the data and the relation between applied pressure and resistance is very well defined. The amount of scatter increases with decreasing applied pressure, however, and at pressures less than 1000-psf (48-kPa) the scatter is so great that it become very difficult to establish the resistance-pressure relation. Based on these

results, a "detection limit" for the sensors was set at 100-ohms. Field resistance readings above this value are therefore considered to be above the detection limit, in which case a value for applied pressure can not be determined.

Figure 5.8 Apparatus used to develop calibration for FSR.

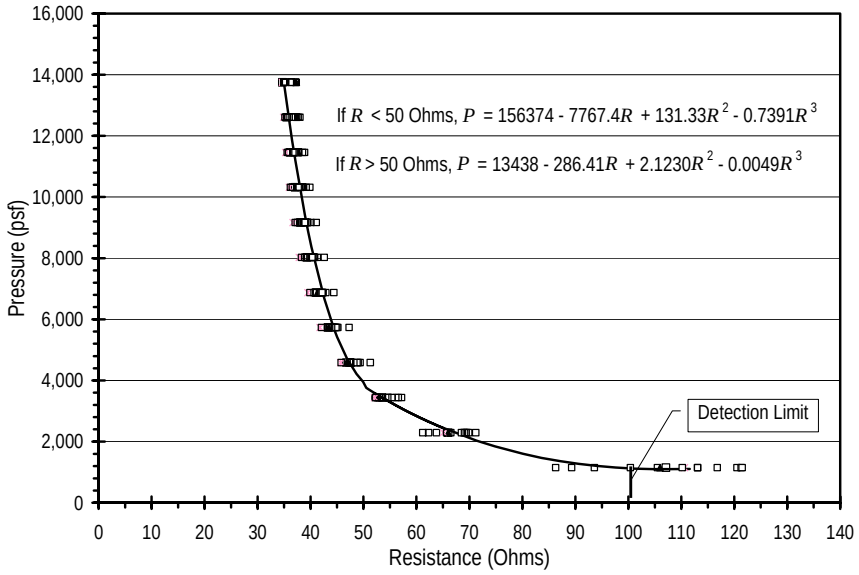

Figure 5.9 Calibration curve for FSR relating measured resistance to applied pressure.

5.4. Measurement of Pore Pressures, Moisture Content, and Soil Suction

Water conditions within each of the slopes were monitored using several types of instrumentation in an attempt to handle the range of possible conditions that might exist at the respective slide areas. Common standpipe piezometers were installed to monitor positive pore water pressures within each slope. Negative pore water pressure, or soil suction, was

monitored using several different types of sensors to directly measure soil suction, or to measure soil moisture content, which can be related to soil suction through a soil-water characteristic curve (SWCC).

5.4.1. Standpipe Piezometers

The standpipe piezometers used at the field sites were generally placed in clusters of two or three standpipes within a single borehole. Each standpipe was screened over different 1- to 2-ft (0.3- to 0.6-m) depth intervals with the intervals hydraulically isolated using bentonite plugs as shown in Figure 5.10. The standpipes were constructed at the MU Geotechnical Engineering laboratories using 0.75-in diameter PVC pipe that was slotted at the requisite locations and then covered with a non-woven geotextile. Standpipe piezometers were then installed at the sites by MoDOT drilling crews with assistance from MU researchers.

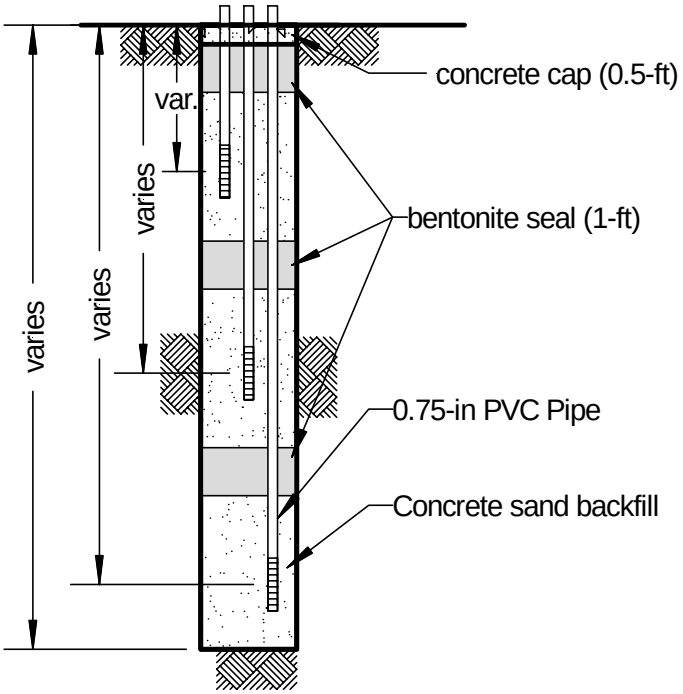

Figure 5.10 General schematic for standpipe piezometers installed at field test sites.

5.4.2. Other Moisture Sensors

In addition to standpipe piezometers, two types of sensors, known as ThetaProbes® and Equitensiometers®, were installed to continuously monitor the water conditions within the slope. The ThetaProbe®, shown in Figure 5.11, consists of four sharpened stainless steel rods that are connected to a waterproof housing which contains the sensor electronics. The probe measures volumetric soil moisture content by responding to changes in the soil's apparent dielectric constant and converting these changes into a DC voltage that can be correlated to volumetric moisture content. The probe responds to the changes in the dielectric constant by generating a 100 MHz sinusoidal signal that extends into the soil by means of the array of four stainless steel rods. A voltage standing wave is formed along an

internal transmission line of the probe from the reflection of the 100 MHz signal, which is affected by the impedance of the rod array. The impedance of the rod array fluctuates with the impedance of the soil, which is a function of the soil's dielectric constant and ionic conductivity. The 100 MHz signal minimizes the effects of ionic conductivity, so that the variation in the impedance is almost solely due to the soil's apparent dielectric constant. Dry soils typically have a dielectric constant between 3 and 5. The dielectric constant of water is approximately 81 and air is 1. Since the dielectric constant of dry soil is typically much less than water, the dielectric constant of soil is primarily determined by its water content. Published studies have shown that there is nearly a linear correlation between the square root of the dielectric constant and volumetric moisture content for most soil types. The volumetric moisture content is the ratio between the volume of water present and the total volume of the sample, expressed either as a percentage of volume (%vol) or a ratio ($m^3.m^{-3}$). Pure water has a ratio of 1.0-$m^3.m^{-3}$ and a completely dry soil would have a ratio of 0.0-$m^3.m^{-3}$. The output signal of the ThetaProbe® is 0- to 1-V DC for a range of soil dielectric constant between 1 and 32, which corresponds to a volumetric soil moisture content of approximately 0.5-$m^3.m^{-3}$. Installation of the ThetaProbe® is simple. The probe is inserted in the soil until the rods are completely covered. The probes are designed to be installed either at the ground surface or buried in a borehole or trench that is carefully backfilled.

Figure 5.11 Instrumentation used to monitor soil water conditions at the I435-Kansas City site and other sites: ThetaProbe® ML2x (bottom left), Equitensiometer® EQ2 (bottom right), THLog® data logger (top center), Profile Probe® PR1/6 and access tube (center), and HH2 readout unit (lower center).

The Equitensiometer® probe, shown in Figure 5.11, is essentially a ThetaProbe® in which the four measuring rods are embedded in a porous material that serves as an equilibrium body. Equitensiometers® measure soil matric potential, which can be thought of as the negative pressure or soil suction required to extract water from between the soil particles. The porous material surrounding the four rods has a known stable relationship between water content and matric potential (i.e. a known SWCC). When the probe is

inserted into the soil, the matric potential of the porous material quickly equilibrates to that of the surrounding soil and the water content of the equilibrium body is measured by the rods of the ThetaProbe®. The measurement recorded by the ThetaProbe® can then be converted into the matric potential of the surrounding soil using calibration curves supplied by the manufacturer for each probe. Installation of the Equitensiometers® requires more care than the ThetaProbe®. The porous material of the Equitensiometer® needs to be thoroughly saturated before the probe is installed and the probe must be installed in a horizontal or slanting angle. Vertical installation of the probe could lead to non-representative readings due to water running down the side of the probe and excessively wetting the surrounding soil. Small changes to the soil structure surrounding the probes should not affect the accuracy of the readings, however, the probes must be in firm contact with the surrounding soil or any gaps filled with a quartz powder suspension to allow the porous material of the probe to properly equilibrate with the surrounding soil. The probes are designed to withstand prolonged installation periods with little maintenance if installed correctly.

ThetaProbes® and Equitensiometers® were installed in a vertical cluster, composed of two ThetaProbes® and two Equitensiometers®, near the center of each slide area as illustrated in Figure 5.12. The sensors were installed in the vertical up-slope face of a 3.3-ft (1-m) deep trench in alternating succession at depths of approximately 8-in (20-cm), 16-in (40-cm), 24-in (60-cm), and 40-in (100-cm). To install each sensor, a 2.5-in (6.4-cm) sampling tube was inserted horizontally approximately 6 inches (15-cm) into the vertical face of the trench to create a hole for the probes as shown in Figure 5.13. ThetaProbes® were pushed into the end of the hole until the rods were fully inserted into the soil, after which the space surrounding the probe was filled with onsite soil. The Equitensiometers® were first submerged in water for a minimum of 24 hours prior to installation in the slope. Equitensiometers® were then placed in the center of the installation hole and the hole was filled with a quartz powder suspension to ensure intimate contact of the probe and the surrounding soil. After all four sensors were installed, the sensors were connected to a THLog® data logger, which supplies power to the sensors and records measurements from the sensors at two hour intervals.

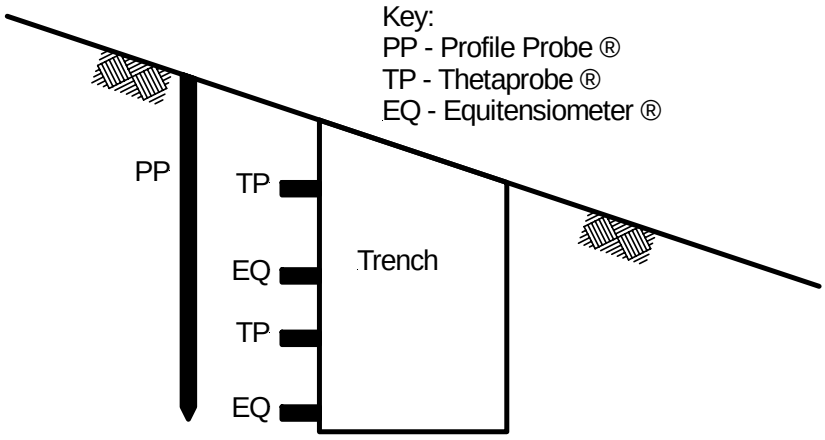

Figure 5.12 Schematic of ThetaProbe® and Equitensiometer® installation.

The final type of moisture instrumentation used is the Profile Probe® shown in Figure 5.11. The Profile Probe® works following the same philosophy as the ThetaProbe®, except that the source and receiver are rings on a slender probe, rather than spikes that are inserted

into the soil. The Profile Probe® PR1/6 contains six sensor sets (source and receiver) to measure moisture content at depths of 4-, 8-, 12-, 16-, 24-, and 40-in (10-, 20-, 30-, 40-, 60-, and 100-cm) simultaneously. Measurements are taken by inserting the Profile Probe® into special composite "access tubes" that are installed in small, pre-drilled holes at the site. The pre-drilled holes are slightly smaller than the access tubes themselves to ensure intimate contact between the tubes and the surrounding soil. Once the access tubes are installed, measurements are taken by simply inserting a Profile Probe® into the access tube and using the HH2 readout unit to store readings for all sensor sets simultaneously as shown in Figure 5.14.

Figure 5.13 Photograph of installation of ThetaProbes® and Equitensiometers® in trench.

5.4.3. Utilization of Pore Pressure/Moisture Sensors

Multiple types of pore pressure and soil moisture sensors were used at each site to account for the potential to have both positive and negative pore water pressures as well as to capture both the spatial and temporal variation of pore pressures. In general, standpipe piezometers were generally installed near the center section of each test area. Readings from these piezometers were taken manually using a simple water level indicator that was inserted into each standpipe during regular field visits. These readings were supplemented with readings from the cluster of ThetaProbes® and Equitensiometers® that were continuously logged to provide information on the temporal variation of moisture conditions. Finally, ProfileProbe® access tubes were generally installed in a distributed pattern across the entire slide area to garner information on the spatial variability of soil moisture conditions during field visits to the respective sites.

Figure 5.14 Photograph of Profile Probe® while taking readings.

5.5. Usefulness of Field Instrumentation

As described in subsequent chapters, the instrumentation used at the respective field test sites was successfully used to develop both a qualitative and quantitative understanding of the performance at the respective sites. However, some types of instrumentation proved to be more useful than others.

Both the slope inclinometers and standpipe piezometers performed exceptionally well and served a critical role in evaluating performance and refining the design method. The strain gages used on instrumented reinforcing members also provide to be quite useful. A limited number of strain gages did not produce reliable measurements following installation, either due to damage during installation or other effects that rendered them ineffective. Fortunately, the instrumentation schemes were generally redundant enough to provide reliable results, although inoperable gages do complicate data reduction and interpretation. With time, additional gages inevitably became inoperable, which in turn required more interpretation, until at some point the amount of reliable data is limited to the point where little meaningful information can be gleaned. In most cases, the time over which meaningful strain gage data was collected for the respective sites was at least two years, or longer in some cases. This period was generally sufficient to permit reasonable interpretation of the behavior of the test sites.

The force-sensing resistors (FSR) intended to provide indications of lateral loads on the reinforcing members did not perform as well. Readings taken for periods of several years generally remained below the detection limit of the sensors so little useful information was gleaned from these gages.

The soil moisture sensors used at the test sites also turned out to provide limited benefits. Data obtained from the clusters of ThetaProbes® and Equitensiometers® did prove useful for establishing trends in soil suctions or soil moisture within the slopes with time. However, as monitoring continued, it became apparent that slope movements were generally occurring at times when pore pressures within the slopes were positive rather than negative.

As such, data from the standpipe piezometers was utilized more extensively in evaluating performance and revising the design method, although the ThetaProbe and Equitensiometer data was collected and reviewed to evaluate suctions between readings of the standpipe piezometers. The ProfileProbe® access tubes and probe, which were intended to provide information on the spatial variability of pore pressures, proved to be even less useful for the project. This result is partially due to the fact that pore pressures at key points in time were generally positive. However, ProfileProbe® measurements also proved to be extremely erratic from one set of readings to the next and were not deemed reliable. Furthermore, a large number of the access tubes became buried over time and could not be located so it was not always possible to consistently acquire data for these devices.

5.6. Summary

In this chapter, the different types of instrumentation utilized at the field test sites has been described. Instrumentation included classical slope inclinometers to monitor lateral deformations; strain gages and force-sensing resistors on select reinforcing members to monitor loads in the members; and standpipe piezometers, ThetaProbes®, Equitensiometers®, and ProfileProbes® to monitor pore pressures within the respective test slopes. Of these, the inclinometers, standpipe piezometers, and strain gages proved to be the most useful for aiding the interpretation of performance and revision of the design method. The remaining information was useful, but of more indirect value.

Chapter 6. I70-Emma Site

The first test site established for the project is the I70-Emma site. During Phase I of the project, two slide areas at this site were stabilized to demonstrate the feasibility of the technique. Two additional slide areas were simply regraded to the original slope geometry to serve as control sections for the stabilized areas. Both control sections subsequently experienced failures while the stabilized areas have not failed. One of these control areas was subsequently selected for stabilization during Phase II to provide for evaluation of the potential to use more widely spaced reinforcement configurations to stabilize surficial slides. In this chapter, the activities undertaken to establish the three test areas at the I70-Emma site are described along with field performance data acquired from instrumentation installed at the test site.

6.1. Site Characteristics

The I70-Emma site is located on Interstate 70 approximately 65 miles (105-km) west of Columbia Missouri and approximately 1 mile north of the city of Emma Missouri. Figure 6.1 shows an air photo of the area indicating the location of the site. The slope is an embankment that forms the eastbound entrance ramp to Interstate 70. The embankment is approximately 22-ft (6.7-m) high with side slopes varying from 2.5H:1V to 2.2H:1V and is composed of mixed lean and fat clays with scattered gravel, cobbles, and construction rubble (concrete and asphalt). Prior to being selected for stabilization as part of this project, the embankment had experienced recurring slides in four areas of the embankment over a decade or more. Figure 6.2 shows a plan view of the site indicating locations of the four slide areas denoted S1, S2, S3, and S4. Figure 6.3 shows a photograph of the south side of the embankment following the failures that occurred prior to stabilization during Phase I. Previous stabilization attempts consisting of regrading the slope, dumping concrete rubble over the crest of the embankment, and replacing soils near the toe with construction rubble were unsuccessful.

Figure 6.1 Air photo of Interstate 70 near Emma Missouri taken March 8, 1997 showing location of I70-Emma site (from USGS).

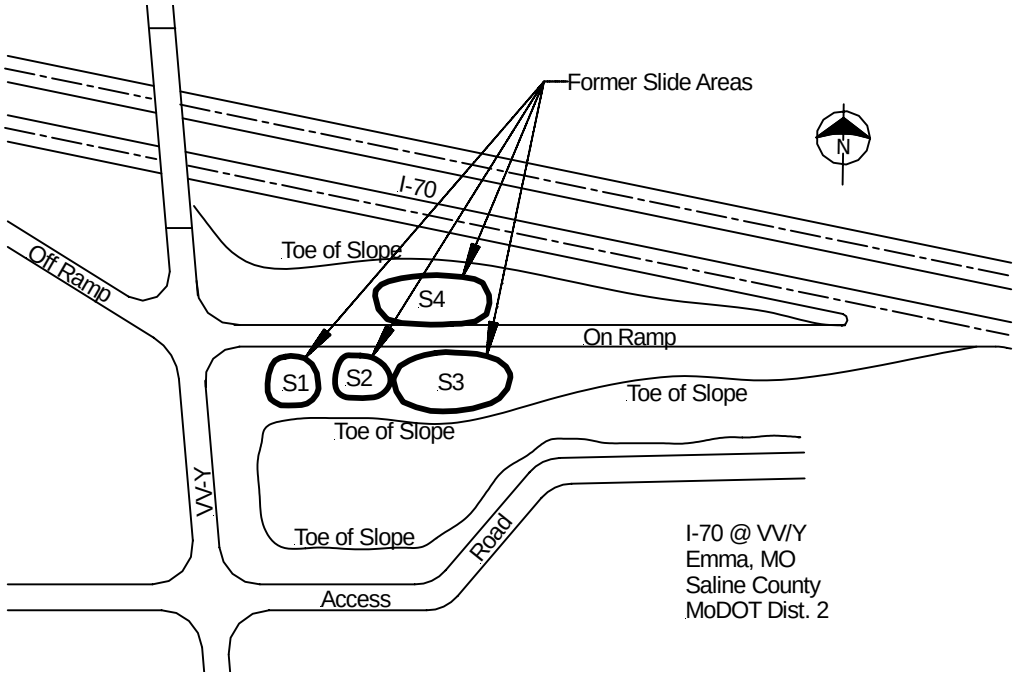

Figure 6.2 Plan view of I70-Emma site showing slide areas S1, S2, S3, and S4.

Figure 6.3 Photograph of south side of embankment at I70-Emma site showing slide areas S1 (left), S2 (center), and S3 (right).

Boring and sampling activities at the I70-Emma site were performed on June 1-3, 1999 prior to stabilization during Phase I. A total of 11 borings were made across the site to depths ranging from 10- to 33-ft (3- to 10-m). A plan view of the site showing boring

locations and boring logs are provided in Appendix A. In each boring, continuous 3-in (7.6-cm) diameter Shelby tube samples were taken, extruded in the field for identification and field testing, and then wrapped in aluminum foil and waxed for transport to the University of Missouri Geotechnical Engineering Laboratories for subsequent laboratory testing. The borings indicate the slope is composed of a mixture of lean to fat clays of variable consistency with scattered fine gravel and cobbles that are presumed to be construction rubble remaining from previous stabilization attempts. Several of the borings made near slide areas S1 and S2 indicated groundwater was present below the elevation of the toe of the slope; all other borings were dry throughout the site investigation. Standard Penetration tests performed near the base of the embankment produced SPT N_{60}-values between 3 and 8. Two other SPT tests performed below the base of the embankment produced N_{60} in excess of 40.

Moisture contents determined from samples taken in the field indicate that field moisture contents were essentially constant with depth throughout the embankment. Measured moisture contents ranged from 14 to 34 percent but the vast majority of values were between 20 and 25 percent. Atterberg limits determined for samples from the site indicate the soils have liquid limits (LL) from 39 to 60, plastic limits (PL) from 19 to 27, and plasticity indices (PI) from 10 to 41. The soils generally classified as either CL or CH in the USCS, although one sample classified as ML. No clear trends were observed in the Atterberg limits for soils from the site which indicates the embankment is composed of an essentially random mixture of soils.

Mohr-Coulomb effective stress shear strength parameters for the Emma site soils were determined from both triaxial compression and direct shear tests. All but two of these tests were performed during Phase II of the project. Figure 6.4 shows the stress paths determined from consolidated-undrained ($\overline{CU}$, $\overline{R}$) and consolidated-drained (CD,S) type triaxial compression tests along with upper bound and lower bound failure envelopes established from the test results for the surficial soils and soils at greater depths. A summary of the drained effective stress strength parameters for the surficial and deeper soils is given in Table 6.1. These tests indicate that the effective stress cohesion intercept, $\bar{c}$, for the surficial soils is equal to approximately 100-psf (4.8-kPa) and the effective stress friction angle, $\bar{\phi}$, is equal to 23 degrees while for the deeper soils $\bar{c}$ ranges from 170- to 365-psf (8.1- to 17.5-kPa) and $\bar{\phi}$ is approximately 25 degrees.

Table 6.1 Summary of Mohr-Coulomb effective stress strength parameters from direct shear and triaxial compression tests on specimens from the I70-Emma test site.

			upper bound		lower bound		direct shear	
Stratum	Depths	Sample Numbers	$\bar{c}$ (psf)	$\bar{\phi}$ (°)	$\bar{c}$ (psf)	$\bar{\phi}$ (°)	$\bar{c}$ (psf)	$\bar{\phi}$ (°)
Surficial clay	< 4.0-ft	274 313	96	23	--	--	202	14
Deeper clay	> 4.0-ft	277, 278 286, 287 284, 289	364	25	170	25	101	14

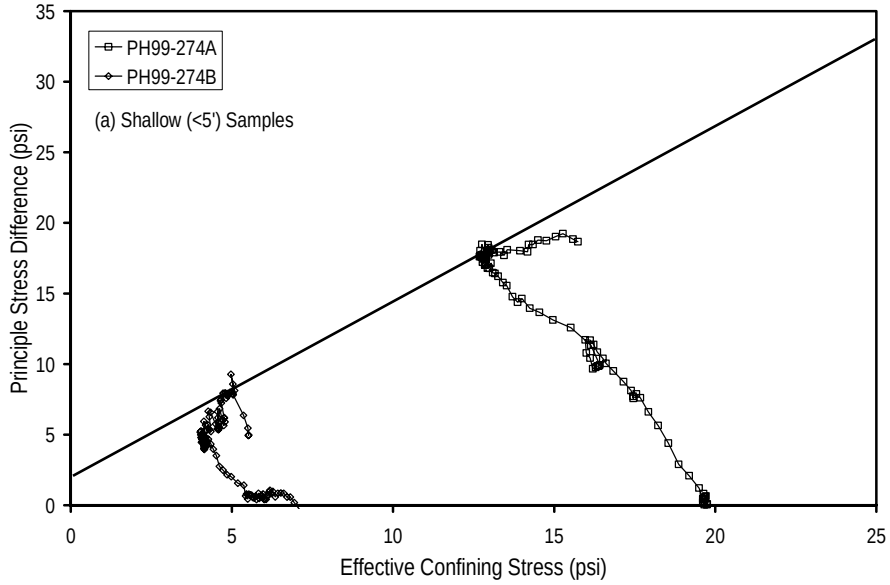

(a)

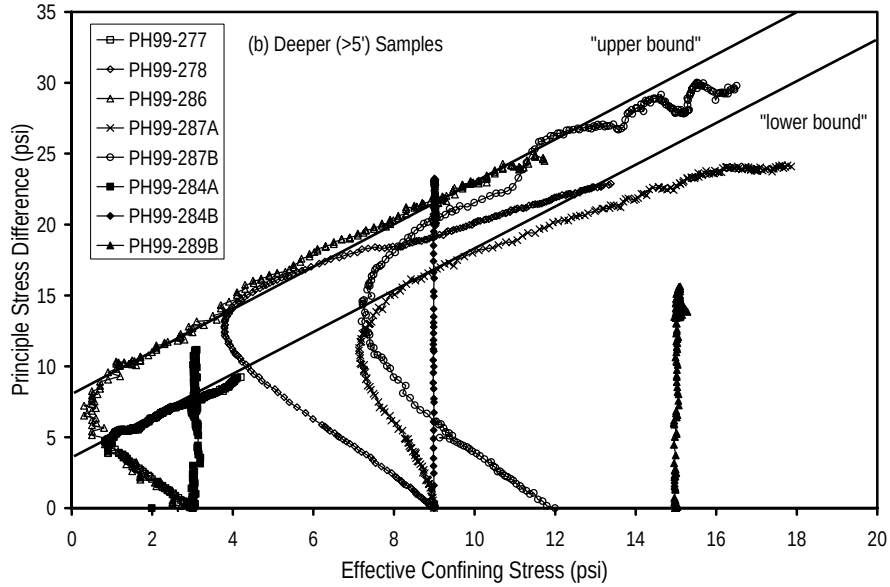

(b)

Figure 6.4 Summary of triaxial test results for specimens from the I70-Emma site: (a) shallow samples and (b) deeper samples.

Figure 6.5 shows the results of the drained direct shear tests on two samples from the I70-Emma site with peak shear strength failure envelopes determined for each sample. Mohr-Coulomb effective stress strength parameters for these envelopes are shown in Table 6.1. These values indicate that the both samples had $\bar{\phi}$ of 14 degrees, a value that is significantly lower than $\bar{\phi}$ obtained from the triaxial test results. Values of $\bar{c}$ ranged from 100- to 200-psf (4.8- to 9.6-kPa).

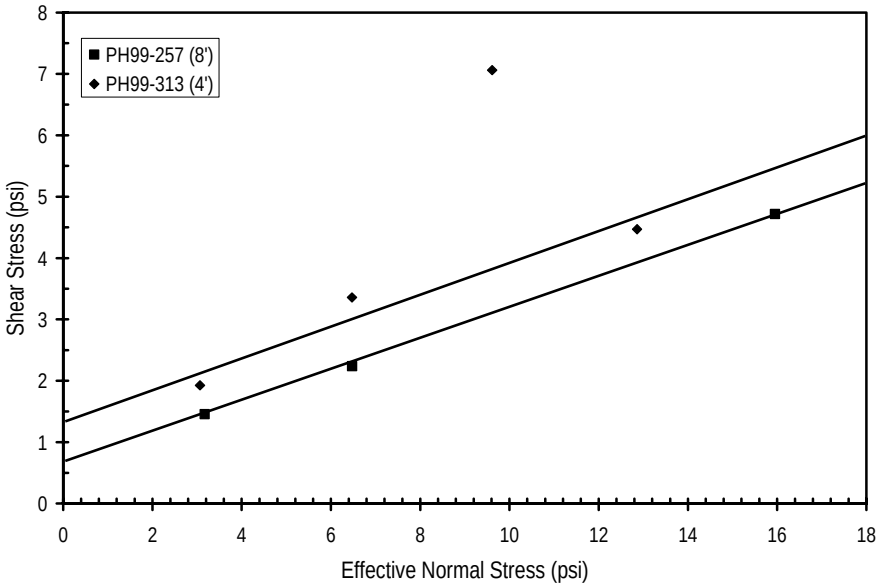

Figure 6.5 Summary of direct shear test results for specimens from the I70-Emma site.

6.2. Selection of Stabilization Schemes

The stabilization schemes utilized at the I70-Emma site in both Phase I and Phase II were established based on a limited number of stability analyses. The following sections described the stability analyses performed and the stabilization schemes selected for slide areas S1 and S2 during Phase I and slide area S3 during Phase II, respectively.

6.2.1. Stabilization Schemes for Slide Areas S1 and S2

The schemes utilized to stabilize slide areas S1 and S2 during Phase I of the project were determined from preliminary analyses performed using back-calculated strength parameters. In these analyses, the slope was assumed to be essentially homogenous and the soil was assumed to have negligible cohesion intercept (i.e. $\bar{c} = 0$) under fully drained conditions. Pore water pressures within the slope were assumed to be negligible. Based on these assumptions, the back-calculated value of $\bar{\phi}$ was determined to be approximately 22 degrees. These conditions were then used to evaluate factors of safety for various reinforcement configurations composed of members placed in a uniform grid across the entire slide area. Factors of safety determined from these analyses ranged from 1.05 for a 6-ft longitudinal by 6-ft transverse (1.8-m by 1.8-m) grid of reinforcement to 1.43 for reinforcement placed on a 1-ft by 1-ft (0.3-m by 0.3-m) grid (Liew, 2000).

The reinforcement configurations selected for stabilization of slide areas S1 and S2 are shown in Figure 6.6. Both selected schemes included members placed on a 3-ft by 3-ft (0.9-m by 0.9-m) staggered grid. However, members for slide area S1 were inclined perpendicular to the face of the slope, while members for slide S2 were inclined vertically. The factor of safety for both of these reinforcement schemes was estimated to be approximately 1.2 based on calculations performed using the back-calculated soil conditions.

Calculations performed subsequent to the installation considering the potential for a perched water condition produced a similar factor of safety.

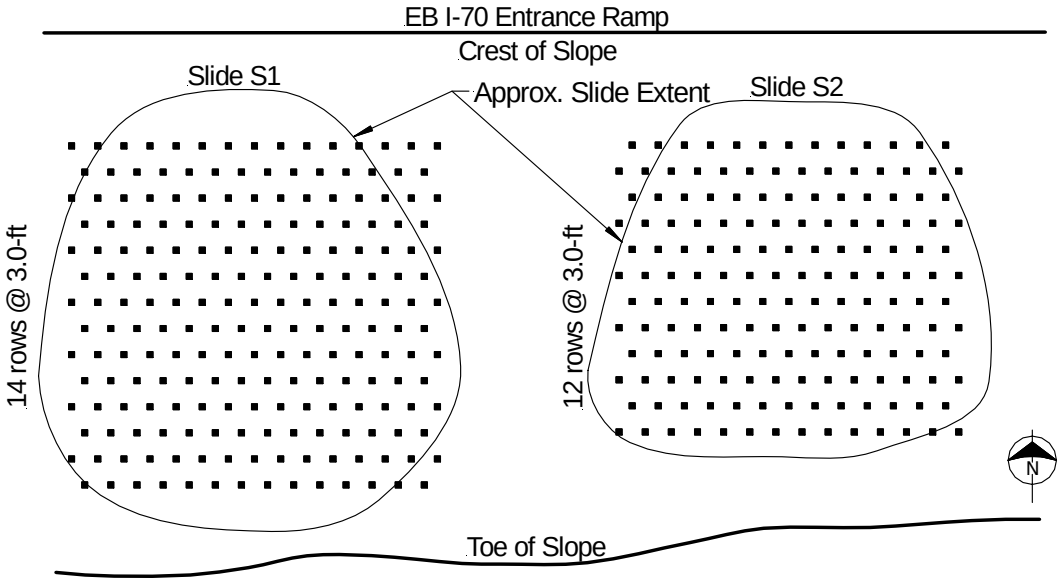

Figure 6.6 Plan view of slide areas S1 and S2 at the I70-Emma site showing selected layout of reinforcing members.

6.2.2. Stabilization Scheme for Slide Area S3

As described subsequently in more detail, the stabilization schemes used for slide areas S1 and S2 proved to effectively stabilize the respective slide areas while the control sections established both failed. Additional stabilization was subsequently undertaken for slide area S3 during Phase II of the project to evaluate the potential for stabilization using more widely spaced reinforcement patterns. Figure 6.7 shows the final selected configurations. The slide area was separated into four sections, denoted Sections A through D, with different reinforcement schemes utilized in each section. In Section A, members were placed on a 4.5-ft by 3.0-ft (1.4-m by 0.9-m) longitudinal (strike direction) by transverse (dip direction) staggered grid. A 4.5-ft by 6.0-ft (1.4-m by 1.8-m) grid was used in Section B, a 6.0-ft by 6.0-ft (1.8-m by 1.8-m) grid was used in Section C, and a 6.0-ft by 4.5-ft (1.8-m by 1.4-m) grid was used in Section D. Slide area S4 was also again regraded to its original slope to serve as a control section during Phase II.

Factors of safety for each of the reinforcement schemes were calculated for two different possible sets of slope conditions as summarized in Table 6.2. The first set of conditions, referred to as stability condition A, was the conditions determined from back-analyses described above. The second set of conditions, stability condition B, considered the two layer profile shown in Figure 6.8 with a perched water condition within the upper layer. For these analyses, the upper layer was assumed to have $\bar{c}$=95-psf (4.5-kPa) and $\bar{\phi}$=15 degrees while the lower layer had $\bar{c}$=310-psf (14.8-kPa) and $\bar{\phi}$=22 degrees and the piezometric line for the upper layer was assumed to be at the ground surface. The factor of safety for both conditions without reinforcement is 1.0. As shown in Table 6.2, factors of

safety calculated for Section A range from 1.10 to 1.16, Section B from 1.03 to 1.10, Section C from 1.01 to 1.06, and Section D from 1.02 to 1.08.

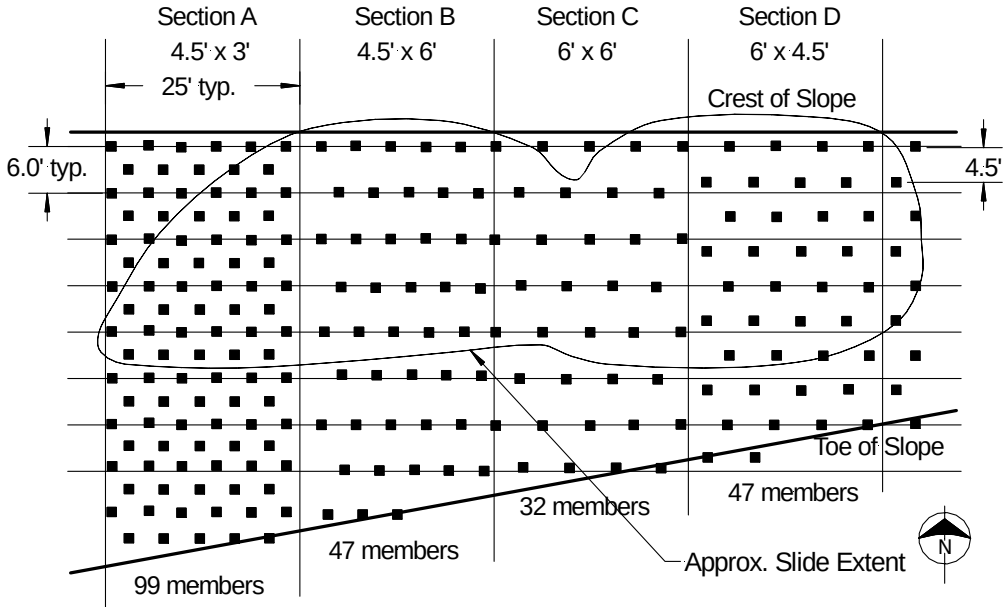

Figure 6.7 Plan view of selected stabilization schemes for slide area S3 at the I70-Emma test site.

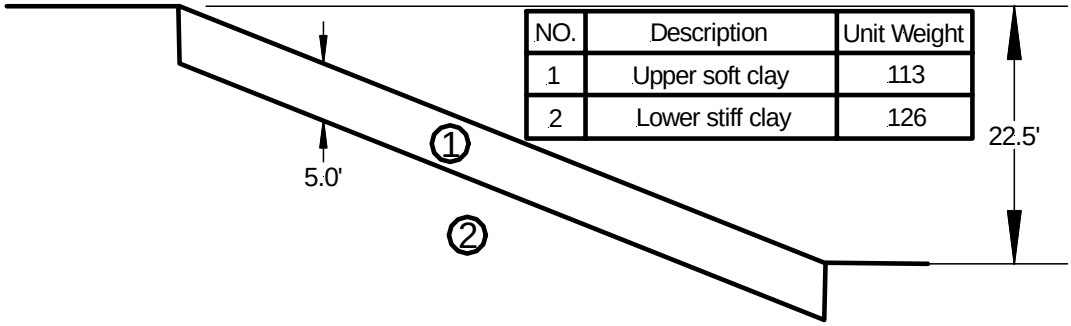

Figure 6.8 Cross-section assumed for stability condition B at the I70-Emma test site.

Table 6.2 Estimated factors of safety for Sections A through D in slide area S3 and slide areas S1 and S2 at the I70-Emma test site

Rein. Spacing (ft)	Slope Section	Factor of Safety for Respective Stability Condition	
		A	B
3.0L x 3.0T [1]	S1, S2	1.20	1.21
4.5L x 3.0T	A	1.16	1.10
4.5L x 6.0T	B	1.10	1.03
6.0L x 4.5T	D	1.08	1.02
6.0L x 6.0T	C	1.06	1.01

[1] L and T denote spacing in longitudinal (strike) and transverse (dip) directions, respectively

6.3. Field Installation

Field installation activities at the I70-Emma site were performed at two different times. Slide areas S1 and S2 were stabilized in October and November 1999 during Phase I of the project. Slide areas S3 and S4 were regraded at the same time to serve as control sections. Both control sections S3 and S4 subsequently failed. Slide area S3 was subsequently stabilized in January 2003 during Phase II. Field installation activities during these two periods are described in more detail in Chapter 10.

6.4. Instrumentation

Several types of instrumentation were installed at the I70-Emma test site during both Phases I and II. The following sections describe the instrumentation installed during each phase of the project.

6.4.1. Instrumentation Installed During Phase I

The instrumentation utilized in slide areas S1 and S2 during Phase I differed somewhat from that used at subsequent test sites. Instrumentation installed during Phase I included instrumented reinforcing members to monitor loads in the reinforcing members, slope inclinometers to monitor lateral deformations in the slope, continuously screened wells to monitor possible positive pore water pressures, and "jet-filled" tensiometers to monitor possible soil suction. Figure 6.9 shows the locations of the various types of instrumentation utilized.

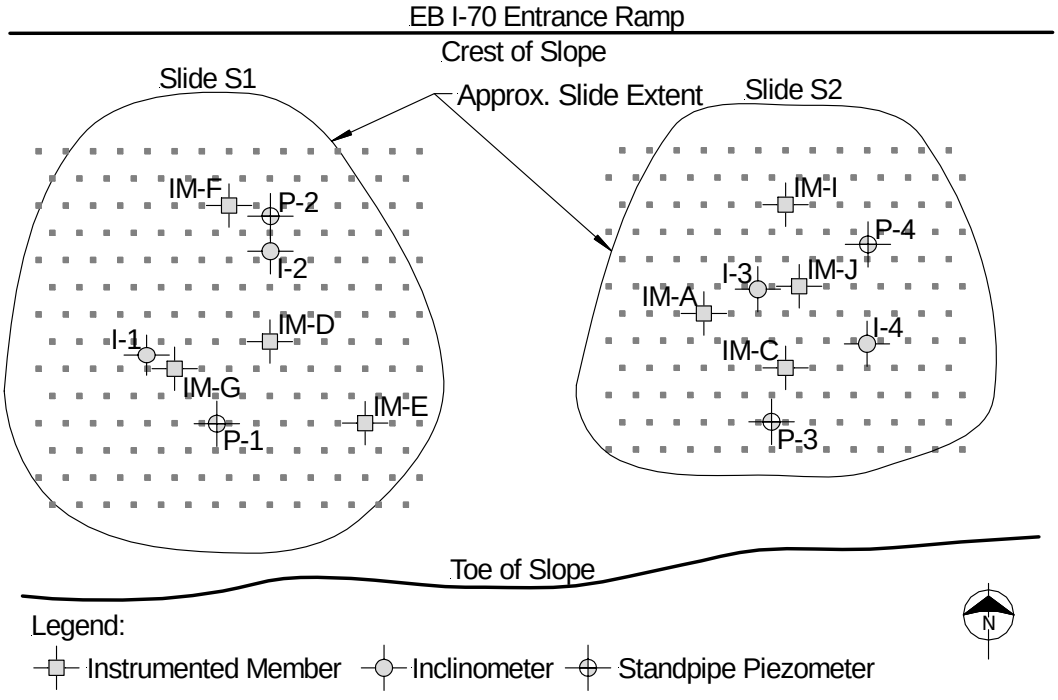

Figure 6.9 Plan view of slide areas S1 and S2 showing locations of instrumentation installed during Phase I at the I70-Emma site.

Ten of the recycled plastic members installed during Phase I were instrumented with 120-ohm electrical resistance strain gages (Vishay Measurements Group part number EP-08-500AF-120). The instrumented reinforcing members were similar to those used at subsequent test sites (Figure 5.1), except that the force-sensing resistors (FSR) were not used and four pairs of "shear gages" were installed on the sides of the members. The instrumented members installed during Phase I also differed from those installed in Phase II in that they were not outfitted with the connections needed to take readings using the data acquisition system subsequently developed in Phase II. Rather, each individual gage was measured by manually connecting bare-ended wires to a Vishay Measurements Group P-3500 "manual" readout unit, which displayed the strain reading for subsequent recording in a log book. As shown in Figure 6.9, four instrumented members, denoted members IM-D, IM-E, IM-F, and IM-G, were installed in slide area S1. Instrumented members IM-A, IM-C, IM-I, and IM-J were similarly installed in slide area S2. Two additional instrumented members, IM-B and IM-H, were installed within slide area S3 (the control slide during Phase I) to monitor the "free-field" behavior of the reinforcing members.

Five slope inclinometers were also installed at the site to monitor deformations in the stabilized areas (S1 and S2) and control section S3. Inclinometer casings installed during Phase I were placed in 4-in (10-cm) diameter boreholes extending approximately 5-ft (1.5-m) below the toe of the slope and backfilled with concrete sand. Two casings were placed in each of the stabilized areas as shown in Figure 6.9. One casing was installed near the center of slide area S3 to monitor the control slide.

Five continuously screened "wells" were also installed at the site to depths extending approximately 5-ft (1.5-m) below the toe of the slope. Two wells were placed in each of the stabilized areas along a line roughly through the center of the areas; one additional well was installed near the center of slide area S3. The wells were complemented with several jet-filled tensiometers installed to depths of up to 4-ft (1.2-m) in close proximity to the wells. No other moisture sensors were installed at the site during Phase I.

6.4.2. Instrumentation Installed During Phase II

Following installation of reinforcing members in slide area S3 during Phase II, additional instrumentation was installed at the site to monitor the performance of the newly stabilized area. Instrumentation installed at this time was generally similar to that installed at the other test sites during Phase II, which included improvements to overcome some of the limitations of the instrumentation installed during Phase I. Figure 6.10 shows a plan view of slide area S3 indicating approximate locations of the instrumentation installed in slide area S3 during Phase II.

Six instrumented reinforcing members, similar to those described in Chapter 5 (Figure 5.1), were installed in slide area S3 during installation of all reinforcing members. All instrumented members were generally installed along a horizontal line passing just above the mid-point of the slope. Instrumented members IM-19 and IM-22 were installed in Section A and Section D, respectively, while two instrumented members were installed in Sections B (IM-17 and IM-24) and C (IM-18 and IM-23) to provide some redundancy in the sections that are most likely to fail.

Slope inclinometer casings were installed in each of the four reinforcement sections on January 27-28, 2003 in close proximity to the instrumented reinforcing members. The

inclinometer casings were installed in 6-in (15-cm) diameter boreholes and backfilled with concrete sand. All casings were extended 19-ft (5.8-m) below grade to provide for adequate anchorage in stable strata.

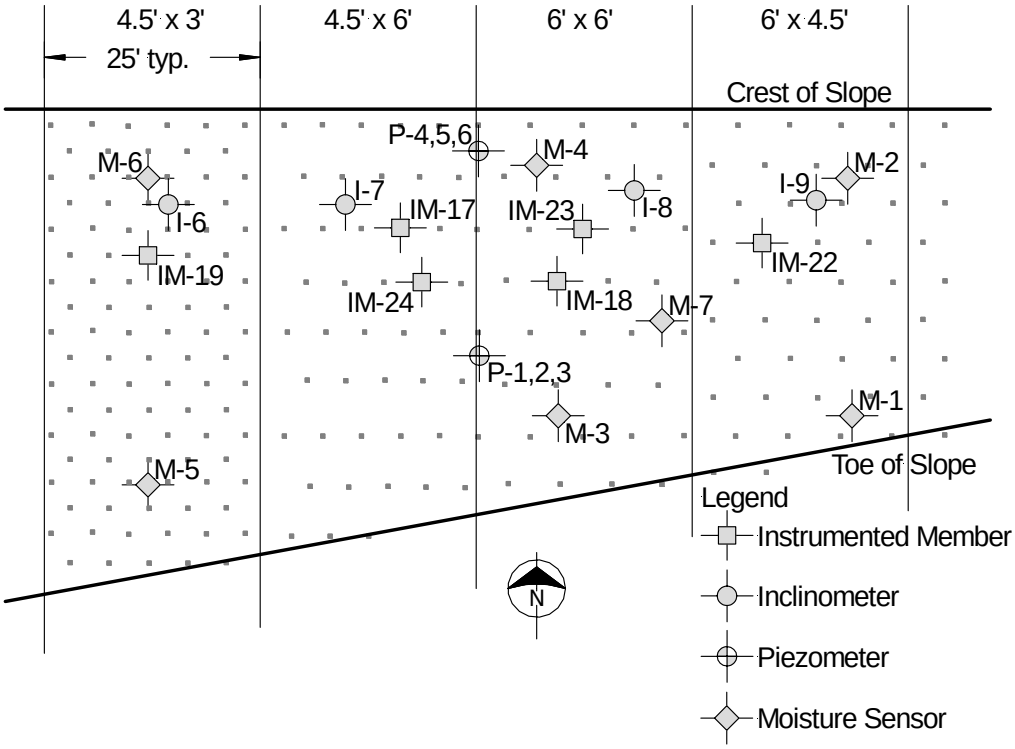

Figure 6.10 Plan view of slide area S3 at the I70-Emma site showing locations of instrumentation during Phase II.

Two clusters of standpipe piezometers similar to the one shown in Figure 5.10 were also installed in slide area S3 at the same time. Both clusters were installed along the slope section between Sections B and C and both contained three piezometers screened at different levels to permit possible perched water conditions to be detected. Piezometers P-1, P-2, and P-3 were placed in a cluster just below the center of the slide area and were screened at depths of 14.5-ft, 9.5-ft, and 4.5-ft (4.4-m, 2.9-m, and 1.4-m), respectively. Piezometers P-4, P-5, and P-6 were installed near the crest of the slope and screened at depths of 14.5-ft, 9.5-ft, and 4.5-ft (4.4-m, 2.9-m, and 1.4-m), respectively.

An array of moisture sensors similar to that described in Chapter 5 was also installed in slide area S3 in May 2003. Seven Profile Probe® access tubes were installed across the slide area at locations denoted M-1 through M-7. In addition, an array of two Thetaprobes® and two Equitensiometers® was installed as illustrated in Figure 5.12 at location M-7 to provide for essentially continuous monitoring of moisture conditions within the slope.

6.5. Field Performance

Instrumentation installed during Phases I and II was monitored from installation through January 2005. Field instrumentation readings were taken at intervals ranging from 4 weeks to 10 weeks. Site precipitation data was obtained from the National Climatic Data

Center for the Sweet Springs, Missouri weather station located approximately 4 miles east of the I70-Emma site. Data presented in the following sections include measured piezometric levels, soil moisture and soil suction measurements, lateral slope displacements, and mobilized loads in the reinforcing members. Results of a field reconnaissance performed following a failure in Sections B and C are also presented.

Because work at the I70-Emma site was performed over two distinct periods, the performance observed during each period is described separately. The first performance period described is based on installations performed in November and December 1999 and extends through December 2002, just prior to installations performed in slide area S3 during Phase II of the project. The second performance period extends from January 2003, when subsequent installations were performed in slide area S3, through January 2005 when monitoring was ceased.

6.5.1. Precipitation at the I70-Emma Site

Figure 6.11 shows daily and monthly precipitation totals recorded at the National Climatic Data Center (NCDC) weather station in Sweet Springs Missouri (Coop ID 238223) since November 1999 along with 50-year monthly averages. The weather station is located approximately 4 miles east of the I70-Emma site. Normal precipitation patterns at the site consist of relatively wet spring seasons, moderate rainfall during the summer and fall months, and relatively dry winter seasons. This pattern has been generally evident throughout the entire monitoring period, although some expected deviations have occurred. The following summarize general trends in precipitation levels recorded at the site:

- November 1999 – March 2001: precipitation was generally at or below 50-year average levels with the single exception of June 2000, which had monthly precipitation approximately 4 inches above normal for June.
- April 2001 – July 2001: precipitation during this period was substantially higher than normal throughout the period with several months of precipitation exceeding monthly averages by 3 to 5 inches.
- August 2001 – November 2003: precipitation during this period was substantially lower than average due to a moderate drought experience in the area; precipitation during May 2002 was higher than normal but precipitation during the remaining months were frequently lower than normal.
- December 2003 – June 2004: precipitation during this period generally followed 50-year average trends although December 2003 precipitation was substantially greater than normal as a result of a significant individual precipitation event on December 10, 2003 (3.5 inch event).
- July 2004 – January 2005: precipitation during this period was substantially higher than 50-year averages, with four months having monthly precipitation totals exceeding 50-year averages by more than 3 inches. The total precipitation recorded between July 1, 2004 and January 31, 2005 was 14 inches greater than the 50-year average for Sweet Springs, Missouri.

Of these periods, the April 2001 – July 2001 and July 2004 – January 2005 periods appear to have been most significant in relation to the performance observed at the I70-Emma site as

they represent extended periods with precipitation significantly above 50-year average levels. In addition to these general trends, several significant individual precipitation events have been observed. These include:

- A 4.7 inch event spanning August 31-September 1, 2003,
- A 3.5 inch event on December 10, 2003, and
- A 3.1 inch event on May 19, 2004

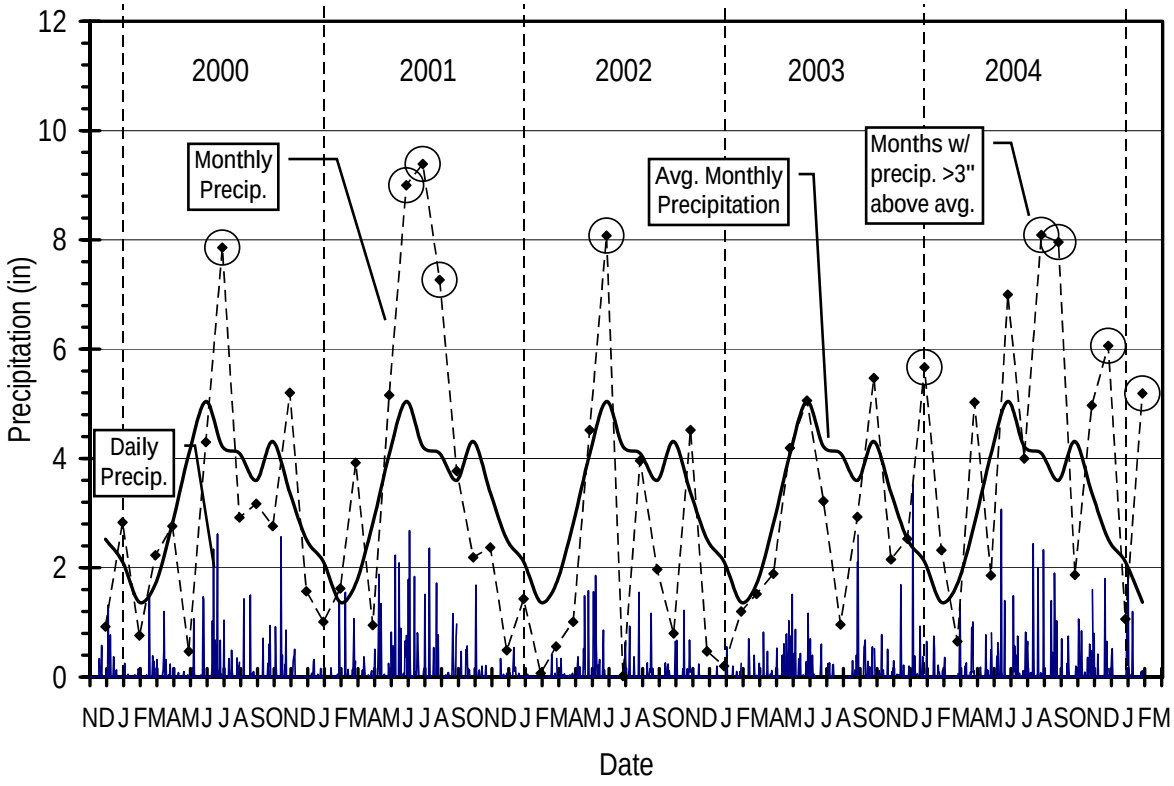

Figure 6.11 Recorded daily, monthly, and 50-year average precipitation at Sweet Springs Missouri weather station near I70-Emma site.

6.5.2. Performance of Slide Areas S1, S2, and S3 – November 1999 to December 2002

6.5.2.a Pore pressure measurements

Unfortunately, neither the continuously screened "wells" nor the standpipe tensiometers installed during Phase I produced reliable estimates of pore pressures in the slope in response to precipitation. The wells have indicated some water is present within the slope. However, because the wells are continuously screened, it has been difficult to interpret the source of this water and the associated pore pressure conditions. The tensiometers have indicated variable soil suctions in response to precipitation at the site. However, since the tensiometers were only monitored at discrete intervals, it has been extremely difficult to correlate the field readings with precipitation events. The tensiometers have also become damaged on several occasions due to freezing temperatures. Results from

these instruments have therefore not been useful for developing an understanding of the pore pressure conditions within the slope to date. As a result, observations regarding performance observed prior to January 2003 had to be related directly to precipitation, or to inferred pore pressures based on the observed precipitation. Improved instrumentation installed during Phase II remedied these problems in many respects for subsequent monitoring.

6.5.2.b Inclinometer measurements

Figure 6.12 shows the lateral deflection profile determined from inclinometer I-2 in slide area S1 at the I70-Emma site. Other inclinometers showed generally similar profiles. However, some problems were experienced with some inclinometers indicating significant "up-slope" movements at depth. These "movements" are attributed to movement of the casing within the borehole as a result of inadequate backfilling of the casings rather than actual movements in the slope. As a result of these problems, inclinometer measurements have been somewhat scattered over time. As shown in the figure, movements have generally been greatest near the ground surface with continuously decreasing movements with depth. This trend was consistent among the remaining inclinometers, although the magnitudes of the overall movements varied somewhat.

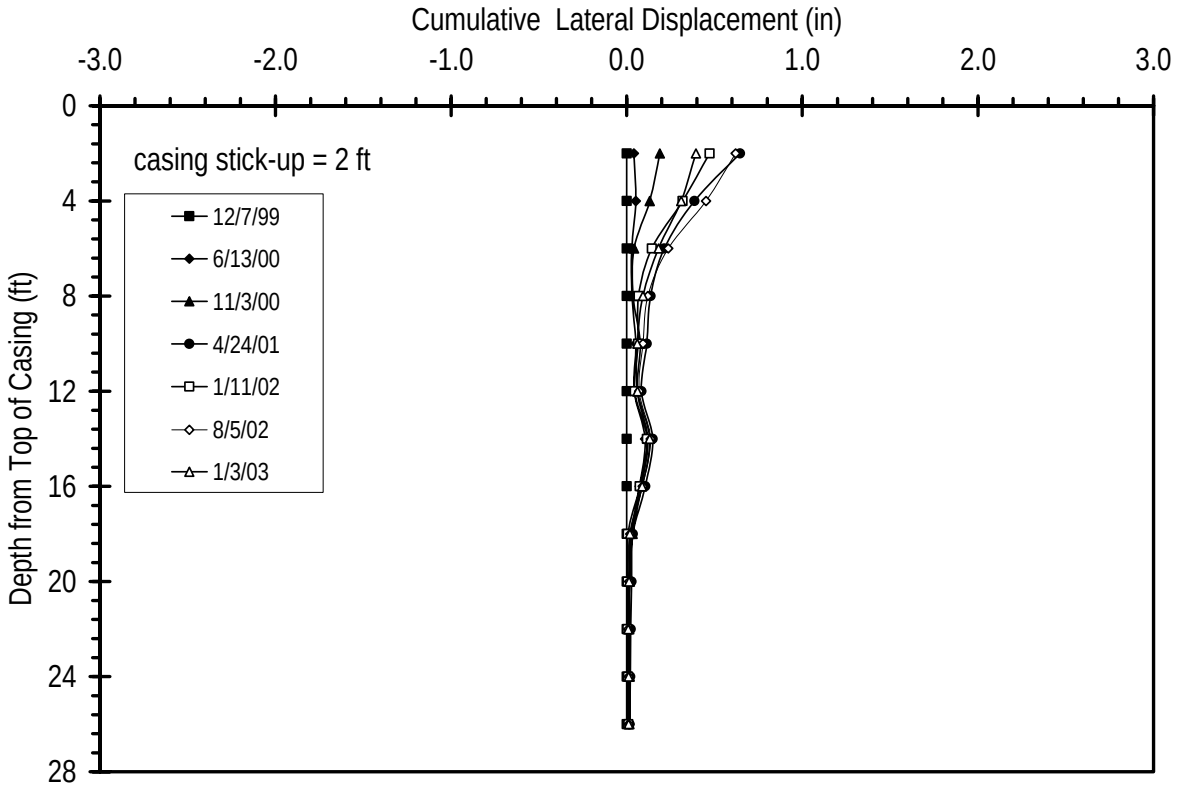

Figure 6.12 Lateral deflection profile for inclinometer I-2 in slide area S1 at I70-Emma site.

Figure 6.13 shows the cumulative deformations determined from inclinometers installed at the site versus time. Although these data are somewhat erratic due to the nature of the casing backfill, the trend in behavior is generally consistent with that observed at other test sites described in subsequent chapters. Movements were generally small during most of

the first year following installation. This is consistent with the lower than normal precipitation experienced at the site during this time. Movements were then observed to increase in early to mid 2001, presumably in response to increased precipitation observed during this time. Lateral movements then remained relatively steady through the end of 2002. Inclinometers I-1, I-3, and I-4 all indicated a significant "jump" in lateral deformations between February and June 2002 following a month of higher than average precipitation. However, this increase in deformation follows a period of apparently up-slope deformations between August 2001 and February 2002, which may simply be scatter in the measurements or movement within the borehole since upslope movements are not considered realistic. This possibility is supported by readings from inclinometer I-2, which has been relatively stable during the same period. Regardless of the reasons for the apparent "up-slope" movements followed by "down-slope" movements, the overall movements indicated by all of the inclinometers at the end of 2003 are similar in magnitude to the overall movements indicated in August 2001, which suggests that significant movements have not occurred since that time. The magnitudes of overall movements vary from less than 0.5-in (1.3-cm) to approximately 1.5-in (3.8-cm) in both areas S1 and S2.

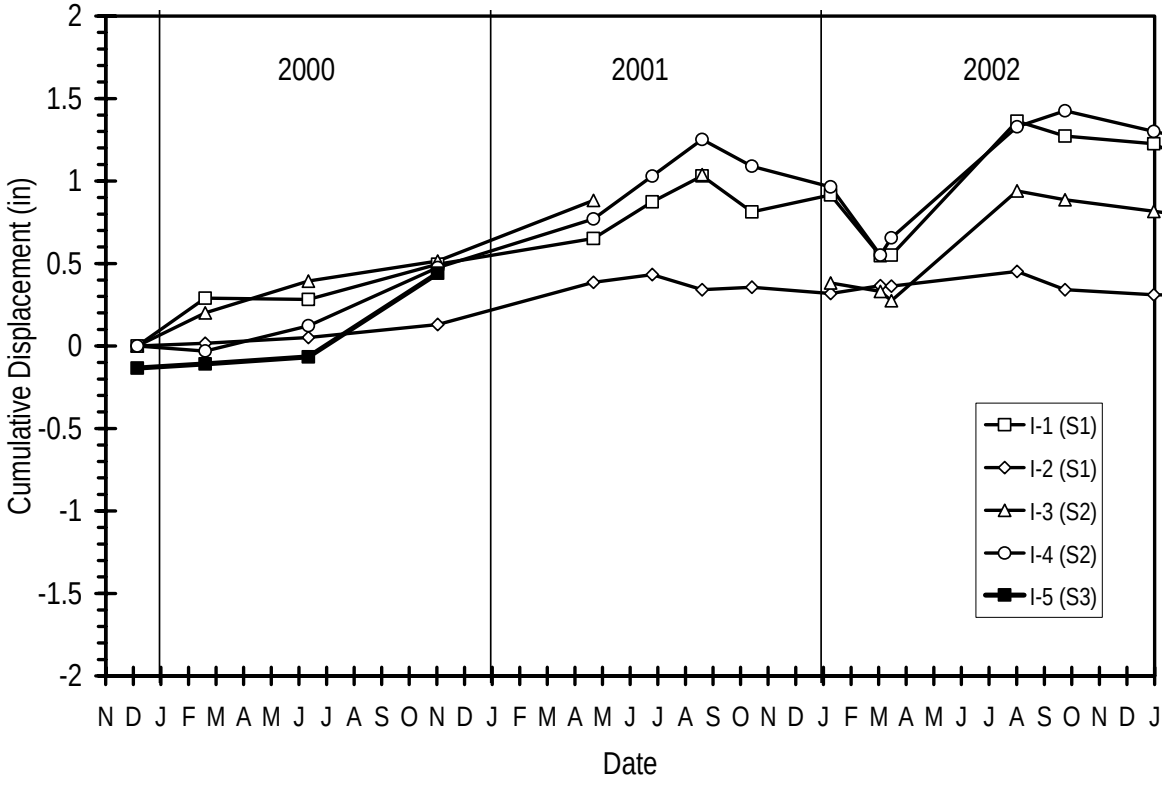

Figure 6.13 Cumulative lateral deflections for inclinometers I-1 through I-5 at depths between 3- to 4-ft for slide areas S1 and S2 at the I70-Emma test site.

The pattern of movements consisting of an initial period of little movement followed by a period of increasing movements, after which movements are generally negligible is consistent with patterns observed at other test sites. It is postulated that this movement

sequence is a combined result of the pore pressure conditions within the slope and mobilization of resistance in the reinforcing members. Just after installation, the slope would be stable without the reinforcing members because of the low pore water pressures within the slope. However, during the first wet period following installation, the stability of the slope decreases in response to increasing pore water pressures. As the stability decreases, the slope begins to move at which point the reinforcing members begin to deflect and provide some resisting loads. With continued higher pore pressures, the slope movement continues until the reinforcing members mobilize loads sufficient to create equilibrium in the slope. At this point, additional movement is resisted by the reinforcing members and movement essentially stops. Upon subsequent wetting and drying cycles, some resistance in the members is already mobilized which prevents significant additional movement unless the pore water pressures become significantly greater than have been experienced since installation. In cases where subsequent pore pressures are greater than previously experienced, additional movement would mobilize the additional resistance required to reach a new equilibrium condition as long as no limit state is reached to produce failure.

Inclinometer I-5 is somewhat of a special case. This inclinometer was installed in slide area S3, which served as a control slide during Phase I. Control slide S3 failed on June 5-6, 2001. The failure occurred just above the location where inclinometer I-5 met the ground surface and the failure "kinked" the inclinometer casing so that no further readings could be taken. Figure 6.13 shows that this inclinometer indicated negligible movements over the first year following installation. However, movements indicated by the inclinometer then increased dramatically over the next few months in response to increased rainfall. The inclinometer was then rendered inoperable in June 2001, when the control slide failed. This pattern of deformation is generally consistent with what would be expected for the observed rainfall patterns and is indicative of the failure. The fact that the remaining inclinometers in the stabilized sections have indicated little additional movements supports the observation that the movements experienced in the stabilized sections were simply movements required to mobilize the resistance in the reinforcing members.

6.5.2.c Instrumented reinforcing members

Readings from instrumented reinforcing members have also been taken on a regular basis. These readings have been processed and interpreted to establish the magnitudes of axial stresses and bending moments mobilized in the reinforcing members at each reading. However, it is important to note that reduction of the strain gage data requires that potentially significant assumptions be made in order to interpret the data. Two basic assumptions that were made include: (1) bending was assumed to be uniform when separating out axial strains from bending strains and (2) all strains were assumed to produce changes in stress (i.e. no creep or thermal strains). While these assumptions may be questioned, it is not clear that other assumptions could be made to reduce the data with the information currently available. Furthermore, there is no compelling evidence to suggest that these assumptions will have a noticeable impact on the interpretations made. Of somewhat more importance in the current context, however, are assumptions made regarding which gages were providing accurate data and which gages were not. To address this issue, several different interpretations have been developed for many of the instrumented reinforcing members (generally denoted as interpretation A, B, C, etc.) and significant effort has been put into selecting the most appropriate of these interpretations that is both reasonable and consistent with observations

from other instrumentation. The interpretations presented in this and subsequent chapters are the ones deemed to be the most appropriate among several different interpretations that can be made.

One particular issue that came to light during interpretation of data from the instrumented reinforcing members is the issue of initial stresses and bending moments imposed during installation. Data obtained from members where readings were taken prior to and just after installation indicate that significant initial stresses and moments were often developed in the members due to the installation process. The existence of such stresses is not difficult to accept given the method of installation. However, the distribution of such stresses is in no way connected to the mechanisms by which load is transferred to the reinforcing members due to slope movements. It is therefore unreasonable to expect that the *overall* stresses and moments determined *including the initial stresses* should have distributions that are consistent with what one would expect from slope movements. However, it is reasonable to expect that the *incremental* stresses imposed *since installation* should have distributions that are consistent with those expected from slope movements. Because both the overall and incremental stresses are of importance in establishing the patterns of behavior in the slopes, two sets of interpretations were made: one set including any initial strains/stresses developed during installation and another that only includes the strains/stresses developed since installation was complete. In the following sections and chapters, the term "overall" is used to refer to stresses and bending moments determined to include any stresses or moments developed during installation (i.e. with reference to the unstressed member prior to installation) while the term "incremental" is used to refer to stresses and bending moments developed since installation (i.e. with reference to the member stresses just after installation).

Readings were taken on all instrumented reinforcing members in slide areas S1, S2, and S3 between December 1999 and January 2004. No initial readings were taken for the reinforcing members prior to installation during Phase I. The results presented here are therefore "incremental" stresses and bending moments induced since installation as discussed in Section 5.3.2. The most reliable data has been obtained from instrumented member IM-G from slide area S1, member IM-C from slide area S2, and member IM-H from slide area S3 (a single member in the control area). The results presented below are therefore for these members.

Figure 6.14 shows the distribution of axial stresses determined for instrumented member IM-G. The observed distribution is generally parabolic with negligible stresses near the two ends of the member and the maximum axial stress near the midpoint of the member. Members IM-C and IM-H had similar distributions of axial stress although the magnitudes of the stresses differ.

Figure 6.15 shows the maximum incremental axial stresses determined for instrumented members IM-G, IM-C, and IM-H plotted as a function of time. The incremental axial stresses are all negative, which indicates tensile stresses/strains since installation. The reason(s) for the development of tensile strains/stresses in the members following installation is not entirely understood, but the trend has been consistently observed at all field test sites. One possible explanation is that the observed tensile strains/stresses are a result of relaxation of compressive stresses induced in the members during installation. Another possible contributor to the tensile strains/stresses could be a result of thermal strains

produced by changes in temperature. However, there is no apparent trend to the strains according to season so this is not believed to be a major contributor to the tensile strains. Regardless of the reason(s), it is important to emphasize that the stresses indicated in Figure 6.15 only indicate negative *changes* in stress as opposed to actual tensile stresses because initial stresses imposed during installation were not measured for instrumented members installed during Phase I.

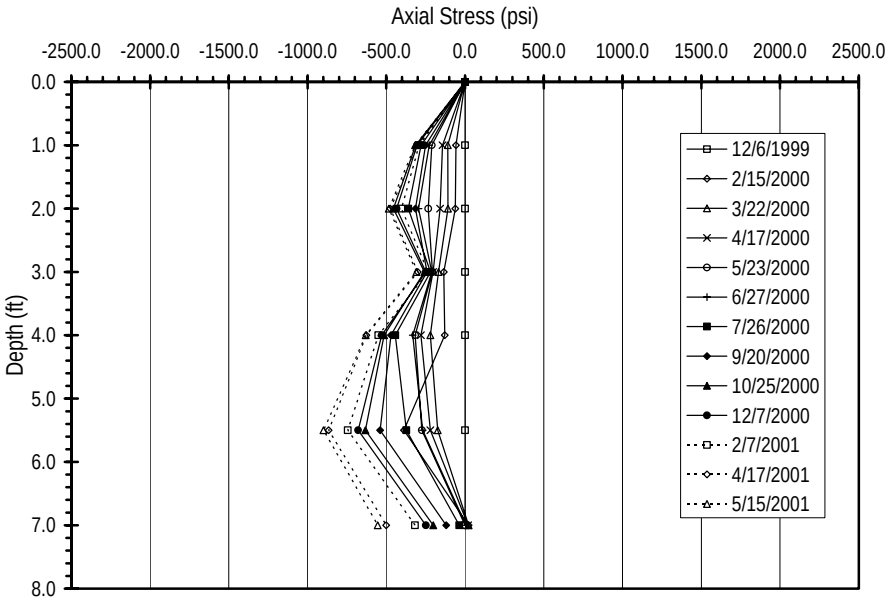

Figure 6.14 Measured incremental axial stress in instrumented member IM-G in slide area S1 at I70-Emma site during Phase I.

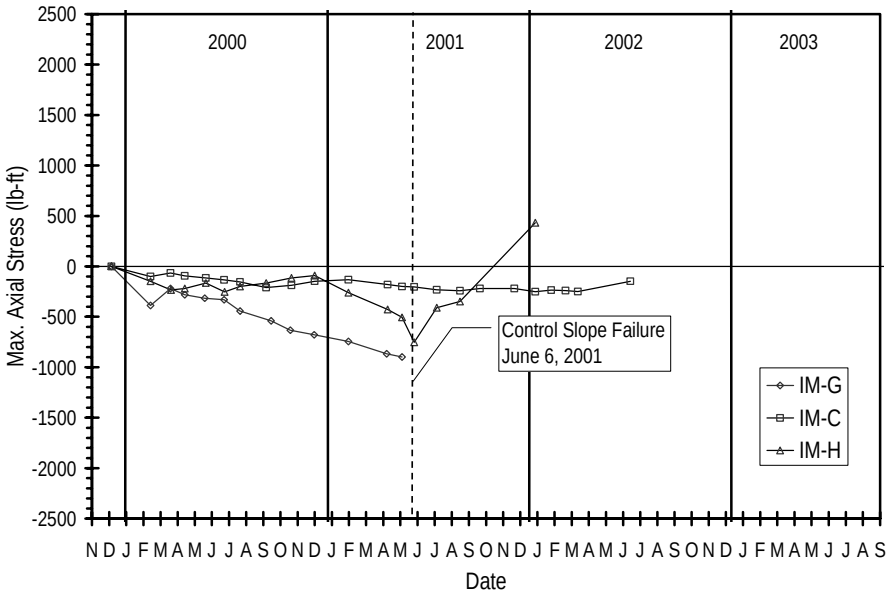

Figure 6.15 Maximum incremental axial stress in instrumented members IM-G, IM-C, and IM-H at I70-Emma test site during Phase I.

It is interesting to note however that member IM-C, which was installed with a vertical orientation in slide area S2, experienced a slight decrease in stress over the first year after installation after which the axial stress has stayed relatively constant. Member IM-G, which was installed perpendicular to the face of the slope, also experienced a gradual decrease in stress over this time, but the magnitude of the incremental stress is much greater. It is believed that the incremental axial stresses developed in member IM-C were significantly lower than member IM-G because slope movements parallel to the face of the slope would tend to resist any axial relaxation for members installed vertically, while slope movements for members installed perpendicular to the slope would not tend to influence the axial stresses. Unfortunately, member IM-G was rendered inoperable in late May 2001 so it is impossible to determine whether the incremental axial stresses in the member would have stabilized. Member IM-H, installed vertically in control slide area S3, behaved similar to member IM-C (also installed vertically) over the first year following installation. However, the incremental axial stresses in IM-H then decreased substantially prior to the failure of slide area S3 on June 5, 2001. This rapid decrease in the incremental axial stresses occurs at the same time as movements in slide area S3 began to accelerate and is believed to be a result of the slope beginning to fail.

Figure 6.16 shows the distribution of bending moments determined for instrumented member IM-H. The distribution is also generally parabolic with negligible moments near the ends of the member and the maximum moment occurring near the midpoint of the member. Moments are generally positive along the entire length of the member. Moment distributions for members IM-G and IM-C were similar in shape but with generally lower magnitudes.

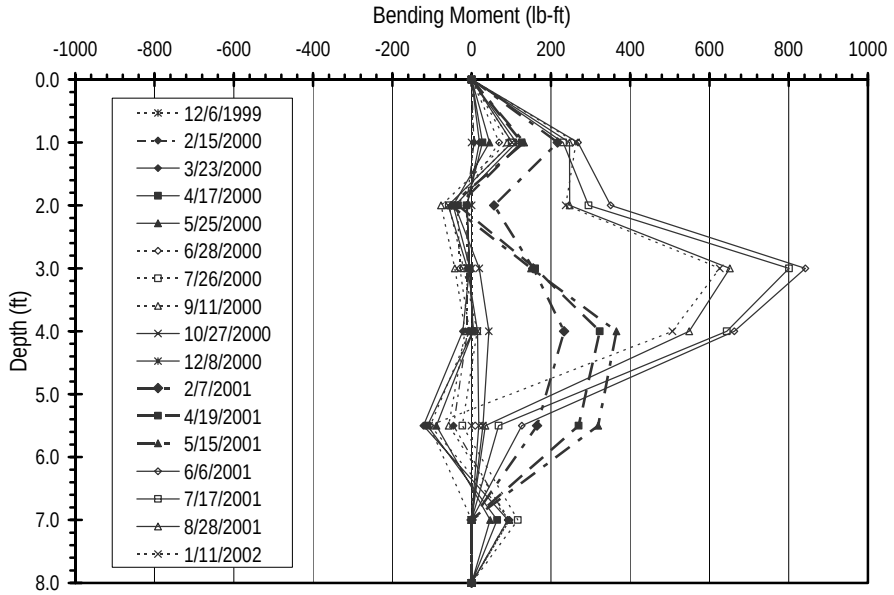

Figure 6.16 Measured bending moments in instrumented member IM-H at I70-Emma test site during Phase I.

Figure 6.17 shows the maximum moments determined for these three members plotted as a function of time. Member IM-C experienced gradually increasing moments during the first 17 months following installation. Then, around the time of the failure of control slide S3, the moments in IM-C increased by a small but noticeable amount. This

sudden increase is believed to be a response to the slope needing additional resistance to maintain equilibrium at the time of the control slide failure. Incremental bending moments since that time have remained essentially constant despite having several periods of heavy rainfall during that time.

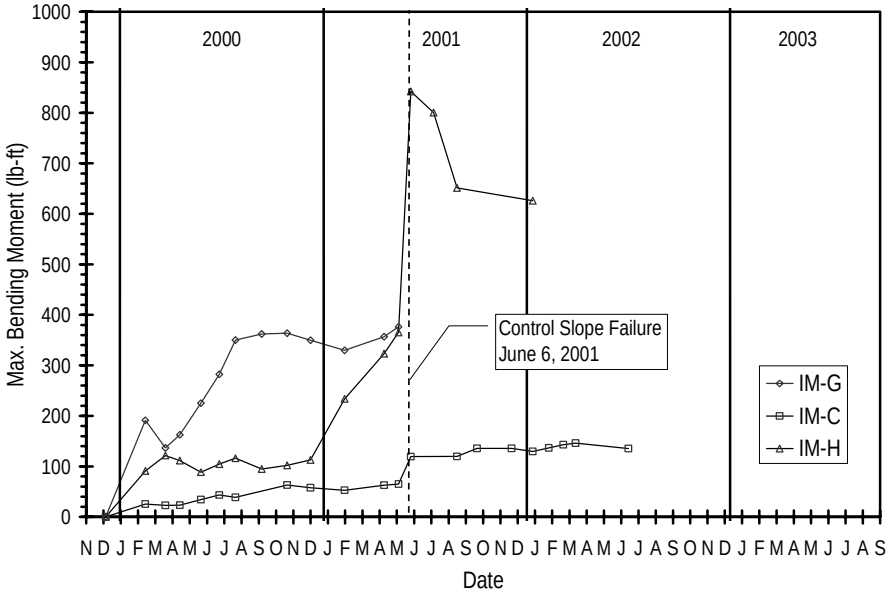

Figure 6.17 Maximum bending moments in instrumented members IM-G, IM-C, and IM-H at I70-Emma test site during Phase I.

In contrast, Member IM-G experienced a relatively rapid increase in the incremental bending moments during the first 8 months following installation after which the incremental bending moments remained essentially constant until, during the three months prior to the failure of the control slopes, the bending moments increased slightly. Unfortunately, IM-G became inoperable just prior to the failure of the control slide. However, the slight increase in bending moments leading up to this time indicates that the reinforcing members were providing additional resistance needed to maintain the equilibrium of the slope. While the incremental bending moments in member IM-G just after the control slide failure are not known, the fact that inclinometers IM-1 and IM-2 have not shown any significant movement since that time suggests that the bending moments would have remained essentially constant.

Member IM-H indicated behavior similar to member IM-C during the first year following installation, although the member had slightly higher bending moments. However, incremental bending moments in member IM-H increased steadily during the 6 months leading up the failure of the control slide, which appear to be a response to the slope needing additional resistance. Readings taken on member IM-H on the day after the failure indicated that a significant increase in bending moments had occurred. This dramatic increase is believed to be in response to the failure of the slope. The magnitude of the bending moments measured just after the failure is approximately 850-lb-ft (1200-N-m), a value which is relatively close to the nominal moment capacity of the recycled plastic members (~1000-lb-ft). Member IM-H was subsequently exhumed in early 2002, when it was determined that the member had fractured at a distance of approximately 5-ft (1.5-m) below the top of the member.

It is interesting to compare the behavior of member IM-G, which was installed perpendicular to the face of the slope, with member IM-C which was installed vertically. Results determined from the field instrumentation indicate that member IM-G experienced greater incremental axial stresses and greater incremental bending moments than member IM-C which was installed vertically. Furthermore, prior to the months leading up to the failure of the control slide, member IM-H, which was also installed vertically, exhibited behavior similar to member IM-C. This evidence suggests that members installed perpendicular to the slope will be subjected to noticeably higher bending moments since slope movements will directly contribute to these moments. In contrast, members installed vertically are subjected to lower incremental bending moments since down-slope movements will tend to produce a compressive axial stress in addition to a bending moment. This postulated load transfer is further supported by the measured axial stresses in the members. Recalling the hypothesis that the observed incremental axial stresses/strain are in fact a result of relaxation of compressive stresses/strains developed during installation, it can be noted that *incremental* axial stresses for members IM-C and IM-H were of smaller magnitude (i.e. less relaxation of stresses) than was observed for member IM-G which was installed perpendicular to the slope and therefore would not experience a significant compressive load as the soil moves down-slope. This postulated load transfer is consistent with that observed at other field test sites.

6.5.3. Performance of Slide Area S3 – January 2003 to January 2005

6.5.3.a Pore pressure measurements

Measured piezometric levels for the I70-Emma site between January 2003 and January 2005 are plotted in Figure 6.18. Piezometers readings consistently indicate a perched water condition in the slope, as evidenced by consistently higher piezometric levels for the upper piezometers than observed for the deeper piezometers. Piezometric levels in the shallower piezometers also appear to respond more to individual precipitation events than to longer term trends, although both are observed. Between March 2003 and November 2003, piezometric levels were relatively constant. Little response was observed for the August 31-September 1, 2003 intense precipitation; however, the piezometers were not read until 30 days after this event. Piezometric levels in piezometers located in the upper portion of the slope were observed to increase in January 2004, likely due to intense precipitation observed on December 10, 2003; piezometric levels for the piezometers in the lower portion of the slope do not appear to immediately respond to this event, but instead increase subsequently suggesting a delayed response or response to different events. Piezometric levels in all shallow piezometers were again slightly elevated in November 2004, presumably in response to elevated precipitation in late 2004. All piezometers were severed during the failure that occurred between November 2004 and January 2005 (see Section 6.5.3.d), thus no data was available following the November 2004 reading.

Figure 6.19 shows measured soil suctions and volumetric water contents measured at the cluster of sensors located near the center of the slide area. These measurements show decreasing pore pressures and water contents during late summer 2003 in response to an extended dry period and subsequent response to the August 31-September 1, 2003 precipitation event. However, since that time the soil suction and water content measurements have not correlated well with observed precipitation patterns and measurements from the piezometers aside from generally showing saturated or near saturated

conditions. Several problems were encountered with the soil moisture and suction sensors during 2004 so the reliability of these measurements is judged to be suspect. More credence has therefore been placed on the piezometer measurements.

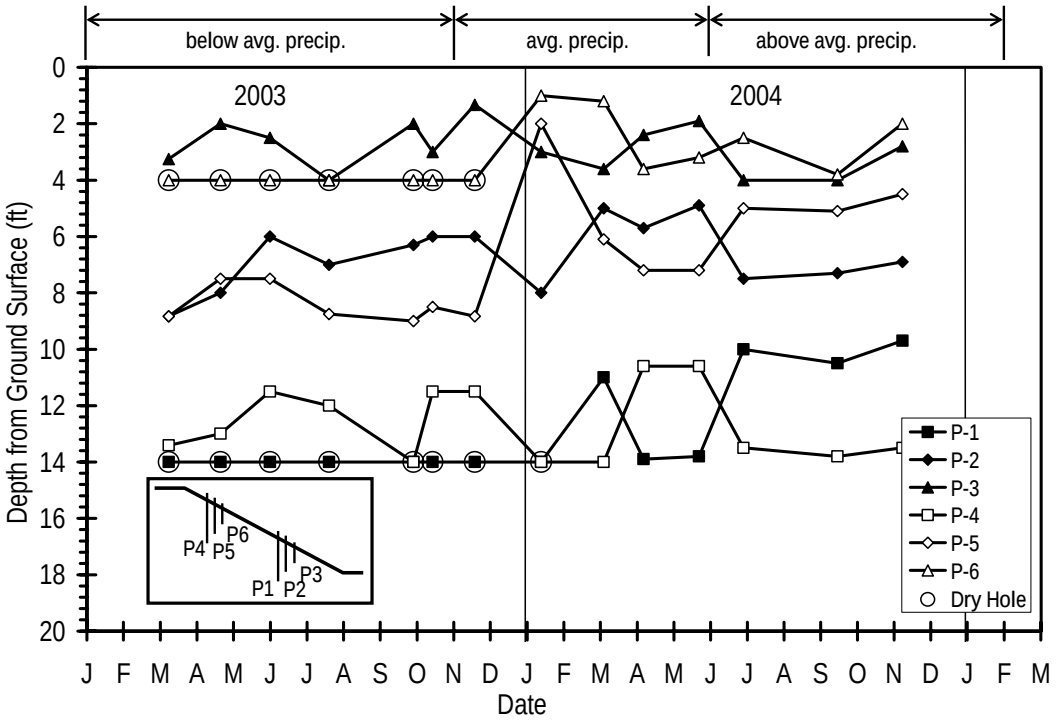

Figure 6.18 Piezometric water levels measured at I70-Emma test site.

6.5.3.b Inclinometer measurements

Figure 6.20 shows measurements of lateral displacement versus depth for inclinometer I-7, which is typical of the general response observed for all inclinometers in slide area S3. As shown in the figure, measured displacements were generally confined to the upper 7 feet of the slope. Little displacement occurred below 8-ft. The large increase in displacement between June 3 and September 30, 2003 is presumed to be due to the initial mobilization of resistance in the reinforcing members. This is followed by marginal additional mobilization of resistance, or perhaps creep, between September 2003 and September 2004. This is in turn followed by substantial additional mobilization and subsequent failure between September 2004 and January 2005.

Measured lateral displacement versus time records determined from all inclinometers at the I70-Emma site are shown in Figure 6.21. Shaded regions in the figure indicate periods of notable displacement where resistance of the reinforcement is presumed to be mobilized. Periods of low, medium, and high precipitation are shown at the top of the figure. All inclinometers at the I70-Emma site indicate higher displacements at shallow depths with little displacement below a depth of 8 feet.

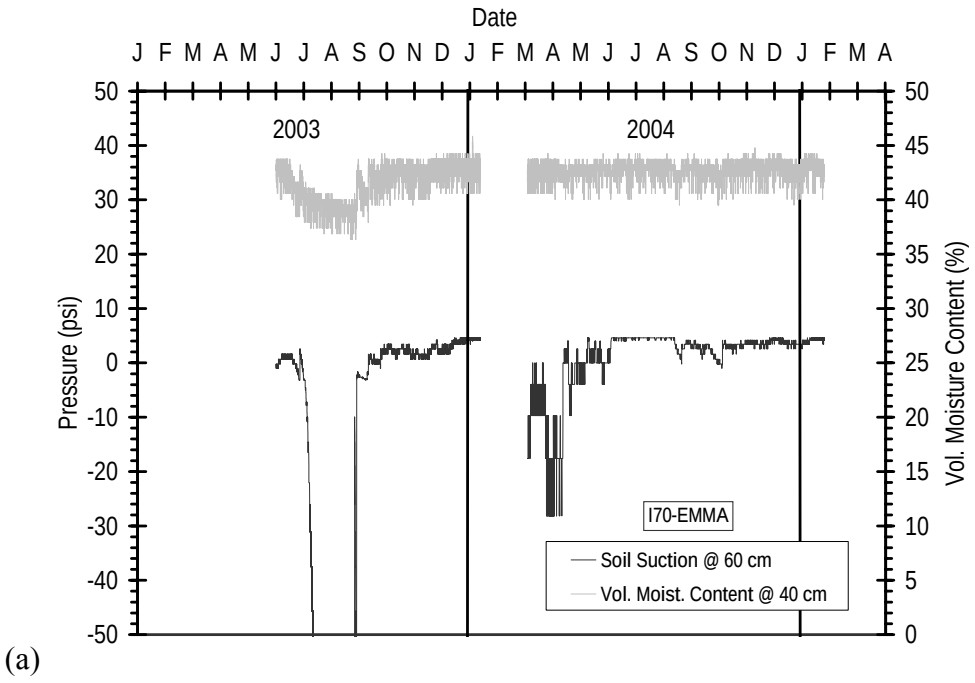

(a)

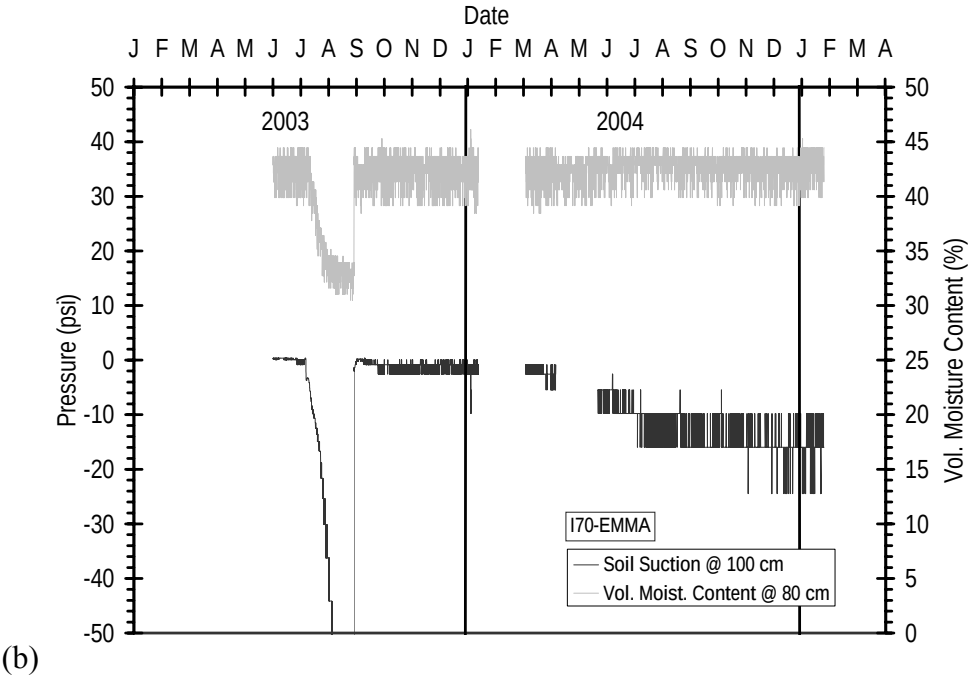

(b)

Figure 6.19. Volumetric moisture content and soil suction measured at I70-Emma test site during Phase II: (a) measurements from shallow sensors, and (b) measurements from deeper sensors.

Inclinometers in Sections B, C, and D exhibited a similar pattern of displacement with time that is consistent with patterns observed at other test sites. Little displacement was observed during the first six months after installation. Between August and October 2003, there was an increase in displacement presumed to be the result of decreased stability and

mobilization of resistance in the reinforcing members. This mobilization is the first shaded region in Figure 6.21. The decrease in stability likely resulted from elevated piezometric conditions due to the 4.5 inches of rainfall that occurred between August 31 and September 1, 2003. This period of mobilization was followed by a period of displacements increasing at a small but relatively constant rate from October 2003 to September 2004. Piezometric levels during this period were generally higher than previously recorded levels, particularly in January and June 2004.

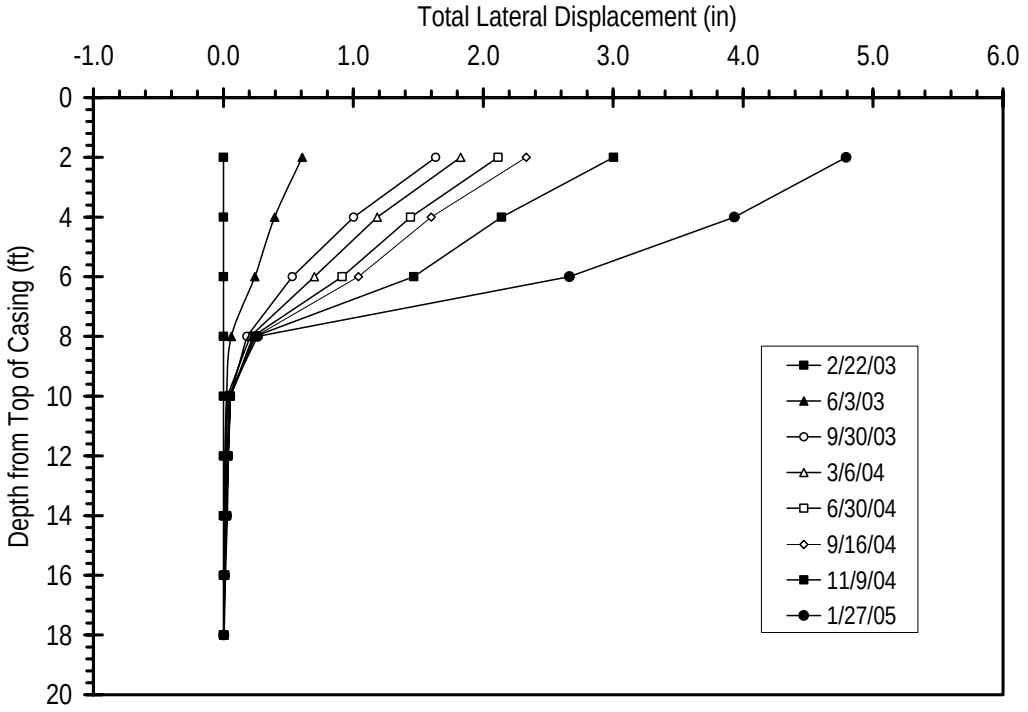

Figure 6.20 Displacement versus depth for inclinometer I-7, Section B, at the I70-Emma test site.

From September 2004 onward, an additional increase in displacements was observed. This second period of movement is attributed to additional mobilization of resistance from the reinforcing members. Piezometric levels were generally observed to increase following the September 2004 readings, likely due to the high precipitation during late summer and fall 2004. Unfortunately, the piezometers were severed due to the slope movements and could not be read following the November 2004 reading. However, given the high precipitation that continued through late 2004 and early 2005, it is likely that the piezometric levels increased above those shown for November 2004.

Deformations measured from Inclinometer I-6 in Section A (Figure 6.21a) were notably smaller than those observed in the other test sections. A slight increase in deformation was observed between August and October 2003, presumably in response to increased precipitation and mobilization of the resistance in the reinforcing members. No such increase in deformation was observed in late 2004. The lack of movements during this time is attributed to the fact that the reinforcing members were more closely spaced in this section.

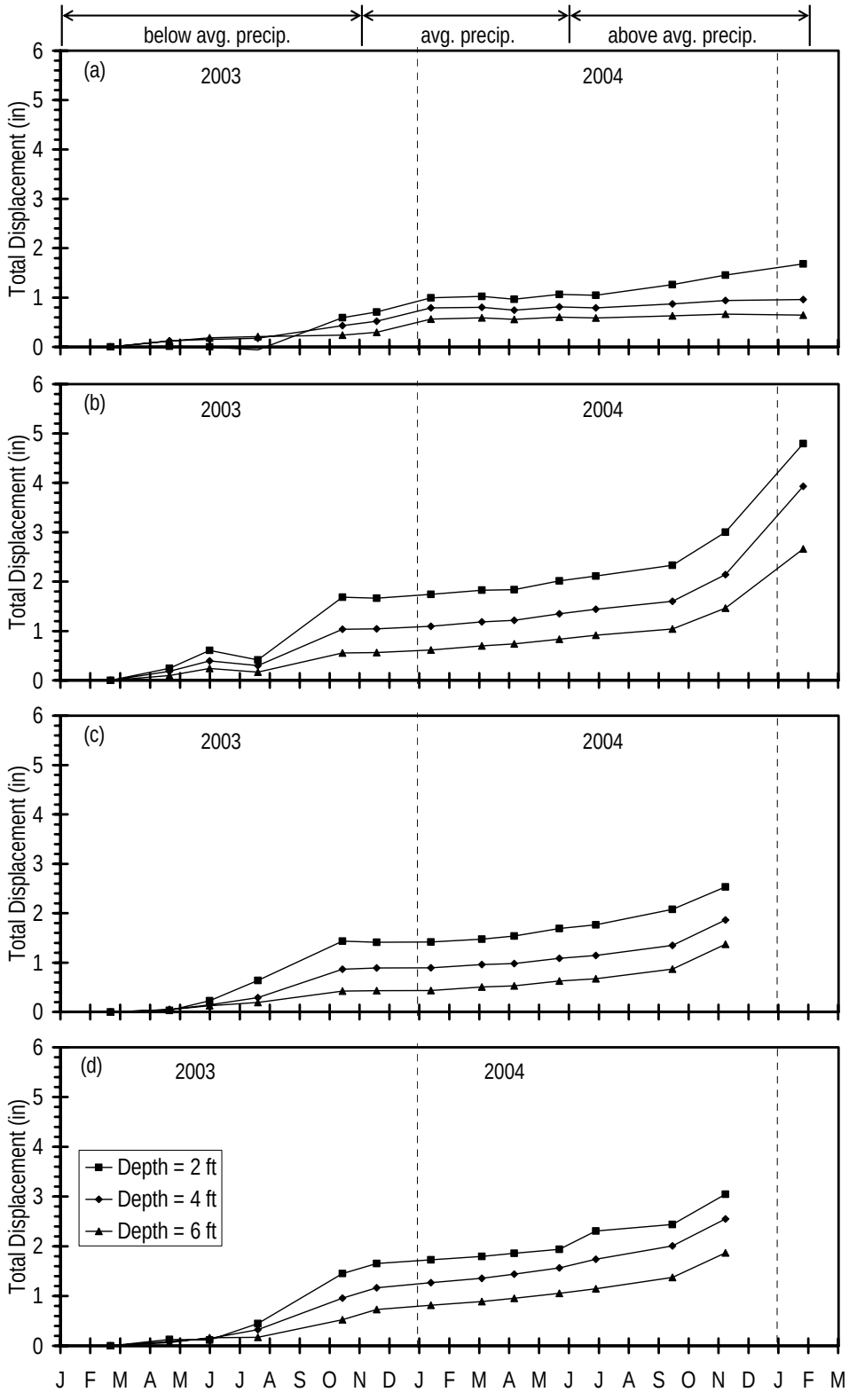

Figure 6.21 Measurement displacements for inclinometers at I70-Emma site: (a) Section A, I-6; (b) Section B, I-7; (c) Section C, I-8; Section D, I-9.

6.5.3.c Mobilized Bending Moments in Reinforcing Members

Reinforcing members instrumented with strain gages were monitored to provide values of stresses and bending moments within the members. The moments are interpreted from strain gage readings, a procedure which requires several assumptions and involves some uncertainty. Nevertheless, the interpreted bending moments provide a measure of the loads being transferred to the reinforcing members. Figure 6.22 shows the interpreted maximum moments for instrumented member IM-24 from Section B along with the measured displacements for the nearest inclinometer (I-7). The figure shows consistency between the interpreted bending moments and the measured displacements, with bending moments generally increasing as a result of slope movement. Similar consistency between deformations and maximum bending moments has been observed at other test sites. There is some uncertainty with the magnitude of the moment on January 27, 2005, as many of the strain gages on this date were broken. The actual moment could be higher than measured.

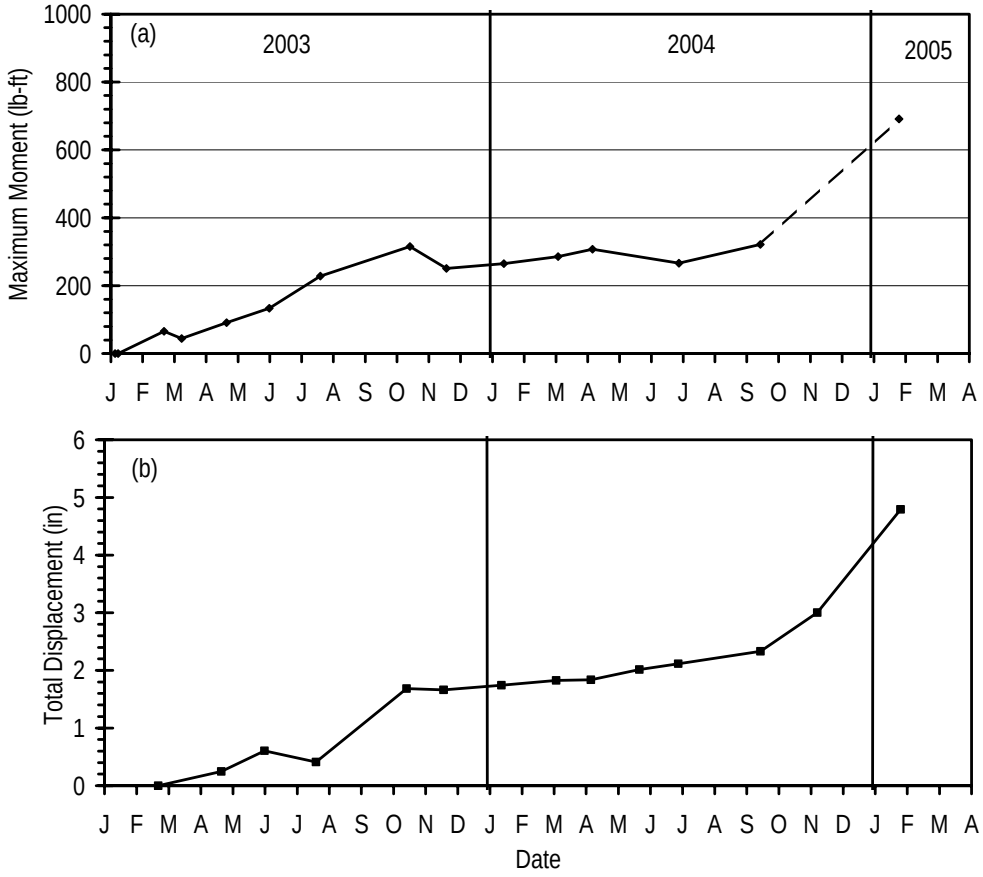

Figure 6.22 Comparison of maximum bending moments and slope displacement: (a) Maximum interpreted moment in IM-24 and (b) Measured displacement (I-7)

6.5.3.d Failure of control area and failure in Sections B and C

Slide area S4 on the opposite side of the embankment, which was used as the control section for monitoring during Phase II, failed between July and September 2004 during an

extended period of well above average precipitation. During this period, deformations in the stabilized sections were observed to increase, but only slightly.

Subsequently, a failure occurred in Sections B and C of slide area S3 between November 2004 and January 2005. A photograph of the failure is shown in Figure 6.23. The failure was confined to sections B and C of slide area S3 as shown in Figure 6.24. The failure was approximately 25- to 30-feet wide and confined to the upper portion of the slope, stopping approximately 10 feet above the toe of the slope. Inclinometers I-8 and I-9 in Sections C and D were pinched off at depths of 7-ft. and 5-ft. respectively. Inclinometer I-7, located just to the west of the failure in Section B, showed a substantial increase in displacements on that date, while inclinometer I-6 in Section A showed little increase in displacement during this period. Piezometers P-1, P-2, and P-3 in the lower portion of the slope were pinched off at a depth of 5-ft. Piezometers P-4, P-5, and P-6 were buried in the slide. No surface expressions of failure were observed in Sections A and D. However, the fact that inclinometer I-9 in Section D was pinched off suggests that substantial deformations did occur in Section D around the time of the failure.

Figure 6.23 Observed failure in slide area S3 at I70-Emma site on January 27, 2005.

The fact that the failure did not extend into Section A is not surprising since that section is more heavily reinforced than other sections. The fact that the failure did not extend into Section D is more surprising given that it is reinforced with members spaced similarly to Section B. However, the slope height in Section D is less than that in the other section, which may have contributed to the lack of an observed failure.

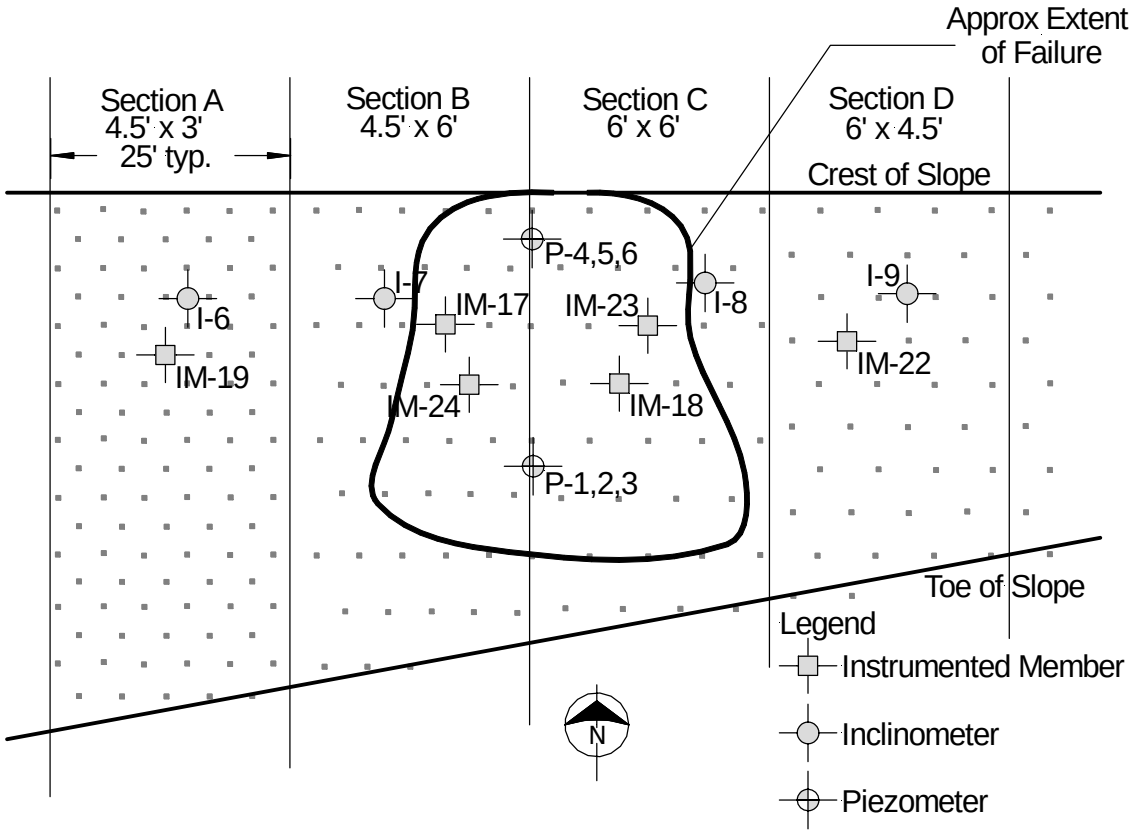

Figure 6.24 Approximate extent of failure at I70-Emma site.

6.5.3.e Post-failure investigations

On March 2, 2005, a backhoe was used to excavate a trench up the center of the failed section to evaluate whether the reinforcing members failed during the slide and the approximate depth of the failure surface. The trench was excavated along the center of the failure, generally aligned with the locations of the piezometers. The depth of the failure surface was not readily apparent during the field investigations. However, all of the recovered members were found to be broken as a result of the failure. Some of the members recovered were broken in multiple pieces and not all pieces could be located. The three members with significant portions of recovery are instrumented members IM-18 and IM-17, and uninstrumented member M-1. The entire length of member IM-18 was recovered. The upper 4.5 feet of member IM-17 and the upper 4.5-ft of member M-1 were recovered. The approximate locations of the exhumed reinforcing members are shown in Figure 6.25. Attempts to extract pins near the top of the slide were unsuccessful, suggesting that these members had not failed.

Member M-1 and the upper section of member IM-18 were excavated using the backhoe to dig a trench along the side of the reinforcing member; the member was then removed from the slope by hand. The lower section of IM-18 and the recovered section of IM-17 were obtained by extraction. A chain was wrapped around the reinforcing member and the backhoe pulled on the chain along the axis of the reinforcing member to extract these sections. This extraction technique is shown in Figure 6.26.

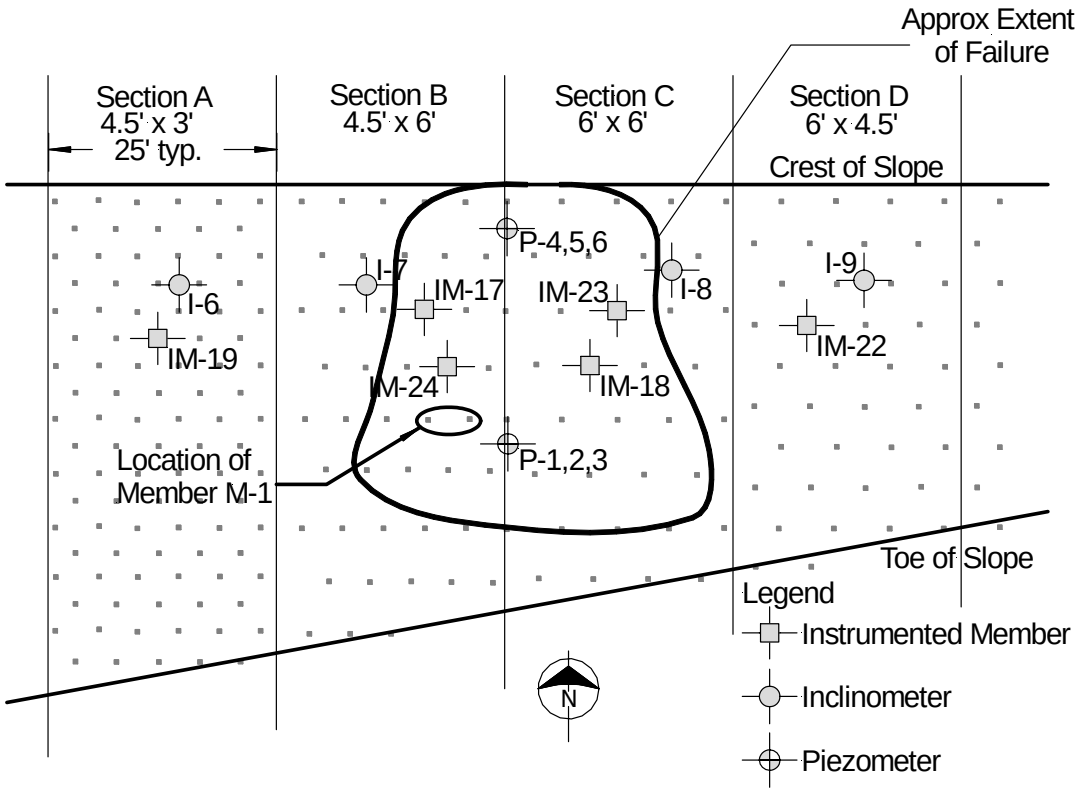

Figure 6.25 Locations of exhumed reinforcing members at I70-Emma site

Figure 6.26 Extraction of reinforcing members using backhoe at I70-Emma site

Figure 6.27 shows member M-1 in the slope during excavation. The upper 3.5-ft. section of the reinforcing member is out of vertical while the lower 1.0-ft. section is horizontal. The remainder of the reinforcing member could not be located. The recovered sections of member M-1 are shown in Figure 6.28. The slight "S-Shape" of the upper section of the reinforcing member should be noted. Additionally, the cracks on the down-hill side of the pin near the failure, as shown in Figure 6.28b, suggest failure of the reinforcement in bending.

Figure 6.27 Photograph of member M-1 in slope during excavation: (a) entire members and (b) close up of fractured section.

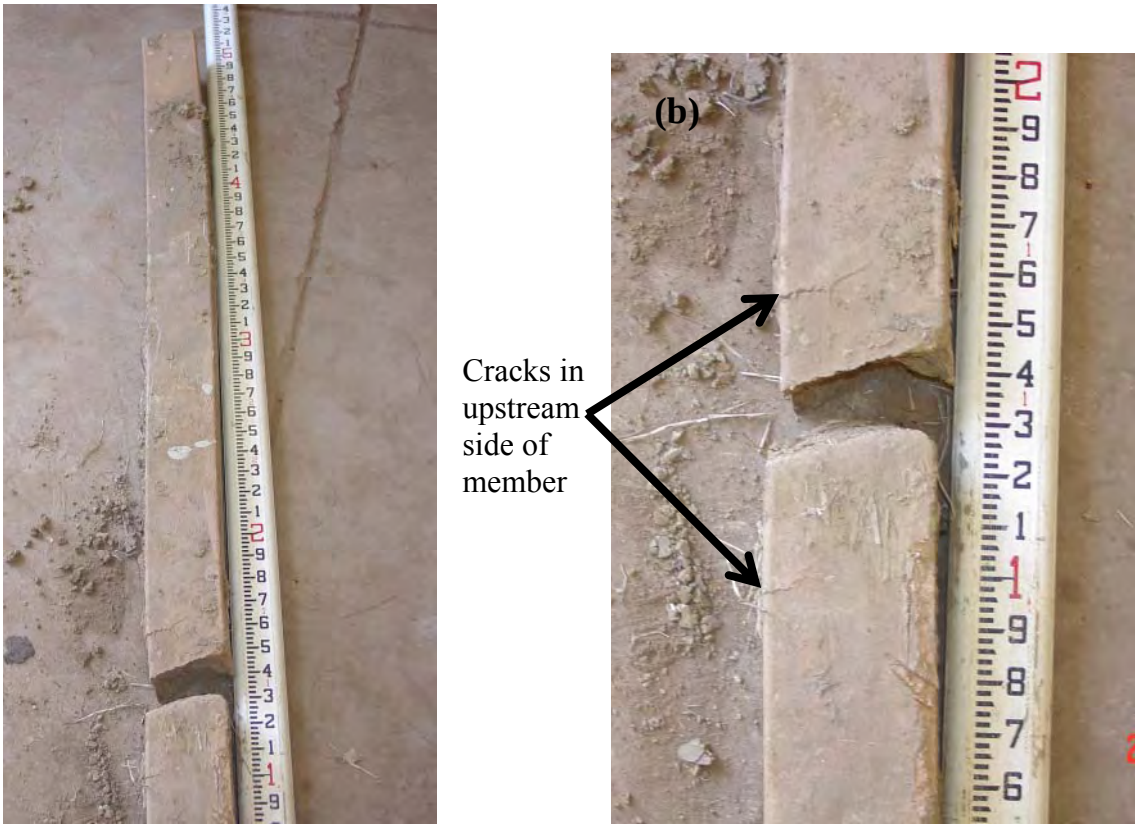

Figure 6.28 Photograph of member M-1 after excavation: (a) full member and (b) close up of failed section.

Instrumented member IM-18 was found to be broken at a depth of 4.5-ft. from the top of the member. The instrumentation cables running the length of the pin were severed which suggest that large deformations occurred. The upper section of member IM-18 is shown in the slope in Figure 6.29. The entire pin after excavation is shown in Figure 6.30. Member IM-17 was also found to be broken at a depth of 4.5-ft.

Figure 6.29 Photograph of member IM-18 during exhumation.

Figure 6.30 Photographs of member IM-18 after excavation: (a) complete member and (b) close up of the failure surface.

6.5.4. Performance of Slide Areas S1 and S2 – January 2003 to January 2005

By January 2003, the strain gages installed on instrumented reinforcing members in slide areas S1 and S2 had deteriorated to the point where little meaningful data could be acquired from continued monitoring of strains. Continued monitoring of these areas was

therefore limited to monitoring lateral deformations using the slope inclinometers. Figure 6.31 shows the measured deformations from inclinometers in these areas through January 2005[1]. While the measured deformations are at times erratic due to inadequate backfilling and potentially due to variations in operator techniques, the data generally show an initial increase in displacements in early to mid 2001 followed by relatively stable values through mid 2003. Measured displacements were then observed to increase in late 2003 and to continue increasing slightly throughout 2004. This response is generally consistent with that observed in slide area S3 (Fig. 6.21). Maximum deformations at the end of monitoring in January 2005 were generally between 1 and 2 inches. Despite the increased deformations observed in 2003 and 2004, no visible surface expressions of failure have been observed in slide areas S1 and S2 to date and the sections appear to be performing well.

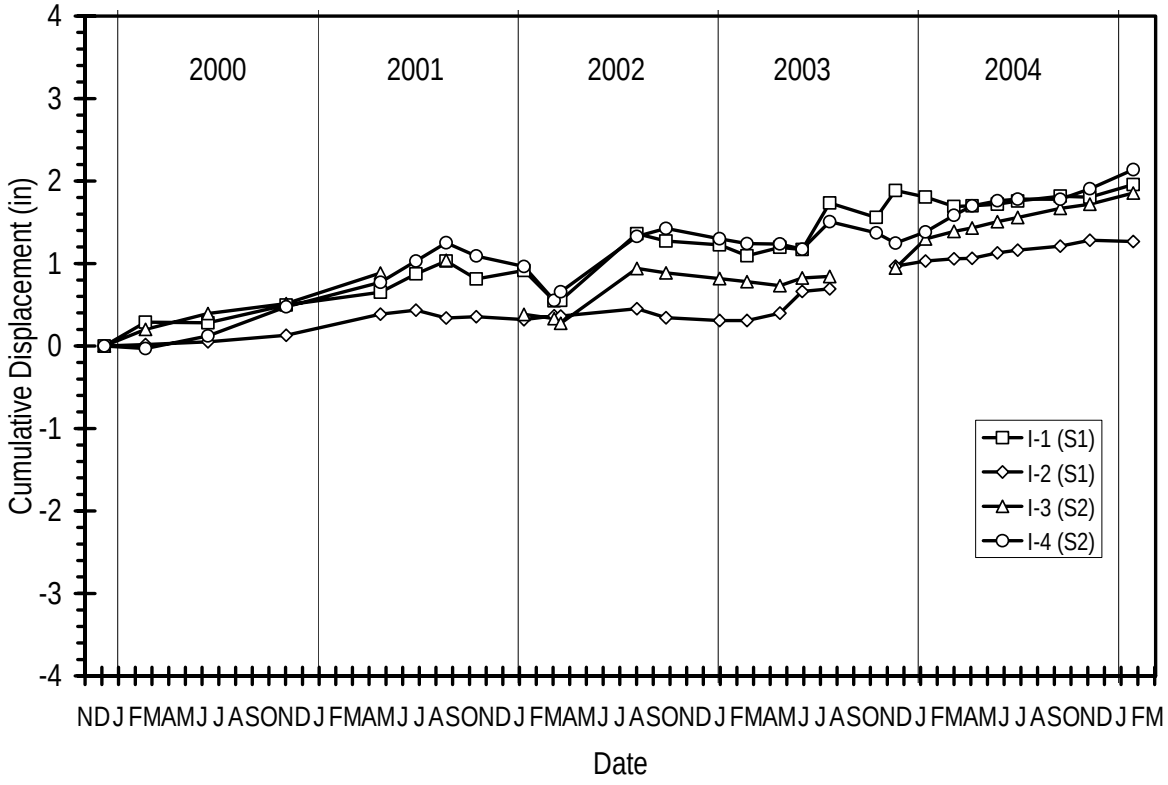

Figure 6.31 Lateral displacements at depths of 3 to 4 feet beneath ground surface for inclinometers I-1 and I-2 in slide area S1 and I-3 and I-4 in slide area S2 at I70-Emma site.

6.5.5. Potential creep in reinforcement

The slight, but steadily increasing deformations observed in inclinometers during the latter half of 2003 and throughout 2004 are indicative of creep type deformations. Because of this potential, creep rates were estimated from the measured displacements by taking the slope of the displacement versus time plots for each inclinometer between October 2003 and

[1] Recall that inclinometer casings installed in slide areas S1 and S2 during Phase I have proven to be less effective than subsequently installed inclinometer casings because of the installation method.

September 2004. These estimated creep rates are summarized in Table 6.3. Estimated creep rates range from a low of 0.03 in/year to a high of 1.06 in/year, but vary substantially both with depth and with member spacing.

Creep rates shown for shallow depths must be considered carefully because they can be influenced by measurement technique and may therefore not be representative of actual movements. As such, the estimates shown for depths of 4 to 6 feet are believed to be more appropriate. Considering these depths and neglecting values for inclinometer I-3, which are considered suspect, the estimated creep rates suggest nominal rates of between 0 and 0.3 in/year for members placed in patterns with 3-ft spacings and rates of 0.5 to 1.0 in/year for members placed at greater spacings.

Table 6.3 Estimated creep rates for I70-Emma site at depths of 2-ft, 4-ft, and 6-ft below ground surface.

Slide Area	Inclinometer (Section)	Member Spacing (ft. x ft.)	Estimated Creep Rate (in/yr)		
			2-ft. depth	4-ft. depth	6-ft. depth
S1	I-1	3.0 x 3.0	0.03	0.07	0.07
	I-2		0.66	0.40	0.22
S2	I-3	3.0 x 3.0	0.99	0.73	0.44
	I-4		0.47	0.33	0.18
S3	A (I-6)	4.5 x 3.0	0.51	0.29	0.29
	B (I-7)	4.5 x 6.0	0.69	0.62	0.51
	C (I-8)	6.0 x 6.0	0.69	0.51	0.47
	D (I-9)	6.0 x 4.5	1.02	1.06	0.84

It is important to emphasize that the creep rates shown in Table 6.3 are estimated and may, in fact, not be a result of actual creep in the members, but instead be a result of additional mobilization of resistance (creep being a phenomenon of displacement at constant load) or other factors. Such alternative explanations are supported by data shown in Figure 6.22, and data from other instrumented members, which show relatively stable bending moments in the instrumented members during the period over which creep rates were estimated. These data therefore do not support the observation that creep is occurring in the reinforcing members but rather that the steady increases in deformation is a product of other factors. Alternative explanations are also supported by the fact that observed precipitation during the period over which creep rates were estimated was generally equal to or greater than 50-year averages. Piezometric levels and soil moisture/suction measurements also suggest that pore pressures were elevated during this period. As such, the steady increases in movements could very well be a result of additional mobilization or other phenomena. Furthermore, Figure 6.31 shows that very little deformation was observed between summer 2001 and summer 2003 suggesting that creep was not significant during this previous monitoring period and, therefore, that alternative explanations for the movements between September 2003 and September 2004 are possible or even likely. Additional discussion regarding the potential for creep is presented in subsequent chapters.

6.6. Summary

The activities performed to establish three separate test areas at the I70-Emma test site were described in this chapter. The site includes four separate slide areas that have experienced repeated failures in the past. Two of these slide areas were stabilized during Phase I while the remaining two slide areas were used as control sections. Both control sections subsequently failed in spring 2001 and one of the former control slide areas was subsequently selected for stabilization during Phase II. The performance of the stabilized areas has been monitored for as long as five years. The performance of the stabilized sections has been consistent with that observed at other sites and consists of a period of little movement, one or more periods of increasing movements that are necessary to mobilize the resistance in the reinforcing members, followed by periods of stable conditions where the resistance provided by the reinforcement is sufficient to maintain equilibrium of the slope. To date, all test sections stabilized using members placed at spacings of 4.5-ft or less have remained stable while control sections without reinforcement have failed. A failure did occur in two stabilized sections where members were placed at spacings as large as 6-ft. Post-failure investigations performed to evaluate the failure revealed that the reinforcing members did fail structurally during the failure. Observations of performance suggest that creep may play a role in the performance of slopes stabilized using recycled plastic members; however, alternative explanations can also explain the observed performance so additional evaluations are necessary to confirm the role of creep.

Chapter 7. I435-Kansas City Sites

The second and third field test sites selected for the project are located in southern Kansas City Missouri in close proximity to one another along Interstate 435 near the Missouri-Kansas border. One site is located at the intersection of I435 and Wornall Road; the second is located at the intersection of I435 and Holmes Road approximately one mile east of the first site. This chapter contains descriptions of the two stabilization sites, the instrumentation used to monitor the sites, and a summary of the field performance of each slope during the monitoring period.

7.1. Site Characteristics

A map showing the locations of the I435-Kansas City sites is shown in Figure 7.1. The I435-Wornall Road test site is located in the northeast quadrant of the intersection of I435 and Wornall Road between I435 and the westbound exit ramp. The I435-Holmes Road test site is located approximately one mile east of the I435-Wornall Road site. The slope lies in the southeast quadrant of the intersection of I435 and Holmes Road between I435 and the eastbound entrance ramp. Both slopes are bridge approach embankments that serve to support I435 as it passes over Wornall and Holmes roads, respectively. A third slope located in the southwest quadrant of the I435-Wornall Road intersection was used as a control section for both of these sites.

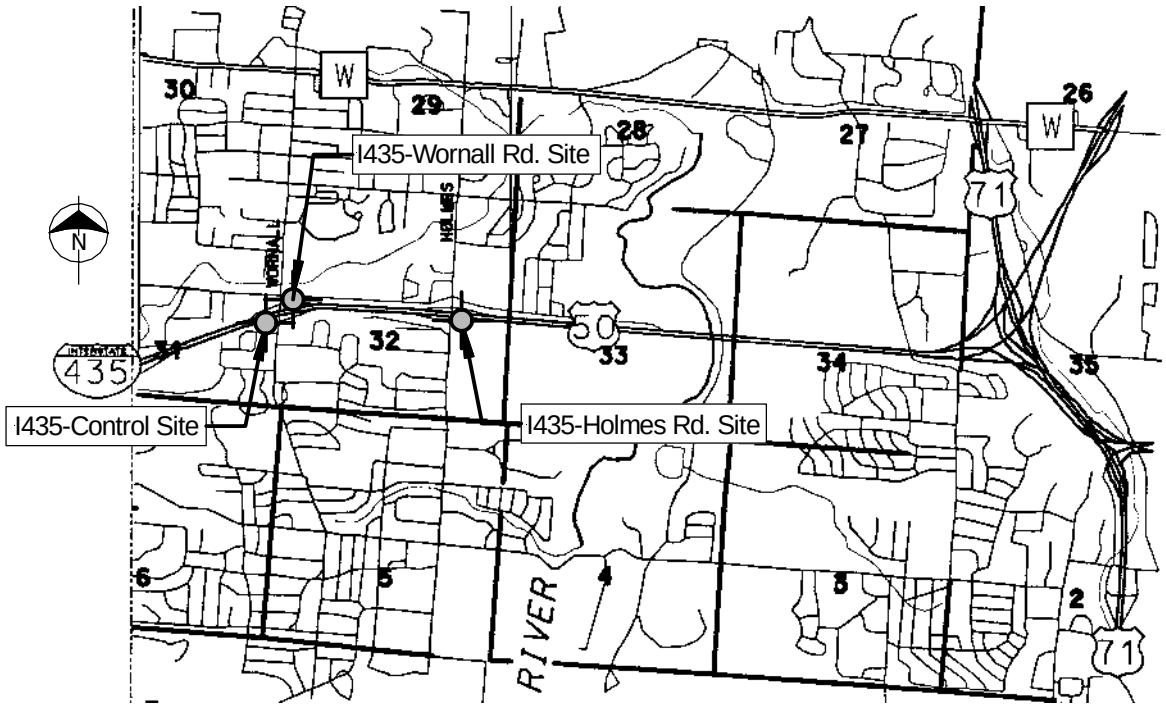

Figure 7.1 Map of southern Kansas City Missouri showing locations of I435-Kansas City test sites.

7.1.1. I435-Wornall Road Site

The I435-Wornall Road embankment is a zoned-fill embankment consisting of a 3- to 5-ft (0.9- to 1.5-m) thick surficial layer of mixed lean to fat clay with soft to medium consistency, overlying stiffer compacted clay shale. The embankment is approximately 32-ft (9.6-m) high with side slopes of 2.2H:1V (horizontal:vertical). The embankment had experienced surficial slides along the interface between the upper clay and the lower compacted clay shale on at least two occasions prior to being selected for stabilization as part of this project. Figure 7.2 shows a photograph of the site following the most recent slide event, which affected approximately 125-ft (38-m) of the embankment (measured parallel to I435). Prior to the most recent slide, extensive ornamental vegetation had been placed on the slope along with 4- to 6-in (100- to 150-mm) of gardening mulch as a part of a neighborhood beautification project. The most recent slide took out a large amount of this vegetation and caused much of the gardening mulch to become mixed with the surficial soils.

Figure 7.2 Photograph of most recent slide at I435-Wornall Road test site, June 20, 2001.

Boring and sampling at the I435-Wornall Road site was performed by MoDOT drilling crews during the period June 25-27, 2001. A total of seven hollow-stem auger borings were made in the slide area to depths varying from 10- to 30-ft (3- to 9-m). A plan view of the site showing boring locations is provided in Appendix B along with logs of all borings. In all but one boring, continuous 3-in (7.6-cm) diameter Shelby tube samples were taken and extruded in the field for visual description and field testing. Samples were then wrapped in aluminum foil and sealed with paraffin for subsequent transportation to the Geotechnical Engineering laboratories at the University of Missouri-Columbia. Obtaining good quality samples at shallow depths within the slide area proved difficult because of the presence of the gardening mulch that had become mixed with the surficial soils. In one boring, Standard Penetration Tests (SPT) were performed at 1.5-ft (0.5-m) intervals until

refusal. SPT N_{60}-values reported for the surficial layer ranged from 0 (weight of hammer) at the surface to 2 at a depth of 4-ft (1.2-m) while values at greater depth ranged from 6 to 16. Auger refusal was generally encountered at a horizontally bedded limestone layer located at depths ranging from 12-ft (3.7-m) near the toe of the slope to 32-ft (9.8-m) at the crest. Groundwater was not observed in any of the boreholes during boring and sampling; however, a groundwater condition was evident from the presence of water on the slope face within the lower third of the slope.

Laboratory tests performed on samples obtained from the I435-Wornall Road test site included natural moisture content tests, Atterberg limits, and triaxial tests. Results of these tests indicate soils from the surficial layer had liquid limits (LL) ranging from 38 to 51 and plasticity indices (PI) from 16 to 34. The compacted shale present below the surficial layer had LL ranging from 29 to 76 and PI from 12 to 51.

Consolidated-undrained ($\overline{CU}$, $\overline{R}$) type triaxial compression tests with pore water pressure measurements were performed on a total of 10 specimens from the I435-Wornall Road site. Stress paths determined from these tests are plotted in Figure 7.3 along with failure envelopes established for surficial (< 4-ft) and deeper (> 4-ft) soils. Mohr-Coulomb strength parameters for these envelopes are summarized in Table 7.1. For the surficial soils (Fig. 7.3a), all tests indicated a consistent effective stress failure envelope with $\overline{c} = 0$ and $\overline{\phi} = 27$ degrees. For deeper soils, three different effective stress failure envelopes were established: a "lower bound" failure envelope, an "upper bound" failure envelope, and an "alternative" failure envelope as shown in Figure 7.3b. For the deeper soils, $\overline{c}$ was found to vary between 0- and 120-psf (5.7 kPa) and $\overline{\phi}$ was found to vary between 23 and 31 degrees.

Table 7.1 Summary of Mohr-Coulomb effective stress strength parameters from triaxial compression tests on specimens from the I435-Wornall Road test site.

			upper bound		lower bound		"alternative"	
Stratum	Depths	Sample Numbers	$\overline{c}$ (psf)	$\overline{\phi}$ (°)	$\overline{c}$ (psf)	$\overline{\phi}$ (°)	$\overline{c}$ (psf)	$\overline{\phi}$ (°)
Surficial clay	< 4.0-ft	38A, 38B 106, 152	0	27	--	--	--	--
Deeper clay	> 4.0-ft	60, 64, 108, 111, 142A, 142B	0	31	0	26	120	23

7.1.2. I435-Holmes Road Site

The I435-Holmes Road site embankment also consists of a surficial layer of mixed lean to fat clay overlying compacted clay shale. The surficial layer varied in thickness between 3- and 6-ft (0.9- to 1.8-m). The site had experienced at least one failure prior to being selected for stabilization as a part of this project. Figure 7.4 shows a photograph of the slope following this slide event. At the location of the slide, the embankment is approximately 15-ft (4.6-m) high with a slope varying from 2.2H:1V near the crest to 2.6H:1V near the toe of the slope.

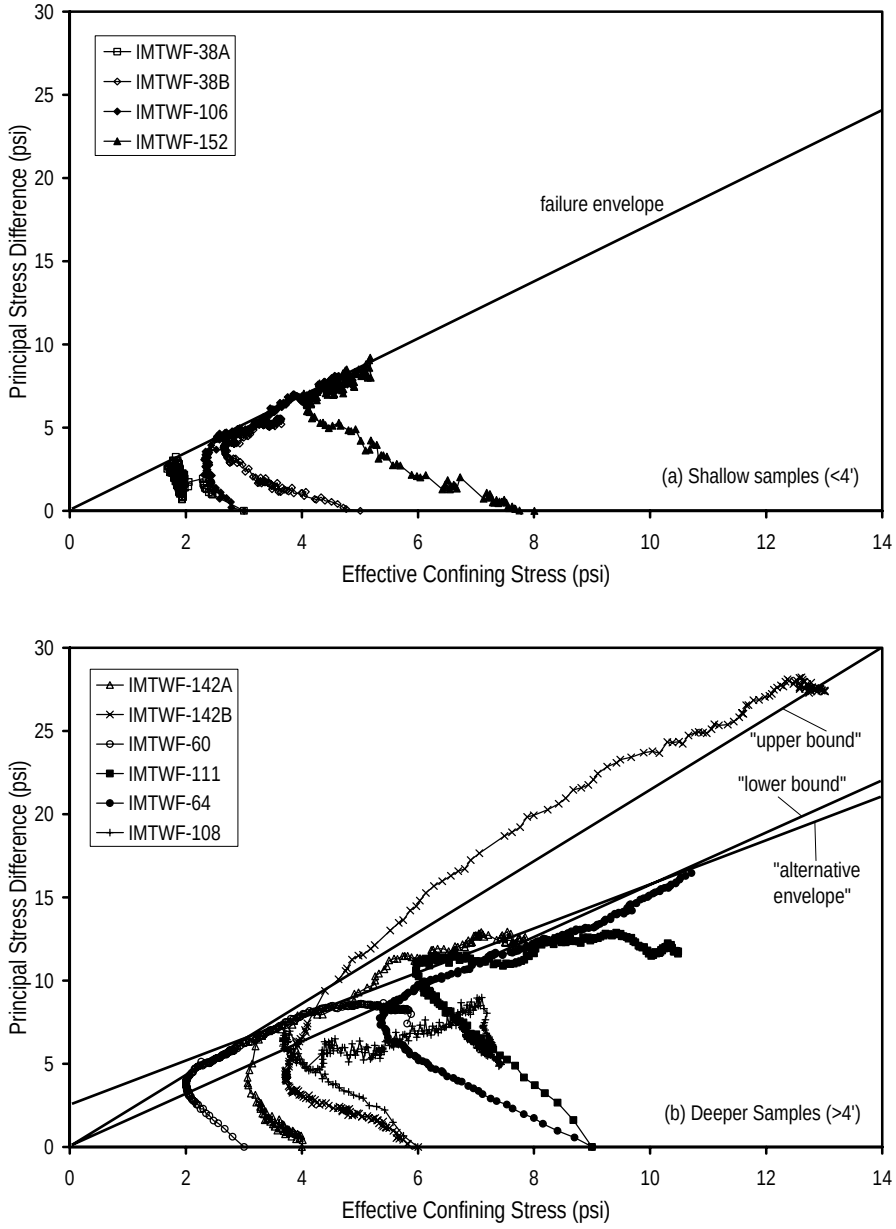

Figure 7.3 Summary of triaxial test results for specimens from I435-Wornall Road site: (a) shallow samples and (b) deeper samples.

No site investigation was performed at the I435-Holmes Road site prior to stabilization. However, one boring made during installation of an inclinometer for the test site was logged on July 11, 2002. Logs from this boring, located near the center of the slide area, indicate that the surficial lean clay material at this location was approximately 4.5-ft (1.4-m) thick and of medium stiff consistency. This layer is underlain by approximately 1-ft (0.3-m) of medium stiff, compacted clay shale, which in turn is underlain by much stiffer clay shale. SPT N_{60}-values determined at depths between 5.3- and 7.8-ft exceeded 100 blows per foot.

Figure 7.4 Photograph of the I435-Holmes Road site prior to stabilization.

7.1.3. I435 Control Slide

A third slide area, located in the southwest quadrant of the intersection of I435 and Wornall Road and shown in Figure 7.5, was selected for use as a control section for both the I435-Wornall and I435-Holmes test sites. One boring was made at this site on July 10, 2002 during installation of instrumentation for the slope. This boring revealed that the stratigraphy of the control slide was similar to that observed for the I435-Wornall Road and I435-Holmes Road slides with 5- to 7-ft of mixed lean to fat clay overlying hard compacted clay shale.

Figure 7.5 Photograph of the I435 Control Slide prior to being regraded for use as a control section.

7.2. Design of Stabilization Schemes

An extensive series of stability analyses were performed to establish the stabilization schemes to be utilized at the respective sites. All analyses were performed using the commercial slope stability software UTEXAS4 (Wright, 2001), which utilizes the limit equilibrium approach. Stability analyses for alternative reinforcement scenarios were performed in general accordance with procedures described in Bowders and Loehr (2003), which is similar to that described in Chapter 2. The following sections describe the stability analyses performed and the stabilization scheme selected for each site.

7.2.1. Stabilization Scheme for I435-Wornall Road Site

The general design cross-section used for the I435-Wornall Road site is shown in Figure 7.6. The ground surface profile was determined from a survey performed for MoDOT following the most recent slide event. The subsurface geometry was assumed to consist of a relatively thin surficial layer overlying compacted clay shale based on results of boring and sampling at the site. The thickness of the surficial layer was varied between 3-ft (0.9-m) and 5-ft (1.5-m) for different analyses.

Because the landscaping mulch became intermixed with the surficial soils during the slide, it was difficult to obtain high quality specimens of the surficial soils for testing. The strength parameters determined for this material were therefore deemed questionable. As a result of this, and the fact that the pore pressure conditions leading to the failure were unknown, a series of back-analyses was performed to establish several plausible sets of conditions that could have led to the failure. All analyses were effective stress stability analyses assuming fully drained, steady state seepage conditions.

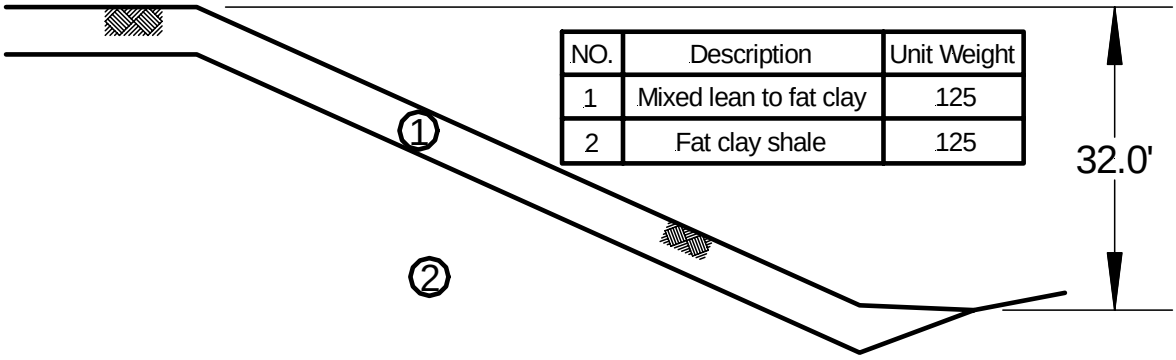

Figure 7.6 Design cross-section for I435-Wornall Road slope.

For the back-analyses, the strength parameters for the compacted clay shale material were taken to be $\bar{c} = 30$-psf and $\bar{\phi} = 27$ degrees based on laboratory tests performed on specimens from near the sliding surface. Several different pore pressure conditions were considered including a case where the pore pressures were assumed to be zero, a case where the pore pressures for both strata were defined by a piezometric surface lying at the ground surface, and a case with "perched" water conditions where pore pressures within the lower stratum were assumed to be zero and pore pressures within the upper stratum were defined by a piezometric surface coincident with the ground surface. For each of these pore pressure conditions and surficial layers of varying thickness, the value of $\bar{c}$ producing a factor of

safety of 1.0 was back-calculated assuming that $\bar{\phi}$ for the surficial soil was either 10 or 20 degrees. For several additional cases, $\bar{c}$ was alternatively assumed to be zero and the value of $\bar{\phi}$ was back-calculated to give a factor of safety of 1.0. The results of all back-analyses were then evaluated with respect to whether they produced a critical sliding surface that was reasonably similar to the observed sliding surface. Conditions that did not produce a reasonable sliding surface were eliminated from further consideration. The conditions that did result in a reasonable critical sliding surface were considered plausible conditions leading to the failure. These conditions are summarized in Table 7.2.

Table 7.2 Summary of plausible conditions leading to the failure at the I435-Wornall Road site.

Stability Case	Thickness of Upper Stratum (ft)	Pore Pressure Condition	Assumed Strength Parameter	Back-calculated Strength Parameter
A	3.0	u=0	$\bar{\phi}$ =10°	$\bar{c}$ =79 psf
B	3.0-5.0[1]	piezo. line – upper stratum	$\bar{\phi}$ =10°	$\bar{c}$ =99 psf
C	3.0-5.0	u=0	$\bar{\phi}$ =20°	$\bar{c}$ =21.5 psf
D	3.0	piezo. line – upper stratum	$\bar{\phi}$ =20°	$\bar{c}$ =64.5 psf
E	5.0	piezo. line – upper stratum	$\bar{\phi}$ =20°	$\bar{c}$ =100 psf
F	3.0-5.0	piezo. line – upper stratum	$\bar{c}$ =0	$\bar{\phi}$ =47°

[1] thickness of upper stratum varies from 3-ft (0.9-m) at crest of slope to 5-ft (1.5-m) at toe

Once the plausible conditions that could have led to the failure were established, analyses were performed to estimate the factors of safety of the slope under a series of different reinforcement scenarios. Factors of safety computed for each of these reinforcement scenarios are summarized in Table 7.3 for each plausible stability case. Based on the results of these analyses, the reinforcement scheme shown in Figure 7.7 was selected for stabilization of the slope. The selected reinforcing scheme included a total of 643 reinforcing members. Reinforcing members were placed on a 3-ft by 3-ft (0.9-m by 0.9-m) staggered grid (with every other row offset by one half the spacing) over the area where previous slides had occurred. Additional reinforcing members were placed on a coarser 3-ft by 6-ft (0.9-m by 1.8-m) grid above the slide area to reduce the potential for future sliding in the upper portion of the slope. The factor of safety for the selected reinforcement configuration was estimated to be between 1.15 and 1.50.

7.2.2. Stabilization Scheme for I435-Holmes Road Site

The I435-Holmes Road slope was stabilized using 3.5-in diameter galvanized steel pipe with 0.188-in (0.48-cm) thick walls. For design purposes, these members are considered to be "strong" members in the sense that the limit resistance for the members is controlled entirely by the strength of the soil rather than by both the strength of the soil and the strength of the reinforcing members as is generally the case for recycled plastic members. These members were therefore selected to compare the overall effectiveness of the respective member types for installation and stabilization.

Table 7.3 Summary of factors of safety determined for the I435-Wornall Road site.

Reinforcement Spacing (ft)	Factor of Safety for Respective Stability Case				
	A	B	C	D	E
3L x 3T[1]	1.50	1.44	1.29	1.28	1.28
3L x 6T	--	--	1.14	1.20	1.12
3L x 3T in middle third; 3L x 6T elsewhere	--	--	1.17	1.31	1.19
3L x 3T in middle third only	--	--	1.09	1.08	1.13
3L x 3T in upper third only	--	--	--	1.00	1.00
3L x 3T in lower third only	--	--	--	1.00	1.00
3L x 6T in upper third only	--	--	--	1.06	1.06
3L x 6T in lower third only	--	--	--	1.05	1.10

[1] L and T denote spacing in longitudinal (strike) and transverse (dip) directions, respectively

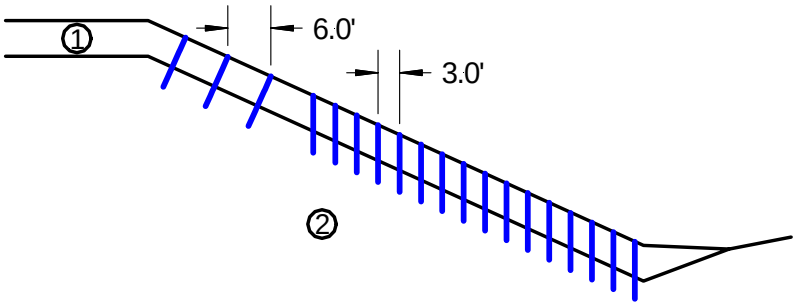

(a) cross-section view

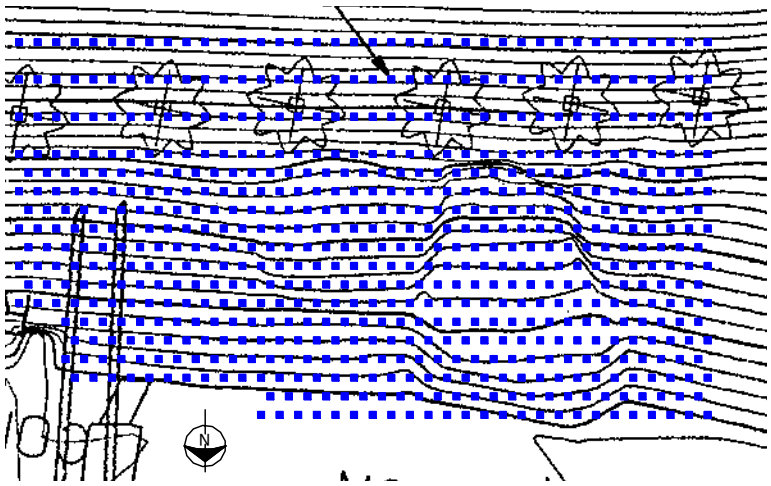

(b) plan view

Figure 7.7 Selected stabilization scheme for the I435-Wornall Road site: (a) cross-section and (b) plan view superimposed on elevation contours of the site established following the most recent slide.

Figure 7.8 shows the assumed design cross-section for the I435-Holmes Road slope. Because no site specific soil property data was available prior to stabilization of the I435-Holmes Road site, no specific stability analyses were performed to select a stabilization scheme for this slope. Rather, the stabilization scheme was selected based on previous experience at the I70-Emma site during Phase I of the project and at the I435-Wornall Road site. The selected stabilization scheme, shown in Figure 7.9, generally consisted of reinforcement placed on a 3-ft by 3-ft (0.9-m by 0.9-m) staggered grid similar to that used at the I70-Emma site during Phase I and at the I435-Wornall Road site. However, given that the previous sliding surface was believed to be greater than 8-ft (2.4-m) deep near the center of the slope, three rows of reinforcement were left out of the grid to reduce costs while still maintaining a reasonable degree of stability against shallower slides in this portion of the slope. The selected stabilization scheme included a total of 276 reinforcing members. Most of these members were to be installed vertically while three of the top four rows of members were inclined perpendicular to the slope to ensure that they extended beyond the observed sliding surface.

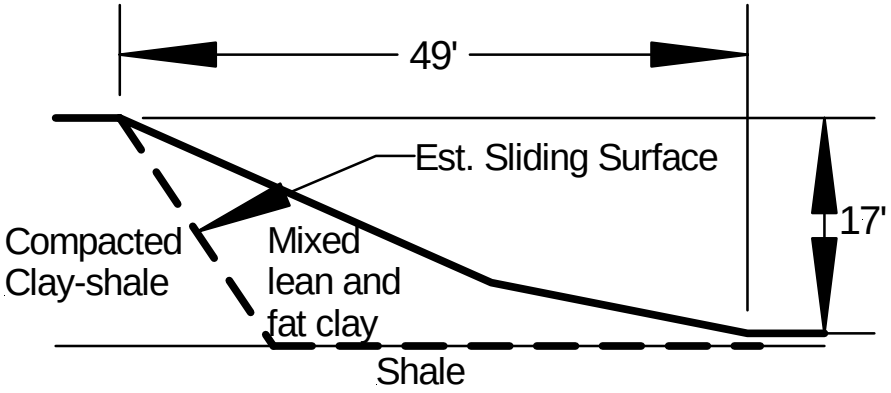

Figure 7.8 Assumed design cross-section for I435-Holmes Road slope.

7.3. Field Installation

Field installation at the I435-Wornall Road test site began in October 2001 and was completed in December 2001, following a delay in delivery of recycled plastic members to the site. Installation at the I435-Holmes Road test site occurred during December 2001 following completion of installation at the I435-Wornall Road site. Details of the installation activities at each of the test sites are provided in Chapter 10.

7.4. Instrumentation

Instrumentation installed at the I435 test sites to monitor performance included slope inclinometers, standpipe piezometers, reinforcing members instrumented with strain gages and force-sensing resistors, and soil moisture and suction sensors. The following sections describe the specific instrumentation installed at each test site.

7.4.1. Instrumentation for the I435-Wornall Road Site

A schematic showing the location of instruments installed at the I435-Wornall Road site is shown in Figure 7.10. The instrumentation at this site included four inclinometers,

four instrumented reinforcing members, two clusters of standpipe piezometers, and an array of moisture instrumentation.

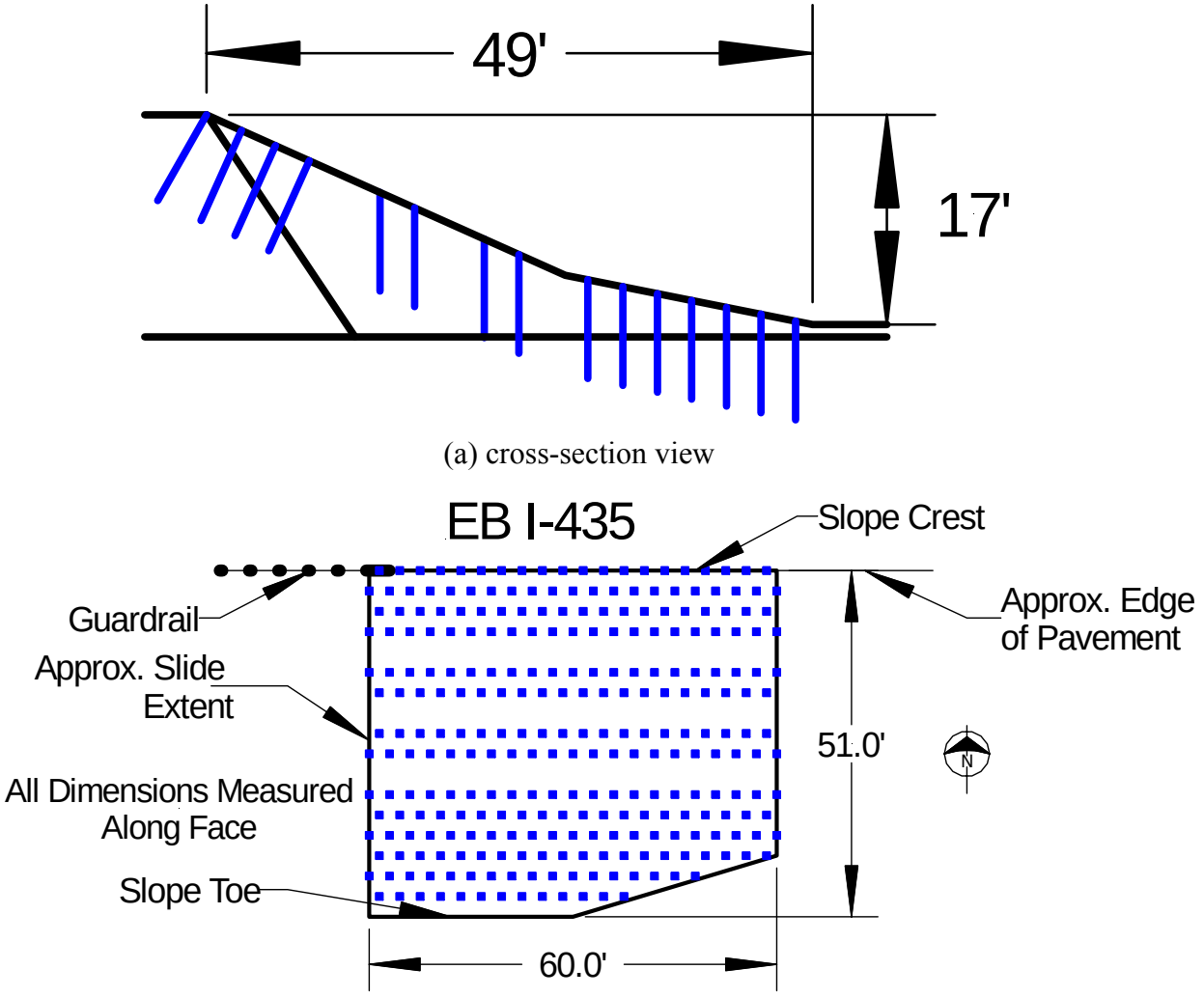

(a) cross-section view

(b) plan view

Figure 7.9 Selected stabilization scheme for the I435-Holmes Road site: (a) cross-section and (b) plan view.

Instrumented reinforcing members were installed during installation of all reinforcing members. Two members, designated members IM-1 and IM-2, were installed near the center of the slide in close proximity to one another. Instrumented member IM-3 was installed downslope of IM-1 and IM-2 while member IM-4 was installed near the center of the western half of the slide area where sliding initiated during the previous failure. Each of the instrumented members was driven to full depth. Wiring from the instrumented reinforcing members was buried in shallow trenches to extend to a weather resistant box located near the center of the site to provide protection for the electrical connections and a convenient location for connecting the data acquisition system.

Slope inclinometer casings were installed on November 27, 2001. Inclinometer I-1 was located near the center of the eastern half of the slide area at about the mid-point of the

slope. Inclinometers I-2 and I-3 were placed near the center of the slide area in close proximity to instrumented reinforcing members IM-1, IM-2, and IM-3. Inclinometer I-4 was placed adjacent to instrumented member IM-4 near the center of the western half of the slide area. Each inclinometer casing was founded in the stiff clay shale but was not extended into the limestone layer lying beneath the shale. Approximate depths for the respective inclinometers are 19.0-ft (5.8-m) for I-1, 26-ft (7.9-m) for I-2, 14.5-ft (4.4-m) for I-3, and 19.5-ft (5.9-m) for I-4. All casings were cut off approximately 0.5-ft (15-cm) above the ground surface.

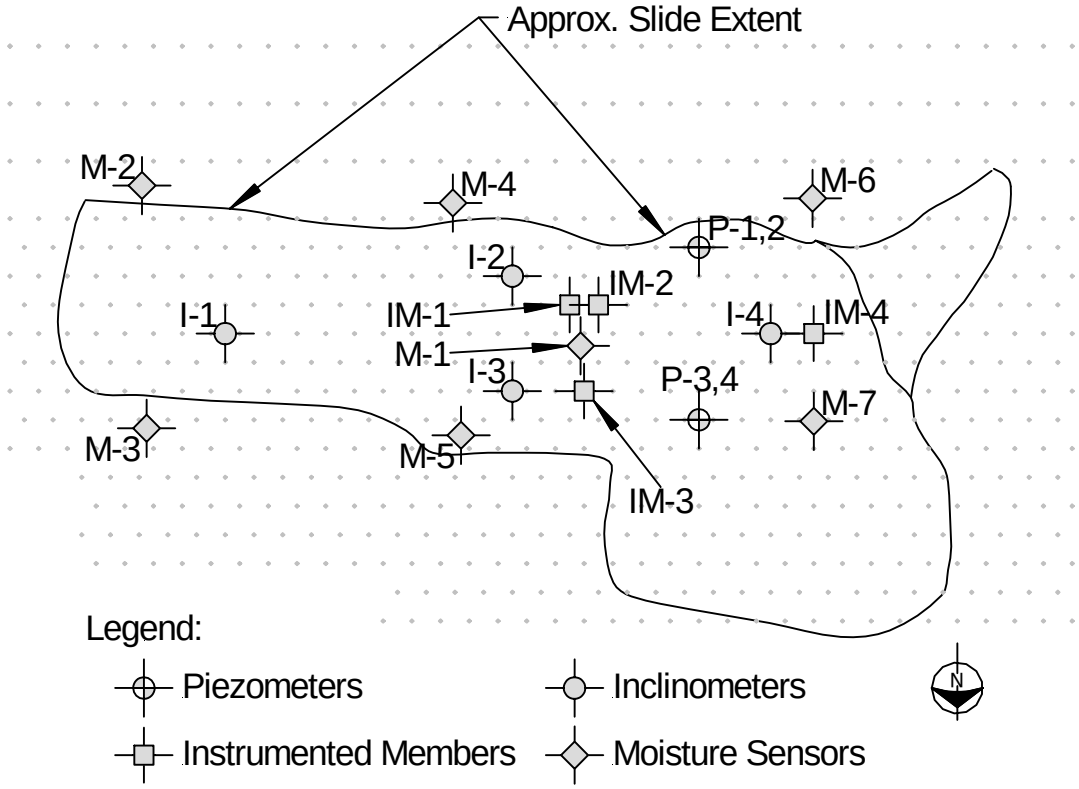

Figure 7.10 Instrumentation layout for I435-Wornall Road site.

Two clusters of standpipe piezometers were also installed in the western half of the slide area on July 10, 2002. One cluster containing piezometers P-1 and P-2 was installed near the location of the head scarp of the previous slide. Piezometer P-1 is screened at a depth of 11.6-ft (3.5-m) and P-2 at 5.0-ft (1.5-m). The second cluster of piezometers is located downslope of the upper cluster near the lower third-point of the slope. In this cluster, piezometer P-3 is screened at 11.0-ft (3.4-m) and P-4 at 4.0-ft (1.2-m).

Moisture instrumentation was installed at seven different locations, designated M-1 through M-7, on August 8, 2002. Profile Probe® access tubes were installed at each of these locations to measure the variation of moisture content with depth at each location at discrete time intervals as well as to establish the variability of moisture contents over the entire slide area. At location M-1, an array of two ThetaProbes® and two Equitensiometers® was installed in close proximity to the Profile Probe® access tube. ThetaProbes® were installed at depths of 8- and 24-in (20- and 60-cm) while Equitensiometers® were installed at depths of

16- and 40-in (40- and 100-cm). Each of these sensors were connected to a field data logger that permitted moisture content and soil suction readings to be taken at two hour intervals, thus enabling for essentially continuous measurement of moisture content and soil suction at location M-1.

7.4.2. Instrumentation for the I435-Holmes Road Site

A schematic of the instrumentation layout for the I435-Holmes Road site is shown in Figure 7.11. The instrumentation consisted of two instrumented steel pipe members, one inclinometer, one cluster of two piezometers, and two Profile Probe® access tubes.

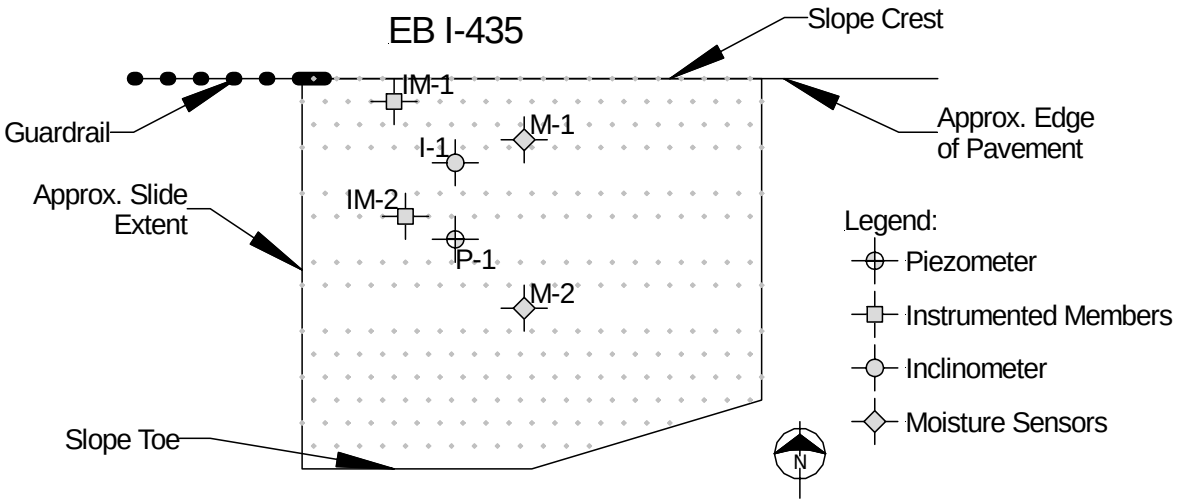

Figure 7.11 Instrumentation layout for I435-Holmes Road site.

The two instrumented members are located in the upper portion of the slope within the western half of the former slide area. Member IM-1 is an inclined member aligned roughly perpendicular to the slope face, while member IM-2 is inclined vertically. Because many of the members at this site could not be driven to full depth, the tips (bottom end) of the two instrumented members were cut off prior to installation to prevent having the members extend significantly above ground level. The length of the members that were cut off was determined from the measured penetrations of the surrounding members. Member IM-1 was cut to a length of 5.9-ft (1.8-m) while member IM-2 was cut to a length of 6.7-ft (2.0-m), eliminating the lowest pair of strain gages for both members.

The inclinometer and piezometers were installed by MoDOT drilling crews on July 11, 2002. The inclinometer casing was extended to a depth of approximately 18-ft (5.5-m) and founded in the stiff shale. The piezometers were installed within a single borehole and screened at different depths. Piezometer P-1 was screened at a depth of 2.5-ft (0.8-m); piezometer P-2 was screened at a depth of 13.0-ft (3.9-m). Profile Probe® access tubes were installed at two locations, designated M-1 and M-2, on October 9, 2002 to monitor water contents in the soils.

7.4.3. Instrumentation for the I435 Control Slope

Instrumentation for the I435 Control slope included one slope inclinometer and three Profile Probe® access tubes installed along a line passing through the center of the former

slide area. The inclinometer casing was installed near the center of the slide area to a depth of approximately 20-ft (6.1-m) on July 11, 2002. The three access tubes were installed on October 9, 2002, with access tube M-1 installed near the toe of the slope, access tube M-2 near the midpoint of the slope, and access tube M-3 near the crest of the slope.

7.5. Field Performance

Instrumentation at the I435-Kansas City test sites was monitored from installation through February 16, 2005. During this time, readings were taken on all field instrumentation at intervals ranging from 1 to 4 months. The measurements have been processed, analyzed, and interpreted to produce the results presented in this section to demonstrate the performance of the stabilized slopes. The instrumentation has, in general, performed well. However, problems were encountered with the soil moisture/soil suction devices beginning in Summer 2003 that rendered the devices inoperable or unreliable. Furthermore, by summer 2005 a sufficient number of strain gages had deteriorated to the point where making reasonable interpretations was extremely difficult if not impossible. Observations from these instruments are therefore limited to the period between installation and summer 2005.

7.5.1. Precipitation at I435-Kansas City Sites

Figure 7.12 shows daily and monthly precipitation totals recorded at the weather station at Lee's Summit Municipal Airport, located approximately 4-miles (6.4-km) east of the test sites. Precipitation patterns observed since installation have been rather typical with relatively heavy precipitation during the Spring and significantly less precipitation throughout the rest of the year. Precipitation during the first few months after installation was generally limited with the exception of a single heavy precipitation event in late January 2002. Precipitation then increased substantially between April and June 2002 with numerous heavy precipitation events and large monthly precipitation, especially in May and early June. Precipitation then decreased dramatically between July 2002 and March 2003 with an exceptionally dry period between July 2002 and February 2003. Precipitation then increased again during Spring 2003, although rainfall levels were not as great as those observed in Spring 2002. Precipitation in 2004 was general at or above 50-year average levels, especially in spring 2004 when monthly precipitation exceeded 50-year averages by more than 3 inches for three out of the five months between March and July of 2004.

7.5.2. Performance of I435-Wornall Road Site

7.5.2.a Pore pressure measurements

Figure 7.13 shows the water levels measured in the piezometers placed in the I435-Wornall Road slope. The first two readings taken are somewhat sporadic and are believed to be a result of the piezometers coming to equilibrium with the surrounding soils rather than a result of the actual water conditions within the slope. After this initial equalization period however, the piezometers appear to be providing reasonable readings. Piezometers P-1 and P-3, which are screened within the lower compacted clay shale, have consistently shown very similar readings with the exception of readings taken in July 2003, March 2004, and January 2005. The July 2003 and March 2004 readings are considered suspect and may be a result of operator error. Readings from piezometers P-2 and P-4, which are screened within the upper stratum, also follow a consistent trend with higher piezometric levels during the spring

months and lower piezometric levels during other parts of the year. These are consistent with observed precipitation records. Piezometric levels in piezometers P-2 and P-4 are also consistently higher than those in piezometers P-1 and P-3, which suggests a perched water condition exists within the upper stratum which is maintained throughout the year. Piezometric levels in piezometer P-4, located near the toe of the former slide area, are also consistently higher than those in P-2. Overall, the perched water condition is maintained at depths ranging from 0 to 2.5-ft below ground surface in the area of P-4 and at depths ranging from 2 to 5-ft below the ground surface higher up on the slope near P-2.

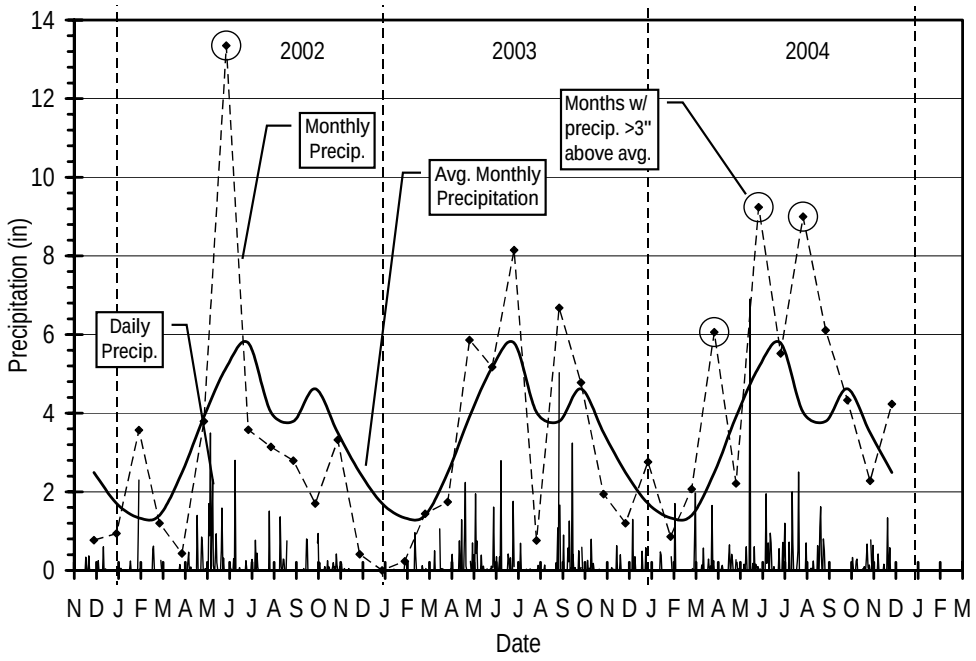

Figure 7.12 Monthly and daily precipitation from Lee's Summit Municipal Airport located 4 miles east of I435-Kansas City sites.

Readings taken for the Equitensiometers®, which measure soil suction directly, have consistently been out of range indicating that the soil has been essentially saturated since the sensors were installed. This further supports the piezometer readings for the shallow piezometers which suggest that positive pore pressures are present within the upper stratum. Readings taken for the ThetaProbes®, which measure volumetric water content, are plotted in Figure 7.14. Readings for both ThetaProbes® indicate increasing water content during Fall 2002. Water contents for the upper ThetaProbe® then decreased between November 2002 and February 2003 while water contents for the lower ThetaProbe® remained essentially constant during this time. Both probes indicate a significant increase in water content in early February 2003 in response to a single heavy precipitation event in late January 2003 followed by generally decreasing water contents since that time. ThetaProbe® readings began to become very erratic in early summer 2003. Readings taken after this time varied substantially and, even when they became more stable, indicated substantially lower volumetric water contents than are considered realistic. The data acquired following summer 2003 is therefore considered unrealistic.

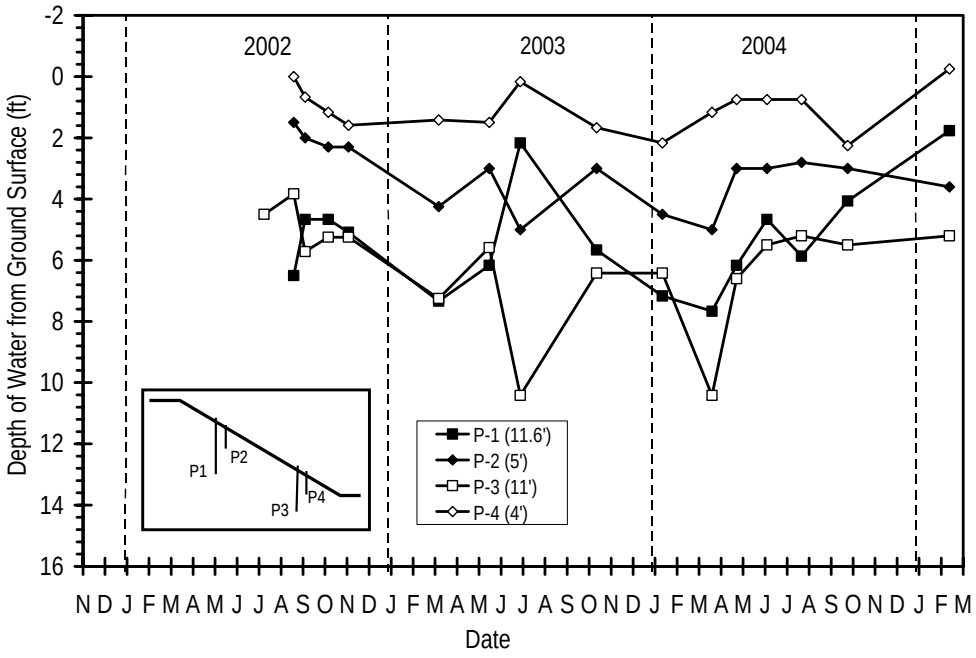

Figure 7.13 Piezometric water levels measured at I435-Wornall Road site.

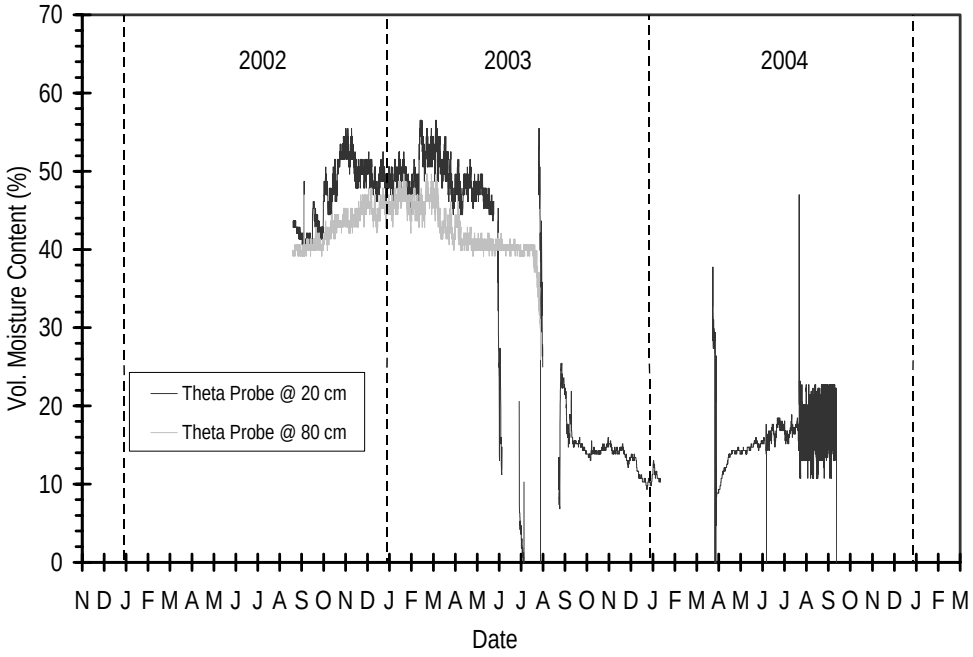

Figure 7.14 Volumetric water content from I435-Wornall Road test site.

7.5.2.b Inclinometer measurements

Lateral deformations determined from inclinometers I-3 and I-4 are plotted in Figures 7.15 and 7.16, respectively. As shown in the figures, two different forms of deflection profiles have been observed in the inclinometers. Inclinometer I-3 indicates that maximum

deformations are occurring near the ground surface with continuously decreasing deformations with depth. Inclinometer I-1 produced a similar profile with lower overall deformations. Inclinometer I-4 also shows that the maximum deformations are at the ground surface. However, I-4 also shows a significant discontinuity in the deformation profile at a depth between 8- and 10-ft (2.4- and 3.0-m), which indicates concentrated deformations at this depth indicative of sliding surface formation. Inclinometer I-2 produced a similar profile with a discontinuity between 10- and 12-ft (3.0- and 3.6-m). The differences in deformation profiles with depth are believed to be due to the different locations of the inclinometers within the slide area. Inclinometers I-4 and I-2 are both located within the central portion of the former slide area where sliding would be expected to be deeper while inclinometer I-3 is located near the toe of the former slide area where sliding would tend to be shallower. Inclinometer I-1 is located in the eastern portion of the former slide area where sliding was observed to be shallower than observed in the primary slide area to the west.

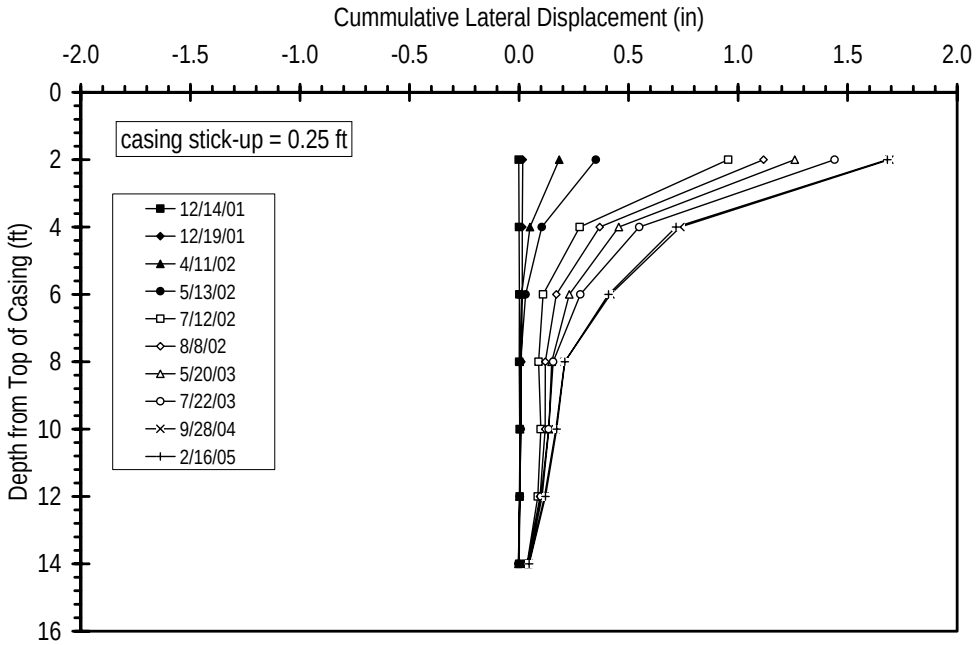

Figure 7.15 Lateral deflection profile for Inclinometer I-3 at I435-Wornall Road test site.

Cumulative deformations for all four inclinometers are plotted as a function of time in Figure 7.17. The deformations plotted are taken at a depth of approximately 4-ft because they are more representative of overall movements and because surficial deformations are sensitive to operator technique and are therefore more scattered. Figure 7.17 shows that all four inclinometers have a similar trend of deformation with time. Little movement was observed during the first few months following installation. Movements then increased substantially in April 2002 and continued to increase throughout the summer until leveling out in August/September 2002. Movements since that time have increased only slightly, presumably in response to increased precipitation and piezometric levels during the spring and early summer months. Maximum deformations for inclinometer I-4 is approximately 1.2

inches, while deformations in inclinometers I-2 and I-3 nominally 0.75-in. Deformations for inclinometer I-1 have been notably smaller.

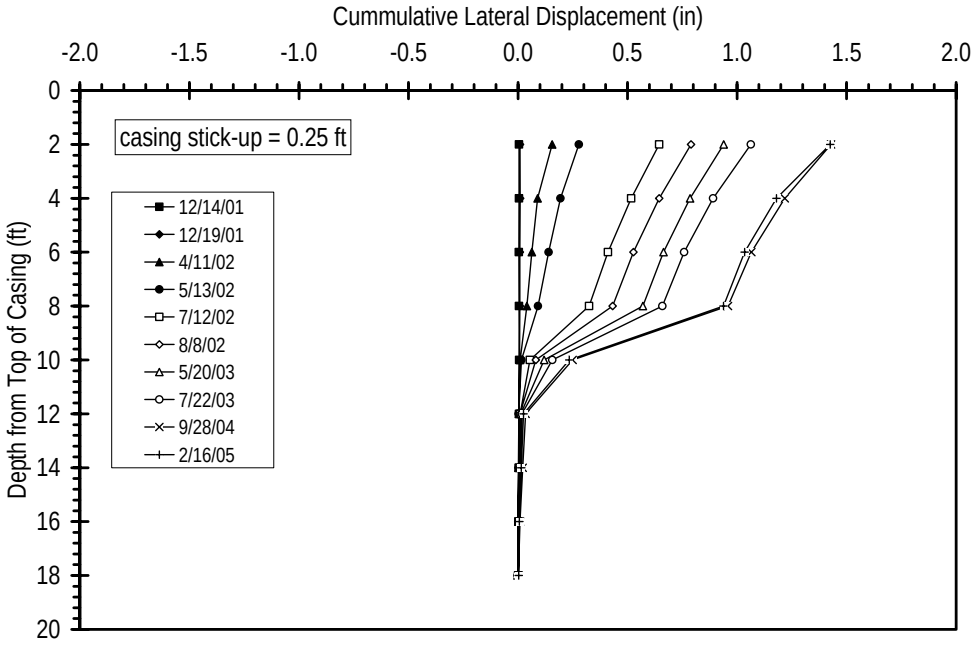

Figure 7.16 Lateral deflection profile for Inclinometer I-4 at I435-Wornall Road test site.

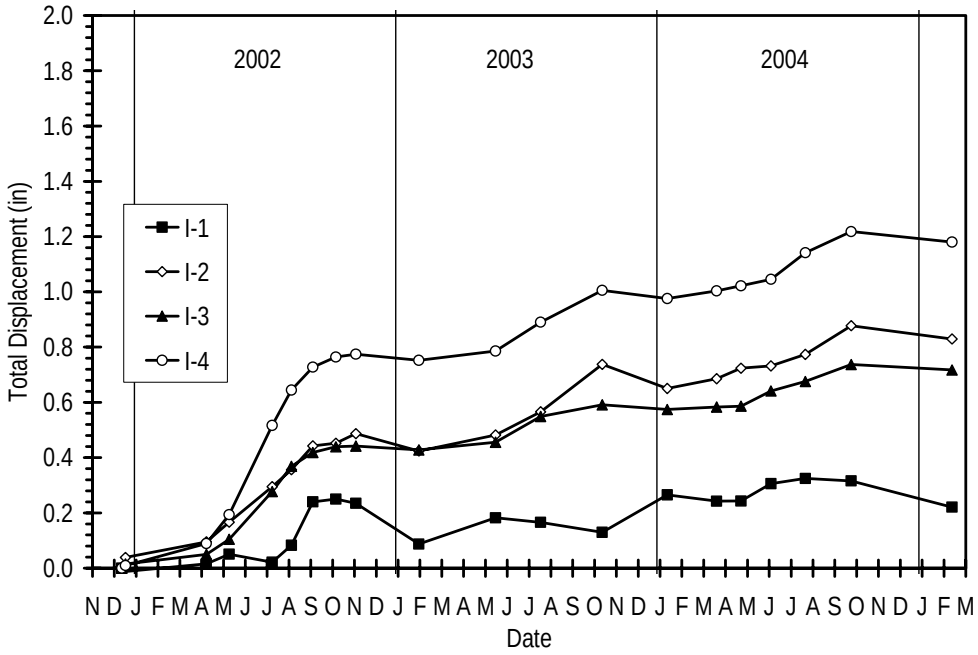

Figure 7.17 Cumulative lateral deflections at depth of 4 feet for inclinometers I-1 through I-4 at the I435-Wornall Road test site.

The pattern of movements observed at the I435-Wornall Road slope is consistent with those observed at the I70-Emma site, with an initial period of little movement followed by a period of increasing movements, after which movements are generally negligible. It is postulated that this movement sequence is a combined result of the pore pressure conditions within the slope and mobilization of resistance in the reinforcing members. Just after installation, the slope would be stable without the reinforcing members because of the low pore water pressures within the slope. However, during the first wet period following installation, the stability of the slope decreases in response to increasing pore water pressures. As the stability decreases, the slope begins to move which causes the reinforcing members to deflect and to begin mobilizing resisting loads. With continued higher pore pressures, the slope movement continues until the reinforcing members mobilize loads sufficient to create equilibrium in the slope. At this point, additional movement is resisted by the reinforcing members and movement essentially stops. Upon subsequent wetting and drying cycles, some resistance in the members is already mobilized which prevents significant additional movement unless the pore water pressures become significantly greater than have been experienced since installation. In cases where subsequent pore pressures are greater than previously experienced, additional movement produces additional mobilization of resistance required to reach a new equilibrium condition. This postulated load transfer is supported by the response observed in the inclinometers at the site.

7.5.2.c Instrumented reinforcing members

Figure 7.18 shows typical distributions of incremental axial stresses determined for the instrumented reinforcing members at the I435-Wornall Road test site. Members IM-1 and IM-2 had distributions of incremental axial stresses like that shown in Figure 7.18a, in which the maximum incremental axial stress is located near the midpoint of the member. In contrast, members IM-3 and IM-4 had distributions like the one shown in Figure 7.18b, with the maximum incremental stresses occurring within the lower portion of the members. Readings from all four instrumented members indicate development of tensile stresses since installation.

The maximum incremental and overall axial stresses in each member are plotted as a function of time in Figure 7.19. This figure shows that all four members had similar responses consisting of an initial period with little change in stress, followed by decreases in stress for a period of time, after which the axial stresses are essentially constant. This response is consistent with that observed in the inclinometers and with the postulated load transfer to reinforcing members. The maximum incremental axial stresses for the four instrumented members ranged from approximately -1000- to -2000-psi (-6900- to -14,800-kPa). These stresses are much greater than those measured at other field sites as described in subsequent chapters. The initial axial stresses developed in the members during installation were generally small (<200 psi).

Results from instrumentation readings indicate that all four members have experienced tensile strains/stresses since installation as shown in Figure 7.19a. The reason(s) for the development of tensile strains/stresses in the members following installation is not entirely understood, but the trend has been consistently observed at all field test sites. One possible explanation is that the observed tensile strains/stresses are a result of relaxation of compressive stresses induced in the members during installation. However, if this were true, it would suggest that the overall magnitude of the axial stresses would remain compressive or

near zero, but would not become significantly negative since there is no apparent loading mechanism to induce tension. However, the data clearly indicate significant overall tensile strains/stresses, which does not support this hypothesis. It is possible that the strain gages may not have accurately captured the full magnitude of the strains induced during installation, which would suggest that the actual overall stresses (including installation induced stresses) were actually shifted by some unknown amount. Another possible contributor to the tensile strains/stresses could be a result of thermal strains produced by changes in temperature. However, there is no apparent trend to the strains according to season so this is not believed to be a major contributor to the tensile strains.

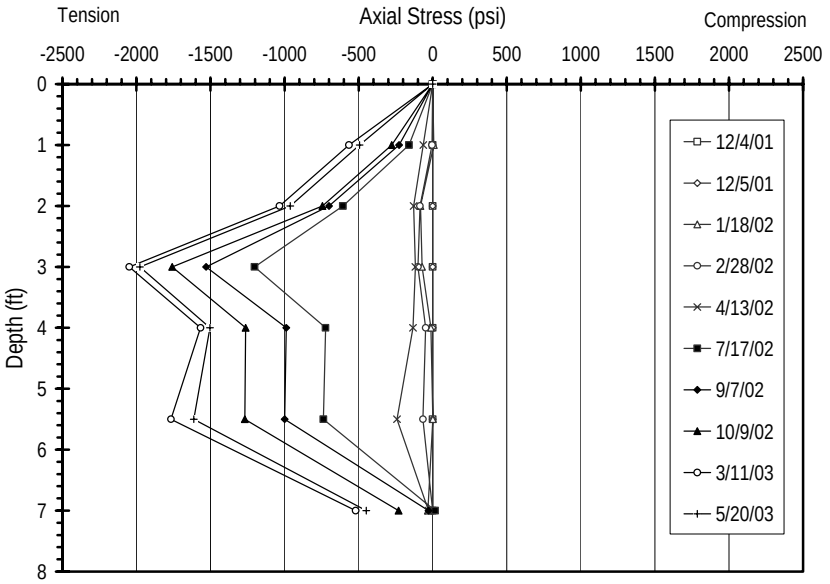

(a) instrumented member IM-1

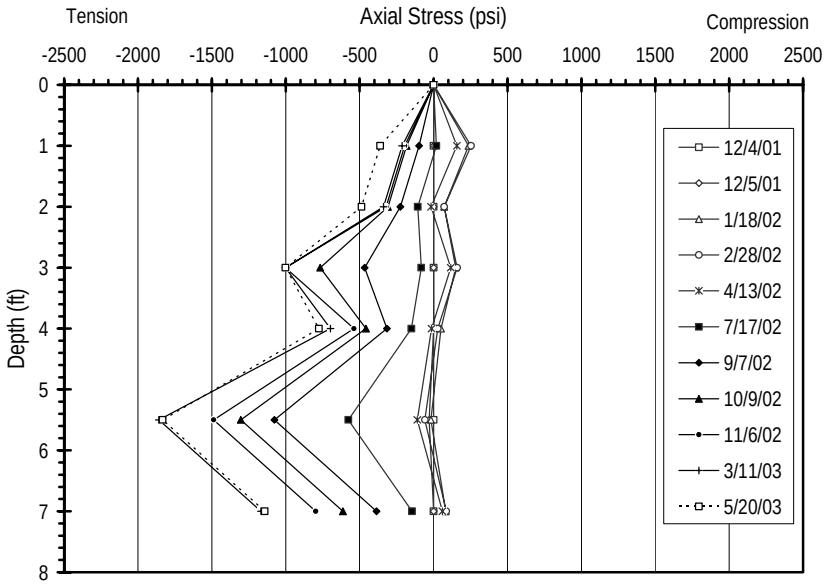

(b) instrumented member IM-3

Figure 7.18 Measured incremental axial stresses in instrumented members at I435-Wornall Road test site: (a) IM-1 and (b) IM-3.

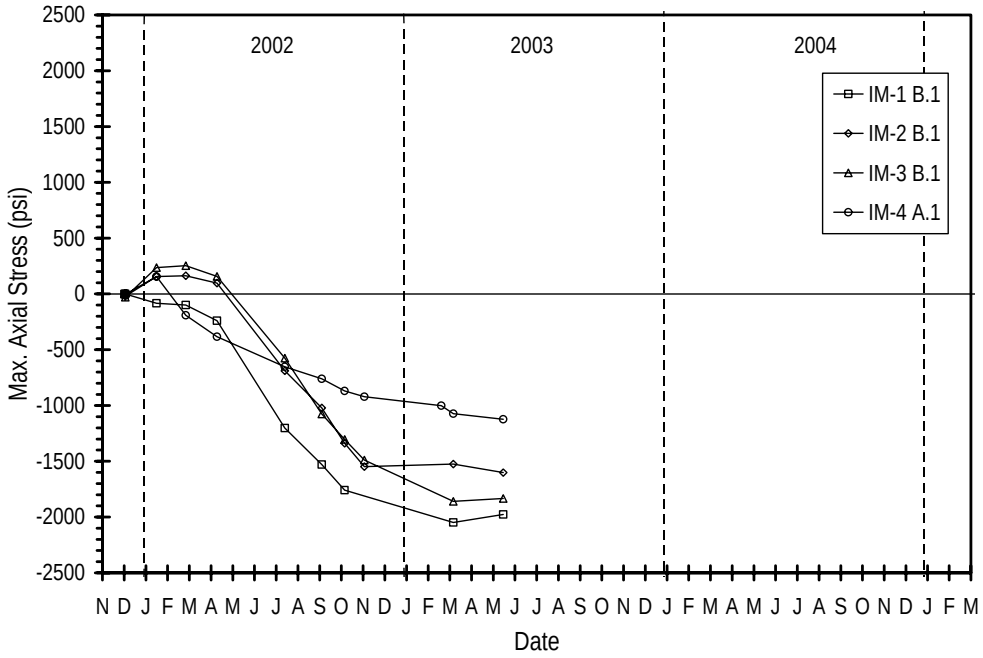

(a) incremental axial stress

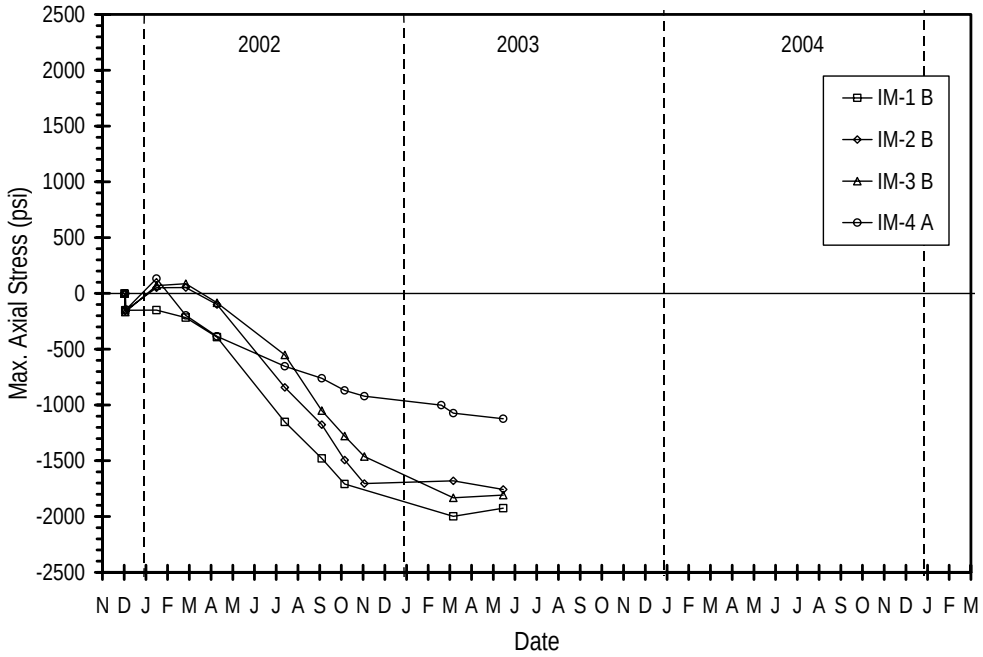

(b) overall axial stress

Figure 7.19 Maximum axial stress in instrumented members at I435-Wornall Road test site: (a) incremental axial stresses, and (b) overall axial stresses.

Figures 7.20 through 7.22 show the incremental distributions of bending moments determined for instrumented members IM-1, IM-2, and IM-4, respectively. The distributions of bending moments for these three members are distinctly different. Member IM-1

developed a roughly parabolic distribution of bending moments with depth, with all moments being negative (implying bending towards the crest of the slope). Member IM-2 also produced a roughly parabolic distribution of bending moments, but with all moments being positive (implying bending towards the toe of the slope). One would expect that the bending moments in these two members would be very similar given their close proximity on the slope so the difference in the sign of the moments is perplexing. Member IM-3, located near the toe of the slope produced a distribution similar to IM-2. Member IM-4 has a different distribution of moments, with positive moments near the top, near zero moments at the center, and positive moments in the lower portion of the member.

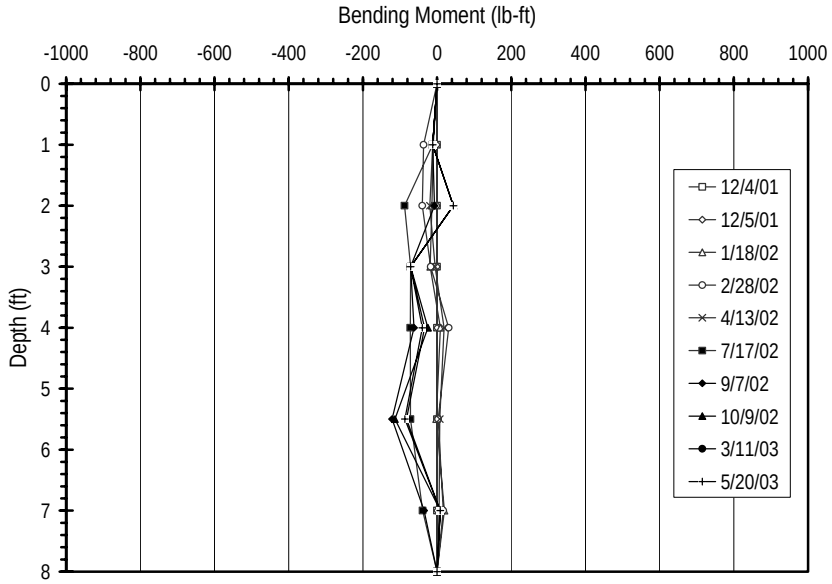

Figure 7.20 Measured incremental bending moments in instrumented member IM-1 at the I435-Wornall Road test site.

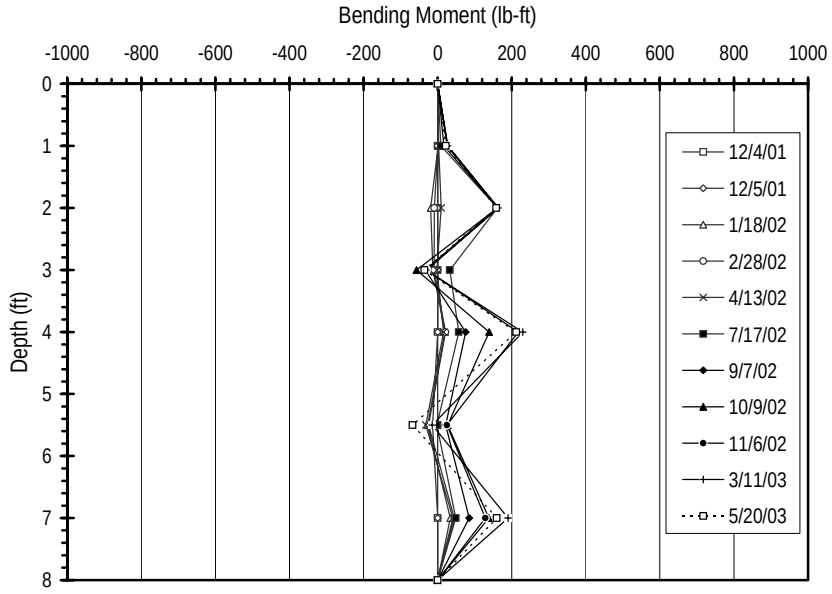

Figure 7.21 Measured incremental bending moments in instrumented member IM-2 at the I435-Wornall Road test site.

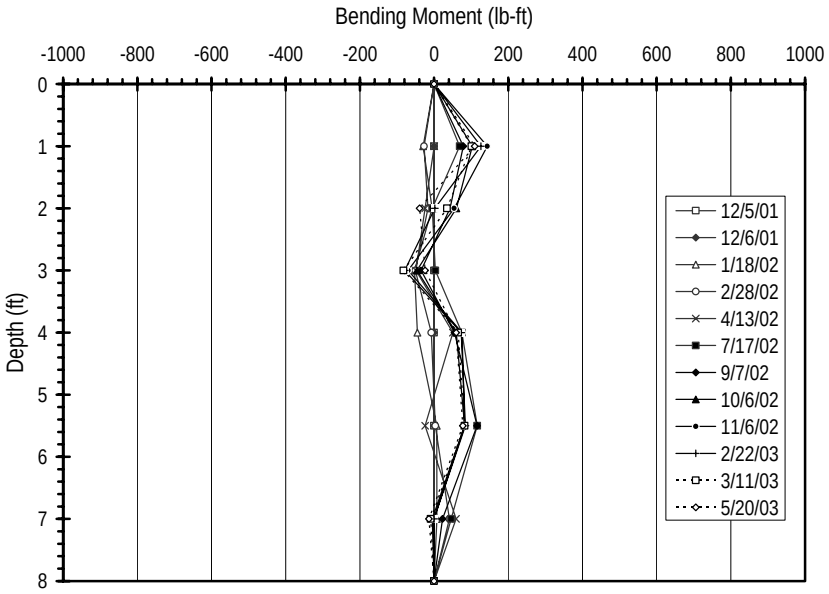

Figure 7.22 Measured incremental bending moments in instrumented member IM-4 at the I435-Wornall Road test site.

Figure 7.23 shows the maximum bending moments determined for each instrumented reinforcing member plotted as a function of time. As shown in Figure 7.23b, the initial bending moments developed during installation generally ranged from 20- to 120-lb-ft (27-160-N-m). Incremental bending moments in each member remained relatively low for several months followed by a period of relatively steady increases in the bending moments during and just following the period of high precipitation between April and June 2002. Since that time the maximum bending moments have remained steady, even during the spring of 2003. Member IM-3, located near the toe of the slope where pore pressures have been highest, has experienced the largest incremental and overall bending moments. However, these moments remain below 500-lb-ft (680-N-m), which indicates that the members have significant excess capacity remaining and are not near failure (nominal capacity is 1000-lb-ft).

To date, readings taken from the FSR on the instrumented reinforcing members have been below the "detection limit" of 1000-psf (50-kPa) discussed previously. While this limits the information provided by these sensors to some extent, these readings at least serve as an upper limit on the magnitude of the lateral pressures being applied to the reinforcing members, which is useful when interpreting the data from the strain gages.

Overall, the performance observed with the different types of instrumentation show a consistent behavioral pattern. Slope movements and mobilized loads in the reinforcing members increased in a consistent manner during the first period where pore water pressures were observed to increase following installation. Since that time, both the loads in the reinforcing members and the deformations observed in the slope have remained essentially constant or increased only slightly.

7.5.3. Performance of I435-Holmes Road and I435-Control Sites

Measured piezometric water levels recorded at the I435-Holmes Road site are plotted

in Figure 7.24. These data again indicate the presence of a perched water condition within the slope. The piezometric levels seem to be somewhat less responsive to rainfall events than those measured at the I435-Wornall Road site, particularly during Spring 2003. Figure 7.25 shows the lateral deformations determined at the I435-Holmes Road site. Lateral movements at this site have generally be limited to less than 0.25-in, while movement at the control sight have been negligible. Measured incremental axial stresses and bending moments in instrumented members in the I435-Holmes Road slope have also been negligible.

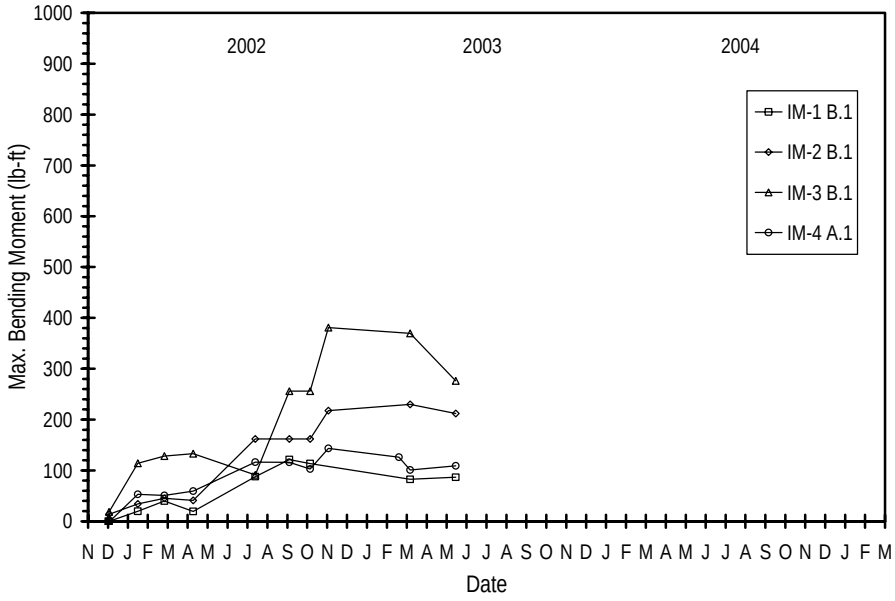

(a) incremental bending moments

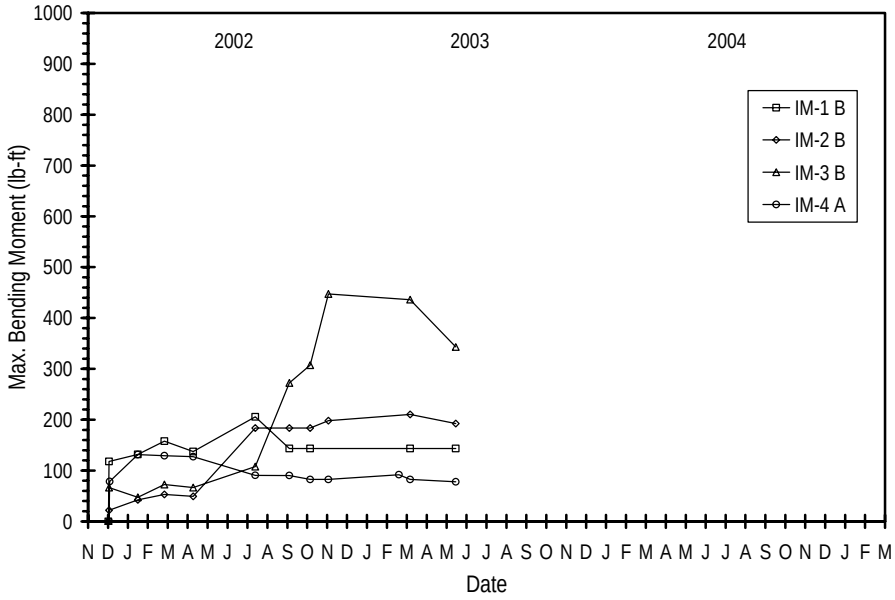

(b) overall bending moments

Figure 7.23 Maximum bending moments in instrumented members at I435-Wornall Road test site: (a) incremental bending moments and (b) overall bending moments.

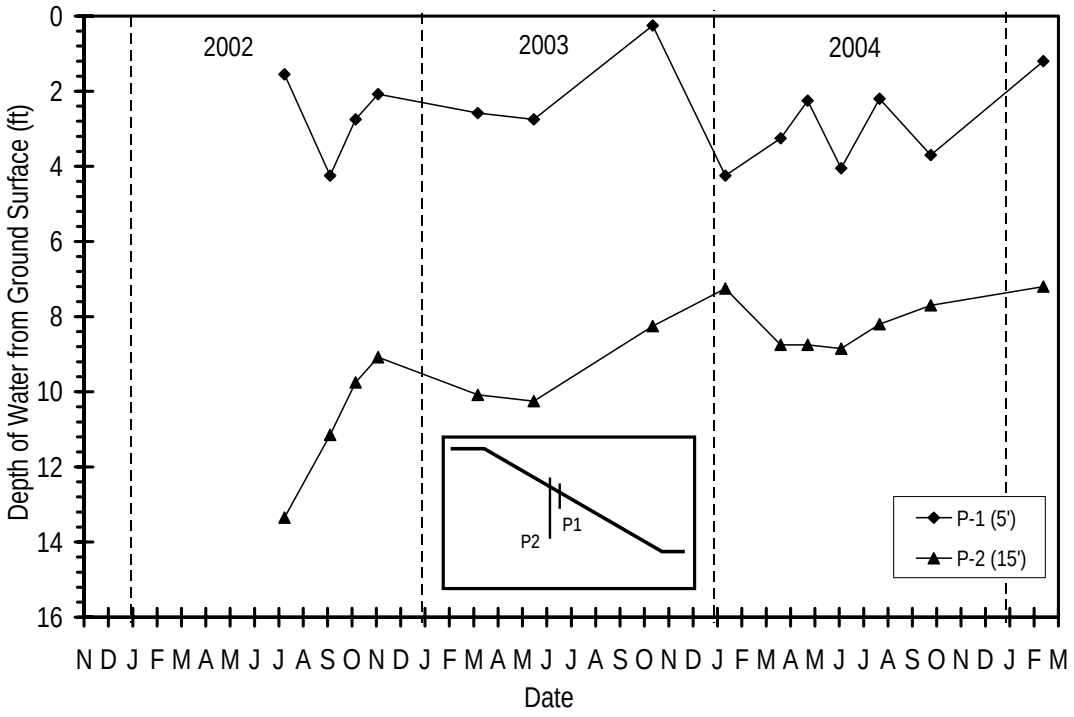

Figure 7.24 Piezometric water levels measured at I435-Holmes Road test site.

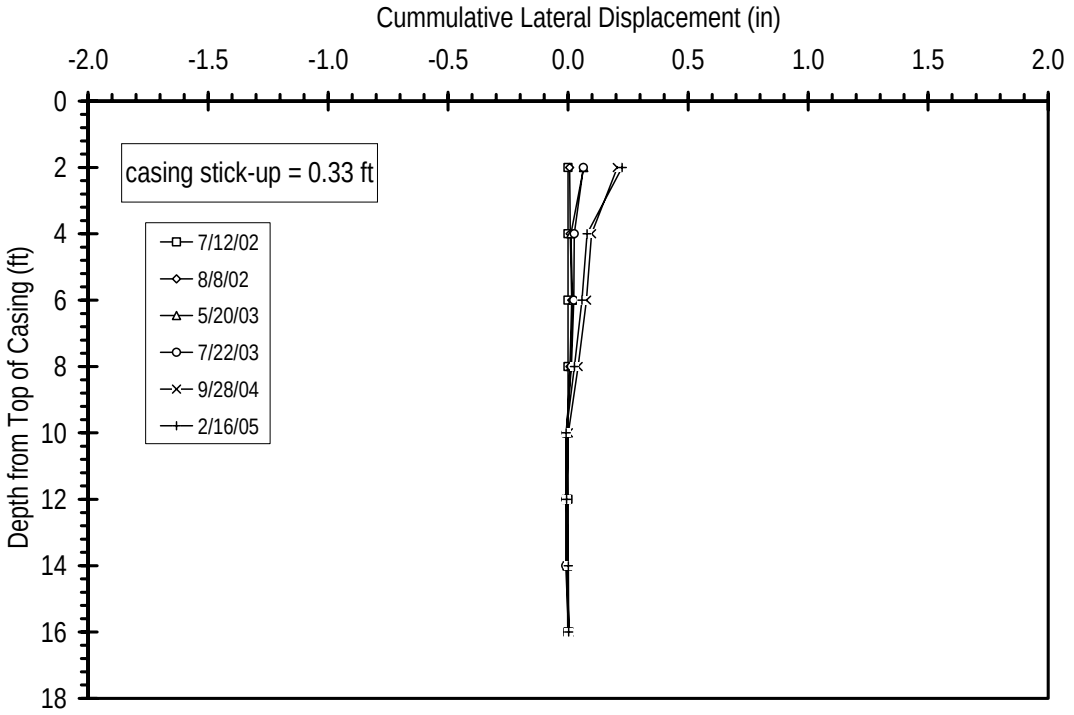

Figure 7.25 Lateral deflection profile for Inclinometer I-1 at I435-Holmes Road test site.

7.6. Summary

In this chapter, the activities undertaken to establish and monitor two stabilized test sections and one control section at the I435-Kansas City sites have been presented. The general characteristics of the three slide areas were described including results from a site investigation and laboratory testing program. An extensive series of stability analyses performed to estimate the stability of the stabilized slopes was then presented and the selected stabilization schemes were described. Finally, results obtained from monitoring the field instrumentation at the site were presented.

Chapter 8. US36-Stewartsville Site

The fourth site stabilized during the project is the US36-Stewartsville site. The site is located in northwest Missouri on U.S. Highway 36, approximately two miles west of the city of Stewartsville. In this chapter, the general characteristics of the site are first described followed by descriptions of the design analyses performed to select the stabilization schemes used at the site and the selected stabilization schemes. The instrumentation scheme used to monitor the performance of the site and the results of instrumentation readings are then presented.

8.1. Site Characteristics

The slope stabilized at the US36-Stewartsville site lies in the median of US36 between the eastbound and westbound sections of the roadway. Figure 8.1 shows an air photo of the site indicating the location of the slope and Figure 8.2 shows a photo of the site following the recent slide event which involved approximately 150-ft (45-m) of the slope (measured parallel to US36). The slope at the site is approximately 29-ft (8.8-m) high with an inclination of 2.2H:1V. The slope is similar to the slopes at the I435-Kansas City sites in that the stratigraphy consists of a surficial layer of soft to medium clay overlying stiff to hard fat clay. However, the slope is an excavated slope rather than an embankment fill. A second, much smaller slide area is located approximately 100-ft (30-m) to the west of the main slide area. This slide area was selected for use as a control slope for the main slide.

Figure 8.1 Air photo of US36-Stewartsville site taken March 26, 1997 showing location of site in the median of US36 (from USGS).

Boring and sampling at the US36-Stewartsville site was performed by MoDOT Soils and Geology crews during the period May 30 to June 7, 2001. A plan view of the site showing the locations of all borings is provided in Appendix C along with all boring logs. A

total of eight 4-in (10-cm) diameter solid stem auger borings were made to depths varying from 10-ft (3-m) to 25-ft (7.5-m). In seven of the borings, continuous 3-in (7.6-cm) diameter Shelby tube samples were taken for field classification and laboratory testing in a manner similar to that described in Chapter 5. The general stratigraphy determined from these borings consists of a 2.5- to 5-ft (0.8- to 1.5-m) thick stratum of soft, moist lean to fat clay overlying very stiff to hard fat clay with scattered gravel to the depths investigated. In the remaining boring, "continuous" Standard Penetration tests (SPT) were performed. SPT N_{60}-values determined from tests in the upper 3.0-ft (0.9-m) of the boring were 0 (weight of hammer). Between 3- and 6-ft (0.9- and 1.8-m), N_{60} ranged from 9 to 11. Below 6-ft (1.8-m), N_{60} increased dramatically and varied between 13 and 20. N_{60} values determined for SPT tests performed in other borings when Shelby tube samples could not be taken showed similarly high SPT N-values within the lower stiff clay. No groundwater was observed in any of the boreholes during the site investigation.

Figure 8.2 Photograph of US36-Stewartsville site taken after the recent slide at the site.

Laboratory testing performed on samples taken from the site included natural moisture contents, Atterberg limits, and triaxial compression tests. Moisture contents varied somewhat across the site, but most borings indicated higher moisture contents in the upper 5- to 10-ft (1.5- to 3.0-m) of the profile below which the moisture content generally decreased to essentially constant values of approximately 20 percent in all borings. Moisture contents in the surficial soils ranged from 18 to 44 percent and averaged about 30 percent.

Atterberg limits for the surficial soils varied substantially. Liquid limits (LL) for the surficial soils ranged from 33 to 69 and plastic limits (PL) varied from 16 to 26; plasticity indices (PI) for these soils ranged from 7 to 44. Most of the surficial samples tested classified as CL soils in the Unified Soil Classification System (USCS), although several samples classified as CH and one sample classified as ML. Atterberg limits for the deeper

soils were more consistent with LL ranging from 41 to 55, PL ranging from 16 to 21, and PI ranging from 21 to 34. All of the deeper soils classified as CL or CH in the USCS.

Consolidated-undrained ($\overline{CU}$, $\overline{R}$) and consolidated-drained (CD, S) type triaxial compression tests were performed on a total of 13 specimens from the US36-Stewartsville site. Figure 8.3 shows the stress paths determined from these tests along with "upper bound" and "lower bound" failure envelopes for specimens taken from depths less than 6-ft (1.8-m) and depths greater than 6-ft (1.8-m), respectively. Mohr-Coulomb effective stress strength parameters for these envelopes are summarized in Table 8.1. Tests on specimens from shallow depths indicate the soil has a small cohesion intercept ($\bar{c}$) and an angle of internal friction ($\bar{\phi}$) between 27° and 29°. Tests on deeper specimens indicate that $\bar{c}$ is between 0- and 211-psf (10.1-kPa) and $\bar{\phi}$ is between 32° and 35°.

Table 8.1 Summary of Mohr-Coulomb effective stress strength parameters from triaxial compression tests on specimens from the US36-Stewartsville test site.

			Upper bound		Lower bound	
Stratum	Depths	Sample Numbers	$\bar{c}$ (psf)	$\bar{\phi}$ (degrees)	$\bar{c}$ (psf)	$\bar{\phi}$ (degrees)
Surficial lean to fat clay	< 6.0-ft	276, 278, 280, 316, 318, 343	42	29	0	27
Deeper stiff clay	> 6-ft	282, 300, 302, 322, 324, 375	211	35	0	32.5

8.2. Design of Stabilization Schemes

An extensive series of stability analyses was performed to select the stabilization schemes to be used at the US36-Stewartsville site. The design cross-section utilized for these analyses is shown in Figure 8.4. The ground surface profile was established from survey data provided by MoDOT and the subsurface geometry was assumed to consist of a 3- to 5-ft (0.9- to 1.5-m) thick, soft surficial layer overlying a layer with much higher strength based on boring logs obtained for the site.

The approach used for the stability analyses was similar to that used for the I435-Wornall Road site wherein a series of back-analyses was performed to establish a range of plausible conditions that could have led to the failure, followed by additional analyses for a variety of different reinforcement configurations to establish factors of safety for possible reinforcement schemes. The range of slope conditions evaluated included cases with zero pore pressures throughout the slope and a perched water condition within the upper stratum for various assumed thicknesses of the upper stratum. Analyses were performed for both the upper and lower bound strength parameters as well as for several other assumed sets of strength conditions falling between the upper and lower bounds. Based on these analyses, the stability cases summarized in Table 8.2 were selected as plausible conditions that could have led to failure of the slope.

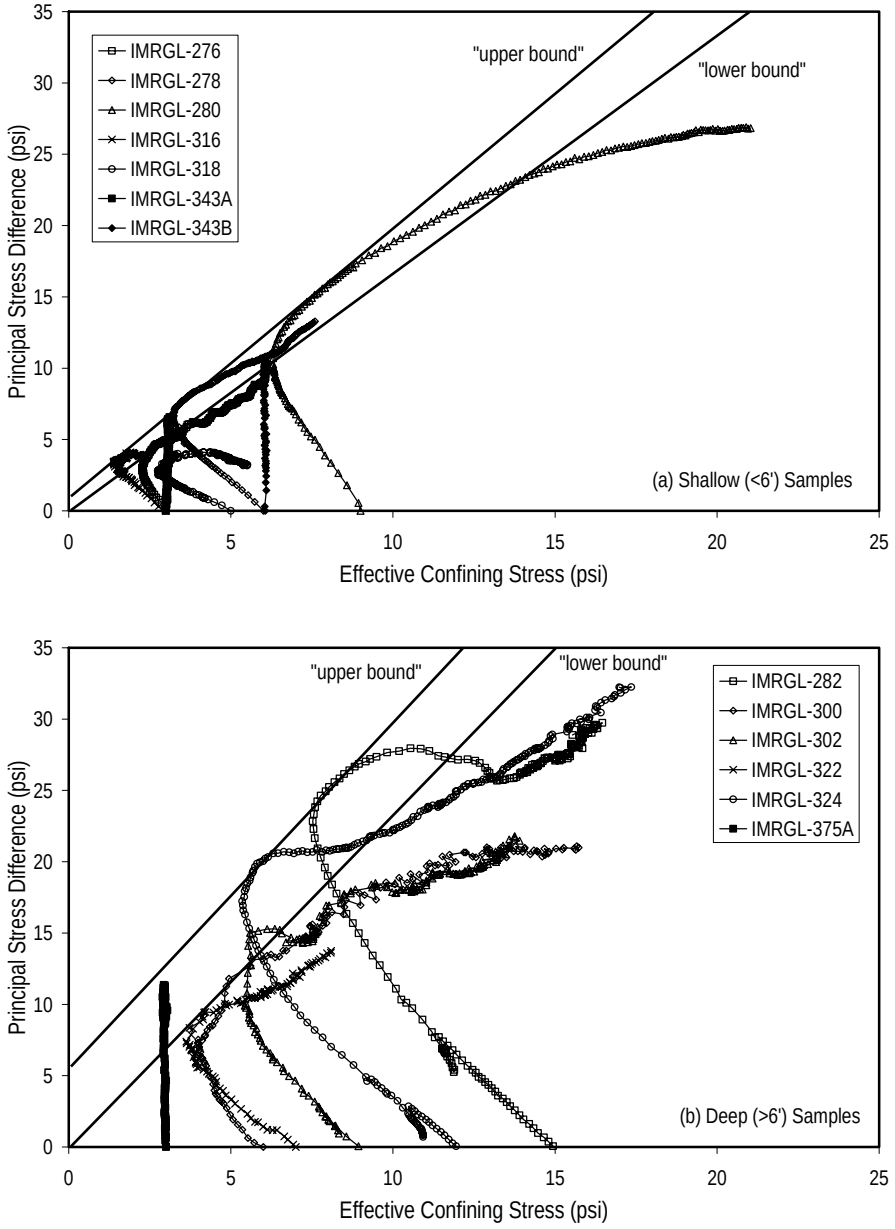

Figure 8.3 Summary of triaxial test results for specimens from US36-Stewartsville site: (a) shallow samples and (b) deeper samples.

Several reinforcement configurations were then evaluated for each of the plausible stability cases. The reinforcement configurations included reinforcing members placed in a uniform grid over the entire slope face with members spaced between 3- and 6-ft (0.9- and 1.8-m) as well as several non-uniform grids with different member configurations in the upper, middle, and lower portions of the slope. Table 8.3 shows a summary of the different configurations analyzed and the resulting factors of safety for the different plausible stability cases considered. The calculated factors of safety ranged from a low of 1.03 for the most widely spaced members considered to 1.30 for the most closely spaced members. In general, factors of safety calculated for the different member configurations using the upper and

lower bound envelopes for the lower stiff clay were identical, which indicates that the critical sliding surface passes only through the upper stratum in all cases.

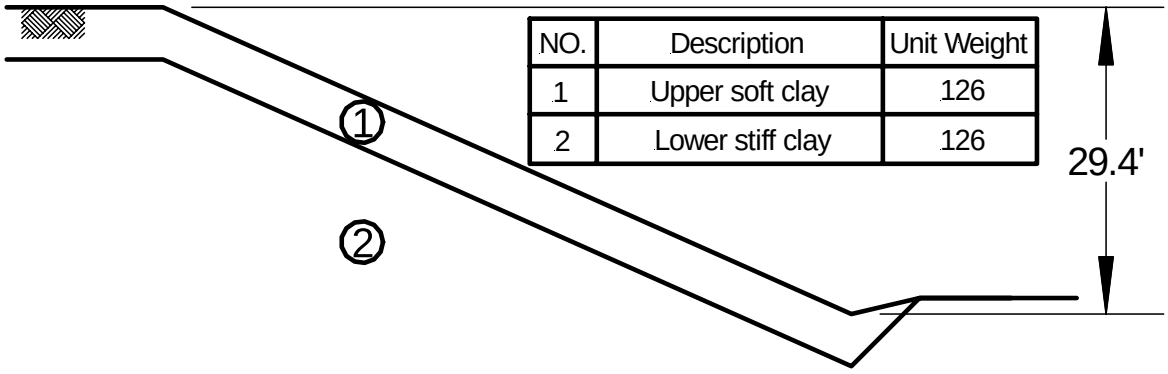

Figure 8.4 Design cross-section for the US36-Stewartsville slope.

Table 8.2 Summary of plausible stability cases leading to the failure at the US36-Stewartsville test site.

Stability Case	Thickness of Upper Stratum (ft)	Pore Pressure Condition	Deeper Stratum Envelope	Upper Stratum	
				Assumed Parameter	Back-calculated Parameter
A	3.0	perched 1 [1]	upper bound	$\bar{\phi}$ =29°	$\bar{c}$ =45 psf
B	5.0	perched 1	upper bound	$\bar{\phi}$ =28°	$\bar{c}$ =76 psf
C	3.0	perched 2 [2]	upper bound	$\bar{c}$ =1-psf	$\bar{\phi}$ =26°
D	5.0	perched 3 [3]	upper bound	$\bar{c}$ =1-psf	$\bar{\phi}$ =26°
E	3.0	perched 1	lower bound	$\bar{\phi}$ =29°	$\bar{c}$ =45 psf
F	5.0	perched 1	lower bound	$\bar{\phi}$ =28°	$\bar{c}$ =76 psf
G	3.0	perched 2	lower bound	$\bar{c}$ =1-psf	$\bar{\phi}$ =26°
H	5.0	perched 3	lower bound	$\bar{c}$ =1-psf	$\bar{\phi}$ =26°

[1] condition with piezometric surface for upper stratum at ground surface and u=0 for deeper stratum
[2] condition with piezometric surface for upper stratum 2-ft below ground surface and u=0 for deeper stratum
[3] condition with piezometric surface for upper stratum 3.3-ft below ground surface and u=0 for deeper stratum

Because the 3-ft by 3-ft (0.9-m by 0.9-m) arrays of reinforcing members used at both the I70-Emma and I435-Wornall Road sites seemed to be sufficient for stabilization of those slopes and because significant costs savings could be realized if more widely spaced arrays of reinforcing members could be shown to be effective, several different configurations of reinforcing members were selected for use at the US36-Stewartsville site. Using more widely spaced arrays of reinforcing members also increases the chances of having a failure at the site, which would greatly facilitate calibration of the design method described in Chapter 2. Figure 8.5 shows a plan view of the site with the selected reinforcement configurations. The slope was divided into four different sections, denoted Sections A through D, with a different configuration selected for each section. Section A had members placed on a 4.5-ft by 3.0-ft (1.4-m by 0.9-m) staggered grid, Section B a 6.0-ft by 6.0-ft (1.8-m by 1.8-m) staggered grid, Section C a 6.0-ft by 4.5-ft (1.8-m by 1.4-m) staggered grid, and Section D a

4.5-ft by 6.0-ft (1.4-m by 1.8-m) staggered grid. All members were to be installed with a vertical orientation. Estimated factors of safety for each of these reinforced sections are summarized in Table 8.4.

Table 8.3 Summary of factors of safety determined for different reinforcement configurations and stability cases for the US36-Stewartsville test site.

Rein. Spacing (ft)	Factor of Safety for Respective Stability Case							
	A	B	C	D	E	F	G	H
3L x 3T [1]	1.12	1.29	1.16	1.30	1.12	1.29	1.16	1.30
4L x 3T	1.08	1.19	1.11	1.20	1.08	1.19	1.11	1.20
3L x 6T	1.04	1.12	1.07	1.14	1.04	1.12	1.07	1.14
5L x 3T	1.07	1.13	1.08	1.15	1.07	1.13	1.08	1.15
5L x 6T	1.03	1.06	1.04	1.08	1.03	1.06	1.04	1.07
4L x 6T	1.04	1.06	1.05	1.09	1.04	1.06	1.05	1.09
3L x 3T and 3L x 6T [2]	1.12	1.19	--	--	--	--	--	--
3L x 3T and 3L x 6T [3]	1.11	1.17	--	--	--	--	--	--

[1] L and T denote spacing in longitudinal (strike) and transverse (dip) directions, respectively
[2] 3L x 3T grid in middle third of slope, 3L x 6T grid elsewhere
[3] 3L x 6T grid for upper and lower four rows of reinforcement, 3L x 3T grid elsewhere

8.3. Field Installation

The main slide area and control slide area were regraded to their original slopes in spring 2002. Installation of reinforcing members was performed during the period April 30 to May 7, 2002. Aside from an issue encountered with defective reinforcing members, which is described in Chapter 10 along with other details of the installation, the installation at the US36-Stewartsville site was completed without incident.

Table 8.4 Summary of estimated factors of safety for each reinforced slope section at the US36-Stewartsville test site.

Slope Section	Reinforcing Scheme	Estimated Factor of Safety
A	4.5L x 3.0T	1.07 – 1.20
B	6.0L x 6.0T	1.03 – 1.08
C	6.0L x 4.5T	1.03 – 1.15
D	4.5L x 6.0T	1.03 – 1.09

8.4. Instrumentation

Several different types of instrumentation were installed at the US36-Stewartsville site to monitor lateral deformations, moisture conditions, and loads in the reinforcing

members. Figure 8.6 shows a schematic of the main slide area indicating approximate locations of the instrumentation installed. Additional instrumentation was also installed in the center of the control section located to the west of the main slide as described below.

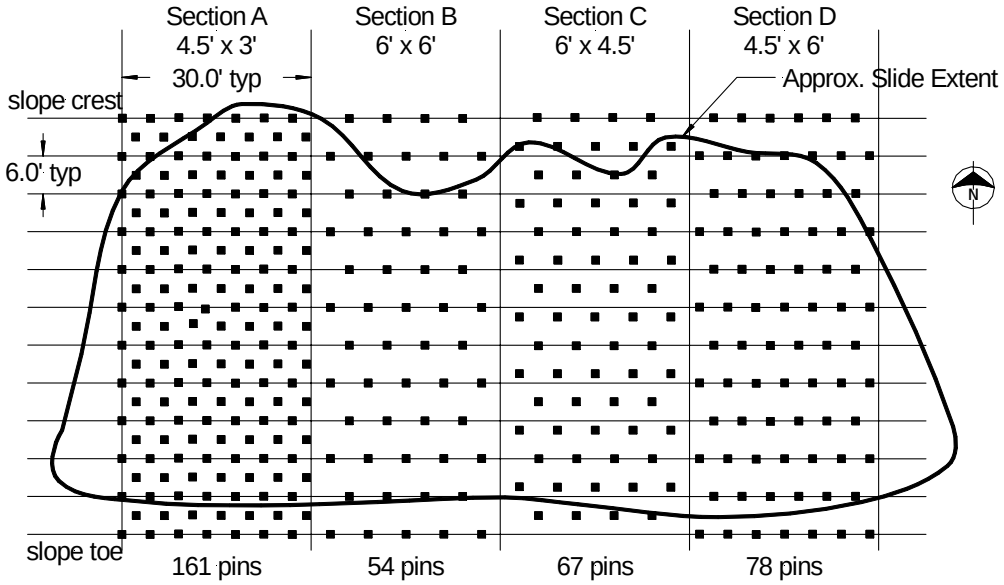

Figure 8.5 Plan view of selected stabilization schemes for US36-Stewartsville site (Note that all members were installed with vertical alignment).

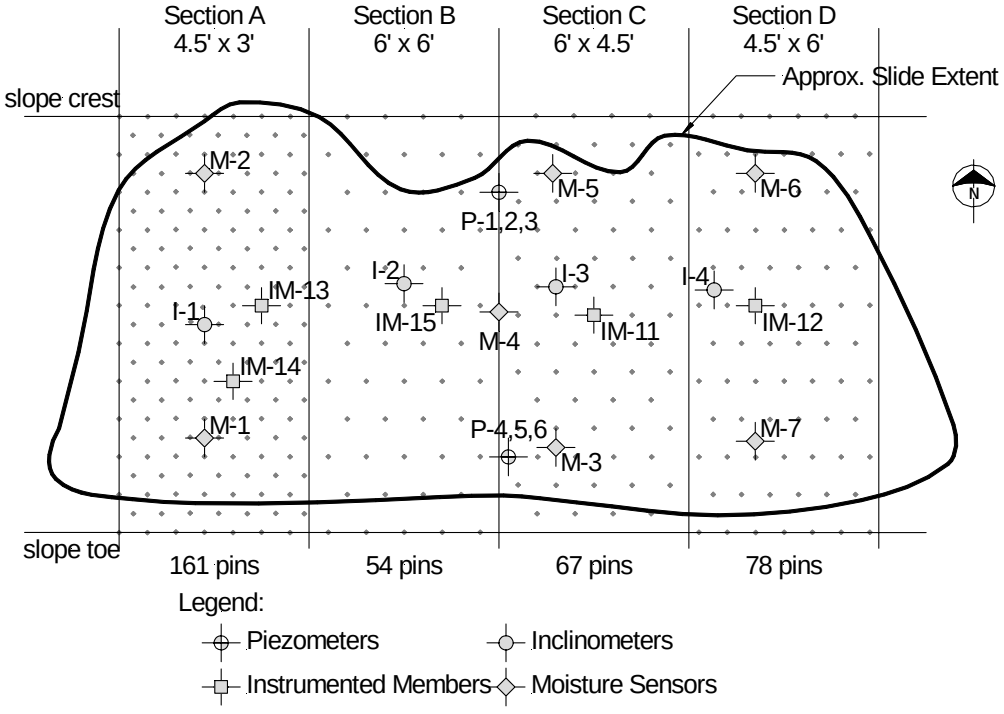

Figure 8.6 Instrumentation layout for US36-Stewartsville site.

Five of the recycled plastic reinforcing members installed in the main slide area were instrumented with strain gages and force-sensing resistors (FSR) as described in Chapter 5. Table 8.5 summarizes the instrumented members installed and the "stick-up" length of the members remaining above ground after installation. Members IM-13 and IM-14 were installed in Section A while members IM-15, IM-11, and IM-12 were installed near the center of Sections B, C, and D, respectively. Two additional instrumented members were installed approximately 10-ft (3-m) apart near the center of the control slide as shown in Figure 8.7 to evaluate the "free-field" behavior of the reinforcing members. One of these members, member IM-7, is a recycled plastic member identical to the other instrumented recycled plastic members. The other member, member IM-9, is a 3.5-in (8.8-cm) diameter steel pipe instrumented with strain gages but no FSR as was done for the steel pipe at the I435-Holmes Road site.

Table 8.5 Summary of "stick-up" for instrumented reinforcing members at the US36-Stewartsville site.

Member Designation	Member Type	Slope Section	Stick-up Length (ft)
IM-11	plastic	C	2.5
IM-12	plastic	D	0.5
IM-13	plastic	A	0.9
IM-14	plastic	A	1.8
IM-15	plastic	B	0.7
IM-7	plastic	Control	0.6
IM-9	steel pipe	Control	0.5

Figure 8.7 Photograph of US36-Stewartsville control slide during installation of instrumented reinforcing members.

Five slope inclinometer casings were installed by MoDOT drilling crews during the period July 7-9, 2002. All casings were installed to a depth of approximately 19-ft (5.8-m) below ground surface to extend below the toe of the slope and ensure adequate founding in the very stiff clay. One casing was installed within each section of the main slide area in close proximity to the instrumented reinforcing members. The fifth casing was installed in the control slide area approximately midway between the two instrumented members.

Two clusters of standpipe piezometers were installed at the site during the same period. Both clusters were placed near the middle section of the slide between Sections B and C. Each cluster contained three piezometers placed within a single borehole. Piezometers P-1, P-2, and P-3 were placed in a cluster located in the upper third of the slope and screened at depths of 14-ft, 9-ft, and 4-ft (4.2-m, 2.7-m, and 1.2-m), respectively (Figure 5.10). Piezometers P-4, P-5, and P-6 were placed in a cluster located in the lower third of the slope and screened at similar depths.

Instrumentation to monitor the moisture conditions and soil suction within the slope was installed at 7 locations across the main slide area on August 23, 2002. As was done at the I435-Wornall Road site, a vertical array of ThetaProbes® and Equitensiometers® was installed at location M-4 near the center of the slide area (Figure 8.6) to establish an essentially continuous record of moisture/suction conditions within the slope. A Profile Probe® access tube was also installed at location M-4. Additional Profile Probe® access tubes were installed at the remaining locations shown in Figure 8.6 (designated M-1 through M-7) to provide data on the vertical and lateral distribution of moisture conditions across the slide area.

8.5. Field Performance

Field performance of the US36-Stewarstville test site was monitored between July 2002 and February 2005. Intervals between readings ranged from two weeks to four months resulting in sixteen sets of readings. Results of field instrumentation readings, including precipitation, piezometers, inclinometers, and instrumented reinforcing members, are presented in the following sections.

8.5.1. Precipitation at the US36-Stewartsville Site

Daily and monthly precipitation data were acquired from the National Climatic Data Center station at Amity, Missouri, located approximately 8 miles north of the site. Daily and monthly precipitation, along with the 50-year average monthly precipitation is shown in Figure 8.8. Measured precipitation was generally near or below the 50-year average for the first two years following installation of reinforcing members at the site. Precipitation increased in early 2004 and has been near or above average since that time. In May 2004, 12.5-in. of precipitation occurred compared to the average monthly precipitation of 4.7-in. This monthly total includes two intense rainfall events measuring almost 4-in. The site was subjected to a similar intense rainfall event in June of 2002.

8.5.2. Piezometers and Moisture Sensors

Measured piezometric levels for the US36-Stewartsville site are shown in Figures 8.9 and 8.10. Piezometers P-2 and P-3, located in the upper third of the slope at depths of 10-feet and 5-feet respectively, have been dry since installation and have been unaffected by precipitation levels except for the reading on February 16, 2005. Levels in piezometer P-1

were variable throughout monitoring and were highest on February 16, 2005. Piezometers P-4, P-5, and P-6 show consistent piezometric levels indicating the presence of a classic unconfined groundwater table. The piezometric levels in P-4 through P-6 have been relatively stable throughout the monitoring period, although the level was slightly elevated during the months of June through September 2004 in response to the elevated precipitation at the site. Piezometric levels on July 26, 2004 were approximately 0.5 feet higher than the previous reading. A failure occurred at the control site after the July 26, 2004 reading in response to the elevated piezometric levels during this period. This suggests that the piezometric conditions experienced at this time were similar to those resulting in the previous failures.

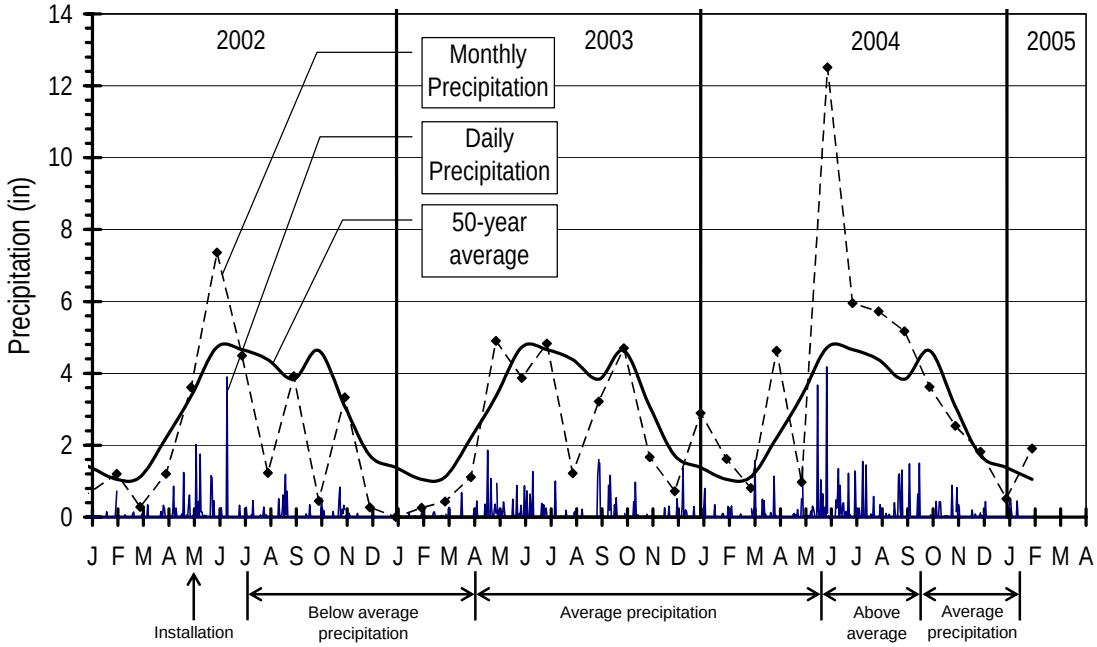

Figure 8.8 Daily, monthly, and average precipitation from NCDC station at Amity Missouri located approximately 8 miles north of the US36-Stewartsville site.

Measurements taken for the soil moisture and soil suction sensors located near the center of the slide area are plotted in Figure 8.11. In contrast to the experience with Equitensiometers® at the I435-Wornall Road test site, the Equitensiometers® at the US36-Stewartsville site have produced excellent data. This is primarily attributed to the fact that the I435-Wornall Road slope has remained very wet and likely saturated since installation while the US36-Stewartsville slope has been unsaturated. The trends in volumetric water content and soil suction have been very similar throughout the period of monitoring, which provides some confidence that the sensors are providing accurate data. The data clearly show several alternating periods of wetting and drying at the site that are generally consistent with the observed precipitation shown in Figure 8.8 and to a lesser extent with the recorded piezometric levels shown in Figures 8.9 and 8.10. Measured volumetric water contents and soil suctions at shallow depth tend to vary more substantially than those measured at deeper depths, but similar trends are exhibited for all sensors. The volumetric water contents

measured at shallow depths are consistently lower than those at deeper depths. This may be a result of variations in soil unit weight (density) which can affect the interpretation of readings from dielectric sensors like the ones used, or may be a true representation of field moisture contents. It is also noteworthy that pore water pressures measured by the deeper sensor tend to respond more slowly to wetting and drying periods than pressures measured by the shallower sensor.

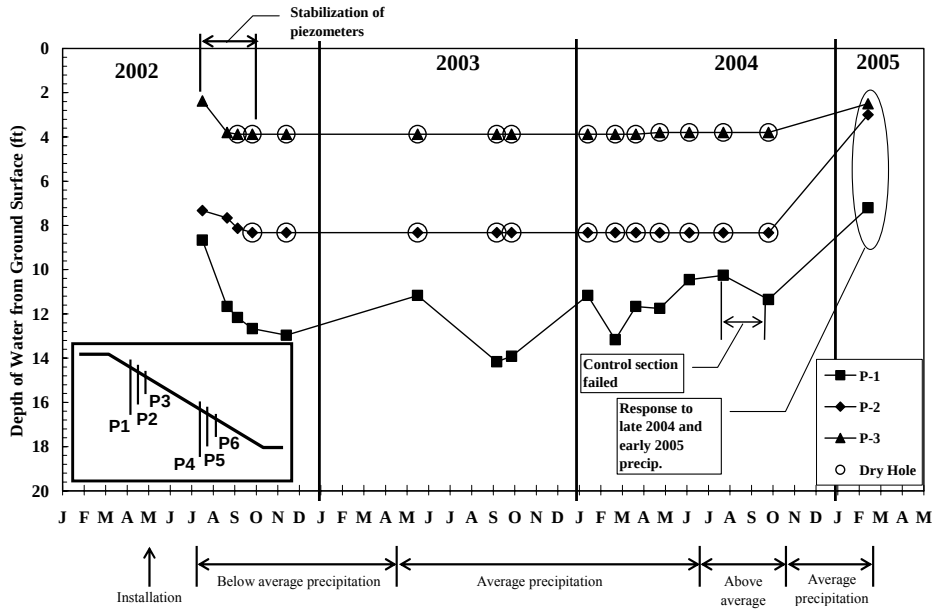

Figure 8.9 Measured piezometric levels for piezometers P-1, P-2, and P-3 at the US36-Stewartsville site.

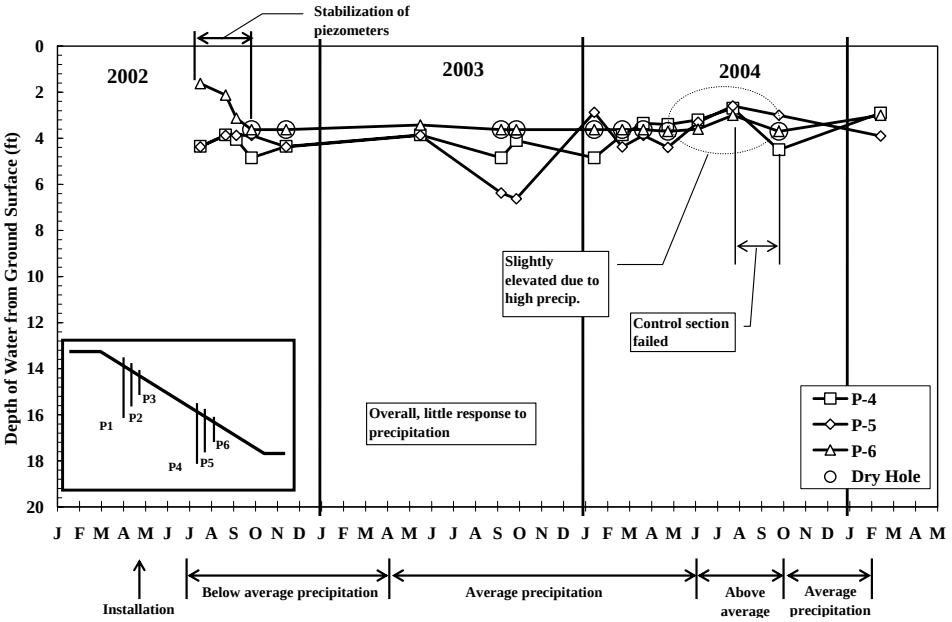

Figure 8.10 Measured piezometric levels for piezometers P-4, P-5, and P-6 at the US36-Stewartsville site.

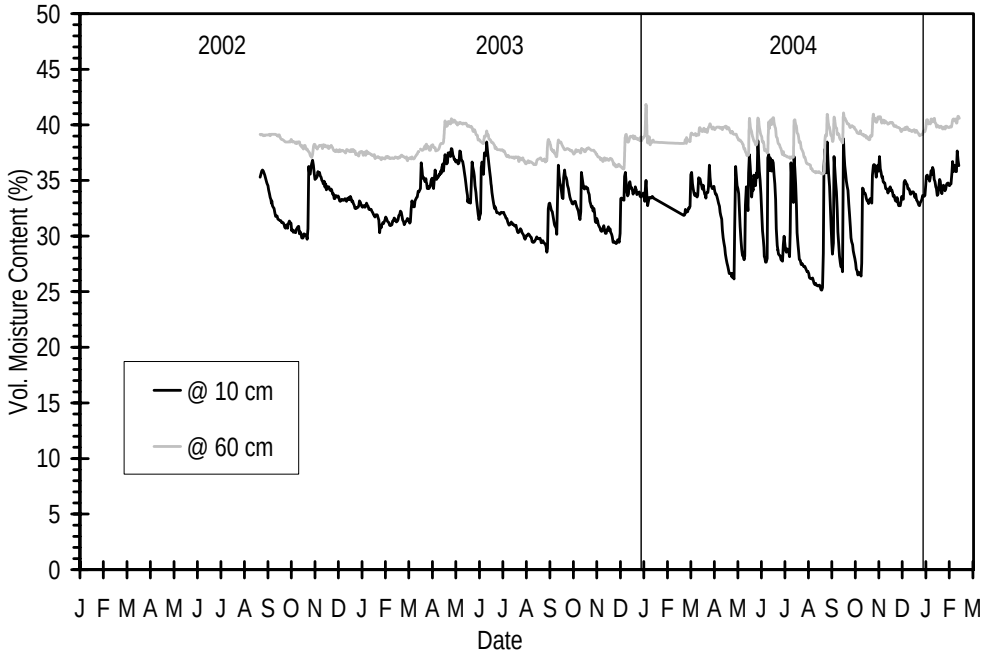

(a) soil moisture sensors

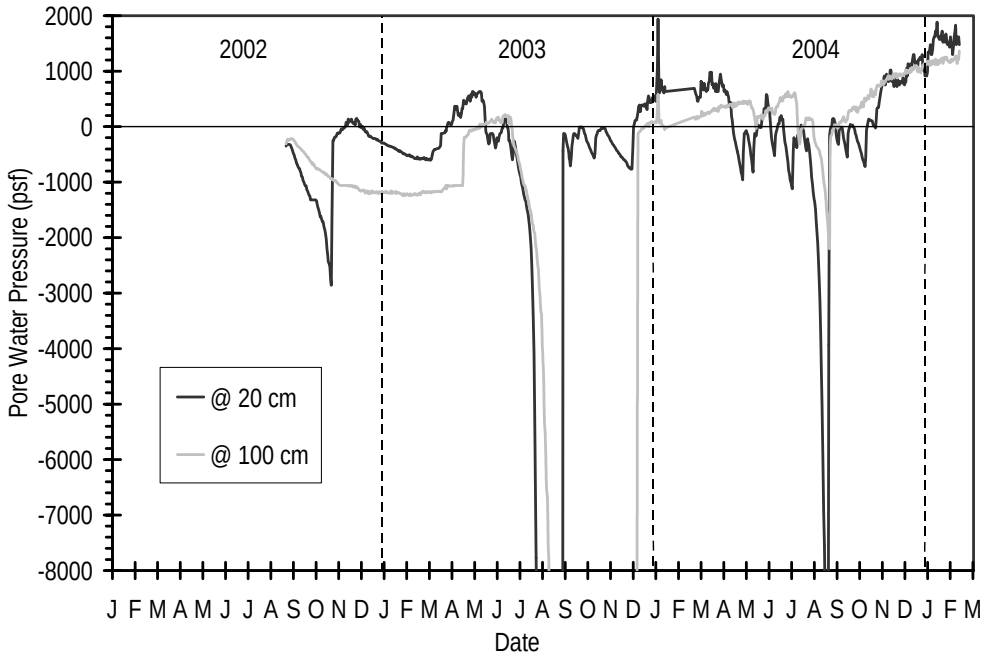

(b) soil suction sensors

Figure 8.11 Soil suction and volumetric water content measurements from the US36-Stewartsville test site: (a) ThetaProbe® sensors and (b) Equitensiometer® sensors.

The three most notable periods observed in Figure 8.11 in terms of stability of the slope are periods with high water contents and pore pressures observed in April to June 2003, December 2003 to June 2004, and September 2004 to January 2005. In each of these

periods, pore pressures within the slope were observed to become positive while pore pressures were generally negative for the remainder of the monitoring period. It should be noted that the accuracy of the sensors for measuring positive pore pressures is substantially degraded compared to their accuracy when measuring negative pore pressures because of the calibration. As such, the magnitudes of the positive pore pressures shown in Figure 8.11 should not be given much credence, but the indication that pore pressures are in fact positive is accurate.

8.5.3. Slope Inclinometers

The displacement versus time for each inclinometer at the US36-Stewartsville site is shown in Figure 8.12. The annotation at the top of the figure correspond to general periods of low (L), medium, (M), and high (H) precipitation.

In each inclinometer, there are four notable periods of displacement similar to observations at the I70-Emma site. Initially, very little displacement occurred following installation for a period of greater than one year. This initial period was followed by an increase in displacement attributed to mobilization of resistance in the reinforcing members. This occurred between June and September 2003 and is shown by the first shaded region in Figure 8.12. Precipitation during this time period was generally similar to or below average monthly values but it does follow a period of increased pore pressures as shown in Figure 8.11. Following this initial mobilization period, displacements remained steady or increased slightly for a period of approximately 10 months. The slight increases in deformations observed in some inclinometers during this time could be attributed to a number of factors including additional mobilization (pore pressures were again elevated between December 2003 and July 2004, potential creep in the reinforcement (discussed subsequently), or simply variability and precision in the inclinometer readings. Following this relatively stable period, additional deformation was again observed starting in September 2004. These movements are attributed to additional mobilization of resistance due to increased precipitation and increased pore pressures in late summer and fall 2004. Overall deformations measured from the respective inclinometers are similar and indicate maximum movements of 1.5 to 2 inches.

Figure 8.13 shows the measured displacement versus depth for inclinometer I-3, which shows that movements have been greatest at the ground surface and have been limited to depths of less than approximately 6 feet. All other inclinometers showed similar patterns of deformations.

The control area of the US-36 Stewartsville slope failed sometime between July 26, 2004 and September 28, 2004. The displacement versus time record for inclinometer I-5, located within the control area, is shown in Figure 8.14. Deformation patterns observed prior to the failure were generally consistent with the behavior shown in Figure 8.12 for inclinometers within the stabilized sections. The magnitudes of the movements in the control slide area were generally slightly greater than those observed in the stabilized sections up to the point when sliding occurred when surficial displacement increased to 9.5 inches. The failure occurred following above average precipitation from May through July and followed periods of increased piezometric levels in piezometers P-4, P-5, and P-6 and increased pore pressures measured by the Equitensiometers (Figure8.11). A subsequent reading on February 16, 2005 indicated that the inclinometer was pinched off at depth of approximately 5 feet.

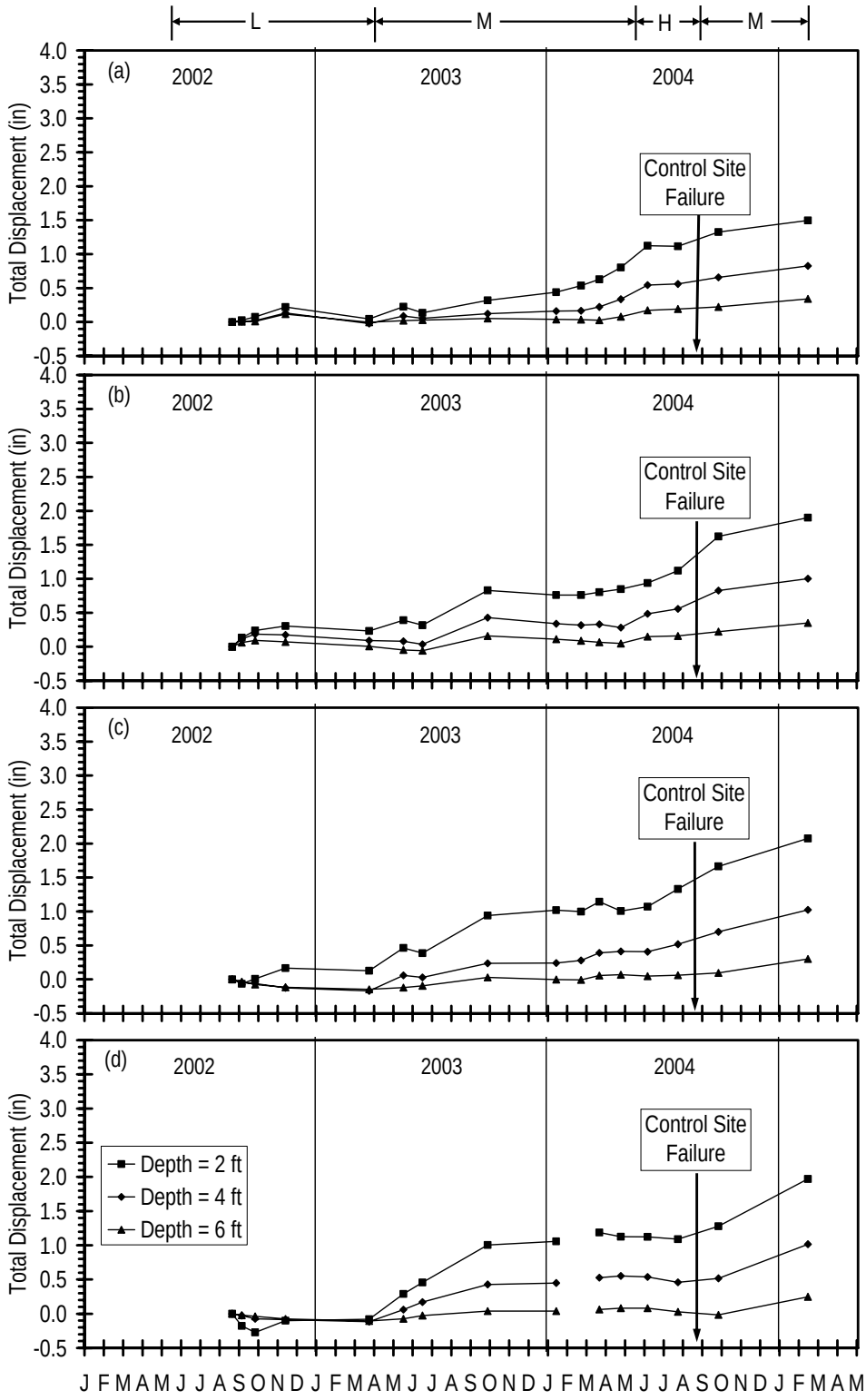

Figure 8.12 Measured displacement versus time for inclinometers at the US36-Stewarstville site: (a) I-1 in Section A, (b) I-2 in Section B, (c) I-3 in Section C, and (d) I-4 in Section D.

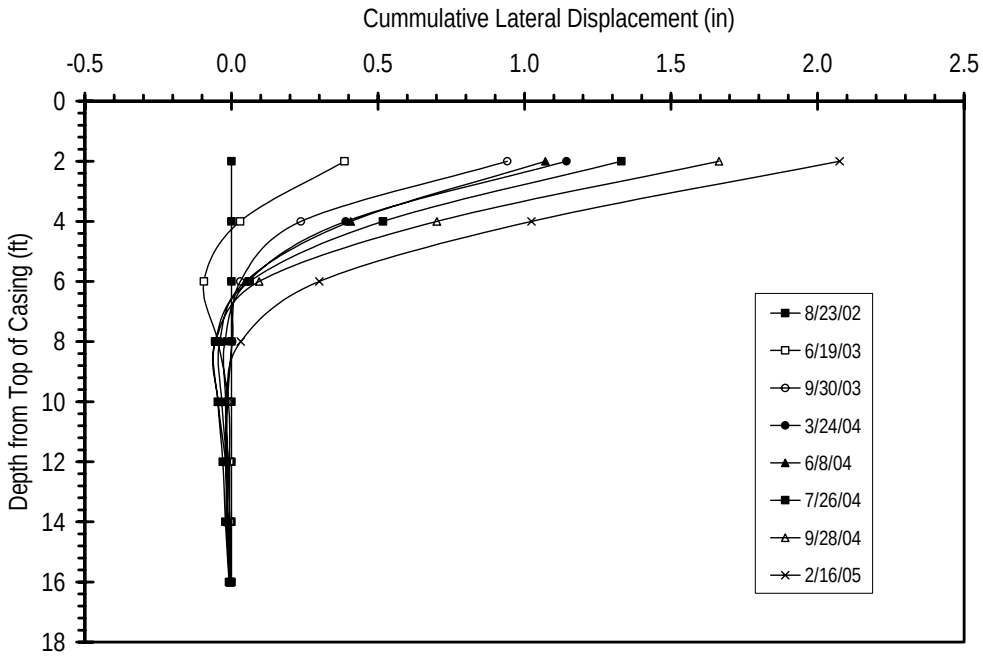

Figure 8.13 Measured displacement versus depth for inclinometer I-3 at the US36-Stewartsville site.

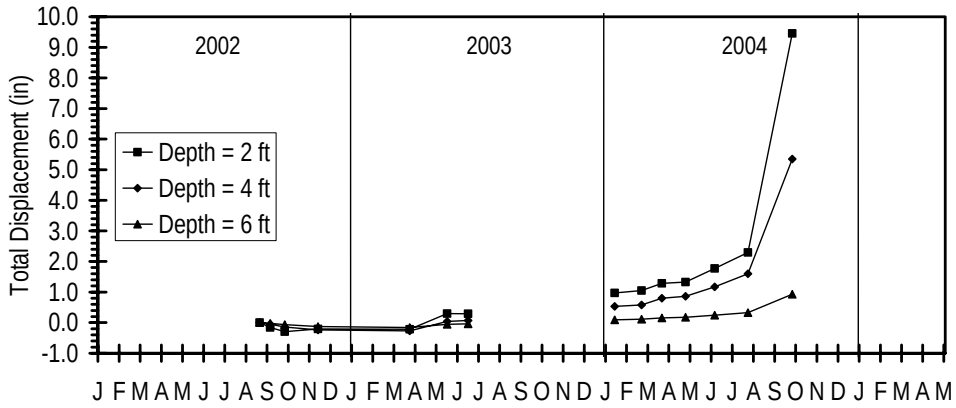

Figure 8.14 Measured displacement versus time for control site at the US36-Stewartsville site.

8.5.4. Instrumented Reinforcing Members

Strain gage readings from instrumented member IM-9 in the US36-Stewartsville control slide area were used to compute moments within the reinforcing member. The maximum computed moments and the deformations measured at the slope surface are plotted versus date in Figure 8.15. As has been consistently observed at the other test sites, the mobilization of bending moments generally coincides with the deformations observed. Moments in the reinforcing member were generally small until the control section failed, although moments did increase in conjunction with increasing movement in the months preceding the failure. The maximum moment increased to the approximate ultimate capacity of the reinforcing members around the time of the control failure. Some time after the

failure, the maximum moment in the reinforcing member decreased, presumably due to relaxation of the stresses and unloading of the reinforcing member following its failure.

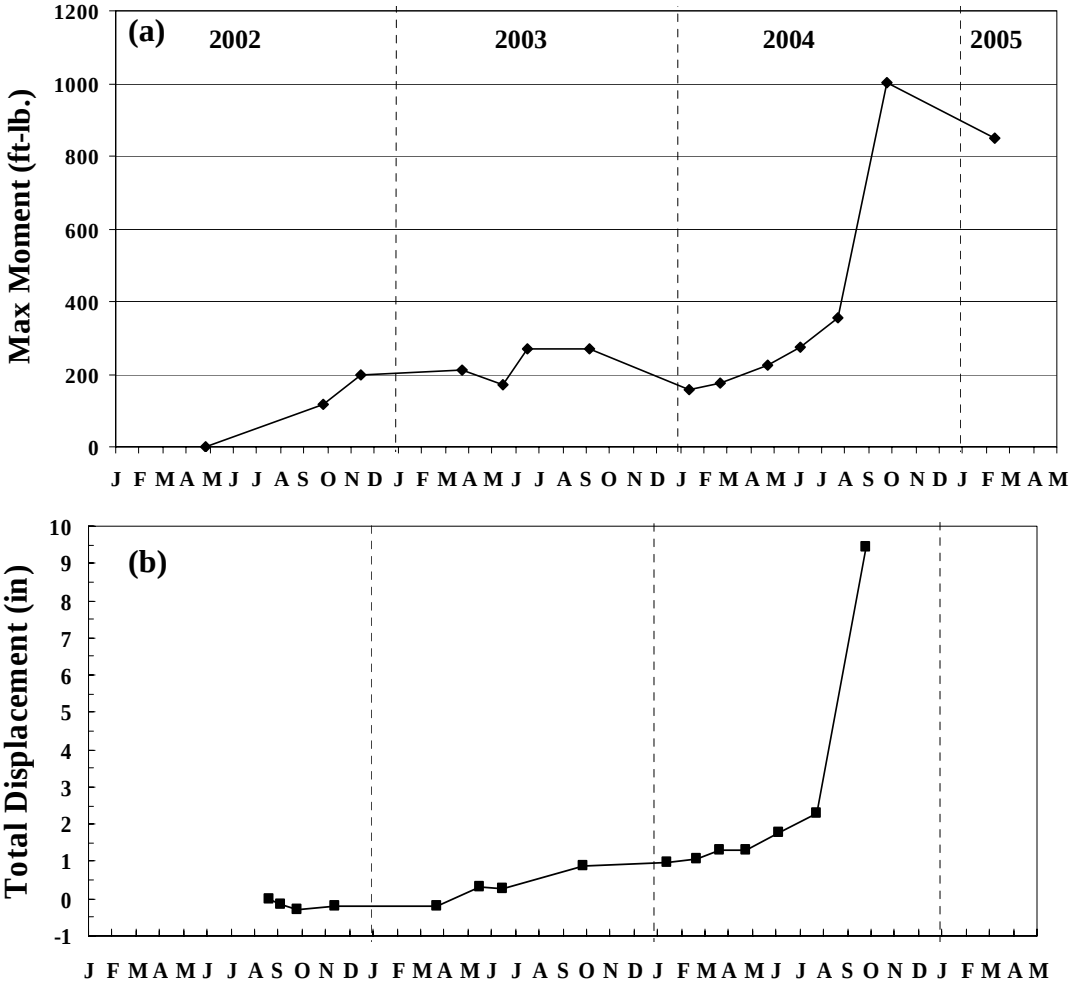

Figure 8.15 Comparison of maximum bending moment and slope displacement in the control area of the US36-Stewartsville site: (a) maximum moment in member IM-9 and (b) surficial displacement

8.5.5. Potential Creep in Reinforcing Members

As was discussed in Chapter 6 for the I70-Emma site, it is possible to interpret some of the deformations observed, particularly those between September 2003 and July 2004, as movements attributable to creep. As such, "creep rates" were estimated from displacement versus time data for each inclinometer for the period between September 2003 and July 2004. The estimated creep rates for the different test sections are summarized in Table 8.6. It is worth noting that the displacement versus time data for the US36-Stewartsville site during this period did not exhibit as clean of a trend as was observed for the I70-Emma site. Estimated creep rates for the US36-Stewartsville site were highest in section A, which had the narrowest reinforcing scheme, while rates in sections B, C, and D were generally similar considering the quality of the data. In general, estimated creep rates for US36-Stewartsville

site were substantially lower than those estimated at the I70-Emma site. If the observed movements are attributable to creep, this could be due to higher mobilized loads at the I70-Emma site.

However, it is important to reiterate that these movements can also be attributed to additional mobilization of resistance. This interpretation is supported by the fact that precipitation levels during portions of this period were above average and that pore pressures measured using the Equitensiometers were elevated during a portion of this period.

Table 8.6 Estimated creep rates for US36-Stewartsville site at depths of 2-ft, 4-ft, and 6-ft below ground surface.

Section	Spacing	Creep rate (in./yr)		
		2-ft.	4-ft.	6-ft.
A	4.5' x 3'	0.58	0.18	0.26
B	6' x 6'	0.15	0.04	0.15
C	6' x 4.5'	0.18	0.29	0.07
D	4.5' x 6'	0.22	0.36	0.11

8.6. Summary

In this chapter, the activities undertaken to construct, instrument, and monitor the performance of the US36-Stewartsville test site have been described. The US36-Stewartsville site was stabilized using a variety of different reinforcement patterns to permit direct comparison of the effectiveness of alternative measures. To date, all of the different stabilization schemes continue to be performing well. Precipitation at the site since installation has been below normal for much of the monitoring period. However, the site has been subjected to periods of average to above average precipitation and to periods where piezometric levels and pore pressures were observed to be slightly elevated. Furthermore, the control slide area located just to the west of the stabilized test sections failed in September 2004, which suggests that the site has been subjected to conditions that are at least as bad as those that caused the original slide. Piezometers P-4, P-5, and P-6 show nearly uniform piezometric levels at three different screen depths, indicating the presence of a classic groundwater table. Piezometers P-2 and P-3, located in the upper third of the slope at depths of 10-feet and 5-feet respectively, have been dry since installation and have been unaffected by precipitation levels except for the reading on February 16, 2005. Surficial displacements of the slope are less than 2-in. in all sections and deformations have been limited to the upper 6 feet of the slope. Similar to other test sites, the site has been subjected to varying displacement: small initial displacements following installation, an increase in displacement resulting from mobilization of resistance in the reinforcing members, a period of constant to slightly increasing displacements, and finally a period of additional displacement for additional mobilization of resistance in the reinforcing members.

Chapter 9. US54-Fulton Site

The final site selected for stabilization during the project is the US54-Fulton test site. The site is located on U.S. Highway 54 approximately 2 miles north of Fulton Missouri, just south of Richland Creek. Activities undertaken to establish the test site are described in this chapter along with results of field performance monitoring activities performed to date.

9.1. Site Characteristics

The slope at the US54-Fulton site is an excavated slope constructed for the approach to the nearby bridge across Richland Creek. The slope is approximately 46-ft (14-m) high at its highest point with an inclination of approximately 3.2H:1V. Figure 9.1 shows an air photo of the area indicating the location of the slope. Prior to being selected for stabilization, the slope experienced a large surficial slide shown in Figure 9.2 that dammed the surface drainage features alongside U.S 54. The slide involved approximately 275-ft (85-m) of the slope measured parallel to US54 and was confined to the lower two-thirds of the slope. The slide appeared to be a retrogressive slide with the primary slide involving the lower half of the slope after which the upper portion of the slope subsequently failed.

Figure 9.1 Air photo of area surrounding US54-Fulton site taken April 3, 1995 showing location of slope selected for stabilization (from USGS).

Boring and sampling for the US54 site took place during the period September 25-October 11, 2000. A total of 12 borings were placed throughout the area of the slide and just to the south of the slide area. A plan view of the site indicating the locations of all borings is provided in Appendix D along with logs of all borings. Continuous 3-inch (7.6-cm) diameter Shelby tube samples were taken in eight of the borings where soil conditions permitted. Where good quality Shelby tube samples could not be acquired, a Standard split spoon

sampler was used to acquire disturbed samples for classification testing. In the remaining four borings, Standard Penetration Tests (SPT) were performed at 18-in (45-mm) intervals. The boring logs and subsequent laboratory testing indicate the soil profile at the US 54 site generally consists of lean to fat clay of variable stiffness with traces of sand and gravel found throughout the depths investigated. The clays are believed to be of glacial origin (ablation till). Fissures were observed in several of the borings at depths exceeding 10-feet (3-m), which indicates that sliding has previously occurred in the clay materials. Gypsum crystallizations were observed in several of these fissures. These fissures were not originally believed to be associated with the current slide as they were located at depths that are not consistent with the observed features of the slide. However, subsequent monitoring described later in this chapter has suggested that, in fact, the observed slide was likely occurring along these fissures. Bedrock was not encountered in any of the borings at the US54 site. Standard Penetration Test (SPT) N_{60}-values measured in the soils less than 8-ft (2.4-m) in depth ranged from 1 to 23, with most values being between 8 and 10. N_{60}-values at greater depths ranged from 10 to 35 with most values in the range of 15 to 25.

Figure 9.2 Photograph of US54-Fulton slope following most recent slide event.

Laboratory testing of samples from the US54 site again consisted of natural moisture content tests, Atterberg limit tests, and consolidated-undrained type triaxial compression tests with pore pressure measurements. Measured moisture contents ranged from 10 to 35 percent. Samples taken from significant depths tended to have relatively consistent moisture contents of approximately 18 to 20 percent, while samples taken from near the surface tended to have highly variable moisture contents. There was some tendency for surficial samples taken from outside the slide area to have lower moisture contents than samples taken from within the slide area, although this observation was not universal.

Results of Atterberg limits tests indicated a general trend of increasing liquid limit (LL) and plasticity index (PI) with depth with essentially constant plastic limits (PL) for all specimens. Liquid limits for soils taken from depths less than 8-ft (2.4-m) ranged from 30 to

45, while LL for samples from greater depths ranged from 40 to 62. Plasticity indices for the surficial soils similarly ranged from 18 to 33 while PI at greater depths ranged from 27 to 45. Plastic limits for all soils varied from 10 to 21 and averaged approximately 16. Surficial samples almost universally classified as CL soils while deeper samples classified as either CL or CH soils.

A total of 11 consolidated-undrained triaxial compression tests were performed on specimens from the US54-Fulton site. Stress paths for each of these tests are plotted in Figure 9.3 for specimens from depths less than and greater than 6-ft (1.8-m), respectively. Based on these tests, three different possible failure envelopes were established for the surficial soils and one failure envelope was established for the deeper soils. Mohr-Coulomb effective stress strength parameters for each of these envelopes are summarized in Table 9.1. These indicate that the deeper soils have a significant effective stress cohesion intercept and an effective stress angle internal friction of 25 degrees. The surficial soils have a much smaller cohesion intercept and an angle of internal friction between 23 and 30 degrees.

Table 9.1 Summary of Mohr-Coulomb effective stress strength parameters from triaxial compression tests on specimens from the US54-Fulton test site.

			upper bound A		upper bound B		lower bound	
Stratum	Depths	Sample Numbers	$\bar{c}$ (psf)	$\bar{\phi}$ (°)	$\bar{c}$ (psf)	$\bar{\phi}$ (°)	$\bar{c}$ (psf)	$\bar{\phi}$ (°)
Surficial clay	< 6.0-ft	402, 405 407, 425 147, 148	0	30	91	25	0	23
Deeper clay	> 6.0-ft	185	230	25	--	--	--	--

9.2. Design of Stabilization Schemes

The stabilization schemes selected for the US54-Fulton site were selected based on a series of stability analyses performed for several plausible sets of slope conditions as was done for the previous test sites. The plausible stability cases were again established based on back-analyses performed for the unreinforced slope. For these analyses, the slope was assumed to be homogenous with strength parameters within the range indicated by the failure envelopes described above. Six different pore water pressure conditions were considered. One pore pressure condition assumed negligible pore pressures throughout the slope (i.e. u=0). Another considered a perched water condition within the upper 4-ft (1.2-m) of the slope as was done for previous sites. The remaining pore pressure conditions were defined by piezometric lines passing from the toe of the slope through different levels of the slope ranging from one-quarter of the height of the slope to the full height of the slope. Based on these analyses, the plausible stability cases summarized in Table 9.2 were established. It is noteworthy that each of the plausible stability cases involve a piezometric surface within the slope.

An extensive series of analyses was then performed to evaluate factors of safety for different reinforcement configurations. The reinforcement configurations considered include uniform arrays installed over the entire slide area with member spacings ranging from 3.0- to 6.0-ft (0.9- to 1.8-m). Several additional configurations with non-uniform arrays were also analyzed. A summary of the factors of safety determined for each of these configurations is provided in Table 9.3. Factors of safety for these configurations range from 1.0 to 1.3.

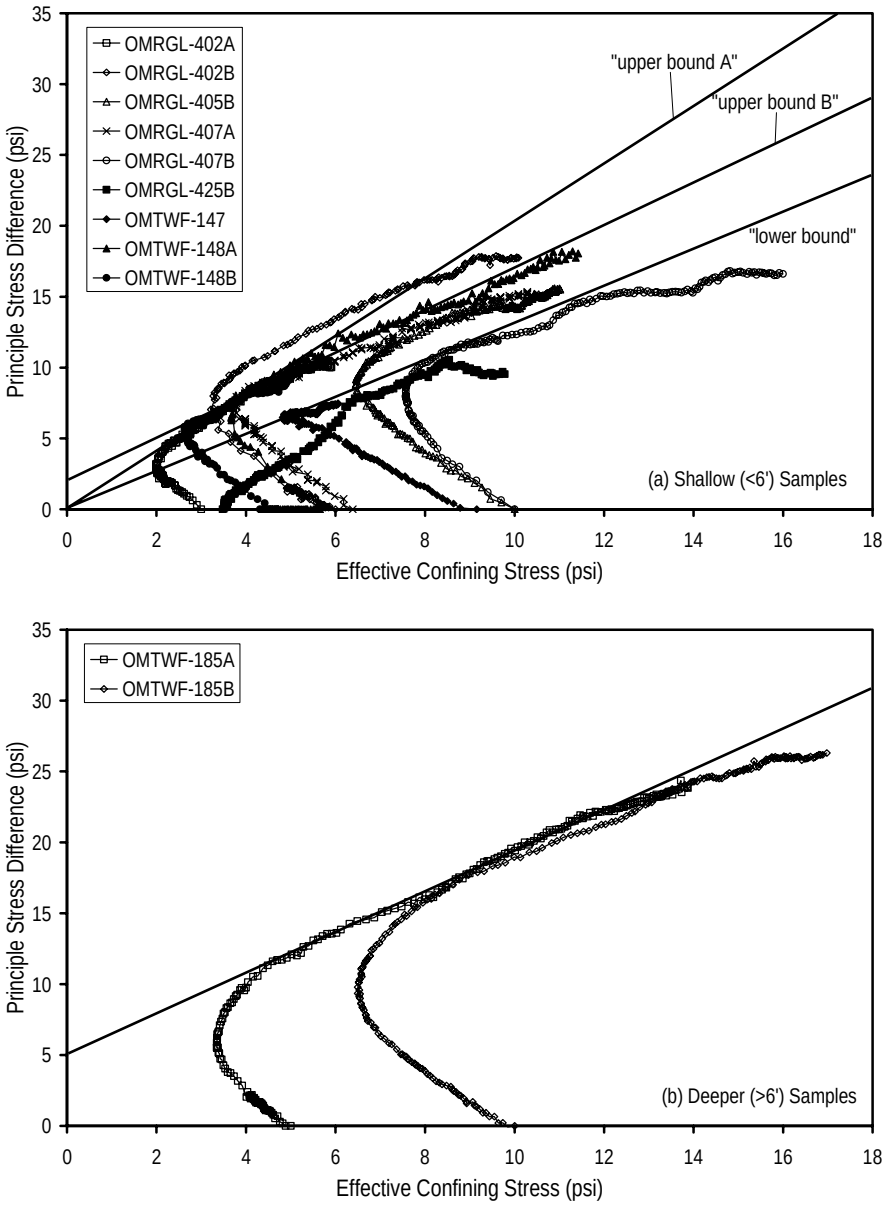

Figure 9.3 Summary of triaxial test results for specimens from the US54-Fulton test site: (a) shallow samples and (b) deeper samples.

The reinforcement configurations selected for use at the US54-Fulton site are shown in Figure 9.4. Several different configurations were again selected to evaluate the effectiveness of alternative stabilization schemes. The slide area was divided into five 40-ft (12.2-m) wide sections, denoted Sections A through E, with a different stabilization scheme

selected for each slope section. A 10-ft (3.0-m) wide "separation" between the different reinforced areas was established to address potential concerns about interaction between adjacent test sections. The selected schemes included members placed in uniform grids with member spacings ranging from 4.5- to 10-ft (1.4- to 3.0-m). Greater member spacings were employed at the US54-Fulton site than at previous sites in an attempt to induce failure in one or more sections to allow for rigorous calibration of the design method. Two non-uniform sections were also utilized to evaluate the potential for using more refined grids in critical areas of the slope with sparser configurations in secondary areas. A summary of the estimated factors of safety for each of the selected configurations is provided in Table 9.4. Estimated factors of safety range from approximately 1.15 for Section A with the most refined reinforcement to essentially 1.0 for Sections D and E with the sparsest reinforcement.

Table 9.2 Summary of plausible stability cases leading to the failure at the US54-Fulton test site.

Stability Case	Piezometric line height[1]	Piezometric line distance[2] (ft)	$\bar{c}$ (psf)	$\bar{\phi}$ (°)
A	mid-height	85	0	28.8
B	quarter-height	33 (on face)	51.8	20.3
C	mid-height	87	51.8	20.3
D	mid-height	110	0	22.4[3]
			51.8	20.3

[1] piezometric line assumed to vary linearly from toe to height noted at distance noted from toe, beyond which it extends horizontally

[2] horizontal distance from toe of slope to point where piezometric line reaches piezometric line height

[3] stability case D employs bi-linear failure envelope using first envelope for confining stresses less than 8.4-psi and the second envelope at greater confining stresses.

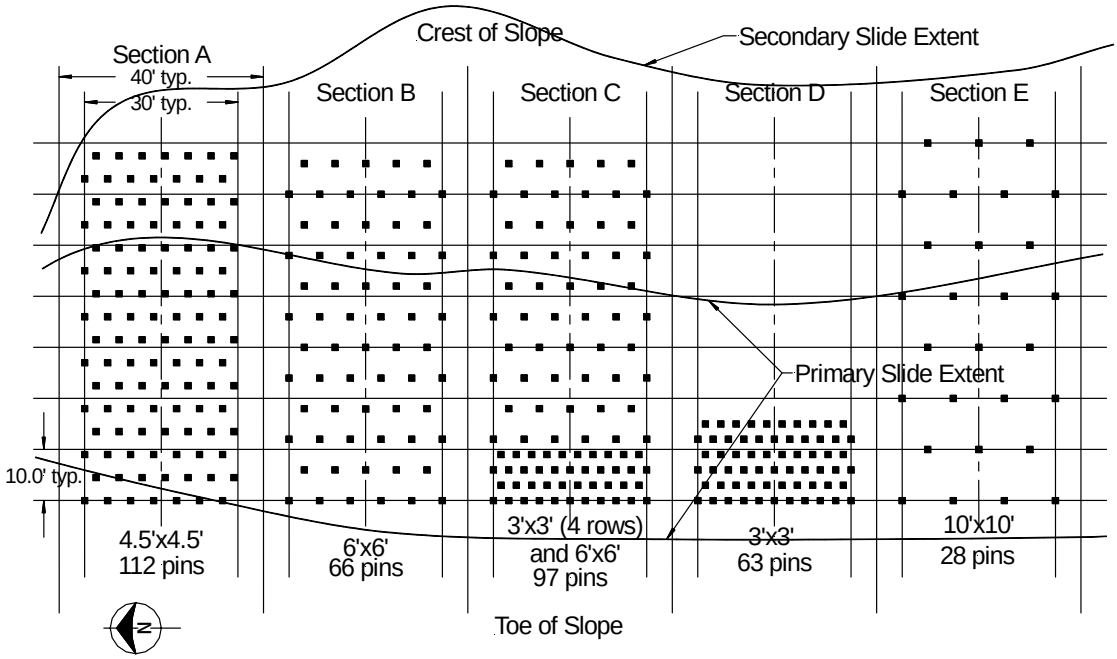

Figure 9.4 Plan view of US54-Fulton site showing selected reinforcement configurations for Sections A through E.

Table 9.3 Summary of factors of safety determined for different reinforcement configurations and stability cases for the US54-Fulton test site.

Rein. Spacing (ft)	Factor of Safety for Respective Stability Case			
	A	B	C	D
3.0L x 3.0T [1]	1.21	1.26	1.16	1.31
4.5L x 3.0T	1.14	1.19	1.10	1.24
6.0L x 3.0T	1.06	1.09	1.07	1.16
3.0L x 6.0T	1.14	1.10	1.07	1.16
4.5L x 6.0T	1.07	1.07	1.04	1.11
6.0L x 6.0T	1.03	1.05	1.03	1.05
3L x 3T on bottom half	1.15	1.24	1.07	1.25
3L x 3T on bottom quarter	1.03	1.09	1.03	1.08
3L x 3T first three rows only	1.00	1.00	1.00	1.02
3L x 3T and 6L x 6T [2]	1.06	1.06	1.03	1.07

[1] L and T denote spacing in longitudinal (strike) and transverse (dip) directions, respectively
[2] 3L x 3T grid on lower three rows, 6L x 6T grid elsewhere

Table 9.4 Summary of estimated factors of safety for each reinforced slope section at the US54-Fulton test site.

Slope Section	Reinforcing Scheme	Estimated Factor of Safety
A	4.5L x 4.5T	1.07 – 1.17
B	6.0L x 6.0T	1.03 – 1.05
C	3.0L x 3.0T (4 rows) 6.0L x 6.0T (rest)	1.03 – 1.07
D	3.0L x 3.0T (6 rows)	1.00 – 1.02
E	10.0L x 10.0T	1.01

9.3. Field Installation

The US54-Fulton site was regraded to the original slope configuration in December 2002. Field installation of the reinforcing member began January 10, 2003 and was completed on January 15, 2003. Details of installation activities and performance are provided subsequently in Chapter 10.

9.4. Instrumentation

Instrumentation utilized at the US54-Fulton test site again consisted of inclinometers, instrumented reinforcing members, standpipe piezometers, and an array of moisture sensors. Figure 9.5 shows a plan view of the site with the locations of all instrumentation indicated. Six instrumented reinforcing members similar to those used at previous sites were installed during installation. Two instrumented members (IM-20 and IM-25) were placed in Section B while one instrumented member was placed in each of the remaining sections. Member IM-16 was placed in Section A, IM-8 in Section C, IM-21 in Section D, and IM-10 in Section E.

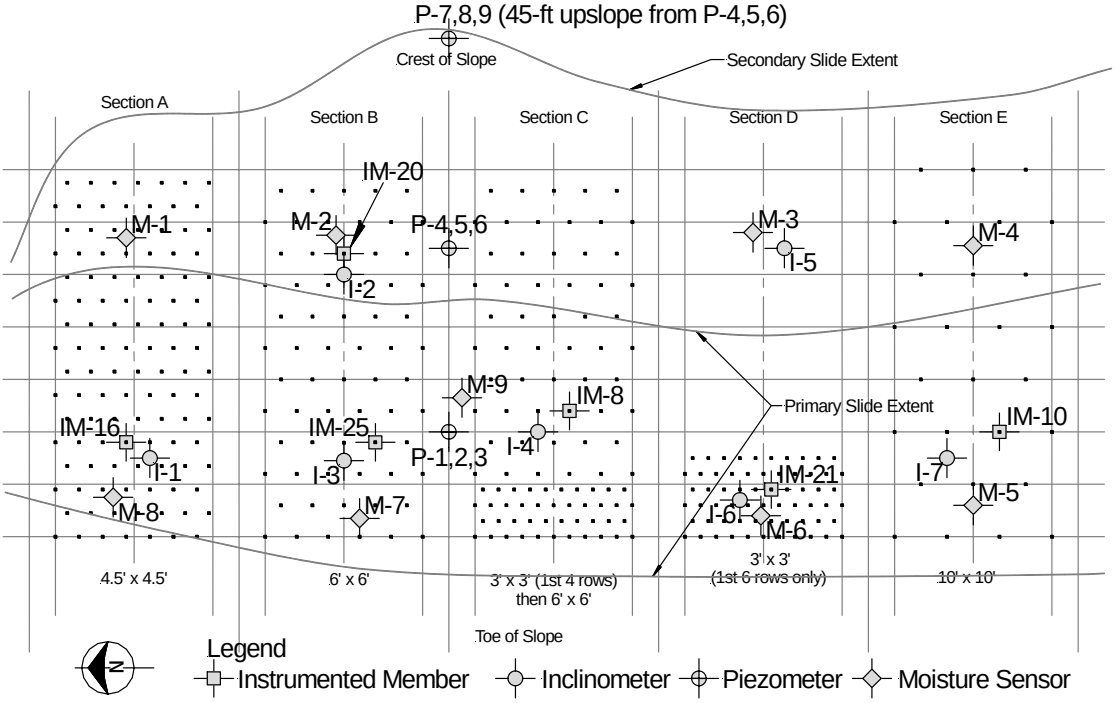

Figure 9.5 Plan view of US54-Fulton test site showing locations of instrumentation.

Seven inclinometer casings were installed at the site on January 29, 2003. All inclinometer casings were installed within 6-in (15-cm) diameter boreholes extending at least 5-ft (1.5-m) beneath the elevation of the toe of the slope. Six of the inclinometer casings were installed in close proximity to the instrumented reinforcing members; one additional casing was installed in the upper portion of Section D to monitor deformations within the unstabilized area of that section.

Three clusters of standpipe piezometers were also installed near the center of the slide area on January 29, 2003. Each cluster contains three piezometers screened at different depths. Piezometers P-1, P-2, and P-3 were installed in a cluster in the lower portion of the slope and screened at depths of 12.5-, 7.5-, and 2.5-ft (3.8-, 2.3-, and 0.8-m) below grade, respectively. Piezometers P-4, P-5, and P-6 were installed near the upper extent of the stabilized area at depths of 17.5-, 7.5-, and 2.5-ft (5.3-, 2.3-, and 0.8-m), respectively. Piezometers P-7, P-8, and P-9 were installed near the upper extent of the stabilized area at depths of 18.5-, 10.5-, and 2.5-ft (5.6-, 3.2-, and 0.8-m), respectively.

In addition to the standpipe piezometers, an array of moisture sensors was installed at the site on June 6, 2003. One array of two ThetaProbes® and two Equitensiometers® was connected to a data logger at location M-9 for essentially continuous monitoring of moisture conditions within the slope. Profile Probe® access tubes were also installed at locations M-1 through M-9 to monitor the vertical and lateral variability of moisture conditions at discrete intervals.

9.5. Field Performance

Field performance at the US54-Fulton site was monitored from February 2003 to January 2005. Readings were taken at intervals ranging from two weeks to three months for a total of 16 sets of readings. Results of field instrumentation readings, including precipitation, piezometric levels, deformations from inclinometers, and loads from instrumented reinforcing members, are presented in the following sections.

9.5.1. Precipitation at the US54-Fulton Test Site

Daily and monthly precipitation data recorded at the National Climatic Data Center weather station in Fulton, Missouri are plotted in Figure 9.6 along with the 50-year average monthly precipitation. In general, precipitation of the site has fluctuated about the average levels with no extended periods of above or below average precipitation. Monthly measured precipitation in September 2003, March 2004, and January 2005 was more than 3-in. above normal. Between February 18, 2004 and March 30, 2004, several events of high precipitation occurred resulting in 7.3 inches of rainfall, including three inches on March 27, 2004. During the first week of January 2005, 4.95 inches of precipitation occurred in Fulton, MO. An additional 1.5 inch of precipitation occurred the following week.

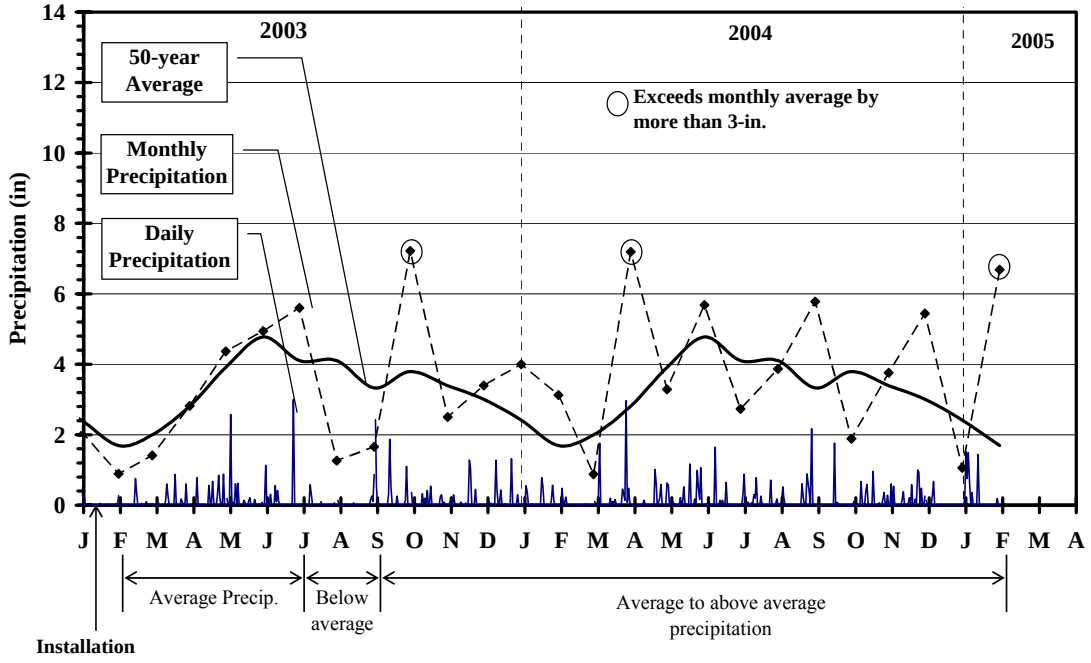

Figure 9.6 Recorded daily, monthly, and 50-year average precipitation from the Fulton Missouri NCDC station approximately 1 mile south of the US54-Fulton site.

9.5.2. Piezometers and Moisture Sensors

Measured piezometric levels for the US54-Fulton site are shown in Figures 9.7 and 9.8. The piezometers located just above the former slide area, P-7, P-8, and P-9, have been dry since installation, as has piezometer P-6 at the middle of the slope. The remaining piezometers at the site have shown little response to high levels of precipitation with exception of the readings on March 30, 2004 and January 20, 2005. Piezometric levels near the slope surface increased by approximately three feet between February 18, 2004 and March 30, 2004 in response to heavy precipitation. A month of similarly high precipitation in September 2003 did not appear to have a significant effect on the piezometric levels within the slope. This could be attributed to the delay in reading the piezometric levels. Data were collected on June 9, 2003 and October 22, 2003, indicating the possibility that potential increased piezometric levels associated with the September 2003 precipitation were not recorded. However, it is also possible that piezometric levels were not significantly affected by this event. Precipitation in July and August 2003 was below average, which could have resulted in the September 2003 precipitation not producing elevated piezometric levels. Furthermore, the precipitation events producing the monthly total in September 2003 were generally small, but frequent, while the monthly precipitation in March 2004 resulted from more intense precipitation events. Additionally, no deformations occurred within the slope following September 2003 which suggest that the piezometric levels did not rise significantly during this time.

Piezometric levels measured on January 20, 2005 were elevated over typical readings but were not as high as the readings on March 30, 2004. The elevated piezometric levels are due to the heavy rainfall during the first week of January. It is possible that the highest piezometric levels resulting from precipitation during this period were not measured due to a lag in readings.

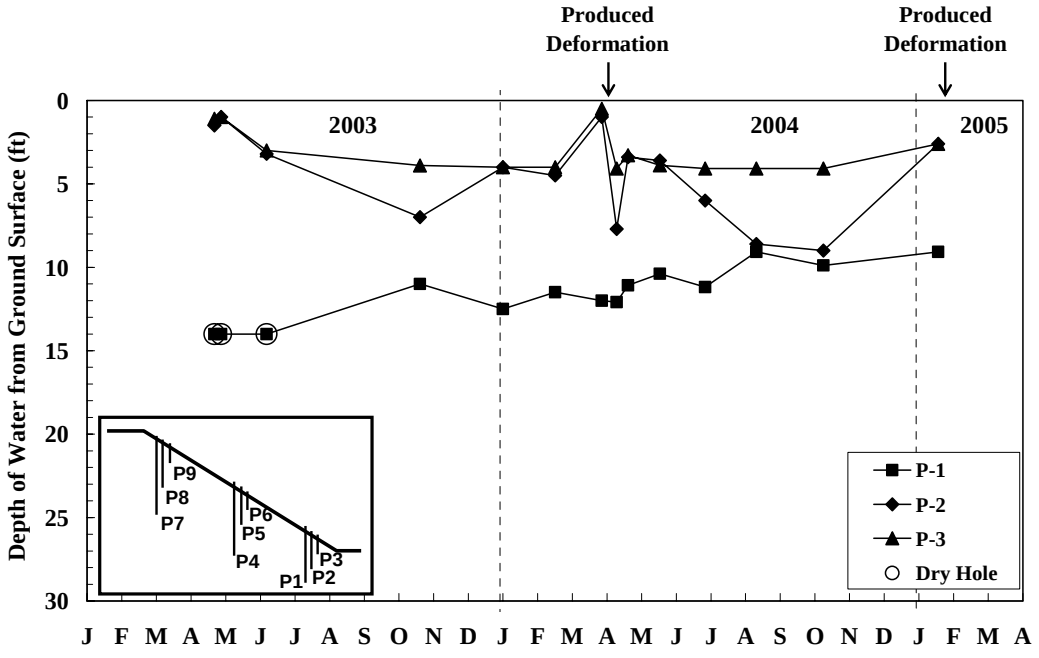

Figure 9.7 Measured piezometric levels for piezometers P-1, P-2, and P-3 near the toe of the slope at the US54-Fulton site.

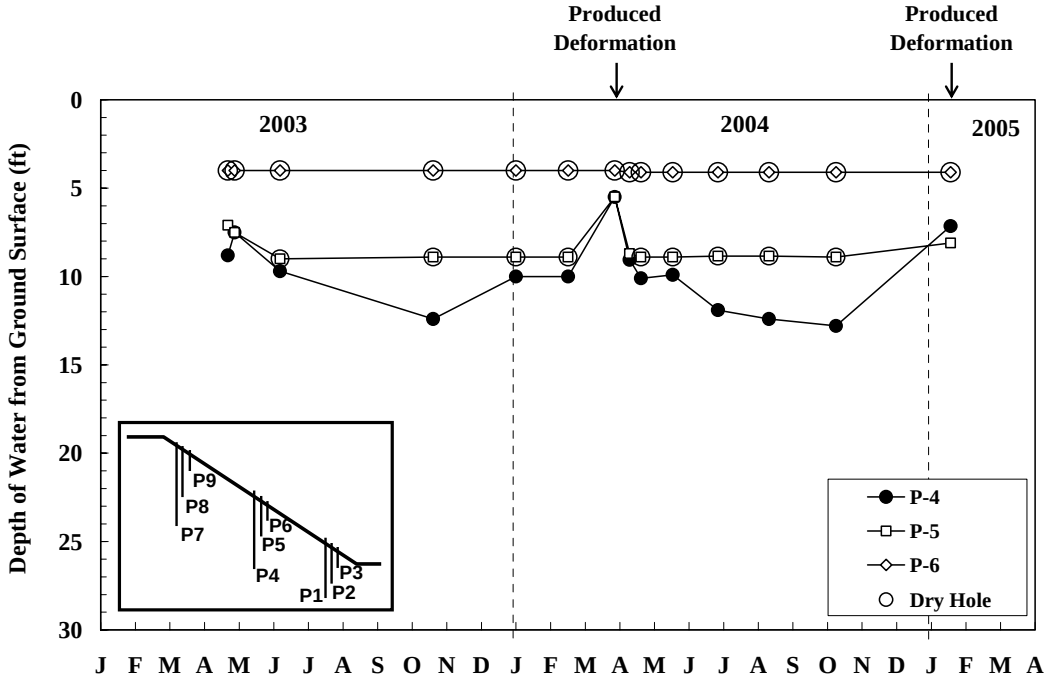

Figure 9.8 Measured piezometric levels for piezometers P-4, P-5, and P-6 at the US54-Fulton site.

Data from the soil moisture and soil suction sensors installed near the center of the slide area at location M-9 are plotted in Figure 9.9. While no data is available prior to mid-June 2003, the data acquired appear consistent and reliable. The exception to this is the Equitensiometer placed at 40 cm below ground, which began providing very sporadic readings in summer 2004. The data indicate several prolonged drying periods in summer 2003 and summer and fall 2004 and a short drying period in February 2004. Between these drying periods pore pressures were generally near zero except for two small "blips" in the record that occurred in late February and late March 2004. These responses are most evident in the ThetaProbe records, but are also apparent in the Equitensiometer record for the sensor located at 40 cm below ground. These blips also correspond to two of the most intense precipitation events during the period that volumetric water content and soil suction were recorded. Combined with observations of elevated levels in piezometers at approximately the same time, these results suggest that the slope at the US54-Fulton site is more sensitive to intense precipitation than to less intense but steady precipitation.

9.5.3. Slope Inclinometers

Measured displacements versus time for each inclinometer at the SU54-Fulton site are plotted in Figure 9.10. Arrows at the top of the figure indicate dates when elevated piezometric levels were observed. The observed displacement versus time at the US54-Fulton site is different than was observed at the other test sites. Rather than having somewhat extended periods of increasing movements followed by stabilized movements as resistance was mobilized in reinforcing members as was generally experienced at other sites, movements at the US54-Fulton site have generally been rather abrupt and have tended to coincide with individual intense precipitation events rather than longer term trends in

precipitation. Deformations between these sporadic events have been negligible and show no indication of creep movements.

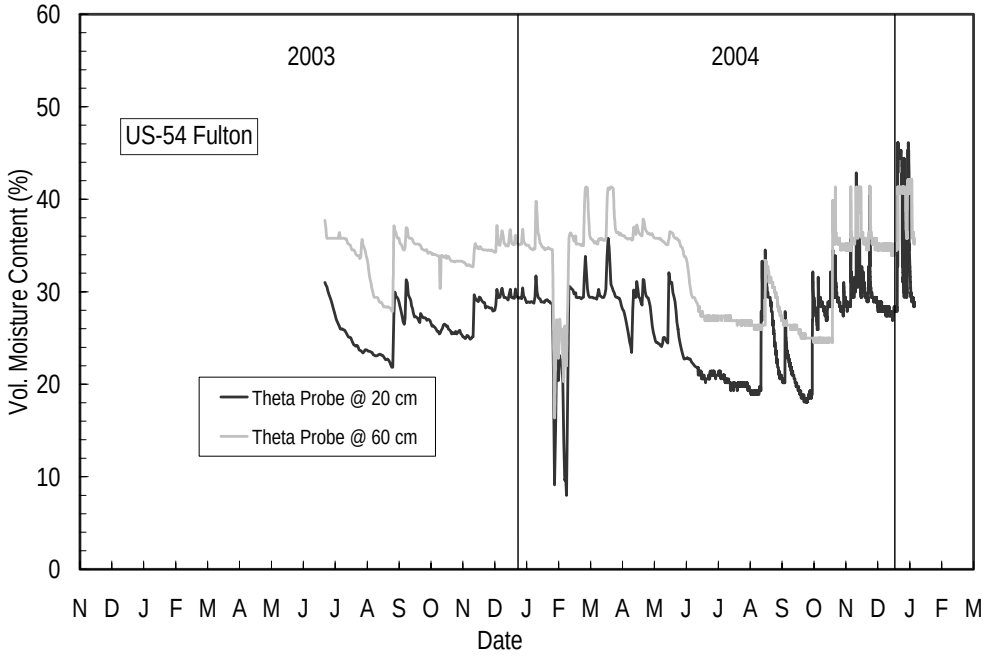

(a) soil moisture sensors

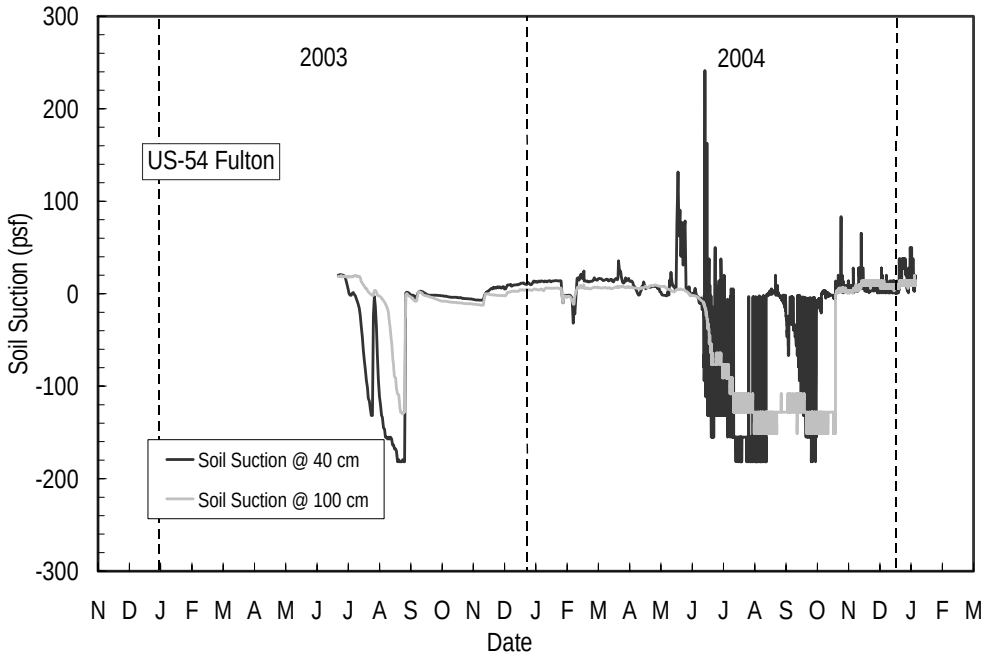

(b) soil suction sensors

Figure 9.9 Soil suction and volumetric water content from the US54-Fulton test site: (a) ThetaProbe™ sensors and (b) Equitensiometer™ sensors.

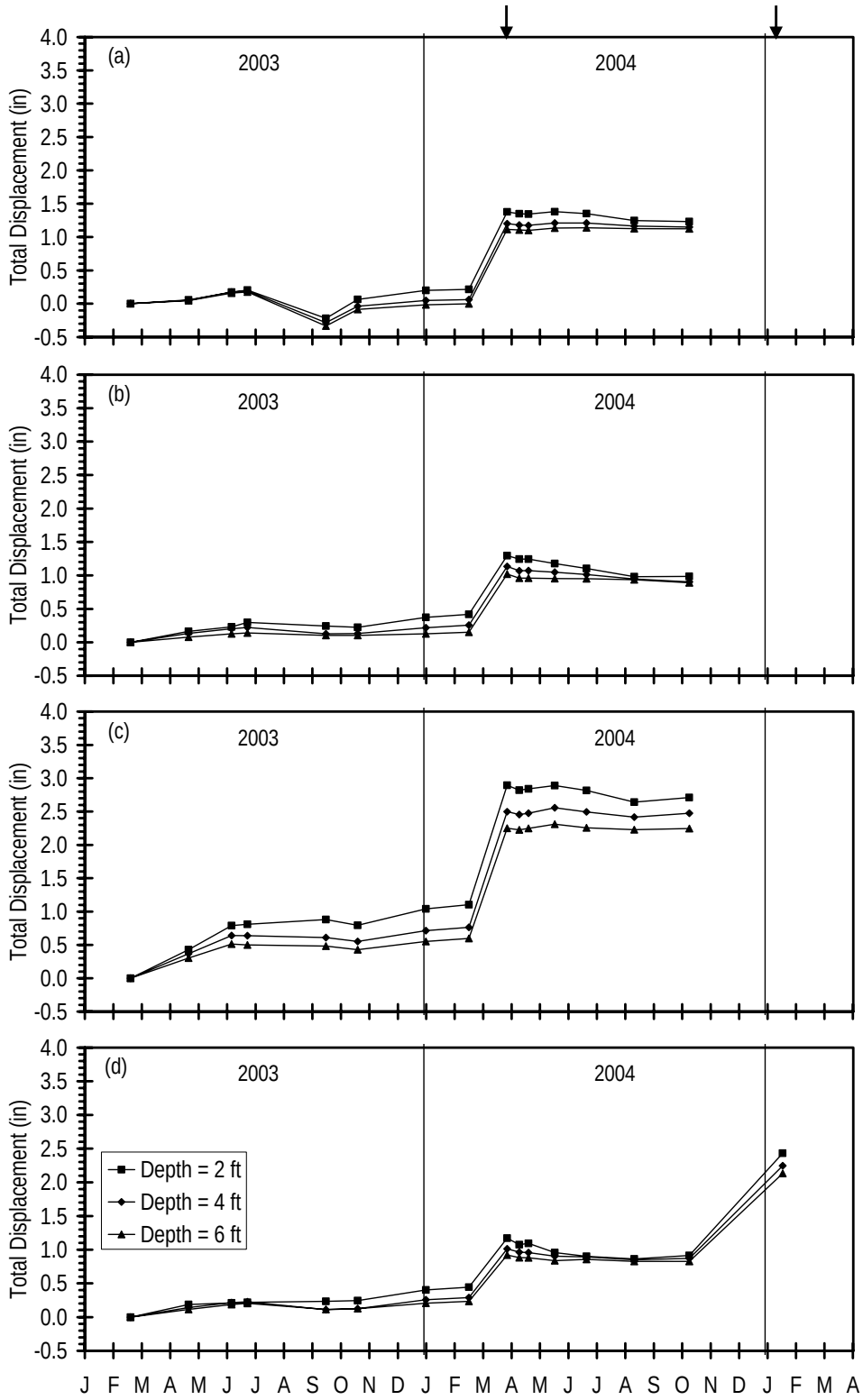

Figure 9.10 Measured displacement versus time for inclinometers at the US54-Fulton site: (a) I-1 in Section A, (b) I-2 in Section B, (c) I-3 in Section B, (d) I-4 in Section C, (e) I-5 in Section D, (f) I-6 in Section D, and (g) I-7 in Section E (cont'd).

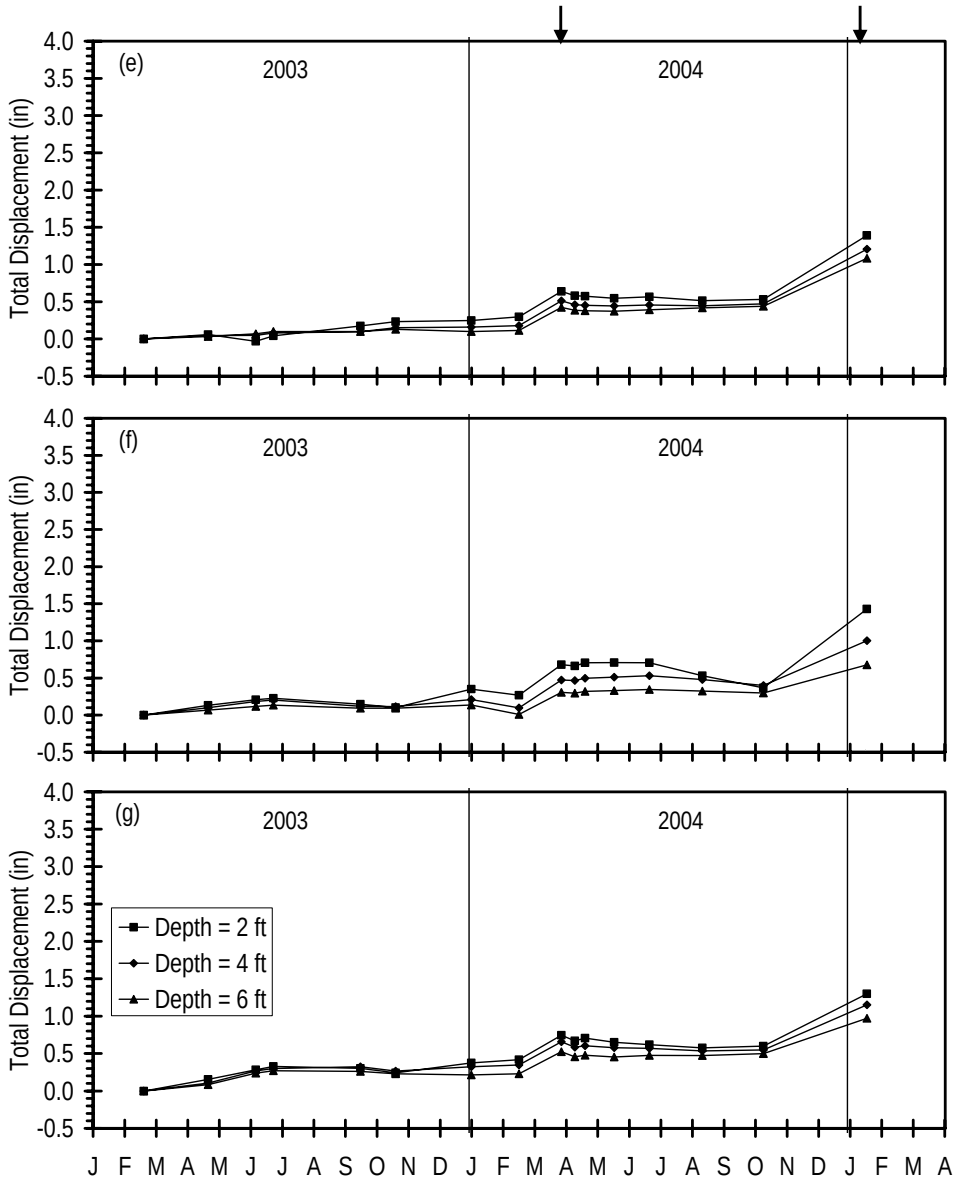

Figure 9.10 Measured displacement versus time for inclinometers at the US54-Fulton site: (a) I-1 in Section A, (b) I-2 in Section B, (c) I-3 in Section B, (d) I-4 in Section C, (e) I-5 in Section D, (f) I-6 in Section D, and (g) I-7 in Section E.

Two instances of deformation have been observed at the US54-Fulton site. The first coincides with an intense precipitation event and associated changes in pore pressures that occurred between February 18, 2004 and March 30, 2004. Following this period of deformation, displacements were highest in inclinometers I-1, I-2, and I-3 in Sections A and B. The second instance of displacement occurred between October 11, 2004 and January 19, 2005. This instance is presumed to be a result of the intense precipitation in January 2005. Inclinometers I-1, I-2, and I-3 were severely deformed during these events at the same time as additional displacements were observed in all other sections. These observations suggest

that previous sliding at the site was initiated in the area of Sections A and B and that the sliding in the remaining sections was secondary.

Figure 9.11 shows the displacement versus depth for inclinometer I-4 in Section C. These data indicate that the sliding surface is located at a depth of approximately 12- to 14-ft, well below the tips of the reinforcing members. Other inclinometers at the US54-Fulton site show sliding zones at depths ranging from 9- to 17-ft. Although there is some movement within the upper 8-ft. of the slope, most of the observed displacement is occurring below the bottom of the reinforcing members, indicating that the reinforcing members are moving down slope with the soil and are not providing significant resistance to sliding at least at the locations of inclinometers. A summary of depths of the sliding and surficial and sliding surface displacements for each inclinometer is provided in Table 9.4.

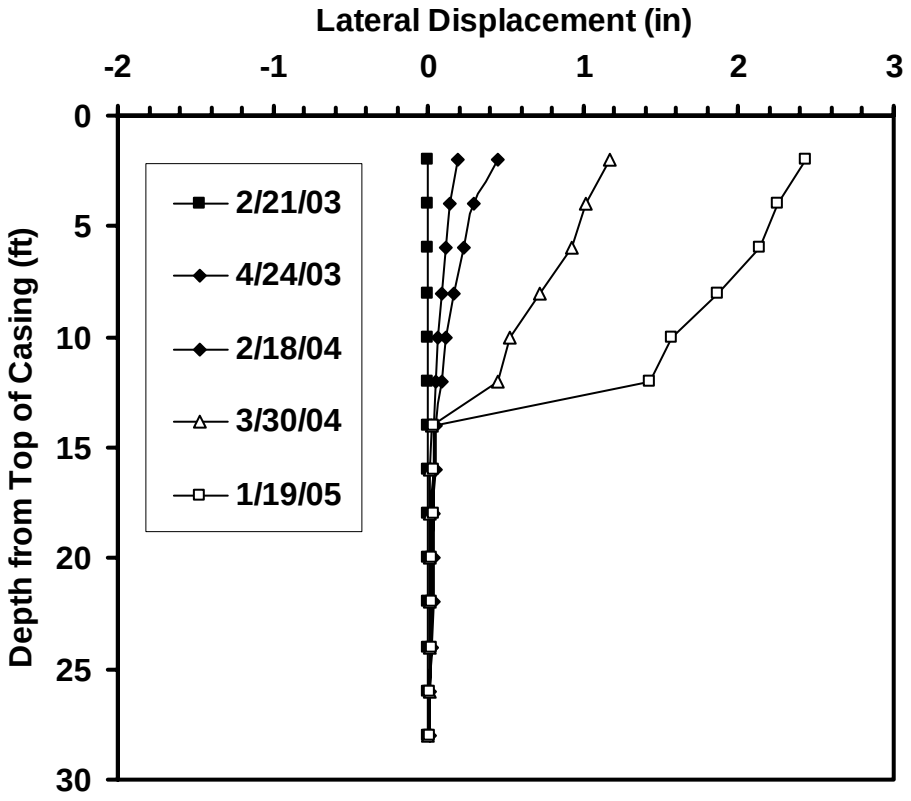

Figure 9.11 Measured displacement versus depth for inclinometer I-4 at the US54-Fulton site.

Despite the large deformations observed in Sections A and B, no obvious surface expressions of failure have been observed. A slight dip in the upper portion of the slope in Section B can be seen, as can a slight bulge in the lower portion of the slope. However, no clear cracks or scarps are visible.

Table 9.4 Summary of observed displacements at surface and at sliding depth for inclinometers at US55-Fulton site.

Incl.	Test Section	Depth of Sliding Surface	Displacement at sliding surface (in)		Displacement at 2-ft (in)	
			3/30/2004	1/19/2005	3/30/2004	1/19/2005
I-1	A	9	1.05	1.38	unable to measure	
I-2	B	17	0.65	1.30	unable to measure	
I-3	B	9	1.98	2.90	unable to measure	
I-4	C	13	0.42	1.17	1.39	2.43
I-5	D	14	0.34	0.64	0.53	1.39
I-6	D	--	--	0.68	--	1.43
I-7	E	13	0.33	0.74	0.71	1.30

9.5.4. Instrumented Reinforcing Members

Strain gage readings from instrumented member IM-25 in Section B of the US54-Fulton site were used to compute moments along the length of the reinforcing member. The maximum moment in reinforcing member IM-25 is plotted versus date in Figure 9.12a, while the displacement versus date for Inclinometer I-3 is shown in Figure 9.12b. The shaded regions indicate periods when displacements were observed to occur. As was observed at previously described sites, increases in bending moments are observed to occur when displacements are observed to increase, and maximum moments are generally constant during periods of little displacement. The magnitude of the maximum bending moments at the US54-Fulton site is somewhat surprising given that the reinforcing members do not intercept the sliding surface based on inclinometer measurements. The fact that some load is being transferred to the reinforcing members suggests that the reinforcement is providing some resistance to sliding along shallow surfaces, and may be contributing to the stability of the slope.

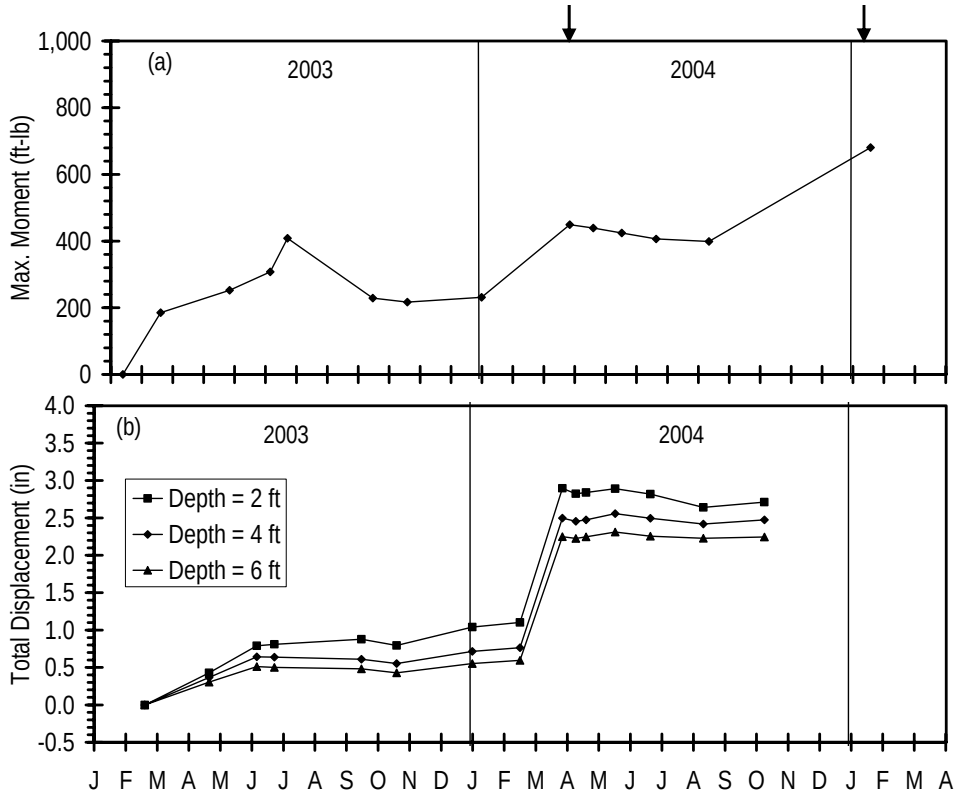

Figure 9.12 Comparison of maximum bending moments and slope displacement: (a) Maximum interpreted moment in IM-25 and (b) measured displacement in inclinometer I-3.

9.6. Summary

Activities undertaken to establish the US54-Fulton test site have been described in this chapter. The slope at the site is a relatively flat, but long excavated slope in ablation till. Five different stabilized sections with different reinforcement configurations were constructed to evaluate the effectiveness of different stabilization schemes. Results obtained from monitoring of field instrumentation at the site indicate that deformations of up to 3 inches have occurred, generally concentrated at depths that exceed the depths of reinforcing members. However, all of the stabilized sections remain stable despite the fact that sliding appears to be occurring largely below the reinforcing members.

Chapter 10. Construction Methods and Performance

In this chapter, field installation activities undertaken to install reinforcing members at each test site are described in detail. Descriptions include the type(s) of equipment used at each site, problems encountered during installation and the actions taken to remedy the problems, and the installation performance as measured by "penetration rates", which indicate the rate of penetration during installation independent of setup time between member installations, and "installation rates" which include setup time.

10.1. Field Installation at I70-Emma Site

Field installation activities at the I70-Emma site were performed at two different times. Slide areas S1 and S2 were stabilized in October and November 1999 during Phase I of the project. Slide area S3, which was used as a control slide area during Phase I, was stabilized in January 2003 during Phase II following the failure of the section when used as a control slide. Field installation activities during these two periods are described in more detail in the following sections.

10.1.1. Installation in Slide Areas S1 and S2

Initial attempts to install reinforcing members at the I70-Emma site occurred on October 18, 1999. The equipment utilized at this time was a Case 580 backhoe with an Okada OKB 305 hydraulic hammer shown in Figure 10.1. While the backhoe mounted hammer was able to drive the recycled plastic members into the slope, it was extremely difficult to get the members installed without damaging them. Installation of 45 members was attempted using the backhoe, but 22 of these were broken during installation. The primary reason for the high incidence of member failure was that the equipment had no means for maintaining the alignment of the hammer and the reinforcing member other than the skill of the operator. As the member was installed, the backhoe boom follows an arc that requires that the hammer be continuously realigned to maintain alignment with the reinforcing member and prevent failure of the members in bending due to the misalignment. Doing so proved exceptionally difficult, particularly since it was difficult to maintain the equipment in a fixed position on the slope. An additional problem with this equipment included having substantial difficulty maneuvering into position on the slope which caused severe rutting and damage to the slope and previously installed reinforcing members. As a result of these problems, use of the backhoe mounted hammer was discontinued.

Installation at the I70-Emma site was resumed in November 1999 using a Davey-Kent DK100B track-mounted hydraulic rock drill shown in Figure 10.2. This rig proved to be much more effective than the backhoe because the rig has a mast that maintains the alignment of the percussion hammer with the reinforcing member. The rig also proved to be much more maneuverable and caused less damage to the slope face, although the rig did have to be tethered to a truck located at the top of the slope when installing members on the steepest areas of the slope. A second rig, an Ingersoll Rand (IR) CM150 pneumatic rock drill shown in Figure 10.2, was also used at the I70-Emma site during this time. However, penetration rates achieved with the IR rig were significantly lower than those achieved with the Davey-Kent rig so its use was limited to installation of only a handful of members.

Figure 10.1 Backhoe mounted hammer used for initial installation attempts at the I70-Emma test site during Phase I.

Using the Davey-Kent rig, a total of 154 members[1] were installed in slide area S1 and 163 in slide area S2 during the period November 11-22, 1999. Members in slide area S1 were installed approximately perpendicular to the slope face while members in slide area S2 were installed vertically. Most members were driven to full depth. However, near the toe of the slope where the soil had been previously excavated and replaced with concrete rubble and/or large aggregate, members generally encountered refusal at depths from 3- to 6-ft (0.9- to 1.8-m). The portions of members remaining above ground were subsequently cut off using a gas-powered chain saw. Figure 10.3 shows a photograph of the site near the end of installation.

While several mechanical problems delayed completion for several days, the overall performance of the track-mounted rig proved acceptable and all 317 members installed at the site were driven in a little over four working days. Table 10.1 summarizes data collected regarding penetration rates during these installations and Figure 10.4 shows a frequency distribution of the measured average penetration rates for members installed in slide areas S1 and S2. Average penetration rates varied from 0.4- to 10.2-ft/min (0.1- to 3.1-m/min) with a mean of 4.4-ft/min (1.3-m/min) when considering data from both slide areas combined. Installation rates including set up time between member installations were relatively low given that this was the first test site, but a peak installation rate of approximately 80 members/day was achieved near the end of installation.

[1] Most of the members planned for installation in the lowest three rows of reinforcement could not be installed because of underground obstacles.

(a) Davey-Kent DK100B track-mounted hydraulic rig

(b) Ingersoll Rand CM150 track-mounted pneumatic rig

Figure 10.2 Photograph of equipment used to install majority of recycled plastic reinforcing members at the I70-Emma test site during Phase I.

10.1.2. Installation in Slide Area S3

Slide area S3 was regraded to the original slope configuration in early Fall 2002. Field installation in slide area S3 at the I70-Emma site took place on January 6-7, 2003. Reinforcing members were installed using two different pieces of equipment shown in Figure 10.5. The first piece of equipment was an Ingersoll Rand (IR) ECM350 track-mounted drill rig. This rig is a pneumatic hammer drill rig similar to the IR CM150 used during Phase I installations at this site and at other test sites. However, the ECM350 rig operates with higher air pressures and the drill mast is attached to an extendable boom that enables it to cover a larger area of the slope without requiring movement of the chassis. The extendable

boom also permitted the equipment to move up the slope "face first" without tipping and eliminated the need to tether the equipment to the guard-rail or other support. The second piece of equipment utilized was a simple drop-weight device, the Daken Farm King, commonly used for driving fence or guard-rail posts mounted on a skid-steer loader. Both types of equipment performed exceptionally well which allowed installation to proceed more rapidly than had been achieved in previous installations.

Figure 10.3 Photograph of I70-Emma test set near the end of installation activities for slide areas S1 and S2.

A total of 199 reinforcing members were installed in slide area S3, 196 of which were recycled plastic members from Batch A10. Three members were 3-in diameter pressure-treated landscaping timbers installed to evaluate the "drivability" of these members. Some slight "brooming" of the landscaping timbers was observed following installation of the timber members. However, the brooming is not expected to be significant in terms of the performance of the members. As was the case in slide areas S1 and S2, members installed near the toe of the slope generally met refusal at depths ranging from 3- to 6-ft (0.9- to 1.8-m) while members driven further up on the slope were driven to full depth. Recycled plastic members were generally driven without any significant problems and the overall installation was completed in less than two working days. Figure 10.6 shows a photograph of the site following the completed installation.

Frequency distributions of the average penetration rates observed for both types of equipment used at slide area S3 are shown in Figure 10.7. Overall, the average penetration rates ranged from under 2-ft/min (0.6-m/min) to over 18-ft/min (5.5-m/min) with a mean of 6.5-ft/min (2.0-m/min) and standard deviation of 4.6-ft/min (1.4-m/min). No significance differences were observed in the installation rates for the two different types of equipment used. Daily installation rates for each rig exceeded 100-members/day indicating that both pieces of equipment were more effective than previously utilized installation equipment.

Table 10.1 Penetration Performance of members installed at I-70 Emma Site

Stabilized Slope (Working Period)	Specimen Batch	Installed length	# Monitored	Penetration Rate (ft/min) Min.	Max.	Avg.	Std Dev.
Slide S1	A1	8 ft	79	0.7	10.2	5.0	2.2
(10/18/1999~11/12/1999)		< 8 ft	11	0.7	2.7	1.6	0.7
		ALL[1]	90	0.7	10.2	4.6	2.4
Slide S2	A1	8 ft	107	1.5	8.7	4.5	1.6
(11/17/1999~11/22/1999)		< 8 ft	43	0.4	7.0	2.4	1.4
		ALL	150	0.4	8.7	3.9	1.8
Slide S3	A10	8 ft	60	2.0	18.5	10.1	4.4
(1/6/2003~1/7/2003)		< 8 ft	88	0.1	17.0	4.1	2.8
		ALL	148	0.1	18.5	6.5	4.6
	A10[2]	ALL	25	1.2	15.0	4.2	2.9
	Timber Pile	ALL	3	2.8	12.3	6.9	4.9

[1]: average results for all monitored pins.

[2]: using drop-weight hammer driving machine.

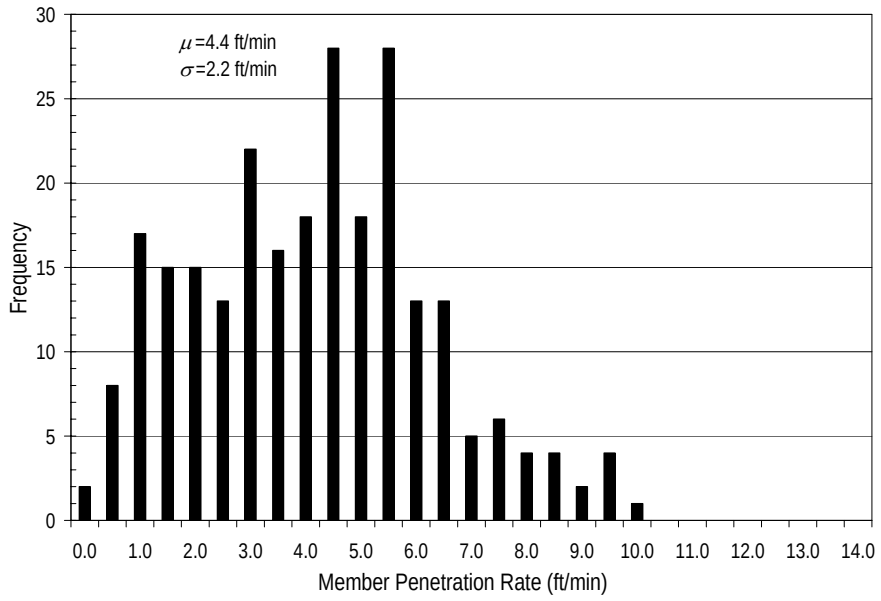

Figure 10.4 Frequency distribution of average penetration rates for recycled plastic members from Batch A2 installed in slide areas S1 and S2 at the I70-Emma test site. (μ=mean, σ=std. dev.)

Figure 10.5 Ingersoll Rand ECM350 pneumatic hammer drill (background) and drop-weight hammer rig (foreground) used to install reinforcing members in slide area S3 at the I70-Emma site.

Figure 10.6 Photograph of slide area S3 at the I70-Emma test site following completion of installation activities.

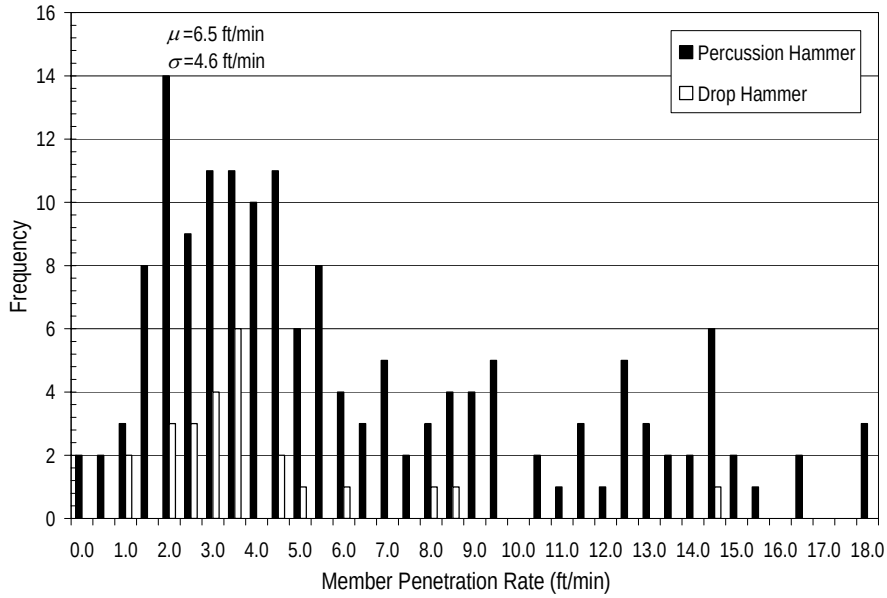

Figure 10.7 Frequency distribution of average penetration rates for recycled plastic members from Batch A2 installed in slide area S3 at the I70-Emma test site. (μ=mean, σ=std. dev.)

10.2. Field Installation at I435-Kansas City Sites

Field installation at the I435-Wornall Road test site began in October 2001 and was completed in December 2001. Installation at the I435-Holmes Road test site occurred during December 2001. The following sections describe installation activities at each of the respective test sites.

10.2.1. Installation at I435-Wornall Road Test Site

The I435-Wornall Road site was regraded to the original slope configuration by MoDOT maintenance crews in early October 2001. Installation of reinforcing members began on October 18, 2001 following several moderate to heavy rainfall events. At this time, noticeable seepage was observed coming from the slope in several locations and several small cracks were observed in the former slide area, which appeared to be an early indication of sliding. Furthermore, the available supply of reinforcing members at this time was not sufficient to complete the installation and additional members were not expected for several weeks. To respond to these observations, the installation plan was modified slightly so that alternating sections of reinforcing members would be installed to provide immediate stabilization across the slide area. These members were installed during the period October 18-30, 2001. The remaining sections of the stabilization pattern were then completed during the period December 5-7, 2001 after additional reinforcing members were acquired. Figure 10.8 shows a photograph of the slope at the completion of field installation. The survey flags in the photograph show the locations of all reinforcing members. Following the installation, the ornamental vegetation was replaced across the site and 4- to 6-in (10- to 15-cm) of landscaping mulch was placed across the slide area.

Figure 10.8 Photograph of I435-Wornall Road site following installation.

The equipment utilized for driving the reinforcing members at the I435-Wornall Road site included a Davey-Kent DK100B track-mounted hydraulic rig and a Ingersoll Rand (IR) CM150 pneumatic rock drill shown in Figure 10.9. A cable and pulley system was developed to assist maneuvering of both rigs on the slope and to prevent tipping of the rigs on the relatively steep slope (2.2H:1V). The Davey-Kent rig was previously utilized at the I70-Emma site during Phase I of the project with a great deal of success. However, significant problems were encountered in traversing the wet areas of the I435-Wornall Road slope with the Davey-Kent rig due to is relatively heavy weight, which caused severe rutting and resulted in the rig becoming stuck on several occasions. The lighter IR rig was therefore used to install the vast majority (590 out of 620) of reinforcing members installed at the site because of its lighter weight and additional maneuverability.

A total of 620 reinforcing members were installed in the slope[2]. Of these, 424 members were from Batch A4, which consisted of compression molded members with a relatively high filler content (primarily sawdust). The remaining members installed at the site were extruded members including 188 members from Batch A5, 3 members from Batch C9, 1 member from Batch B7, and 1 member from Batch B8. In addition to these members, three 3.5-in (9-cm) diameter steel pipe members (schedule 40) were also installed to evaluate the drivability of these members as compared to the recycled plastic members. Members in the 3-ft by 3-ft (0.9-m by 0.9-m) staggered grid were generally driven vertically while members in the 3-ft by 6-ft (0.9-m by 1.8-m) grid at the top of the slope were generally installed perpendicular to the slope face. Four of the recycled plastic members installed at the site were instrumented members as described in Section 5.3.

[2] Several members originally included in the design layout were not installed because they fell below the toe of the slope or because they may have impacted a culvert running through the embankment on the eastern edge of the stabilized area.

(a) Davey-Kent DK100B track-mounted hydraulic rig

(b) Ingersoll Rand CM150 track-mounted pneumatic rig

Figure 10.9 Equipment used to install reinforcing members at the I435-Wornall Road site: (a) Davey Kent rig and (b) Ingersoll Rand rig.

A second problem encountered during installation was that penetration rates for the reinforcing members dropped dramatically when the reinforcing members encountered the stiff compacted clay shale fill. Depths to the stiffer clay shale varied from approximately 5-ft (1.5-m) at the toe of the slope to greater than 8-ft (2.4-m) at the crest of the slope. To avoid inflicting significant damage to the reinforcing members, installation was halted when the

penetration rate dropped below approximately 3-in per minute (1.2-cm/min). At the same time, every effort was made to ensure that at least 6-in (15-cm) of penetration was achieved after reaching the stiffer soil to ensure that adequate resistance to sliding was available. The lengths of reinforcing members remaining above ground were removed using a gasoline-powered chain saw.

A summary of penetration performance for the I435-Wornall site and Holmes site is shown in Table 10.2. Figure 10.10 shows a frequency distribution of the average penetration rate, calculated as the total length of penetration divided by the total time of penetration, for 502 of the reinforcing members installed at the I435-Wornall Road site. All members included in the distribution are from Batches A4 and A5. As shown in the figure, penetration rates ranged from 0.5- to 14-ft/min (0.2- to 4.2-m/min) with an average penetration rate of 5.4-ft/min (1.6-m/min). This corresponds to an average driving time of 1.5 minutes for 8-ft (2.4-m) long members. Penetration rates for limited numbers of recycled plastic members from other batches (B7, B8, and C9), as well as steel pipe members, produced penetration rates that were similar to those observed for members from Batches A4 and A5 as shown by the arrows in Figure 10.10. The similarity in penetration rates for members with widely different stiffness suggests that member stiffness has a limited influence on penetration rate. Additional details regarding the relative penetration rates observed for different types of members can be found in Bowders et al (2003).

Table 10.2 Penetration Performance of members installed at I435-Wornall Road and I435-Holmes Road Sites

Stabilized Slope (Working Period)	Spec. Batch	Installed length	# Monitored	Penetration Rate (ft/min)			
				Min.	Max.	Avg.	Std Dev
I435 Wornall	A4	< 8 ft	251	1.0	13.4	4.4	2.1
(10/18/2001~12/7/2001)		ALL[1]	384	1.0	13.7	5.2	2.4
	A5	8 ft	49	3.8	9.7	6.6	1.4
		< 8 ft	61	2.2	13.0	6.0	2.0
		ALL	110	2.2	13.0	6.3	1.8
	B7	< 8 ft	1	- -	- -	6.0	- -
	B8	8 ft	1	- -	- -	3.3	- -
	C9	< 8 ft	3	3.5	12.0	6.7	4.6
	Steel Pipe	8 ft	3	4.8	6.9	5.9	1.0
I435 Holmes	A5	< 8 ft	6	3.1	5.8	4.6	1.0
(12/14/2001~12/20/2001)	Steel Pipe	< 8 ft	216	0.4	13.2	5.0	2.1

[1]: average results for all monitored pins.

Installation rates – the rate of installation including "set up" time between members – varied dramatically during installation of the reinforcing members. Several modifications to the driving equipment were evaluated during the first few days of installation. Installation

rates during these trials were generally very low because of the trial and error process required for evaluating the equipment. After several days of trials, installation rates increased dramatically and approached the installation rates that were achieved at the I70-Emma site during Phase I. The peak installation rate achieved at the I435-Wornall Road site was 114 pins per day with an average installation rate of approximately 80 pins per day (excluding the initial trials undertaken during the first days of installation).

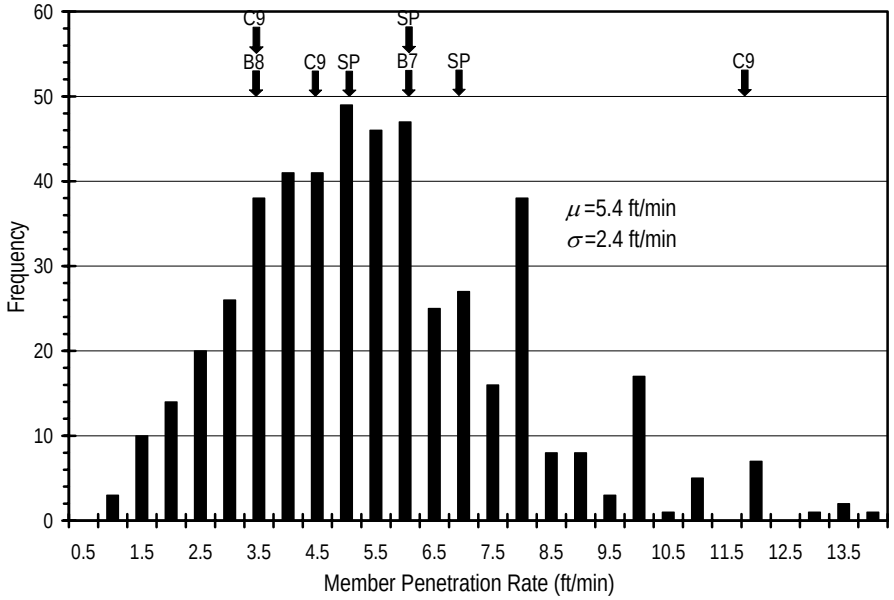

Figure 10.10 Frequency distribution of average penetration rates for recycled plastic members from Batches A4 and A5 installed at the I435-Wornall Road site. (μ=mean, σ=std. dev.)

10.2.2. Installation at I435-Holmes Road Test Site

Installation at the I435-Holmes Road site was performed during the period December 14-20, 2001 using the same IR CM150 rig used for installation at the I435-Wornall Road site. A total of 262 members[3] were installed at the site including 256 galvanized steel pipes and 6 recycled plastic members from Batch A5 for comparative purposes. Two of the steel pipe members were instrumented as described in Section 5.3.

Figure 10.11 shows a photograph of the site just after completion of the installation. Unlike the I435-Wornall Road site, the I435-Holmes Road site was not regraded to its original slope prior to installation. Instead, reinforcing members were installed such that the top of the members would lie at the anticipated ground surface after the site was regraded. Members installed near the crest of the slope generally did not meet refusal while members installed in the middle and lower portions of the slope met refusal at depths ranging from 4- to 8-ft (1.2- to 2.4-m). This suggests that the compacted clay shale stratum was shallower than originally assumed for selection of the stabilization scheme. Members that could not be installed to the requisite depth were cut off at the appropriate location using an acetylene

[3] Several members included in the original design layout were again eliminated during field layout and installation because they fell beyond the extent of the slide.

torch or a portable band saw. Following installation, any void space within the pipes that did not become plugged with soil during installation was filled with bagged cement grout to prevent accumulation of water within the pipes.

Figure 10.11 Photograph of I435-Holmes Road site just after installation.

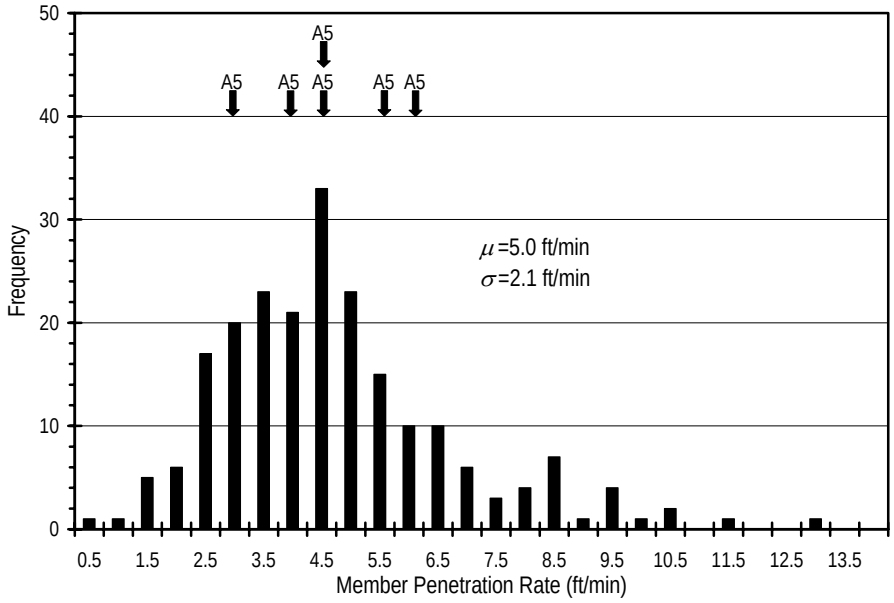

Figure 10.12 Frequency distribution of average penetration rates for galvanized steel members installed at the I435-Holmes Road site. (μ=mean, σ=std. dev.)

Penetration rates were recorded for 218 of the steel pipes and all 6 plastic members. As shown in Figure 10.12, the average penetration rate for the steel pipes was 5.0-ft/min (1.5-m/min) with a standard deviation of 2.1-ft/min (0.6-m/min) while the average

penetration rate for the plastic members from Batch A5 was 4.6-ft/min (1.4-m/min), only slightly lower than that observed for the steel members. These observations again suggest that member stiffness has only a limited effect in determining field installation rates. The peak installation rate (including set up time between members) was again near 100 members per day, with an average installation rate of approximately 80 members per day.

Overall, use of steel reinforcing members provided little benefit over use of recycled plastic members in terms of constructability. Penetration rates observed for the steel members were slightly greater than those observed for recycled members. However, the steel members are significantly heavier (approximately 70-lb.) than recycled plastic members (approximately 45-lb.) and are more difficult to cut off when refusal is met during installation. As a result, overall installation rates observed for steel and recycled plastic members were comparable. Thus, there appears to be little advantage to using steel members from an installation point of view, although there may be some advantages (or disadvantages) in terms of their effectiveness for long-term stabilization.

10.3. Field Installation at US36-Stewartsville Site

The main slide area and control slide area at the US36-Stewartsville site were regraded to their original slopes in spring 2002. Installation of reinforcing members was performed during the period April 30 to May 7, 2002. The equipment utilized at the US36-Stewartsville site was the Ingersoll Rand (IR) CM150 rig that was previously utilized at the I435-Wornall Road and I435-Holmes Road sites (Figure 10.9b). Because of the steep slope and the fact that the guardrail for the westbound lanes was located approximately 20-ft (6-m) back from the crest of the slope, the rig was tethered to a truck located between the guardrail and the crest of the slope to help control the rig during driving. Otherwise, the rig performed well. Figure 10.13 shows a photograph of the site near the end of installation.

Figure 10.13 Photograph of US36-Stewartsville site nearing the completion of installation.

A total of 360 recycled plastic members from Batch A6 were installed at the site. Only 59 of the members installed were driven to full depth; most of these were located near

the crest of the slope. Members installed near the toe of the slope generally reached refusal at depths between 4- and 5-ft (1.2- and 1.5-m) while members installed further up the slope reached refusal at progressively greater depths. In cases where members could not be installed to full depth, effort was made to ensure that the members penetrated at least 6-in (15-cm) into the stiffer stratum to provide adequate anchorage. The portions of the members left above grade were then cut off using a chain saw.

One problem experienced during installation was that several members installed early in the installation sequence split apart along the mid-plane of the member and shattered once they had penetrated several feet into the ground. Inspection of the remaining members on site revealed small cracks on the ends of some members as shown in Figure 10.14 that were apparently developed during the manufacturing process. The entire stock of members was therefore inspected and all pallets containing members with cracks were returned to the manufacturer. Approximately 21 members from these pallets were installed along the easternmost portion of Section D prior to remedying the problem. However, no further problems were experienced with the remaining members and no significant defects were observed in subsequent batches of reinforcing members used for the remaining sites.

Figure 10.14 Photographs of defective recycled plastic members damaged during installation.

Average penetration rates were determined for 208 members installed at the site. A summary of these measurements is provided in Table 10.3 and Figure 10.15 shows a frequency distribution of the average penetration rates determined for these members. The mean of all penetration rates was 5.2-ft/min (1.6-m/min) with a standard deviation of 3.2-ft/min (1.0-m/min). Installation rates (including set up time) achieved at the US36-Stewartsville site were again relatively slow during the initial phases of installation, but increased significantly once the problem encountered with the defective members was

addressed. The peak installation rate achieved at the US36-Stewartsville site was 93 members in one day, with an average rate of 70 members/day.

Table 10.3 Driving Performance of members installed at US36-Stewartsville Site

Stabilized Slope (Working Period)	Specimen Batch	Installed length	# Monitored	Penetration Rate (ft/min) Min.	Max.	Avg.	Std Dev
US36 Stewartsville	A6	8 ft	40	2.7	16.0	8.3	4.1
(4/30/2002~5/7/2002)		< 8 ft	166	1.7	16.9	4.4	2.3
		ALL[1]	206	1.7	16.9	5.2	3.2

[1]: average results for all monitored pins.

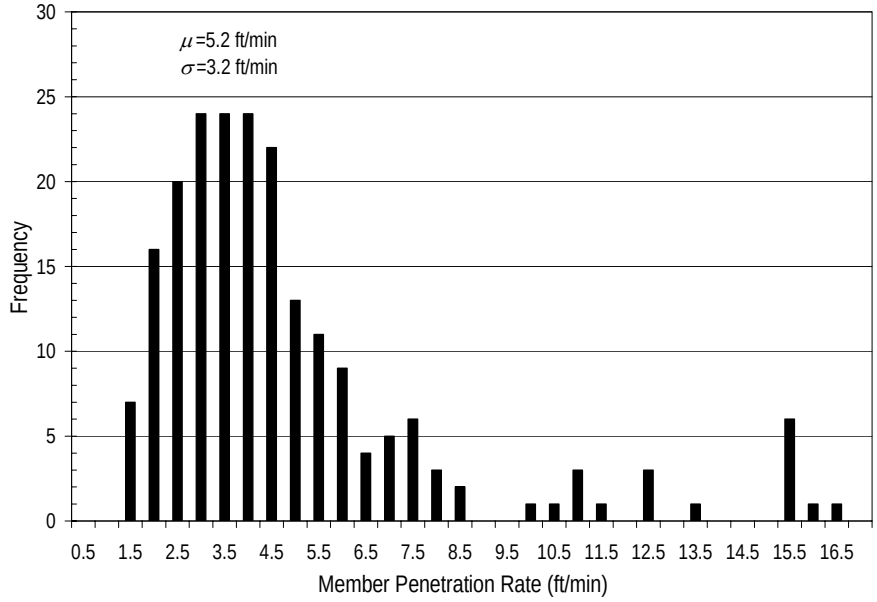

Figure 10.15 Frequency distribution of average penetration rates for recycled plastic members from Batch A5 installed at the US36-Stewartsville site. (μ=mean, σ=std. dev.)

Upon completion of installation, the slope was left unseeded for several weeks and heavy rains caused some minor erosion of the slope, which exposed a number of reinforcing members to depths of an inch or more. The exposed lengths were subsequently cut off as close to the ground surface as possible. Weeds and some grass grown from seed spread at the site have become somewhat established, which has helped to reduce erosion to some extent but minor erosion continues to occur during heavy rain events.

10.4. Field Installation at US54-Fulton Site

The US54-Fulton site was regraded to the original slope configuration in December 2002. Field installation of the reinforcing member began January 10, 2003 and was completed on January 15, 2003. The equipment utilized for installation was the Ingersoll

Rand CM350 that was utilized at the I70-Emma site during Phase II (Figure 10.5). This equipment was able to maneuver on the relatively flat (3.2H:1V) slope without the need for a tether.

A total of 373 recycled plastic members from Batch A10 were installed in the slope over four days. Three additional 3-inch (7.6-cm) diameter landscaping timbers were also installed to evaluate the drivability of timber members. In general, members installed near the top of the reinforcement pattern and members installed near the toe of the slope reached refusal at depths ranging from 3- to 7-ft (0.9- to 2.1-m), while members installed in the middle portion of the slope did not meet refusal. No significant differences were observed in the drivability of the recycled plastic and timber members.

Figure 10.16 shows a photograph of the site near the end of installation. Aside from a minor mechanical problem that delayed installation for one afternoon, the rig was able to install members at a significantly higher pace than was possible at previous sites. The peak installation rate achieved at the site was 141 members/day and all members were installed in just over three working days.

Table 10.4 shows a summary of installation measures for the US54-Fulton site and Figure 10.17 shows a frequency diagram of the average penetration rates observed for members driven at the US54-Fulton site. Average penetration rates ranged from 0.6-ft/min (0.2-m/min) to over 20-ft/min (6.1-m/min), with a mean rate of 6.6-ft/min (2.0-m/min). The penetration rates observed at the I70-Emma Slide S3 site and US54-Fulton site during Phase II are somewhat higher than those observed at previous sites, which contributed to increased installation rates at these sites. However, the high installation rates observed at these sites are believed to be primarily due to decreases in "set-up" time between member installations as a result of the ease of maneuvering on the slope and the extendable boom.

Figure 10.16 Photograph of US54-Fulton test site near the end of installation.

Table 10.4 Driving Performance of members installed at US54-Fulton Site

Stabilized Slope (Working Period)	Specimen Batch	Installed length	# Monitored	Penetration Rate (ft/min) Min.	Max.	Avg.	Std Dev
US54 Fulton	A10	8 ft	143	1.4	27.6	9.6	5.8
(1/10/2003~1/15/2003)		< 8 ft	223	0.6	14.5	4.7	2.5
		ALL[1]	366	0.6	27.6	6.6	4.8
	Timber Post	< 8 ft	3	3.6	9.6	6.4	3.0

[1]: average results for all monitored pins.

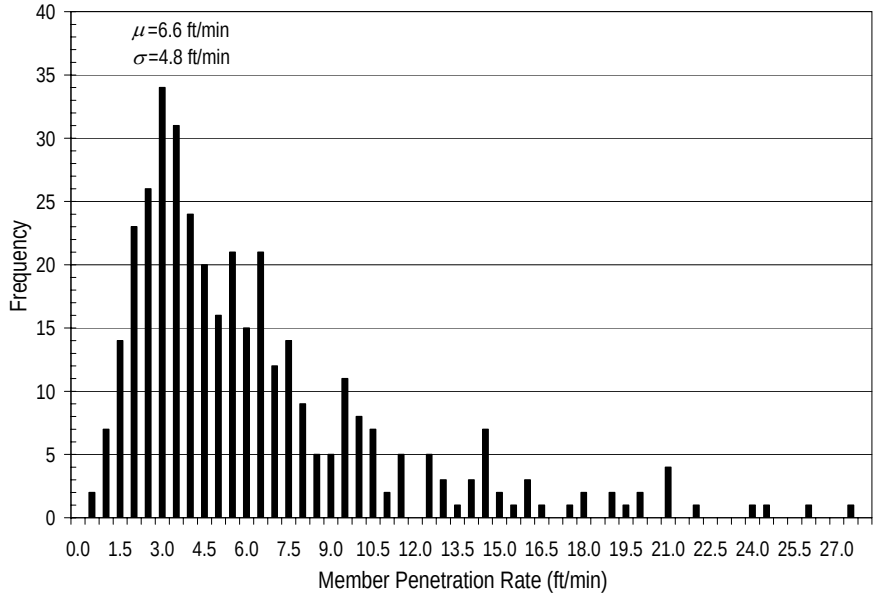

Figure 10.17 Frequency distribution of average penetration rates for recycled plastic members from Batch A10 installed at the US54-Fulton test site. (μ=mean, σ=std. dev.)

10.5. Comparison of Installation Performance

Figure 10.18 shows the average penetration rates achieved at each of the field test sites and Figure 10.19 shows the peak installation rates for the sites. The sites are listed in chronological order (from the first project to the most recent one). In general, installation performance generally improved with time both in terms of penetration rates as well as overall installation rates. Peak average penetration rates exceeded 6.0 ft/min (1.8 m/min) while peak installation rates exceeded 100 members per day for a single piece of installation equipment. Some of the improvement in installation performance is attributed to acquisition of experience by installation crews over time. However, later installations also utilized equipment that was better suited to the task, e.g. use of extendable booms, etc. Later installations at the I70-Emma site and the US54-Fulton sites also did not require tethering of the installation equipment which produced improvements in both penetration rates and

installation rates. It is notable that the strength and stiffness of the recycled plastic members generally decreased as installation progressed in the chronological order so there is little correlation of member strength and stiffness with installation rates.

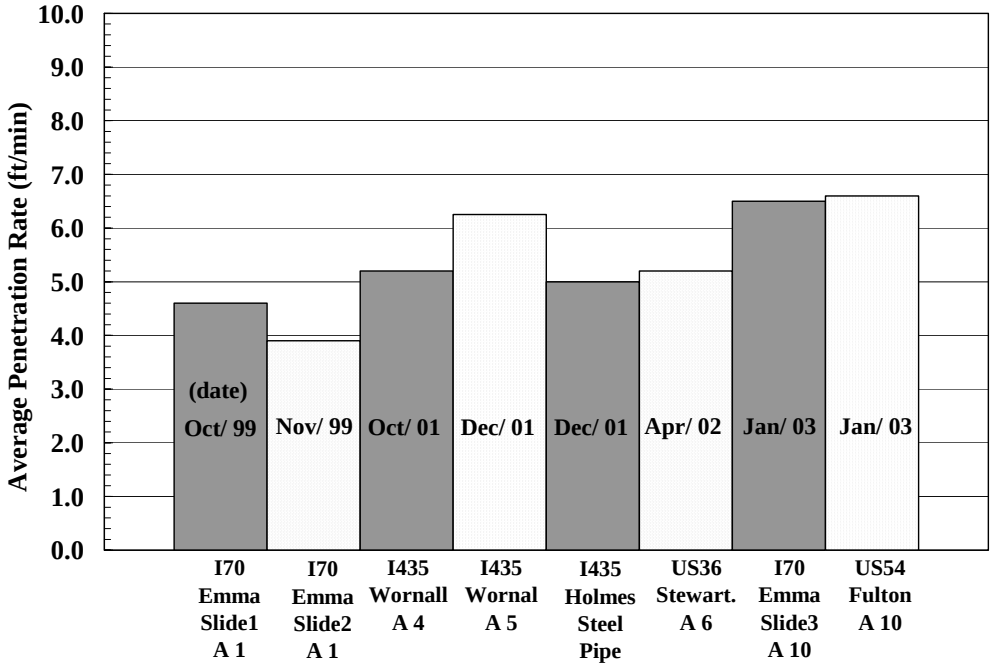

Figure 10.18 Average penetration rate versus installation sequence of seven slopes.

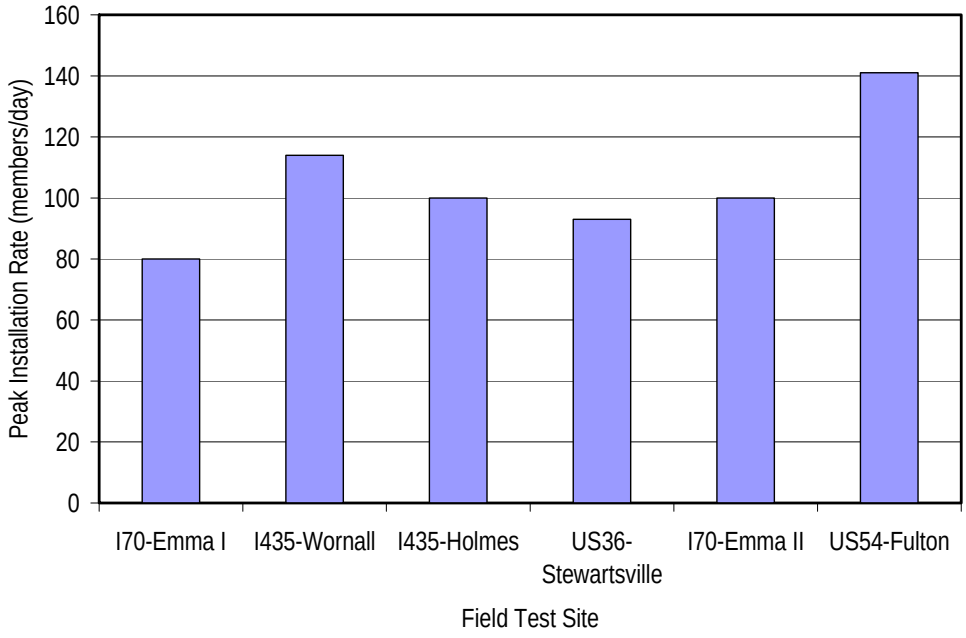

Figure 10.19 Peak installation rates achieved at respective field tests sites using one installation rig.

10.6. Summary

This chapter has described installation activities at the respective field test sites. Several different pieces of installation equipment have been successfully used to install recycled plastic members as well as similarly sized steel pipe and a limited number of similarly sized timber posts. All equipment utilized consisted of some form of percussion or impact hammering device to install the members in the ground. The common feature among the equipment that was successfully utilized for installation is that the equipment has a means for maintaining the alignment between the percussion or impact hammer and the member being installed to prevent damage to the member during installation. Using this type of equipment, average penetration rates (rate of penetration into the ground exclusive of set up time) reach 6 feet per minute and peak installation rates reached over 140 members per day for a single piece of equipment. Penetration rates across all sites averaged approximately 4 feet per minute and the average installation rate was approximately 100 members per day. Analysis of the installation data showed that there is little correlation between achievable penetration rates and the strength or stiffness of the reinforcing members. Overall installation efficiency also tended to improve with the experience of the installation crews.

Chapter 11. Evaluation and Calibration of Design Method

The general methodology for analysis of slopes stabilized with recycled plastic reinforcement described in Chapter 2 provides the basis for rigorous analysis of possible stabilization schemes. However, as described in Section 2.7, several specific issues remain unresolved. These issues include which method for predicting the limit soil pressure is most appropriate, what impact does member inclination have, and what effect, if any, does creep have on the appropriate estimation of member capacity. The field performance data acquired from the field test sites provides the basis upon which to evaluate and in fact calibrate the general analysis method so that the method predicts performance consistent with observed field performance. The procedures used to calibrate the analysis method are described in this chapter. Application of the calibration procedures to each test site is also presented. Finally, conclusions reached from collective evaluation of the calibration analysis are discussed and recommendations for improvements to the existing method are provided.

11.1. Method of Calibration

The main objective of calibrating the analysis method presented in Chapter 2 is to allow for better future design of slopes with "weak" reinforcing members. As discussed in Chapter 2, the primary source of uncertainty in the existing design method is predicting the magnitude of the resistance provided by the reinforcement. The focus of the calibration analyses has therefore been on improving methods for predicting the resistance in the reinforcement. Two procedures were used to evaluate/calibrate the analysis method depending on whether a failure was experienced in a specific test section.

11.1.1. Calibration Procedure for Failed Test Sections

In cases where a failure occurred in a test section, the calibration procedure follows classical back-calculating methods used for all slopes, but focuses on the resistance provided by the reinforcement rather than the shear strength parameters, pore pressure conditions, or other input parameters. For sites experiencing a failure through the reinforced section of the slope, the calibration procedure consists of the following steps:

1. Establish the as-built cross section for each test section based on construction records and previous site investigations.
2. Using classical back-calculation techniques and available information on shear strength parameters and piezometric conditions, establish parameters believed to have produced the original failure in the unreinforced slopes.
3. Develop baseline limit resistance curves for reinforcing members based on conditions established in Step 2 and the existing "baseline" analysis method.
4. Evaluate the baseline (theoretical) factor of safety for the as-built (reinforced) slope using best estimates of shear strength parameters at the time of failure and pore water pressures at the time of failure.
5. If the baseline factor of safety is not equal to unity, develop alternative limit resistance functions for the reinforcing members and evaluate the factors of safety for the as-built reinforced slope using those limit resistance functions.

Limit resistance functions producing a factor of safety of unity are possible calibration methods.

Like all back-calculation analyses, this calibration procedure is not unique. There may be several plausible and logical ways to vary the limit resistance to produce a factor of safety of unity. Additionally, the conditions within the slope at the time of failure are not certain so there is some uncertainty involved in the calibration. However, uncertainties associated with conditions within the slope can be significantly reduced through the use of extensive field instrumentation (e.g. piezometers, inclinometers, etc) as has been done in this project, so these uncertainties have been minimized to the extent possible. Uncertainties associated with the non-uniqueness of the calibrations cannot be completely eliminated. However, it is believe that by performing calibrations for several different test sites, it is likely that the most appropriate calibration procedure can be identified as the one that produces results that are consistently good for a variety of sites.

11.1.2. Calibration Procedure for Sections Where No Failure Occurred

If a failure does not occur, it is not possible to use traditional back-calculation procedures to evaluate and calibrate the design procedure because the factor of safety for the test section is never truly known (as in the case of failure). However, the analysis procedure can still be calibrated by relating the theoretical factors of safety from alternative procedures to slope deformations measured in the field to establish a "field performance function," and subsequently extrapolating this function to a failure condition (to be established). The procedure used is illustrated in Figure 11.1 and includes the following steps:

1. Establish the as-built cross section for each test section based on construction records and previous site investigations.
2. Using classical back-calculation techniques and other available information on shear strength parameters and piezometric conditions, establish parameters believed to have produced the original failure in the unreinforced slopes.
3. Evaluate baseline factors of safety for the as-built reinforced slope for key dates or conditions during the monitoring period using the existing analysis procedure and best estimates for shear strength parameters and piezometric conditions. This step is illustrated in Figure 11.1a.
4. Establish nominal slope deformations for each of the key conditions from inclinometer data (Figure 11.1b).
5. Plot the baseline factors of safety computed in Step 3 as a function of slope deformations for the same date/condition established in Step 4 to establish the baseline performance function. The performance function relates the theoretical factor of safety computed using a particular procedure to the deformation experienced in the field as shown in Figure 11.1c.
6. Establish a tolerable deformation limit to serve as a failure condition. This limit can be established from judgment or, preferably, from field data indicating the magnitude of deformations experienced in similar slopes prior to observation of notable signs of a failure. In the present work, field data presented in Chapters 6 and 9 suggest that a reasonable limit is on the order of 2.5- to 3-in.

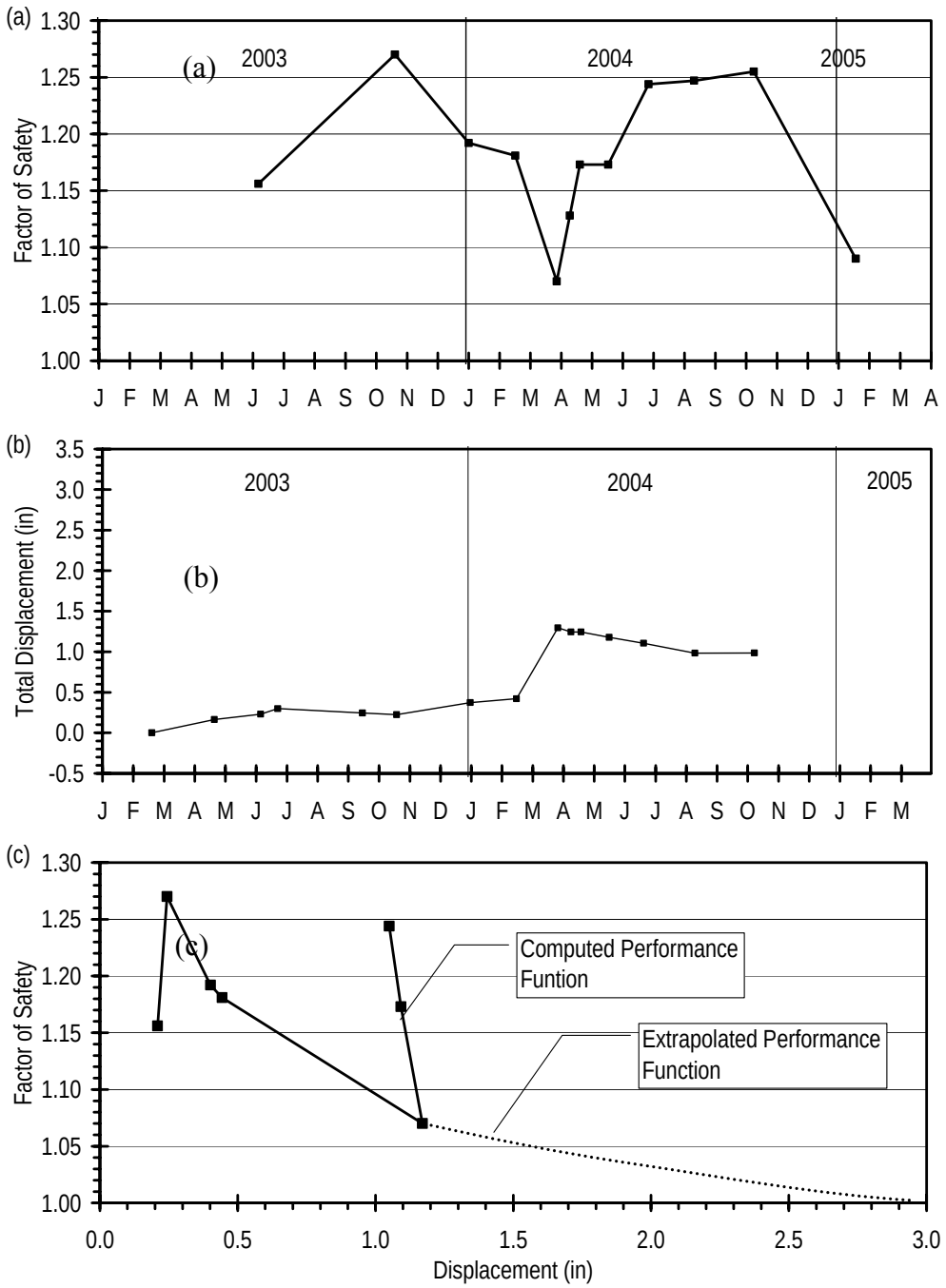

Figure 11.1 Illustration of performance function development: (a) Baseline factor of safety versus date, (b) deformation versus date, and (c) computed and extrapolated performance function

7. Extrapolate the field performance function to a factor of safety of unity as shown in Figure 11.1c to evaluate whether the baseline method predicts a factor of safety of unity at the tolerable deformation limit.

8. Calibrate the procedure by varying the limit resistance for the reinforcing members until the extrapolated performance function intersects the F=1.0 axis

at the tolerable deformation limit. If the extrapolated performance function does not produce a factor of safety of unity at the deformation limit, alternative limit resistances are used to establish alternative performance functions. Procedures that result in performance functions that, when extrapolated to a factor of safety equal to 1.0, produce the tolerable deformation limit are possible calibrated analysis methods. If the initial extrapolated performance function predicts a factor of safety of 1.0 at the deformation limit, no calibration is needed.

The procedure described includes all the uncertainties associated with traditional back-calculation plus some additional ones. First and foremost among these is that there is obviously some uncertainty associated with the shape of the extrapolated function. Previous work by Parra (2004) and field monitoring by others indicates a greater increase in deformations at smaller factors of safety so a simple linear extrapolation will generally not be suitable and will be unconservative. Results of the analysis presented subsequently for the field test sites presented in this report where failure has occurred confirm this observation. However, the shape of the performance function evaluated to date, including those that have reached failure, has generally been consistent so it is possible to perform a reasonable extrapolation using this information. The uncertainty associated with the extrapolation is also reduced as the slope is subjected to more and more deleterious conditions that produce lower factors of safety and larger deformations, which decreases the required amount of extrapolation. Secondly, there is some uncertainty involved with establishing an appropriate deformation limit to serve as the failure criterion. Again, this uncertainty can be reduced by having data on deformations leading up to failure at sites where failure occurs.

Despite these uncertainties, the method at least allows field performance data to be utilized to improve design methods when no failure occurs, thereby providing for logical and prudent advances to conventional design.

11.2. Required Data for Calibration of Limit Resistance

Whether failure occurs or not, realistic evaluation and calibration of the limit resistance using the procedures described above requires that other sources of errors (e.g. errors in soil shear strength parameters or pore pressure conditions) in the stability analyses be reduced or eliminated to the extent possible. For the stability conditions evaluated in this work, this requires accurate assessment of both the shear strength parameters and pore pressure conditions within the test slopes as a function of time throughout the monitoring period. In the present work, this has been accomplished in several ways. Uncertainties in soil shear strength parameters have generally been minimized by performing extensive laboratory tests to establish the most likely values of shear strength parameters as well as the possible ranges of these parameters as described in Chapters 6 through 9. Similarly, uncertainties in pore pressure conditions were minimized by measuring piezometric conditions at the field sites over extended periods of time to establish the actual pore pressures in the field at specific monitoring dates. Without both accurate soil shear strength data and pore pressure measurements at key times during the monitoring period, the calibrations would be subject to additional uncertainties which could render the results inaccurate. As such, knowledge of both shear strength parameters and pore pressure conditions is a critical piece to evaluation and calibration of methods for predicting limit resistance of the reinforcing members.

11.3. Establishment of Acceptable Performance Limit

In cases where failure has not occurred in the field, it is necessary to establish an acceptable performance limit, beyond which the slope will be considered to have failed. The most logical basis for establishing this limit is slope lateral displacement. In the presented work, an acceptable performance limit of slope lateral displacement was established based on observations made at several of the test sites. Review of measured lateral deformations for test sections at the various test sites reveals that several sections have experienced deformations (measured at the ground surface) of up to 3 inches without exhibiting significant surface expressions of failure such as scarps and bulges in the slopes. Such movements therefore appear to be within tolerable performance limits. Furthermore, inclinometer measurements for test or control sections that have failed also suggest that movements observed prior to the onset of failure have approached 3 inches. The acceptable performance limit utilized throughout the analyses described in this chapter has been 3-inches of deformation measured at the ground surface.

11.4. Calibration for I70-Emma Site

The following sections describe calibration analyses performed based on the performance observed at the I70-Emma site. Because pore pressure measurements acquired in slide areas S1 and S2 at this site during Phase I were deemed unreliable (recall that continuously screened wells were used instead of standpipe piezometers), calibration analyses were only performed for slide area S3 based on the performance observed during Phases II and III of the project.

11.4.1. Site Characteristics Used in Analysis

As-built profiles for each test section were developed based on site surveys, boring logs, and construction records. Each profile consisted of an upper surficial layer overlying a deeper stratum. As-built profiles for each section are shown in Figure 11.2. Coordinates of the slope surface and material interface can be found in Appendix E. Two possible sets of shear strength parameters, deemed Case 1 and Case 2, were used for analyses at the I70-Emma test site as summarized in Table 11.1. These strength parameters are slightly below those determined from laboratory tests; however, stability analyses performed using measured strengths and piezometric conditions did not produce a factor of safety of 1.0 for the unreinforced case so the strength parameters were reduced slightly to produce a factor of safety of 1.0. The results presented in this section are based on the Case 1 strength parameters as they were deemed to be most reasonable.

Table 11.1 Soil strength parameters used for calibration analyses for I70-Emma site.

	Upper Layer		Lower Layer	
Stability Case	c'	ϕ'	c'	ϕ'
Case 1	70	21.5	170	25
Case 2	95	16.5	170	25

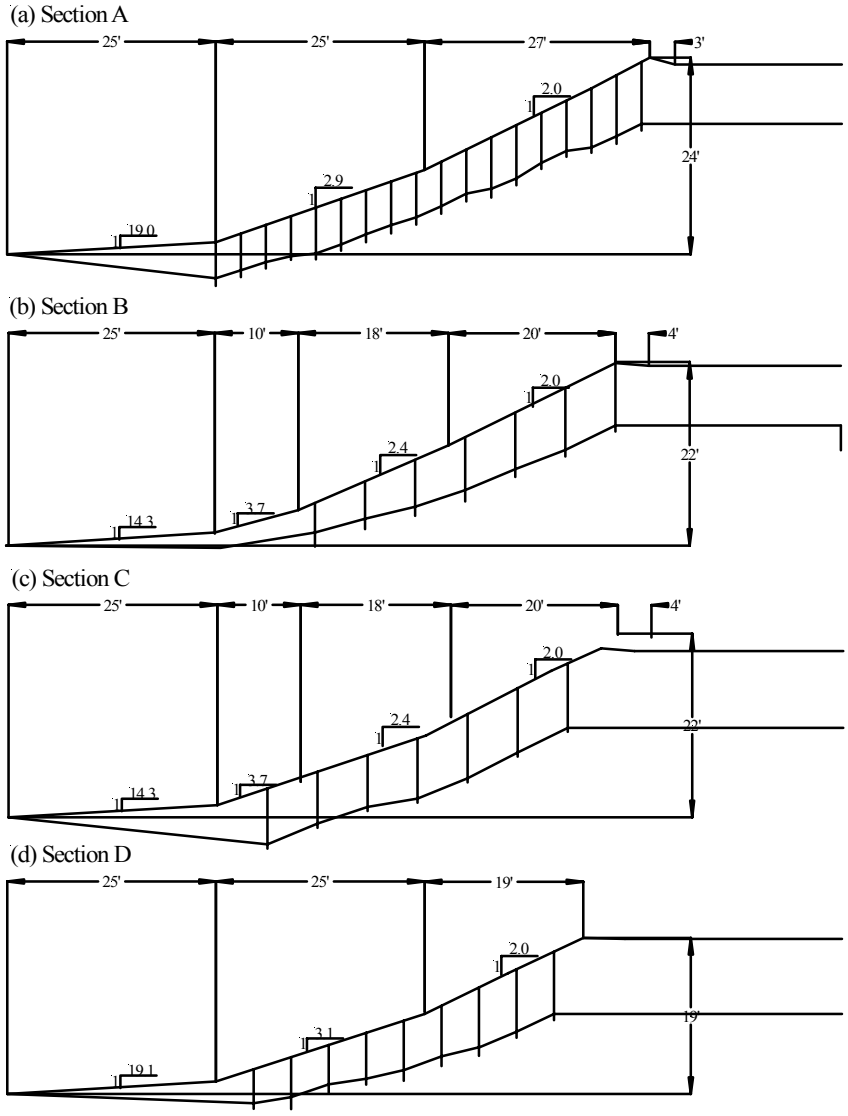

Figure 11.2 As-built cross sections for I70-Emma site: (a) Section A, (b) Section B, (c) Section C, and (d) Section D.

Piezometric conditions for the respective monitoring dates were established based on measured piezometric levels. The piezometric surfaces used in the analyses are shown in Figure 11.3; coordinates of these surfaces can be found in Appendix E. The piezometers were located within extent of the slide that occurred in winter 2004 and were broken as a result of the soil movement. Readings therefore could not be taken on January 27, 2005. Three different estimated piezometric conditions were therefore used for this date based on the observed precipitation and previously recorded piezometric conditions. The following piezometric conditions were used for the January 27, 2005 reading:

1. Entire measured 1/14/04 piezometric surface moved up 0.5-ft.

2. 1/14/04 measured piezometric readings at slope crest. Readings at toe elevated 1.0-ft.
3. Entire measured 1/14/04 piezometric surface moved up 1.0-ft.

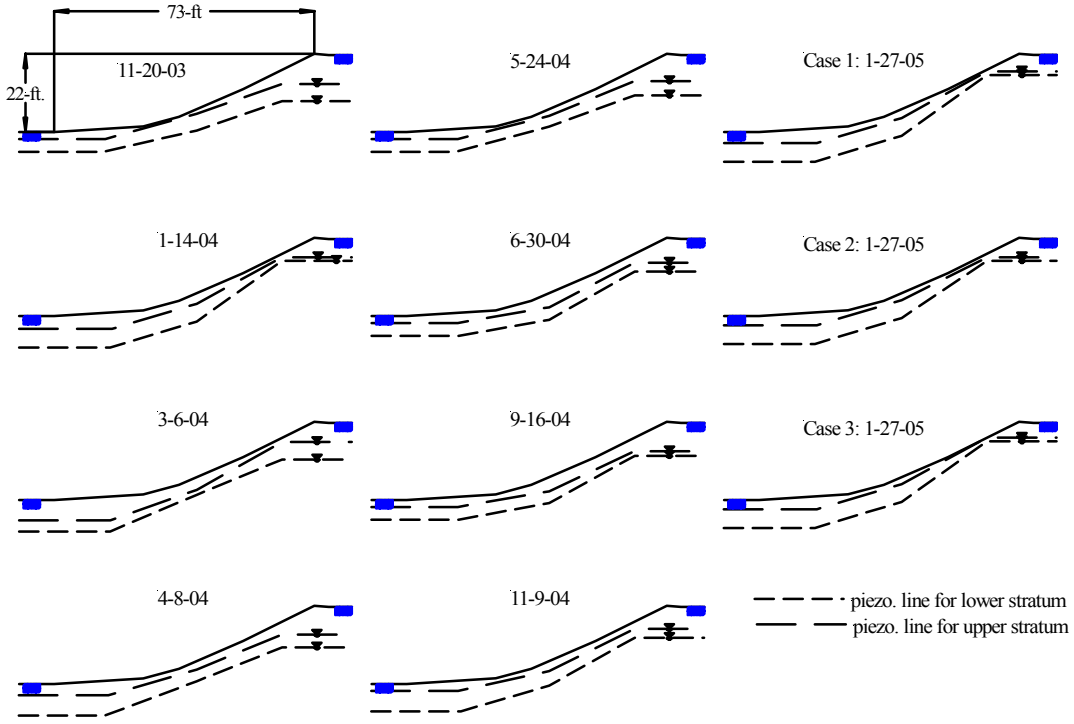

Figure 11.3 Piezometric surfaces used for calibration analyses for I70-Emma site.

11.4.2. Theoretical Field Performance

As previously discussed in Chapter 6, a failure occurred in Sections B and C of the I70-Emma site between November 9, 2004 and January 27, 2005. Since the failure was confined to sections B and C, the factors of safety computed for Sections B and C for the conditions at the time of the failure must be equal to 1.0, while the factors of safety for Sections A and D must be greater than 1.0 since those sections did not fail.

The failure allows the use of traditional back-calculation procedures to evaluate the lateral resistance provided by the reinforcing members in Sections B and C. The procedures evaluated for the I70-Emma site include: (1) using the baseline lateral resistance, (2) using the baseline lateral resistance factored by a constant value, and (3) considering both axial and lateral resistance.

Baseline limit resistance curves were developed as described in Chapter 2 for each set of soil conditions, arrangement of reinforcing members, and each length of reinforcing member installed (in 0.5-ft. increments). A comparison of the baseline limit resistance curves for members with different longitudinal spacing and soil conditions is shown in Figure 11.4 for an 8-ft. long reinforcing member.

The computed baseline factors of safety for each section are plotted in Figure 11.5 as a function of date. The range in factors of safety shown for the final date (January 27, 2005) is due to the three estimated piezometric conditions analyzed (recall piezometers were severed in the failure prior to the January 27, 2005 reading). The computed factors of safety suggest that Sections A and D both have substantially greater stability than Sections B and C. The stability in Section A is greater due to the more closely spaced arrangement of reinforcing members in this section. The increase in stability is to some extent offset by the geometry of the slope, with section A being taller than other sections. The stability in Section D is higher than sections B and C due to the lower slope height. The factors of safety also suggest that, depending on the piezometric conditions used, the existing method is reasonably accurate to slightly unconservative since the theoretical factors of safety for the failed sections are near or slightly above 1.0 around the time of the failure.

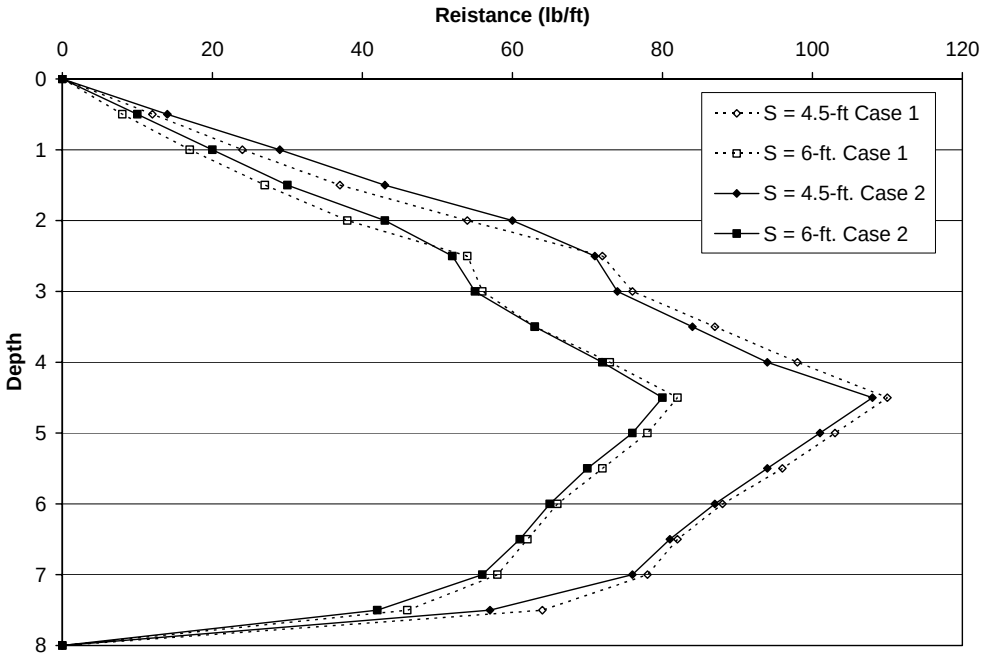

Figure 11.4 Baseline limit resistance curves for 8-ft. member at I70-Emma site

11.4.3. Calibration Using Factored Lateral Resistance

Stability analyses were performed using alternative limit resistance values established by increasing and decreasing the baseline limit resistance by a constant factor along the entire length of the reinforcing member. Factoring of the limit resistance curve for the I70-Emma test site was performed using the following factors: 0.9, 0.75, 0.5, 0.25, 0.1, and 0; where a factor of 0 represents an unreinforced condition. This form of factoring has the effect of varying both the limit soil pressure as well as the member capacity. The computed factors of safety for each section using these reduction factors for piezometric conditions 1 and 3 are shown in Figure 11.6. Results shown in Figure 11.6 for piezometric Condition 1 indicate the limit resistance must be reduced to between 0% and 30% of the resistance computed using Ito and Matsui's theory in order to predict failure of the failed sections. This seems unrealistic, so it is likely that piezometric Condition 1 is not representative of the conditions

at failure. In contrast, results from piezometric Condition 3 indicate that the limit resistance must be reduced to between 70% and 100% to predict F = 1.0 for Sections B and C. This result seems more plausible and suggests that the limit resistance must be between 70% and 100% of the resistance computed using the Ito and Matsui theory in order for the analysis method to predict the failures that occurred in Sections B and C. Use of factored limit resistances between 70% and 100% of that computed using Ito and Matsui's theory for Sections A and D results in factors of safety greater than 1.0, which gives some credence to the plausibility using the factored resistances to predict the stability of the reinforced slopes. Use of more deleterious piezometric condition than Condition 3 would suggest that the limit resistance must be higher than that computed using the Ito and Matsui theory to produce F = 1.0.

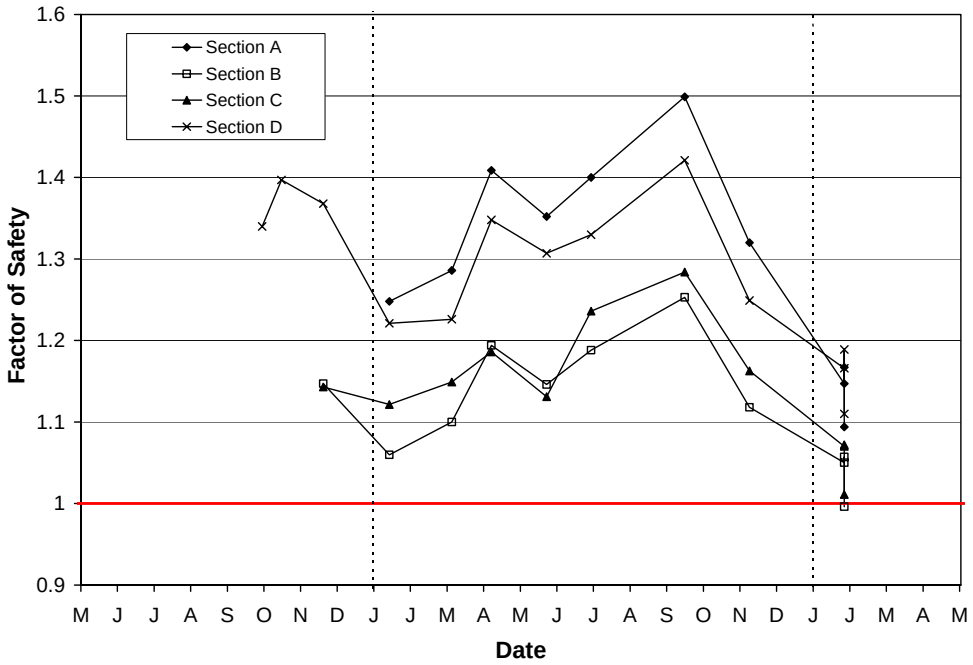

Figure 11.5 Baseline factors of safety for each section at I70-Emma site.

The varying slopes and intercepts of the curves in Figure 11.6 is a result of the fact that the inclination and height of the slope vary from section to section. Some of the variability in factors of safety in Figure 11.6 is therefore due to the slope geometry. The curve for Section A is also steeper than the other sections for additional reasons. First, the slope height is greater in Section A making it less stable without reinforcement and more sensitive to the resistance provided by the reinforcement. Second, Section A is reinforced using a more closely spaced pattern of reinforcement (4.5-ft. x 3-ft.) that includes more reinforcing members than other sections. Thus a 20% decrease in resistance for members in Section A results in a greater overall decrease in stability than occurs when reinforcing members are more widely spaced. The factors of safety for Section D are generally higher than those of Sections B and C because Section D has a smaller slope height. However, Section D produces a similar trend (slope) in factors of safety as the resistance is decreased because it has a similar pattern of reinforcement.

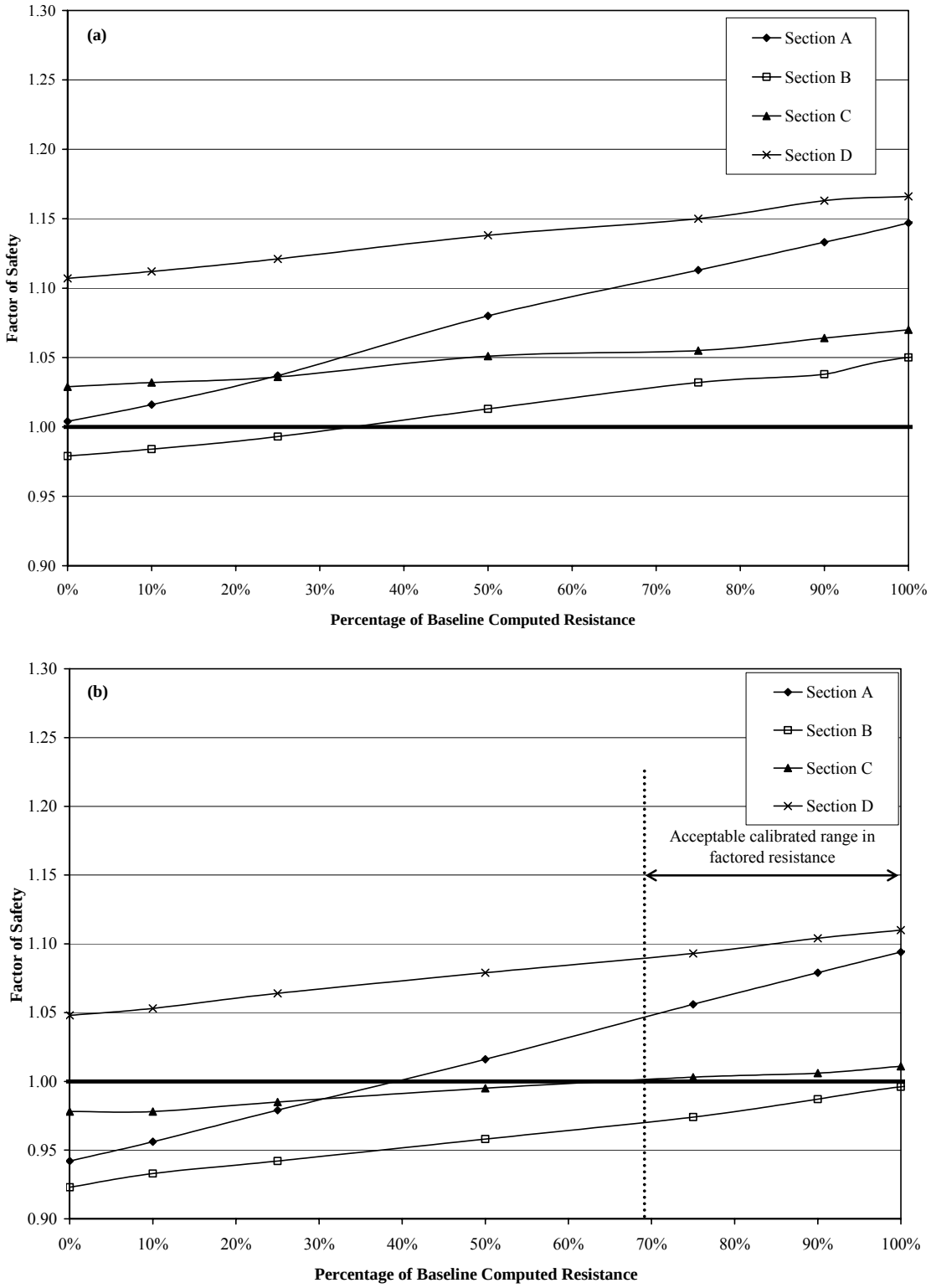

Figure 11.6 Factors of safety at I70-Emma site using factored limit resistance curves for: (a) piezometric condition 1 and (b) piezometric condition 3.

11.4.4. Calibration Using Combined Axial and Lateral Resistance

Calibration analyses were also performed considering that the resistance from the reinforcement has an axial component in addition to the lateral resistance. For these analyses, the axial component was taken to be proportional to the lateral component, and was defined using an inclined resultant force with an inclination θ. In all cases, the lateral force was held constant and equivalent to the baseline limit resistance. Angles of inclination, θ, were measured with respect to the horizontal. Positive angles are inclined above the horizontal and produce a compressive force in the reinforcing member while negative angles are inclined below the horizontal and produce a tensile force as shown in Figure 11.7. Inclinations used in these analyses were 80°, 45°, 30°, 15°, -15°, -30°, -45°, and -80°. The angles of 80° and -80° were selected to provide insight into a situation in which most of the resistance provided by the reinforcing members is axial as opposed to lateral.

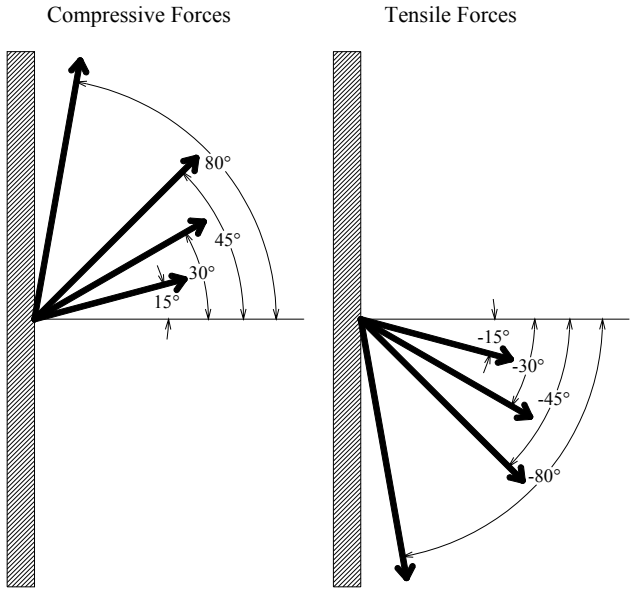

Figure 11.7 Illustration of inclined resisting forces considered for calibration based on the performance of the I70-Emma site.

The variation in factor of safety with inclination of the resultant force is shown in Figure 11.8. As shown in the figure, negative resistance force inclinations, or tensile forces in the reinforcing members tend to increase stability, while compressive forces (positive inclinations) tend to decrease the stability of the slope. Overall, there was little effect on stability except for the cases where the resisting forces were inclined at ± 80°. The corresponding magnitude of the axial stress in the reinforcing member for an inclination of ± 80° is approximately 50 psi. This is well below the ultimate compressive strength of 2800 psi and tensile strength of 1300 psi of the members, so it is at least plausible that axial resistance could be used to calibrate the analysis method. However, limitations of the software used in this work prevented further evaluation of this possibility. Further investigation of the interaction between axial and lateral resistance is therefore still needed.

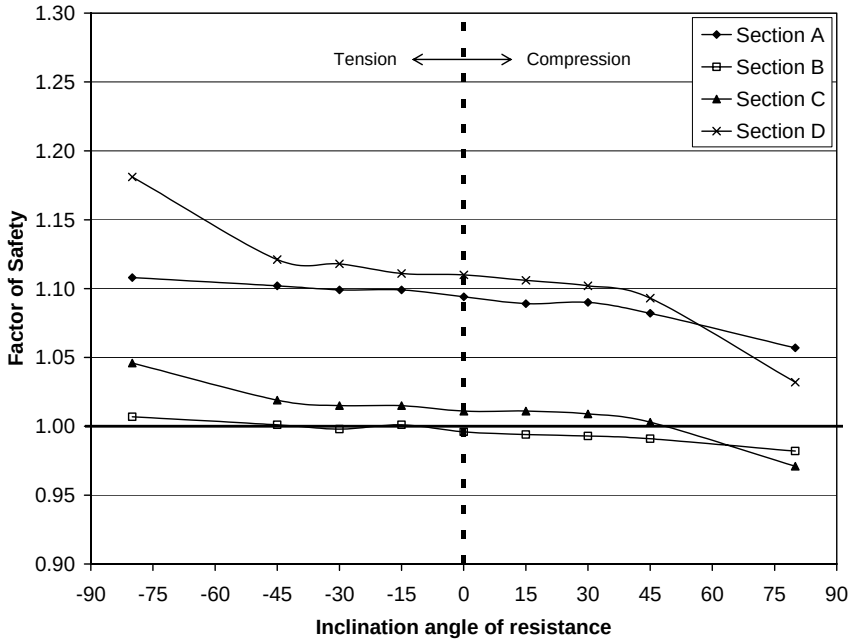

Figure 11.8 Stability at I70-Emma site including axial and lateral resistance

11.4.5. Calibration Using Reduced Moment Capacity

The final modification to current procedures considered for the I70-Emma site was to use limit resistance curves computed using a reduced moment capacity along with the limit soil pressure computed using the Ito and Matsui theory. This approach was evaluated because it was deemed plausible that reinforcing members could degrade within the slope over extended periods of time due to creep or other causes. Calibration analyses were performed for reduced moment capacities of 500 ft-lb and 250 ft-lb.

Figure 11.9 shows the limit resistance curves computed for the nominal moment capacity of 900 ft-lb. and the reduced moment capacities of 500 ft-lb and 250 ft-lb. As the moment capacity decreases, the depth over which structural failure is the controlling limit state increases and the lower the maximum resistance provided by the reinforcing member. For a moment capacity of 250 ft-lb, structural failure is the controlling limit state for almost 90% of the length of the reinforcing member for an 8-ft long member. For a moment capacity of 500 ft-lb, structural failure controls resistance for approximately 75% of the length of the member, while structural failure only controls the limit resistance 60% of the length of the member when the nominal measured moment capacity of 900 ft-lb is used. The maximum possible resistance provided by the reinforcing member also decreases from approximately 125 lb/ft for the nominal moment capacity of 900 ft-lb. to approximately 25 lb/ft for a moment capacity of 250 ft-lb. Such changes can have a significant effect on the predicted stability of reinforced slopes.

The modified limit resistance curves shown in Figure 11.9 were used in stability analyses to evaluate the effects of potential reduced strengths of the reinforcing members for calibrating the analysis procedure. The computed factors of safety from these analyses are shown in Figure 11.10. These results indicate that the analysis method can be calibrated

using moment capacities somewhere between the nominal moment capacity of 900 ft-lbs and a reduced moment capacity of 500 ft-lbs (approximately 50% of the nominal capacity).

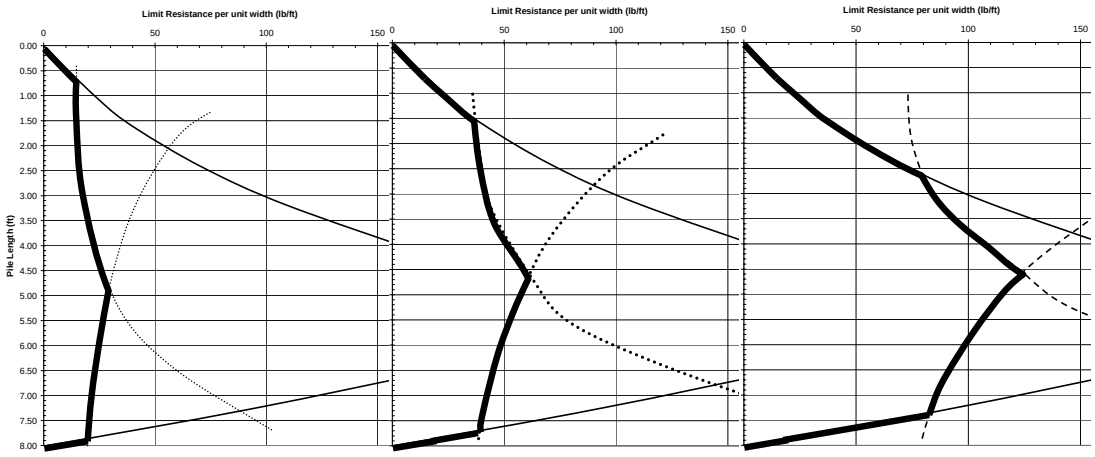

Figure 11.9 Limit resistance curves for (a) moment capacity of 250 ft-lb, (b) moment capacity of 500 ft-lb, and (c) moment capacity of 900 ft-lb.

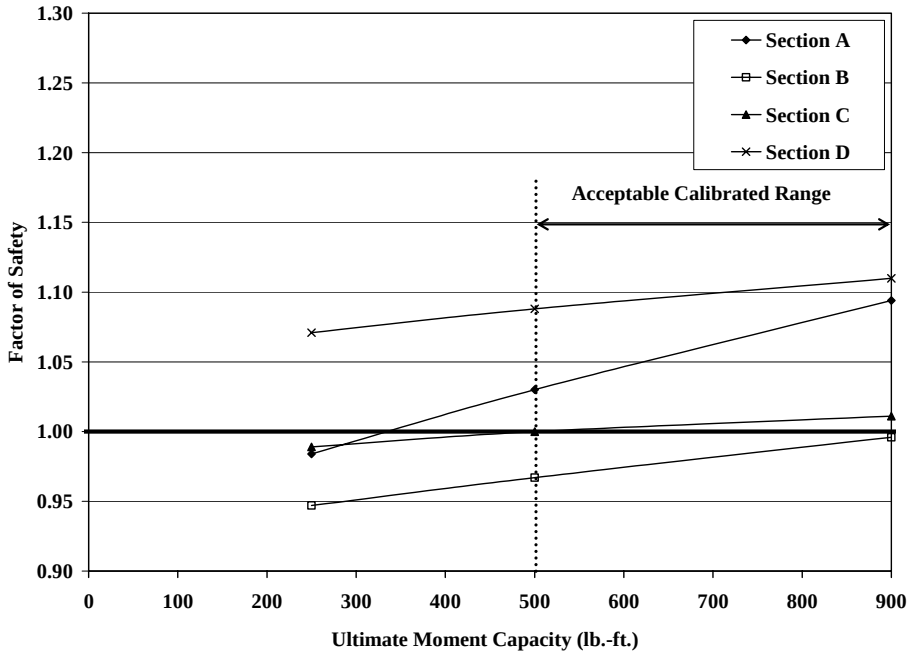

Figure 11.10 Computed factors of safety using reduced moment capacities for I70-Emma site.

Further analyses were performed to determine if the analysis method could be calibrated using limit soil pressures greater than those from Ito and Matsui's theory combined with reduced moment capacities. Stability analyses were performed using reduced moment capacity of the reinforcing members while increasing the limiting soil pressure to

300% of that computed using Ito and Matsui's method. The increase in limiting soil pressure was found to have little effect on the computed factors of safety when reduced moment capacities were used because the length over which the limit soil pressure is the controlling limit state is small. For significant effect to be observed, the critical sliding surface would need to pass through the length of the reinforcing member over which the limit soil pressure is the controlling limit state and this did not occur.

11.4.6. Calibration Using Baseline Resistance

The calibration method established for use in cases where failure did not occur was applied to Section B at the I70-Emma site, which did fail, to provide an evaluation of the procedure to calibrate when a failure does not occur. Figure 11.11 shows the performance function determined using the existing (baseline) analysis procedure described in Chapter 2. The performance function was established using the theoretical factors of safety from Figure 11.5 with the corresponding displacements from Inclinometer I-7 from Figure 6.22b. Figure 11.11 shows that very little displacement is observed during periods when the factor of safety is increasing while displacements increase as the factor of safety decreases. The figure also shows the typical shape of the field performance curve that is similar to that observed by Parra (2004). The figure also shows that the field performance curve intersects the F=1.0 axis at a displacement of approximately 4.0-in which suggests that the tolerable deformation limit of 3.0-in use subsequently is conservative.

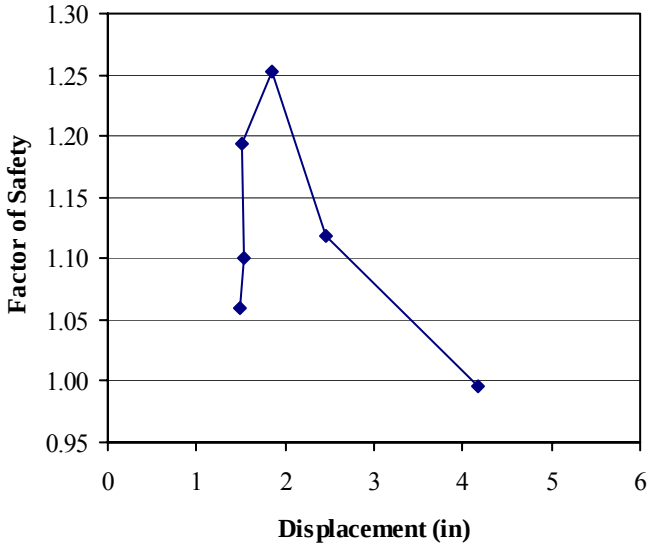

Figure 11.11 Baseline field performance curve for Section B at I70-Emma site.

11.4.7. Summary of I70-Emma Site Analyses

Calibration analyses performed for the I70-Emma site using factored limit resistance curves, inclusion of axial and lateral resistance, and using reduced moment capacities for the reinforcing members met with variable success. The inclusion of axial resistance did not have a significant affect on stability over the range evaluated, which suggests that using axial and lateral resistance is not an effective approach for calibration and that axial resistance does not play a major role over the conditions evaluated. However, these analyses were

limited by the capabilities of the software used and other available software so additional evaluations using alternative software are needed to further evaluate the potential for calibration using both axial and lateral resistances.

Conversely, calibration using factored limit resistance curves indicated field performance can be reasonably predicted using limit resistances between 70% and 100% of the resistance computed using the Ito and Matsui theory. Calibrations performed using reduced moment capacities for the reinforcing member were also successful and suggest that capacities between 50 and 100% of the measured capacities are appropriate. The latter calibration using reduced moment capacities is appropriate when used in conjunction with the Ito and Matsui method for predicting the limit soil pressure as well as for use with other methods for predicting the limit soil pressure (e.g. Broms method or the Poulos and Davis method).

11.5. Calibration for US36-Stewartsville Site

11.5.1. Site Characteristics Used in Analyses

Analyses for the US36-Stewartsville site were performed using a layered soil profile for the main slope and the control section. The control section of the US36-Stewarstville test site failed between July 26, 2004 and September 28, 2004. Shear strength parameters c' and ϕ' were back calculated using the control section profile along with the measured piezometric levels from the July 26, 2004 readings. Two possible sets of back-calculated strength parameters are summarized in Table 11.2.

Table 11.2 Back-calculated shear strength parameters for US36-Stewartsville site.

Stability Case	Upper Layer		Lower Layer	
	c'	ϕ'	c'	ϕ'
Case 1	10	24.3	105	33
Case 2	20	22.9	105	33

As-built cross-sections for Sections A, B, C, and D are shown in Figure 11.12, while the piezometric surfaces used for all monitoring dates are shown in Figure 11.13. Coordinates of the slope cross sections, material interfaces, and piezometric levels are provided in Appendix E.

11.5.2. Theoretical Field Performance

Since no failure has occurred at the US36-Stewartsville site, the second calibration procedure using the field performance functions was used for calibration. Baseline factors of safety computed using the established shear strength parameters, measured piezometric levels, and limit resistance computed using the baseline method are plotted in Figure 11.14 for the Case 2 strength parameters. In general, the computed factors of safety showed little variation throughout the monitoring period with the exception of those for the July 26, 2004 and February 16, 2005 readings, where elevated piezometric levels were observed. Unfortunately, the lack of variations in the observed factor of safety limits the number of points that can be used to define the field performance function, which makes the extrapolation more difficult. Figure 11.15 shows the baseline field performance functions for

each test section. Because only two points are generally available to define the field performance curves, linear extrapolation was used for all calibrations.

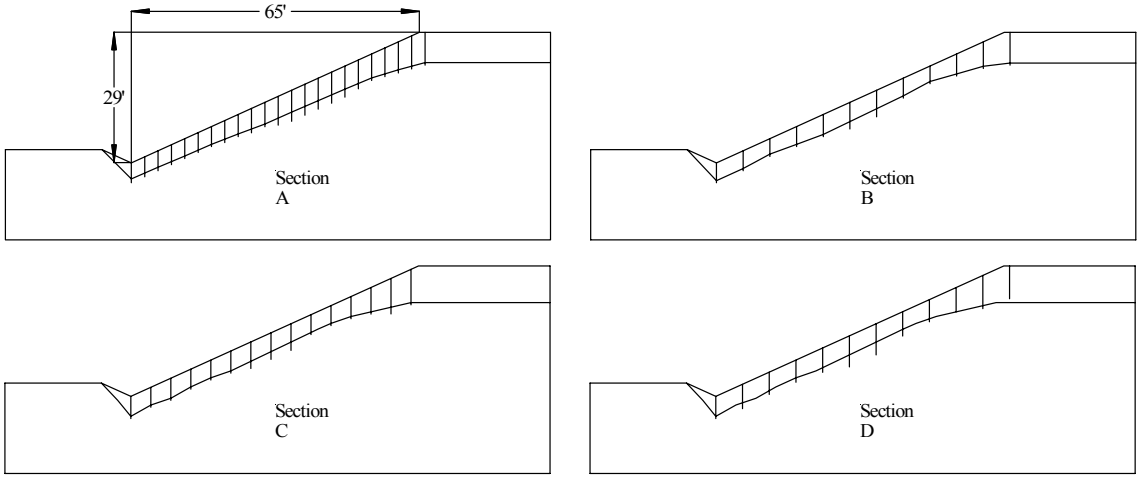

Figure 11.12 As-built cross sections for US36-Stewartsville site.

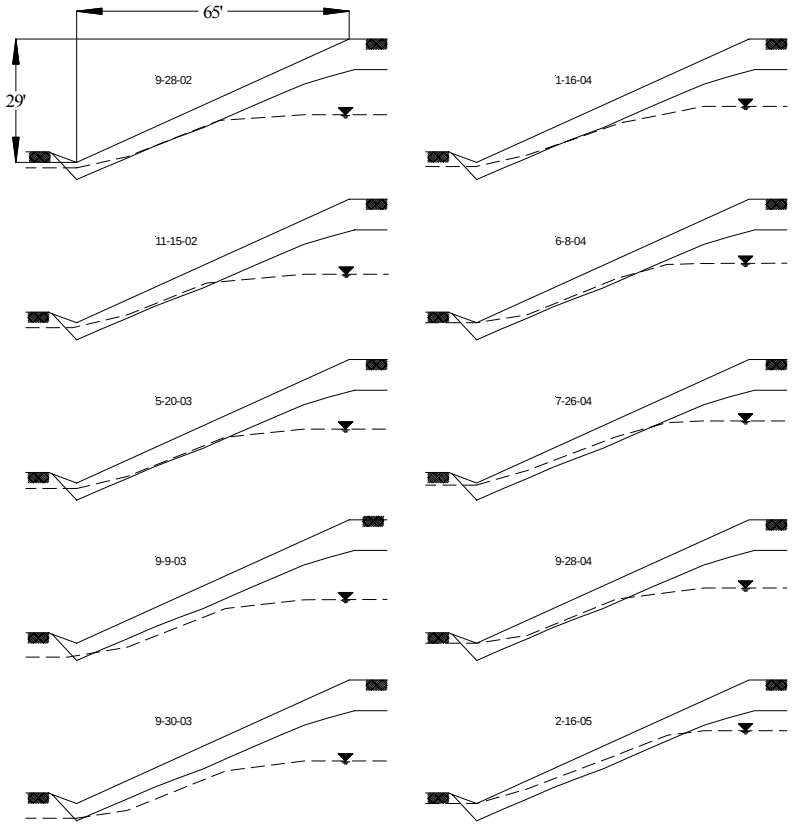

Figure 11.13 Piezometric surfaces used for calibration analysis at US36-Stewartsville site.

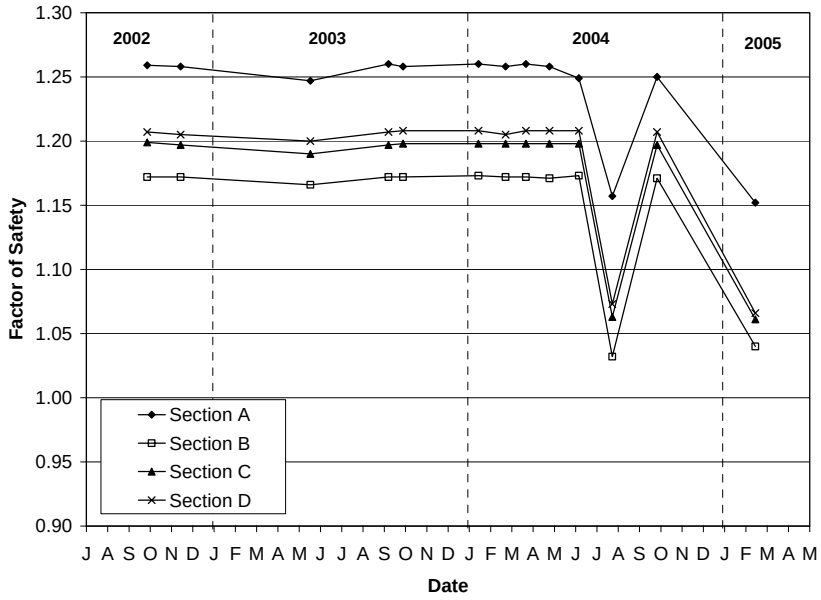

Figure 11.14 Computed performance at US36-Stewartsville site

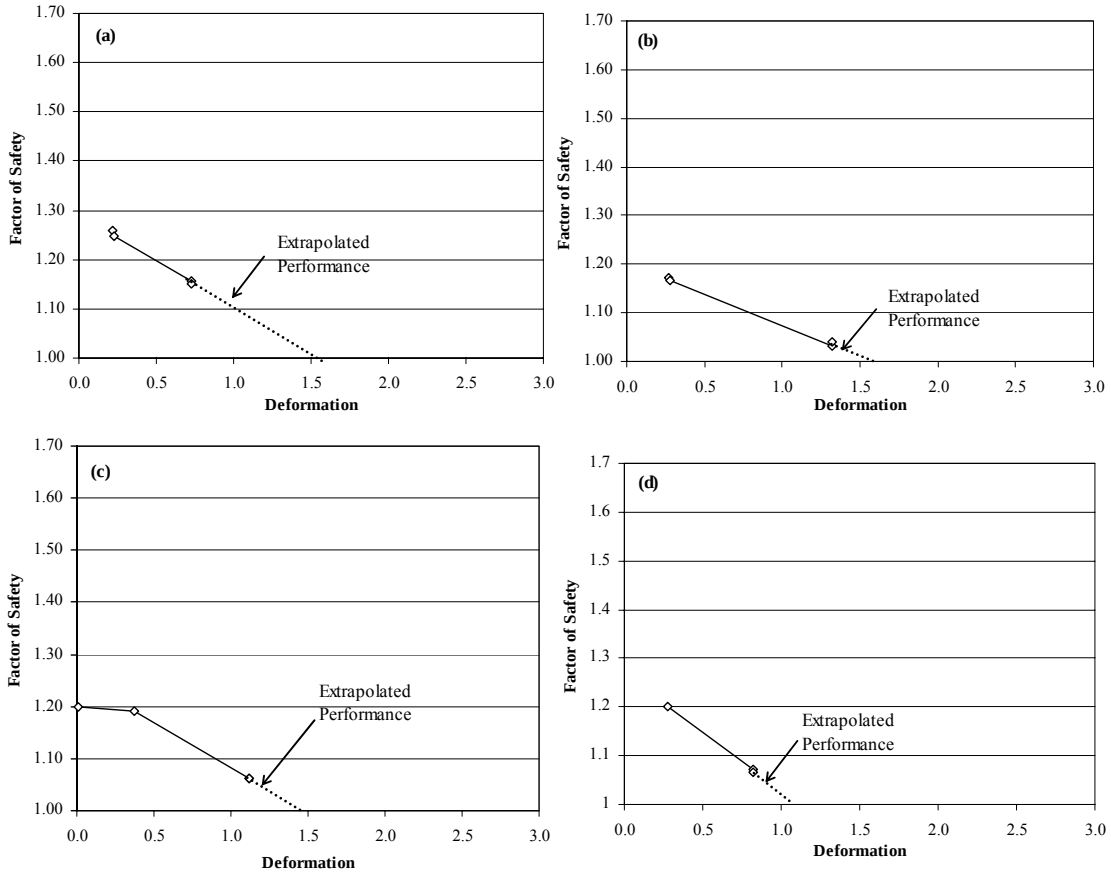

Figure 11.15 Performance functions from calibration analysis using baseline limit resistance for US36-Stewartsville site: (a) Section A, (b) Section B, (c) Section C, and (d) Section D.

11.5.3. Calibration Using Factored Lateral Resistance

In the first attempt at calibration for the US36-Stewartsville site, the limit resistance curves for the reinforcing members were factored by a constant amount to determine the level of resistance in the reinforcing members that would result in prediction of failure at the tolerable deformation limit of approximately 3-in. Since the extrapolated baseline performance functions indicate deformations of less than 3-in. at F =1.0, the resistance provided by the reinforcing members must be greater than that computed using Ito and Matsui's method. Analyses were therefore performed for limit resistances between 200% and 500% greater than the baseline values.

The performance functions determined from these analyses for each section of the US36-Stewartsville test site are shown in Figure 11.16. These results indicate that the limit resistance required to predict failure at the tolerable deformation limit is between 200% to 500% of the limit resistance computed using Ito and Matsui's theory and the nominal moment capacity of the member.

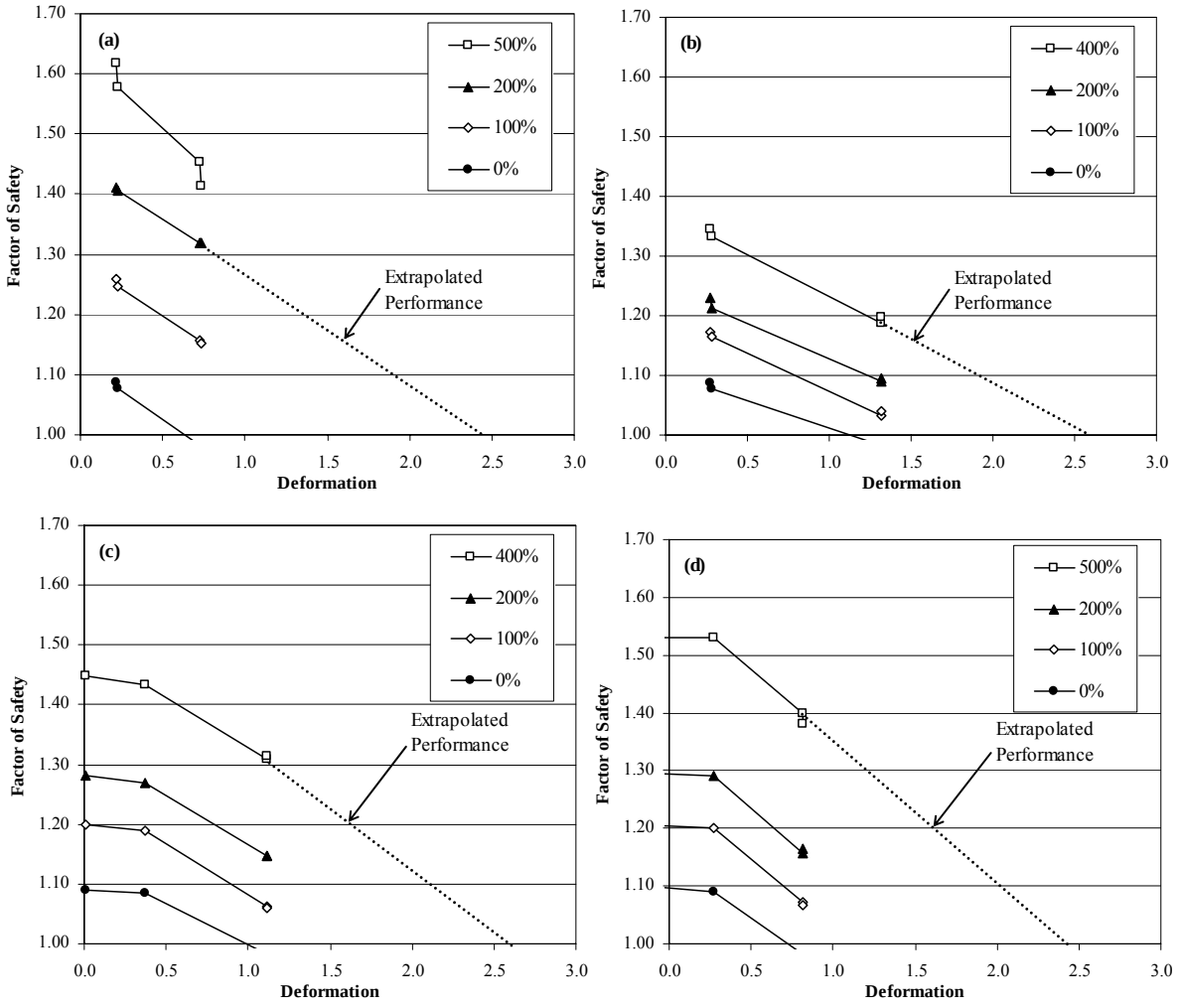

Figure 11.16 Performance functions from calibration analysis using factored limit resistance for US36-Stewartsville site: (a) Section A, (b) Section B, (c) Section C, and (d) Section D.

However, at least two issues arise when considering these results. First, the use of linear extrapolation of the performance function is generally unconservative in that more resistance is required to produce a calibrated procedure that would be needed if the curve was extrapolated in a shape similar to that observed for other sites. Secondly, while it is certainly plausible that the actual limit soil pressure is much greater than predicted by Ito and Matsui's method, it is not logical that the bending resistance of the reinforcement is significantly greater than measured in laboratory tests. Both of these observations suggest that the actual resistance provided by the reinforcement is some what lower than what is predicted by these calibrations. While the field performance can be matched using the factored limit resistance curves determined above, it is unlikely that such modifications to the analysis procedure are representative of what is actually occurring in the field and alternative means of calibration should be considered.

11.5.4. Calibration Using Axial and Lateral Resistance

An alternative method of calibration considered for the US36-Stewartsville site was to include an axial component of resistance in addition to the lateral resistance. Angles of inclination of the resultant force measured with respect to the horizontal used in these analyses were 80°, 45°, 30°, 15°, -15°, -30°, -45°, and -80°. Again, positive angles act above the horizontal and produce compressive forces in the reinforcing member while negative angles act below the horizontal and produce tensile forces. Results of these analyses again showed little variation in stability with the addition of either compressive or tensile axial resistance over the range considered, which suggests that calibration cannot be achieved using this approach and, furthermore, that axial resistance is not a substantial contributing factor to stability for the range of conditions employed at this site. Additional analyses incorporating larger axial forces and/or axial forces that are not proportional to the lateral resistance are needed to further evaluate whether calibration can be accomplished using this approach.

11.5.5. Summary of US36-Stewartsville Site Analysis

Calibration analyses performed for the US36-Stewartsville site using factored limit resistance curves and the inclusion of axial and lateral resistance in the reinforcing members produced mixed results. Inclusion of axial resistance did not have a significant affect on stability over the range evaluated. Results of analyses using factored limit resistance curves indicate that resistance of between 200% and 500% of the baseline resistance is needed to predict F = 1.0 at the tolerable deformation limit. However, this result is believed to be somewhat unconservative and it is likely that lower resistances are more appropriate.

11.6. US54-Fulton Site Analysis

11.6.1. Site Characteristics Used in Analyses

Analyses for the US54-Fulton site were performed using two separate profiles: a uniform soil profile and a layered soil profile with a weaker layer of surficial soil. These profiles were developed based on the site investigation, laboratory tests, and construction records. A summary of the range in soil strength parameters used in the analyses is provided in Table 11.3. Measured piezometric conditions used are shown in Figure 11.17. Coordinates of the piezometric surfaces are provided in Appendix E.

Table 11.3 Summary of shear strength parameters used for US54-Fulton site.

Stability Case	Upper Layer		Lower Layer	
	c'	ϕ'	c'	ϕ'
Case 1	20	20.2	50	20.2
Case 2	20	20.6	20	22.6
Case 3	50	18.6	50	18.6

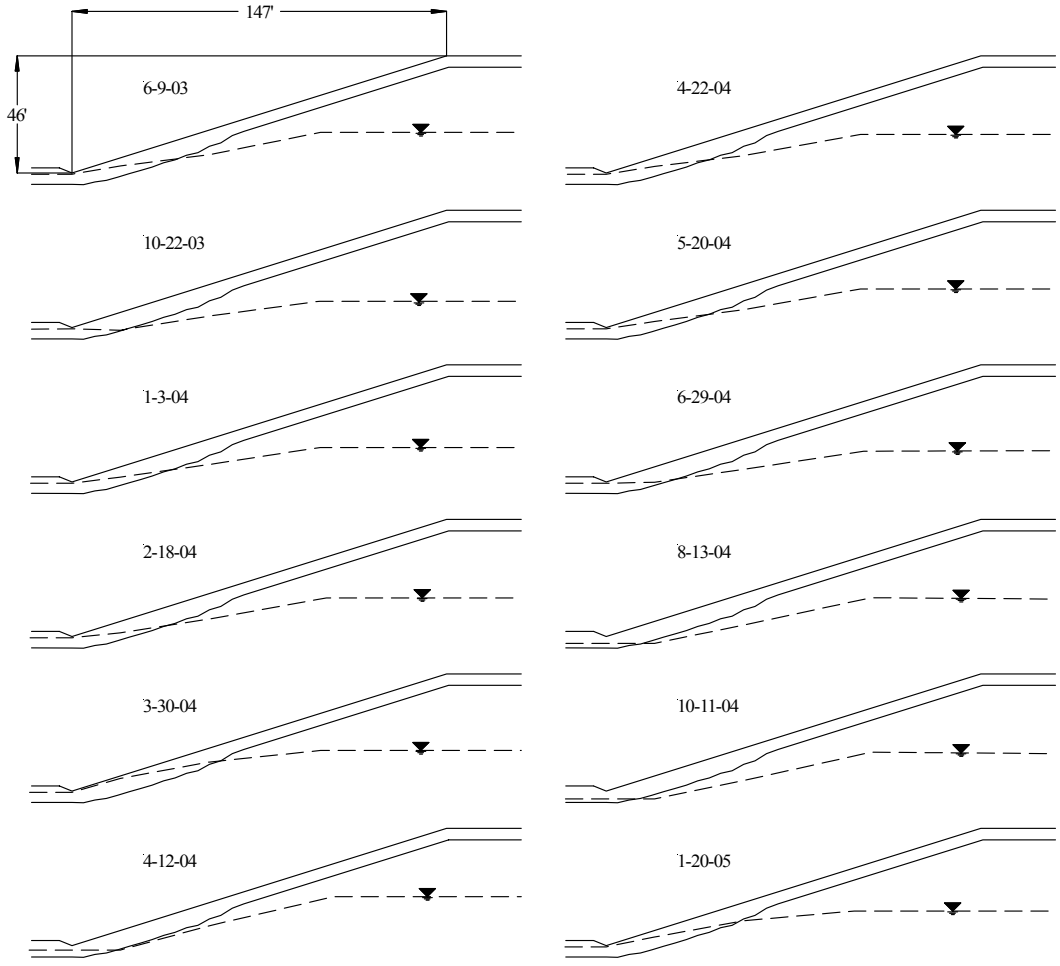

Figure 11.17 Piezometric surfaces used for analysis for the US54-Fulton site.

Inclinometer measurements from the US54-Fulton site indicate movement is occurring at depths ranging from 9- to 17-ft, well below the tips of the reinforcing members. Boring logs developed prior to stabilization indicated the possible presence of an old failure surface at depths ranging from 8 to 15-ft, and it appears that sliding is occurring along this deep surface rather than along shallow surfaces are was originally expected. Since the sliding is primarily occurring at depths well below the tips of the reinforcement, the US54-

Fulton site is not useful for calibration of the analysis procedure for the reinforced slopes. However, since the slope at the US54-Fulton site has experienced movement, it provides an opportunity to evaluate the procedure for calibration when a failure has not occurred for what is effectively an unreinforced slope (or very lightly reinforced due to the reinforcement at the toe).

Factors of safety computed using Case 1 soil strength parameters and the baseline analysis method for the reinforced and unreinforced condition are plotted in Figure 11.18. The results indicate that the reinforcement is providing little improvement with the exception of the March 30, 2004 results. On this date, the piezometric conditions were high enough that the critical sliding surface from the stability analysis in the unreinforced case was entirely in the surficial soil. Inclusion of reinforcement resulted in a deeper critical sliding surface, which passed through a few of the reinforcing members near the toe of the slope. On all other dates, the critical sliding surfaces for the unreinforced and reinforced conditions generally falls outside of the reinforced zone. The critical sliding surfaces for the reinforced and unreinforced conditions for April 12, 2004 are shown in Figure 11.19. As shown, the failure surfaces are very similar and thus only minimal improvement occurs with the inclusion of resistance for a few reinforcing members.

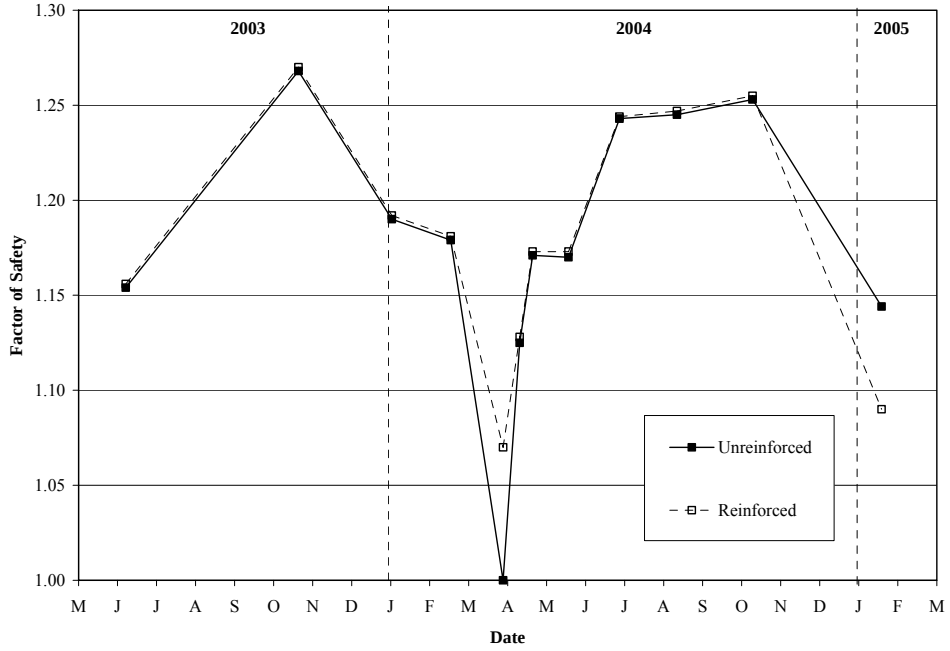

Figure 11.18 Factor of safety versus date for US54-Fulton Site

Figure 11.20 shows the baseline performance function determined for the US54-Fulton site. As has been observed at other sites, the performance function is generally vertical during periods when the factor of safety is increasing, but shows increasing displacements when the factor of safety becomes lower than previously experienced. The performance function also suggests that a tolerable deformation of approximately 3.0-in. is reasonable and that the baseline analysis method is producing factors of safety that are reasonably consistent with the observed field performance.

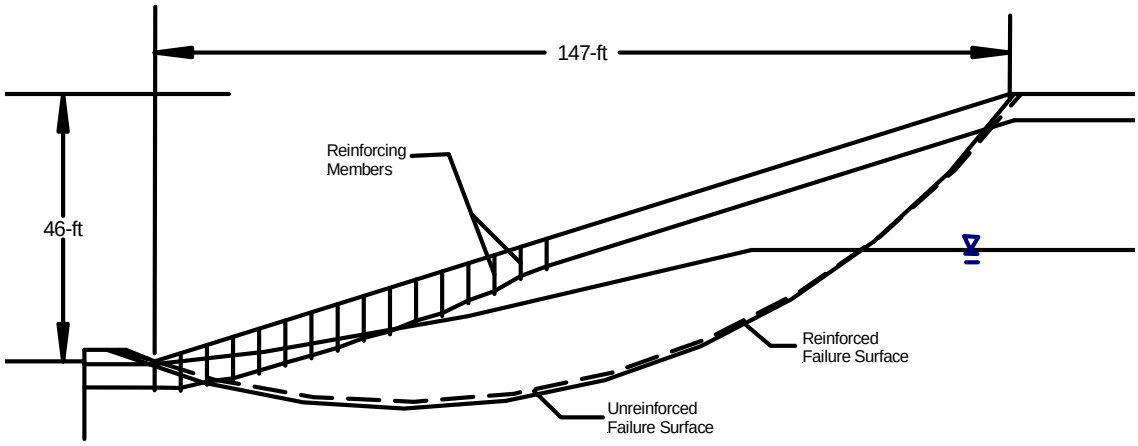

Figure 11.19 Failure surfaces for reinforced and unreinforced cases at US54-Fulton site 4-12-04

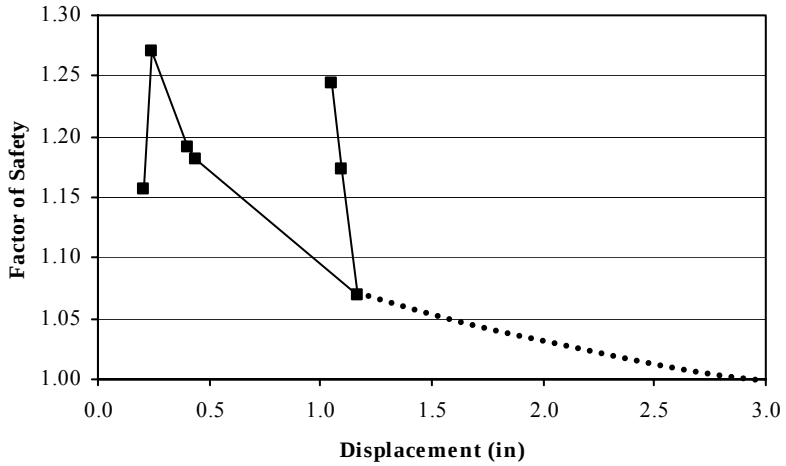

Figure 11.20 Baseline field performance function Section A at the US54-Fulton site.

11.7. Calibration for I435-Wornall Road Site

This section describes the analyses made to calibrate the analysis methodology based on field data and performance documented for the I-435 Wornall Road site from December 2001 through May 2003, as described in Chapter 7.

11.7.1. Site Characteristics Used in Analyses

The "as-built" cross-section for the I-435 Wornall Road site was established based on boring logs and a site survey made prior to stabilization, and from installation records indicating the depth of penetration of the reinforcing members. The "as-built" cross-section includes three different strata, as shown in Figure 11.21. The upper stratum consists of soft to medium clay with thickness from 3-ft near the crest of the slope to 3.5-ft near the middle of the slope, and reducing to a minimum of 1-ft at the toe of the slope. The middle stratum

consists of stiff clay varying in thickness from 12-ft to 16-ft in the upper two thirds of the slope and gradually decreasing to 3.5-ft in thickness near the lower portion of the slope. Underlying the stiff clay is a hard clay shale and limestone. Figure 11.21 also shows the actual length of the reinforcing members installed, which varied from 8-ft (full penetration) in the upper two-thirds of the slope to 3.5-ft near the toe.

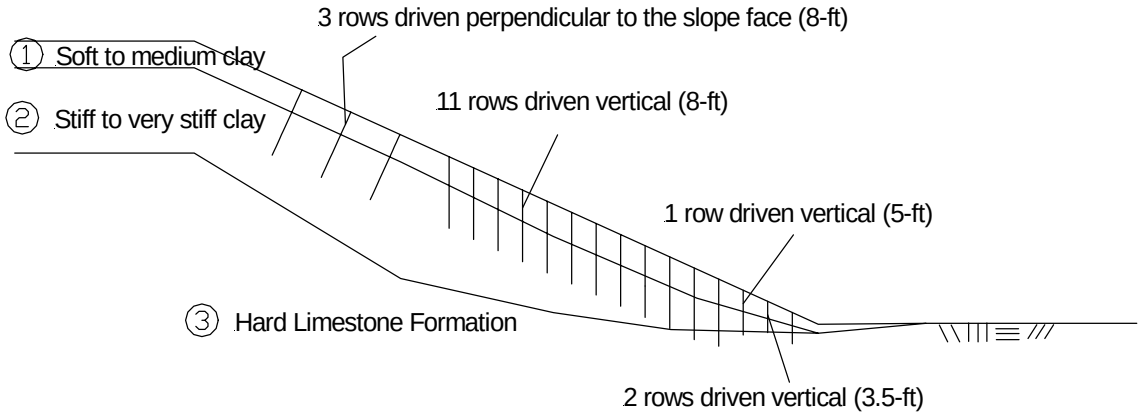

Figure 11.21 As-built section established for I-435 Wornall Road site.

The soil shear strength parameters used for all stability analyses necessary to calibrate the analysis methodology were the same parameters reported in Table 7.1. Two different combinations of strength parameters were considered for the upper and intermediate strata. The first combination was referred to as Case A, and considered the set of upper bound strength parameters for the upper and middle strata, respectively. The second combination was referred to as Case B and considered the upper bound parameters for the upper stratum and the lower bound parameters for the middle stratum. Evaluating the factor of safety for different soil strength combinations produced a range of factors of safety for a given soil pressure condition. Limit resistance distributions based on the different combinations of soil strength parameters were subsequently recalculated for the different member lengths and orientation with respect to the slope, again using Ito and Matsui's method.

Pore pressure conditions for the I-435 Wornall Road site were established based on precipitation records and measured piezometric levels at the site. Unfortunately, the first piezometer data was recorded in August 2002, after the first period of heavy precipitation at the site following installation. Since the primary "loading period" for the reinforcing members was prior to this date, piezometric data for the selected performance intervals had to be extrapolated based on trends in precipitation observed in the months preceding the monitoring program.

Figure 11.22 shows the monthly precipitation observed at the site and the measured piezometric data. Piezometric levels for each stratum for the respective time intervals were established by first relating the measured piezometric levels to observed precipitation. This relation was then used to establish piezometric levels during spring 2002 from observed precipitation during spring 2002. The piezometric levels established this way are shown in Figure 11.23.

Additional assumptions were necessary to indicate the location of the piezometric levels in the toe and crest areas since piezometric data was only available for two specific

locations near the middle of the slope. For all the analyses made, one of the assumptions was that the location of the piezometric levels in the upper stratum coincided with the toe of the slope, and the location of the piezometric levels in the middle stratum was at 1-ft below the toe elevation. The other assumption was that the location of the piezometric levels in the upper stratum coincided with the interface of the upper and middle stratum at the slope crest, and the piezometric level in the middle stratum coincided with the interface between the middle and the lower stratum at the slope crest. The piezometric levels used in the different stability analyses for the calibration method are shown in Figure 11.24.

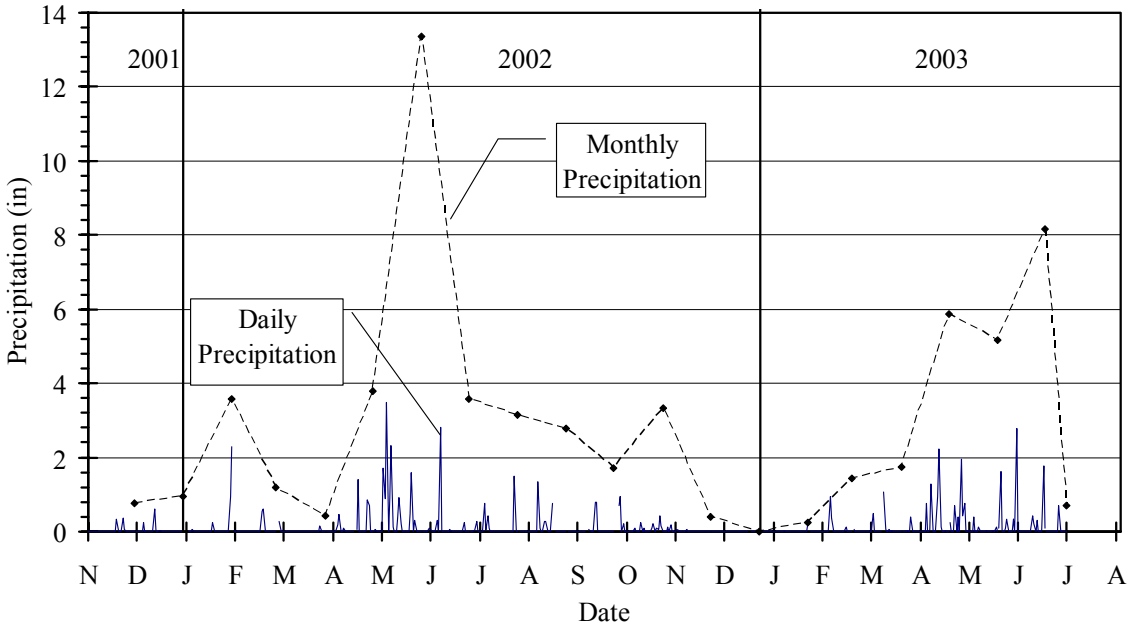

a) monthly precipitation

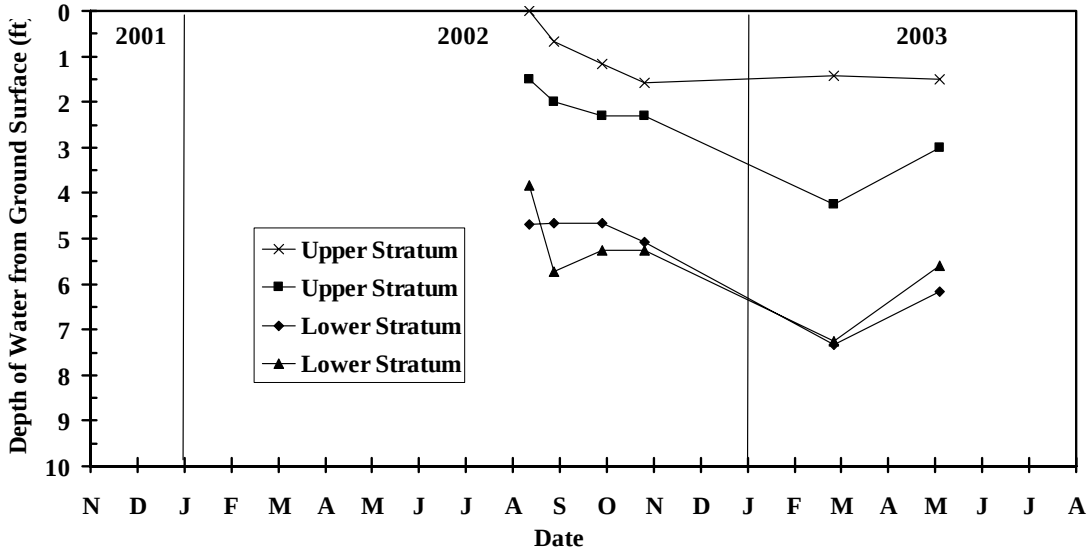

b) measured piezometric data

Figure 11.22 Piezometric data evaluated at I-435 Wornall Road site, a) monthly precipitation data, b) measured piezometric data.

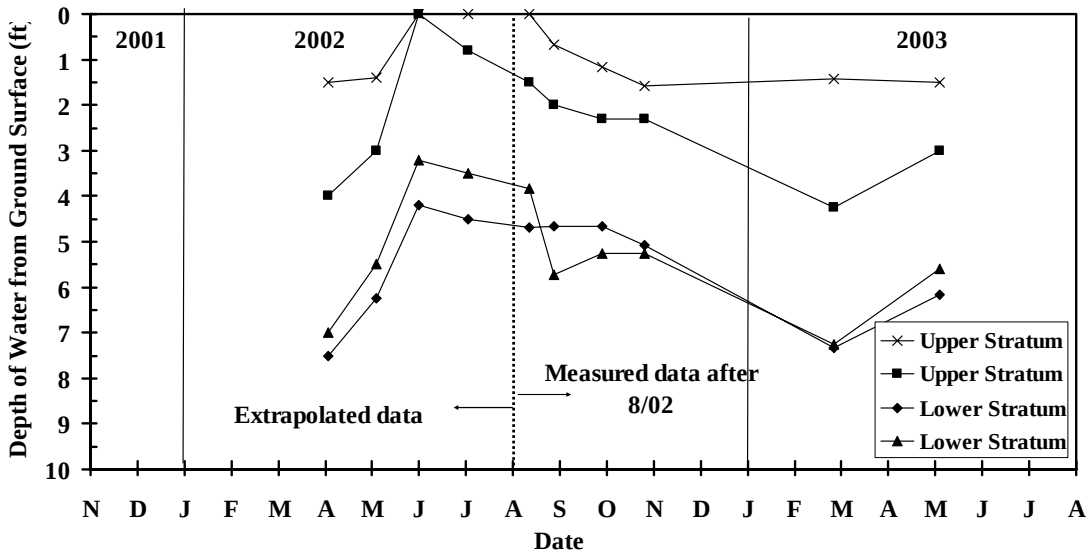

Figure 11.23 Extrapolated piezometric levels established from trends in precipitation data.

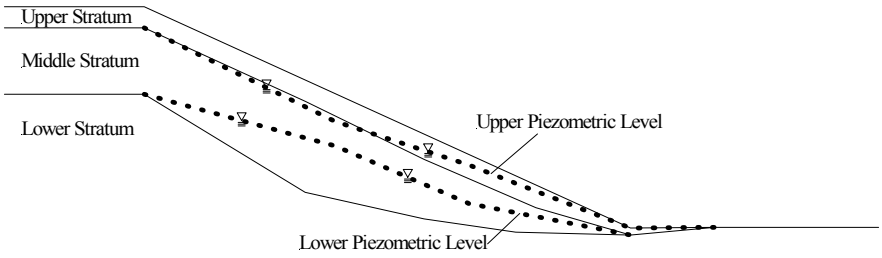

(a) 4/11/02

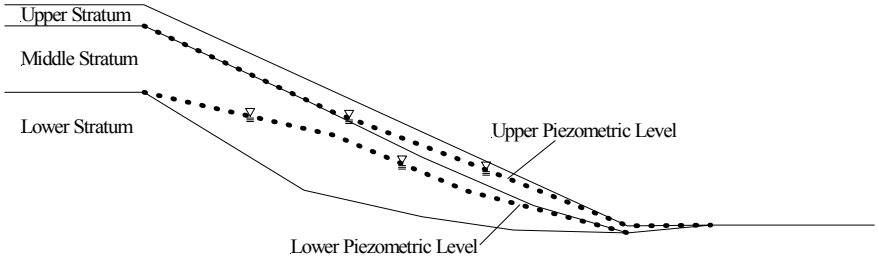

(b) 5/13/02

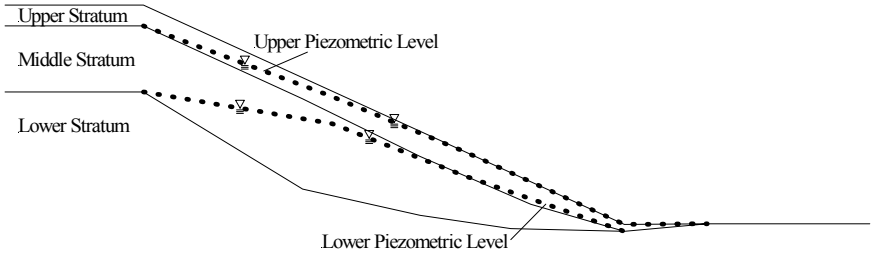

(c) 7/12/02

Figure 11.24 Piezometric surfaces used in the different stability analyses for the calibration method, a) 4/11/02, b) 5/13/02, c) 7/12/02.

The measured lateral displacements from Inclinometer I-3, installed near the middle of the slope at I-435 Wornall site, were selected as the more representative data for the site. The measured displacement data representing the total cumulative displacement near the ground surface, as shown in Figure 11.25, was used for establishing the "theoretical performance function".

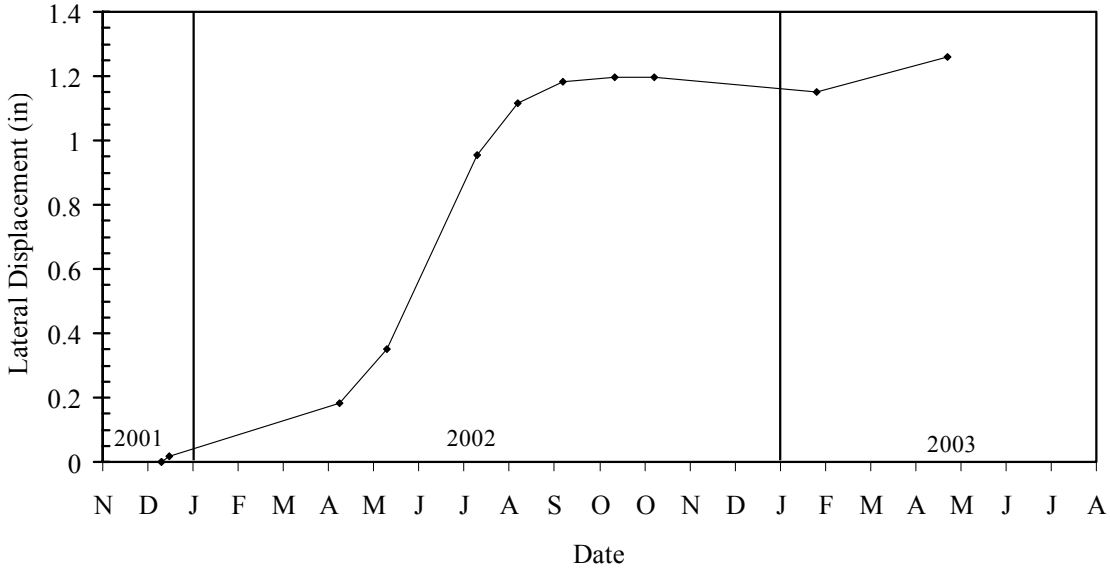

Figure 11.25 Slope lateral displacement measured from Inclinometer I-3

11.7.2. Theoretical field performance

Stability analyses were performed for the period between April 2002 and October 2002 to determine the variation in theoretical factor of safety of the slope for the pore pressure conditions established for the respective dates. The results of the stability analyses consistently indicated a critical surface passing beyond most of the reinforcing members and tangent to the interface between the middle and lower strata at the lowest point. Figure 11.26 shows an example of the critical surface obtained for Case B parameters on April 2002. A summary of the computed factors of safety is presented in Table 11.4. Computed factors of safety are also shown in Figure 11.27, and were consistently greater for Case A strength parameters. The trend in computed factor of safety showed a decrease from April through June 2002, after which the factor of safety increased slightly as a result of decreasing piezometric levels.

Figure 11.28 shows the interpretation made to extrapolate the factors of safety following the period of April 2002 through July 2002. Data corresponding to 6/10/02 was disregarded for not correlating well to the measured lateral displacement and therefore not providing the most realistic trend in factor of safety. Extrapolation including the data taken on 6/10/02 would predict lateral deformations at failure (FS=1) that are less than the lateral deformations measured to date in the inclinometers. The data after 7/12/02 was extrapolated by means of a power function. The performance function for Case A strength parameters indicates approximately 3.9-in of slope displacement for a factor of safety of unity (FS=1). The performance function for Case B parameters indicates about 1.7-in of displacement for FS=1.

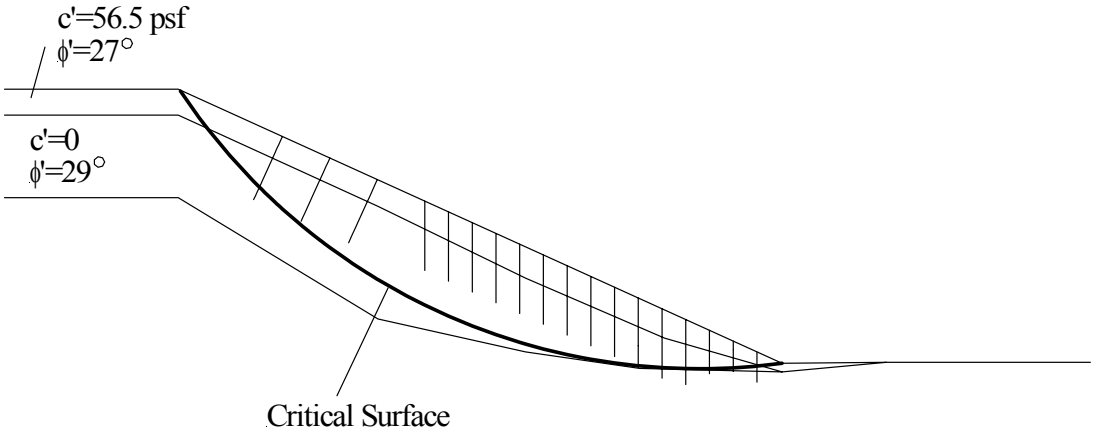

Figure 11.26 Critical sliding surface for Case B parameters, and piezometric levels recorded on 4/13/02 at I-435 Wornall Road site.

Table 11.4 Summary of theoretical factors of safety obtained from evaluations of "as-built" geometry for different time intervals and different soil strength parameters.

Date	Factor of Safety	
	Case A	Case B
4/11/2002	1.35	1.25
5/13/2002	1.27	1.17
6/10/2002	1.14	1.05
7/12/2002	1.15	1.06
8/22/2002	1.16	1.07
10/9/2002	1.18	1.09

Case A – Upper bound-Upper bound
Case B – Upper bound-Lower bound

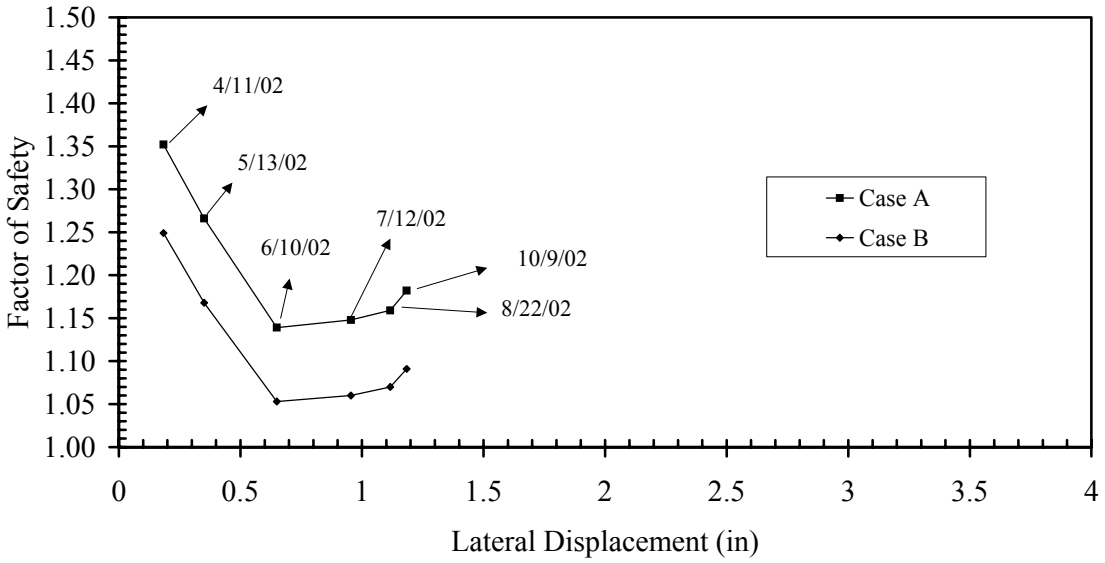

Figure 11.27 Computed factors of safety for actual conditions.

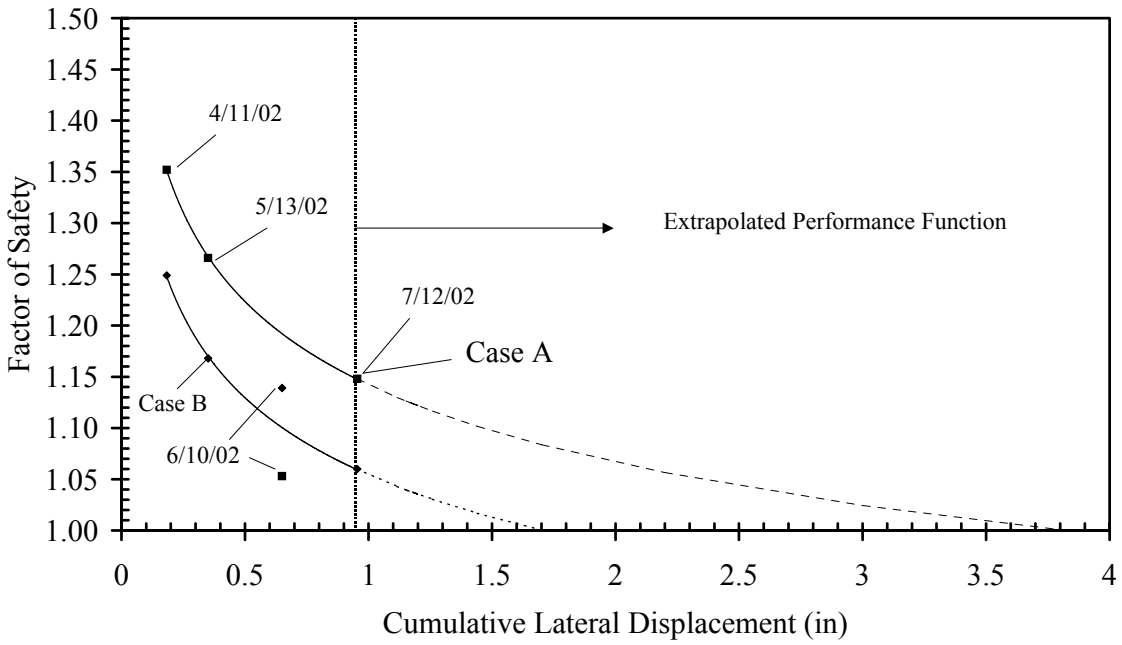

Figure 11.28 Computed factor of safety versus lateral displacement measured in I-3 showing extrapolated performance function after 7/12/02.

Based on an acceptable performance limit of approximately 3-in, Figure 11.28 suggests that, when the baseline analysis methodology produces a factor of safety of unity, expected slope lateral displacements are between 1.5- and 3.5-in depending on the strength parameters used. This suggests that the baseline analysis methodology is somewhat conservative when considering Case B soil strength parameters determined from laboratory tests. When considering Case A parameters, the performance function for the current procedure indicates a factor of safety of unity for lateral displacements close to 3.5-in, which suggest that the current procedure predicts factors of safety that are reasonably consistent with existing field performance data.

11.7.3. Calibration Using Factored Limit Resistance

The actual analysis methodology was initially calibrated by gradually increasing the limit resistance for all the reinforcing members by a constant factor and calculating new performance functions using the modified limit resistance until matching the predetermined, 3-in displacement criterion at failure. Results of these analyses indicate that the distribution of limit resistance along each individual reinforcing member, based on Ito and Matsui's method, must be increased by a factor of 3 to produce a performance function that indicates a lateral deformation of 3-in for FS=1, as shown in Figure 11.29.

11.7.4. Calibration Using Combined Axial and Lateral Capacity

Attempts were again made to calibration the analysis method by incorporating axial resistance in addition to the lateral resistance computed using the baseline analysis method. However, as was the case with similar attempts for the I70-Emma site, these attempts proved unsuccessful because of numerical instabilities and problems encountered when performing

these analyses that produce unrealistic results. Additional details regarding these analyses are provided in Parra (2004).

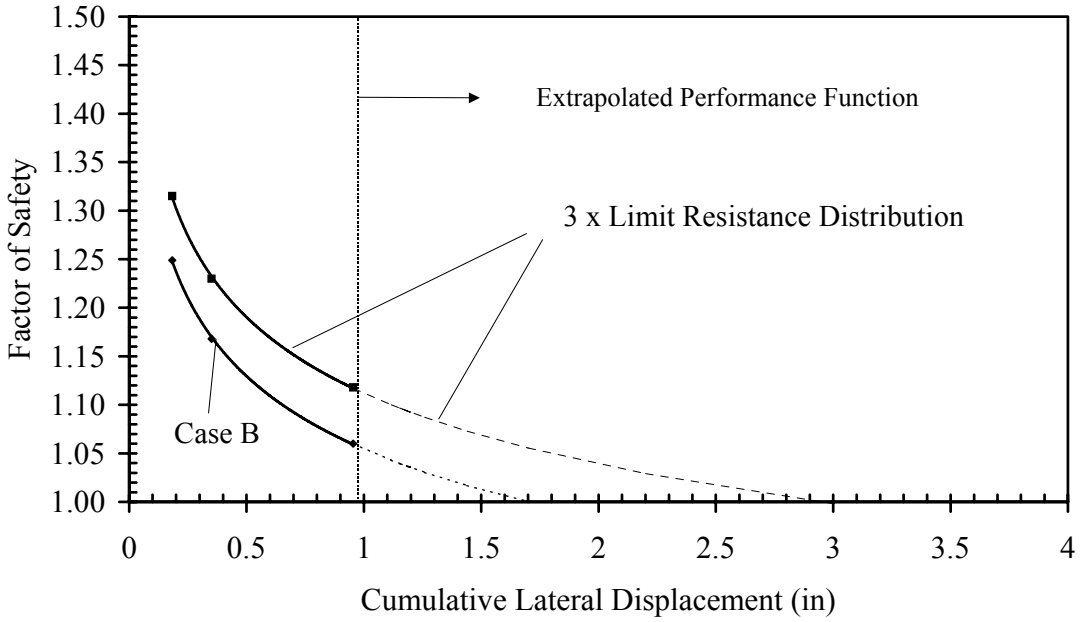

Figure 11.29 Factors of safety resulting from calibration of analysis methodology using factored limit resistance.

11.8. Summary of Results from Calibration Analyses

The analyses described in previous sections have provided useful guidance for development of recommendations for performing rigorous stability analyses for slopes stabilized with recycled plastic reinforcement. The following sections summarize key observations from these analyses:

11.8.1. Factoring baseline resistance by a constant amount

Analyses for the I70-Emma site indicate that the calibrated resistance is between 70% and 100% of the resistance computed using Ito and Matsui's limit soil pressure and using laboratory measured capacities for the reinforcing members (i.e. the "baseline" resistance). In contrast, analyses for the US36-Stewartsville site indicate the calibrated resistance is between 200% and 500% of the baseline resistance. However, the limited data available for calibration based on performance of this site required use of linear extrapolation, which may lead to overestimation of the calibrated resistance. Finally, analyses performed for the I435-Wornall site suggest that the calibrated resistance is between 100% and 300% of the baseline resistance while analyses for the US54-Fulton site suggest that the baseline resistance is reasonably consistent with the observed field performance.

11.8.2. Factoring limit soil pressure

Analyses for the I70-Emma site and the US36-Stewartsville site both indicate that the computed factors of safety are not sensitive to the value of the limit soil pressure. This suggests that modification of the method for computing the limit soil pressure is not an effective approach for calibration of the baseline resistance and further that the choice of

method for computing the limit soil pressure is not critical *for the application of using recycled plastic reinforcement* (it may be important for other member types with higher bending capacities). These findings also suggest that the structural capacity of the reinforcement is often the controlling factor for stability, in contrast to what has been concluded previously (Loehr et al, 2000).

11.8.3. Reduced moment capacity

Analyses for the I70-Emma site, where failure of two test sections did occur, indicate that calibrated limit resistances can be computed using reduced moment capacities for the reinforcing members. Results obtained suggest that, at least for the relatively sparse reinforcement patterns utilized in the failed sections, member capacities should be reduced by between 0% and 45% of the nominal measured capacities. These results are supported by the fact that reinforcing members exhumed following the failure were found to be fractured at the approximate location of the measured maximum moments.

Analyses for the other test sites produce mixed observations. Results for both the I435-Wornall Road site and the US54-Fulton site suggest that calibrated resistance can be computed using the nominal measured capacities of the reinforcing members, or perhaps even capacities slightly greater than the nominal measured capacities. Analyses for the US36-Stewartsville site suggest that calibrated resistance should be computed using member capacities that exceed the nominal member capacities by between 200 to 500%. However, it is important to re-emphasize that the results of calibrations for the US36-Stewartsville site are based on limited data that required linear extrapolation, which can produce unconservative results. As such, the results for the US36 site should be given less credence than results from other sites unless additional data is acquired to confirm the observations provided.

11.8.4. Incorporation of axial load in reinforcing members

Analyses presented indicate that it is not possible to calibrate the method using both axial and lateral loads within the range and for the conditions considered. These observations also suggest that axial resistance provided by the reinforcing members is either very low, or has little effect on the overall stability of the stabilized slopes. However, limitations of the software used prevented complete evaluation of this approach so additional work is needed to resolve this issue.

11.9. Recommended Methods for Analysis of Slopes with Recycled Plastic Reinforcement

Based on the accumulation of evidence summarized above, the following recommendations are made for future analysis of slope stabilization schemes utilizing recycled plastic reinforcement:

1. Use of Broms' (1964) method for predicting the limit soil pressure under fully drained conditions is recommended for use in predicting the limit resistance of recycled plastic reinforcing members.
2. Axial resistance should continue to be ignored as long as the member inclinations are restricted to between being oriented vertically and being oriented perpendicular to the face of the slope.

3. For members to be installed at spacings of 3-ft or less, the limit resistance should be computed based on the nominal measured capacity of the reinforcing member. For members to be installed at greater spacings, the limit resistance should be computed using a reduced member capacity equal to 60% of the nominal measured capacity.

It is certainly possible that additional knowledge regarding load transfer in reinforced slopes in general, or additional experience with use of recycled plastic reinforcement in particular, may lead to modifications to these recommendations. However, the recommendations above are supported by the preponderance of evidence available from the field testing program at this time.

Chapter 12. Summary and Conclusions

This report has documented activities undertaken to evaluate the use of recycled plastic reinforcing members for stabilization of surficial slope failures over a seven year period. This chapter includes a brief summary of items included in the body of the report along with a number of broad conclusions drawn from the project activities. Recommendations for implementation of the technique on a widespread basis are also presented.

12.1. Summary

The report is organized in twelve chapters, each of which covers a different aspect of the project. Chapter 1 of the report included a brief section describing the motivation behind the project entitled "Slope Stabilization Using Recycled Plastic Pins". Relevant background information regarding the overall scope of the three phase project effort was then presented followed by a description of the scope of this report and other documentation prepared as a part of the project.

The general methodology for rigorous analysis of the stability of slopes stabilized using recycled plastic reinforcement is described in Chapter 2. This chapter includes specific procedures for calculation of resistance provided by recycled plastic members. Additionally, descriptions of several unresolved issues related to specific application of the design method are discussed.

Results of evaluations to establish the properties and behavior of recycled plastic members were described in Chapter 3. The chapter includes information regarding sources of recycled plastic lumber and general characteristics of the products currently available along with descriptions of several laboratory test standards developed for use with recycled plastic lumber. Tests performed for a total of 13 different batches of members from three different manufacturers were summarized and the special issues of creep, strain rate effects, and degradation of the member properties upon exposure to a variety of conditions were addressed.

The process for selection of the field test sites and the field instrumentation used to monitor performance at the respective test sites were described in Chapters 4 and 5, respectively. In Chapter 4, the general criteria used to screen candidate sites and to make the final site selections were described. General characteristics of the selected test sites were then presented. Chapter 5 describes the different types of measurements needed to monitor performance of the stabilized and control test sections at the field test sites and then describes the specific instrumentation used at the sites.

In Chapters 6 through 9, the activities undertaken to establish each of the respective test sites are described along with a summary of observations from field performance monitoring of the sites. Activities undertaken to establish three different test areas on I-70, at what is referred to as the I70-Emma site, were described in Chapter 6. Activities for two test sites located in southern Kansas City and referred to collectively as the I435-Kansas City sites were presented in Chapter 7. Activities at the US36-Stewartsville site located in northwest Missouri were described in Chapter 8. Finally, activities for the US54-Fulton test site in central Missouri were described in Chapter 9.

Chapter 10 describes the construction methods used to install recycled plastic reinforcement at each of the respective test sites. The performance and efficiency of installation at each site are also described and compared among the different sites. Chapter 11 then describes a series of "calibration" analyses performed to establish appropriate guidance for application of the general design methodology based on the performance observed at the different field test sites. Specific recommendations are then provided based on the results of these analyses. Finally, this chapter provides a summary of the entire report along with broad conclusions derived from the overall project effort.

12.2. Conclusions

In any large project such as the one described in this report, numerous notable observations and conclusions can be made regarding many of the activities performed. While all of these observations and conclusions are important, some have limited significance in terms of the overall objectives of the project while others specifically relate to the overall objectives and have more far reaching implications. Observations and conclusions drawn from the project that have limited implications have been made within each of the respective chapters and will not be repeated here. However, several broad overall conclusions drawn from collective review of all project efforts warrant additional attention and are therefore summarized here. These broad conclusions include:

1. The technique of using recycled plastic reinforcement to stabilize surficial slope failures in excavated and embankment slopes has proven to be effective at providing long-term stabilization. To date, slopes stabilized as a part of this project have been in place for up to six years. Control sections established at several of the sites have failed, which demonstrates that these sites have very likely been subjected to conditions that are at least as bad as those that caused the original failures and that the installed reinforcement is in fact providing additional stabilization.
2. Observations from field instrumentation measurements taken at the field test sites provide a consistent picture of how the reinforcement effects stabilization. The observed performance has generally followed a three-stage behavioral pattern. In the first stage, the stabilized slopes are observed to experience little movement and little resistance is provided by the reinforcing members. In Stage 2, slope movements are observed to increase substantially in response to increased pore water pressures within the slope at the same time as loads in the reinforcing members are observed to increase. These movements are believed to simply be movement required to mobilize resistance in the reinforcing members. Finally, Stage 3 is characterized by diminishing movement that is simultaneously accompanied by stabilization of the loads in the reinforcing members. This stage is believed to be a result of the slope and reinforcement coming to equilibrium.
3. The required spacing of reinforcing members depends on the specific conditions encountered at a particular site. A "standard" reinforcement pattern that appears to be sufficient for the vast majority of cases encountered consists of a distributed pattern of reinforcing members placed across the entire slide area on a staggered grid with members spaced at 3-ft centers. In some cases, appropriate stabilization

can also be accomplished with members placed at greater spacing. The latter is especially true if site specific analyses are performed.

4. Recycled plastic reinforcing members can be efficiently and reliably installed using either a percussion hammer found on many drilling rigs or a simple drop-weight type of hammer. Experience acquired to date has shown that the critical feature of installation equipment is having a mast to maintain the alignment between the hammer and the reinforcing member.
5. Costs for stabilization of slopes using recycled plastic reinforcing members were relatively consistent throughout the project. Nominal costs for materials and installation are approximately $40/member with the costs being approximately equally split between material costs and installation costs. Unit costs per unit area of the slope face vary significantly with the spacing of the reinforcing members. Costs for stabilization using reinforcing members spaced at 3-ft (0.9-m) are nominally $4.50/ft^2 ($50/m^2). In contrast, costs for stabilization using reinforcing members spaced at 4.5-ft are nominally $2.00/ft^2 ($18/m^2).
6. The general design approach developed as a part of this project is suitable for design of stabilization schemes using recycled plastic reinforcement.
7. Field performance data acquired at the respective test sites provide a strong basis for "calibration" of the general design methodology to establish specific recommendations for application of the analysis method for future design. Recommendations developed based on these analyses include:
   - that Broms' (1964) method be used for predicting the limit soil pressure,
   - that axial resistance be ignored in the analyses,
   - that the member capacity used for prediction of member resistance be taken as the nominal measured capacity when members are to be placed at spacings of 3-ft or less and as 60% of the nominal measured capacity when members are to be placed at spacings greater than 3-ft.
8. The material properties of recycled plastic members vary with the manufacturing process used and the specific blend of constituents used.
9. The properties of all recycled plastic members are dependent on the specific loading rate adopted for testing and the magnitude of loading rate effects can vary from product to product. As such, care must be applied when reviewing material properties from different manufacturers and for different products to ensure that acceptable performance can be achieved with a particular product.

12.3. Recommendations for Implementation

The performance observed at the field test sites has provided a strong track record of success in stabilizing surficial slope failures using recycled plastic reinforcing members. This track record clearly supports and justifies more widespread implementation of the technique to address the considerable nuisance slide problem. However, several practical challenges to widespread implementation remain that must be carefully considered and addressed if the technique is to become widely utilized.

The primary challenges associated with more widespread implementation generally arise from the necessity to use the competitive bidding process for both acquisition and installation of recycled plastic reinforcing members. Competitive bidding for acquisition of recycled plastic products is a challenge because of the variability of recycled plastic products available on the market today, which leads to the potential for acquiring unacceptable product if care is not taken in establishing *and enforcing* appropriate specifications. Effective specifications are, in turn, challenging because current ASTM specifications for recycled plastic products do not produce sufficient criteria because of loading rate effects described in Chapter 3. Material properties reported based on current ASTM standards are not appropriate for use in design (due to loading rate effects) and, since loading rate effects may be different for different products, it is not generally possible to simply "apply a correction" because each product may have a different correction. To address this problem, project investigators have developed a draft material specification (Bowders et al., 2003) that provides several alternative means for suppliers to account for loading rate effects so that owners can be confident in the quality of the product without placing undue burdens on suppliers that may prevent them from entering the market.

Competitive bidding for installation services is also a challenge because of the potential for damage of recycled plastic reinforcing members during installation coupled with the desire on the part of installation contractors to install members as efficiently as possible. Attention must therefore be paid to the installation equipment and installation techniques used by contractors to ensure that members are not subject to significant damage during installation. Recommendations in this regard are provided in Loehr and Bowders (2006) and in the accompanying short-course notes. In general, preference should be given to installation techniques that impose high frequency, low amplitude blows to the members as opposed to low frequency, high amplitude blows, which could impose excessive stresses on the members during installation. Specific criteria for hammer energy, frequency, and force are difficult to establish at this time, but with additional experience such criteria can be developed to aid in establishing appropriate construction specifications. In the interim, a prudent approach is to require contractors to demonstrate the effectiveness of equipment that differs substantially from that used in this project through a series of "test drives" at the site being stabilized.

Finally, because the technique of using recycled plastic reinforcement is new, there is likely to be some hesitancy on the part of suppliers and installers to enter into the market of providing products and installation services because of uncertainties regarding the magnitude of the market and risks involved with construction. To remedy this, it is strongly recommended that MoDOT, or other owners considering use of the technique, establish an incentive program of one form or another to provide motivation for use of the new technique. Such an incentive program could include cost-sharing on projects, provision of recycled plastic members, or provision of installation services, as a few examples to allow agency, material supplier, and contractor personnel to become comfortable with the technique and to work out inevitable issues that will arise when implementing a new technique.

References

American Plastics Council (2002), *2001 National Post-consumer Plastics Recycling Report*, R. W. Beck, Inc. Washington, D.C.

Ang, E.C. (2005), *Numerical Investigation of Load Transfer Mechanism in Slopes Reinforced with Piles*, thesis submitted to the faculty of the University of Missouri in partial fulfillment of the requirements for Ph.D. degree, 154 pp.

Ang, E.C., J.E. Loehr, and D.E. Smith (2005), "Numerical investigation of limit soil pressure for design of pile stabilized slopes," *Prediction, Analysis, and Design in Geomechanical Applications*, Proceedings of the 11th International Conference of IACMAG, Torino, Italy, G. Barla and M. Barla, Editors, Patron Editore, Vol. 2, pp. 319-326.

ASTM (1997), "Standard Test Methods for Compressive and Flexural Creep and Creep-Rupture of Plastic Lumber and Shapes," *ASTM International*, D 6112.

ASTM (2003), "Standard Test Method for Compressive Properties of Plastic Lumber and Shapes," *ASTM International*, D6108.

ASTM (2005), "Standard Test Methods for Flexural Properties of Unreinforced and Reinforced Plastic Lumber and Related Products," *ASTM International*, D 6109.

Birley A.W., B. Haworth, and J. Batchelor (1991), *Physics of Plastics*, Oxford University Press, New York.

Bowders, J.J., and J.E. Loehr (2000), "Slope Stabilization with Recycled Plastic Pins," *Geotechnical News*, Canadian Geotechnical Society and United States National Society, BiTech Publishers Ltd., Richmond, British Columbia, Canada, Vol. 18, No. 1.

Bowders, J.J., J.E. Loehr, H. Salim, and C-W Chen (2003), "Engineering Properties of Recycled Plastic Pins for Use in Slope Stabilization," *Transportation Research Record: Journal of the Transportation Research Board*, Transportation Research Board, TRR 1849, pp. 39-46.

Bowders, J.J., J.E. Loehr, and C-W Chen (2003), *Evaluation of Recycled Plastic Products in Terms of Suitability for Stabilization of Earth Slopes*, Final Report to Missouri Department of Transportation and Recycled Materials Resource Center, Project RI98-007c, Report RDT 03-019, 125 pp.

Bowders, J.J., C-W Chen, H. Salim, J.E. Loehr, and J.W. Owen (2006), "Creep Behavior of Recycled Plastic Lumber in Slope Stabilization Applications," *Journal of Materials in Civil Engineering*, ASCE, (in press).

Breslin, V.T., U. Senturk, and C.C. Berndt (1998), "Long-term Engineering Properties of Recycled Plastic Lumber Used in Pier Construction," *Resources Conservation and Recycling*, Vol. 23, pp. 243-258.

Broms, B.B. (1964), "Lateral resistance of piles in cohesionless soil," *Journal of the Soil Mechanics and Foundations Division*, ASCE, Vol. 90, No. SM3, pp. 123-156.

Bruce, A.H., G.R. Brenniman, and W.H. Hallenbeck (1992), *Mixed Plastics Recycling Technology*, Noyes Data Corporation, Park Ridge.

Chandler, K.S. (2005), *Calibration of Resistance Provided by Slender Reinforcing Members in Earth Slopes*, thesis submitted to the faculty of the University of Missouri in partial fulfillment of the requirements for M.S. degree, 140 pp.

Chen, C-W (2003), *Engineering Properties of Recycled Plastic Pins for Use in Slope Stabilization,* thesis submitted to the faculty of the University of Missouri in partial fulfillment of the requirements for M.S. degree, 118 pp.

Ito, T., and T. Matsui (1975), "Methods to estimate lateral force acting on stabilizing piles," *Soils and Foundations*, Vol. 15, No. 4, pp. 43-59.

Koerner, R.M., Y.H. Halse, and A.E. Lord (1990), "Long-term durability and aging of geomembranes," *Waste Containment Systems: Construction, Regulation, and Performance, Geotechnical Special Publication*, No. 26, pp. 106-137.

Koerner, R.M. (1998), *Designing with Geosynthetics,* 4th Ed, Prentice Hall, New Jersey.

Lampo, R.G. and T.J. Nosker (1997), *Development and Testing of Plastic Lumber Materials for Construction Applications*, Report TR 97/95, US Army Construction Engineering Research Laboratories, Champaign, Illinois.

Liew, W. (2000), *Stability Analysis of Slopes Reinforced with Recycled Plastic Pins*, thesis submitted to the faculty of the University of Missouri in partial fulfillment of the requirements for M.S. degree, 208 pp.

Loehr, J.E., J.J. Bowders, J.W. Owen, L. Sommers, and W. Liew (2000), "Stabilization of Slopes Using Recycled Plastic Pins," *Transportation Research Record: Journal of the Transportation Research Board*, National Academy Press, No. 1714, Paper No. 00-1435, pp. 1-8.

Loehr, J.E., J.J. Bowders, and H. Salim (2000), *Slope Stabilization Using Recycled Plastic Pins – Constructability*, Missouri Department of Transportation, MoDOT RDT 00-007, 74 pp.

Loehr, J.E. (2000), "Stabilization of Infrastructure Slopes Using Recycled Plastic Pins," Extended Abstract published in *Proceedings of Transportation Systems 2000 Workshop*, U.S. Department of Defense, San Antonio, Texas, February 28 – March 3.

Loehr, J.E. (2002), "Stabilization of Slopes with Recycled Plastic Pins," Proceedings of the NSF Workshop on Geotechnical Composite Systems, Roanoke, Virginia, July 28-29, 2002, Extended Abstract, pp. 40-43.

Loehr, J.E., and J.J. Bowders (2003), *Slope Stabilization Using Recycled Plastic Pins: Phase II – Assessment in Varied Site Conditions*, Missouri Department of Transportation, RDT 03-016, 214 pp.

Loehr, J.E., T.W. Fennessey, and J.J. Bowders (2003), "Mechanical Stabilization of Earth Slopes Using Recycled Materials," *Proceedings of Beneficial Use of Recycled Materials in Transportation Applications*, AWMA, November 13-15,2001, Washington, D.C., pp. 413-422.

Loehr, J.E., Parra, J.R., E-C Ang, and J.J. Bowders (2004), "Design Method for Slope Stabilization Using Recycled Plastic Pins," *Proceedings of Geo-Trans 2004: Geotechnical Engineering for Transportation Projects*, M.K. Yegian and E. Kavazanjian, Editors, ASCE, GSP 126, Vol. 1, pp. 723-731.

Loehr, J.E., J.J. Bowders, C-W Chen, K.S. Chandler, P.H. Carr, and T.W. Fennessey (2004), "Slope Stabilization Using Recycled Plastic Pins," *Proceedings of the 55th Highway Geology Symposium*, Robert Henthorne, Editor,

Loehr, J.E., and J.J. Bowders (2005), *Design and Construction Guidance for Slope Stabilization Using Recycled Plastic Reinforcement*, participant handouts for ½-day workshop, Fall 2005.

Loehr, J.E., and J.J. Bowders (2006), *Guide for Design and Construction of Slope Stabilization Measures Using Recycled Plastic Reinforcement*, Missouri Department of Transportation, 44 pp.

McLaren, M.G. (1995), "Recycled Plastic Lumber and Shapes: Design and Specifications," *Proceedings of the 13th Structures Congress*, Vol. 1, ASCE, pp. 819-833.

Osman, H.E., D.J. Elwell, G. Glath, and M. Hiris (1999), "Noise Barriers Using Recycled-Plastic Lumber," *Transportation Research Record: Journal of the Transportation Research Board*, No. 1670, Paper No. 99-2100, pp. 49-58.

Parra, J.R., J.E. Loehr, D.J. Hagemeyer, and J.J. Bowders (2003), "Field Performance of Embankments Stabilized with Recycled Plastic Reinforcement," *Transportation Research Record: Journal of the Transportation Research Board*, Transportation Research Board, TRR 1849, pp. 31-38.

Parra, J.R. (2004), *Evaluation of Uncertainties in the Resistance Provided by Slender Reinforcement for Slope Stabilization*, thesis submitted to the faculty of the University of Missouri in partial fulfillment of the requirements for Ph.D. degree, 370 pp.

Parra, J.R., E.C. Ang, and J.E. Loehr (2004), "Sources of Uncertainty in Lateral Resistance of Slender Reinforcement Used for Slope Stabilization," *Proceedings of Geo-Support 2004: Drilled Shafts, Micropiling, Deep Mixing, Remedial Methods, and Specialty Foundation Systems*, J.P. Turner and P.W. Mayne, Editors, ASCE, GSP 124, pp. 187-198.

Poulos, H.G., and E.H. Davis (1980), *Pile foundation analysis and design*, John Wiley and Sons, New York.

Sommers, L., J.E. Loehr, and J.J. Bowders (2000), "Construction Methods for Slope Stabilization Using Recycled Plastic Pins," *Proceedings of the Mid-Continent Transportation Symposium*, Iowa State University, Ames, Iowa, May 15-16, pp. 254-258.

Sommers, L. (2001), *Reliability-based Analysis of Three Alternative Methods for Repair of Surficial Slope Failure*, thesis submitted to the faculty of the University of Missouri in partial fulfillment of the requirements for M.S. degree, 169 pp.

Timoshenko S.P., and J.M. Gere (1972), *Mechanics of Materials*, VanNostrand, New York.

Transportation Research Board (1996), *Landslides: Investigation and Mitigation*, TRB Special Report 247, A.K. Turner and R.L. Schuster editors, National Academy Press, 673 pp.

Appendix A. Boring Logs for I70-Emma Site

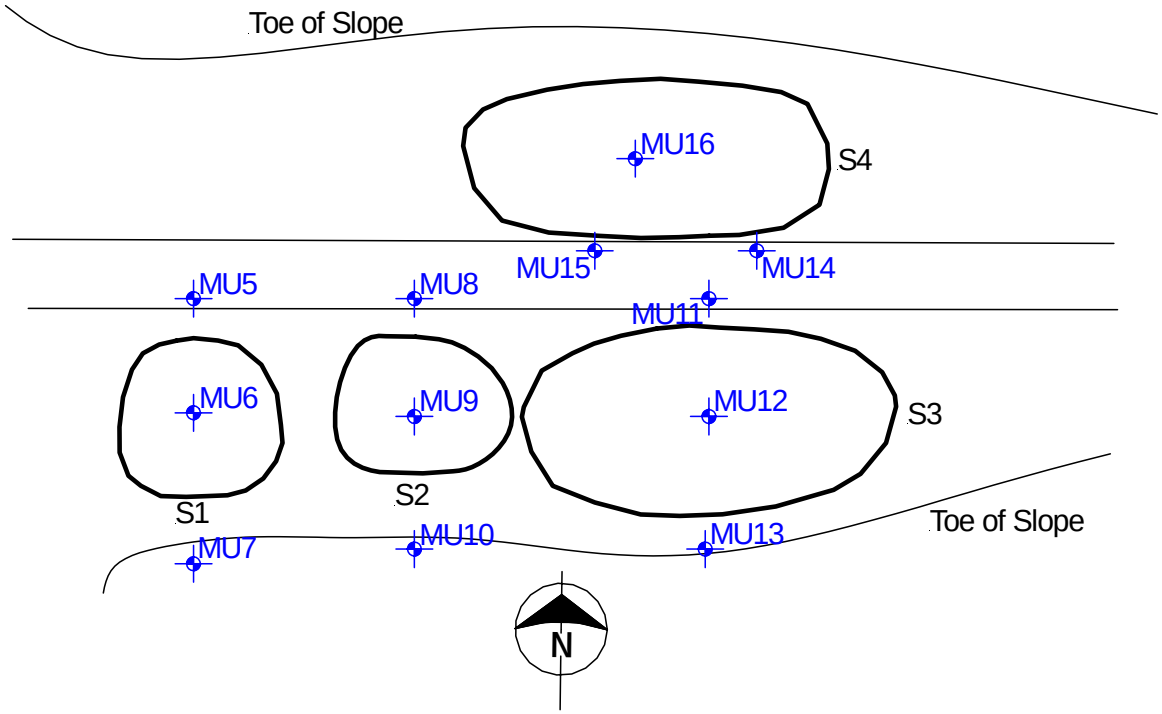

Figure A.1 Plan view of I70-Emma site showing approximate boring locations.

University of Missouri - Columbia

Civil & EnvironmentalEngineering Department -Geotechnical Group

Project Name: I-70 - Emma Site | **Project NO: Test 7**

Location: Eastbound on-ramp @ Jct. Rt. Y & I-70 | **Boring Number: MU5**

Ground Elevation: | **Logged By: A. Miller**

Drilling Date: 6/1/1999 | **Driller: Lamberson**

Weather: Sunny | Auger Method: | Driller's Hole NO: L-99-24

Conditions: | SPT Hammer Efficiency: | Drilling Equip: Failing 1500 G7889

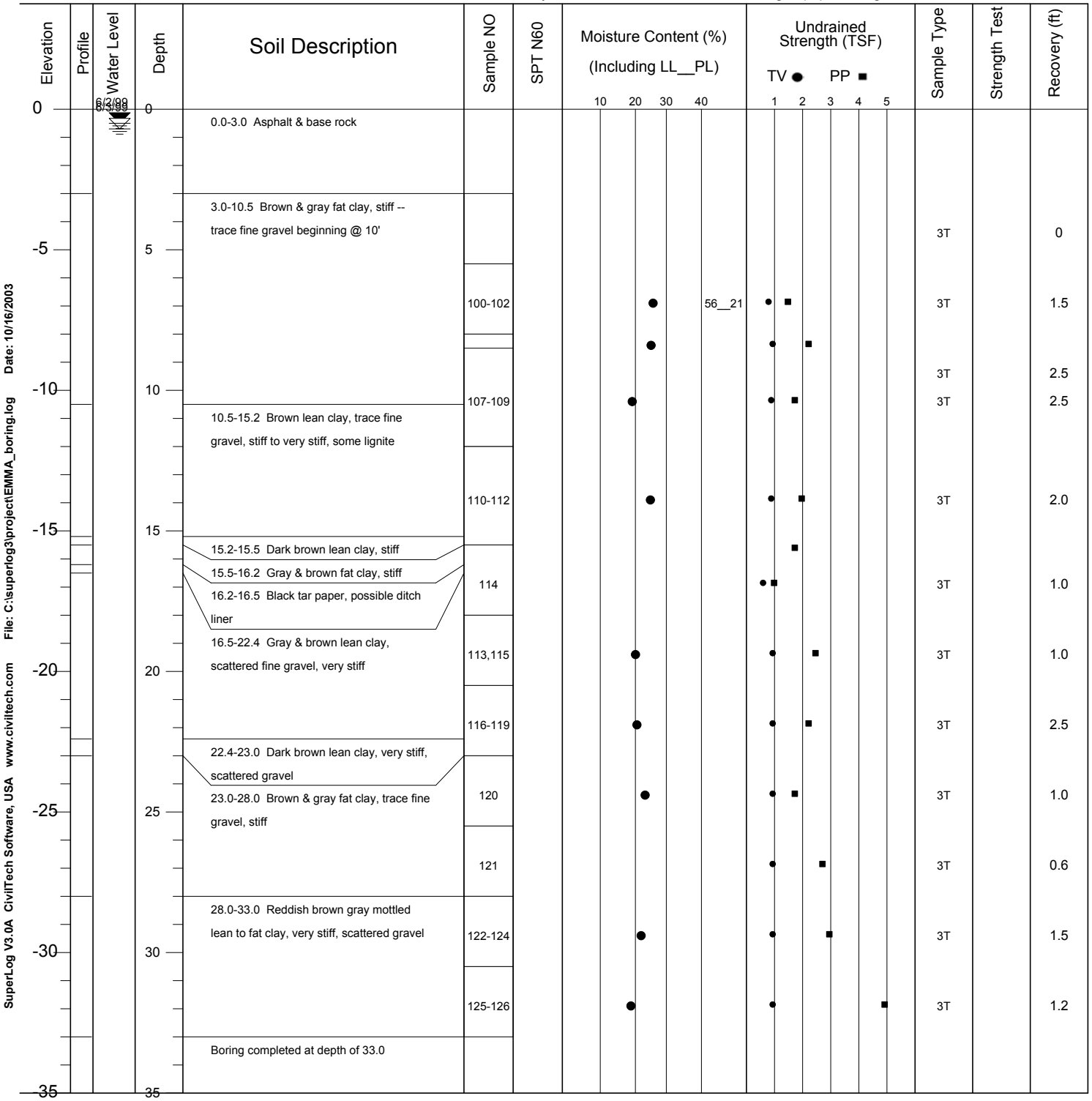

--water table artificially high due to drilling method

SuperLog V3.0A CivilTech Software, USA www.civiltech.com File: C:\superlog3\project\EMMA_boring.log Date: 10/16/2003

University of Missouri - Columbia

Civil & EnvironmentalEngineering Department -Geotechnical Group

Project Name: I-70 - Emma Site | **Project NO: Test 7**

Location: Eastbound on-ramp @ Jct. Rt. Y & I-70 | **Boring Number: MU6**

Ground Elevation: | **Logged By: P. Hilchen**

Drilling Date: 6/1/1999 | **Driller: Varnes**

Weather: Overcast with occasional showers | Auger Method: | Driller's Hole NO: Y-99-38

Conditions: | SPT Hammer Efficiency: | Drilling Equip: Sonco 4000

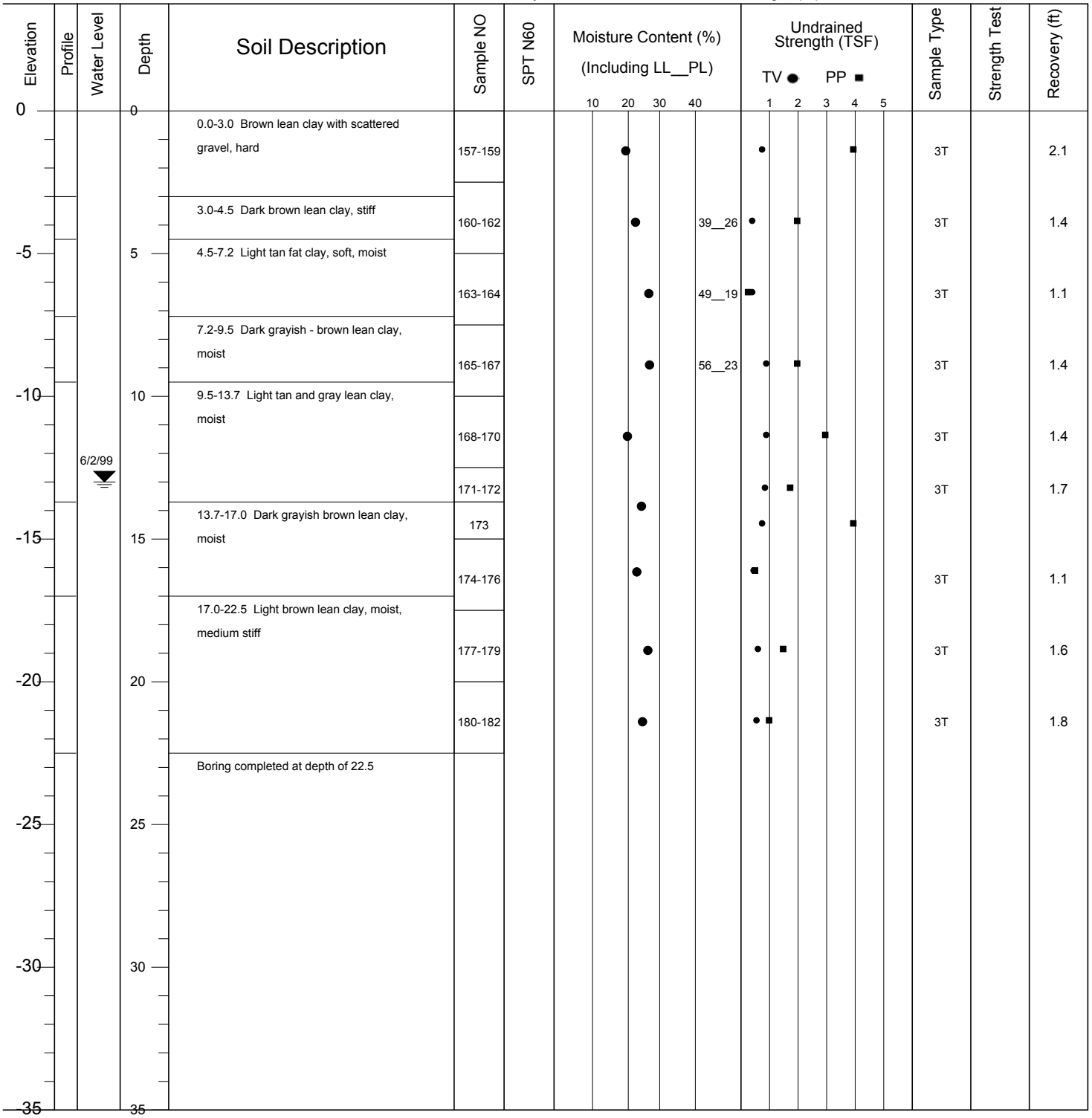

University of Missouri - Columbia

Civil & EnvironmentalEngineering Department -Geotechnical Group

Project Name: I-70 - Emma Site | **Project NO: Test 7**

Location: Eastbound on-ramp @ Jct. Rt. Y & I-70 | **Boring Number: MU7**

Ground Elevation: | **Logged By: Hilchen**

Drilling Date: 6/1/1999 | **Driller: Dodds**

Weather: Cloudy with occasional showers | Auger Method: | Driller's Hole NO: V-99-36A

Conditions: | SPT Hammer Efficiency: | Drilling Equip: CME 850 G7950

Elevation	Depth	Soil Description	Sample NO	SPT N60	Sample Type	Recovery (ft)
0	0	0.0-2.5 Concrete and Rubble			3T	
		2.5-3.8 Light brown fat clay, moist, stiff	203,205		3T	1.9
		3.8-4.5 Dark brown fat clay, moist, stiff				
-5	5	4.5-5.7 Light brown lean clay, moist	204		3T	
			206		3T	
		5.7-7.9 Dark gray lean clay, moist, hard	207-208		3T	
					3T	0.4
		7.9-10.0 Dark grayish - brown lean clay, moist, medium stiff	209		3T	
-10	10	Boring completed at depth of 10				
-15	15					
-20	20					
-25	25					
-30	30					
-35	35					

Water Level: GWT not encountered

Moisture Content (%) (Including LL__PL): 10 20 30 40

Undrained Strength (TSF): TV ● PP ■ 1 2 3 4 5

Strength Test

SuperLog V3.0A CivilTech Software, USA www.civiltech.com File: C:\superlog3\project\EMMA_boring.log Date: 10/16/2003

University of Missouri - Columbia

Civil & EnvironmentalEngineering Department -Geotechnical Group

Project Name: I-70 - Emma Site | **Project NO: Test 7**

Location: Eastbound on-ramp @ Jct. Rt. Y & I-70 | **Boring Number: MU8**

Ground Elevation: | **Logged By: Miller**

Drilling Date: 6/1/1999 & 6/3/1999 | **Driller: Lamberson**

Weather: Partly Cloudy, 80 deg. | Auger Method: | Driller's Hole NO: L-99-25

Conditions: | SPT Hammer Efficiency: | Drilling Equip: Failing 1500 67889

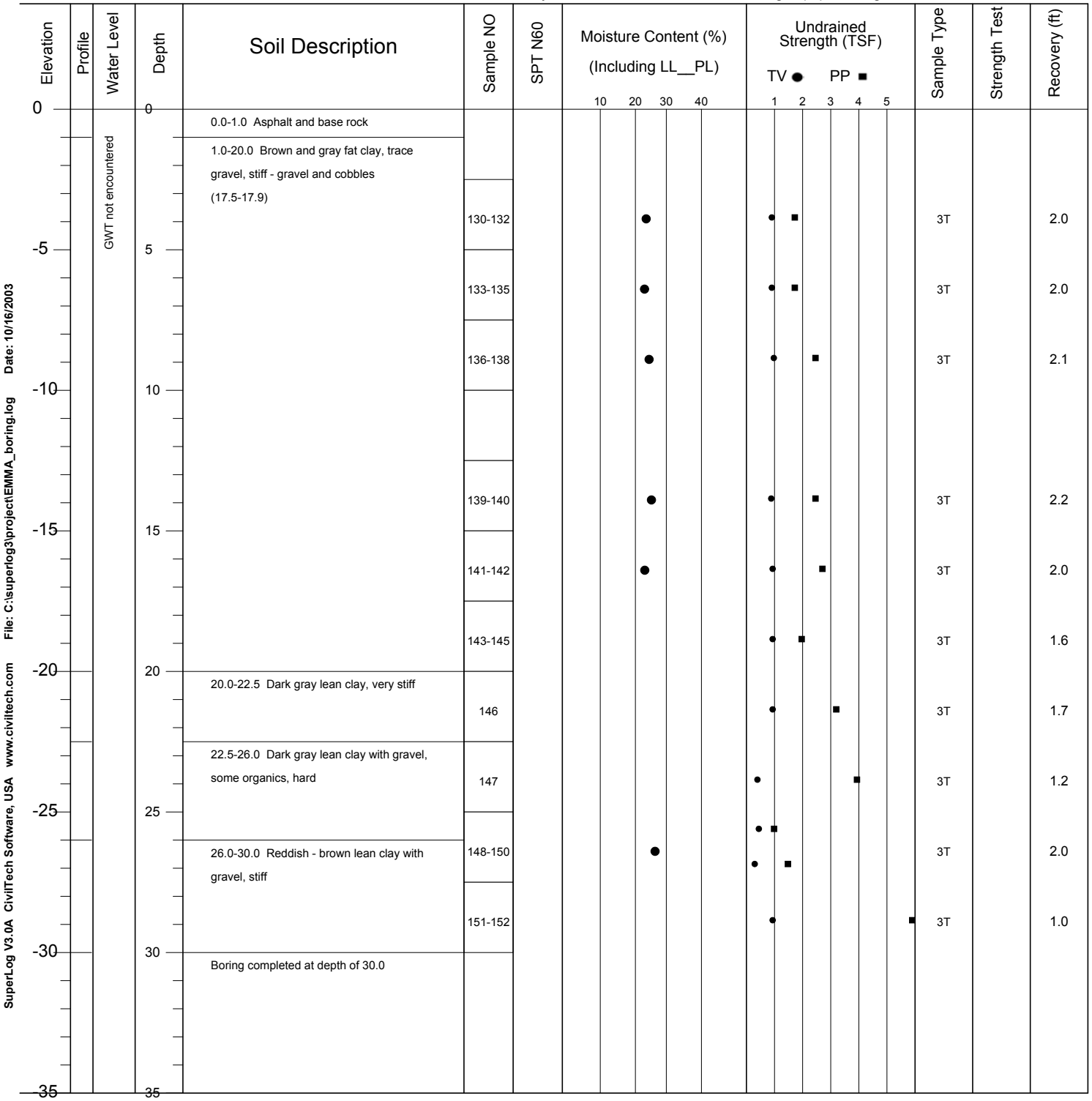

SuperLog V3.0A CivilTech Software, USA www.civiltech.com File: C:\superlog3\project\EMMA_boring.log Date: 10/16/2003

University of Missouri - Columbia

Civil & EnvironmentalEngineering Department -Geotechnical Group

Project Name: I-70 - Emma Site | **Project NO: Test 7**

Location: Eastbound on-ramp @ Jct. Rt. Y & I-70 | **Boring Number: MU9**

Ground Elevation: | **Logged By: Hilchen**

Drilling Date: 6/1/1999 | **Driller: Varner**

Weather: Cloudy with occasional showers | Auger Method: | Driller's Hole NO: Y-99-39

Conditions: | SPT Hammer Efficiency: | Drilling Equip: Simco 4000 G6944

Elevation	Depth	Soil Description	Sample NO	SPT N60	Moisture Content (%) (Including LL__PL)	Undrained Strength (TSF) TV ● PP ■	Sample Type	Strength Test	Recovery (ft)
0	0	0.0-4.5 Light brown lean clay, moist, hard to medium stiff	183-184				3T		1.1
			185				3T		0.6
-5	5	4.5-7.0 Tan and gray fat clay with silt, moist, soft	186-188		52__21		3T		1.5
		7.0-12.0 Tan and gray fat clay with silt, moist, laminated layers of gray and tan fat clay	189-191				3T		1.2
-10	10		192-194				3T		1.5
		12.0-12.5 Dark gray lean clay with reddish - brown Mg nodules, moist					3T		
		12.5-13.5 Cobbles and concrete							
-15	15	13.5-18.2 Gray and tan fat clay, moist, medium stiff to stiff	195-197				3T		0.7
			198-200				3T		2.0
-20	20	-- shelby tube refusal @ 18.2	201-202				3T		0.7
		Boring completed at depth of 20.7							
-25	25								
-30	30								
-35	35								

Water Level: 6/2/99

Refusal @ 18.2 -- cleaned out to 20.0

(Sample not used 12.5-15.0)

SuperLog V3.0A CivilTech Software, USA www.civiltech.com File: C:\superlog3\project\EMMA_boring.log Date: 10/16/2003

University of Missouri - Columbia

Civil & EnvironmentalEngineering Department -Geotechnical Group

Project Name: I-70 - Emma Site | **Project NO: Test 7**

Location: Eastbound on-ramp @ Jct. Rt. Y & I-70 | **Boring Number: MU10**

Ground Elevation: | **Logged By: Hilchen**

Drilling Date: 6/1/1999 | **Driller: Dodds**

Weather: Cloudy with occasional showers | Auger Method: | Driller's Hole NO: V-99-36B

Conditions: | SPT Hammer Efficiency: | Drilling Equip: CME 850 G7950

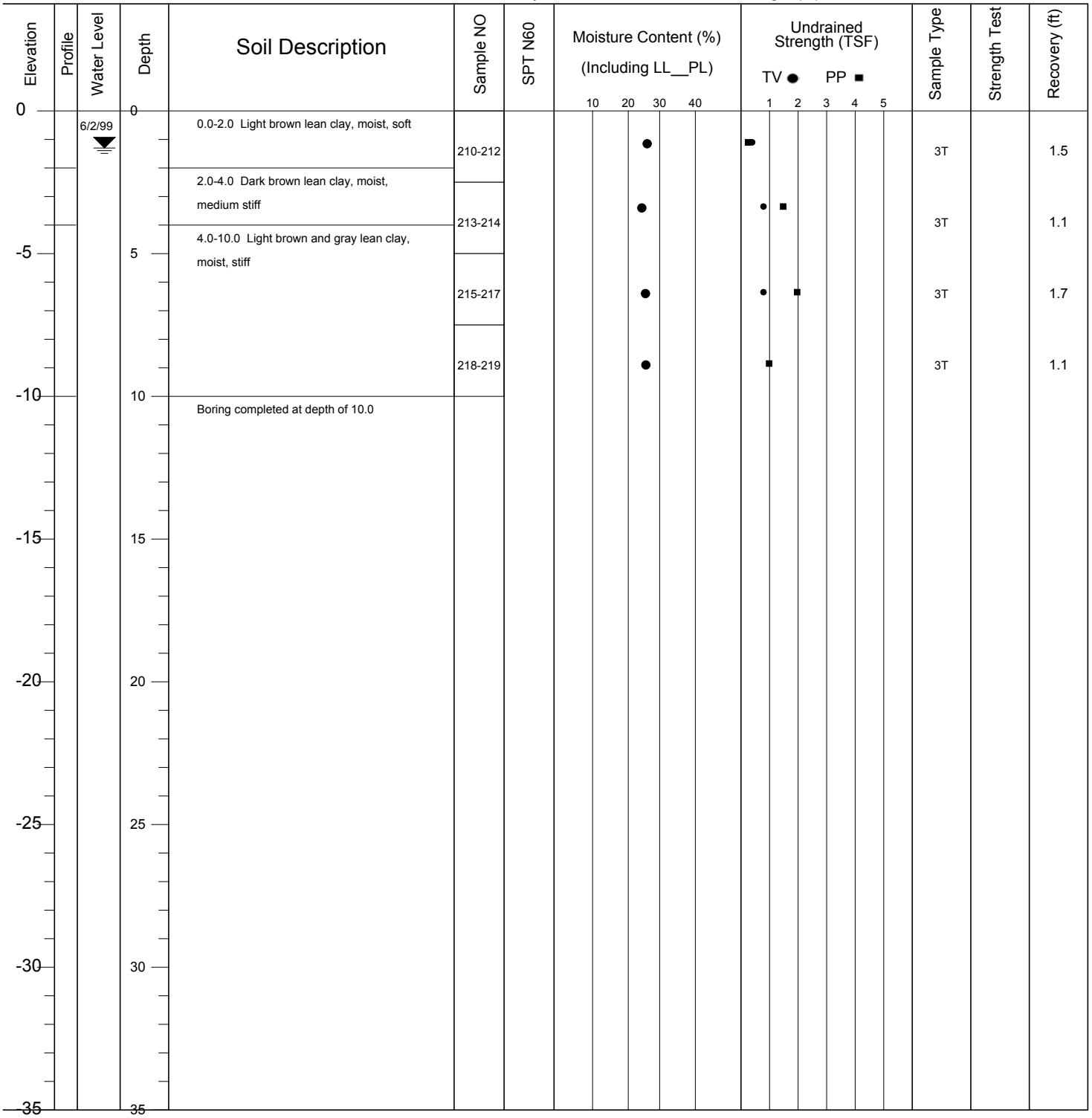

SuperLog V3.0A CivilTech Software, USA www.civiltech.com File: C:\superlog3\project\EMMA_boring.log Date: 10/16/2003

University of Missouri - Columbia

Civil & EnvironmentalEngineering Department -Geotechnical Group

Project Name: I-70 - Emma Site | **Project NO: Test 7**

Location: Eastbound on-ramp @ Jct. Rt. Y & I-70 | **Boring Number: MU11**

Ground Elevation: | **Logged By: Hilchen**

Drilling Date: 6/2/1999 | **Driller: Dodds**

Weather: Clear & 80 deg | Auger Method: | Driller's Hole NO: V-99-36C

Conditions: | SPT Hammer Efficiency: | Drilling Equip: CME 850 G7950

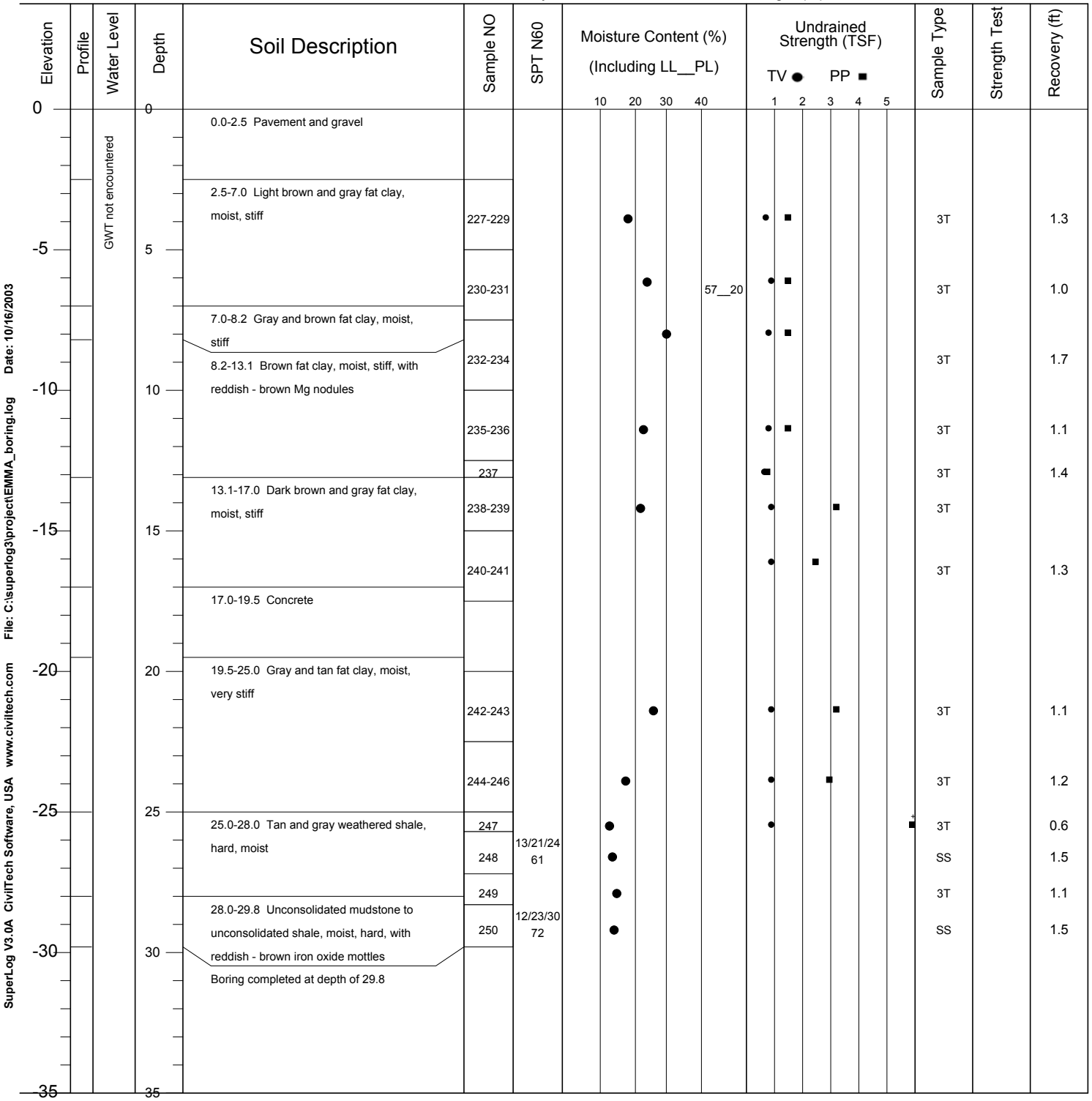

SPT corrected N60 values given below blow sequence

Shelby tube refusal at 28.3' -- sample too disturbed for use

University of Missouri - Columbia

Civil & EnvironmentalEngineering Department -Geotechnical Group

Project Name: I-70 - Emma Site | **Project NO: Test 7**

Location: Eastbound on-ramp @ Jct. Rt. Y & I-70 | **Boring Number: MU12**

Ground Elevation: | **Logged By: Hilchen**

Drilling Date: 6/2/1999 | **Driller: Varner**

Weather: Clear 80's | Auger Method: | Driller's Hole NO: Y-99-40

Conditions: | SPT Hammer Efficiency: | Drilling Equip: Simco 4000 TR-2 G6944

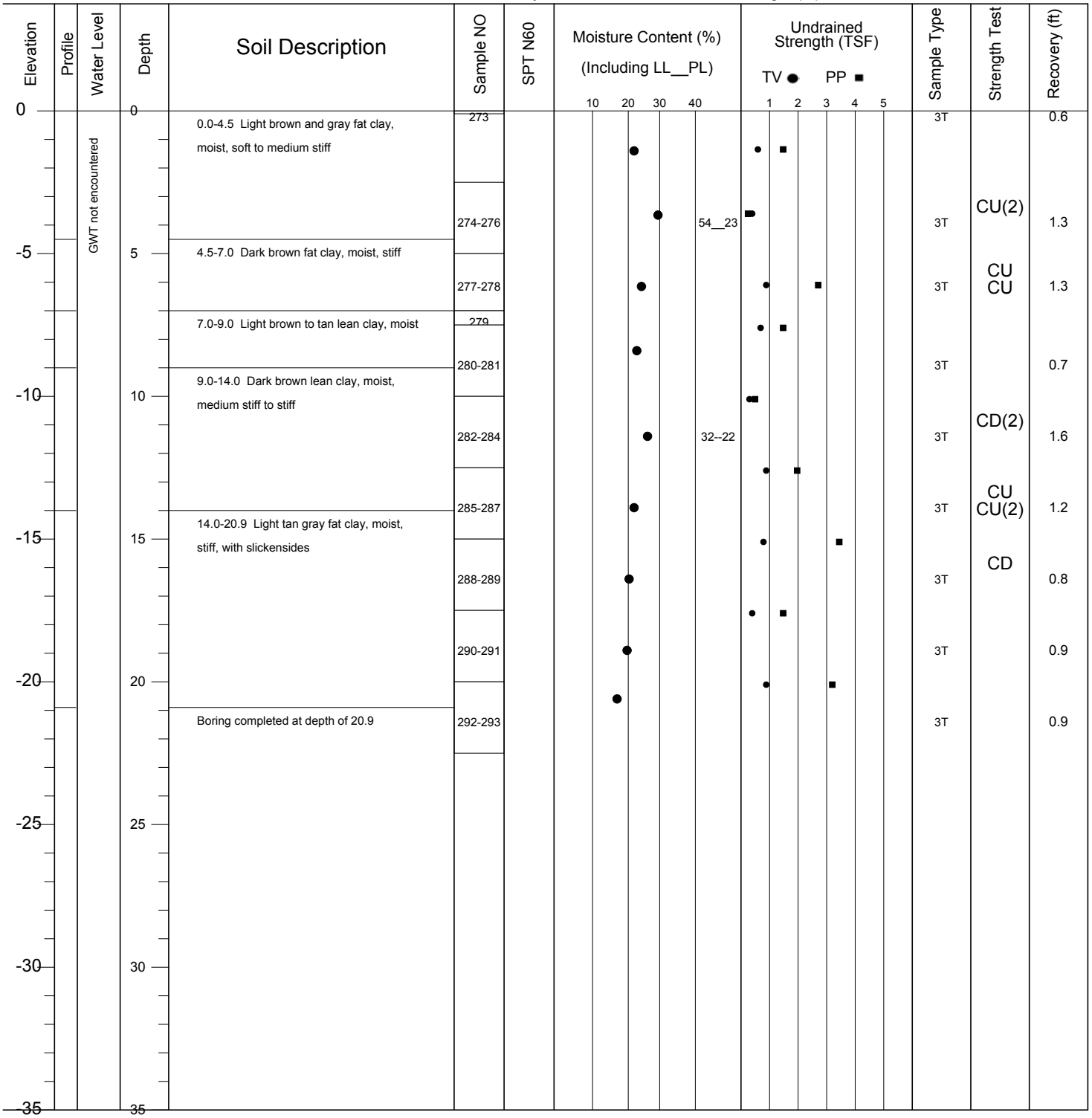

University of Missouri - Columbia

Civil & EnvironmentalEngineering Department -Geotechnical Group

Project Name: I-70 - Emma Site | **Project NO: Test 7**

Location: Eastbound on-ramp @ Jct. Rt. Y & I-70 | **Boring Number: MU13**

Ground Elevation: | **Logged By: Hilchen**

Drilling Date: 6/1/1999 | **Driller: Dodds**

Weather: Cloudy with occasional showers | Auger Method: | Driller's Hole NO: V-99-36C

Conditions: | SPT Hammer Efficiency: | Drilling Equip: CME 850 G7950

Elevation	Profile	Water Level	Depth	Soil Description	Sample NO	SPT N60	Moisture Content (%) (Including LL__PL)	Undrained Strength (TSF) TV ● PP ■	Sample Type	Strength Test	Recovery (ft)
0		GWT not encountered	0	0.0-2.5 Rubble and concrete, free water at 1.5'			10 20 30 40	1 2 3 4 5	3T		
-5			5	2.5-6.1 Brown and reddish brown lean clay, very stiff	220-221				3T		2.5
					222-224				3T		1.4
-10			10	6.1-9.5 Greenish gray fat clay, moist	225-226				3T		1.2
-15			15	Boring completed at depth of 9.5							
-20			20								
-25			25								
-30			30								
-35			35								

(0.0-2.5) No recovery -- rock, gravel, and concrete

SuperLog V3.0A CivilTech Software, USA www.civiltech.com File: C:\superlog3\project\EMMA_boring.log Date: 10/16/2003

University of Missouri - Columbia

Civil & EnvironmentalEngineering Department -Geotechnical Group

Project Name: I-70 - Emma Site | **Project NO: Test 7**

Location: Eastbound on-ramp @ Jct. Rt. Y & I-70 | **Boring Number: MU14**

Ground Elevation: | **Logged By: Hilchen**

Drilling Date: 6/2/1999 | **Driller: Dodds**

Weather: Clear & Sunny, breezy, mid 80's | Auger Method: | Driller's Hole NO: V-99-37

Conditions: | SPT Hammer Efficiency: | Drilling Equip: CME 850 G7950

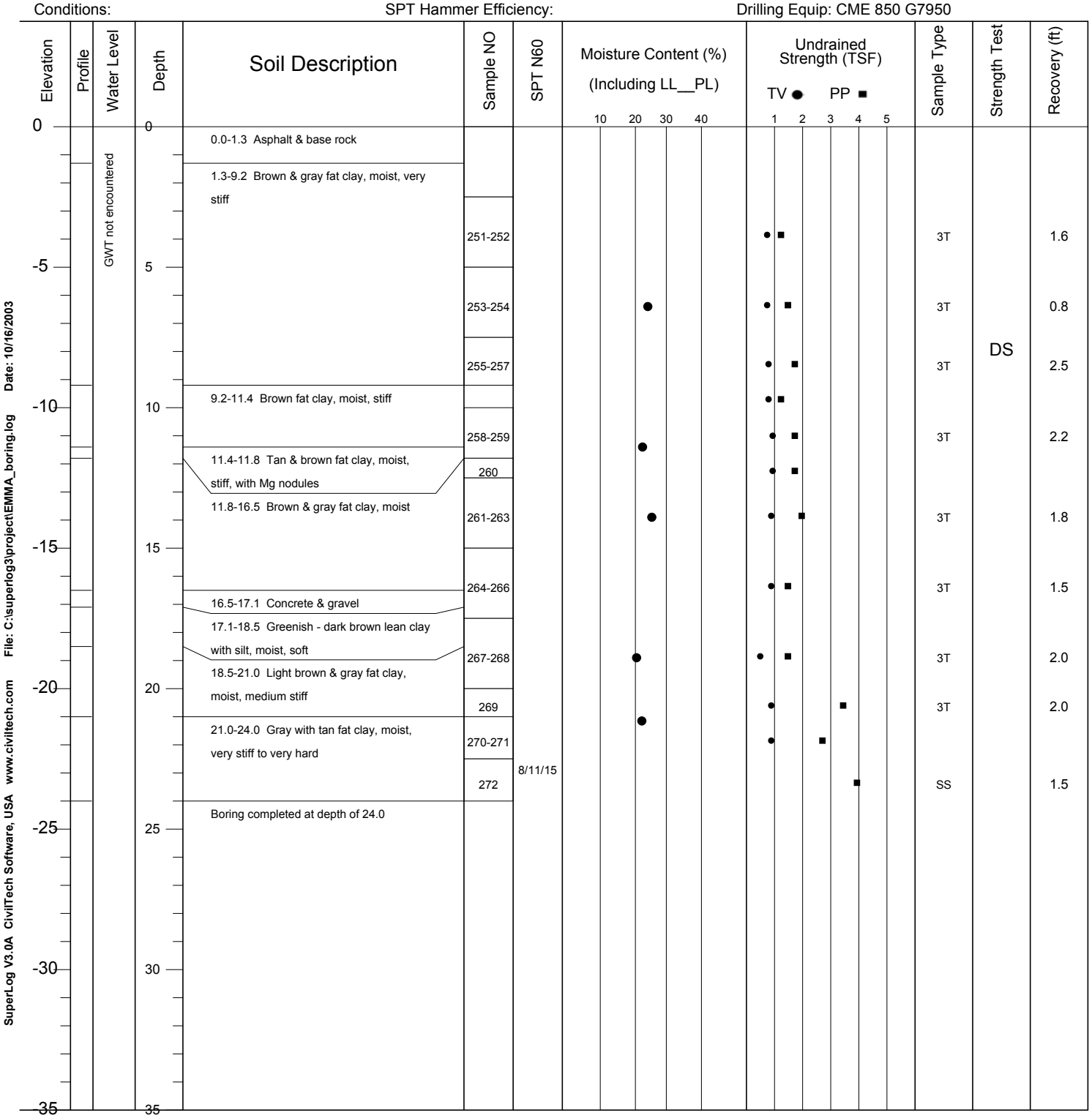

SuperLog V3.0A CivilTech Software, USA www.civiltech.com File: C:\superlog3\project\EMMA_boring.log Date: 10/16/2003

0.0-2.5 --- too much pavement & gravel to recover a sample

SPT corrected N60 value not given, just the blow sequence

DS--Direct Shear Test

University of Missouri - Columbia

Civil & EnvironmentalEngineering Department -Geotechnical Group

Project Name: I-70 - Emma Site | **Project NO: Test 7**

Location: Eastbound on-ramp @ Jct. Rt. Y & I-70 | **Boring Number: MU15**

Ground Elevation: | **Logged By: Miller**

Drilling Date: 6/2/1999 | **Driller: Lamberson**

Weather: Sunny, 80's | Auger Method: | Driller's Hole NO: L-99-27

Conditions: | SPT Hammer Efficiency: | Drilling Equip: Failing 1500 G7889

Elevation	Depth	Soil Description	Sample NO	SPT N60	Moisture Content (%) (Including LL__PL)	Undrained Strength (TSF) TV ● PP ■	Sample Type	Strength Test	Recovery (ft)
0	0	0.0-1.4 Asphalt & base rock							
		1.4-18.5 Gray & brown fat clay, trace fine gravel, stiff -- scattered gravel beginning @ 13.0	210-212				3T		2.5
-5	5		213-215		56__23		3T		2.3
			216-218				3T		2.1
-10	10		219-221				3T		2.1
			222-224				3T		1.6
-15	15		225-227				3T		1.6
			228				3T		1.0
-20	20	18.5-22.5 Dark brown lean clay, scattered gravel layers, medium stiff	229	1/1/2			SS		1.5
		22.5-25.0 Reddish - brown lean clay, trace fine gravel, hard	230				3T		0.5
-25	25	25.0-27.5 Gray shaley clay, scattered gravel, hard	231-232				3T		1.2
		27.5-28.5 Red weathered sandstone, hard	233	10/18/27			SS		1.5
-30	30	Boring completed at depth of 28.5							
-35	35								

Water Level: 6/3/99

3T refusal @ 18.8 -- cleaned out to 20.0'

3T refusal @ 27.0

SuperLog V3.0A CiviliTech Software, USA www.civiltech.com File: C:\superlog3\project\EMMA_boring.log Date: 10/16/2003

University of Missouri - Columbia

Civil & EnvironmentalEngineering Department -Geotechnical Group

Project Name: I-70 - Emma Site | **Project NO: Test 7**

Location: Eastbound on-ramp @ Jct. Rt. Y & I-70 | **Boring Number: MU16**

Ground Elevation: | **Logged By: Hilchen**

Drilling Date: 6/2/1999 | **Driller: Varner**

Weather: Clear & Sunny, mid 80's | Auger Method: | Driller's Hole NO: Y-99-42

Conditions: | SPT Hammer Efficiency: | Drilling Equip: Simco 4000 TR-2 G6944

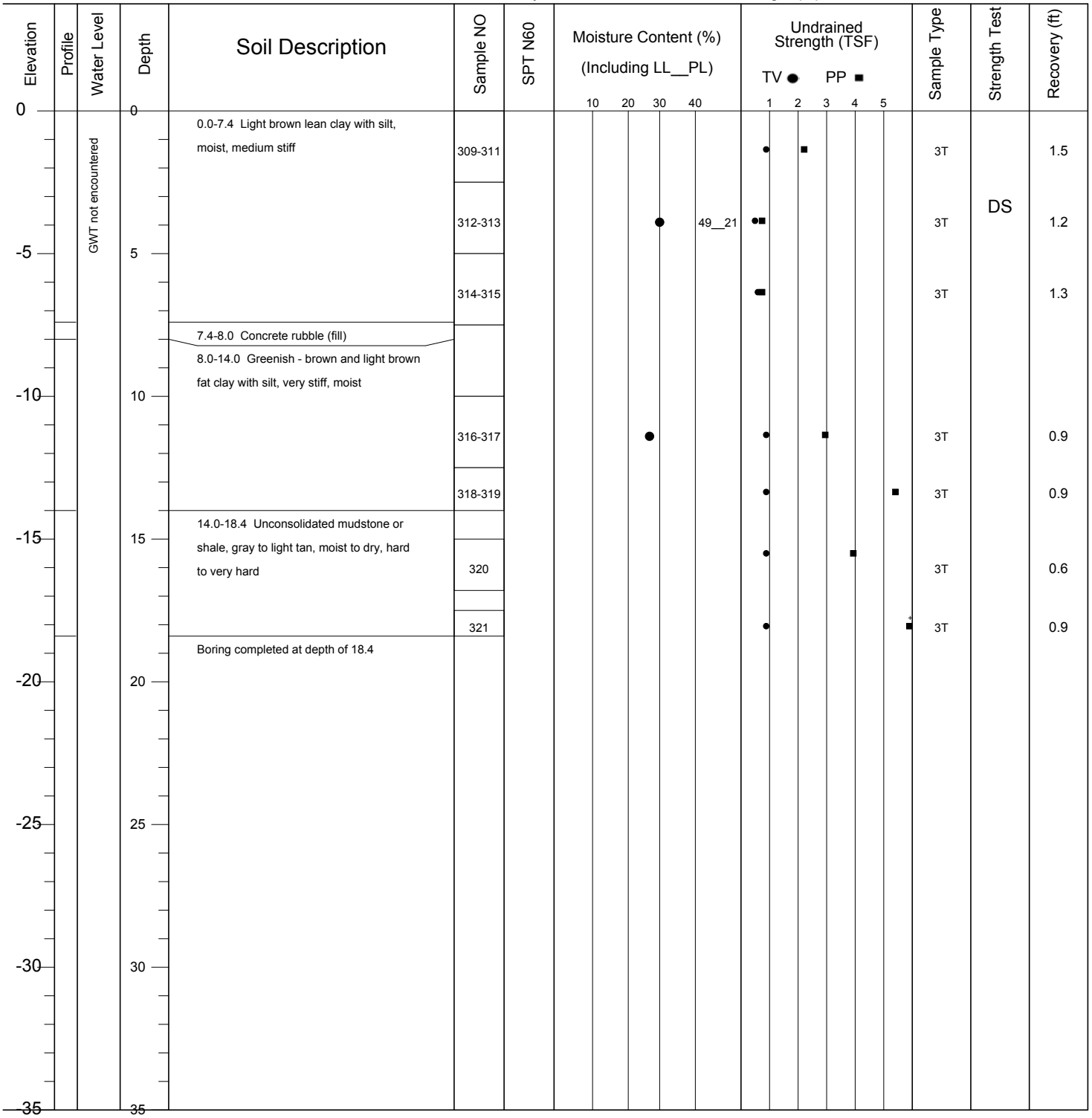

3T refusal @ 14.0' -- cleaned out to 15.0'

3T refusal @ 15.8' -- cleaned out to 17.5'

DS--Direct Shear Test

SuperLog V3.0A CivilTech Software, USA www.civiltech.com File: C:\superlog3\project\EMMA_boring.log Date: 10/16/2003

University of Missouri - Columbia

Civil & EnvironmentalEngineering Department -Geotechnical Group

Project Name: I-70 - Emma Site | **Project NO: Test 7**

Location: Eastbound on-ramp @ Jct. Rt. Y & I-70 | **Boring Number: MU17**

Ground Elevation: | **Logged By: Hilchen**

Drilling Date: 6/2/1999 | **Driller: Varner**

Weather: Clear, Sunny | Auger Method: | Driller's Hole NO: Y-99-41

Conditions: | SPT Hammer Efficiency: | Drilling Equip: Simco 4000 TR-2 G6944

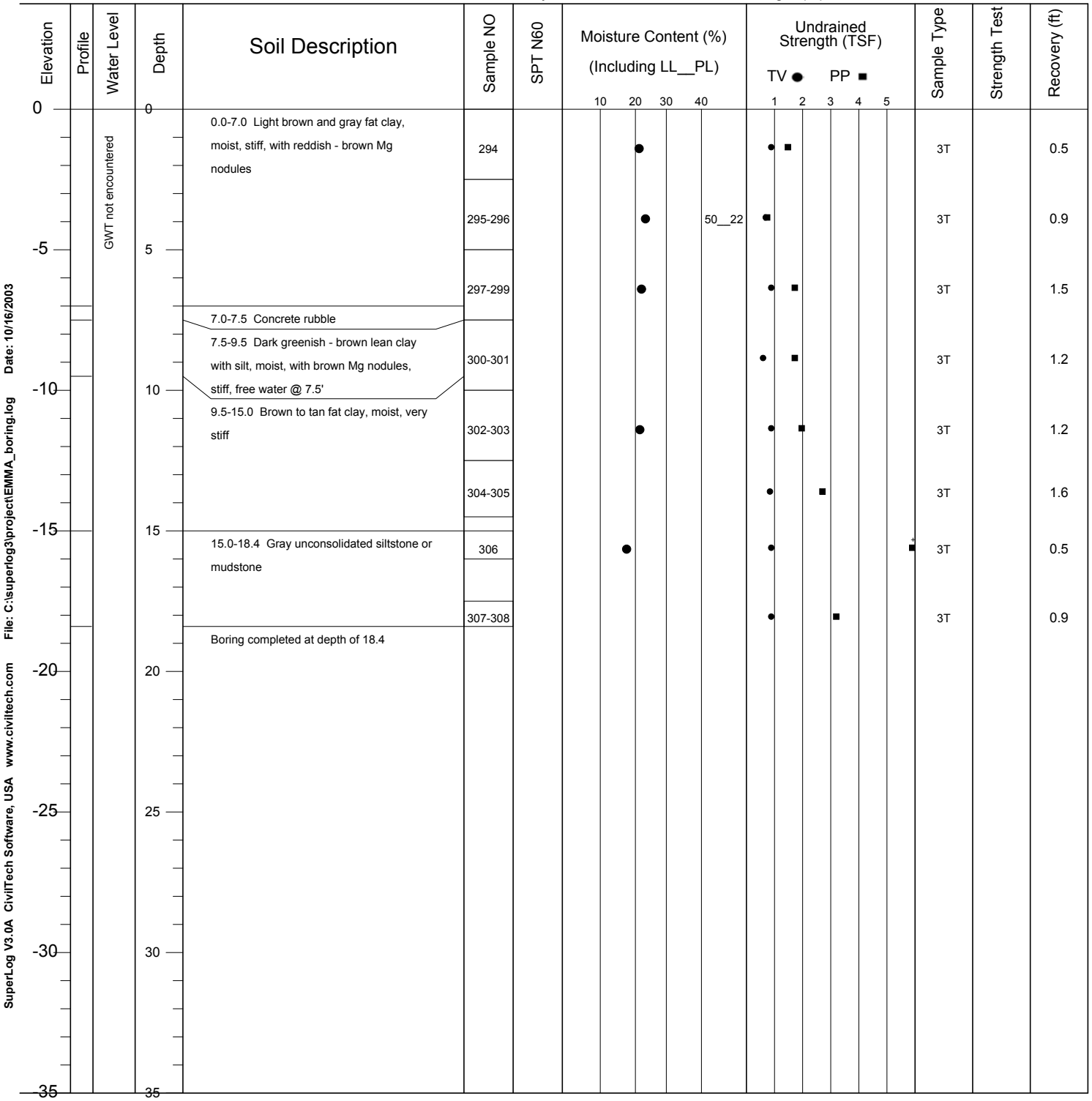

3T refusal @ 14.5' -- cleaned out to 15.0'

3T refusal @ 16.0' -- cleaned out to 17.5'

SuperLog V3.0A CivilTech Software, USA www.civiltech.com File: C:\superlog3\project\EMMA_boring.log Date: 10/16/2003

Appendix B. Boring Logs for I435-Kansas City Sites

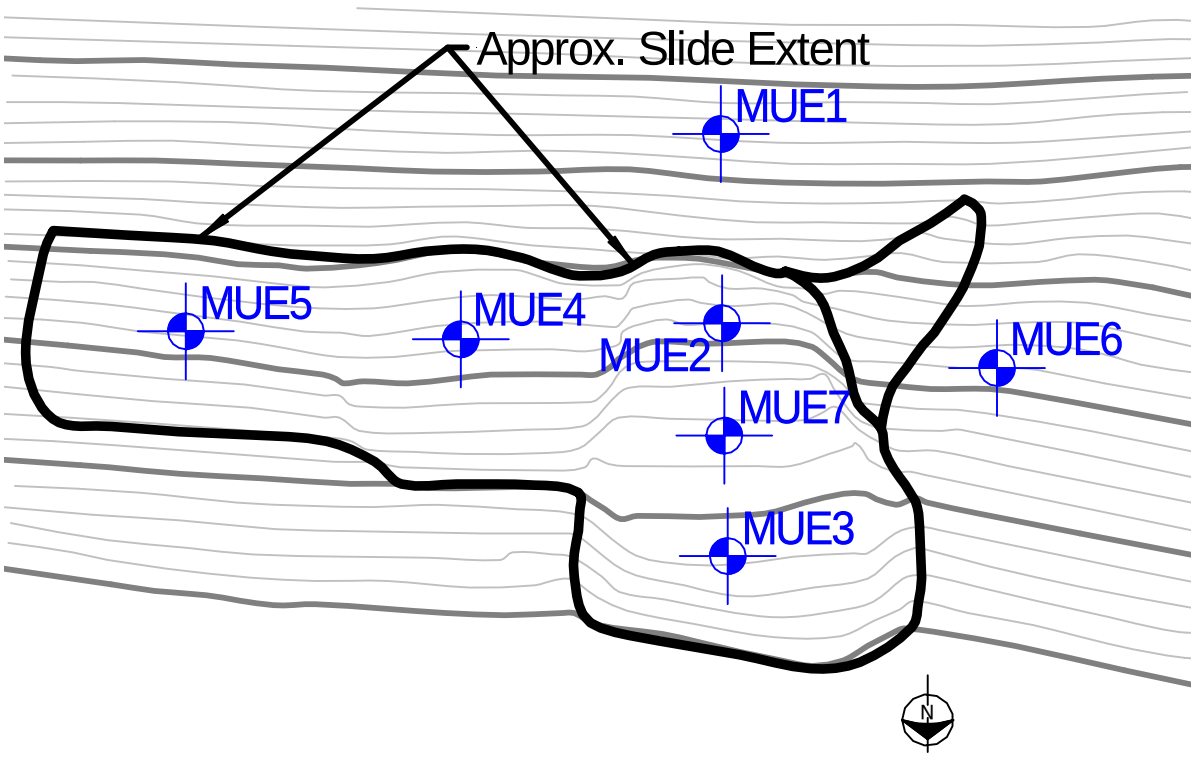

Figure B.1 Plan view of I435-Wornall Road site showing approximate boring locations.

University of Missouri - Columbia

Civil & EnvironmentalEngineering Department -Geotechnical Group

Project Name: I-435 - Kansas City Site | **Project NO: RI98-007B/SPRID55**

Location: I-435 & Wornall Road | **Boring Number: MUE1**

Ground Elevation: 846.0 | **Logged By: Fennessey**

Drilling Date: 6/26/2001 | **Driller: Murray**

Weather: Sunny, Hot | Auger Method: 4" Hollow Stem | Driller's Hole NO: Y-01-71

Conditions: | SPT Hammer Efficiency: | Drilling Equip: Versa-Drill G8641

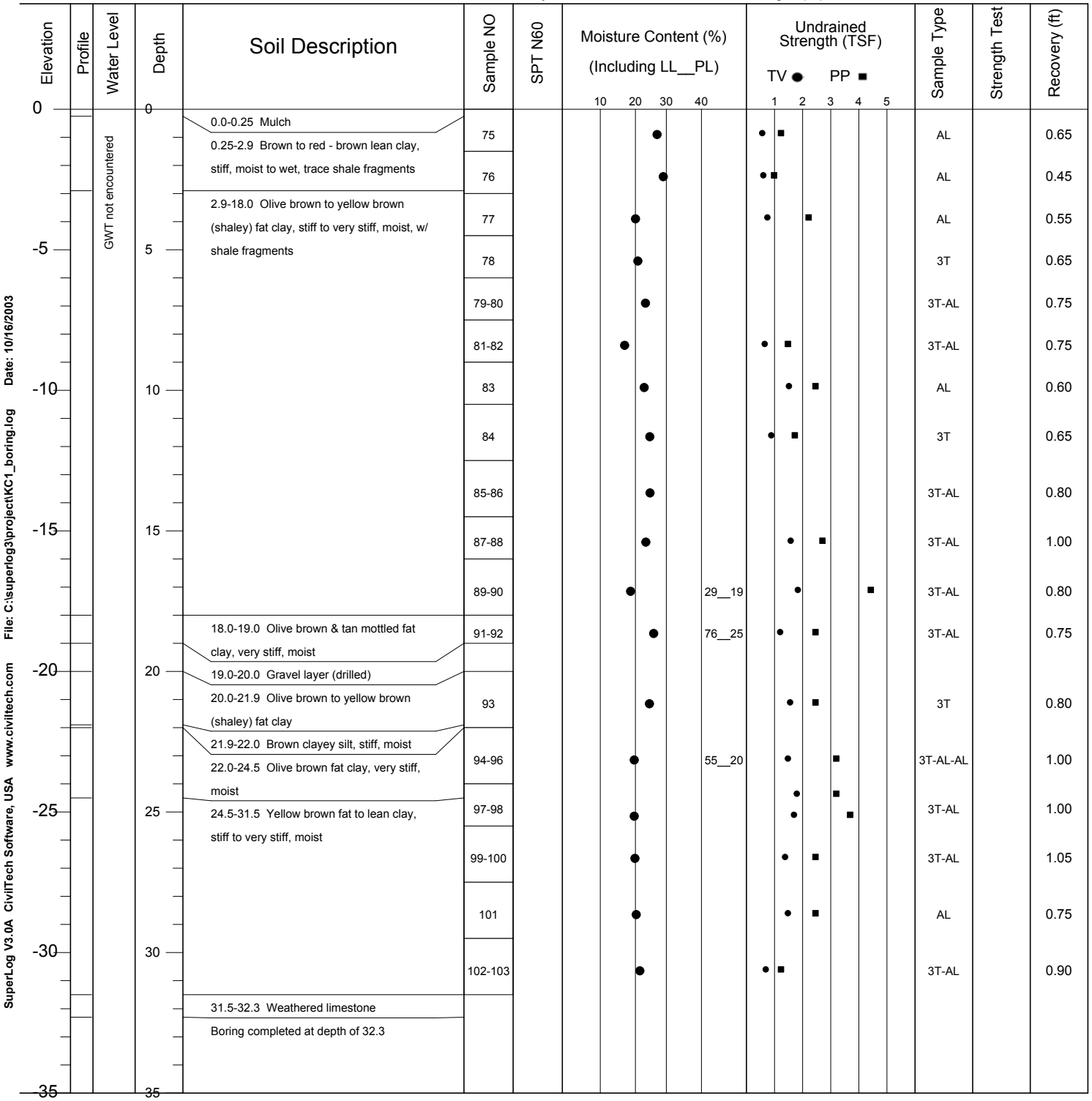

AL--Sample taken for Atterberg Limits

CU--Consolidated Undrained Compression Test

SuperLog V3.0A CivilTech Software, USA www.civiltech.com File: C:\superlog3\project\KC1_boring.log Date: 10/16/2003

University of Missouri - Columbia

Civil & EnvironmentalEngineering Department -Geotechnical Group

Project Name: I-435 - Kansas City Site | **Project NO: RI98-007B/SPRID55**

Location: I-435 & Wornall Road | **Boring Number: MUE2**

Ground Elevation: 838.2 | **Logged By: Fennessey**

Drilling Date: 6/26/2001 | **Driller: Murray**

Weather: Partly Cloudy, Hot | Auger Method: 4" Hollow Stem | Driller's Hole NO: Y-01-72

Conditions: | SPT Hammer Efficiency: | Drilling Equip: Versa-drill G8641

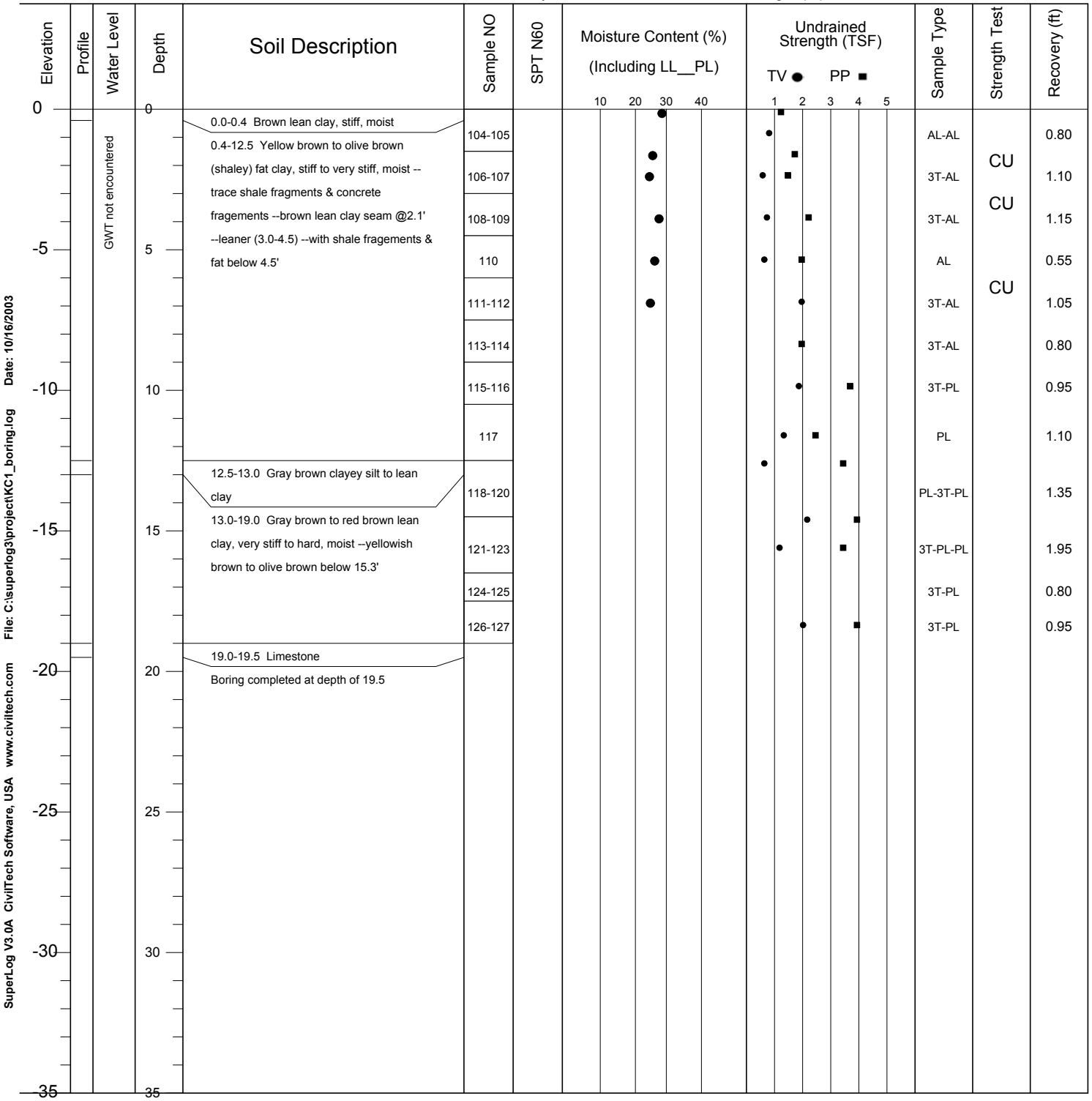

SuperLog V3.0A CivilTech Software, USA www.civiltech.com File: C:\superlog3\project\KC1_boring.log Date: 10/16/2003

AL--Sample taken for Atterberg Limits

PL--Sample placed in plastic bag to preserve moisture

CU--Consolidated Undrained Compression Test

University of Missouri - Columbia

Civil & EnvironmentalEngineering Department -Geotechnical Group

Project Name: I-435 - Kansas City Site | **Project NO: RI98-007B/SPRID55**

Location: I-435 & Wornall Road | **Boring Number: MUE3**

Ground Elevation: 828.7 | **Logged By: Fennessey**

Drilling Date: 6/27/2001 | **Driller: Murray**

Weather: Sunny, Hot | Auger Method: 4" Hollow Stem | Driller's Hole NO: Y-01-74

Conditions: | SPT Hammer Efficiency: | Drilling Equip: Versa-drill G8641

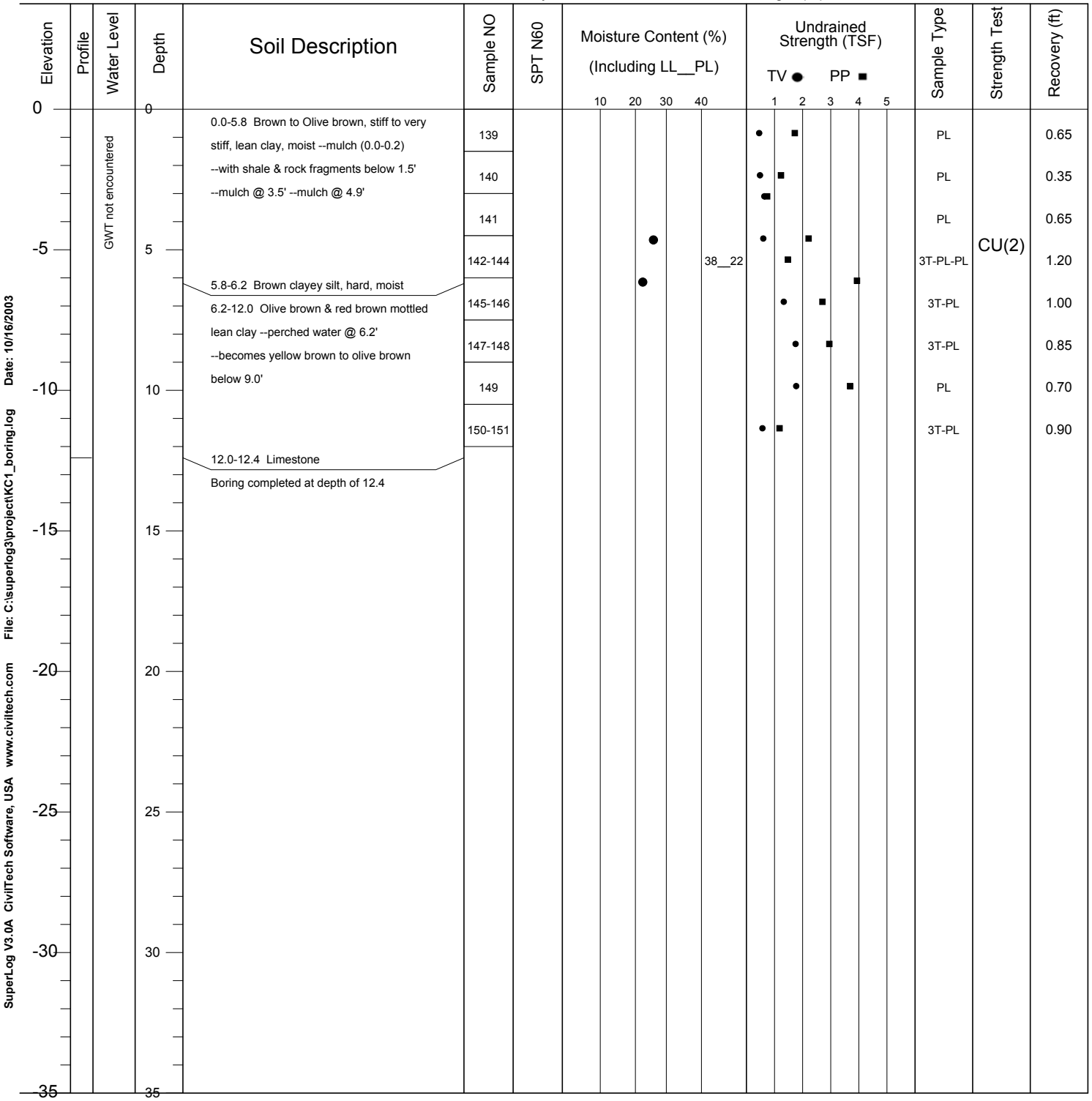

PL--Sample placed in plastic bag to preserve moisture

CU--Consolidated Undrained Compression Test

SuperLog V3.0A CivilTech Software, USA www.civiltech.com File: C:\superlog3\project\KC1_boring.log Date: 10/16/2003

University of Missouri - Columbia

Civil & EnvironmentalEngineering Department -Geotechnical Group

Project Name: I-435 - Kansas City Site | **Project NO: RI98-007B/SPRID55**

Location: I-435 & Wornall Road | **Boring Number: MUE4**

Ground Elevation: 837.7 | **Logged By: Fennessey**

Drilling Date: 6/26/2001 | **Driller: Murray**

Weather: Sunny, Warm | Auger Method: 4" Hollow Stem | Driller's Hole NO: Y-01-70

Conditions: | SPT Hammer Efficiency: | Drilling Equip: Versa-drill G8641

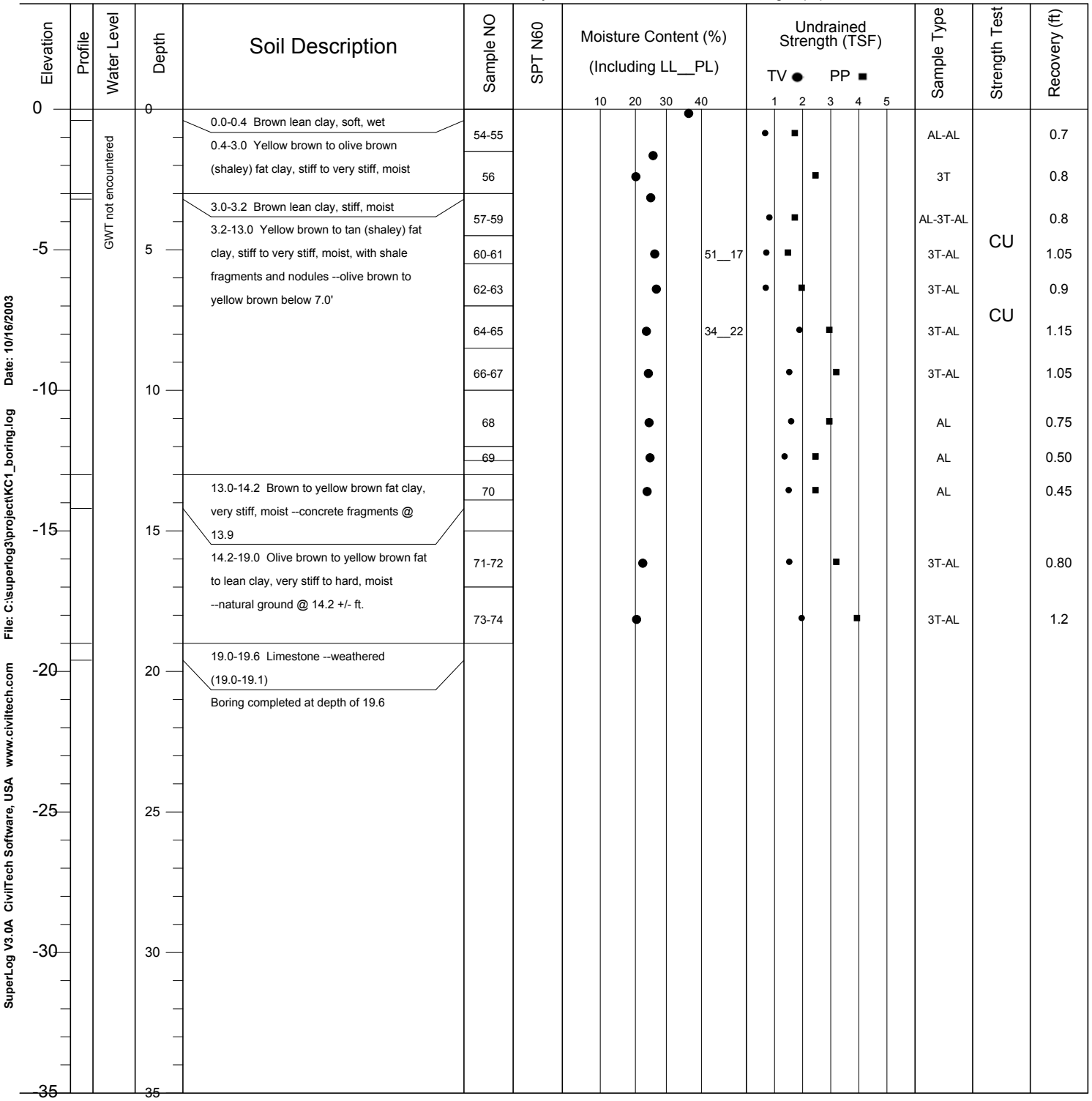

3T refusal @ 12.5' --cleaned out to 13.0'

3T refusal @ 13.9' --cleaned out to 15.0'

University of Missouri - Columbia

Civil & EnvironmentalEngineering Department -Geotechnical Group

Project Name: I-435 - Kansas City Site | **Project NO: RI98-007B/SPRID55**

Location: I-435 & Wornall Road | **Boring Number: MUE5**

Ground Elevation: 837.5 | **Logged By: Fennessey**

Drilling Date: 6/25/2001 | **Driller: Murray**

Weather: Sunny & Hot | Auger Method: 4" Hollow Stem | Driller's Hole NO: Y-01-69

Conditions: | SPT Hammer Efficiency: | Drilling Equip: Versa-drill G8641

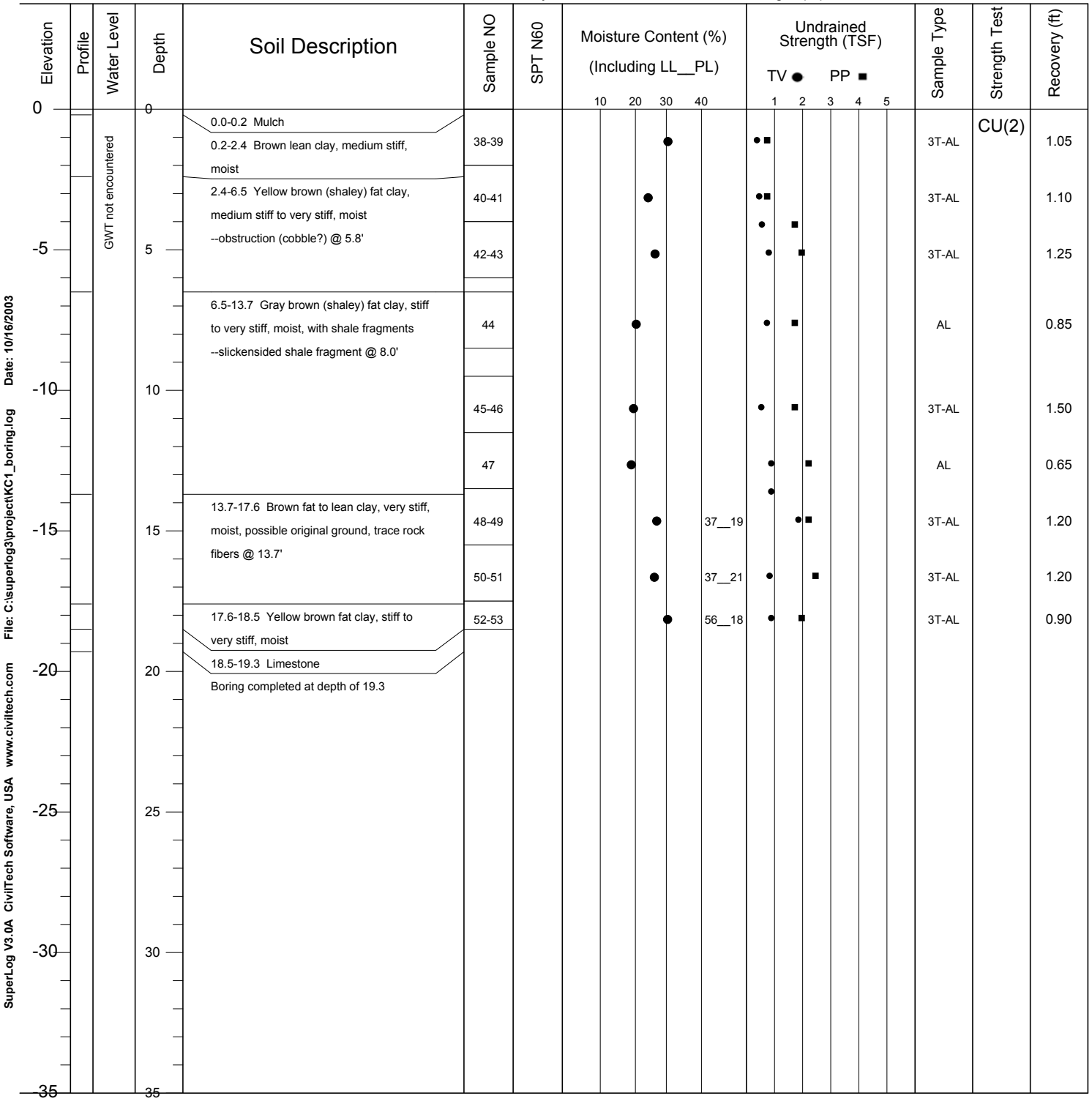

damaged 3T (4.0-6.0) -- drilled out obstruction from 6.0-6.5

--drilled out obstruction from 8.5-9.5

SuperLog V3.0A CivilTech Software, USA www.civiltech.com File: C:\superlog3\project\KC1_boring.log Date: 10/16/2003

University of Missouri - Columbia

Civil & EnvironmentalEngineering Department -Geotechnical Group

Project Name: I-435 - Kansas City Site | **Project NO: RI98-007B/SPRID55**

Location: I-435 & Wornall Road | **Boring Number: MUE6**

Ground Elevation: 832.7 | **Logged By: Fennessey**

Drilling Date: 6/27/2001 | **Driller: Murray**

Weather: Overcast, showers, and sunny | Auger Method: 4" Hollow Stem | Driller's Hole NO: Y-01-75

Conditions: | SPT Hammer Efficiency: | Drilling Equip: Versa-drill G8641

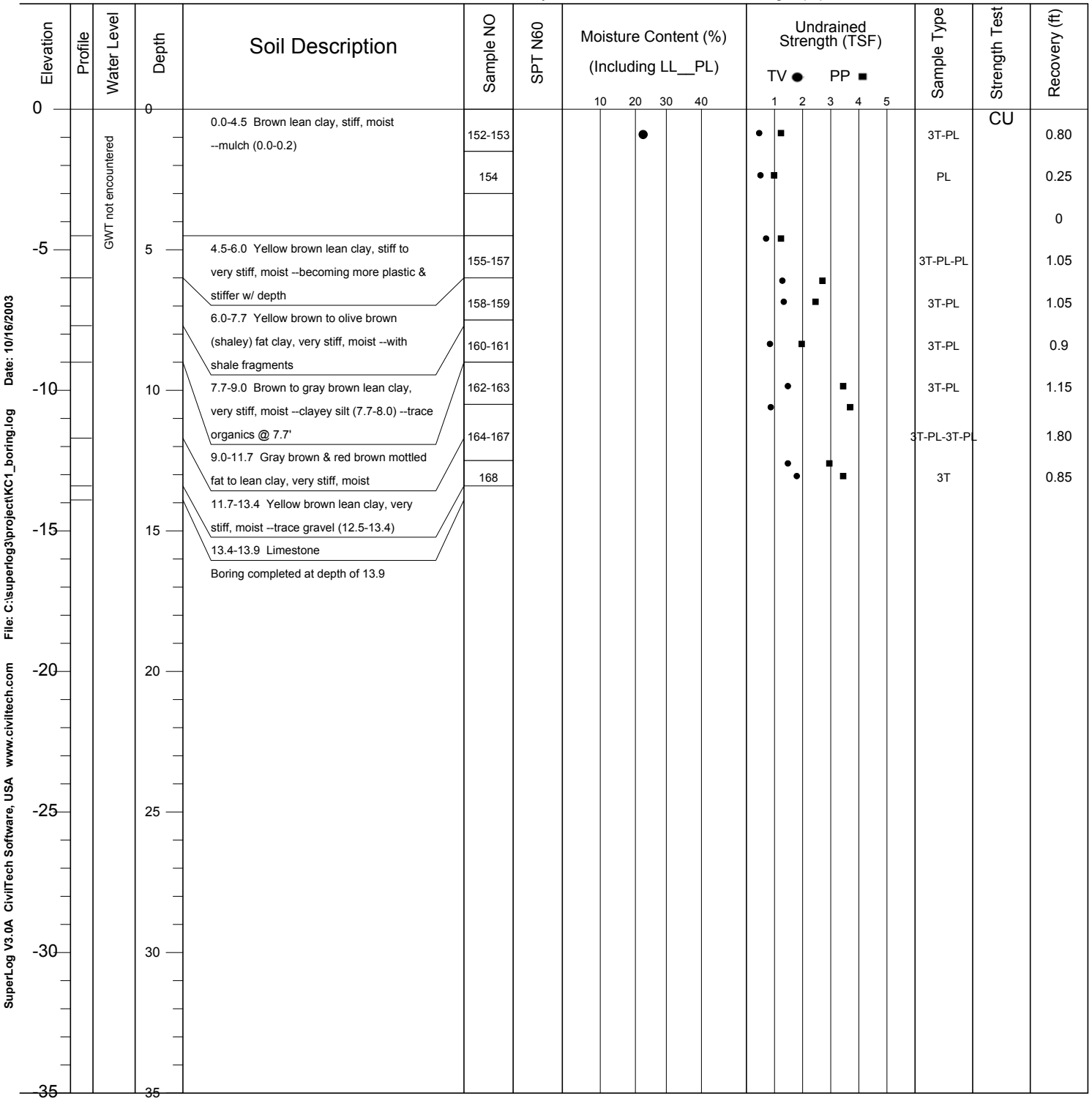

SuperLog V3.0A CivilTech Software, USA www.civiltech.com File: C:\superlog3\project\KC1_boring.log Date: 10/16/2003

PL--Sample placed in plastic bag to preserve moisture

CU--Consolidated Undrained Compression Test

No sample recovered (3.0-4.5)

University of Missouri - Columbia

Civil & EnvironmentalEngineering Department -Geotechnical Group

Project Name: I-435 - Kansas City Site | **Project NO: RI98-007B/SPRID55**

Location: I-435 & Wornall Road | **Boring Number: MUE7**

Ground Elevation: 831.3 | **Logged By: Fennessey**

Drilling Date: 6/27/2001 | **Driller: Murray**

Weather: Sunny, Warm | Auger Method: 4" Hollow Stem | Driller's Hole NO: Y-01-73

Conditions: | SPT Hammer Efficiency: | Drilling Equip: Versa-drill G8641

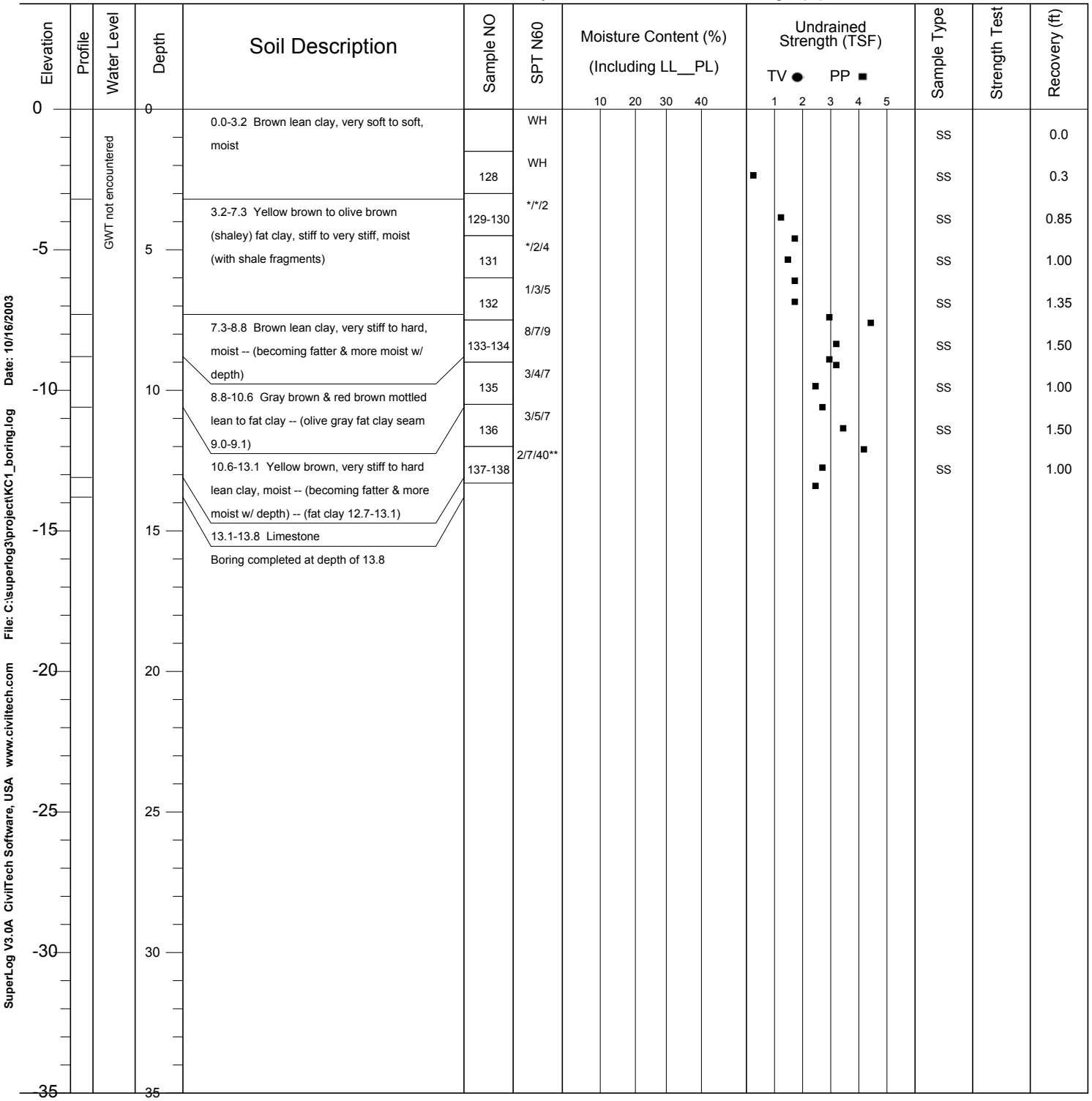

SuperLog V3.0A CivilTech Software, USA www.civiltech.com File: C:\superlog3\project\KC1_boring.log Date: 10/16/2003

WH--Sampler pushed 18" by the weight of the hammer

* Sampler pushed 6" by the weight of the hammer

** The 40 blows only moved the sampler 3.5"

Plastic bag samples were also taken from each 1.5' increment

University of Missouri - Columbia

Civil & EnvironmentalEngineering Department -Geotechnical Group

Project Name: I-435 - Kansas City Site | **Project NO: RI98-007B/SPRID55**

Location: I-435 & Wornall Road | **Boring Number: Control Slope SW Quadrant**

Ground Elevation: 8' above toe of slope | **Logged By: B. Temme**

Drilling Date: 7/10/2002 | **Driller: K. Barnett**

Weather: Sunny 85 deg | Auger Method: 4" Hollow Stem | Driller's Hole NO: B-02-56

Conditions: | SPT Hammer Efficiency: | Drilling Equip: Versa drill G8690

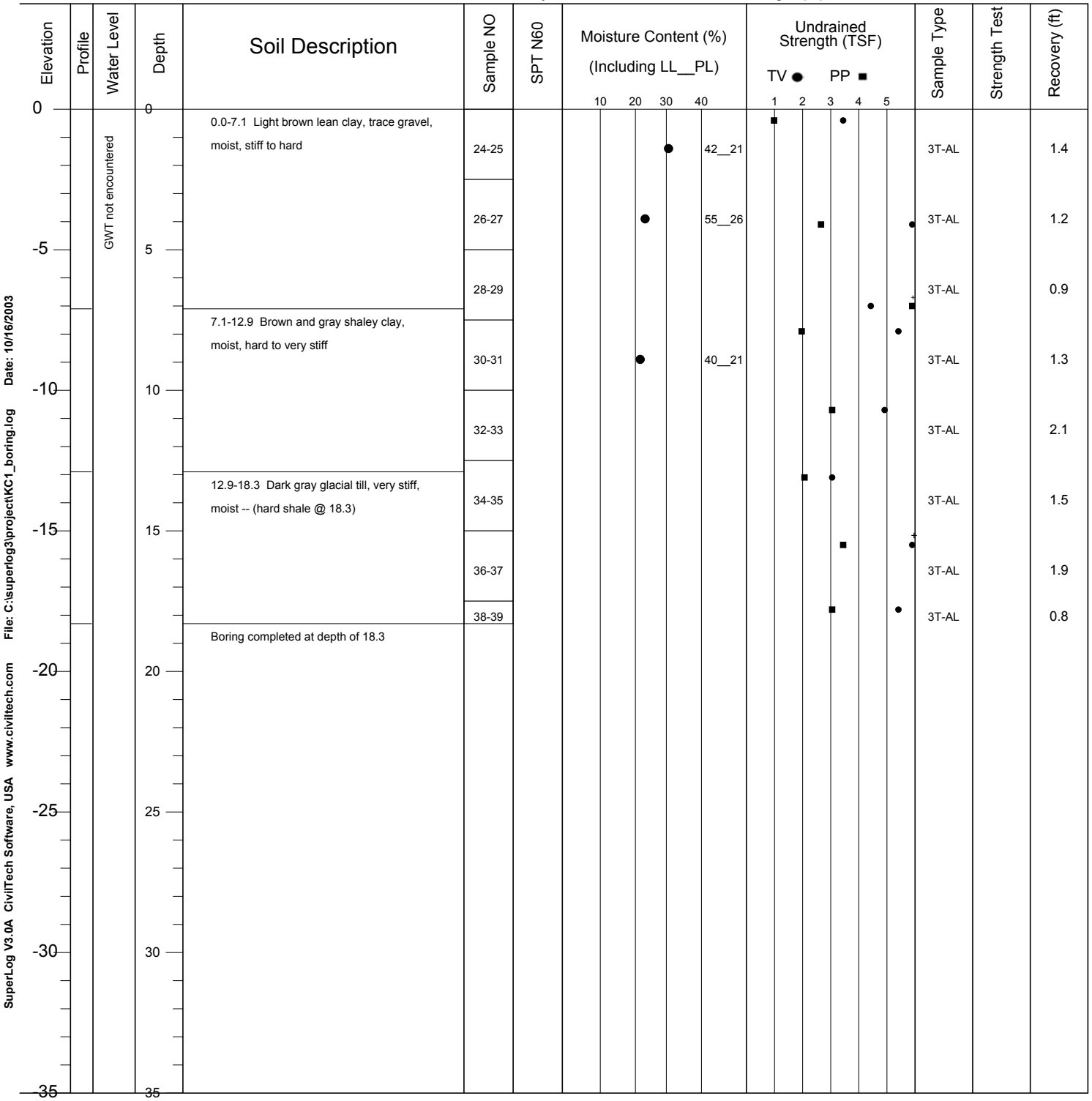

SuperLog V3.0A CivilTech Software, USA www.civiltech.com File: C:\superlog3\project\KC1_boring.log Date: 10/16/2003

University of Missouri - Columbia

Civil & EnvironmentalEngineering Department -Geotechnical Group

Project Name: I-435 Kansas City Site | **Project NO: RI98-007B**

Location: I-435 & Holmes Road | **Boring Number: Steel Pin Slope -- SE Quadrant**

Ground Elevation: 10' above toe, offset 6' downslope | **Logged By: R. Temme**

Drilling Date: 7/11/2002 | **Driller: K. Barnett**

Weather: Overcast, 70 deg | Auger Method: 4" Hollow Stem | Driller's Hole NO: B-02-57

Conditions: | SPT Hammer Efficiency: | Drilling Equip: Versa drill G8690

Elevation	Depth	Soil Description	Sample NO	SPT N60	Sample Type	Recovery (ft)
0	0	0.0-4.3 Brown lean clay, medium stiff, moist	40-41		3T-AL	1.1
			42-43		3T-AL	2.1
-5	5	4.3-19.0 Gray shale, very soft, moist -- (refusal @ 5.3')			AL	0.3
				14/27/40* 100+	SS	1.0
				27/40** 100+	SS	0.3
-10	10					
-15	15					
-20	20	Boring completed at depth of 19.0				
-25	25					
-30	30					
-35	35					

Moisture Content (%) (Including LL__PL): 10 20 30 40

Undrained Strength (TSF): TV ● PP ■ 1 2 3 4 5

Water Level: GWT not encountered

Strength Test:

SPT corrected N60 values given below blow sequence

* No advance

** Advanced only 2"

Appendix C. Boring Logs for US36-Stewartsville Site

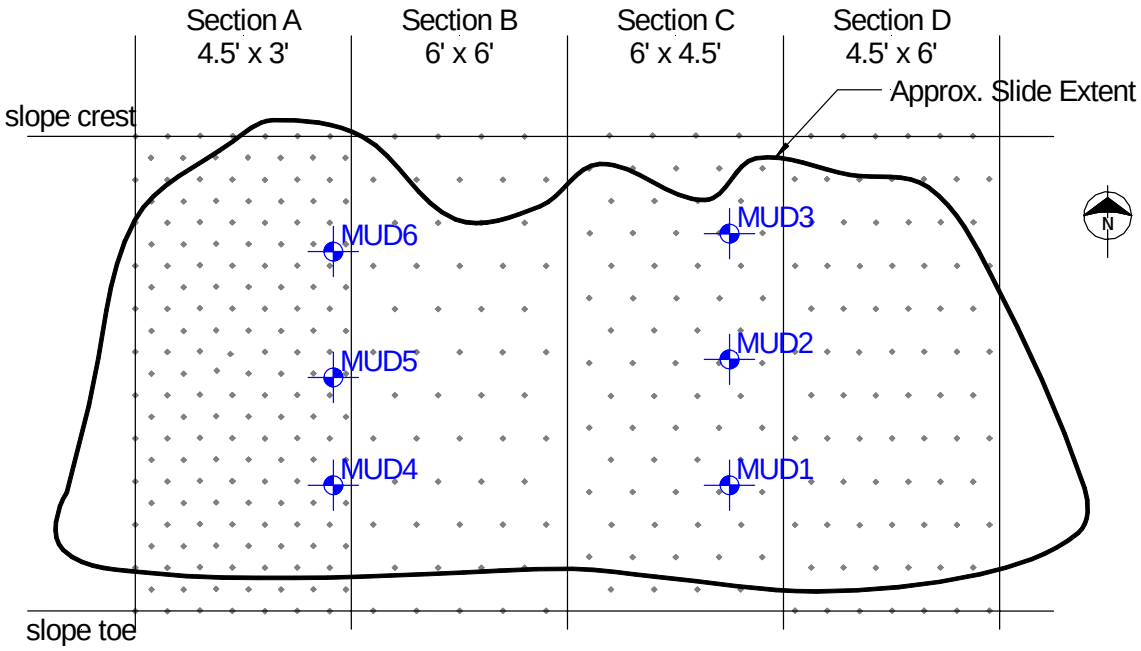

Figure C.1 Plan view of US36-Stewartsville site showing approximate boring locations.

University of Missouri - Columbia

Civil & EnvironmentalEngineering Department -Geotechnical Group

Project Name: US-36 Stewartsville Site | **Project NO: SPROID5S**

Location: Between eastbound & westbound US-36 | **Boring Number: MUD1**

Ground Elevation: | **Logged By: Less**

Drilling Date: 5-30-2001, 6/4/2001 | **Driller: Murray/Hees**

Weather: Cloudy, Raining | Auger Method: 4" Hollow Stem | Driller's Hole NO: Y-01-55

Conditions: | SPT Hammer Efficiency: | Drilling Equip: Versa Drill 4000TR-2 G8641

Elevation	Depth	Soil Description	Sample NO	SPT N60	Moisture Content (%) (Including LL__PL)	Undrained Strength (TSF) TV ● PP ■	Sample Type	Strength Test	Recovery (ft)
0	0	0.0-2.5 Brown to gray fat mottled clay, medium stiff, moist	275-276		45__16		AL-3T	CU	1.1
		2.5-4.5 Gray fat clay, trace gravel, medium stiff, moist	277-278		46__21		AL-3T	CU	1.7
-5	5	4.5-10.5 Gray to brown mottled lean clay, brittle, medium stiff to hard	279-280		40__19		AL-3T	CU	1.9
			281-282				AL-3T	CU	1.7
-10	10		283-284				AL-3T		1.7
		10.5-15.1 Tan lean clay with gray mottling, trace gravel, stiff to very stiff, moist	285-286				AL-3T		1.9
		--Refusal 12.4-12.9, cleaned with auger	287-288				AL-3T*		0.5
			289-290				AL-3T		1.2
-15	15		291-292				AL-3T		1.0
		Boring completed at depth of 15.1							
-20	20								
-25	25								
-30	30								
-35	35								

Water Level: GWT not encountered

Note: 5/30/2001 lost tube in hole @ 11.6' -- moved over to the east 2.0' on 6/4/2001 & resumed drilling back at 10.5'

* No sample recovered

University of Missouri - Columbia

Civil & EnvironmentalEngineering Department -Geotechnical Group

Project Name: US-36 Stewartsville Site | **Project NO: SPROID5S**

Location: Between eastbound & westbound US-36 | **Boring Number: MUD2**

Ground Elevation: | **Logged By: Less**

Drilling Date: 6/5/2001 | **Driller: Murray**

Weather: Cloudy 70-75 deg | Auger Method: 4" Hollow Stem | Driller's Hole NO: Y-01-57

Conditions: | SPT Hammer Efficiency: | Drilling Equip: Versa Drill 4000TR-2 G8641

Elevation	Depth	Soil Description	Sample NO	SPT N60	Moisture Content (%) (Including LL__PL)	Undrained Strength (TSF) TV ● PP ■	Sample Type	Strength Test	Recovery (ft)
0	0	0.0-2.5 Tan to gray fat clay, soft to medium stiff, moist	315-316		69__24		AL-3T	CU	1.1
		2.5-7.5 Gray fat clay, medium stiff, moist	317-318		52__21		AL-3T	CU	1.7
-5	5		319-320		65__24		AL-3T		2.0
		7.5-9.0 Gray lean clay, medium stiff to stiff, moist	321-322		51__20		AL-3T	CU	2.0
-10	10	9.0-11.7 Tan to gray lean clay with gravel, stiff to very stiff, moist	323-324		41__20		AL-3T	CU	1.8
			325-326				AL-3T		1.9
		11.7-14.0 Gray to tan lean clay, mottled with gravel, moist	327-328				AL-3T		1.3
-15	15	14.0-20.5 Tan to brown lean clay, trace gravel, moist, very stiff	329-330				AL-3T		1.5
			331-332				AL-3T		2.0
			333-334				AL-3T		1.5
-20	20		335-336				AL-3T		1.5
		Boring completed at depth of 20.5							
-25	25								
-30	30								
-35	35								

Water Level: GWT not encountered

Moisture Content (%) (Including LL__PL): 10 20 30 40

Undrained Strength (TSF) TV ● PP ■: 1 2 3 4 5

SuperLog V3.0A CivilTech Software, USA www.civiltech.com File: C:\superlog3\project\US-36_boring.log Date: 10/16/2003

University of Missouri - Columbia

Civil & EnvironmentalEngineering Department -Geotechnical Group

Project Name: US-36 Stewartsville Site | **Project NO: SPROID5S**

Location: Between eastbound & westbound US-36 | **Boring Number: MUD3**

Ground Elevation: | **Logged By: Less**

Drilling Date: 6-4-2001-6/5/2001 | **Driller: Hees/Murray**

Weather: Cloudy, Windy, Cool, 68 deg | Auger Method: 4" Hollow Stem | Driller's Hole NO: Y-01-56

Conditions: | SPT Hammer Efficiency: | Drilling Equip: Versa Drill 4000TR-2 G8641

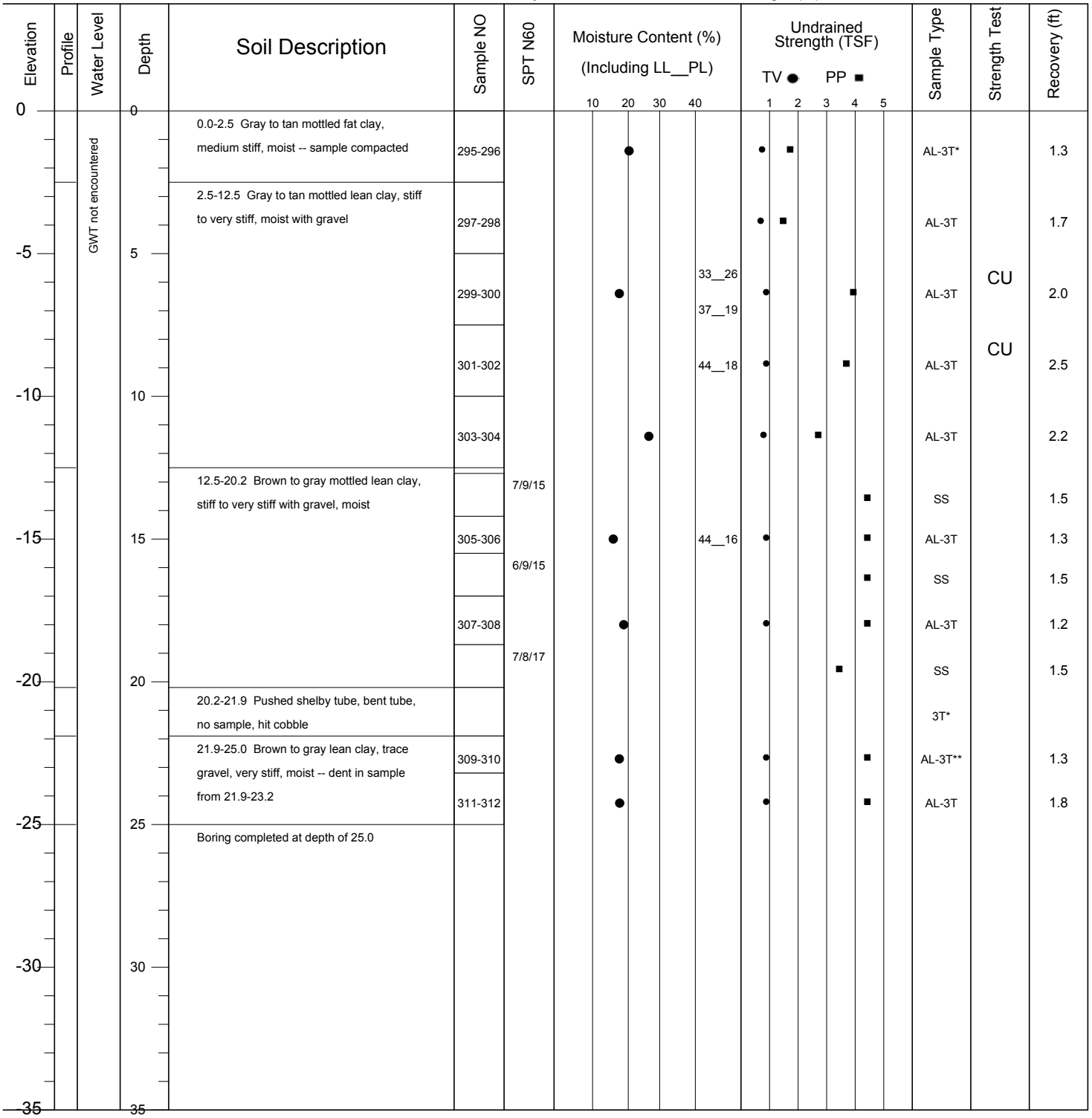

* Shelby tube refusal -- no sample

** Damaged shelby tube sample

SuperLog V3.0A CivilTech Software, USA www.civiltech.com File: C:\superlog3\project\US-36_boring.log Date: 10/16/2003

University of Missouri - Columbia

Civil & EnvironmentalEngineering Department -Geotechnical Group

Project Name: US-36 Stewartsville Site | **Project NO: SPROID5S**

Location: Between eastbound & westbound US-36 | **Boring Number: MUD4**

Ground Elevation: | **Logged By: Less**

Drilling Date: 6/6/2001 | **Driller: Murray**

Weather: Cloudy, Rainy, 68 deg | Auger Method: 4" Hollow Stem | Driller's Hole NO: Y-01-60

Conditions: | SPT Hammer Efficiency: | Drilling Equip: Versa Drill 4000TR-2 G8641

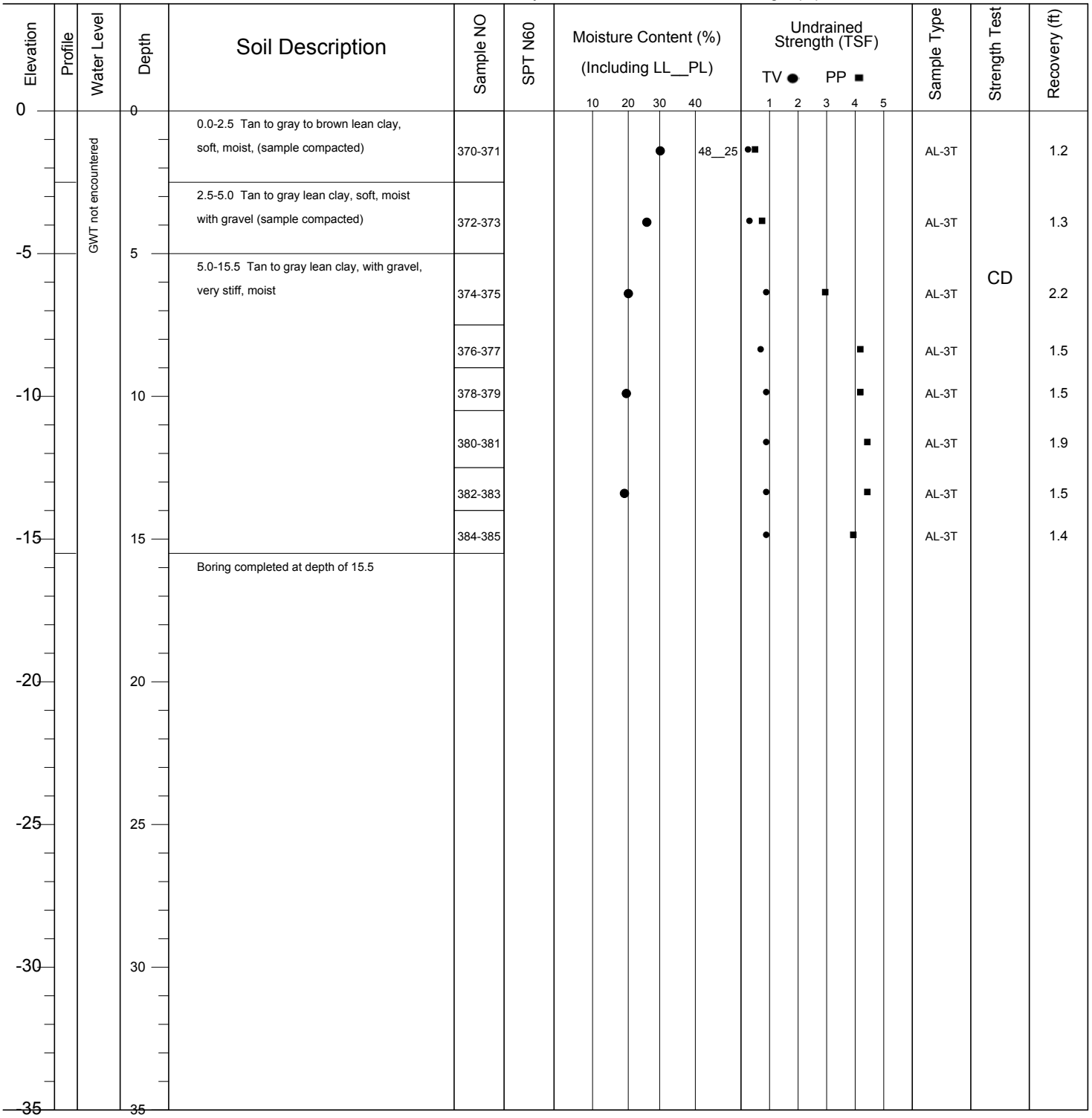

SuperLog V3.0A CivilTech Software, USA www.civiltech.com File: C:\superlog3\project\US-36_boring.log Date: 10/16/2003

University of Missouri - Columbia

Civil & EnvironmentalEngineering Department -Geotechnical Group

Project Name: US-36 Stewartsville Site | **Project NO: SPROID5S**

Location: Between eastbound & westbound US-36 | **Boring Number: MUD5**

Ground Elevation: | **Logged By: Less**

Drilling Date: 6/6/2001 | **Driller: Murray**

Weather: | Auger Method: 4" Hollow Stem | Driller's Hole NO: Y-01-59

Conditions: | SPT Hammer Efficiency: 75 | Drilling Equip: Versa Drill 4000TR-2 G8641

Elevation	Depth	Soil Description	Sample NO	SPT N60	Sample Type
0	0	0.0-2.5 Brown to gray mottled fat clay, soft, moist		WH	SS
				WH/1	SS
		2.5-9.0 Brown to gray lean clay with gravel, stiff to very stiff, moist		2/3/4 9	SS
-5	5			2/3/6 11	SS
				3/7/9 20	SS
				4/5/8 16	SS
		9.0-10.5 Tan to gray lean clay with gravel, moist		3/3/7 13	SS
-10	10	10.5-13.5 Tan to gray lean clay, sandy, with gravel, moist		3/6/9 19	SS
				3/6/8 18	SS
		13.5-15.0 Tan to gray lean clay, with gravel, very stiff, moist		3/6/8 18	SS
-15	15	15.0-16.5 Brown lean clay, very stiff, moist		4/6/8 18	SS
		16.5-18.0 Brown to gray mottled lean clay, very stiff, moist		4/7/9 20	SS
		18.0-21.0 Brown lean clay, sandy, trace gravel, moist		3/6/8 18	SS
-20	20			4/5/8 16	SS
		Boring completed at depth of 21.0			
-25	25				
-30	30				
-35	35				

Moisture Content (%) (Including LL__PL): 10 20 30 40

Undrained Strength (TSF): TV ● PP ■ 1 2 3 4 5

Strength Test | Recovery (ft)

WH -- Weight of hammer penetrated soil

SuperLog V3.0A CivilTech Software, USA www.civiltech.com File: C:\superlog3\project\US-36_boring.log Date: 10/16/2003

University of Missouri - Columbia

Civil & EnvironmentalEngineering Department -Geotechnical Group

Project Name: US-36 Stewartsville Site | **Project NO: SPROID5S**

Location: Between eastbound & westbound US-36 | **Boring Number: MUD6**

Ground Elevation: | **Logged By: Less**

Drilling Date: 6/5/2001 | **Driller: Murray**

Weather: Sunny, Warm 75-80 deg | Auger Method: 4" Hollow Stem | Driller's Hole NO: Y-01-58

Conditions: | SPT Hammer Efficiency: | Drilling Equip: Versa Drill 4000TR-2 G8641

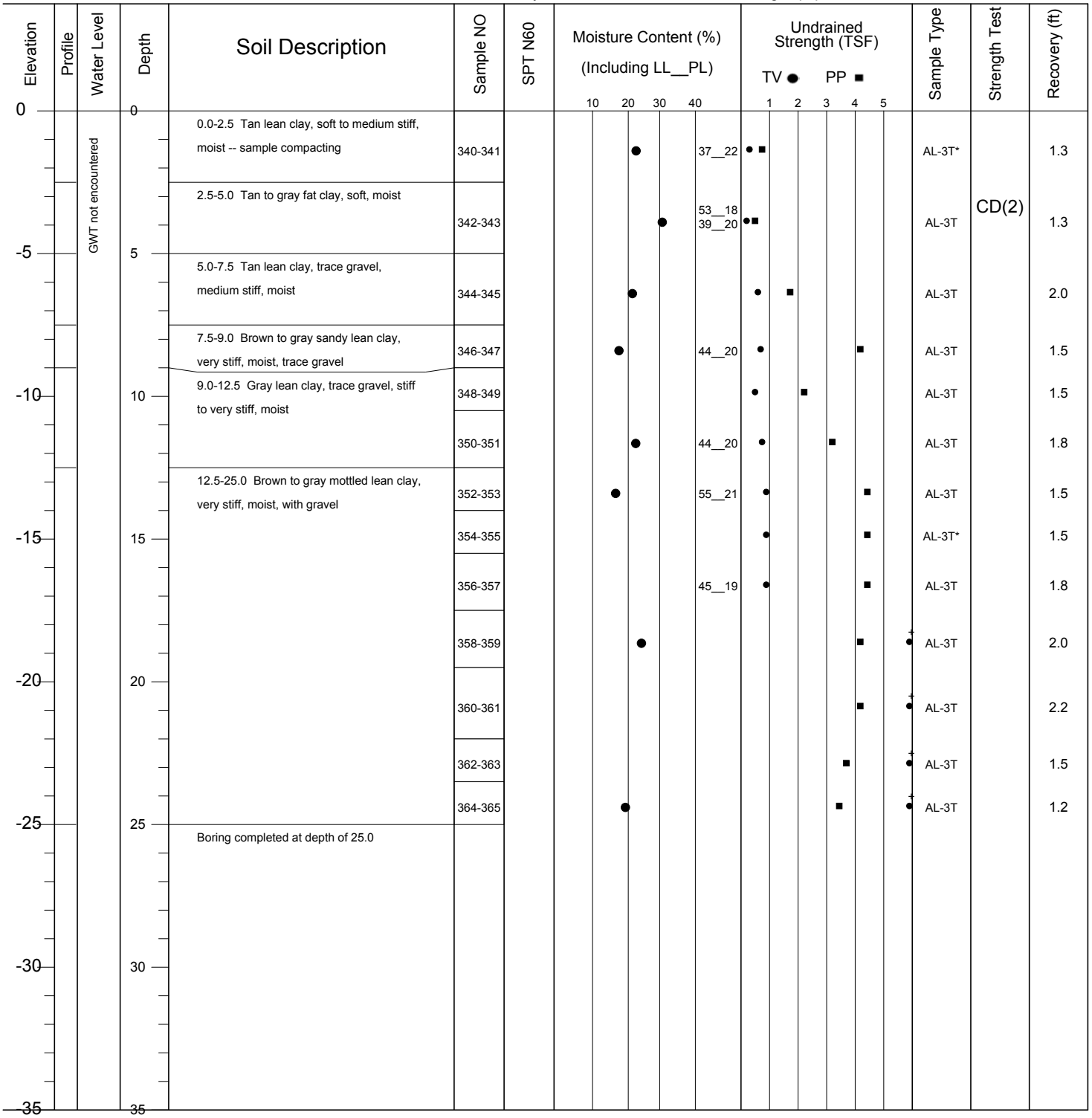

* Shelby Tube damaged --- no sample

SuperLog V3.0A CivilTech Software, USA www.civiltech.com File: C:\superlog3\project\US-36_boring.log Date: 10/16/2003

University of Missouri - Columbia

Civil & EnvironmentalEngineering Department -Geotechnical Group

Project Name: US-36 Stewartsville Site | **Project NO: SPROID5S**

Location: Between eastbound & westbound US-36 | **Boring Number: MUD7**

Ground Elevation: | **Logged By: Less**

Drilling Date: 6/6/2001 | **Driller: Murray**

Weather: Sunny 80-85 deg | Auger Method: 4" Hollow Stem | Driller's Hole NO: Y-01-61

Conditions: | SPT Hammer Efficiency: | Drilling Equip: Versa Drill G8641

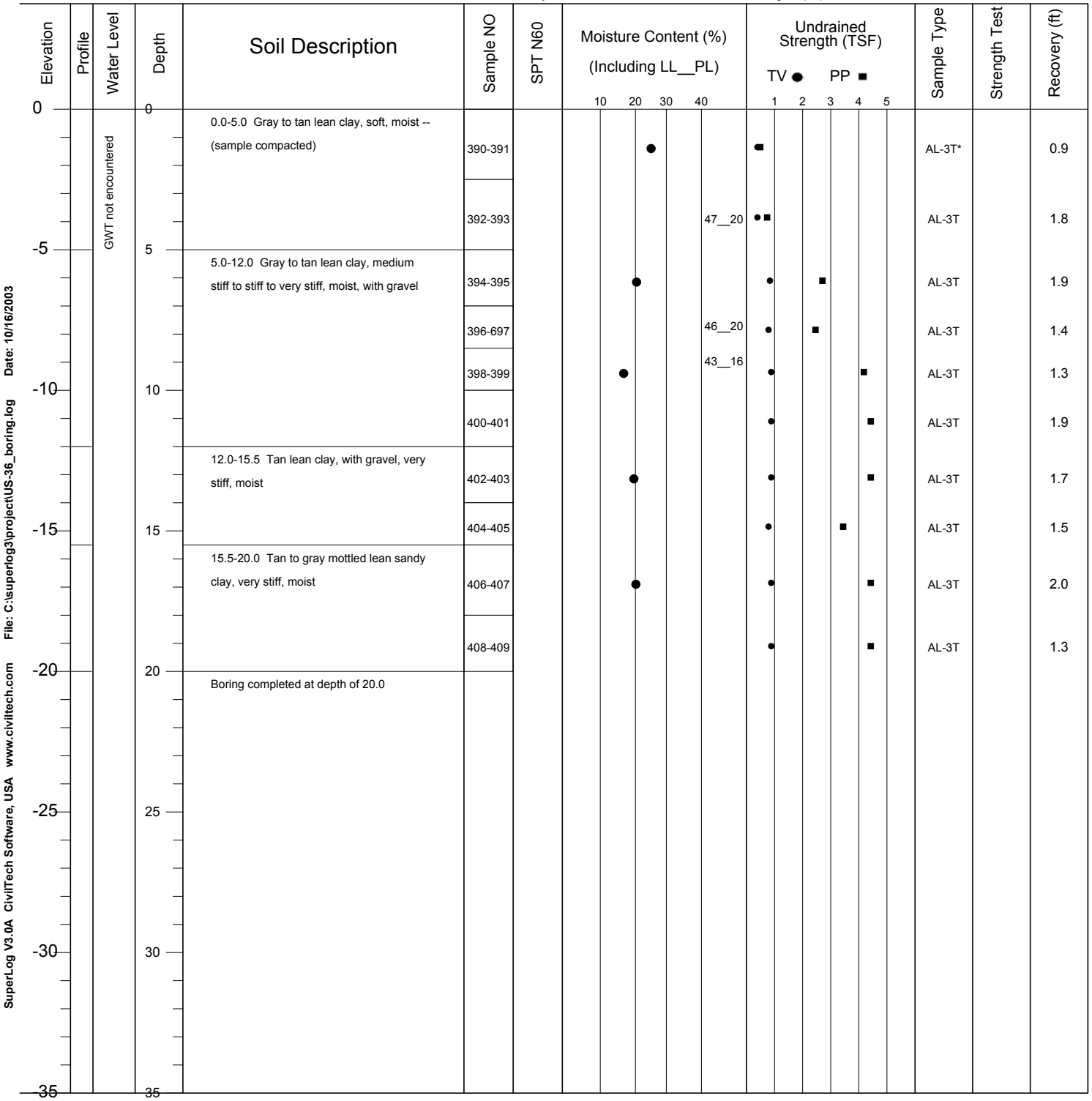

SuperLog V3.0A CivilTech Software, USA www.civiltech.com File: C:\superlog3\project\US-36_boring.log Date: 10/16/2003

* Tube damaged, no sample

University of Missouri - Columbia

Civil & EnvironmentalEngineering Department -Geotechnical Group

Project Name: US-36 Stewartsville Site | **Project NO: SPROID5S**

Location: Between eastbound & westbound US-36 | **Boring Number: MUD8**

Ground Elevation: | **Logged By: Less**

Drilling Date: 6/7/2001 | **Driller: Murray**

Weather: Cloudy, Humid, 70 deg | Auger Method: 4" Hollow Stem | Driller's Hole NO: Y-01-62

Conditions: | SPT Hammer Efficiency: | Drilling Equip: Versa Drill 4000TR-2 G8641

Elevation	Depth	Soil Description	Sample NO	SPT N60	Moisture Content (%) (Including LL__PL)	Undrained Strength (TSF) TV ● PP ■	Sample Type	Strength Test	Recovery (ft)
0	0	0.0-2.5 Brown to gray fat clay, soft, moist	415-416		58__23		AL-3T		1.2
		2.5-7.0 Gray to tan mottled lean clay, with gravel, stiff to very stiff, moist	417-418				AL-3T		1.9
-5	5		419-420				AL-3T		1.5
		7.0-10.0 Tan to gray mottled lean clay, trace gravel, very stiff, moist	421-422		47__21		AL-3T		1.3
-10	10		423-424				AL-3T		1.4
		Boring completed at depth of 10.0							
-15	15								
-20	20								
-25	25								
-30	30								
-35	35								

GWT not encountered

Moisture Content (%) (Including LL__PL): 10 20 30 40

Undrained Strength (TSF) TV ● PP ■: 1 2 3 4 5

SuperLog V3.0A CivilTech Software, USA www.civiltech.com File: C:\superlog3\project\US-36_boring.log Date: 10/16/2003

Appendix D. Boring Logs for US54-Fulton Site

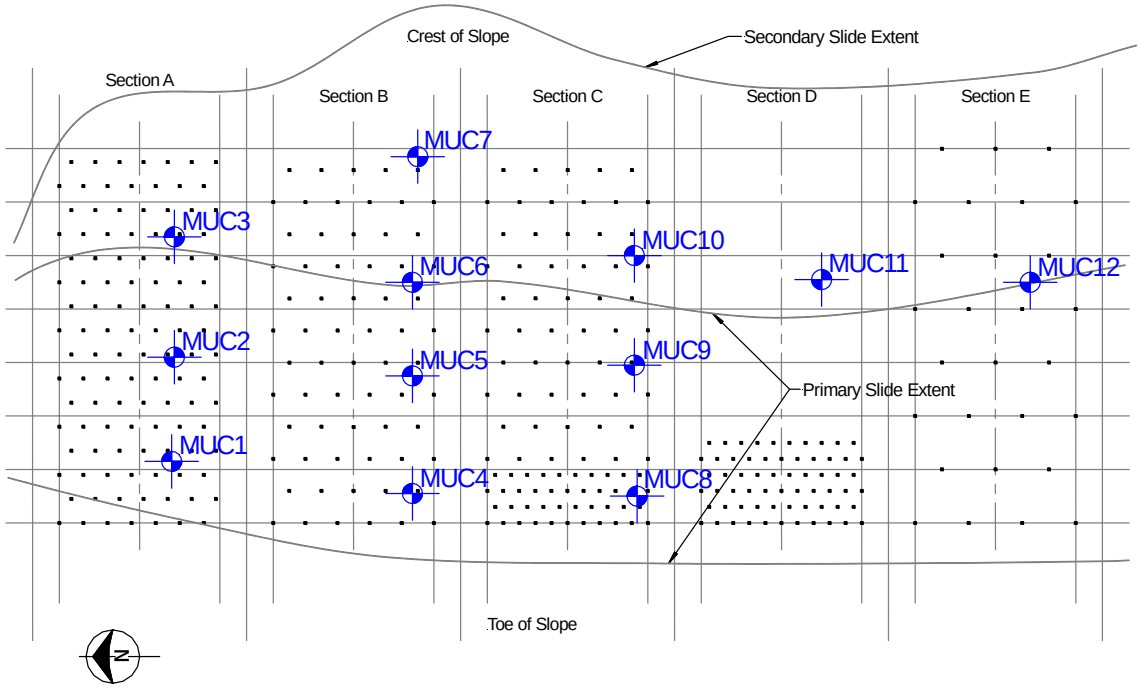

Figure D.1 Plan view of US54-Fulton site showing approximate boring locations.

University of Missouri - Columbia

Civil & EnvironmentalEngineering Department -Geotechnical Group

Project Name: US 54 - Fulton Site | **Project NO: 906 RDT RI98-701**

Location: 500 ft South of Richland Creek | **Boring Number: MUC-1**

Ground Elevation: | **Logged By: Fennessey**

Drilling Date: 9/25/2000 | **Driller: Hess**

Weather: Overcast, Mild | Auger Method: 4" Hollow Stem | Driller's Hole NO: Y-00-106

Conditions: | SPT Hammer Efficiency: | Drilling Equip: Versa Drill G8641

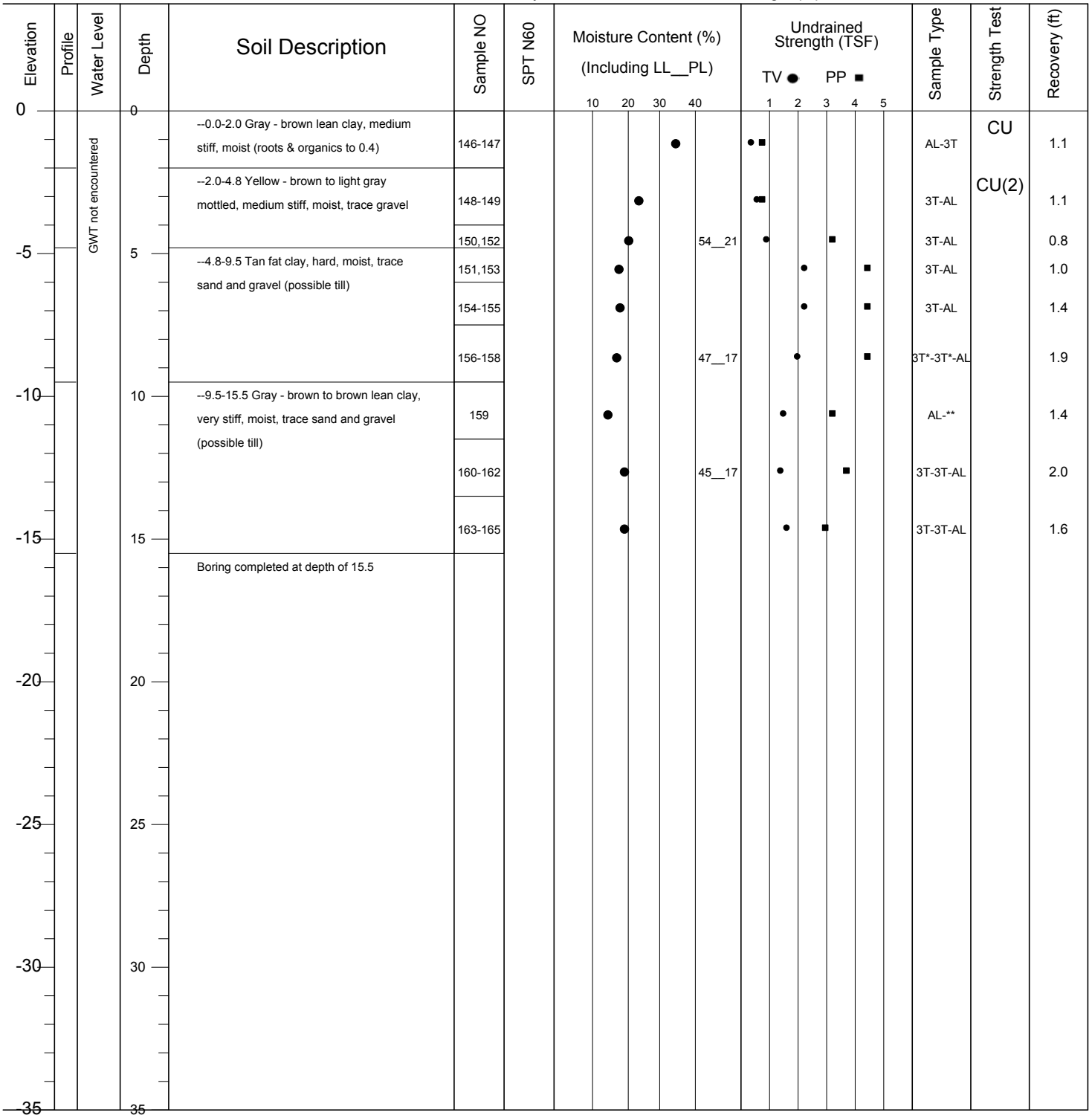

SuperLog V3.0A CivilTech Software, USA www.civiltech.com File: C:\superlog3\project\US-54_boring.log Date: 10/16/2003

* Partially disturbed (creased on side) ** damaged tube

3T--3" dia. shelby tube AL--bag sample for Atterberg Limits

Note: Shelby Tube refusal at 7.5 ft.

University of Missouri - Columbia

Civil & EnvironmentalEngineering Department -Geotechnical Group

Project Name: US 54 - Fulton Site | **Project NO: 906 RDT RI98-701**

Location: 500 ft South of Richland Creek | **Boring Number: MUC-2**

Ground Elevation: | **Logged By: Fennessey/Parra**

Drilling Date: 9/25/2000 - 9/26/2000 | **Driller: Hess**

Weather: | Auger Method: 4" Hollow Stem | Driller's Hole NO: Y-00-107

Conditions: | SPT Hammer Efficiency: 75 | Drilling Equip: Versa Drill G8641

Elevation	Depth	Soil Description	Sample NO	SPT N60	Moisture Content (%) (Including LL__PL)	Undrained Strength (TSF) TV ● PP ■	Sample Type	Strength Test	Recovery (ft)
0	0	--0.0-3.0 Brown lean clay, scattered snad, dry to moist	166	1/1/ 1			SS		0.8
			167	2/3/4 9	38__18		SS		1.4
		--3.0-4.1 Gray - brown lean clay, medium stiff to stiff, moist, trace sand	168	3/3/4 9			SS		1.35
-5	5	--4.1-6.5 Gray lean clay, medium stiff to stiff, moist, trace sand	169	3/3/4 9	39__21		SS		1.5
		--6.5-9.5 Gray - brown to dark yellow - brown lean clay, medium stiff to stiff, moist, trace sand	170	2/4/4 10			SS		.75
			171	3/4/7 14			SS		.95
-10	10	--9.5-20.5 Olive and light gray lean clay, very stiff to hard, moist, trace to scattered sand and gravel	172	5/5/8 16	50__18		SS		1.5
			173	6/7/11 23			SS		1.5
			174	5/10/11 26			SS		1.5
-15	15		175	5/8/10 23	47__17		SS		1.5
			176	8/9/9 23			SS		1.2
			177	5/7/11 23			SS		1.5
-20	20		178	5/8/9 21	45__17		SS		1.5
		Boring completed at depth of 20.5							
-25	25								
-30	30								
-35	35								

GWT not encountered

3T--3" dia. shelby tube AL--bag sample for Atterberg Limits

Note: SPT corrected N60 values given below blow sequence

--Cleaned out at 16 ft and stopped for day -- restarted 8:30 am 9/26

University of Missouri - Columbia

Civil & EnvironmentalEngineering Department -Geotechnical Group

Project Name: US 54 - Fulton Site | **Project NO: 906 RDT RI98-701**

Location: 500 ft South of Richland Creek | **Boring Number: MUC-3**

Ground Elevation: | **Logged By: Fennessey**

Drilling Date: 9/26/2000 | **Driller: Hess**

Weather: Clear, Warm | Auger Method: 4" Hollow Stem | Driller's Hole NO: Y-00-108

Conditions: | SPT Hammer Efficiency: | Drilling Equip: Versa Drill G8641

Elevation	Depth	Soil Description	Sample NO	SPT N60	Moisture Content (%) (Including LL__PL)	Undrained Strength (TSF) TV ● PP ■	Sample Type	Strength Test	Recovery (ft)
0	0	--0.0-0.7 Brown to tan lean clay, medium stiff, dry, with root and organics					**		
		--0.7-3.6 Gray - brown lean clay, dry, hard, trace gravel & sand	179				AL		1.8
			180		36__15		**-AL		1.5
-5	5	--3.6-12.0 Gray - brown with tan & black mottled lean clay, stiff to very stiff, moist with trace sand and gravel	181-182		37__15		3T-AL		1.2
			183-184				3T-AL		0.8
			185-186		39__16		3T-AL	CU(2)	0.9
-10	10		187-188				3T-AL		1.0
		--12.0-13.7 Gray lean clay, very stiff, moist, trace sand and gravel	189-190		40__13		3T-AL		1.3
		--13.7-21.3 Olive - brown with brown & gray mottled lean clay, very stiff to hard, moist, trace sand					AL		
-15	15		192-193		62__17		3T-AL		1.5
			194-195				3T-AL		1.6
			196-197				3T-AL		1.0
			198-199		48__15		3T-AL		0.8
-20	20		200-201				3T-AL		1.7
		Boring completed at depth of 21.3							
-25	25								
-30	30								
-35	35								

** sample grooved by rock, did not keep 3T sample

3T--3" dia. shelby tube AL--bag sample for Atterberg Limits

3T refusal at 17.4, 18.5, 19.5, 21.3 ft.

University of Missouri - Columbia

Civil & EnvironmentalEngineering Department -Geotechnical Group

Project Name: US 54 - Fulton Site | **Project NO: 906 RDT RI98-701**

Location: 500 ft South of Richland Creek | **Boring Number: MUC-4**

Ground Elevation: | **Logged By: Less**

Drilling Date: 10/2/2000 | **Driller: Hees**

Weather: Sunny, Mild | Auger Method: 4" Hollow Stem | Driller's Hole NO: Y-00-113

Conditions: | SPT Hammer Efficiency: | Drilling Equip: Versa Drill 4000 TR-2

Elevation	Depth	Soil Description	Sample NO	SPT N60	Moisture Content (%) (Including LL__PL)	Undrained Strength (TSF) TV ● PP ■	Sample Type	Strength Test	Recovery (ft)
0	0	--0.0-0.9 Brown to tan lean clay	401		10 20 30 40	1 2 3 4 5	AL	CU(2)	1.7
		--0.9-7.6 Brown lean clay, medium stiff, trace gravel, moist gray mottling @ 5.5 ft.	400,402				AL-3T		1.7
			404-405				AL-3T	CU	1.3
-5	5		406-407				AL-3T	CU(2)	2.0
			408-409				AL-3T		1.5
		--7.6-11.5 Brown fat clay, with gravel, stiff to very stiff, moist with gray mottles	410-411				AL-3T		1.5
-10	10		412-413				AL-3T		1.8
			414				AL		0.4
		--11.5-16.0 Brown lean clay with gravel, stiff to very stiff, moist, abundant gravel 11.7 to 12.5 (too heavy to sample), trace black and gray mottles	415				AL		
			416-417				AL-3T		1.6
-15	15		418-419				AL-3T		1.5
		Boring completed at depth of 16.0							
-20	20								
-25	25								
-30	30								
-35	35								

10/2/00

3T--3" dia. shelby tube AL--bag sample for Atterberg Limits

Refusal at 11.7, cleaned out to 12.5

Sample damaged (14.5-16.0)

SuperLog V3.0A CivilTech Software, USA www.civiltech.com File: C:\superlog3\project\US-54_boring.log Date: 10/16/2003

University of Missouri - Columbia

Civil & EnvironmentalEngineering Department -Geotechnical Group

Project Name: US 54 - Fulton Site | **Project NO: 906 RDT RI98-701**

Location: 500 ft South of Richland Creek | **Boring Number: MUC-5**

Ground Elevation: | **Logged By: Fennessey**

Drilling Date: 9/28/2000 | **Driller: Hees**

Weather: Clear, Warm | Auger Method: 4" Hollow Stem | Driller's Hole NO: Y-00-112

Conditions: | SPT Hammer Efficiency: | Drilling Equip: Versa Drill G8641

Elevation	Depth	Soil Description	Sample NO	SPT N60	Moisture Content (%) (Including LL__PL)	Undrained Strength (TSF) TV ● PP ■	Sample Type	Strength Test	Recovery (ft)
0	0	--0.0-3.5 Tan and brown lean clay, very stiff, moist, --brown and dry to 0.3 ft. w/ organics	272-273		45__14		3T-AL		1.2
			275				3T		0.9
		--3.5-9.3 Gray - brown with tan & gray mottles, lean clay, trace sand, very stiff and moist, --hard w/ brown mottles below 6.0	276				AL		
-5	5		277-278		40__15		3T-AL		0.9
			279-280				3T-AL		1.4
			281-282		48__17		3T-AL		1.1
-10	10	--9.3-14.0 Gray lean clay, trace sand and gravel, very stiff, moist	283				AL		
			284-286		41__10		3T-3T-AL		1.6
		10/2/00 ▼	287				AL-**		1.3
-15	15	--14.0-19.9 Olive - gray & gray fat clay, trace to scattered gravel & sand, very stiff to hard, moist, --limestone and chert gravel @ 15.8, --gravelly 16.6-17.3	288-289				3T-AL		1.5
			290		53__16		AL		0.4
			291				AL-**		0.6
			292				AL-**		0.8
			293	9/12/14 33	52__16		SS		1.5
-20	20	Boring completed at depth of 19.9							
-25	25								
-30	30								
-35	35								

3T--3" dia. shelby tube AL--bag sample for Atterberg Limits

Refusal at 15.5, 15.8, 16.6

** Shelby tube crushed by cobble (too disturbed for 3T sample)

Note: SPT corrected N60 values given below blow sequence

SuperLog V3.0A CivilTech Software, USA www.civiltech.com File: C:\superlog3\project\US-54_boring.log Date: 10/16/2003

University of Missouri - Columbia

Civil & EnvironmentalEngineering Department -Geotechnical Group

Project Name: US 54 - Fulton Site | **Project NO: 906 RDT RI98-701**

Location: 500 ft South of Richland Creek | **Boring Number: MUC-6**

Ground Elevation: | **Logged By: Fennessey**

Drilling Date: 9/26/2000 - 9/27/2000 | **Driller: Hees**

Weather: Clear & Warm both days | Auger Method: 4" Hollow Stem | Driller's Hole NO: Y-00-109

Conditions: | SPT Hammer Efficiency: | Drilling Equip: Versa Drill G8641

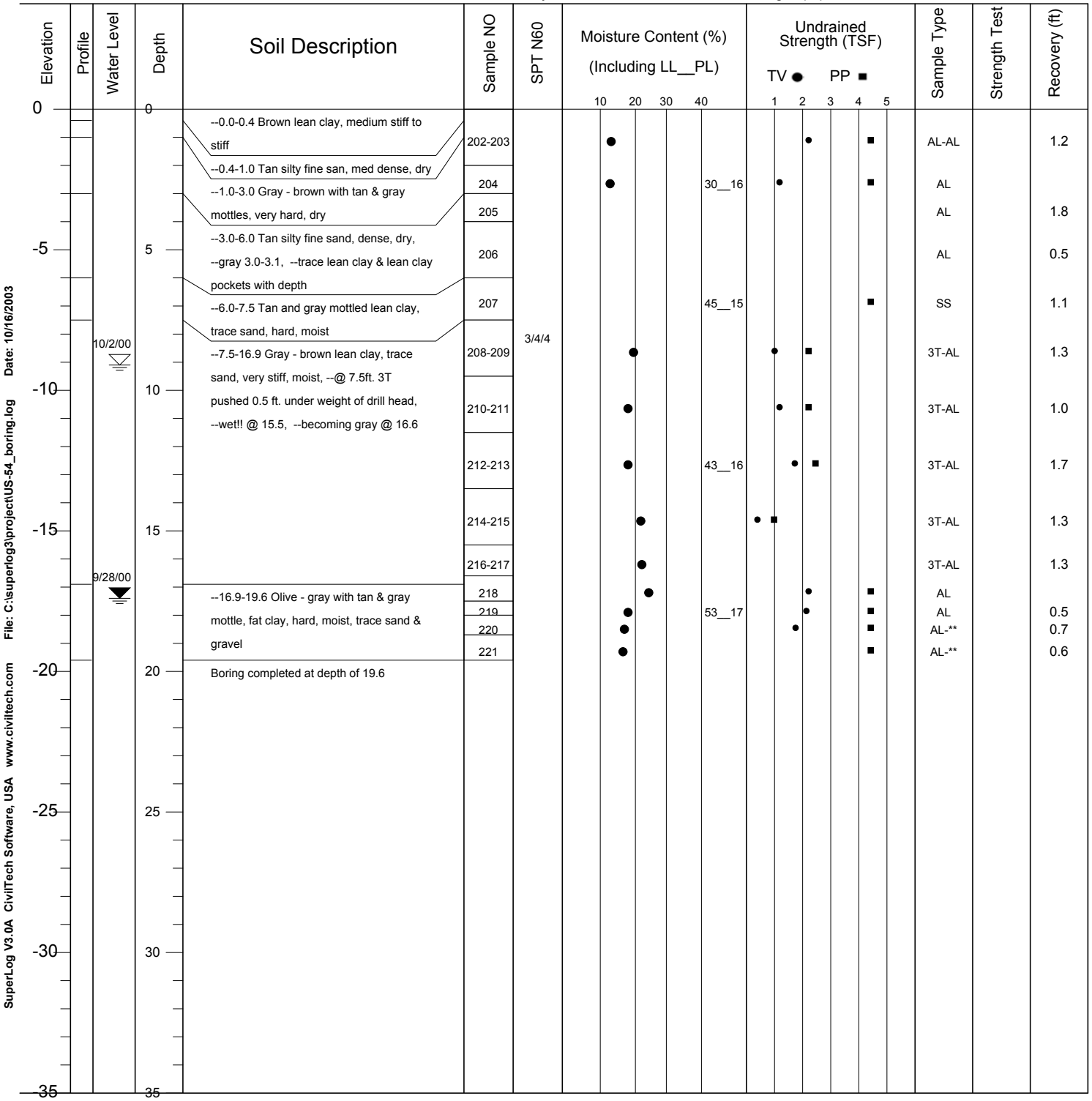

3T--3" dia. shelby tube AL--bag sample for Atterberg Limits

SS-- Split Spoon sampler Stopped for day @ 11.5 ft.

--3T Refusal @ 18.0 & 19.6 (3T Refusal @ 18.7 drilled out to19.0)

** Sample too disturbed for 3T

SuperLog V3.0A CivilTech Software, USA www.civiltech.com File: C:\superlog3\project\US-54_boring.log Date: 10/16/2003

University of Missouri - Columbia

Civil & EnvironmentalEngineering Department -Geotechnical Group

Project Name: US 54 - Fulton Site | **Project NO: 906 RDT RI98-701**

Location: 500 ft South of Richland Creek | **Boring Number: MUC-7**

Ground Elevation: | **Logged By: Fennessey**

Drilling Date: 9/27/2000 | **Driller: Hees**

Weather: Clear, Warm | Auger Method: 4" Hollow Stem | Driller's Hole NO: Y-00-110

Conditions: | SPT Hammer Efficiency: | Drilling Equip: Versa Drill G8641

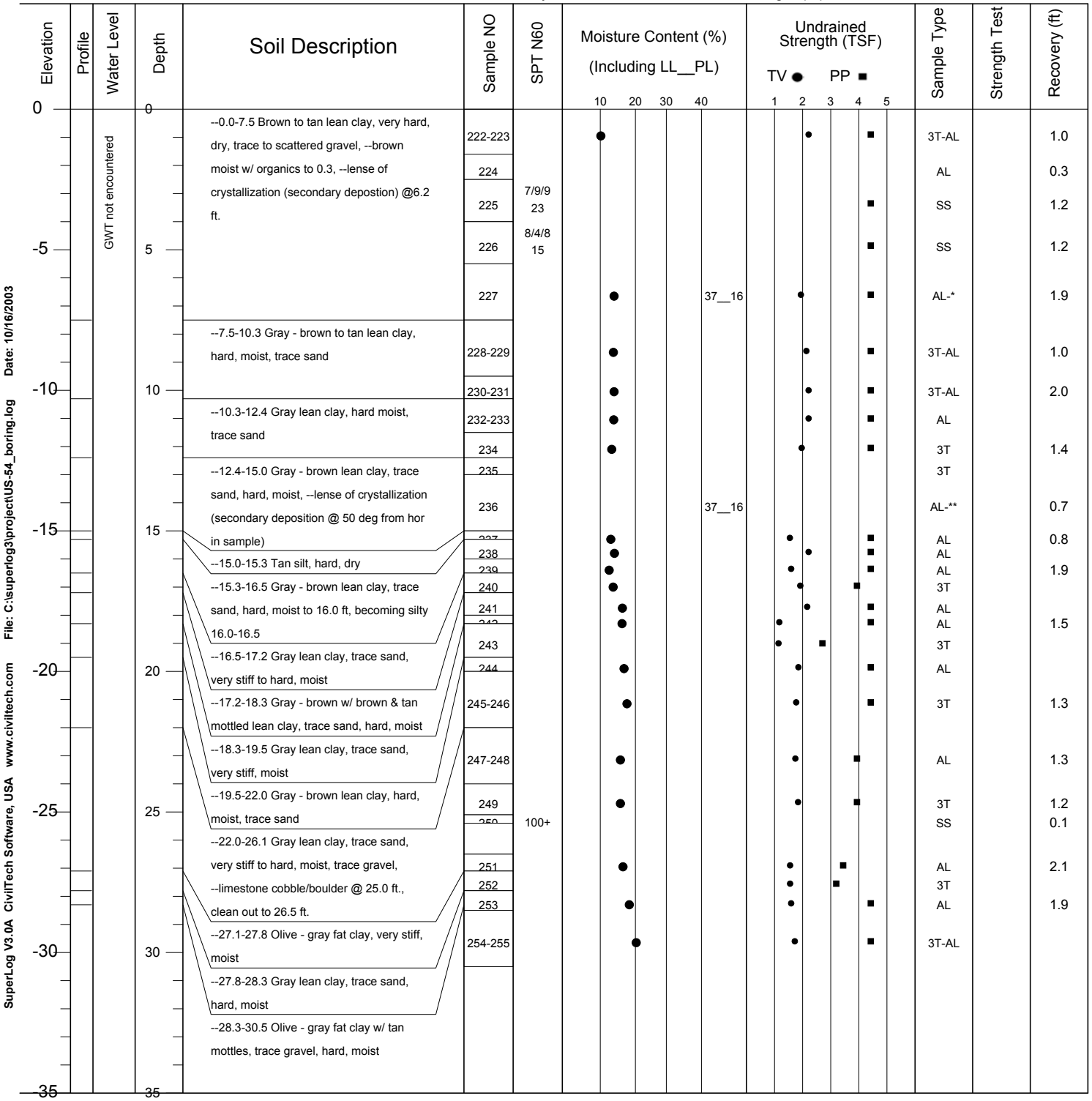

SuperLog V3.0A CivilTech Software, USA www.civiltech.com File: C:\superlog3\project\US-54_boring.log Date: 10/16/2003

* sample too dry and broken for 3T

** collapsed by gravel, no undist sample, poor quality

3T--3" dia. shelby tube AL--bag sample for Atterberg Limits

SS--Split Spoon

University of Missouri - Columbia

Civil & EnvironmentalEngineering Department -Geotechnical Group

Project Name: US 54 - Fulton Site | **Project NO: 906 RDT RI98-701**

Location: 500 ft South of Richland Creek | **Boring Number: MUC-8**

Ground Elevation: | **Logged By: Less**

Drilling Date: 10-2-2000 | **Driller: Hees**

Weather: Sunny, Warm | Auger Method: 4" Hollow Stem | Driller's Hole NO: Y-00-114

Conditions: | SPT Hammer Efficiency: | Drilling Equip: Versa Drill 4000TR-2

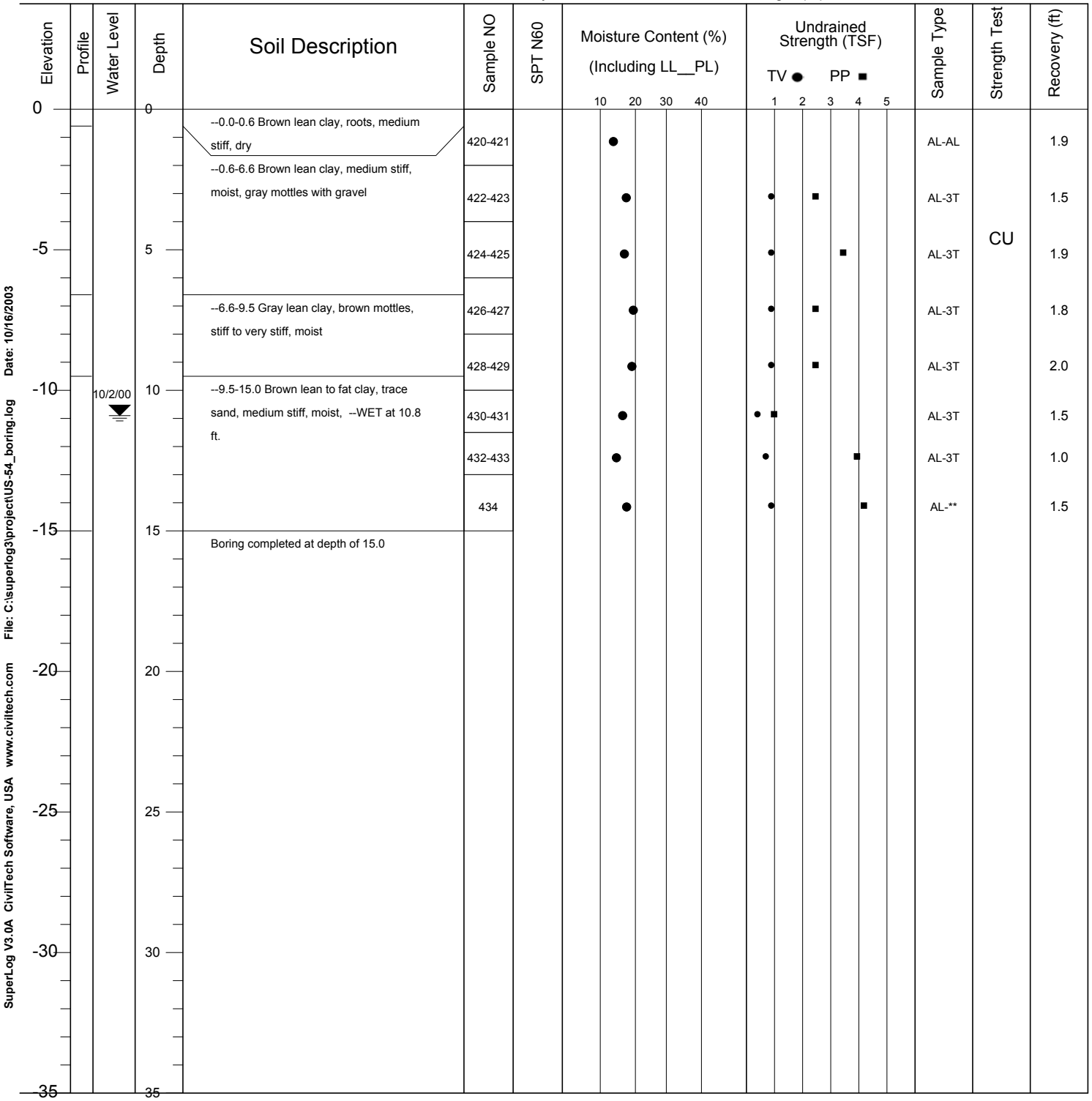

SuperLog V3.0A CivilTech Software, USA www.civiltech.com File: C:\superlog3\project\US-54_boring.log Date: 10/16/2003

3T--3" dia. shelby tube AL--bag sample for Atterberg Limits

Refusal at 11.5, cleaned out to 12.0

** final 3T sample damaged (13.0-15.0) did not keep

University of Missouri - Columbia

Civil & EnvironmentalEngineering Department -Geotechnical Group

Project Name: US 54 - Fulton Site | **Project NO: 906 RDT RI98-701**

Location: 500 ft South of Richland Creek | **Boring Number: MUC-9**

Ground Elevation: | **Logged By: Fennessey**

Drilling Date: 9/27/2000 - 9/28/2000 | **Driller: Hees**

Weather: | Auger Method: 4" Hollow Stem | Driller's Hole NO: Y-00-111

Conditions: | SPT Hammer Efficiency: 75 | Drilling Equip: Versa Drill G8641

Elevation	Profile	Water Level	Depth	Soil Description	Sample NO	SPT N60	Moisture Content (%) (Including LL__PL) 10 20 30 40	Undrained Strength (TSF) TV ● PP ■ 1 2 3 4 5	Sample Type	Strength Test	Recovery (ft)
0		GWT not encountered	0	--0.0-3.0 Light brown to tan lean clay, trace sand, hard to very stiff, moist, --brown with organics to 0.2	256	1/2/3 6			SS		1.2
					257	2/3/3 8			SS		1.4
				--3.0-8.0 Gray - Brown with tan & brown mottled lean clay, trace sand, very stiff, moist	258	3/3/6 11			SS		1.4
-5			5		259	3/5/7 15			SS		1.2
					260	4/6/12 23			SS		1.0
				--8.0-9.6 Gray lean clay, trace sand, very stiff, moist	261	5/8/8 20			SS		0.2
-10			10	--9.6-10.5 Gray - brown lean clay, trace sand, very stiff, moist	262	4/5/8 16			SS		1.4
				--10.5-13.0 Gray lean clay, trace sand, very stiff to hard, moist	263-264	4/6/7 16			SS		0.4
					265	3/4/6 13			SS		1.6
				--13.0-13.5 Gray - brown with tan mottled lean clay, trace sand & gravel, very stiff, moist	266						
-15			15		267	2/3/5 10			SS		1.6
				--13.5-21.0 Tan & gray - brown fat clay, trace gravel, stiff to hard, moist, --with brown mottles & trace sand and gravel below 19.4	268	3/4/7 14			SS		1.5
					269	3/7/10 21			SS		1.6
					270	5/5/9 18			SS		1.5
-20			20		271	5/9/12 26			SS		1.5
				Boring completed at depth of 21.0							
-25			25								
-30			30								
-35			35								

SS- split spoon sampler

Note: SPT corrected N60 values given below blow sequence

Stopped for day @ 10.5 ft.

University of Missouri - Columbia

Civil & EnvironmentalEngineering Department -Geotechnical Group

Project Name: US 54 - Fulton Site | **Project NO: 906 RDT RI98-701**

Location: 500 ft South of Richland Creek | **Boring Number: MUC-10**

Ground Elevation: | **Logged By: Newton**

Drilling Date: 10-10-2000 | **Driller: Barnett**

Weather: Cool & Clear (50 F) | Auger Method: 4" Hollow Stem | Driller's Hole NO: 0-00-59

Conditions: | SPT Hammer Efficiency: | Drilling Equip: Versa Drill 4000TR-2

Elevation	Depth	Soil Description	Sample NO	SPT N60	Moisture Content (%) (Including LL__PL)	Undrained Strength (TSF) TV ● PP ■	Sample Type	Strength Test	Recovery (ft)
0	0	--0.0-0.4 Black lean clay, medium stiff --0.4-12.2 Brown lean clay with gray and black mottles, scattered gravel, very stiff to hard, --gravelly 9.6-10.0	621		10 20 30 40	1 2 3 4 5	3T		1.1
			620,622				AL,SS		1.3
-5	5		623-624				3T-AL		1.1
			625				AL		1.0
			626-627				3T-AL		1.6
-10	10		628-629				3T-AL		1.5
		--12.2-14.2 Yellowish brown mottled lean clay with scattered gravel, very stiff, gypsum crystals present @12.0	630-631				3T-AL		1.6
-15	15	--14.2-16.2 Dark brown lean clay with black mottles, stiff, scattered gravel and fine sand present, --sandy brown @ 16.0	632,637				3T-3T		1.5
		--16.2-20.0 Brown gravelly lean clay with lignite and reddish brown sandy seams, --gravelly @18	633-634				3T-AL		1.4
-20	20	Boring completed at depth of 20.0	635-636				AL-3T		2.1
-25	25								
-30	30								
-35	35								

GWT not encountered

AL--bag sample for Atterberg Limits

3T--3" diameter Shelby Tube

SS--Split Spoon Sampler

University of Missouri - Columbia

Civil & EnvironmentalEngineering Department -Geotechnical Group

Project Name: US 54 - Fulton Site | **Project NO: 906 RDT RI98-701**

Location: 500 ft South of Richland Creek | **Boring Number: MUC-11**

Ground Elevation: | **Logged By: Newton**

Drilling Date: 10/10/2000 | **Driller: Barnett**

Weather: | Auger Method: 4" Hollow Stem | Driller's Hole NO: 0-00-60

Conditions: | SPT Hammer Efficiency: | Drilling Equip: Versa Drill G7211

Elevation	Depth	Soil Description	Sample NO	SPT N60	Sample Type
0	0	--0.0-4.8 Dark brown and gray mottled lean clay with and few fine gravels and lignites, very stiff	640	4/7/8	SS
			641	4/5/7	SS
			642	4/7/9	SS
-5	5	--4.8-9.0 Light brown and gray mottled lean clay with scattered fine gravel and lignite, very stiff to hard, --gypsum crystals and sand seams @6.0	643	6/9/9	SS
			644	4/7/6	SS
			645	3/7/8	SS
-10	10	--9.0-10.8 Brown lean clay with scattered fine gravel, stiff	646	5/10/15	SS
		--10.8-16.3 Brown and gray sandy lean clay, very stiff with scattered fine gravel and lignite	647	4/9/15	SS
			648	4/8/11	SS
-15	15		649	5/10/13	SS
			650	5/9/15	SS
		--16.3-19.8 Brown sandy lean clay, stiff to very stiff with scattered fine gravel, --gypsum crystals & sand seams @ 18.0	651	7/11/15	SS
			652	6/13/18	SS
-20	20	--19.8-21.0 Light brown sandy lean clay with fine gravel and lignite, very stiff			
		Boring completed at depth of 21.0			
-25	25				
-30	30				
-35	35				

Moisture Content (%) (Including LL__PL): 10 20 30 40

Undrained Strength (TSF): TV ● PP ■ 1 2 3 4 5

Strength Test | Recovery (ft)

SS--Split Spoon Sampler

SPT corrected N60 values not given -- just original blow sequence

University of Missouri - Columbia

Civil & EnvironmentalEngineering Department -Geotechnical Group

Project Name: US 54 - Fulton Site | **Project NO: 906 RDT RI98-701**

Location: 500 ft South of Richland Creek | **Boring Number: MUC-12**

Ground Elevation: | **Logged By: Newton**

Drilling Date: 10/11/2000 | **Driller: Barnett**

Weather: | Auger Method: 4" Hollow Stem | Driller's Hole NO: 0-00-61

Conditions: | SPT Hammer Efficiency: | Drilling Equip: Versa Drill G7211

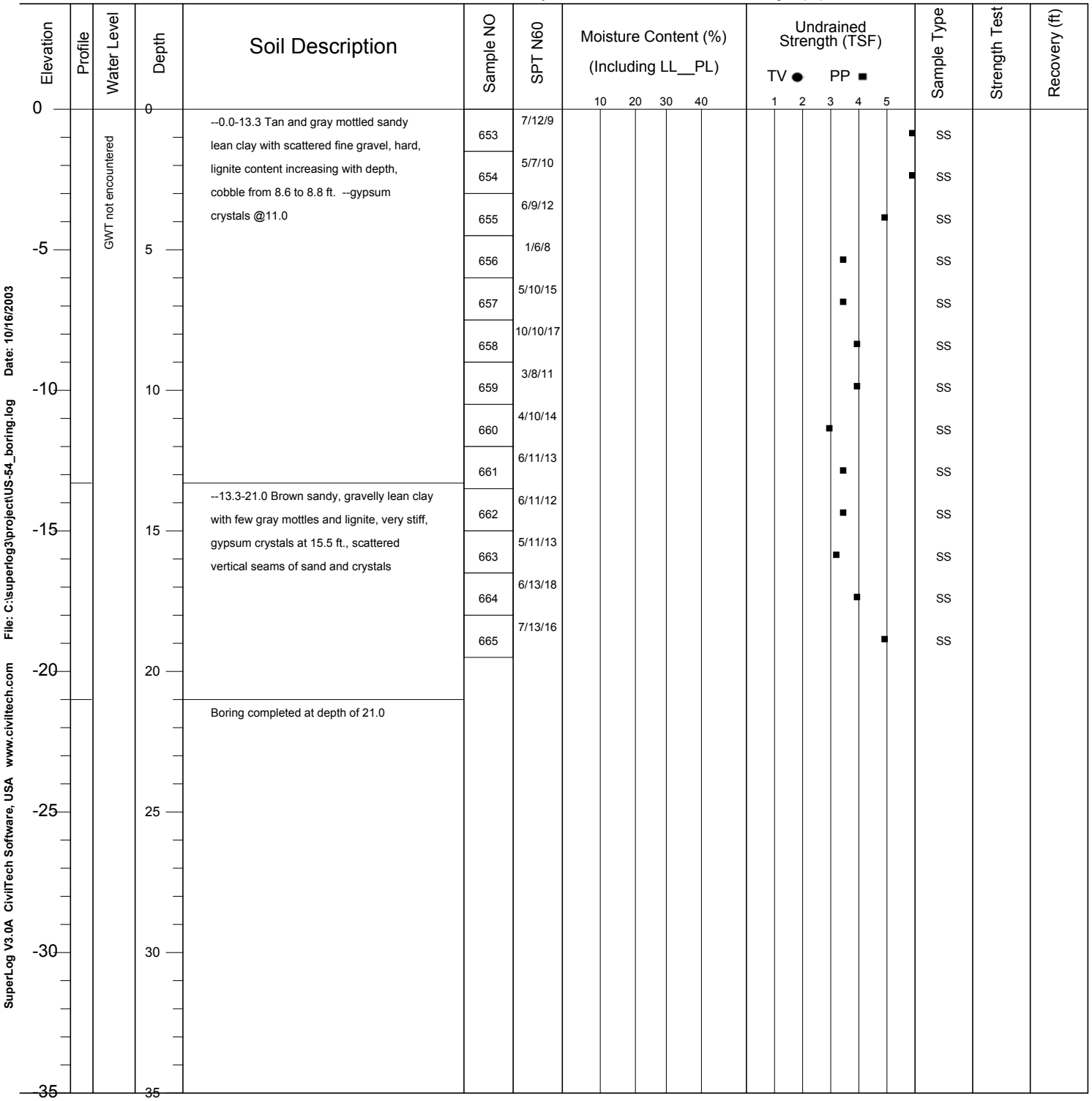

SS--Split Spoon Sampler

SPT corrected N60 values not given, just original blow sequence

SuperLog V3.0A CivilTech Software, USA www.civiltech.com File: C:\superlog3\project\US-54_boring.log Date: 10/16/2003

Appendix E

Slope Stability Model Coordinates

I70-Emma Slope Coordinates
(all coordinates in units of feet)

Section A

Slope Surface (x,y)	Slope Interface (x,y)	Reinforcement Coordinates (x,y)		
		x	y_{top}	y_{bot}
-50,0	0,0	25	1.44	-3.81
0,0	25,-2.89	28	2.48	-2.77
25,1.44	28,-1.92	31	3.53	-1.72
50,10.14	34,-0.95	34	4.57	-0.68
77,23.65	34,0.14	37	5.62	-0.63
80,22.83	40,1.18	40	6.66	0.41
100,22.83	43,2.40	43	7.7	1.45
100,-50	46,3.50	46	8.75	2.5
-50,-50	49,4.44	49	9.79	3.54
	52,5.77	52	11.12	4.87
	55,7.30	55	12.59	6.34
	58,7.43	58	14.06	6.81
	61,9.12	61	15.54	8.29
	64,10.98	64	17.01	10.26
	67,12.43	67	18.48	11.73
	70,12.83	70	19.95	12.2
	73,14.21	73	21.54	13.29
	76,15.67	76	23.12	14.87

Section B

Slope Surface (x,y)	Slope Interface (x,y)	Reinforcement Coordinates (x,y)		
		x	y_{top}	y_{bot}
-50,0	0,0	37	5.15	-0.1
0,0	25.71,-0.28	43	7.74	1.99
25,1.58	37,0.53	49	10.34	3.59
35,4.28	43,2.82	55	13.06	5.31
53,12.07	49,4.29	61	16.02	8.27
73,21.82	55,6.41	67	18.98	10.73
77,21.65	61,9.17	73	21.97	13.72
100,21.65	67,11.48			
100,-50	73,14.47			
-50,-50				

Section C

Slope Surface (x,y)	Slope Interface (x,y)	Reinforcement Coordinates (x,y)		
		x	y_{top}	y_{bot}
-50,0	0,0	31	3.49	-3.76
0,0	31,-3.76	37	5.49	-1.26
25,1.48	37,-0.68	43	7.5	0.75
50,9.84	43,1.20	49	9.51	1.76
65,17.63	49,2.24	55	12.44	4.19
71,20.33	55,4.44	61	15.55	7.30
75,20	61,7.70	67	18.53	10.28
100,20	67,10.65			
100,-50				
-50,-50				

Section D

Slope Surface (x,y)	Slope Interface (x,y)	Reinforcement Coordinates (x,y)		
		x	y_{top}	y_{bot}
-50,0	0,0	29.5	2.97	-1.78
0,0	29.5,-1.11	34	4.43	-1.82
25,1.5	34,-1.45	38.5	5.9	0.15
50,9.64	38.5,1.15	43	7.36	1.11
69,18.78	43,1.84	47.5	8.83	1.58
74,18.66	47.5,2.43	52	10.62	3.37
100,18.66	52,4.52	56.5	12.82	4.57
100,-50	56.5,5.32	61	15	6.75
-50,-50	61,7.50	65.5	17.13	8.88
	65.5,9.63			

I70-Emma Piezometric Surface Coordinate Pairs
(all coordinates in units of feet)

	Section A		Section B		Section C		Section D	
	Upper	Lower	Upper	Lower	Upper	Lower	Upper	Lower
1/14/2004	-50,-4.77	-50,-9.98	-50,-3.58	-50,-8.85	-50,-4.03	-50,-9.48	-50,-3.23	-50,-7.47
	21.09,-4.77	21.09,-9.98	16.22,-3.58	15.69,-8.85	22.75,-4.03	22.75,-9.48	16.60,-3.23	16.60,-7.47
	49,6.79	49,1.79	40,3.44	40,-1.56	46,5.5	46,0.5	38.5,1.86	38.5,-2.10
	71,19.5	71,18.5	64,16.5	64,15.5	64,16.1	64,15.1	62.5,14.7	62.5,13.7
	100,19.5	100,18.5	100,16.5	100,15.5	100,16.1	100,15.1	100,14.7	100,13.7
3/6/2004	-50,-4.77	-50,-9.98	-50,-5.72	-50,-8.85	-50,-4.03	-50,-9.48	-50,-3.23	-50,-7.47
	21.09,-4.77	21.09,-9.98	15.74,-5.72	15.69,-8.85	22.75,-4.03	12.27,-9.48	21.25,-3.23	16.60,-7.47
	49,6.19	49,4.79	40,2.84	40,1.44	46,4.9	46,3.5	38.5,2.30	38.5,0.9
	71,19.3	71,14.4	64,16.3	64,11.4	64,15.9	64,11	62.5,14.5	62.5,9.6
	100,19.3	100,14.4	100,16.3	100,11.4	100,15.9	100,11	100,14.5	100,9.6
4/8/2004	-50,-3.45	-50,-7.02	-50,-3.16	-50,-8.85	-50,-4.03	-50,-9.48	-50,-3.23	-50,-7.47
	21.43,-3.45	21.71,-7.02	15.23,-3.16	14.35,-8.85	14.5,-4.03	15.25,-9.48	14.65,-3.23	16.60,-7.47
	49,7.39	49,4.09	40,4.04	40,0.74	46,6.1	46,2.8	38.5,3.50	38.5,0.2
	71,16.9	71,13.3	64,13.9	64,10.30	64,13.5	64,9.9	62.5,12.1	62.5,8.5
	100,16.9	100,13.3	100,13.9	100,10.30	100,13.5	100,9.9	100,12.1	100,8.5
5/24/2004	-50,-3.25	-50,-6.61	-50,-1.96	-50,-5.53	-50,-4.03	-50,-6.79	-50,-3.23	-50,-7.47
	16.75,-3.25	21.54,-6.61	14.38,-1.96	13.82,-5.53	10.78,-4.03	16.26,-6.79	16.05,-3.23	16.60,-7.47
	49,7.89	49,4.89	40,4.54	40,1.54	46,6.6	46,3.6	38.5,4.0	38.5,1.0
	71,17.3	71,13.3	64,14.3	64,10.30	64,13.9	64,9.9	62.5,12.5	62.5,8.5
	100,17.3	100,13.3	100,14.3	100,10.30	100,13.9	100,9.9	100,12.5	100,8.5
6/30/2004	-50,-4.77	-50,-6.70	-50,-1.96	-50,-5.53	-50,-4.03	-50,-9.48	-50,-3.23	-50,-7.47
	21.09,-4.77	21.19,-6.70	14.38,-1.96	14.66,-5.53	22.75,-4.03	22.75,-9.48	18.59,-3.23	20.92,-7.47
	49,5.79	49,2.29	40,2.44	40,-1.06	46,4.5	46,1.0	38.5,1.9	38.5,-1.6
	71,18	71,15.5	64,15	64,12.5	64,14.6	64,12.1	62.5,13.2	62.5,10.7
	100,18	100,15.5	100,15	100,12.5	100,14.6	100,12.1	100,13.2	100,10.7
9/16/2004	-50,-4.77	-50,-9.98	-50,-1.96	-50,-5.53	-50,-4.03	-50,-9.48	-50,-3.23	-50,-7.47
	21.09,-4.77	21.09,-9.98	14.38,-1.96	14.66,-5.53	22.75,-4.03	22.75,-9.48	14.65,-3.23	16.60,-7.47
	49,5.79	49,2.49	40,2.44	40,-0.86	46,4.5	46,1.2	38.5,1.90	38.5,-1.4
	71,16.7	71,15.4	64,13.7	64,12.4	64,13.3	64,12.0	62.5,11.9	62.5,10.6
	100,16.7	100,15.4	100,13.7	100,12.4	100,13.3	100,12.0	100,11.9	100,10.6
11/9/2004	-50,-4.77	-50,-9.98	-50,-1.96	-50,-7.61	-50,-4.03	-50,-9.48	-50,-3.23	-50,-7.47
	21.09,-4.77	21.09,-9.98	14.38,-1.96	15.23,-7.61	22.75,-4.03	22.75,-9.48	14.65,-3.23	16.60,-7.47
	49,5.79	49,2.49	40,3.64	40,-0.46	46,5.7	46,1.6	38.5,3.1	38.5,-1.0
	71,18.5	71,16	64,15.5	64,13	64,15.1	64,12.6	62.5,13.7	62.5,11.2
	100,18.5	100,16	100,15.5	100,13	100,15.1	100,12.6	100,13.7	100,11.2
1/27/2005 Case 1	-50,-4.27	-50,-9.48	-50,-3.08	-50,-8.35	-50,-3.53	-50,-8.98	-50,-2.73	-50,-6.97
	21.09,-4.27	21.09,-9.48	16.22,-3.08	15.69,-8.35	22.75,-3.53	22.75,-8.98	16.60,-2.73	16.60,-6.97
	49,7.29	49,2.29	40,3.94	40,-1.506	46,6.0	46,1.0	38.5,2.36	38.5,-1.6
	71,20	71,19	64,17	64,16	64,16.6	64,15.6	62.5,15.2	62.5,14.2
	100,20	100,19	100,17	100,16	100,16.6	100,15.6	100,15.2	100,14.2
1/27/2005 Case 2	-50,-3.77	-50,-8.98	-50,-2.58	-50,-7.85	-50,-3.03	-50,-8.48	-50,-2.23	-50,-6.47
	21.09,-3.77	21.09,-8.98	16.22,-2.58	15.69,-7.85	22.75,-3.03	22.75,-8.48	16.60,-2.23	16.60,-6.47
	49,7.79	49,2.79	40,4.44	40,-0.56	46,6.5	46,1.5	38.5,2.86	38.5,-1.10
	71,19.5	71,18.5	64,16.5	64,15.5	64,16.1	64,15.1	62.5,14.7	62.5,13.7
	100,19.5	100,18.5	100,16.5	100,15.5	100,16.1	100,15.1	100,14.7	100,13.7
1/27/2005 Case 3	-50,-3.77	-50,-8.98	-50,-2.58	-50,-7.85	-50,-3.03	-50,-8.48	-50,-2.23	-50,-6.47
	21.09,-3.77	21.09,-8.98	16.22,-2.58	15.69,-7.85	22.75,-3.03	22.75,-8.48	16.60,-2.23	16.60,-6.47
	49,7.79	49,2.79	40,4.44	40,-0.56	46,6.5	46,1.5	38.5,2.86	38.5,-1.10
	71,20.5	71,19.5	64,17.5	64,16.5	64,17.1	64,16.1	62.5,15.7	62.5,14.7
	100,20.5	100,19.5	100,17.5	100,16.5	100,17.1	100,16.1	100,15.7	100,14.7

US36-Stewartsville Slope Coordinates
(all coordinates in units of feet)

Slope Surface (x,y)	Section A				Section B			
	Slope Interface (x,y)	Reinforcement Coordinates (x,y)			Slope Interface (x,y)	Reinforcement Coordinates (x,y)		
		x	y_{top}	y_{bot}		x	y_{top}	y_{bot}
-50,3	-6.6,3	0	0.00	-4.50	0,-4	0	0.00	-4.50
-6.6,3	0,-3.6	3	1.36	-3.14	6,-1.27	6	2.73	-1.77
0,0	6,-0.97	6	2.73	-1.77	12,1.95	12	5.45	1.45
64.7,29.4	12,1.55	9	4.09	-0.41	18,4.18	18	8.18	3.68
114.7,29.4	18,4.18	12	5.45	0.95	24,6.41	24	10.91	5.91
114.7,-50	24,6.51	15	6.82	2.32	42,15.09	30	13.64	7.64
-50,-50	30,8.74	18	8.18	3.68	48,18.32	36	16.36	10.36
	36,11.41	21	9.55	4.55	54,20.05	42	19.09	14.59
	41.98,14.03	24	10.91	5.91	60,21.77	48	21.82	17.82
	48,16.61	27	12.27	6.77	66,22.50	54	24.55	19.55
	54,19.15	30	13.64	8.14		60	27.27	21.27
	60,20.97	33	15.00	8.50		66	29.40	22.00
	66,22.6	36	16.36	9.36				
	114.7,22.6	39	17.73	10.73				
		42	19.09	12.09				
		45	20.45	13.45				
		48	21.82	14.82				
		51	23.18	16.68				
		54	24.55	18.55				
		57	25.91	19.41				
		60	27.27	20.27				
		63	28.64	21.14				
		66	29.40	22.00				

Slope Surface (x,y)	Section C				Section D			
	Slope Interface (x,y)	Reinforcement Coordinates (x,y)			Slope Interface (x,y)	Reinforcement Coordinates (x,y)		
		x	y_{top}	y_{bot}		x	y_{top}	y_{bot}
-50,3	0,-4.5	0	0.00	-5.00	0,-4.5	0	0.00	-5.00
-6.6,3	4.5,-1.94	4.5	2.05	-2.45	4.5,-1.94	6	2.73	-2.77
0,0	9,-0.41	9	4.09	-0.91	9,-0.41	12	5.45	0.45
64.7,29.4	13.5,2.14	13.5	6.14	1.64	13.5,2.14	18	8.18	3.18
114.7,29.4	18,4.18	18	8.18	3.68	18,4.18	24	10.91	5.41
114.7,-50	22.5,5.73	22.5	10.23	5.23	22.5,5.73	30	13.64	6.64
-50,-50	40.5,14.41	27	12.27	6.27	40.5,14.41	36	16.36	9.36
	45,16.45	31.5	14.32	8.32	45,16.45	42	19.09	13.59
	49.5,18	36	16.36	10.36	49.5,18	48	21.82	16.82
	54,19.05	40.5	18.41	13.91	54,19.05	54	24.55	19.05
	63,21.14	45	20.45	15.95	63,21.14	60	27.27	19.77
		49.5	22.50	17.50		66	29.40	22.00
		54	24.55	18.55				
		58.5	26.59	18.59				
		63	28.64	20.64				

US36-Stewartsville Piezometric Surface Coordinate Pairs
(all coordinates in units of feet)

	All Sections (x,y)
9/28/2002	-50,-0.82
	-0.13,-0.82
	12,1.85
	33.88,10.5
	54,11.84
	114.7,11.84
11/15/2002	-50,-1.19
	-0.93,-1.19
	12,1.85
	30.91,9.44
	54,11.54
	114.7,11.54
5/20/2003	-50,-0.84
	0,-0.84
	12,2.05
	35.27,11.38
	54,13.34
	114.7,13.34
9/9/2003	-50,-3.32
	-2.08,-3.32
	12,-0.95
	35.43,8.27
	54,10.34
	114.7,10.34
9/30/2003	-50,-3.32
	-2.08,-3.32
	12,-1.15
	35.43,8.27
	54,10.64
	114.7,10.64
1/16/2004	-50,-0.98
	-0.16,-0.98
	12,1.75
	34.38,9.43
	54,13.34
	114.7,13.34
2/24/2004	-50,0
	0,0
	12,1.85
	34.38,9.43
	54,11.34
	114.7,11.34

	All Sections (x,y)
3/24/2004	-50,-0.98
	-0.16,-0.98
	12,1.85
	34.38,9.43
	54,12.84
	114.7,12.84
4/27/2004	-50,-0.98
	-0.16,-0.98
	12,1.85
	34.38,9.43
	54,12.74
	114.7,12.74
6/8/2004	-50,0
	0,0
	12,1.85
	33.26,10.52
	45.17,13.86
	54,14.09
	114.7,14.25
7/26/2004	-50,0
	0,0
	12,3.45
	33.26,11.52
	45.17,14.86
	54,15.29
	114.7,15.29
9/28/2004	-50,0
	0,0
	12,1.85
	33.26,11.52
	54,13.14
	114.7,13.14
2/16/2005	-50,0
	0,0
	12,3.45
	45.37,16.26
	54,17.34
	114.7,17.34

US54-Fulton Slope Coordinates
(all coordinates in units of feet)

Section A				
Slope Surface (x,y)	Slope Interface (x,y)	Reinforcement Coordinates (x,y)		
		x	y_{top}	y_{bot}
-50,2	-50,-4.35	0	0.00	-5.00
-5,2	0,-4.50	4.5	1.41	-5.09
0,0	4.5,-4.58	9	2.81	-3.69
147,2.46	9,-3.5	13.5	4.22	-3.28
250,46	13.5,-2.93	18	5.63	-2.38
250,-100	18,-1.62	22.5	7.03	-0.97
-50,-100	22.5,-0.27	27	8.44	0.44
	27,1.01	31.5	9.84	1.84
	31.5,2.34	36	11.25	4.25
	36,4.00	40.5	12.66	4.66
	40.5,5.16	45	14.06	6.56
	45,7.00	49.5	15.47	7.47
	49.5,7.97	54	16.88	9.88
	54,11.38	58.5	18.28	11.28
	58.5,11.83	63	19.69	14.19
	63,14.66	67.5	21.09	15.59
	67.5,16.35			

US54-Fulton Piezometric Surface Coordinate Pairs
(all coordinates in units of feet)

	Section A (x,y)
6/9/2003	-50,-0.5
	0,-0.5
	19,2.74
	54,7.18
	97.65,15.92
	250,15.92
10/22/2003	-50,-0.5
	0,-0.5
	19,-1.06
	54,4.48
	97.39,10.32
	250,10.32
1/3/2004	-50,-0.5
	0,-0.5
	19,1.94
	54,6.88
	97.49,13.56
	250,13.56
2/18/2004	-50,-0.5
	0,-0.5
	19,1.44
	54,6.88
	99.93,15.13
	250,15.13
3/30/2004	-50,-0.5
	0,-0.5
	19,4.94
	54,11.38
	97.65,15.92
	250,15.92
4/12/2004	-50,-0.5
	0,-0.5
	19,1.64
	54,7.78
	102.77,19.17
	250,19.17

	Section A (x,y)
4/22/2004	-50,-0.5
	0,-0.5
	19,2.54
	54,6.78
	99.93,15.13
	250,15.13
5/20/2004	-50,-0.5
	0,-0.5
	19,2.34
	54,6.98
	99.93,15.13
	250,15.13
6/29/2004	-50,-0.5
	0,-0.5
	19,-0.6
	54,4.98
	101.17,12.07
	250,12.07
8/13/2004	-50,-2.75
	0,-2.66
	19,-2.66
	54,4.48
	104.12,15.25
	250,15.25
10/11/2004	-50,-3.1
	0,-3.1
	19,-3.1
	54,4.1
	104.12,15.25
	250,15.25
1/20/2005	-50,-0.5
	0,-0.5
	19,3.34
	54,9.73
	97.49,13.56
	250,13.56

APPENDIX F – STANDARD SPECIFICATION FOR RECYCLED PLASTIC PINS USED TO STABILIZE SLOPES

1 SCOPE

1.1 This specification covers recycled plastic lumber, produced from industrial by products and post-consumer waste materials, for use as slender member units for stabilization of earthen slopes.

1.2 This specification provides minimum engineering properties for the recycled plastic members to be considered for use in slope stabilization. Also provided are the testing protocols to be used to determine the engineering properties of candidate recycled plastic members. Alternative methods are provided for qualifying the recycled plastic members.

2 REFERENCED DOCUMENTS

2.1 *ASTM Standards*

- ASTM D6108 (1997a), "Standard Test Method for Compressive Properties of Plastic Lumber and Shapes," Section 8, Vol. 8.03.
- ASTM D6109 (1997b), "Standard Test Method for Flexural Properties of Unreinforced and Reinforced Plastic Lumber," Section 8, Vol. 8.03.
- ASTM D6111 (1997c), "Standard Test Methods for Bulk Density and Specific Gravity of Plastic Lumber and Shapes by Displacement," Section 8, Vol. 8.03.
- ASTM D6112 (1997d), "Standard Test Methods for Compressive and Flexural Creep and Creep-Rupture of Plastic Lumber and Shapes," Section 8, Vol. 8.03.

2.2 Other Documents

- Loehr JE, Bowders JJ and Salim H (2000) "Slope Stabilization Using Recycled Plastic Pins – Constructability," *Final Report*, RDT 00-007, Research Investigation 98-007, Missouri Department of Transportation, 74pp.
- Loehr JE, Bowders JJ (2003) "Slope Stabilization Using Recycled Plastic Pins: Phase II - Assessment in Varied Site Conditions" *Final Report*, RDT 03-016, Research Investigation 98-007B, Missouri Department of Transportation.

3 GENERAL DESCRIPTION

3.1 Slender recycled plastic pins (RPPs) can be used to stabilize earthen slopes by driving the RPPs into the face of the slope to intercept the sliding surface and "pin" the slope.

3.2 Recycled plastic pins (RPPs) are manufactured from industrial by-products or post-consumer waste consisting predominantly of polymeric materials (usually high or low density polyethylene).

3.3 Typically, recycled plastic pins are composed of the following: High Density Polyethylene (HDPE) (55 percent to 70 percent), Low Density Polyethylene (LDPE) (5 percent to 10 percent), Polystyrene (PS) (2 percent to 10 percent), Polypropylene (PP) (2 percent to 7 percent), Polyethylene-terephthalate (PET) (1 percent to 5 percent), and varying amounts of additives (sawdust, fly ash, and other by-products) (0 percent to 5 percent).

3.4 Two main processes are commonly used to produce recycled plastic pins: compression molding and extrusion forming.

3.4.1 In compression molding, the constituent waste streams are pulverized, blended together, heated until partially melted, and then compression formed in molds. In this process, the raw material is compressed into desired shapes and dimensions and is cured with heat and pressure.

3.4.2 Extrusion forming includes steps similar to compression molding; however, the molten composite material is forced through a die of the desired cross-section for the member being produced in lieu of compression into a mold. An advantage of the extrusion process is that it is relatively easy to manufacture members of any desired length while the compression molding process requires different molds for each different member length.

3.5 Recycled plastic pins acceptable for slope stabilization applications must meet the strength, flexure and durability criteria outlined in Section 4.

4 REQUIRED PROPERTIES

4.1 Recycled plastic pins specified for slope stabilization application must meet the criteria specified in Table 1. The parameters must be determined in accordance with the testing protocols listed and described in Section 5.

4.2 The design compressive strength must be equal to or greater than 1500 psi at less than or equal to five percent strain measured at a strain rate of 0.00003 in/in/min.

4.3 The design flexural strength must be equal to or greater than 1200 psi at less than or equal to two percent center strain measured at a crosshead motion rate of 0.02 in/in/min.

Table 1 – Minimum Properties for Recycled Plastic Pins Utilized in Slope Stabilization Applications.

<table>
<tr><th>Property</th><th>Minimum Requirements</th></tr>
<tr><td>Uniaxial Compressive Strength, σ_c (ASTM D6108)</td><td>A. $\sigma_c \geq$ 1500 psi, axial strain $\leq$ five percent, strain rate = 0.00003 in/in/min,
or
Alt A1. Develop expression for the strain rate effects and correct measured strength to the design strain rate, or
<table>
<tr><th>Strain Rate (in/in/min)</th><th>No. of Compression Tests</th></tr>
<tr><td>0.03</td><td>2</td></tr>
<tr><td>0.003</td><td>2</td></tr>
<tr><td>0.0003</td><td>2</td></tr>
</table>
Alt A2. $\sigma_c \geq$ 3750 psi, axial strain $\leq$ five percent, strain rate = 0.03 in/in/min.</td></tr>
<tr><td>Flexural Strength, σ_f (ASTM D6109)</td><td>B. $\sigma_f \geq$ 1200 psi, center strain $\leq$ two percent, rate of crosshead motion = 0.02 in/min, or
Alt B1. $\sigma_f \geq$ 2000 psi, center strain $\leq$ two percent, rate of crosshead motion = 1.9 in/min.</td></tr>
<tr><td>Durability - Environmental Exposure</td><td>C. Polymeric Constituent > 60% of mass of product, or
Alt C1. Less than 10% reduction in compressive strength after 100 days exposure.</td></tr>
<tr><td>Durability - Creep</td><td>D. No bending failure during 100 days under a constant load that produces an extreme fiber stress not less than 50% of the design compressive stress, or
Alt D1. Testing and Arrhenius modeling showing that the RPPs do not fail during the desired design life for the facility.</td></tr>
</table>

5 TEST METHODS

5.1 The measured strengths of RPPs are greatly influenced by the strain rate. The assumed field strain rate is on the order of 0.00003 in/in/min, which correlates with a compressive failure of a standard 3.5-in. x 3.5-in. RPP under a continuous rate of deformation for one week. Measured compressive strength of the RPP decreases as the strain rate used in the test decreases. The rate of decrease in strength is a function of the material type. For the RPPs tested in one program, the average decrease in strength was about 20 percent per log cycle decrease in the strain rate, i.e., an RPP with a compressive strength of 1000 psi at a strain rate of 0.03 in/in/min will show a compressive strength of 600 psi if tested at a strain rate of 0.0003 in/in/min. Due to the dependence on strain rate, it is imperative to make the required minimum strengths a function of the testing strain rate.

5.2 The “design” compressive (1500 psi) and flexural (1200 psi) strengths (measured at field strain rates), presented in Table 5.1, represent the required minimum mechanical properties for RPPs to be used in stabilization of slopes. The values are used in design of the stabilized field slopes and are determined at the field strain rate of 0.00003 in/in/min. Ideally, all RPP specimens should be tested at the field strain rate; however, from a practical perspective testing at this strain rate requires about one week per compression specimen which is not practical for production facilities.

5.3 Alternatives for qualifying an RPP material include:

5.3.1 (Alt A1) - Establish a compressive strength versus strain rate behavior and estimate the compressive strength at the field strain rate, or

5.3.2 (Alt A2) - A compressive strength of 3750 psi (25.9 MPa) or better when tested at the ASTM D6108 strain rate of 0.03 in/in/min (0.03 mm/mm/min). The latter value represents the increase in strength realized by the 3-order of magnitude increase in strain rate, i.e., above the field strain rate of 0.00003 in/in/min, using a reasonable upper-bound for strain rate effects.

Because Alt. A2 uses an upper-bound, most manufacturers will find that they can meet the specification more easily by establishing strain rate effects for their specific products rather than using the default relation assumed for Alt. A2.

5.4 The second part of the specification for mechanical properties is the required minimum flexural strength of 1200 psi at less than or equal to two percent center strain, when tested in four-point flexure using a crosshead displacement rate of 0.02 in/min (results in a strain rate of 0.00003 in/in/min).

5.4.1 (Alt B1) - If the ASTM D6109 crosshead deformation rate of 1.9 in/min is used, the required flexural strength is at least 2000 psi at less than or equal to two percent center strain. Again, the increase in required strength for the higher deformation rate is due to the effect that loading rate has on the resulting strength of the RPP.

5.5 In addition to mechanical properties, the candidate RPPs must meet several durability criteria. Recycled plastic materials can have significant variability with respect to constituents and manufacturing processes. The durability of the finished product will influence its suitability for application to slope stabilizations. Two durability facets, environmental degradation and creep, must be considered.

5.5.1 To address environmental degradation, the polymeric content of the RPPs should be greater than 60 percent of the mass to reduce the effect of environmental exposures.

5.5.2 To address the issue of creep, the RPP should not fail (break) under a cantilever bending load that generates an extreme fiber stress of 75 percent of the ultimate tensile strength when subjected to the load for 100 days.

5.5.3 Exposure testing and Arrhenius modeling are offered as alternate means to qualify a material’s durability properties.

5.6 It should be noted that in any slope stabilization design using RPPs, the designer can vary the stabilization scheme through variation of the number, location, strength and stiffness of the RPPs. The designer can also change the parameters by changing the factor of safety desired for the stabilized slope. Thus, the designer has numerous options for stabilization schemes and as such the required engineering properties of the RPPs could vary considerably.

APPENDIX G – STANDARD SPECIFICATION FOR CONSTRUCTION OF SLOPE STABILIZATION MEASURES USING RECYCLED PLASTIC REINFORCEMENT

Description. This work shall consist of installing recycled plastic pins into a soil slope either vertically or perpendicular to the soil slope as specified by the engineer on a staggered grid pattern for slope stabilization as shown on the attached plans.

Material. Recycled plastic pins, commonly referred to as "plastic lumber", consist of nominal 4 in. x 4 in. x 96 in. members made from recycled plastic, filler and other minor materials. Recycled plastic pins will be Commission furnished. Contractor shall pick up the pins from the MoDOT Maintenance Facilities listed below. Contractor will be allowed to mobilize operations from the maintenance facility indicated below where the pins are stored.

Site	Maintenance Facility	Contact Person	Contact No.

[Indicate the specific maintenance facility that will be used for storage of the pins and mobilization here for the particular contract that is being let for bids]

Construction Requirements. The Contractor shall furnish all labor, materials (except pins), equipment, and tooling required for installation of recycled plastic pins at the sites indicated on the plans. In advance of installation, MoDOT will be responsible for establishing base line survey stakes and intermediate layout markers at the site. At least 10 working days in advance of the start of installation, the Contractor shall contact the designated MoDOT contact established at the preconstruction conference to coordinate the base line staking and intermediate layout markers. The Contractor shall submit a written work plan outlining the installation method, equipment and tooling to be utilized to the engineer prior to starting the project. If base line staking and/or intermediate layout marks become unusable due to weather, construction or other cause, the contractor shall notify the engineer, and the engineer shall remark the base lines and intermediate marker locations. The contractor shall exercise reasonable care not to unnecessarily disturb or obliterate the base line markings and intermediate layout markings provided by the engineer. If remarking is required due to contractor's failure to exercise reasonable care, or if repeated unnecessary requests for remarking are made by the contractor even though the markings are visible and usable, the contractor may be responsible to the commission for the reasonable cost of such remarking.

The Contractor shall install each pin within 6 in. of the location as shown on the plans. The recycled plastic pins shall be installed vertically or perpendicular to the soil slope as specified by the engineer into the soil slope by a method of driving or hammering or by other methods approved by the engineer. Prior to installation at each location, the alignment of installation equipment and pin shall be checked to ensure the pins will be installed as specified.

The Contractor will be responsible for accessing the existing slope and stabilizing his equipment on the existing slope as necessary to maintain alignment and location during installation of the pins. The pins shall be installed to their full length into the soil unless refusal is encountered at shallower depth and installation is accepted as determined by the engineer. Care shall be exercised to not chip, split, broom or otherwise damage any pin during installation. The pins shall be installed such that the top of the completed installation is flush with or slightly below

existing ground surface. Any accepted pins installed to less than full depth and any damaged pins that can not be readily extracted shall be cut off with a chain saw or other appropriate device to be flush with or slightly below existing ground surface.

Driving Equipment. Recycled plastic pins shall be driven with power-driven hammers. Power-driven hammers will be defined as hammers operated by hydraulics, air or mechanical drop methods. Maximum allowable hammer energy for driving recycled plastic pins shall be 2000 ft-lb.

Test Drives. The contractor shall perform a test drive of the recycled plastic pins at locations specified by the engineer to demonstrate the contractor's ability to drive recycled plastic pins.

Test drives shall be performed with the same type of equipment as will be used for driving the recycled plastic pins at the project location. Test drives not conducted at the project location shall be cut off, or pulled and backfilled as approved by the engineer.

In general, it is permissible for some areas within the overall slope stabilization project to have no members or to have compromised members (partial penetration or broken at some depth) provided that the area is surrounded by intact, fully-penetrating members. The area with compromised members shall be small relative to the overall project area. The engineer shall determine if the area with compromised members is acceptable; however, an estimate of acceptable size might be up to ten percent of the total project area. Any pin broken or damaged by reason of internal defects, by improper driving, or driven outside of the pin's proper location, shall be cut off flush with the ground surface. Some members may break as they are nearing full penetration. They should remain in place and the portion above the ground surface should be cut off. The engineer can decide to drive a replacement pin immediately adjacent to the broken one or to simply continue with the installation scheme. Up to ten percent broken members, provided they are not concentrated in one location, should not compromise the stability of the scheme.

Recycled plastic members that can not be fully embedded shall be cut off at the ground surface using a chain saw or other appropriate device approved by the engineer. The pins should be cut as close to flush with the ground surface as possible so that the pins do not interfere with mowing and landscaping activities.

The top of the recycled plastic pins shall be protected against damage during driving. The procedure incident to the driving of pins shall not subject pins to excessive and undue abuse.

Site Cleanup. After all of the pins are installed at the project location, the site shall be cleaned of all debris. All pin lengths remaining above ground shall be cut off flush with the ground surface. All excess pin lengths that are cut off and all other trash and debris resulting from the pin installation process shall be the responsibility of the contractor for proper disposal at no cost to the Commission.

Repair and re-vegetation of the slope damaged by the pin installation equipment shall be the responsibility of the Commission. The Commission reserves the right to halt pin installation if

soil or weather conditions are such that, in the opinion of the engineer, excessive damage to the soil slope is occurring.

Pin Cut-Offs. No direct payment will be made for pin cut-offs.

Payment. Payment will be made on a per installed pin basis less a replacement cost of $25 for each pin in excess of 4 per site damaged by the Contractor.

No direct payment will be made for incidental items necessary to complete the work unless specifically provided as a pay item in the contract.

Test Drives. Test drives will be paid for at the contract unit price.

Missouri Department of Transportation
Organizational Results
P. O. Box 270
Jefferson City, MO 65102

573.751.3002
1 888 ASK MODOT
rdtcomments@modot.mo.gov
www.modot.org/services/rdt